



कविकुलगुरु

Kavikulaguru Kalidas Sanskrit University
Ramtek, Dist. Nagpur, Maharashtra

Vol. X- Issue I (III) (January-June 2023)

ISSN - 2277-7067

Peer Reviewed

**Journal of
Fundamental &
Comparative Research**

UGC CARE Listed Journal

शोधसंहिता

New Research Frontiers

Principal
Poona College of Arts, Science & Commerce
Camp, Pune-411001
Principal Office

January-June 2023

Volume - X Issue I (III)

Research Journal
ISSN No. 2277-7067

Journal of Fundamental & Comparative Research

शोधसंहिता

A Peer Reviewed Bi-annual Interdisciplinary Research
Journal of the University

UGC CARE Listed Journal
New Research Frontiers

- Patron -

Prof. Shrinivasa Varkhed
Vice Chancellor

- Chief Editor -

Prof. Madhusudan Penna
Director, Research & Publication

- Editor -

Dr. Rajendra C. Jain
Dept. of Sanskrit Language & Literature



कविकुलगुरु कलिदास

**KAVIKULAGURU KALIDAS SANSKRIT UNIVERSITY
RAMTEK**


PRINCIPAL

Paona College of Arts, Science & Commerce
Camp, Pune-411001
Principal Office



INDEX

1	IMPACT OF TECHNOLOGICAL INNOVATION ON BUSINESS PERFORMANCE: A SYSTEMATIC REVIEW OF LITERATURE USING PRISMA FRAMEWORK Zafar Ahmed Khan, Dr. Shakeb Ahmed Mumtaz Husain	1
2	HOLIDAY EFFECT IN INDIAN STOCK MARKET: AN EMPIRICAL STUDY OF NSE NIFTY SECTORAL INDICES Mr. Suraj Prakash Tavekar, Dr. Sri Ram Padyala, Ms. Pinky Yadav	7
3	LEADERSHIP STYLE MATTER ON PUBLIC AND PRIVATE EMPLOYEES PERFORMANCE (EVIDENCE FROM ETHIOPIAN BANKS) Bruk Gonfa Worku	18
4	INDIAN TOURISM INDUSTRY: PROSPECTS AND CHALLENGES Mohammad Shadab Hussain	28
5	A STUDY ON HUMAN RESOURCE DEVELOPMENT IN CO-OPERATIVE ORGANISATION Yewale Hambirao Bhagwan	35
6	COVID -19 PANDEMIC- A SAGA OF INCONVENIENCES AND CHALLENGES AMONG PREGNANT WOMEN IN RURAL AREAS OF GOA. Ms Archana Narayan Kanekar alias Shivani Shivdatt Shirodkar	38
7	A STUDY ON HR AUDIT ORGANIZATION SYSTEMS IN UTKPL PUNE. Dr. Anjum Sayyad, MR. Nisar Shaikh.	45
8	WOMEN'S ENTREPRENEURSHIP IN STARTUP INDIA CAMPAIGN: PROBLEMS AND DIFFICULTIES Dr. Neha Devidas Nalawade	52
9	INTERLINKAGE BETWEEN E WASTE HANDLING PRACTICES AND SUSTAINABILITY IN IT INDUSTRY: AN EMPIRICAL STUDY Mohd Talha Ahmad, Dr. Amol Murgai	57
10	A STUDY OF VARIOUS RESULT-ORIENTED EMPLOYEE TRAINING METHODS FOR ORGANIZATIONS Prof. (Dr.) Aftab Anwar Shaikh, Chitra Viswanathan Iyer	67
11	AN EVALUATION OF WOMEN'S PERCEPTION IN USING PLASTIC MONEY FOR PAYMENT Dr. Mohammed Fazil Shareef	73
12	A STUDY OF ROLE OF PUNE DISTRICT CENTRAL COOPERATIVE BANK IN PUNE DISTRICT Jagtap Shradha Tusbar	82
13	WORK LIFE BALANCE: AS A BEST PRACTICE MODEL OF HUMAN RESOURCE MANAGEMENT Amrin Adkar	86
14	NEP 2020: MULTIDISCIPLINARY APPROACH IN COMMERCE EDUCATION Dr. Lamture Nagesh T	93
15	PHARMACEUTICAL MARKETING STRATEGY AND PROSPECTS OF SMALL AND MEDIUM SCALE PHARMACEUTICAL COMPANIES Akbar Raza khan, Roshan Kazi	99
16	AN EMPIRICAL STUDY OF MERGER BETWEEN E-TAILER AND SUPERMARKETS -A Case Study of Goa Mr. Jitendra Rabada, Prof. Guntur Anjana Raju	105
17	THE IMPACT OF GIG WORK ON ENTREPRENEURSHIP IN INDIA: CHANGING THE LANDSCAPE Mr. Sushil Madanrao Gangane	119

PRINCIPAL
Poona College of Arts, Science & Commerce
Camp, Pune-411001
Principal Office



AN EVALUATION OF WOMEN'S PERCEPTION IN USING PLASTIC MONEY FOR PAYMENT

Dr. Mohammed Fazil Shareef

Ph.D. MBA., M.Com. NET.(Management) SET. (Commerce), Poona College of Arts Science and Commerce, Pune

ABSTRACT

In Modern Indian Banking Sector various innovative products are introduced. In banking financial inclusion the bank provides financial products and services with affordable cost, speedy, usage facility to Business organization and individuals. While financial inclusion was introduced in that more focused was given to promoting the electronic payment methods as well as plastic money in India. In this paper the main objective is to understand the perception of women's in order to analyses usage factors in pune city. This study is based on primary and secondary data were researcher used Questionnaire and observation methods to getting accurate responses. For analysis statistical tools are used Government of India took initiative to make cashless society with the help of digitization in banks, Varied types of plastic cards provided by banks in India like ATM cards, Debit Cards, Credit Cards and smart cards are mentioned. The study additionally highlights the role of those cards as electronic payment tool to be utilized by customers and discusses clearing and settlement method of those cards. Financial institutions with launching new innovative products as well as plastic money such as Debit Cards, Credit cards. This research study is also provide useful information regarding changes in banking industry also gives future insightness about innovative banking practices.

KEYWORDS: Banking Instruments, Debit Card, Credit Card.

1. INTRODUCTION

In India's economic growth and development banks are playing very essential role. Banks providing various facilities such as Capital for businesses, industrial development, agricultural development, credit facilities, transfer of money, investment, saving, and also provide financial advisory services. As government initiated the financial inclusion in all over the country. Financial inclusion defined as "where individuals and business have access to useful and affordable financial products and services that meet their needs that are delivered in a responsible and sustainable way. "Banks are also took steps to bringing the new innovative practices. Banks tried to initiate innovative and effective payment systems and functioning of smooth financial activities. Now day's digital methods of payment systems are more secure and efficient. In Indian Banking the Plastic Money is innovative product. It is a modern and convenient method for payments and doing transactions. Most of the Indians are preferred to use plastic money. This change in payment process is very important. Plastic money holders transact with riskless and also manage their large amount very easily. Under plastic money following cards like Debit cards, credit cards, automatic teller machines cards, smart cards, etc. are issued by the financial institutes. The advantage of plastic money cards are like Credit or Debit cards made easy to buy things from anywhere, through this purchase anything from anyplace without spending money on fare or cash transition, there is no time wastes for making payments, extra and advance safety while doing transactions. Some



limitations are also in plastic money such as while purchasing some shops that accept credit cards of a specific company only, the regional disputes is also main reason to not get facilitate, high Interest Rates on cards, credit cards fraud etc.

2. LITERATURE REVIEW

A review of theoretical and empirical literature for the research study is an integral part of any research work. Hence, an efforts are taken in this to present a review of various studies relating to plastic money cards (debit card, credit card etc.) as reported by experts, professionals and researchers. It shows the gap between what is done and what should be done in future. It makes a path for further research.

Slocum, J. and Mathews (1970) in their study "Social class and income indicators of consumer credit behavior" they stated the influence in USA of social and income variables on credit card selection and usage among cardholders. They defined lower higher and middle social economic classes. Peoples of the lower socio-economic class tend to use their cards for installment financing. Upper classes tend to use their cards as a convenient method of payment, the middle class feels that they should save money and postpone purchases. It also showed that age, sex and marital status are the significant factors of credit card selection and its usage.

Manideep Kaur and Kamalpreet Kaur (2008) The article "Development of Plastic Cards Market: Past, Present and Future Scenario in Indian Banks" described the Indian banking sectors various problems regarding of information technology as all the groups of bankers have now understood essence of requirement for their growth in future for having the strong advancements in e-payments methods. This can considered as beginning for bright future of plastic in India's economic scenario.

Syed Ali Raza (2016) his paper has attempted to understand the preference and attitude of plastic money holder of Hyderabad city. The survey was performed on 200 respondents. It was found that customer very well known about the concept of plastic money and its usage, and have been using it since long time. Debit card is most preferred mode of payment than various others card because it controls hobbits of over spending. According to the author respondents' are showing their interest in various ways as well as modes which they are eager to learn new techniques of modern banking.

Ms. Pinki (2017) in an article researcher gave an information into the factors which impacted the choice of people between paper money and the plastic money. It has been observed from the paper that 50% respondents were using plastic money and remaining was still not aware about the use of plastic money. The implementation of Security Pin and digital signatures should be made much secured to disallowing of misuse of plastic card.

Bhawna Mukaria (2018) the researcher discussed about various schemes and policies related with government such as Digital India and Pradhan Mantri Jan Dhan Yojna, in order to promote non-cash modes of payment. She also explained the challenges and futures regarding plastic money in India. This Study was mainly based on secondary data. It was suggested that the requirement of



high IT infrastructure, security concerns, lack of technological awareness are the main obstacle in the way of cashless economy.

3. STATEMENT OF PROBLEM:

In Indian economic scenario banking plays an important role for economic growth as well as development. For the increasing financial inclusion in India banks create infrastructural system to expanding the businesses, reduce the risk and as well as capture the market through introducing new innovative payment methods. There are lots of new innovative methods which helps to make secure payment systems. Plastic cards are introduced for secure payments and advancement in technology. The researcher has chosen the usage of debit and credit card and perception amongst the women's of using this plastic cards in pune city. It also aims to identifying the driving factors behind the behavior women regarding promoting the financial inclusion through plastic money with respect to debit and credit cards in pune only.

4. OBJECTIVES OF THE STUDY:

1. To study the concept Plastic Money Cards.
2. To study the benefits of plastic money in the economy.
3. To understand the perceptions about plastic money card of women's in pune city.
4. To analyze the relationship between plastic money and occupation of users of plastic money.

5. RESEARCH STUDY OF HYPOTHESIS:

- H0: There is no relationship among using of debit /credit card and occupation of the card holder.
H1: There is relationship among using of debit / credit card and occupation of the card holder.

6. RESEARCH METHODOLOGY:

The present research paper is based on Primary as well as secondary data. As this study is based on analysis.

The universe of the survey is the working and non-working women working in Pune City. The sample size for the study is 170 respondents, all age group. Questionnaire of research study was filled from persons known to the researcher therefore researcher used a convenience sampling method. The questionnaire was given after enquiring of the usage of cards. Appropriate statistical tools have been employed. The data collected was analyzed using the SPSS (Statistical package for Social Science) tools like percentage and Chi Square test is used to get prove the hypothesis. Tables and Graphs are used to represent the data. In Secondary data researcher used various books, Reference books of financial inclusion, banking scenario in India, international and national journals, scholarly articles, government publications, reference papers in print and online related to the topic.

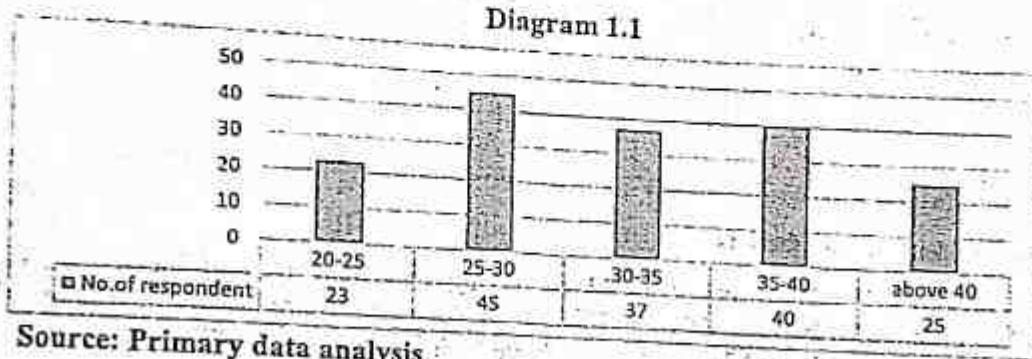


7. LIMITATIONS OF STUDY:

Due to Time constraint researcher mainly focused on the perception regarding selected plastic money card such as Debit card, Credit card have been considered for the study. Data Collection was limited to working and non-working women of in Pune City only. Method used in sampling and data collection analysis which has its own pros and cons.

8. INTERPRETATION AND ANALYSIS:

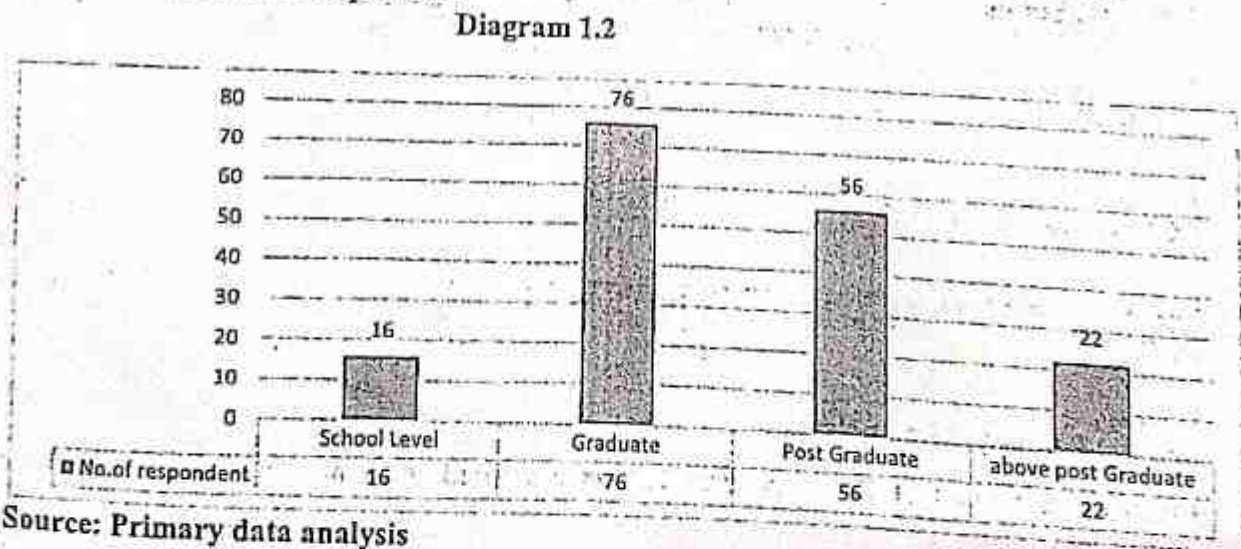
I. Age of the respondent



Source: Primary data analysis

Interpretation: Out of 170 respondent, 23 respondents are between the age group 20-25, 45 are between age group 25-30, 37 respondents are age group between 30-35, between 35-40 age group 40 respondents and above 40 age group 25 respondents.

II. Education of the respondent



Source: Primary data analysis



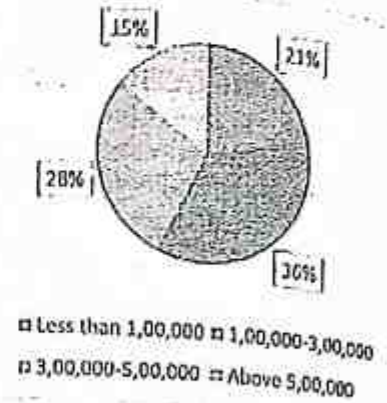
Interpretation: Out of 170 respondents 22 are above post graduates, 56 are postgraduates, graduates are 76 and 16 respondent completed till school level education.

III. Income of the respondent

Table 2.1

Income	No. of Respondent	Percentage
Less than 1,00,000	43	21.33
1,00,000-3,00,000	57	36
3,00,000-5,00,000	47	28
Above 5,00,000	23	14.66 %
Total	170	100 %

Diagram 1.3



Source: Primary data analysis

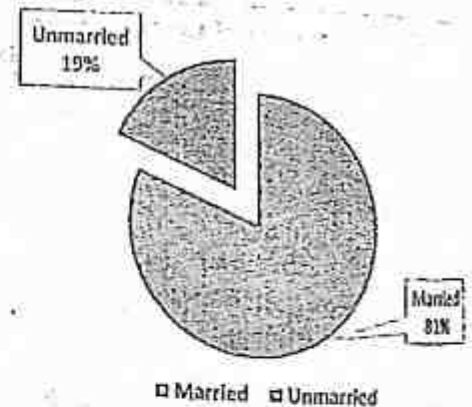
Interpretation: In 170 respondents 43 are having less than 100000 income annually. 57 respondents income is between 100000-300000. 47 respondents are having their annual income between 300000- 500000 and 23 respondents have their income above 500000.

IV. Marital Status of the respondent

Table 2.2

Marital Status	No. of Respondent	Percentage
Married	124	81%
Unmarried	46	19%
Total	170	100 %

Diagram 1.4



Source: Primary data analysis

Interpretation: Out of 170 respondent 124 were married and remaining 46 respondent were unmarried.



V. Trends of respondents Doing Job or Not.

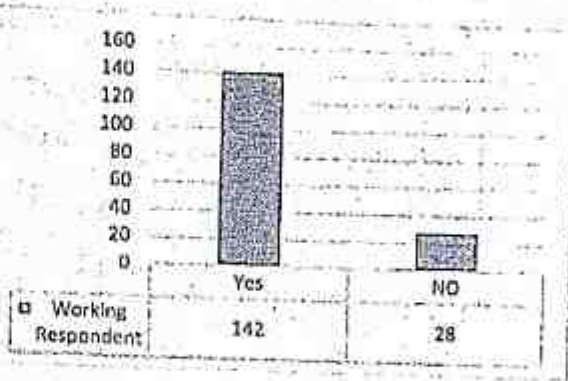
Table 2.2

	No. of Respondent	Percentage
YES	142	83.52%
NO	28	16.47%
Total	170	100 %

Source: Primary data analysis

Interpretation: Out of 170 women respondents 142 were working in various sectors and 28 were not working anywhere.

Diagram 1.4



V. Respondent usage of debit and credit Cards

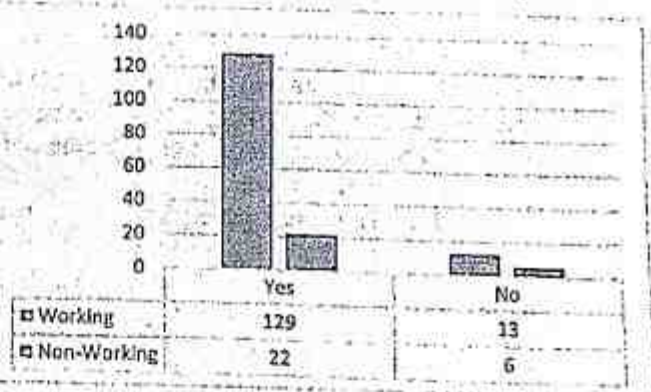
Table 2.3

	Working	Non- Working
YES	129	22
NO	13	06
Total	142	28

Source: Primary data analysis

Interpretation: Out of 170 respondents 142 working womens 129 respondent tell us on usage of debit and credit card, 13 respondents not used the cards. Out of 28 non-working women 22 were used the plastic cards and 6 were not used plastic cards.

Diagram 1.5



PRINCIPAL

Poona College of Arts, Science & Commerce
Camp, Pune-411001
Principal Office

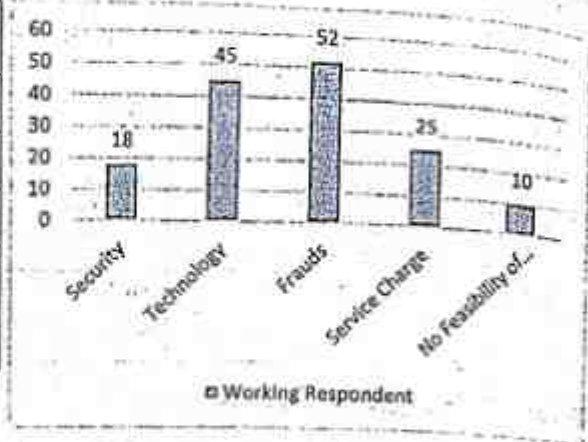


VI. Respondent persuasion about problems while use of debit and credit Cards

Table 2.4

Impact factors	No. of Respondent	Percentage
Security	28	16.47
Technology	45	26.47
Service charge	57	33.52
Frauds	27	15.88
No Feasibility of Services	13	7.64

Diagram 1.5



Source: Primary data analysis

Interpretation: In Table 2.4 170 respondent they give feedback about the impactful factors in debit and Credit card. 28 respondent mentioned the security factor, 45 respondents were mentioned technological factor, 57 mentioned their consent about service charges of using plastic money cards, 27 respondents respond regarding fraud issues and 13 women respondents for no feasibility of services.

9. TESTING OF HYPOTHESIS

The relationship among the women and carrying the Debit or credit card is analyzed through Chi-Square method using SPSS. The results are below:

H0: There is no relationship among using of debit /credit card and occupation of the card holder.

H1: There is relationship among using of debit /credit card and occupation of the card holder.

Table 2.5

Women		Number of Users debit /Credit card				Total
		Debit card	credit card	Both	No Card	
Working	Count	76	24	28	0	128
	Expected	77.12	25.76	25.12	0	
Non-working	Count	16	4	6	16	42
	Expected	15.84	4.16	8	14	
Total		92	28	34	16	170

Source: Computed data using SPSS (Output)

PRINCIPAL

Poona College of Arts, Science & Commerce
Camp, Pune-411001 Page | 79
Principal Office



Result of Chi-Square Tests

Table 2.6

	Value	df	Asymp. Sig. (2-sided)
Pearson Chi-Square	12.013	3	.0160
Likelihood Ratio	16.454	3	.009
Linear-by-Linear Association	3.831	1	.0596
N of Valid Cases	170		

Source; SPSS output

From the above Table it is found that the significant value of the chi-square value of 12.013 for the 3 degrees of freedom is 0.016 which is less than 0.05. Hence the null hypothesis is not accepted and Hypothesis H1 is accepted. It is concluded that there is a relationship between occupation and number of withdrawals.

10. FINDINGS AND SUGGESTIONS:

Following are the findings from this research study. Use of debit cards and credit cards maximum by young generation. Old age women respondents are not ready to use latest technological changes regarding payment. Researcher also found Plastic money is commonly and effectively used by educated people if proper training is given to all then the use of cards will increase. Most of the non-working women are used debit cards for shopping but very less are used credit cards. The cards of non-working women who are not using debit cards are preferred over credit cards by both working and non-working women. Researcher suggested awareness should create about related with advancement of payment technology, security of transaction and give proper instruction or training using the plastic money cards. Collaboration of bank and government especially for the non-working women. Unnecessary paper formality should be reduced to encourage the use of credit card. In order to increase the use of plastic money, number of POS and ATM should be increased. The corresponding servers should be high in speed and capacity to provide high speed and uninterrupted experience for the users. Also the machines should be established in secured places. It is suggested that to popularize the use of plastic money amongst non-working women, easy banking and supportive staff leads to the miracle changes in present scenario.

CONCLUSION:

Government of India's initiative regarding "Financial Inclusion Scheme". This scheme is launched to introduce new financial instrument and services which give boost banking payment methods. In this paper an attempt has been made to evaluate the perception of working and non-working women towards debit and credit cards. It was felt that a large number of non-working women prefer to use cash for transaction purpose. The institute should use innovative strategy to increase the percentage of usage of debit cards as well as credit cards. If methods of payments are sustained through the acceptance of customer who use the cards effectively and wisely. Increasing awareness about the payment methods such as debit cards, credit cards. Also financial institutes ensure about the satisfaction which is very necessary to increase the use of this cards.



REFERENCES:

- [1] A.Sarangapani and T. Manath, (July 2008) 'Implementation and challenges', E-business, Volume XIV page 54.
- [2] Dr. A.Vinayagamoorthy, (Feb 2008) 'Globalization and recent trends in Banking', Banking Finance, Volume IV (page 9-14).
- [3] Dr. S. Arumugasmy and P. Shenbagavalli, (May 2008) 'Growth and development of ATM', Banking Finance, Volume V (page 39-44).
- [4] Shashi K.Guptha and Nisha Aggarwal, (2008) 'Financial Services' Ludhiana Kalyani Publishing House ISBN 9789327240832 (13).
- [5] V.A. Avadani, (2010) 'Marketing of financial services' 3rd Edition (2015) Himalaya Publishing House, New Delhi.
- [6] Desai Vasant (2012) "Financial markets and financial services", ISBN 978-93-5202-298-4, Himalaya Publishing House, New Delhi.
- [7] Sharma, A., Karim, S. F., & Jain, V. (2015) "An Evaluation of Consumer Perception and Attitude towards the Usage of Plastic Money in India". International Journal of Science Technology and Management (page 80-86).
- [8] Syed Ali Raza (July 2016) "Analysis the Use of Plastic Money in Hyderabad City, Sindh Province" American International Journal of Research in Humanities, Arts and Social Sciences, ISSN (Print) 2328-3734, ISSN (Online): 2328-3696 (page 99-103).
- [9] Mr. Rohit Malagi and Mrs. Harshala Shelar (January 2017) "Increasing the Trend of Shopping because of Plastic Money in Western Maharashtra" International Journal for Innovative Research in Science & Technology| Volume 3 | Issue 08 | January 2017 ISSN (online): 2349 (page 72-77).
- [10] Ms. Pinki (July 2017), "To Study Customer Choice between Paper Currency and Plastic Money" International Journal of Engineering Sciences & Research Technology, ISSN: 2277-9655 (page 777-779).
- [11] Bhawna Mukaria (February 2018) "PLASTIC MONEY: PROSPECTIVE AND CHALLENGES" International Journal of Engineering and Management Research, Vol.5 (Iss.2): February, 2018 ISSN: 2454-1907 (page 117-125).
- [12] E. Megha, Swathi Prathap and M.B. Krishna (2018) "A Study on Impact of Demonetization on Increased Use of Plastic Money-with Special Reference to Ernakulam District" International Journal of Pure and Applied Mathematics Volume 119 No. 10 2018, (page 679-688).
- [13] www.globalcard.com.au/product.
- [14] www.icmrindia.org.
- [15] www.investopedia.com

PRINCIPAL

Poona College of Arts, Science & Commerce
Camp, Pune-411001
Principal Office

anvesak

A biannual Journal

2023



**Sardar Patel Institute of
Economic and Social Research**

PRINCIPAL

Poona College of Arts, Science & Commerce

Campus, Poona-411001

Phone: 020-26121111



anveṣak

A bi-annual journal

Vol.53, No.1 January - June 2023

ISSN: 0378-4568

Edition-II



Sardar Patel Institute of Economic and Social Research

Thaltej Road, Ahmedabad - 380 054, India

Phone: (079) 2685 0598, Fax: (079) 2685 1714

Website: www.spiesr.as.in, Email: info@spiser.ac.in

PRINCIPAL

Poona College of Arts, Science & Commerce

Camp, Pune-411001


Principal Office



CONTENTS

1.	USE OF KAIZEN TECHNIQUE IN INFORMATION TECHNOLOGY SECTORS TO ENHANCE PRODUCTIVITY IN PUNE REGION	Ansari Nasrin Husen, Dr. M. G. Mulla	1-5
2.	NEW PARADIGMS IN INDIAN FOREIGN POLICY (1990-2022)	Ahmad Shamshad	6-13
3.	A STUDY ON ENTREPRENEURSHIP & START UP	Jadhav Sonali, L., Dhumal S.R, Doshi S.S	14-17
4.	NEW AI CHATBOT - "ChatGPT"	Priya Jaysing Nimbalkar, Aparna Sanjay Kadam, Aparna Sanjay Kadam	18-21
5.	CUSTOMER RELATIONSHIP MANAGEMENT IN COOPERATIVE BANKS: AN EMPIRICAL STUDY OF NASHIK CITY	Dr. Asha Dadasaheb Kadam	22-25
6.	AN EMPIRICAL STUDY ON PRESENT STATUS OF RICKSHAW DRIVERS IN NASHIK CITY	Dr. Motiram B. Wagh	26-32
7.	GIG ECONOMY: BOON OR BANE FOR WORKERS	Dr. Noel Parge	33-37
8.	GIG ECONOMY – EMPLOYERS PERSPECTIVE	Dr. Noel Parge	38-41
9.	DIGITAL MARKETING PRACTICES BY ONLINE PHARMACIES IN INDIA	Dr. Khalid Arshad, Dr. Aftab Alam	42-50
10.	CHANGING SCENARIO OF RURAL MARKETING- AN OVERVIEW	Dr. Mohammed Fazil Shareef	51-55
11.	INDO-OMAN RELATIONS: LOOKING BACK WITH SATISFACTION, LOOKING AHEAD WITH CONFIDENCE.	Dr. Zoheb Hasan	56-59
12.	TO STUDY THE PROGRESSION & DEVELOPMENT OF INDIAN BANKING	Aadil Omer Bade, Dr. Shirsi Rajendra Shiyoyi	60-66
13.	INFLATION IN INDIA: CAUSES & REMEDIES	Vishal Balawant Gaikwad, Harshwardhan Shrikant Kulkarni	67-70
14.	OPINION MINING TECHNIQUES	Abdul Samad Riyaz Ahmed Khan	71-73
15.	A COMPARATIVE STUDY ON CORPORATE SOCIAL RESPONSIBILITY (CSR) PRACTICES OF STATE BANK OF INDIA & HDFC BANK	Ramajan Varunkar, Dr. Rakesh Suran	74-79
16.	MSME'S IN INDIA: PROBLEMS & THE FUTURE IN POST-COVID PANDEMIC	Dr. Lanjure Nagesh Topanna	80-85

Mumbai


PRINCIPAL
 Poona College of Arts, Science & Commerce
 Camp, Pune-411001
 Principal Office

CHANGING SCENARIO OF RURAL MARKETING- AN OVERVIEW

Dr. Mohammed Fazil Shareef

Poona College of Arts Science and Commerce, Pune

Abstract

India is a predominantly agricultural country, with agriculture and agricultural-related activities accounting for the vast majority of the country's economic activity. For a long time, agriculture in India was the largest contributor to the country's GDP. Marketing is a centuries-old concept. It has been assumed since the beginning of time that no one has all of the resources required to meet his or her needs. This paper attempted to assess the impact on rural marketing of various infrastructure developments made by governments (both state and federal) over the last few decades. The study's findings indicate a positive impact on the availability and turnover of branded daily consumption goods. All stakeholders stand to benefit, including the government, shopkeepers, and village consumers, and their attitudes toward branded goods are gradually changing. This will undoubtedly aid in the future economic development of the rural area.

Keywords: Rural marketing, Marketing, Scenario, Development, Rural Sector

Introduction

India is an agriculture-dominated country, with agriculture and agricultural-related activities accounting for the majority of the country's economic activity. For a long time, Indian agriculture was the largest contributor to India's Gross Domestic Product. However, in recent years, the Industrial sector, which includes both manufacturing and services, has surpassed the pivotal position in GDP.

According to the 2011 population census, India's population was 1,210,854,977, while Maharashtra's population was 11,23,72,972, with the following rural-urban split. Rural areas account for 68.4 percent of India's population, and migration from rural to urban areas continues for a variety of reasons. When compared to previous decades, the rate of population growth has slowed in recent years. Maharashtra's population is divided into rural and urban areas, according to the 2011 census.

State	Total population	Rural Population	Urban Population	Rural Pop. Percentage	Urban Pop. Percentage
Maharashtra	11,23,72,972	6,15,45,441	5,08,27,511	54.77	45.23

Source: <http://www.censusindia.gov.in/2011census>

Rural Marketing in Historical Perspective:

The concept of marketing is an ancient one. Since the dawn of time, it has been assumed that no one has all the resources necessary to meet his or her needs. One may have a surplus in one area while lacking in another. As a result, someone with surplus must sell it to someone who needs it and exchange it for whatever surplus he or she has. This was the evolution of marketing, which means marketing in exchange for goods and services. In terms of the rural marketing segment, grocers were used to market primarily locally made products that were of lower quality when compared to branded goods. In the absence of adequate purchasing power, village consumers chose low-quality products. Proper packaging was also lacking in the past, with weights and the date of packing not being mentioned on the packaging.

Rural Development in the last three decades:

Given the above demographic situation in India, both the Government of India and the Maharashtra State Government have prioritised socioeconomic development by investing significant resources in infrastructure development. This has given the rural area a new lease on life in terms of education, healthcare, communication, roads, electricity provision, irrigation potential, and so on. On the education front, we now see that almost every taluka has an arts, science, and commerce college, so rural students who were previously denied higher education now have access to it. Because this facility is nearby, village girls who want to pursue higher education no longer need to relocate to urban areas.

On the communication front, all of the villages are now well connected by all-weather roads to the district headquarters and nearby towns. This improvement in the roads has paved the way for public transportation to gain traction. All-weather roads have also had an impact on the development potential of rural areas. The villagers can now transport their agricultural produce to a nearby town for marketing purposes, as well as agricultural input from these towns, because transportation is now available.

On the human healthcare front, we now see that there has been a significant improvement in the village's sanitation arrangements. There has also been an improvement in the availability of clean drinking water in the villages. This has a two-way impact on the villagers' way of life. On the one hand, improved sanitation has improved the health of the villagers, and on the other hand, the village now has a general medical practitioner. Some specialists also charge a weekly or on-demand visit to a rural clinic or private hospital. Every taluka has a primary health care centre with expert doctors and other nursing staff. The changed healthcare scenario has also influenced the villagers' perceptions of the quality of the products they purchase from the village's grocery stores and medical shops.

The increase in irrigation potential, either through canal extension or by constructing Shet Tali under the Maharashtra government's Jalyukt Shivar Yojana, has increased the availability of water supply. The villagers' cropping patterns have shifted as a result of the availability of a reliable water source. Depending on the proximity to a nearby town, they are now cultivating cash crops such as sugarcane, horticultural crops, and vegetables. Dairy activity has also increased as a result of the all-weather roads; now, almost every village has a dairy society. Banking facilities in rural areas enable farm mechanisation, and other credit needs of the rural masses are now met locally. All of these developments have a positive impact on the villagers' ability to generate income. As a result, the villagers' purchasing power has increased. The economic movement has gained traction. The turnover of consumer products, particularly branded consumer products, has increased significantly. Electricity is now available in all of the villages.

Objectives of the study

The author had established the following broad objectives for this study:

- 1) To investigate the changes that has occurred in the field of rural marketing over the last three decades.
- 2) To investigate the factors that contributed to the shift in the rural marketing environment.

Research Methodology

The universe identified for this research study was two talukas in the Pune district, namely

- 1) Haveli 2) Maval.

Each taluka was assigned two villages, one with the highest population and the other with a middle-sized population.

The following Taluka wise villages were visited:

UGC Care Group-I Journals

Taluka	Name of the village	Taluk a	Name of the village
Haveli	1. Ambee 2. Kirkitwadi 3. Khadakwasala 4. Donje 5. Khanapur 6. Malkhed 7. Sonapur	Velhe	1) Kauran (Bk) 2) Nigade 3) Osade 4) Panshet 5) Rule

The primary data was acquired from the randomly designated stakeholders, which included village residents as well as the proprietors of local grocery and medical stores. While identifying the consumers of the village, care was also made to guarantee that it represents a cross section of the consumers. As a result, factors such as gender, education level, economic condition, occupation, and so on were taken into consideration. 100 residents of the community were recognised as customers, along with eight shop owners. When the entire research population is taken into consideration, the size of the sample can be considered sufficiently representative. The responses were compiled with the help of a comprehensive questionnaire that was sent to the respondents. The questionnaire was designed with the aims of this study in mind at every step of the process.

Data analysis discussion

The gender of the consumer influences their needs for groceries and other goods, so gender data was obtained, and it was discovered that 67 of the total 80 consumer respondents were male, while 13 were female.

The respondents' educational backgrounds also have an impact on grocery marketing and the medical needs of village consumers. According to the data gathered, 8 of the total 80 respondents were illiterate, 42 had studied up to the XII standard, 17 held a diploma / ITI, and 13 were graduates/post graduates. It means that 90 percent of the total sample's respondents were fairly educated.

The respondents' occupations were classified as follows: out of 80 respondents, 57 were pursuing Agriculture as their economic activity, accounting for 71.25 percent, 13 were employed, accounting for 16.25 percent, and 10 were pursuing higher education.

Major Findings

A questionnaire with a provision of obtaining responses on certain relevant aspects including the statements given in the Likert scale was administered on the randomly identified respondents. The data so obtained was consolidated and the same was interpreted. Major findings have been enumerated herein below:

1. Infrastructural development in rural areas has occurred over the last two decades, particularly in the areas of all-weather roads, the opening of a primary health centre, the availability of a local healthcare facility, increased irrigation coverage, pure-drinking availability, the opening of a high school, and so on. As a result, the rural area experienced socioeconomic development.
2. The villages are now linked to the district headquarters and nearby cities. The availability of state-run buses has enabled villagers to transport their agricultural produce to urban/metropolitan areas and to purchase agricultural inputs from the city.
3. The rural youth can now use S.T. connectivity to seek jobs in the city and return to the rural area without disrupting their rural settlement.

4. A medical clinic and a few grocery stores have opened nearby, and a bank branch has been financing the rural masses. Because of the presence of the bank nearby, the government credit-input schemes are also being implemented in the rural area.
5. A dairy society has been established in the area, paving the way for the development of dairy activities, allowing farmers to earn liquid cash at regular intervals through activities related to agriculture.
6. All of these developments have had a positive impact on the villagers' earnings, and their purchasing power has increased significantly.
7. In terms of rural market development, it has been discovered that new grocery stores and medical clinics have opened in villages as a result of all-weather roads, mobile connectivity, and bank financing.
8. Previously, villagers preferred buying locally manufactured and in consumer goods in loose form, but now branded quality goods are available in rural areas. The villagers prefer to purchase branded items.
9. Marketing firms are also developing small packaging in sachet forms to meet the needs of consumers who have limited financial resources.
10. A variety of new items in the daily consumable segment are now available, providing consumers with options.
11. The vendors' participation in the weekly bazaar in the nearby town has increased.
12. The villagers no longer need to travel to the nearby town for certain branded goods because they are now available locally.
13. Because electricity is available in villages, rural consumers gain brand awareness of new products with new utility through colourful television advertisements.
14. In terms of shopkeepers, they are not required to obtain branded goods from a nearby city/town. The companies are ensuring that the necessary products are supplied on time.
15. When a new product is introduced, marketing firms pay special attention to creating door-to-door campaigns for consumer goods.
16. Marketing firms are now displaying and promoting their products at village fairs that are held on a regular basis.

Suggestions

1. Given the positive impact of infrastructure developments on rural commerce, it should continue to improve the current level of infrastructure.
2. The government should extend the reach of banks into unbanked villages.
3. The government should improve electricity supply and avoid frequent outages. This will aid in improving the villagers' connectivity with the rest of the world.
4. Shopkeepers should also increase the variety of daily consumption items in small packaging, such as breathing and washing soaps, tooth pastes, shampoos, tea, coffee, and so on.
5. The government should ensure that roads are safe to travel on and that they are repaired on time.

Conclusion

According to the findings of this study, improvements in rural infrastructure have a positive impact on rural economic activity and have increased the purchasing power of the rural masses. Improved healthcare facilities and other infrastructure, such as the provision of pure drinking water and the

Opening of medical shops, have greatly aided the villagers. The villagers' approach to education, healthcare maintenance, and the establishment of cooperative institutions such as primary cooperative credit societies and Milk Collection societies has boosted rural economic development. Further infrastructure development will ensure the pace of development, and rural marketing will be improved. This will strengthen rural economic development even further, and will eventually have an impact on India's GDP. Rural marketing has promising future development prospects.

References

Journal Article

- 1) Aarti Joshi (2011)
- 2) Ahmed M., Vol1, Issue3, December, 162-172 (2017)
- 3) Dr. Joseph Kesari, Abhishek Kumar Srivastava (2015)
- 4) Manpreet Kaur Volume 2, Issue (June 2013)

Books

- 1) Rakesh Bhasin, Ombir Singh, Suvarna Agarwal, Thakkar Publications, Delhi (2018)
- 2) Purshoutam warje, (2013), 3rd edition, by Dorling Kindersley (India) Pvt. Ltd. Noida
- 3) Ranbir Singh Gulia, Ombir Singh, Suvijna Awasthi, Wisdom Publications, Delhi (2011)

Conference Proceedings

- 1) Shokla Pritesh kumar Y. 2013. Indian Journal of Research, Vol. 2, Issue 2, February 2013, pp 49-52

PRINCIPAL

Poona College of Arts, Science & Commerce
Ganga Purna-411001
Principal Office

anvesak

A biannual Journal

2023



**Sardar Patel Institute of
Economic and Social Research**

anveşak

A bi-annual journal

Vol.53, No.1 January - June 2023

ISSN: 0378-4568

Edition-I



Sardar Patel Institute of Economic and Social Research

Thaltej Road, Ahmedabad - 380 054. India

Phone: (079) 2685 0598, Fax: (079) 2685 1714

Website: www.spiesr.as.in, Email: info@spiser.ac.in

CONTENTS

1.	हरियाणा में गैर-संस्थागत माइक्रो-क्रेडिट प्रदाताओं से उधार लेने वाले लोगों की समस्याओं का आर्थिक व सामाजिक विश्लेषण	डॉ. संतोष कुमारी	1-4
2.	KNOWLEDGE MANAGEMENT, INNOVATIONS AND ENTREPRENEURSHIP IN MSMEs OF HEALTHCARE INDUSTRY	Kartikay Mahajan, Dharamveer Narwal	5-13
3/	जनपद हरिद्वार का सामान्य भूमि उपयोग : एक अध्ययन	डॉ० अमित कश्यप	14-21
4.	THE ADOPTION OF MODERN INFORMATIONAL TOOLS BY SEBI TO DETER INSIDER TRADING	Prof. (Dr.) Mahendra Tiwari, Asst. Prof. Deepshikha Sharma	22-25
5.	उत्तराखण्डी लोक संगीत के वाहक बेडा समुदाय का सामाजिक-सांस्कृतिक अध्ययन	रविन्द्र कुमार स्नेही, प्रो० गीताली पडियार	26-33
6.	RISK MANAGEMENT PRACTICES OF PUBLIC AND PRIVATE SECTOR BANKS	Ruby Sharma, Dr. Munish Goyal	34-41
7.	ECONOMICS IN HOUSEHOLDS	Dr. Shirish N. Bhosale	42-45
8.	E- BUSINESS	Dr. Shivanand B. Bhanje, Umashankar G. Nadargi	46-50
9.	BANKING SYSTEM TRANSITION FROM A COMPARATIVELY CLOSED ECONOMY TO A MARKET ECONOMY	Milind Patil, Dr. Gulnawaz Usmani	51-62
10.	TO STUDY THE IMPACT OF DIGITAL MARKETING ON CONSUMER BUYING BEHAVIOUR	Dr. Deepa Nathwani	63-67
11.	ISSUES AND POSSIBILITIES IN MARKETING OF AGRICULTURAL COMMODITIES	Poonam Jadhav, Dr. Shubhangi Auti	68-73
12.	A DESCRIPTIVE STUDY OF THE GLOBALIZATION AND NATION IN PRE AND POST COVID-19	Dr. Vishal Bhaware, Dr. Anil Adsule	74-83
13.	A STUDY OF TREND ANALYSIS OF FOREIGN DIRECT INVESTMENT (FDI) IN CONTEXT OF GLOBAL ECONOMIC SCENARIO IN INDIA	Dr. Mahendra R. Agale, Umesh S. Bharatiya	84-92
14.	COMPANIES IN THE PHARMACEUTICAL INDUSTRY IN PUNE ARE CHALLENGED BY THE COMPLEX WEB OF PERFORMANCE APPRAISAL AND PROMOTION	Dr. Rizwan Sayed LH Sayed	93-95
15.	INNOVATION IN REAL ESTATE: A STUDY OF SUSTAINABILITY	Osama Mohammed Hanif Shaikh , Dr. Rama Venkatachalam	96-101
16.	AN ANALYTICAL STUDY OF PERFORMANCE OF PRIVATE BANKS AND ITS CHALLENGES	Dr. Sham Sharad Kharat	102-107

COMPANIES IN THE PHARMACEUTICAL INDUSTRY IN PUNE ARE CHALLENGED BY THE COMPLEX WEB OF PERFORMANCE APPRAISAL AND PROMOTION

Dr. Rizwan Sayed I.H Sayed

Asst. Professor, Poona College of Arts, Science and Commerce, Pune

Abstract

There is a growing awareness that unique competencies can only be attained by having highly developed employee skills, unique organisational cultures, and unique management processes and systems. In order to achieve such recognitions, HR plays a pivotal role, and the performance appraisal process is one of the most important aspects of the HR process that is connected to the aforesaid objective. Within the scope of this study, an effort was made to gain an understanding of the performance appraisal procedures utilised by pharmaceutical companies in Pune.

Keywords: Performance appraisal, Pharmaceutical Company

Introduction

In today's highly competitive and global marketplace, it's not enough to differentiate a product or service from competitors or to be the market leader in cost; one must also be able to draw on a company's unique abilities or core competencies. Attracting and retaining talented, efficient workers is now considered one of a company's core competencies. Staff must be knowledgeable and efficient because the pharmaceutical industry requires highly specialised, technical, and scientific knowledge and skills, as well as a zero-tolerance policy for quality products and services. Human resources departments often use performance appraisal to ensure employees are talented and efficient. HR departments help achieve such goals.

Review of literature

Performance appraisal is a structured formal interview between a subordinate and supervisor, usually annual or semi-annual, in which the subordinate's work performance is examined and discussed to identify strengths, weaknesses, and opportunities for improvement and skill development. Performance appraisal is defined as: Performance appraisal is an annual or semi-annual interview between a subordinate and supervisor. The performance assessment process compares an employee's past and present performance to their performance standard (Garry Dessler 1999). Performance appraisal conjures up many evaluation methods. Forms are just one part of evaluation. An employee's performance evaluation assumes that the employee knows the criteria and has received feedback to improve. Always aim to improve individual and firm performance (Garry Dessler 1999).

Objective of the Study

The objectives of this study are:

- To study the pharmaceutical industry's appraisal system
- To examine employees' opinions of the company's appraisal system
- To analyse the findings and draw some conclusions to improve the company's performance appraisal process.

Research Methodology

Responses from 400 employees of Pharmaceutical companies of Pune city has been collected.

Hypothesis:

Vol.53, No.01 January-June 2022

Null Hypothesis: There is a no significant relationship between promotion and performance appraisal.
Alternate hypothesis: There is a significant relationship between promotion and performance appraisal.

Correlations		Performance	
		Appraisal	Promotion
Spearman's rho	Performance Appraisal	Correlation Coefficient	1.0
		Sig. (2-tailed)	.89
	Promotion	Correlation Coefficient	.89
		Sig. (2-tailed)	.005
		N	400

It was determined through the use of the Spearman's rank-order correlation test in SPSS 26 that there was a strong positive correlation between Performance Appraisal and Performance. This correlation was statistically significant ($r_s = 0.89$ and $P = 0.005$, which is less than 0.05). As a result, it can be concluded that there is a connection between the two.

Thus Alternative hypothesis is accepted and null hypothesis is rejected.

Findings of the study:

Most pharmaceutical companies use younger workers. This industry employs more men than women. Most employees are married. Pharmacists make between Rs. 16000 and Rs. 25000, with few earning more than Rs. 41000. Pharmaceutical workers need a bachelor's degree, but many continue post-grad degrees and few become scientists or PhDs. Only a small minority of pharma companies hire temporary workers.

Performance is continuously monitored, and high-performing employees are promoted. Performance-based incentives and compensations are fixed. Employee performance depends on such incentives. Good workers get paid family vacations, electronics, and other perks.

Employees are reviewed regularly and promoted fairly in this industry. This exam helps organisations evaluate employees' ability to meet goals. Pharmacists get raises after performance reviews.

Performance assessments sometimes promote workers. 400 respondents said this performance review approach helps employees define and achieve goals and share their obligations. Pharmaceutical executives and co-workers do not criticise.

Conclusion

Evaluations of an individual's past performance are what are considered when deciding whether or not to recommend a promotion for that person. These evaluations form the basis for promotion decisions. The performance reviews of an employee at a pharmaceutical company in Pune are the sole factor used to determine whether or not that employee would be considered for promotion. According to the responses, a performance evaluation system that is comparable to this one enables workers to share their duties and to both define and achieve their goals in the workplace. The mechanism for evaluating employees' performances enables this to be achievable.

References

1. Available online on www.ijpqa.com. International Journal of Pharmaceutical Quality Assurance 2016; 7(3): 55-61.
2. Collegegrad.com/industries
3. Ind.org/executive-training-program

INDEX

1	AN ANALYTICAL STUDY OF THE RELATIONSHIP BETWEEN VARIOUS FACTORS OF ONLINE ADVERTISING AND ITS INFLUENCE ON THE CUSTOMERS' CHOICES WHILE PURCHASING ONLINE Dr. Hamid Lakdawala	7
2	THE IMPACT OF COVID-19 ON BANKING SECTOR: AN INDIAN VIEWPOINT Mr. Armaan Shaikh, Mr. Heena Shaikh	13
3	A STUDY OF CAPITAL MARKETS WITH SPECIAL REFERENCE TO PAYTM Dr. Memon Ulhas Yousuf	16
4	THE IMPACT OF SOFTWARE PIRACY IN INFORMATION TECHNOLOGY Dr. Madhukar P. Aghav	20
5	INNOVATIVE DEVELOPMENT IN THE FIELD OF SUPPLY CHAIN MANAGEMENT Dr. Memon Ulhas Yousuf, Qureshi Shaikh Nawaz Shaikh Nazneer	25
6	DIGITAL MARKETING: TRENDS, CHALLENGES, AND BEST PRACTICES FOR BUSINESS SUCCESS Prof. Sayyad Azharuddin, Zubair Amamullah Motiwala	31
7	INNOVATIVE DEVELOPMENT IN THE FIELD OF HUMAN RESOURCE MANAGEMENT Dr. Padmapani Bhagwan Sawani	36
8	RECENT DEVELOPMENT IN THE FIELD OF MARKETING Dr. Katar Ganesh. N	41
9	INNOVATIVE DEVELOPMENT IN THE FIELD OF FINANCE AND ACCOUNTING Dr. Vinod Ratnam Bansale	46
10	INNOVATIVE DEVELOPMENT IN ISLAMIC BANKING Dr. Sohel Memon	51
11	TO STUDY THE PARAMETERS OF THE EMPLOYEE PRODUCTIVITY IN AN ORGANIZATION Garima Vinay Panchbhair, Dr. Milind Arun Peshave	57
12	THE MOST EFFECTIVE SOCIAL MEDIA TECHNIQUES TO INCREASE CUSTOMER ENGAGEMENT Dr. Aftab Anwar Maqbool Shaikh, Dr. Sayyad Vakeel Ahmad Munaf Ali, Armaan Shaikh	64
13	INFLUENCE OF BRAND REPUTATION ON CUSTOMER FIRST IMPRESSION Dr. Aftab Anwar Maqbool Shaikh, Dr. Sayyad Vakeel Ahmad Munaf Ali	74
14	A CRITICAL ANALYSIS OF INDIA'S GOODS AND SERVICES TAX Dr. Sayyad Vakeel Ahmad Munaf Ali, Dr. Aftab Anwar Maqbool Shaikh	81
15	PROBLEMS AND PROSPECTS OF BANKING SECTOR IN INDIA Dr. Rizwan Sayed M. Sayed	84
16	BEST WEBSITE TO POST A PROPERTY FOR SALE/RENT IN INDIA & 12 LEGAL DOCUMENTS YOU WILL COME ACROSS IN YOUR HOME PURCHASE JOURNEY Venkatesh Narayan Tidake, Dr. Peerzade Riyasat Aminuddin	89
17	AN ANALYSIS OF RIGHTS ISSUE AND ITS IMPACT ON SHAREHOLDERS' WEALTH IN INDIAN LISTED COMPANIES Mr. Jitendra Rabada, Ms. Riancy Mascarenhas, Ms. Elisha Da Costa	95
18	IMPACT OF COVID-19 ON TEACHING-LEARNING EVALUATION OF STUDENTS IN INDIA Dr. Priyanka S. Patil, Mr. Sidharth R. Patil	



A CRITICAL ANALYSIS OF INDIA'S GOODS AND SERVICES TAX

Dr. Sayyad Vakeel Ahmad Munaf Ali

Assistant Professor and Research Guide, Poona College of Arts, Science and Commerce, camp, Pune-411001.

Dr. Aftab Anwar Maqbool Shaikh

Principal of Poona College of Arts, Science and Commerce, camp, Pune-411001.

Abstract Historically, indirect taxes have played a significant role in India's fiscal system. Prior to the implementation of tax changes in the nineties, the primary contributor to the government's coffers came through indirect taxation. The widespread poverty in India was cited as the primary reason for the country's dependence on indirect forms of taxation. Consequently, expanding the direct tax base was constrained by structural barriers. Cascading and skewed taxes on the production of goods and services are hallmarks of India's indirect taxation system, which in turn reduces productivity and slows economic growth. This is one of the reasons why India's economic development is so much slower than that of other wealthy countries. A simple tax known as the goods and services tax is necessary to eliminate the infinite number of taxes that exist under the existing system, some of which are charged by the centre while the rest are imposed by the states, and to reduce the burden on taxpayers. Current taxation procedures include an unlimited number of taxes, only a small subset of which are collected centrally (GST). This article presents a comprehensive analysis of the Value added Tax, including its rationale, its model, its pros and cons, and its effects on the Indian economy.

Keywords—GST, Indian Governance, Taxes, India's Fiscal System.

INTRODUCTION

In recent decades, India's economy has been among those with the highest rates of growth. Several reasons, including market reforms, a flood of foreign direct investment, rising foreign currency reserves, a thriving IT and real estate industry, and a robust capital market, have contributed to this expansion. Indirect taxes have always played a crucial role in India's tax system. (Smith et al., 2022) Before-tax changes were enacted in the 1990s, indirect taxes brought in the lion's share of tax money. The main rationale for relying heavily on indirect taxes was that expanding the base of direct taxes was difficult since the bulk of the people in India was impoverished. Cascading and distorted taxes on the production of goods and services are hallmarks of India's indirect taxation system, which in turn dampens productivity and slows economic progress. It is time for a simplification of the current tax system, which imposes an overwhelming number of taxes on citizens but collects just a fraction of its revenue from the federal government. Goods and services tax would accomplish this (GST). There has been a growth in the number of MNEs (multinational corporations) operating in India and, as a result, a rise in the volume of commerce between the country and others. This opens up a lot of possibilities for the government to reform the tax system. Goods and services tax would accomplish this (GST). This article examines the rationale behind the Goods and Services Tax, the GST Model, its benefits and drawbacks, and the effect it has had on the Indian economy. (Lyeonov et al., 2023)

OBJECTIVE

The research aimed to fulfill the following objectives:

- To study the goods and services tax (GST), its structure, and its components



- Challenge of the goods and services tax (GST).
- Divisions of GST and advantages of the GST

METHODOLOGY

Earlier versions of the constitution granted the central government the authority to impose an excise charge on manufactured goods and a service tax on the provision of services. In the same vein, it grants the state government the authority to impose the value-added tax (VAT) that corresponds to the state tax on the sales of products. Due to the exclusive distribution of fiscal authorities, the indirect tax system in the nation has been subject to manipulation. In addition to that, the sale of products inside the state was subject to a centralized tax. In addition, a few governments impose an entrance tax on the purchase of products inside their respective jurisdictions. Therefore, in order to solve this issue, the government at this stage has implemented a single taxation system that incorporates all taxes into itself. This is done to avoid the various issues that are associated with the taxation system, and as a result, this control is now in the hands of only one person. Goods and services are subject to a tax known as GST. It is a replacement for direct taxes collected by the federal and state governments of India and is implemented as an indirect tax throughout the whole country.

The Goods and Services Tax (GST), Its Structure, and Its Components

Over the last two decades, India's tax collection system has seen a number of changes. The Goods and Services Tax applies to anything that is produced, sold, or purchased on a national basis (GST). The Goods and Services Tax, or GST, is projected to have far-reaching consequences on the tax system of India and is largely regarded as one of the most significant tax changes attempted in India since the nation earned independence. Consolidating and simplifying the many taxes now charged on the manufacturing, distribution, and consumption of products and services is the primary objective of this reform. This will eventually replace the existing convoluted system of taxation. The Goods and Services Tax, or GST for short, is one of the most comprehensive plans for tax reform. The ultimate goal is to create a global market free of monetary restrictions so that all countries may participate. Paying the national sales tax in India is consistent regardless of whether you are buying or renting. in accordance with According to (van der Enden & Klein, 2020)

The Goods and Services Tax (GST) will replace all existing indirect taxes, making their collection and management more simpler. The existing system of many taxes being imposed on an identical product at various periods will be replaced with a consistent, one tax across the board, through inputs to outputs, thanks to the Goods and Services Tax (GST) taxation law. It spells the end of the current order of things. The Goods and Services Tax (GST) is built on the principle of "One Country, One Tax" in an effort to streamline taxes. The Goods and Services Tax will replace many of the existing indirect taxes paid to the federal government and individual states (GST). This is due to its widespread use throughout the whole value chain, from the procurement of inputs to the ultimate distribution of the finished product. The Dual-GST model used in this jurisdiction consists of the CGST and the Goods and Services Taxes imposed by the individual states (SGST). The Central Goods and Services Tax will eventually replace the many indirect taxes now levied by the federal government. These taxes include the central excise duty, central sales tax, service tax, special additional charge on customs, and counter-veiling expenses (CGST). The SGST, if completely implemented, will subsume a variety of other state taxes, including as the state value-added tax, the state purchase tax, the state luxury tax, the state octroi, and the state gaming tax. In addition to the GST, there is also an interstate sales tax called the Integrated Goods and Service Tax (IGST). The Products and Services Tax (GST) is not a new tax, but rather a method of tracking international transactions and assigning tax collection responsibilities to the country in which final consumption of the goods or provision of the service occurs. (Dharmayanti, 2023)



The Effects of GST in India: The most prominent GST reform had a significant influence on the Indian economy, as well as on small, medium, and big firms, in addition to the average Indian citizen and the Indian government. In general, it has left an indelible imprint on the economic landscape of India.

Since it was first implemented, the Goods and Services Tax (GST) has had an impact on the daily lives of billions of people throughout India. The effect is like riding a roller coaster since there have been rate additions as well as substantial relaxations from previous taxes. It is true that this innovative tax reform has made the taxation system easier to understand, but it also comes with its own challenging move. Let's take a look at a few pieces of data to get a better idea of how the Goods and Services Tax (GST) reform in India has affected the country. (Palmer)

- An enlargement of the tax base as an increasing number of taxpayers have switched to the GST regime, there has been a significant expansion of the tax base as well as a modification in the compliance stances of taxpayers.
- Revenue Collections: Without a doubt, the quantity of revenue collected went through a meteoric climb as a direct result of the introduction of an internet taxation system, which rendered tax evasion impossible.
- Rationalization of Rates: In order to rationalize the rates that are applicable to the different items that fall under GST, the government made a number of significant initiatives. For example, although there used to be 19% of things that fell under the 28% GST slab, there are now just 3% of items that fall under that particular slab. That indicates the government is making a concerted effort to reduce the GST rates on a variety of goods.
- E-way Bill System: Despite having been plagued by a number of technological issues, the GST compliance process has recently been transformed into a more efficient operation.
- Requirements posed by taxpayers: In response to the requirements posed by taxpayers, the government has made significant changes to better accommodate the requirements of taxpayers.

The combination of these several elements has resulted in a simpler taxation system that has, to a significant degree, assisted in the reduction of tax evasion. (van der Enden & Klein, 2020)

According to recent studies, the Goods and Services Tax (GST) has resulted in an increased need for 1.3 million qualified financial professionals. As a direct result of this, a flood of possibilities has been created for those who have an interest in accounting, finance, and taxes. Additionally, this paves the way for new opportunities for those who are interested in the expansion and development of their careers. The government is aware that individuals get more anxious as the dates for tax payment deadlines draw near. In addition, the new tax system and the requirements for complying with it made life more complicated for individuals all throughout the country. As a result, the government came up with the idea of GST Practitioners as a means to alleviate the burdens placed on taxpayers as a result of the Goods and Services Tax (GST). These GST Practitioners could act as representatives of taxpayers and assist with the filing of returns and other GST compliance requirements. Now, if you are curious about how to become a GST Practitioner and are contemplating the subject, the first step you should do is to enroll in the GST Course. These classes may be taken offline or online, and there are groups that meet throughout the week as well as on the weekends. (Saxena, 2020)



CHALLENGE

There seem to be certain fundamental flaws in the GST model enforced by the union government that may render it ineffectual in achieving the intended objective.

- One country, one tax is a flawed premise that cannot be applied to India in the form of GST. After the introduction of GST, there are 31 taxes instead of the previous 32 (service tax, excise duty, sale tax, including 29 state VAT taxes); these 31 taxes are made up of IGST, CGST, and 29 SGST, creating a complex tax system that goes against the idea of "one nation, one tax."
- Another fundamental concept behind GST implementation is that a single rate of taxation is not viable in India since, according to the 101st amendment to the constitution, Article 246 A says that the parliament and legislative assembly may levy taxes on goods and services. As a result, not only the union government but also the state governments had the authority to set their own GST rates. Article 279 A of the constitution specifies that the GST council has only advisory powers; it is now up to state governments to impose their own GST rates, which distorts the country's whole GST uniformity rate scheme. (2020)
- The government established the goods and services tax network (GSTN), which is in charge of creating the GST portal to provide services such as GST registration, GST return filing, IGST settlement, and so on, which need a strong IT network. It is well acknowledged that India is still in its infancy in terms of IT network connection.
- The lack of trained and competent labor with up-to-date GST topic knowledge has resulted in an increased workload for experts across industries.
- The Indian insurance industry is still underdeveloped, with fewer than 10% of the population insured. This was the motivation behind the government initiative "Pradhan Mantri Jeevan Bima Yojana," but with the implementation of GST, insurance premiums have increased by 300 basis points, making it difficult for insurance companies to enter the market and acting as a detriment to insurance awareness campaigns. The government program "Pradhan Mantri Jan Dhan Yojna" undertaken by the government that every citizen has a bank account would encounter challenges since the levy on financial services has been hiked by 3% in the new goods and services tax system.
- However, although the government is making strides toward a digital India, the telecommunications industry is facing a major challenge, telecom services are getting costlier as telecom services will attract a GST tax rate of 18% which is 3% higher than the previous service tax rate, even when India's rural tele density is not even 60%.
- The GST administration aims to exclude petroleum items from GST, despite the fact that petroleum products have been a key contributor to inflation in India. (Shukla & Kumar, 2019)
- Because they can't afford to hire dedicated IT and accounting staff to keep track of and file GST forms, small businesses are finding the GST tax rate assessment and the resulting increase in operating costs to be particularly perplexing.

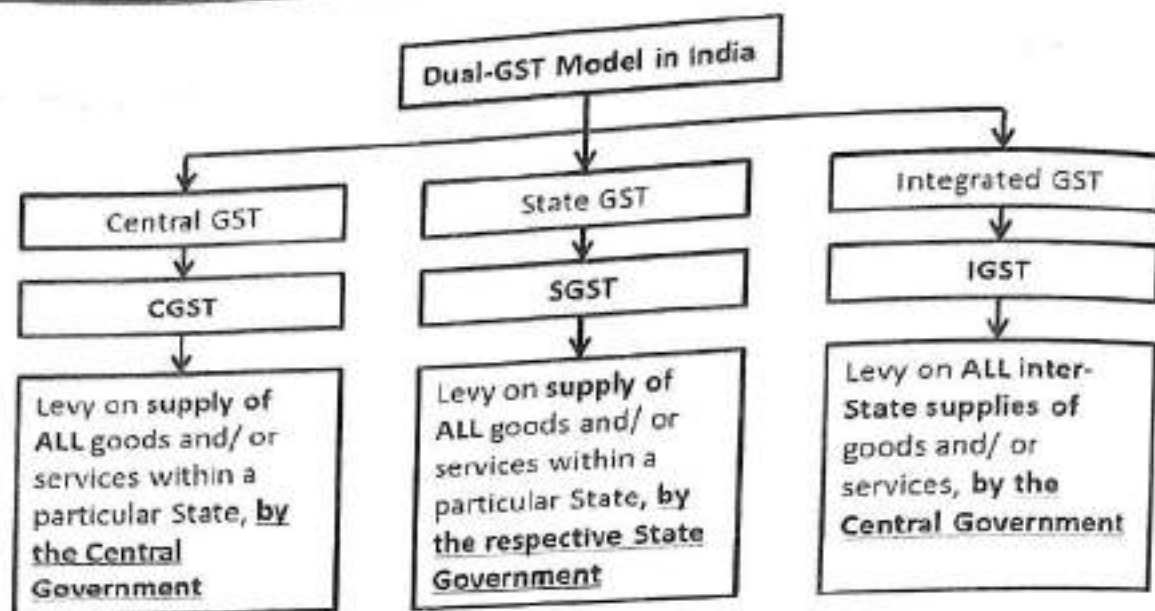


FIGURE 1. GST MODEL

I. DIVISIONS OF GST AND ADVANTAGES OF THE GST

➤ Divisions of GST

The recently enacted Goods and Services Tax (GST) law replaced many different forms of indirect taxes with itself, and it may be broken down into four distinct categories. These are the four categories:

- A central tax on goods and services is referred to as the CGST. It applies to retailers and wholesalers doing business inside the state. Any taxes that are paid will be distributed to the entity that serves as the central authority.
- A state tax on goods and services is referred to by its acronym, SGST.
- It applies to retailers and wholesalers who do business inside the state. The amounts of taxes that are paid will be distributed among the several governmental authority bodies.
- An integrated goods and services tax is what is meant by the abbreviation "IGST." It is relevant to vendors that operate in both commerce beyond state lines and import and export transactions. The amount of taxes that are paid will be distributed to both the state and the central authority body.
- The Union Territory Goods and Services Tax (UTGST), if the transaction is connected to any union territory (Smith et al., 2022)

➤ Advantages of the GST

The implementation of the GST has resulted in a number of advantages all over the world. The primary objective is to preserve the country's existing tax structure while simultaneously fostering economic growth and expanding exports. The following is a summary of some of the advantages that the GST offers.

- The Goods and Services Tax (GST) establishes a nationwide single market.
- Encourages investment from other countries
- Contributes to the establishment of consistent taxes
- Contributes to the enhancement of production and encourages entry into the global market.
- The tax burden for small businesses is either nonexistent or little.
- When customers shop at locally owned and operated businesses, they get several benefits. (Palmer)

Month	GST Collection in Rs. Crs
April	113865
May	100289
June	99939
July	102000
August	98202
September	91916
October	95380
Total	701591

FIGURE 2: - MONTHLY GST COLLECTIONS IN INDIA IN FY2020-21 (IN RS. CRS)

CONCLUSION

Goods and Services Tax (GST) was enacted to modernise India's indirect tax system. Consolidating federal and state levies into one might prevent cascading or double taxation and promote a single national market. The tax's apparent ease of administration bodes well for its eventual adoption and implementation. The Goods and Services Tax (GST) is predicted to provide companies an edge in the marketplace and encourage the growth of e-commerce. By establishing a single market and lowering taxes, the Goods and Services Tax (GST) would significantly alter India's economic climate. The current tax system would undergo significant changes in many respects, including organisation, collection, payment, compliance, use, credit, and reporting. Companies everywhere are moving swiftly to the dynamic global economy. As the global economy expands and diversifies, there is a need for harmonised national tax systems and laws. If efforts are adopted to promote awareness and keep abreast of pricing before the GST is implemented, there may be less reluctance to implementing the anti-profiteering clause. For the GST to regain the trust of the public and business community, it may be necessary to form a committee to deal with any and all problems, establish an audit unit whose only mandate is to check for anti-profiteering, or adopt laws outlining the specific actions that are illegal. For a nationwide launch to succeed, a solid IT network and infrastructure are also required. The creation of a nationwide computer network has only started. As a result, the government has begun the National Digital Literacy Mission to help people improve their skills in this area. The implementation of GST necessitates a re-evaluation of the original goals. The "One Nation, One Tax, and One Market" goal of GST can never be achieved until these issues are addressed. Input tax credit set-offs, service tax set-offs, and the unification



of multiple taxes have all been shown to be beneficial to businesses and consumers alike under the proposed Goods and Services Tax (GST). It's also important to highlight the many industries and fields of study that have benefited from GST.

REFERENCES

- [1] Dharmayanti, N. (2023). The effect of tax office service quality and taxpayer income on land and Building Tax Compliance. *JAK (Jurnal Akuntansi) Kajian Ilmiah Akuntansi*, 10(1), 48-64. <https://doi.org/10.30656/jak.v10i1.4927>
- [2] How tax administrations can relate to tax service providers. (2016). *Rethinking Tax Services*, 73-88. <https://doi.org/10.1787/9789264256200-8-en>
- [3] Lyeonov, S., Tiutiunyk, I., Vasekova, M., Oleksandr Dziubenko, & Samchyk, M. (2023). Tax, investment, institutional and social channels of economic shadowing: Challenges for macro-financial stability and good governance. *Public and Municipal Finance*, 11(1), 128-144. [https://doi.org/10.21511/pmf.11\(1\).2022.11](https://doi.org/10.21511/pmf.11(1).2022.11)
- [4] Palmer, C. (n.d.). Good tax policy on shaky ground? an assessment of tax policy responses to natural disasters. <https://doi.org/10.26686/wgtn.17059994.v1>
- [5] Shukla, S., & Kumar, R. (2019). Role of trust in adoption of online good service tax filing in India. *Vikalpa: The Journal for Decision Makers*, 44(3), 99-114. <https://doi.org/10.1177/0256090919877333>
- [6] Slemrod, J. (2008). Is tax reform good for business? is a pro-business tax policy good for America? *Fundamental Tax Reform*, 142-170. <https://doi.org/10.7551/mitpress/9780262042475.003.0008>
- [7] Smith, N., Idris, M., Schüür, F., & Ko, R. (2022). Data for good, what is it good for?: Challenges, opportunities, and data innovation in service of refugees. *Harvard Data Science Review*. <https://doi.org/10.1162/99608f92.a6dbaef3>
- [8] van der Enden, E., & Klein, B. (2020). Good tax governance? ...govern tax good! *SSRN Electronic Journal*. <https://doi.org/10.2139/ssrn.3610858>



A STUDY ON ATTITUDE OF CONSUMERS TOWARDS GREEN FMGC PRODUCTS

Dr. Aftab Anwar Shaikh

Professor and Principal Department: Commerce Institute: Poona College of Arts Science and
Commerce District: Pune City: Pune
State: Maharashtra

Name: Dr Jyoti Rani

Designation: Associate Professor Department: Nutrition and Dietetics Institute: Chandigarh
University, Gharuan, Mohali District: Mohali City: Mohali State: Punjab

Dr Rishi JP

Designation: Associate Professor Department: Mechanical Engineering Institute: Vidyavardhaka
college of Engineering Mysuru District: Mysuru City: Mysuru State: Karnataka

Lt. Dr. CHARLY JEROME

Designation: Assistant Professor Department: English Institute: KPR Institute of Engineering
and Technology District: Coimbatore City: Coimbatore State: Tamil Nadu

Dr. R. RAJASEKARAN

Assistant Professor Department of Commerce NIFT - TEA College of Knitwear Fashion Tirupur

Dillip Narayan Sahu*

*Assistant Professor, Department of MCA, Gangadhar Meher University, Odisha, India.

Email-id: Dillip1seminar@gmail.com

Abstract

Introduction: Understanding customer attitude regarding Green FMGC products. Marketing organization has described green marketing as the marketing of products that are meant to keep the world environment safe and sound

Literature review: The concept of green products, their effects on customers, challenges associated with green product usage, and probable solutions for the challenges have been discussed. The number of consumers who prefer to use green sustainable products is increasing gradually with time. The theory of green purchase behaviour has been discussed

Methodology: Includes information related to the survey participants, and information collection which is used for the study.

Findings and Discussion: It has been found that consumers are more likely to buy products from companies that are associated with green product distribution and manufacturing. The more time has passed people's perception of green products has changed for the better. Eco-friendly purchases are not in trend today because they are fashionable it's because they are essential for a cleaner and greener earth and sustainable aspects of the future

Conclusion: The number of consumers who prefer to use green sustainable products is increasing gradually with time. Compared to 2009 when 52% of the general public was neutral to a company's environmental effects 60% of people today care about environmental issues and they are more likely to buy products from that company which leaves a less carbon footprint

Keywords: *Green products, Sustainable products, Consumers buying habit*

Introduction

Marketing organization has described green marketing as the marketing of products that are meant to keep the world environment safe and sound. It includes a large range of activities which incorporates modification of products, and production methods alteration. The number of consumers who prefer to use green sustainable products is increasing gradually with time. In 2011 only 49% of people were inclined to use green products (Sethi, 2020). The number gradually increased to 54% in 2015 and 57% in 2018. It shows the gradual acceptance of green sustainable products all over the world (Jain, 2020).

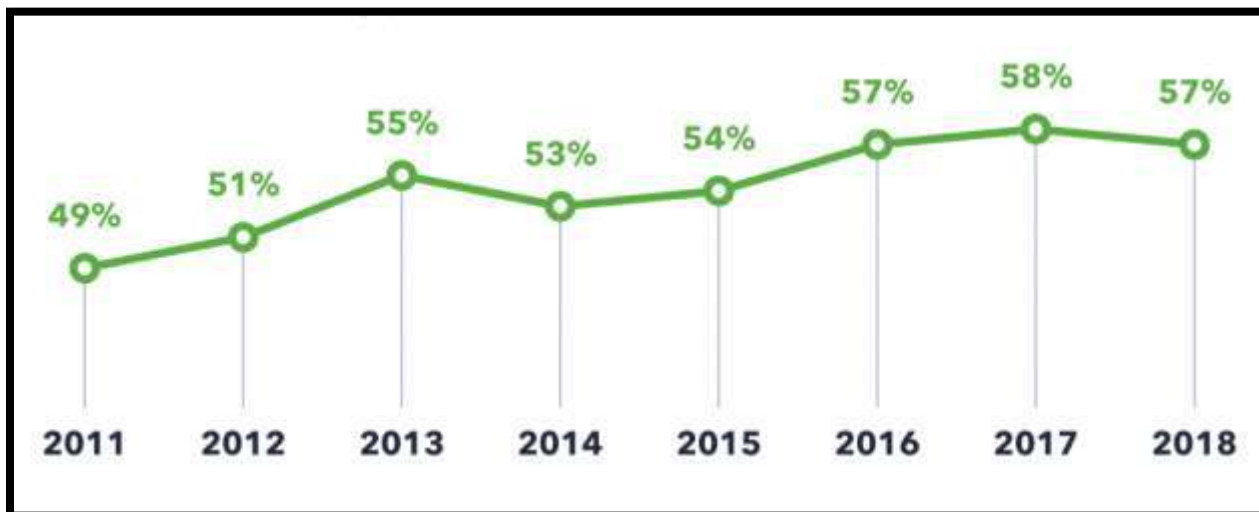


Figure 1: Gradual increase in consumer interest in green sustainable product usage

(Source: Influenced by Tran, 2020)

From the above figure it's evident that from 2011 to 2018 there has been a gradual uprising in the number of consumers who decided to use green products. The goal of the study is to find out consumer attitudes towards the use of green products usage. Compared to 2009 when 52% of the general public was neutral to a company's environmental effects 60% of people today care about environmental issues and they are more likely to buy products from that company which leave a less carbon footprint. 58% of people feel like they are more likely to purchase their

goods from a green company repeatedly. 44% of people felt like they engage more in conversation with their family and relatives about companies that deal with green products (Walia, 2020). 33% of people felt they were less concerned with product prices as long as they were supplied with green sustainable products.

Aim

The following are the research objectives

- To describe the concept of green FMGC products in global markets
- To analyze the impact of green FMGC products on consumers' buying habit
- To identify some of the issues regarding the use of green FMGC products
- To discuss the probable solutions for the challenges regarding the usage of green products

The research questions are a following

- What are green FMGC products and their importance?
- How to analyze the impact of green FMGC products on consumer buying habits?
- What are issues that may arise during the use of green products?
- What could be the solutions to tackle the challenges regarding green product use?

Literature Review

Concept of Green FMGC products

These are the products that are created and manufactured by sustainable technology and cause no environmental negative effects or hazards. As overviewed by Kumar, 2020 today green sustainable products have been able to capture the market quickly and enjoy a much greater share of growth globally. Products which were termed as sustainable were able to grow way faster and quicker than other products. Consumers felt sustainability of products and goods was most important to them. 55% of consumers were willing to pay more for more eco-friendly product purchase options (Tran, 2020).



Figure 2: Steps in green product manufacture and distribution

(Source: Influenced by Tran, 2020)

The above figure shows the steps in green product manufacture and distribution and people are more likely to invest their money in products which less or not likely to harm the environment and these products are doing much better in the market than their counterparts (Negi, 2020). Compared to 2009 when 52% of the general public was neutral to a company's environmental effects 60% of people today care about environmental issues and they are more likely to buy products from that company which leaves a less carbon footprint.

The impact of green FMGC products on consumers' buying habit

Multinational products manufacturing and distribution companies are researching day and night about the market share of various products. A Green FMGC product has created a reputation for not harming the environment and has become a popular choice in people's purchasing options (Kartawinata, 2019). Consumers are more self-aware now and they are looking to decrease their carbon footprint and choosing options that help them do so. Products which have earned a Climate Safe certification have seen 3.6 billion dollars worth of trades in the year 2021 which was more than double that in 2020. 78% of people think environmental safeguards as vital and they would prefer to modify their buying habits to match those goals. 64% of people have shown significant interest in modifying their lifestyle choices (Maharani, 2020).

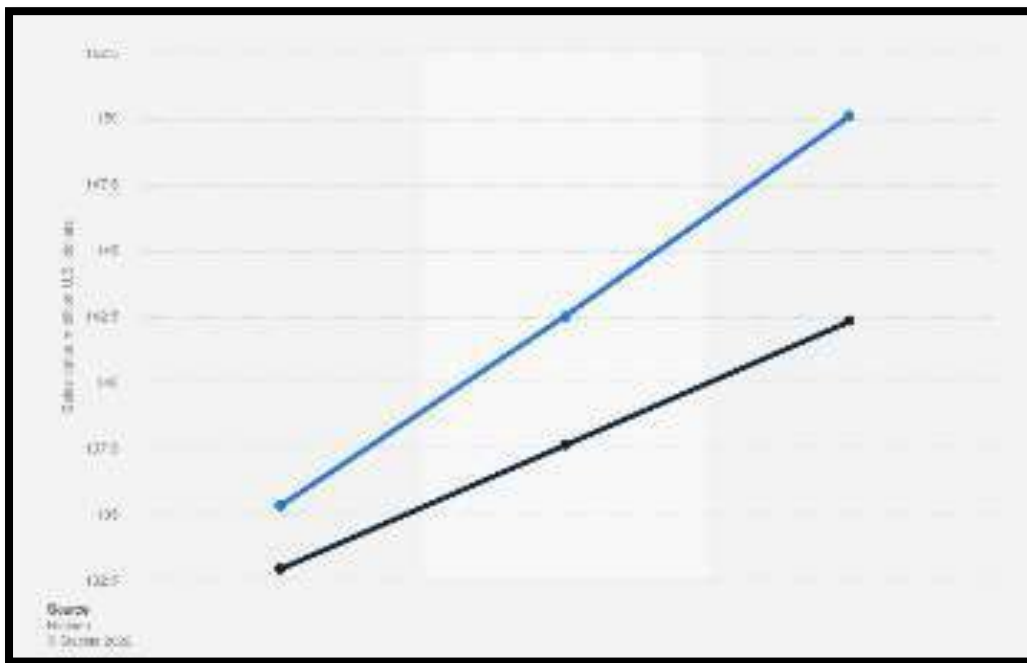


Figure 3: Value of green sustainable products

(Source: Influenced by Tran, 2020)

Figure 3 shows the current and old data of sustainable products in the market and both are showing as increase. However, the current which is blue one is showing comparatively more increased in the trend. The more time has passed people's perception of green products has

changed for the better (Amani, 2020). Eco-friendly purchases are not in trend today because they are fashionable it's because they are essential for a cleaner and greener earth and sustainable aspects of the future.

Challenges associated with the usage of green products

Green FMGC products have a significant role in protecting the environment and decreasing the carbon footprint. Most of the time to manufacture green environmentally safe products companies has to significantly alter their manufacturing division to match the conditions which can result in increased production costs (Mirza, 2020). Green products are often on the costlier side and most people will choose from cheaper options. There is often no standardization to verify manufactured products as green or organic which may create confusion among consumers. Shareholders of a company and investors often need to be patient to view the environment as a larger-picture investment chance (Gupta, 2020). This approach can delay immediate results which may be frustrating. Green product marketing is a concept which is still in the cradle and needs a lot of fine-tuning before it can become viable.

Probable steps to mitigate the issues associated with green products usage

The companies need to spread awareness about the environmental issues that they are trying to advertise their products with. Consumer knowledge and education are very much needed. Transparency in business dealings and genuineness can help and helps to get noticed in the global market (Patnaik, 2020). Customers need to be reassured about their money's worth or they are more likely to overlook the good effects of products.

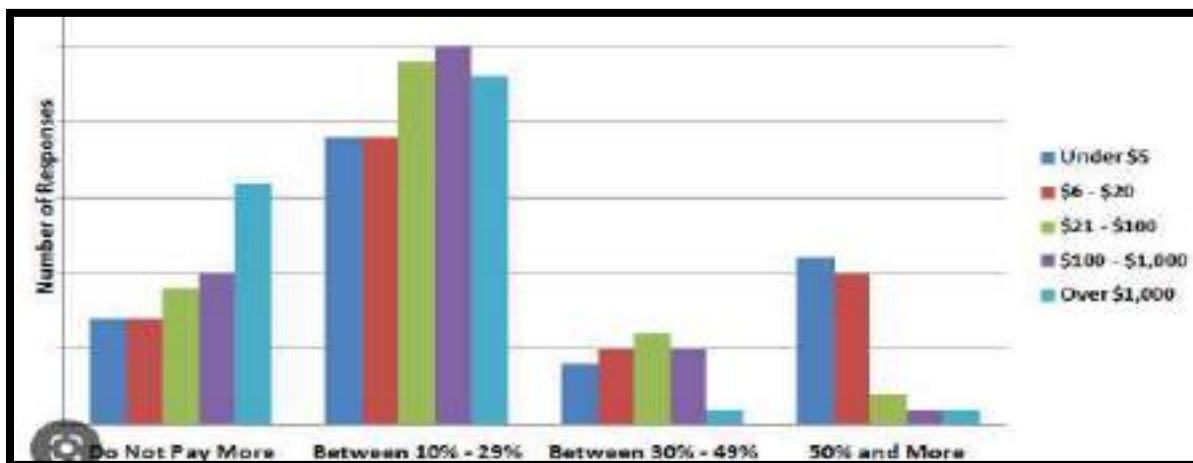


Figure 4: Customer buying habits with green products

(Source: Influenced by Tran, 2020)

Figure 4 shows the customer buying habits with green products in customer surveys and participation is necessary to make way for new products in the market. People are more likely to invest their money in products which less or not likely to harm the environment and these products are doing much better in the market than their counterparts (Sahoo, 2020). The more time has passed people's perception of green products has changed for the better.

Theory of Green Purchase Behavior

The more time has passed people's perception of green products has changed for the better. Eco-friendly purchases are not in trend today because they are fashionable it's because they are essential for a cleaner and greener earth and sustainable aspects of the future (Yanine, 2020). The figure given below shows the green purchasing behavior of consumers. Compared to 2009 when 52% of the general public was neutral to a company's environmental effects 60% of people today care about environmental issues and they are more likely to buy products from that company which leave a less carbon footprint



Figure 5: Green Customer purchasing behavior

(Source: Influenced by Tran, 2020)

Methodology

The job in the analysis makes compiling the information from source as make use of primary quantitative information collection from people. In this section the job makes a systematic illustration of the data. The more time has passed people's perception of green products has changed for the better (Sahoo, 2020). Eco-friendly purchases are not in trend today because they are fashionable it's because they are essential for a cleaner and greener earth and sustainable

aspects of the future. People are more likely to invest their money in products which less or not likely to harm the environment and these products are doing much better in the market than their counterparts.

Findings and Discussion

Hypotheses testing

Hypotheses 1

H1: There is a connection between Customer Attitude changes and Conservative Lifestyle choices

H0: There is no connection between Customer Attitude changes and Conservative Lifestyle choices
H0: There is no connection between Customer Attitude changes and Conservative Lifestyle choices

Hypothesis 2

H2: There is a connection between Customer Attitude and Green FMGC products

H0: There is no connection between Customer Attitude and Green FMGC products

Hypothesis 3

H3: There is a connection between Customer Attitude and Social responsibilities to Environment

H0: There is no connection between Customer Attitude and Social responsibilities to Environment

Demographic Data

Age

What is your age?				
	Frequency	Percent	Valid Percent	Cumulative Percent
Valid	5	8.3	8.3	8.3
20-25	36	60.0	60.0	68.3
26-40	19	31.7	31.7	100.0
Total	60	100.0	100.0	

Table 1: Age Analysis
 (Source: SPSS)

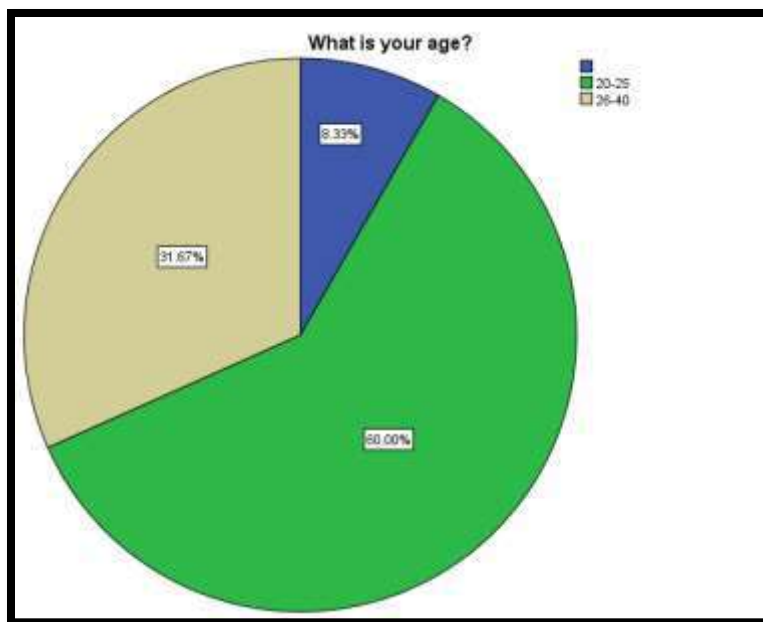


Figure 6: Age Analysis
(Source: SPSS)

There are 31.67 per cent of people belong to the 20 to 25 years age group and the majority of 60 per cent of the people in the age group of 26 years to 40 years.

Gender

What is your gender?				
	Frequency	Percent	Valid Percent	Cumulative Percent
Valid	5	8.3	8.3	8.3
Female	8	13.3	13.3	21.7
Male	47	78.3	78.3	100.0
Total	60	100.0	100.0	

Table 2: Gender Analysis
(Source: SPSS)

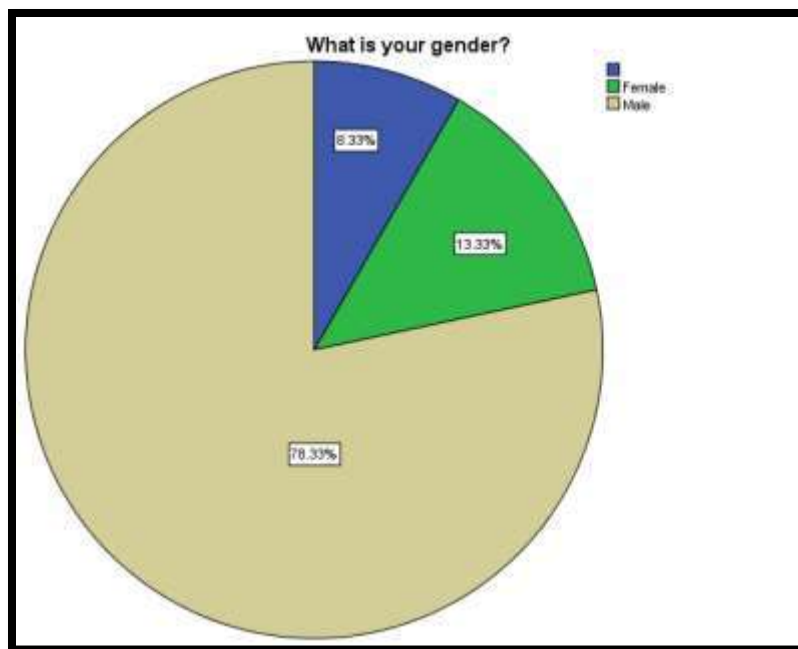


Figure 7: Gender Analysis
(Source: SPSS)

There are 78.33% of people who have participated in the survey are male and 13.33% of people who have participated in the survey are females.

Monthly Income

What is your monthly income?				
	Frequency	Percent	Valid Percent	Cumulative Percent
Valid	5	8.3	8.3	
20000- 30000	25	41.7	41.7	
30000-50000	4	6.7	6.7	
Below 20000	26	43.3	43.3	1
Total	60	100.0	100.0	

Table 3: Income Analysis
(Source: SPSS)

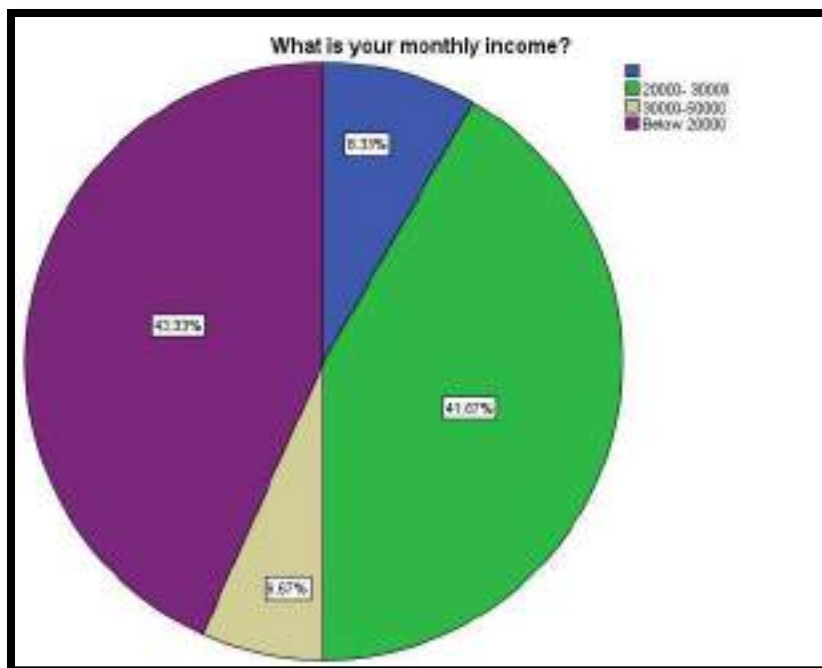


Figure 8: Monthly Income Analysis

(Source: SPSS)

43.33% of people have an income less than 20000, and 41% of people have an income range between 20000 and 30000.

Data Analysis

Hypothesis 1

Model	R	R Square	Adjusted R Square	Std. Error of the Estimate	Change Statistics					Durbin-Watson
					R Square Change	F Change	df1	df2	Sig. F Change	
1	.999 ^a	.998	.998	.08816	.998	21760.451	1	53	.000	2.169

Model		Sum of Squares	df	Mean Square	F	Sig.
1	Regression	168.115	1	168.115	21760.451	.000 ^a
	Residual	.412	53	.008		
	Total	168.527	54			

Model		Unstandardized Coefficients		Standardized Coefficients	t	Sig.
		B	Std. Error	Beta		
1	(Constant)	.030	.035		.858	.395
	IV1	.066	.005	.999	147.514	.000

Table: Hypothesis 1 and its regression analysis

(Source: SPSS)

The table that has been represented above is essential for the examination of the regression model that has been used for data scaling and study analysis hypothesis. Multiple regression testing is essential for testing the information that is taken into consideration for information verification in statistical studies (Gunawardana, 2020). The information is required to identify the alteration. The value of R and the square of R is put in the model summary which is required for analysis. A value between - 1 to +1 shows a positive impact. Here the value of R is found to be 0.980 which shows a higher frequency of correlation. The significance value is found to be 0.000 which is lesser than 0.05 and has been determined that the statistical significance of all information.

In the Anova table, the value of significance is found to be 0.000 which means significant. The variable's behaviour in this study is supposed to predict with the assistance of Square of R. It could be described that customer attitude changes with conservative lifestyle choices.

Hypothesis 2

Model Summary^b

Model	R	R Square	Adjusted R Square	Std. Error of the Estimate	Change Statistics					Durbin-Watson
					R Square Change	F Change	df1	df2	Sig. F Change	
1	.990 ^a	.980	.979	.25449	.980	2564.611	1	53	.000	2.316

□

ANOVA^a

Model		Sum of Squares	df	Mean Square	F	Sig.
1	Regression	166.095	1	166.095	2564.611	.000 ^b
	Residual	3.432	53	.065		
	Total	169.527	54			

Coefficients^a

Model		Unstandardized Coefficients		Standardized Coefficients	t	Sig.
		B	Std. Error	Beta		
1	(Constant)	.259	.097		2.684	.010
	IV2	.961	.019	.990	50.642	.000

Table: Hypothesis 2 and its regression analysis
(Source: SPSS)

The table that has been represented above is essential for the examination of the regression model that has been used for data scaling and study analysis hypothesis. Multiple

regression testing is essential for testing the information that is taken into consideration for information verification in statistical studies. The information is required to identify the alteration (Pareek, 2020). The value of R and the square of R is put in the model summary which is required for analysis. A value between - 1 to +1 shows a positive impact. Here the value of R is found to be 0.980 which shows a higher frequency of correlation. The significance value is found to be 0.000 which is lesser than 0.05 and has been determined that the statistical significance of all information.

In the Anova table, the value of significance is found to be 0.000 which means significant. The variable's behaviour in this study is supposed to predict with the assistance of Square of R. It could be described that customer attitude changes with conservative lifestyle choices.

Hypothesis 3

Model Summary^c

Model	R	R Square	Adjusted R Square	Std. Error of the Estimate	Change Statistics					Durbin-Watson
					R Square Change	F Change	df1	df2	Sig. F Change	
1	1.000 ^a	1.000	1.000	.00000	1.000	2478.55	1	53	.150	2.134 ^b

ANOVA^a

Model		Sum of Squares	df	Mean Square	F	Sig.
1	Regression	169.527	1	169.527	2478.55	.150 ^b
	Residual	.000	53	.000		
	Total	169.527	54			



Coefficients^a

Model		Unstandardized Coefficients		Standardized Coefficients	t	Sig.
		B	Std. Error	Beta		
1	(Constant)	.000	.000			.150
	IV3	1.000	.000	1.000	2.478	

Table: Hypothesis 3 and its regression analysis
(Source: SPSS)

The table that has been represented above is essential for the examination of the regression model that has been used for data scaling and study analysis hypothesis. Multiple regression testing is essential for testing the information that is taken into consideration for

information verification in statistical studies. The information is required to identify the alteration (Hamangoda, 2020). The value of R and the square of R is put in the model summary which is required for analysis. A value between -1 to $+1$ shows a positive impact. Here the value of R is found to be 0.980 which shows a higher frequency of correlation (Schramm, 2020). The significance value is found to be 0.000 which is lesser than 0.05 and has been determined that the statistical significance of all information. In the Anova table, the value of significance is found to be 0.000 which means significant. The variable's behaviour in this study is supposed to predict with the assistance of Square of R. It could be described that customer attitude changes with conservative lifestyle choices.

Discussion

The study creates a meaningful impact in ways of estimating the consumer attitude towards green product usage (Thomas, 2020). The number of consumers who prefer to use green sustainable products is increasing gradually with time. In 2011 only 49% of people were inclined to use green products. The number gradually increased to 54% in 2015 and 57% in 2018. It shows the gradual acceptance of green sustainable products all over the world (Adrita, 2020). The more time has passed people's perception of green products has changed for the better. Eco-friendly purchases are not in trend today because they are fashionable it's because they are essential for a cleaner and greener earth and sustainable aspects of the future. Compared to 2009 when 52% of the general public was neutral to a company's environmental effects 60% of people today care about environmental issues and they are more likely to buy products from that company which leave a less carbon footprint.

Conclusion

The number of consumers who prefer to use green sustainable products is increasing gradually with time. Multinational products manufacturing and distribution companies are researching day and night about the market share of various products. A Green FMGC product has created a reputation for not harming the environment and has become a popular choice in people's purchasing options. Consumers are more self-aware now and they are looking to decrease their carbon foot print and choosing options that help them do so.

Reference

- Adrita, U.W., 2020. Consumers' actual purchase behaviour towards green product: a study on Bangladesh. *International Journal of Business Innovation & Research*, 21(3), pp.311-323. <https://www.inderscienceonline.com/doi/abs/10.1504/IJBIR.2020.105923> Retrieved on 24th April 2023
- Al-Quran, A.Z., Alhalalmeh, M.I., Eldahamsheh, M.M., Mohammad, A.A., Hijjawi, G.S., Almomani, H.M. & Al-Hawary, S.I., 2020. Determinants of the Green Purchase Intention in Jordan: The Moderating Effect of Environmental Concern. *International Journal of Supply Chain Management*, 9(5), pp.366-371. <https://www.researchgate.net/profile/Dr->

- Mohammad-Alhalalmeh/publication/363090722_Determinants_of_the_Green_Purchase_Intention_in_Jordan_The_Moderating_Effect_of_Environmental_Concern/links/630dbd12acd814437fe97be1/Determinants-of-the-Green-Purchase-Intention-in-Jordan-The-Moderating-Effect-of-Environmental-Concern.pdf
https://www.academia.edu/download/80956450/IJM_11_12_342.pdf Retrieved on 24th April 2023
- Bashir, H., Jørgensen, S., Pedersen, L.J.T. & Skard, S., 2020. Experimenting with sustainable business models in fast moving consumer goods. *Journal of Cleaner Production*, 270, p.122302. Retrieved on 24th April 2023
- Colombage, V.K. & Galahitiyawe, N.W., 2020. Basic human values & customer perceived values towards green purchase intention. https://www.theseus.fi/bitstream/handle/10024/336795/Nguyet-Anh_Tran.pdf?sequence=2 Retrieved on 24th April 2023
- Gloria, J., Rajan, U. & Suresh, S., 2020. A STUDY ON CUSTOMER PERCEPTION OF GREEN ADVERTISING IN ECO-FRIENDLY CONSUMER GOODS. *International Journal of Management (IJM)*, 11(12). Retrieved on 24th April 2023
- Gunawardana, T.S.L.W., 2020. Green consumer values: Consumer's lifestyle towards eco-friendly products & purchase intention in the Fast Moving Consumer Goods (FMCG) sector. <http://repo.lib.jfn.ac.lk/ujrr/handle/123456789/2615> Retrieved on 24th April 2023
- Hamangoda, D.R., 2020. GREEN BEHAVIOR OF SRI LANKAN URBAN CONSUMER-THEORETICAL & EMPIRICAL APPLICATIONS IN FAST MOVING CONSUMER GOODS (FMCG) SECTOR. <http://repository.kln.ac.lk/handle/123456789/22860>
<https://www.sciencedirect.com/science/article/pii/S0959652620323490>Worasubhakorn, P. & Soratana, K., 2020. Environmental Criteria for Third Party Logistics (3PL) Transportation Service Selection towards Green Supply Chain: A Case of Fast Moving Consumer Goods Company. In *RSU International Research Conference*. Retrieved on 24th April 2023
- Kartawinata, B.R., Maharani, D., Pradana, M. & Amani, H.M., 2020, August. The role of customer attitude in mediating the effect of green marketing mix on green product purchase intention in love beauty & planet products in indonesia. In *Proceedings of the International Conference on Industrial Engineering & Operations Management* (Vol. 1, pp. 3023-3033). <http://www.ieomsociety.org/detroit2020/papers/616.pdf> Retrieved on 24th April 2023
- Mirza, A. & Gupta, A., A Study on Consumers Perception towards Green FMCG Products: With Reference To Lucknow city in Uttar Pradesh. https://www.researchgate.net/profile/Ashish-Gupta-142/publication/350048663_A_Study_on_Consumers_Perception_towards_Green_FMCG_Products_With_Reference_To_Lucknow_city_in_Uttar_Pradesh/links/604dcffd45851

- 5e529a815dd/A-Study-on-Consumers-Perception-towards-Green-FMCG-Products-With-Reference-To-Lucknow-city-in-Uttar-Pradesh.pdf Retrieved on 24th April 2023
- Pareek, A. & Mathur, N., GREEN MARKETING: A STUDY TO ANALYSIS THE AWARENESS OF CONSUMER TOWARDS GREEN PRODUCT. https://www.researchgate.net/profile/Anupam-Pareek-4/publication/351661999_GREEN_MARKETING_A_STUDY_TO_ANALYSIS_THE_AWARENESS_OF_CONSUMER_TOWARDS_GREEN_PRODUCT/links/60a3e23d92851c9e8de84/GREEN-MARKETING-A-STUDY-TO-ANALYSIS-THE-AWARENESS-OF-CONSUMER-TOWARDS-GREEN-PRODUCT.pdf Retrieved on 24th April 2023
- Patnaik, A., Sahoo, S.K., Sahoo, A.K., Yanine, F.F. & Sukchai, S., 2020, February. Empirical Study on various Factors Influencing Green Business Practices. In *2020 International Conference on Renewable Energy Integration into Smart Grids: A Multidisciplinary Approach to Technology Modelling & Simulation (ICREISG)* (pp. 137-142). IEEE. <https://ieeexplore.ieee.org/abstract/document/9174546/> Retrieved on 24th April 2023
- Rahman, M.S., Ara, M.A., Alim, M.A., Jee, T.W. & Lim, R.T.H., 2020. Consumers' Actual Purchase Behaviour towards Green Products in Bangladesh. *Malaysian Journal of Consumer & Family Economics*, 25, pp.92-120. https://www.researchgate.net/profile/Md-Abdul-Alim-5/publication/347147321_Consumers'_Actual_Purchase_Behaviour_towards_Green_Products_in_Bangladesh/links/5fd85b77a6fdccdb8c9c93d/Consumers-Actual-Purchase-Behaviour-towards-Green-Products-in-Bangladesh.pdf Retrieved on 24th April 2023
- Rathnayake, P., Siyambalapitiya, J. & Perera, K., 2020. Investigation of the Impact of Green Marketing Tools on Customer Purchase Intention of Fast Moving Consumer Goods: With Special Reference to the Youth Sector. In *Proceedings of the International Conference on Marketing Management*. https://www.researchgate.net/profile/Piyumi-Rathnayake/publication/347711652_Investigation_of_the_Impact_of_Green_Marketing_Tools_on_Customer_Purchase_Intention_of_Fast_Moving_Consumer_Goods_with_Special_Reference_to_Youth_Sector/links/5fe3531245851553a0e3d7d4/Investigation-of-the-Impact-of-Green-Marketing-Tools-on-Customer-Purchase-Intention-of-Fast-Moving-Consumer-Goods-with-Special-Reference-to-Youth-Sector.pdf Retrieved on 24th April 2023
- Reference
- Schramm, L.S., 2020. *Consumer attitudes towards green products in the fast-moving consumer goods category in Germany* (Doctoral dissertation). <https://run.unl.pt/handle/10362/104089> Retrieved on 24th April 2023
- Sethi, V. & Jain, A., 2020. The role of subjective norms in purchase behaviour of green FMCG products. *International Journal of Technology Transfer & Commercialisation*, 17(2-3), pp.219-241. Retrieved from

- <https://www.inderscienceonline.com/doi/abs/10.1504/IJTTC.2020.109407> Retrieved on 24th April 2023
- Thomas, M.S.S. & John, M.A., 31. A Study on Customers Perception towards Green Products. *Edited book title: Emerging Trends in Business & Management: Issues & Challenges (Volume 2)*, p.204. https://www.researchgate.net/profile/Usha-Poojary/publication/347937437_Customer_Satisfaction_towards_E-Commerce_System_Services/links/5fe8d903a6fdccdb80ca091/Customer-Satisfaction-towards-E-Commerce-System-Services.pdf#page=216 Retrieved on 24th April 2023
- Tran, N.A., 2020. Customer Perspective Towards Green Consumption in Vietnam. https://www.theseus.fi/bitstream/handle/10024/336795/Nguyet-Anh_Tran.pdf?sequence=2 Retrieved on 24th April 2023
- Walia, S.B., Kumar, H. & Negi, N., 2020. Impact of br& consciousness, perceived quality of products, price sensitivity & product availability on purchase intention towards 'green' products. *International Journal of technology management & sustainable development*, 19(1), pp.107-118. https://intellectdiscover.com/content/journals/10.1386/tmsd_00018_1 Retrieved on 24th April 2023
- Walia, S.B., Kumar, H. & Negi, N., 2020. Impact of socio-demographics on consumers' attitude & purchase intention towards 'eco-friendly' products. *International Journal of technology management & sustainable development*, 19(3), pp.361-371. Retrieved on 24th April 2023
- Yadav, M., 2020. *STUDY OF FACTORS INFLUENCING CONSUMERS' PURCHASING DECISION OF ECO-FRIENDLY PRODUCTS IN FMCG SECTOR* (Doctoral dissertation). http://www.dspace.dtu.ac.in:8080/jspui/bitstream/repository/18191/1/2k18_MBA_053_Manvi%20Yadav.pdf Retrieved on 24th April 2023

Appendices

Appendix 1: Survey Questions

Surveylink:

<https://docs.google.com/forms/d/e/1FAIpQLSe8ohBimy59K1mLOkOHZOcIskACGyzdtG85Hq5EZz00lcji-w/closedform>

1. What is your age?
2. What is your gender?
3. What is your monthly income?
4. It is safe to use recycled products for the customer satisfaction process
5. Recycled products create a change in environment
6. It is wise to consume a product first when it's about to be expired
7. Extra care can be taken to avoid food wastage while preparing meal
8. Recycling is a cost effective to be a viable option
9. It is better to refill a bottle of liquid soap or shampoo instead of buying a new one

10. It is better to consume packaged food before the best before date
11. Environmental problems can be solved by cooperating with other people
12. Supporting environmental policies while casting votes in election is a good idea

of personalisation in a help. Information management shows how exceptional the digital stage is to answer constantly and rapidly to customer needs. First-request develops are shaped from the reflected parts of the two builds.

The India public were educated from the beginning to use the technology to get the COVID-19 vaccination, making the base populace very appropriate to answer the review issue. Thus, the example is less helpless against the supportive of progress predisposition that is normal in development studies, which holds that individuals will generally embrace change and development with a good 404 substantial respondents were used to gather. Members were given severe privacy guidelines, which diminished the opportunity of a social attractiveness predisposition. An extensive collinearity assessment strategy was embraced to check for neurotic co linearity to diminish the probability of normal technique predisposition. The whole co linearity test yielded difference expansion factors (VIFs) that were under 3.3. Accordingly, the outcomes show that there is minimal possibility that the model has normal strategy inclination. Because of its advantages as far as test dissemination and size, a part based underlying condition model was used to break down the dataset to assess the exploration model and the connected hypotheses. Utilizing way gauging estimations and a case-wise substitution missing methodology, the model was processed utilizing Smart PLS 3.0. The standard blunder assessments were performed utilizing a nonparametric bootstrapping with 5000 replications and individual level changes

3.2 Hypothesis

H1.1. The perceived price barrier (value barrier) has a negative impact on the intention to use the digital platform service.

H1.2. The intention to use the digital platform service is adversely affected by the usability barrier (perceived complexity).

H1.3. The intention to use the digital platform service is negatively impacted by the perceived security risk barrier.

H1.4. The self-image barrier has a detrimental impact on the intention to use the digital platform service.

H1.5. The requirement for human interaction, a tradition barrier, has a detrimental impact on the intention to use the digital platform service.

4. RESULTS

200 people who took the survey—2/3 of whom were female and 1/3 of whom were male—completed it on average in 12 minutes. There were 100 legitimate responses. 40% of the population is under 46 years old, 50% is between 25 and 40, and 10% is over 68. 26% of the respondents worked in the healthcare sector, and 50% had a university degree. Age and health accounted for 35% of all immunizations, according to the national vaccination classification, making them the two most important factors. 86% of respondents indicated positive or neutral satisfaction with government as the provider of the immunization, and 85% said they would use digital health services in the future (Rasheed et. al2021). 11% of users said they were prejudiced and concerned about technology, while 10% of users thought the digital vaccine platform was challenging to use. 83 percent of respondents (positive/neutral) believed that the configuration of digital platforms was appropriate for their problem (personalization), 83 percent believed that it kept them informed (communication), and 76 percent believed that it responded quickly (data management). The majority of respondents gave the digital vaccination platform extremely high praise in the configuration areas of personalization (by 52%) and communication (by 53%) (See Table 1).

Table 1: Descriptive Results of Digital Vaccination Management Survey

Variable	Description	M	SD
Duration	Time to fill out survey.	609	356
Age	(1–4) <46, (5–6) 46–67, (7–8) >67	5.70	1.63
Gender	(1) male, ..., (5) female	3.45	1.77
Education	(1–5) school/job, (6–7) B./Master	4.23	1.92
Healthcare w	1 (yes), 2 (no)	3.56	2.12
Priorisat. Group	(1–4) age, (5) care, (6) health, (7) job	1.23	2.65

Satis_3	Satisfied with vaccination process	5.63	1.12
Intent_Adopt_2	intend to use dig service in future	4.99	1.23
Usabilit_Barr_1	digital portal was easy to use	6.12	2.66
Te_Anx_Barr_2	not using d. tech. to avoid errors	4.23	2.74
Personal_1	portal appropriate for concern	5.23	1.86
Commun_1	portal keeps me well informed	6.74	2.77
Data_R_Man_1	portal responded quickly	5.23	2.68

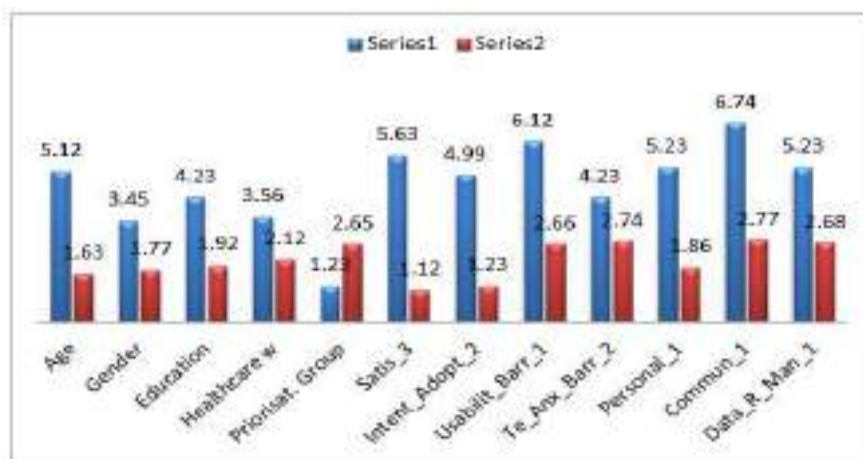


Figure 1: Results of the Digital Vaccination Management Survey in Brief

The viability of the estimating develops was surveyed by testing them without underlying linkages to affirm our reception model. Then, a develop explicit exploratory head part examination was performed. Marker trustworthiness for all designs is proposed by the pointer loadings, which reliably outperformed 0.708 (Abdul et al., 2021). Then, Cranach’s alpha was determined so that each develop might perceive how dependable it was. The discoveries were over 0.7, which is a sufficiently dependable outcome. The typical fluctuation removed (AVE), which was acquired in the wake of looking at joined legitimacy and the separate, surpassed the negligible degree of 0.5. Results from the examination with the squared intercorrelation of the builds were in like manner adequate. The recommended research model’s course coefficients and meanings were assessed utilizing the primary model (see Table 2 for further data).

Table 2: Results from Structural Equation Modelling.

Item	Image Barr	Indivi dual Inertia	Perceived Dependence B.	Perceive d Value Barrier	Security Risk Barr	Technology Anxiety Barr	Tradi tion Barr	Usabi lity Barr	Intenti on to Adopt
Commu nication	-0.185	-0.120	-0.312	-0.099	0.007	-0.168	0.058	- 0.068	
Data Manage ment	-0.123	-0.008	-0.032	-0.098	-0.085	-0.162	0.118	- 0.245	
Personal ization	0.265	-0.163	0.131	-0.131	-0.136	0.156	0.079	0.099	
Intention to adopt	-0.261	0.030	-0.106	0.109	0.090	0.095	- 0.058	- 0.052	-0.05
Age									-0.32
Educati on									-0.08
Gender									
Vaccina tion Timing									0.02

With values ranging from 0.10 to 0.51, the measured R2 confirms an adequate match between the data and the model. The VIFs were processed while considering the chance of multicollinearity at the underlying level, yet they generally fell beneath the fundamental limit of five. The following stage was to compute the standardized root-mean-square lingering (SRMR = 0.08), which was used to assess the model's fit. The worth is adequate with the safer limit for covariance-based underlying condition modelling, regardless of whether the nature of this marker has not yet been totally affirmed for PLS-based primary condition modelling. We examined the effect of utilitarian, mental, and individual impediments on the expectation to embrace (ItA) digital vaccination services for the principal set of hypotheses (see Table 3).

Table 3: The findings of hypothesis H1 focused on adoption difficulties.

Hypothesis	Structural Relation	Original Sample	M	SD	t	P
H1	Usability Barrier (Rev) ->ItA	-0.236	-0.322	0.012	4.231	0.0001***
H2	P. Value Barrier ->ItA	-0.156	-0.215	.0451	3.551	0.170
H3	Security Risk Barrier ->ItA	-0.312	-0.125	.0233	4.361	0.008**
H4	Image Barrier (Rev) ->ItA	-0.344	-0.362	.0145	5.126	0.001***
H5	Tradition Barrier ->ItA	-0.356	-0.251	.0344	5.888	0.400

5. DISCUSSION

5.1 Platform Services for Vaccination Processes—Implications for Further Research

This study proposed a changed reception model that makes sense of stage services for vaccination services, as well as by and large for new digital health services, instead of the opposition model of Mani and Chouk which was initially created for estimating the acceptance of new advances in shopper products markets. This study offers observational help for the model's relevance. In view of the three stage design areas of customization, correspondence, and information management, eight deterrents to the agreeableness of digital vaccination services were found. Most of variable loadings support the model.

The usability barrier should be listed as the main influencing element since it has the greatest impact on adoption intention. In the end, this investigation confirms Ram and Sheth's findings. The second most significant element, the major image barrier, supports the results of researchers like Laukkanen, who found that people may avoid using digital innovations if their identities do not match the functions that are being presented for them. However, image is frequently seen as a network of associations, particularly in the context of commercial communication, from which expectations emerge that are not always connected to one's own self-concept. To fully understand the impact of image on innovation acceptability, more research is required. Interestingly, neither tradition nor technical weaknesses (perceived dependency and technological fear) have a substantial impact on our approach. Only image does.

It's rather striking the way that little worth matters. This differentiations with purchaser items statistical surveying, where it has been exhibited that one of the principal factors impacting acceptance of a development is seen esteem, which is characterized as the shortfall of money related and execution esteem Concentrates on digital innovations that tended to COVID-19 likewise uncovered that the biggest effect on technology reception was anticipated execution (as an intermediary for esteem) The worth of the inoculation is very perfect (given the risk of mortality from COVID-19 and given the re-established opportunity of monetary activity), and there is no other option (however COVID-19 testing might be a brief substitute), which is one defence that may be given. Subsequently, the worth in the conventional significance of a cost benefit proportion isn't as significant in this present circumstance. A substitute clarification has to do with the elements of the mandatory India healthcare framework, where patients are not informed the expenses of medicines, drugs, immunizations, and so forth, therefore such expenses are not imbued in their recollections.

Despite the fact that latency has been shown to be a central point impacting the reception of developments this study has not distinguished a significant effect. Lawmakers and professionals have over and again asked the newbies and antibody defaulters to immunize to drive up vaccination rates during the COVID-19 pandemic. This vaccination reluctance inertia is not apparent in our analysis. Future research is needed to determine if this conclusion can be generalized to the healthcare system or if it is uniquely related to factors like the general population's subjective perception of COVID-19's lethality

5.2 Platform Services for Vaccination Processes—Implications for Management and Policy

How to manage a pandemic and optimize the quick uptake of linked health services is a crucial concern for pandemic managers and policy makers. In order to manage vaccination operations, this paper suggests a digital vaccination service paradigm. The configuration areas of customization, communication, and data management are useful ideas to take into account while implementing such services, since they all significantly affected the adoption hurdles. Although not all hurdles had a substantial impact on the vaccine candidates' decision to adopt, the cumulative impact of all barriers should not be disregarded.

Our research indicates that usability and functionality are quite important. The main influencing element for configuring platform services should be noted as the usability since it had the most impact on adoption intention. The click flow (see Appendix A.6) appears to be crucial in determining whether consumers on digital health platforms convert or bounce. As a result, using a patient-centred approach, the management and design of the assistance provided throughout the digital vaccination experience is of paramount importance. The largest effect of personalisation on usability may be seen throughout the whole model. The ability to shape a help as per the demands and inclinations of the subjects supports its practicality for the user and ought to subsequently reduce related originations of development obstruction, making customization the main concern for strategy producers and pandemic-battling officials.

Usability, image, perceived dependency, and technology anxiety are the most common effects of communication, the second area of platform configuration, on adoption obstacles. The administration of vaccinations depends heavily on information processing on platform services since healthcare sectors have a predominate risk-avoidance attitude. This relates to the creation, dissemination, and updating of information. People can assess the worth of an invention because they can compare it to the harmful status quo and grasp its qualities more clearly with detailed information. Correspondence offers designated data to separate boundaries (e.g., convenience), coordinate user inclinations with stage arrangement (i.e., separate the picture hindrance), and separate the apprehension about specialized shortcomings (i.e., separate the reliance on technology and uneasiness obstructions). It essentially influences whether or not an individual would acknowledge a digital help mentally. In India, the data cycle was conveyed not just on the site of the bureaucratic health service yet in addition on the specific site, <https://social.niti.gov.in/> (got to on March 23, 2022), with clarification and direction, as well as a continuous interaction with email updates, data connections, course direction, SMS updates, and a check list for the vaccination cycle in the assigned vaccination places.

6. CONCLUSION

Internationally, COVID-19 has become a top priority because to its widespread effects, and all nations have made every effort to contain the dreadful situation to the best of their abilities. The use of vaccines is a crucial tactic that may help avoid the disease's horrifying effects and lower mortality rates (Mbiine et al., 2021)The planning, obtaining, distributing, and pricing of the vaccinations were major responsibilities of the federal government, while the state governments concentrated on carrying out the program. The central government's monopoly on vaccine procurement led to large purchases at discounted prices. Vaccine makers, however, quoted higher costs for the state governments and private health units while keeping relatively cheap rates for the central government as a result of the implementation of liberalized policies, which also resulted in differential pricing. The initiative was hastened by the following adjustment to the vaccine strategy, which increased the central government's engagement in procurement. Dependence on the private sector for vaccination distribution did not considerably help the program go through more quickly.

REFERENCES

1. Saw, Y.E.; Tan, E.Y.Q.; Liu, J.S.; Liu, J.C. Predicting Public Uptake of Digital Contact Tracing During the COVID-19 Pandemic: Results from a Nationwide Survey in Singapore. *J. Med. Internet Res.* 2021, 23, e24730.
2. Smith, I.M.; Bayliss, E.; Salisbury, H.; Wheeler, A. Operations management on the front line of COVID-19 vaccination: Building capability at scale via technology-enhanced learning. *BMJ Open Qual.* 2021, 10, e001372.
3. Kis, Z.; Kontoravdi, C.; Shattock, R.; Shah, N. Resources, Production Scales and Time Required for Producing RNA Vaccines for the Global Pandemic Demand. *Vaccines* 2021, 9, 3

4. Kim, D.; Lee, Y.J. Vaccination strategies and transmission of COVID-19: Evidence across advanced countries. *J. Health Econ.* 2022, 82, 102589.
5. Kitagawa, T.; Wang, G. Who should get vaccinated? Individualized allocation of vaccines over SIR network. *J. Econom.* 2021, 232, 109–131.
6. Radonjic-Simic, M.; Mahrt, C.; Niemand, S.; Speck, A.; Windrich, M. Decentralized Open Platform for Vaccination—A India Example: COVID-19-Vacc. *J. Open Innov. Technol Mark. Complex.* 2021, 7, 186.
7. Xu, Z.; Qu, H.; Ren, Y.; Gong, Z.; Ri, H.J.; Zhang, F.; Chen, X.; Zhu, W.; Shao, S.; Chen, X. Update on the COVID-19 Vaccine Research Trends: A Bibliometric Analysis. *Infect. Drug Resist.* 2021, 14, 4237–4247.
8. Asadullah, A.; Faik, I.; Kankanhalli, A. Digital Platforms: A Review and Future Directions. In *Proceedings of the 22nd Pacific Asia Conference on Information Systems, PACIS 2018, Yokohama, Japan, 26–30 June 2018*; p. 248.
9. Hermes, S.; Riasanow, T.; Clemons, E.K.; Böhm, M.; Krcmar, H. The digital transformation of the healthcare industry: Exploring the rise of emerging platform ecosystems and their influence on the role of patients. *Bus Res.* 2020, 13, 1033–1069.
10. Collis, A.; Garimella, K.; Moehring, A.; Rahimian, M.A.; Babalola, S.; Gobat, N.H.; Shattuck, D.; Stolow, J.; Aral, S.; Eckles, D. Global survey on COVID-19 beliefs, behaviours and norms. *Nat. Hum. Behav.* 2022, 6, 1310–1317.
11. Fagherazzi, G.; Goetzinger, C.; Rashid, M.A.; Aguayo, G.A.; Huiart, L. Digital Health Strategies to Fight COVID-19 Worldwide: Challenges, Recommendations, and a Call for Papers. *J. Med. Internet Res.* 2020, 22, e19284.
12. Woldeyohannes, H.O.; Ngwenyama, O.K. Factors Influencing Acceptance and Continued Use of mhealth Apps. In *HCI in Business, Government and Organizations. Interacting with Information Systems*; Nah, F.F.H., Tan, C.H., Eds.; Lecture Notes in Computer Science; Springer: Berlin/Heidelberg, India, 2017; pp. 239–256.
13. Rasheed, J.; Jamil, A.; Hameed, A.A.; Al-Turjman, F.; Rasheed, A. COVID-19 in the Age of Artificial Intelligence: A Comprehensive Review. *Interdiscip. Sci. Comput. Life Sci.* 2021, 13, 153–175.
14. Syed Abdul, S.; Ramaswamy, M.; Fernandez-Luque, L.; John, O.; Pitti, T.; Parashar, B. The Pandemic, Infodemic, and People’s Resilience in India: Viewpoint. *JMIR Public Health Surveill.* 2021, 7, e31645.
15. Mbiine, R.; Nakanwagi, C.; Lekuya, H.M.; Aine, J.; Hakim, K.; Nabunya, L.; Tomusange, H. An Early Warning Mobile Health Screening and Risk Scoring App for Preventing In-Hospital Transmission of COVID-19 by Health Care Workers: Development and Feasibility Study. *JMIR Form Res.* 2021, 5, e27521.
16. Nishtar, S. Public – private 'partnerships' in health – a global call to action. *Health Res Policy Sys* 2, 5 (2004). <https://doi.org/10.1186/1478-4505-2-5>
17. CII and KPMG. 2009. “The Emerging Role of PPP in Indian Healthcare Sector.” Policy Paper. Available online at: www.ibef.org/download/PolicyPaper.pdf.
18. Ravindran, T. S. (2010). Privatisation in reproductive health services in Pakistan: three case studies. *Reproductive Health Matters*, 18(36), 13-24.
19. Tekin, P. S., & Çelik, Y. (2010). Analysing public-private partnership policy as a financing method in Turkey health sector with political mapping. In *7th Biennial Conference in Organisational Behaviour in Health Care, Mind the Gap: Policy and Practice in the Reform of Health Care (Vol. 62)*.

20. Sekhri, N., Feachem, R., & Ni, A. (2011). Public-private integrated partnerships demonstrate the potential to improve health care access, quality, and efficiency. *Health affairs*, 30(8), 1498-1507.



सत्यं शिषं सुन्दरम्
Estd. 1949

Journal of
The Maharaja Sayajirao University of Baroda

Certificate of Publication

Certificate of publication for the article titled:

A COMPARATIVE STUDY OF FILE FORMAT, MANIPULATION, MEASURING AND
ANALYSIS OPTIONS PROVIDED BY PROTEIN STRUCTURE VISUALIZATION TOOLS

Authored by

Shaheda N. Ansari

Department of Computer Science, AKIS, Poona College of Arts, Science and Commerce,
Camp, Pune-411001(MS)

Volume No .57 No.1(II) 2023

Approved in

Journal of The Maharaja Sayajirao University of Baroda

ISSN : 0025-0422

(UGC CARE Group I Journal)

MSU of Baroda
Editor

Journal MSU of Baroda

A COMPARATIVE STUDY OF FILE FORMAT, MANIPULATION, MEASURING AND ANALYSIS OPTIONS PROVIDED BY PROTEIN STRUCTURE VISUALIZATION TOOLS

Shaheda N. Ansari

Department of Computer Science, AKIS, Poona College of Arts, Science and Commerce,
Camp, Pune-411001(MS)

ABSTRACT

The generation of a protein structure is much difficult than the generation of a protein sequence. However, the protein structure gives much more insight in the function than its sequence. Therefore, a number of methods have been proposed for the computational prediction of protein structure from its sequence. Tools are need by the researchers for loading, displaying, analyzing and manipulating sequence data. For visualize a protein whose structure has been known many tools have been developed. Seven commonly used freely available protein structure visualization tools viz. RasMol, Chime, Protein Explorer, Swiss-Pdb Viewer, WebMol, MOLMOL and Cn3D were downloaded during present course of investigation. The study is performed on these softwares for- different input, output file format; manipulation options in the structure and sequence; and different measuring and analysis capabilities provided by these softwares.

Keywords: amino acid, structure, function, visualization etc.

INTRODUCTION

The 3D structure of protein (Anfinsen, 1973) is determined from the amino acid sequence, which is related to its function. An amino acid sequence alteration can bring about changes in the stability and folding of the protein (Lorch *et al.*, 1999; Lorch *et al.*, 2000), interaction of the protein with other molecules (Rignall *et al.*, 2002; Ung *et al.*, 2006) and change in functional levels (Tiede *et al.*, 2006) or overall function of the protein as well. An amino acid sequence mutation may alter the structure of a protein but it does not necessarily alter its function, although, the mutation at specific sites such as conserved residues can bring about a change in the structure and function of the protein (Prabantu *et al.*, 2021).

In the Protein Data Bank (PDB) (Berman *et al.*, 2000) solved structures are usually deposited. There is a large gap between the number of proteins we know the structure of since it is possible to derive a proteins sequence from the sequence of the gene that codes for that protein and sequencing is much faster than solving protein structures experimentally. Also, the majority of these proteins remain uncharacterized, i.e. we have no information about what this proteins function is, where it is located in the cell and with what other proteins it interact. Much can be learned of a protein by knowing its three-dimensional structure and since solving protein structures is a difficult problem, generating protein structures through computational means would allow us to bridge the gap between the number of known protein sequences and known protein structures.

The advances in computer graphics technologies and availability of structural data together have pushed development of computational tools for molecular visualization and analysis (Lesk and Hardman, 1982). The usage of graphical presentations greatly helps to successfully describe, communicate or understand structural concepts related to various biological phenomena (Sánchez-Ferrer *et al.*, 1995). The visualization of 3D structure of proteins is critical in many areas like, protein modeling, drug design. This is because that the 3D structure of a protein determines its interaction with other molecules, hence its function, and the relation of the protein to other known proteins. Each way of visualization highlights a different aspect of the protein molecule (Shirky, 2000). Growing number of new structure data in Protein Data Bank open new ways for collaboration, thus emphasizes the need for visualization tools that are portable. Moreover, studying the interaction between protein molecules may also require visualizing huge number of atoms, thus researchers also need tools that are capable of loading and displaying this huge amount of data (Can *et al.*, 2003). Many tools have been developed to visualize a protein whose structure

has been known. Some of these tools are: RasMol (Sayle and Milner-White, 1995), Chime (MDL Information Systems, Inc.), Protein Explorer (Martz, 2002), Swiss-PDB viewer (Kaplan and Littlejohn, 2001), WebMol (Walther, 1997), MOLMOL (Koradi *et al.*, 1996), and Cn3D (Wang *et al.*, 2000). The study was performed on these softwares for various display capabilities (Ansari and Sayyed, 2011), different properties and coloring styles provided by softwares (Sayyed and Ansari, 2013), and different viewing and selection options provided by softwares (Ansari, 2018).

MATERIALS AND METHODS

Seven free structure visualization tools were downloaded for visualizing the 3D structure of proteins:

RasMol (<http://www.rasmol.org/>)

Chime (<https://www.umass.edu/microbio/chime/getchime.htm>)

Protein Explorer (<https://www.umass.edu/microbio/chime/registfrm/downlpe.htm>)

Swiss-PDB viewer (<http://www.expasy.org/spdbv/>)

WebMol (<https://github.com/dirkwalther/webmol>)

MOLMOL (<https://sourceforge.net/projects/molmol/>)

Cn3D (<https://www.ncbi.nlm.nih.gov/Structure/CN3D/cn3dinstall.shtml>)

Structure data files were downloaded from the Protein Data Bank (<https://www.rcsb.org/>) and NCBI (<http://www.ncbi.nlm.nih.gov/>).

The study was performed on these seven softwares to see sources of the input file supported by the softwares. In order to see a molecular structure an atomic coordinate data file for that structure must be loaded. Hence formats of the input and output files supported by the softwares were studied.

The study was performed to see whether the softwares have the facilities to add or removes amino acids, bonds, H-bonds; and mutate the amino acid. These might be useful to fine-tune an image before a final rendering (e.g. by adding or removing H-bonds), or to discard a part of a protein to save truncated proteins. Studying mutations by using software can be very useful to quickly evaluate their putative effects before actually performing them in the lab.

Software's were observed for different measuring and analysis capabilities provided by them such as measuring distance between two selected atoms, angle of three selected atoms, torsion or dihedral angle of four selected atoms, and total number of chains, groups, atoms, bonds, H-bonds, SS-bonds, helices, strands and turns in the loaded protein.

RESULTS AND DISCUSSION

The results summarized in Table 1 shows that RasMol and MOLMOL can open 3-D structure file from local disk only where as Chime, Protein Explorer, Swiss-PDB Viewer WebMol and Cn3D can opens file from local disk as well as from URL. The format of the input file supported by RasMol are PDB, Alchemy, MOL2, MOL, XYZ, CHARMM, and MOPAC; by Chime are PDB, and MOL; Protein Explorer and WebMol opens only PDB format files; Swiss-PDB Viewer opens PDB, mmCIF and MOL file formats; MOLMOL opens PDB, ANG, COR, MOL2, XYZ and SEQ; and Cn3D can CN3, CDD, Binary ASN and ASCII ASN. Being studying the input file formats supported by the softwares it was observed that all these software supports PDB files except Cn3D. Cn3D does not read PDB-format files directly, but instead uses NCBI's MMDB structure database. RasMol can save files in PDB, BMP, GIF, EPSE, PPM, RAST and Alchemy formats; Chime in PDB and MOL; Protein Explorer save as MolSlides; Swiss-PDB Viewer can save in BMP, PDB and POV; WebMol has no save option. MOLMOL can save in PDB, ANG, COR, Sequence, BMP, JPEG, PNG, FM, PS EMF, TIF, POV, RIB and WRL and Cn3D in CN3, CDD, Binary ASN, ASCII ASN and PNG.

Table 1 : Source of Input File, Input and Output File Formats for protein structure visualization tools.

Software	Source of Input File	File Format	
		Input	Output
RasMol	Local Disk	PDB Alchemy MOL2 MOL XYZ CHARMm MOPAC	PDB BMP GIF EPSF PPM RAST Alchemy
Chime	Local Disk URL	PDB MOL	PDB MOL
Protein Explorer	Local Disk URL	PDB	MolSlide
Swiss-Pdb Viewer	Local Disk URL	PDB mmCIF MOL	BMP PDB POV
WebMol	Local Disk URL	PDB	PDB
MOLMOL	Local Disk	PDB ANG COR MOL2 XYZ SEQ	PDB ANG COR Sequence BMP JPEG PNG FM PS EMF TIF POV RIB WRL
Cn3D	Local Disk URL	CN3 CDD Binary ASN ASCII ASN	CN3 CDD Binary ASN ASCII ASN PNG

The results obtained in Table 2 summarized that only Swiss-PDB Viewer and MOLMOL have the facilities to add and remove amino acids, bonds, and hydrogen bonds and can mutate amino acids.

Table 2 : Manipulation in the Structure and Sequence for protein structure visualization tools.

Software	Amino acid			Bond		Hydrogen Bond	
	Add	Remove	Mutate	Add	Remove	Add	Remove
RasMol	N	N	N	N	N	N	N
Chime	N	N	N	N	N	N	N
Protein Explorer	N	N	N	N	N	N	N
Swiss-Pdb Viewer	Y	Y	Y	Y	Y	Y	Y
WebMol	N	N	N	N	N	N	N
MOLMOL	Y	Y	Y	Y	Y	Y	Y
Cn3D	N	N	N	N	N	N	N

Y = YES, N = NO

The results summarized in Table 3 shows that RasMol, Chime, Protein Explorer and WebMol can display distance between two selected atoms, angle of three selected atoms and torsion angle of four selected atoms, MOLMOL displays only distance and torsion angle but not the angle, Cn3D do not displays distance, angle and torsion angle. Information about the loaded protein molecule like total number of chains, groups, atoms, bonds, H-bonds, SS-bonds, residues forming helices, strands and turns can be obtained in RasMol and Protein Explorer but not in Chime, Swiss-PDB Viewer and Cn3D. WebMol shows only information about total number of chains, residues, SS-bonds and shows fraction of helices and strands. MOLMOL gives information about total number of chains, residues, atoms and bonds only.

Table 3 : Measuring and analysis options supported by protein structure visualization tools.

Software	Distance	Angle	Torsion Angle	Total Number								
				Chains	Groups	Atoms	Bonds	H-bonds	SS-bonds	Helices	Strands	Turns
RasMol	Y	Y	Y	Y	Y	Y	Y	Y	Y	Y	Y	Y
Chime	Y	Y	Y	N	N	N	N	N	N	N	N	N
Protein Explorer	Y	Y	Y	Y	Y	Y	Y	Y	Y	Y	Y	Y
Swiss-Pdb Viewer	Y	Y	Y	N	N	N	N	N	N	N	N	N
WebMol	Y	Y	Y	Y	Y	N	N	N	Y	Shows Fraction	Shows Fraction	N
MOLMOL	Y	N	Y	Y	Y	Y	Y	N	N	N	N	N
Cn3D	N	N	N	N	N	N	N	N	N	N	N	N

Y = YES, N = NO

SUMMARY AND CONCLUSION

Being studying these protein structure visualization softwares it has been observed that Structure visualization tools should support different input file formats also it provides options to save the open structure in different output file formats. It should not only display the molecular images but should contain structure analysis, computation and manipulation tools like in the loaded molecule it should display number of atoms, residues, chains, bonds, H-bonds, disulphide bonds, alpha helices, beta sheets and turns. It should compute distance, angle, and torsion angle. It should be able to add or remove atom, amino acid, bond and H-bond. Also, it should have facility to mutate amino acid.

REFERENCES

- Anfinsen, C. B.**, 1973, 'Principles that govern the folding of protein chains', *Science*, **181**:223–230.
- Ansari, S. N.**, 2018, 'A comparative study of different viewing and selection options provided by protein structure visualization tools', *Bioscience Discovery*, **9**(1): 53-58.
- Ansari, S. N. and Sayyed, I.**, 2011, 'A Comparative Study of Protein Structure Visualization Tools for Various Display Capabilities', *Bioscience Discovery*, **02**(2):222-226.
- Berman, H. M., Westbrook, J., Feng, Z., Gilliland, G., Bhat, T. N., Weissig, H., Shindyalov, I. N. and Bourne, P. E.**, 2000, 'The Protein Data Bank', *Nucleic Acids Res*, **28**:235–242.
- Can, T., Wang, Y., Wang, Y., –F. and Su, J.**, 2003, 'FPV: fast protein visualization using Java 3D', *Bioinformatics*, **19**(8):913-922.
- Kaplan, W. and Littlejohn, T. G.**, 2001, 'Swiss-PDB Viewer (Deep View)', *Briefings in Bioinformatics*, **2**:195–197.
- Koradi, R., Billeter, M. and Wuthrich, K.**, 1996, 'MOLMOL: a program for display and analysis of macromolecular structures', *J Mol Graphics* **14**:51-55.
- Lesk, A. M. and Hardman, K. D.**, 1982. 'Computer-generated schematic diagrams of protein structures', *Science*, **216**(4545):539-40.
- Lorch, M., Mason, J. M., Clarke, A. R., and Parker, M. J.**, 1999, 'Effects of core mutations on the folding of a beta-sheet protein: implications for backbone organization in the I-state', *Biochemistry*, **38**: 1377–1385.
- Lorch, M., Mason, J. M., Sessions, R. B., and Clarke, A. R.**, 2000, 'Effects of mutations on the thermodynamics of a protein folding reaction: implications for the mechanism of formation of the intermediate and transition states', *Biochemistry*, **39**: 3480–3485.
- Martz, E.**, 2002, 'Protein Explorer: easy yet powerful macromolecular visualization', *Trends Biochem. Sci.*, **27**:107–109.
- Prabantu, V.M., Naveenkuma, N. and Srinivasan, N.**, 2021, 'Influence of Disease-Causing Mutations on Protein Structural Networks', *Frontiers in Molecular Biosciences*, **7**:1-11.
- Rignall, T. R., Baker, J. O., McCarter, S. L., Adney, W. S., Vinzant, T. B., Decker, S. R., et al.**, 2002, 'Effect of single active-site cleft mutation on product specificity in a thermostable bacterial cellulase', *Appl. Biochem. Biotechnol.* **98**:383–394.
- Sánchez-Ferrer, A., Núñez-Delicado, E. and Bru R.**, 1995, 'Software for reviewing biomolecules in three dimensions on the Internet', *Trends Biochem Sci.* , **20**(7):286-8.
- Sayle, R. A. and Milner-White, E. J.**, 1995, 'RASMOL: biomolecular graphics for all', *Trends Biochem Sci.*, **20**:374-376.
- Sayyed, I. and Ansari, S. N.**, 2013, 'A Comparative Study of Different Properties Provided by Protein Structure Visualization Tools', *International Journal of Basic and Applied Chemical Sciences*, **3**(1):1-6.
- Shirky, C.**, 2000, 'SevenWays of Looking at a Protein', *FEED Magazin*.
- Tiede, S., Cantz, M., Spranger, J., and Braulke, T.**, 2006, 'Missense mutation in the N-acetylglucosamine-1-phosphotransferase gene (GNPTA) in a patient with mucopolipidosis II induces changes in the size and cellular distribution of GNPTG', *Hum. Mutat*, **27**: 830–831.
- Ung, M. U., Lu, B., and McCammon, J. A.**, 2006, 'E230Q mutation of the catalytic subunit of cAMP-dependent protein kinase affects local structure and the binding of peptide inhibitor', *Biopolymers*, **81**(6):428–439.
- Walther, D.**, 1997, 'WebMol – a Java-based PDB viewer', *Trends Biochem Sci.*, **22**:274–275.
- Wang, Y., Geer, L. Y., Chappay, C., Kans, J. A. and Bryant, S. H.**, 2000, 'Cn3D: sequence and structure views for Entrez', *Trends Biochem. Sci.*, **25**:300–302.

Impact Factor – 7.367

ISSN-2349-638x



**Aayushi
International Interdisciplinary
Research Journal (AIIRJ)**

PEER REVIEWED & INDEXED JOURNAL

Special Issue No.121

**Women Empowerment in India :
Journey of 75 Years**

Chief Editor

Dr.Pramod P. Tandale

Editor

Prof. Rajani Shikhare

IMPACT FACTOR

SJIF 7.367

For details Visit our website

www.aiirjournal.com

Sr. No.	Name of the Author	Title of Paper	Page No.
1.	Dr Jayashri T Birdavade-Bhandwaladar	Empowerment of Women: Role of Government	1
2.	Dr.Kavitha.D	Challenges and Provisions for Women Empowerment in India	6
3.	Dr.Akthar Parveen	Role of Rearing Practices in Developing Gender Equality	11
4.	Mr. Kalipadha Debnath Dr. Md. Tarique Anwer	Social And Political Perspective of Women Empowerment With Special Referrence to Agartala Municipal Area	14
5.	Dr. Ajay Patil	Role of NGO in Women's Empowerment	18
6.	Muthamma K.K.	Women Empowerment in India through Schemes and Laws: An Analysis	22
7.	Dr. Sanjay Bhagwat Salunke	Women Empowerment and Sustainable Development Goal 5	27
8.	Dr. J. B. Kangane	Women Empowerment A Need of Society	30
9.	Dr. Ahmad Shamshad	Self-Help Groups and Women Empowerment: - Issues and Challenges	34
10.	Dr. Pravin Sonune	From Independence to Equality: Assessing Policies and Challenges for Gender Equality and Women's Empowerment in India Since 1947	38
11.	Dr. Gulnawaz Usmani	Women Empowerment: A health Perspective	41
12.	Dr. Ahilya Bharatrao Barure	Rethinking: Indian Literature, Women and Indian Independence	44
13.	Dr. Tandale S. S.	Strategies to Improve Women in Society and Family	47
14.	Autade Pratibha Yedurao	Gender Competitors in Indian Budgeting	50
15.	Hanmant B. Helambe	A study of Government Schemes for Women Empowerment	54

Women Empowerment: A health Perspective

Dr. Gulnawaz Usmani

Assistant Professor
Department of Economics
Poona College of Arts, Science & Commerce
Camp, Pune, Maharashtra-01
Email: nawaz1717@gmail.com

Abstract

Development is very crucial for the human development. Women empowerment is a serious issue in the development process. Education and Health care accessibility is very limited to rural women; hence facing poor standard of health. The constitution of India empowers the state to adopt various measures for the upliftment of women. Empowerment of women is an important agenda in the development efforts on a country.

Keywords: Women; Empowerment; Health; Education

Introduction

The role of women in the process of development has been widely acknowledged (Malhotra, & Schuler, 2005). Almost all the countries of the world have committed to provide equal opportunities to female in each and every field of social and cultural interest (Baqi, et. al., 2017). According to Food and Agriculture Organization (FAO), the International Fund for Agricultural Development (IFAD) and the World Food Programme (WFP) women and girls play a crucial role in achieving the 2030 Agenda for the Sustainable Development, in particular, the goal of eradicating hunger and extreme poverty. Despite this rural women have limited economic resources, have less access to health and education services, limited job security etc. (Keshavarz, et. al., 2013). Again and again, women contributions in the economic growth and development have been relegated. The empowerment of women has relied on improving women's control over their economic resources and on the strengthening their job security (Mehra, 1997).

India has also approved various national and international human rights instruments committing to secure equality for women (Hathaway, 2007). The constitution of India empowers the state to adopt various measures for the upliftment of women (Mokta, 2014). Empowerment of women is an important agenda in the development efforts on a country (Fernós, 2010). There has been significant shift in approach of the Government of India towards

the development of women especially rural women (Agarwal, 1989).

Empowerment of Women

Empowerment is a multi-directional concept (Galiè, & Farnworth, 2019). Women's empowerment is a process in which women gain an equal share of control over resources like financial, knowledge, information, ideas and control over decision-making in the home, society and nation (Mandal, 2013, May). According to the Country Report of Government of India, "Empowerment means moving from a position of enforced powerlessness to one of power".

Education of Women

Education is the most powerful instrument of changing women position in the society (Kasiviswanathan, et. al., 2022). Education reduces inequalities and also acts as a means to improve their living standard and social status within the family and society (Sreedhar, & Kumar, 2018). In order to encourage education among women schools, colleges and even universities were established exclusively for women in the country. To bring more equal status of education among men and women Government provide a package of scholarships, concessions in fee, mid-day meals, school dress, books etc. to the girl children especially from marginalized sections of the society (Ali, 2016). As a result women's literacy rate has grown over the three decades.

Health:

Health status of women is very pity as compared with that of men because of their limited access to healthcare, sufficient nutrition,

reproductive facilities, and to issues of fundamental rights of person (Vainik, 2008; Usmani, & Ahmad, 2016). According to the World Health Organization, 585,000 women die every year, over 1,600 every day, from causes related to pregnancy and childbirth. The maternal mortality ratio in India is 167 per 1,00,000 live births (SRS, 2015). Table 1 presented the percentage of access to health services in India and its major states. Though the percentage of access is well but it needs more serious concern, especially in the least developed states.

Table 1- Maternal health Services by States:

States	ID*	Full ANC**	TT***	PNC****
AP	91.1	38.2	97.1	77.9
ASM	74.2	25.2	90.2	7
BR	65.3	9.6	88.6	6.4
GUJ	87.9	25.7	87.6	47.5
HAR	76.4	9.7	85.1	23.5
KAR	92	33.4	93.2	75.6
KER	99.4	53.6	95.1	94
MP	78.1	12.1	88.9	60.3
MAH	90.3	24.4	89.9	77.1
ORS	81.3	24.6	95.8	10.5
PUJ	80.4	15.5	95.3	15.6
RAJ	82.7	8.6	82.6	9.5
TN	99.3	35.2	96.4	94.7
UP	62.1	2.7	81.3	12.1
WB	76.3	21.2	96	9.1
INDIA	78.7	19.7	89.8	39.3

Source: Rapid Survey on Children (RSOC), 2013-14, Ministry of Women and Child Development, Government of India.*Institutional Deliveries, **Antenatal Care, ***Tetanus Toxoid, ****Postnatal Care

Major Handicaps In The Empowerment Of Rural Women

1. Limited Access to Resources
2. Limited Access to input and credit
3. Inadequate Technical Competency
4. Poor participation in family or society decision making
5. Poor Gender Consideration
6. Limited Exposure to the mass media

Women Empowerment Programmes

Against the patriarchal ideology of society, the women and girls need special commitment to enjoy their rights and participation in the decision making process. With the objective of bringing about the development of women and improving their status in the society government of India implemented various programmes.

The various programmes of women development are as follows:

- Self Help Groups
- Group Development Programmes
- Capacity Building Programme
- Income Generation Programmes
- Credit and Savings Mobilisation Programmes

These programmes have been shown an impressive result in the development of women and in improving their access to education, healthcare, and other socio-culture institution and thus improve their social status in the society.

Conclusion

Though women make half of the world population, they have remained as an oppressed group from the beginning of the history. Though there are some societies those regard women as superior in the family and community, but most of societies of the world have been treating them as second class citizens. Reasons may be religious and cultural and physical structure of the society, that forced women to remain as dominated group around the world, especially in the developing countries. Even in the most developed countries which boast the best human rights situation in their country, women's participation in almost all fields is very negligible because of male dominance ideology. In many countries, women are kept as 'slaves' and within the boundary of home as they are not allowed to go outside without permission and also not to participate in any social and political activities.

In a society like ours, empowerment of different section of the societies are becoming serious concerns and to address it planners, managers, social scientist all over the world have started deliberating and devising way out like anything. In this direction genders issues are dominating over other vulnerable issues like

poverty, class conflicts, communities, ethnic issues etc. In ensuring an egalitarian development gender equity still remains as a pertinent question as it has been for the thousands of years of human civilization.

References

1. **Adick (1995):** Basic Education for Women and girls in rural areas; Agriculture and Rural Development. 2:
2. **Agarwal, B. (1989).** Rural women, poverty and natural resources: sustenance, sustainability and struggle for change. *Economic and Political weekly*, WS46-WS65.
3. **Ali, M. (2016).** Gender Inequality and Empowerment of Women through Education. *International Journal in Management & Social Science*, 4(2), 73-79.
4. **Awasthi, O. N. (1993):** Education Development in India, *Journal of Education and Social Change* 7: 1.
5. **Baqi, S., Albalbeesi, A., Iftikhar, S., Baig-Ansari, N., Alanazi, M., & Alanazi, A. (2017).** Perceptions of gender equality, work environment, support and social issues for women doctors at a university hospital in Riyadh, Kingdom of Saudi Arabia. *PloS one*, 12(10), e0186896.
6. **Fernós, M. D. (2010).** *National mechanism for gender equality and empowerment of women in Latin America and the Caribbean*. ECLAC.
7. **Galiè, A., & Farnworth, C. R. (2019).** Power through: A new concept in the empowerment discourse. *Global Food Security*, 21, 13-17.
8. **Gopalan, S. (1992).** Monitoring and Evaluation of the training programmes for women, function areas in rural Development.
9. **Usmani, G., & Ahmad, N. (2016).** Women's health status and child health. *Social Science Review*, 2(2), 95-103.
10. **Hathaway, O. A. (2007).** Why do countries commit to human rights treaties?. *Journal of Conflict Resolution*, 51(4), 588-621.
11. **Hernader (1993):** Cultural contributions as a complement to economic incentives for people involve in sustainable development project un rural areas; Landscape and Urban Planning,
12. **Kasiviswanathan, K., Alagesan, M., & Banupriya, K. (2022).** Women Empowerment: Role of Education in India. *Dogo Rangsang Research Journal*, 12(5), 46-51.
13. **Keshavarz, M., Karami, E., & Vanclay, F. (2013).** The social experience of drought in rural Iran. *Land use policy*, 30(1), 120-129.
14. **Malhotra, A., & Schuler, S. R. (2005).** Women's empowerment as a variable in international development. *Measuring empowerment: Cross-disciplinary perspectives*, 1(1), 71-88.
15. **Mandal, K. C. (2013, May).** Concept and Types of Women Empowerment. In *International Forum of Teaching & Studies* (Vol. 9, No. 2).
16. **Sreedhar, N., & Kumar, B. R. (2018).** Analytical Approach on Women Education in India. *American International Journal of Social Science Research*, 2(2), 12-15.
17. **Mehra, R. (1997).** Women, empowerment, and economic development. *The Annals of the American Academy of Political and Social Science*, 554(1), 136-149.
18. **Mokta, M. (2014).** Empowerment of women in India: A critical analysis. *Indian Journal of public administration*, 60(3), 473-488.
19. **Vainik, J. (2008).** The reproductive and parental rights of incarcerated mothers. *Family Court Review*, 46(4), 670-694.



**SARDAR PATEL INSTITUTE OF
ECONOMIC AND SOCIAL RESEARCH**

anvesak

A bi-annual journal

CERTIFICATE OF PUBLICATION

This is to certify that the paper entitled

**GIG WORKERS IN PUNE: OPPORTUNITIES
AND CHALLENGES**

Authored by

Dr. M. Shahid Jamal Ansari

University Grants Commission

Approved Journal

vol. 53 No.01

in

Anvesak A bi-annual Journal

UGC Care Group - 1

ISSN: 0378-4568

January-June 2023

Impact Factor: 6.20



A bi-lingual journal

GIG WORKERS IN PUNE: OPPORTUNITIES AND CHALLENGES

Saquib Ali Shahid Ali Khan

Research Scholar, AKI's Poona College of Arts, Science and Commerce

Dr. M. Shahid Jamal Ansari

Assistant Professor, AKI's Poona College of Arts, Science and Commerce

Abstract

The gig economy has experienced rapid growth in recent times, providing a substantial source of income for urban dwellers. This research investigates the socioeconomic characteristics, working conditions, and income trends of gig workers located in Pune, India. The study is based on a survey conducted in 2022, which involved 200 gig workers in Pune. The findings reveal that gig workers in Pune face numerous challenges, including inadequate compensation, prolonged working hours, job insecurity, and limited access to social security. The paper's conclusion highlights policy recommendations for enhancing the socioeconomic status and working conditions of gig workers in Pune.

Introduction

The gig economy has emerged as a substantial employment opportunity in various countries, including India. Typically, gig workers do not maintain a conventional employer-employee relationship, instead opting for temporary or contractual work facilitated by online platforms. This trend has been propelled by multiple factors such as technological advancements, evolving consumer preferences, and the necessity for workforce adaptability.

In India, the gig economy has rapidly expanded in recent years, offering significant earning prospects to numerous individuals, particularly in urban locales. The city of Pune, located in the western state of Maharashtra, has emerged as a prominent hub for gig work, with numerous individuals engaging in a diverse range of such jobs.

In order to explore policy implications for enhancing the socioeconomic position of gig workers in Pune, this article looks at their socioeconomic profiles, working circumstances, and income patterns.

Literature Review

Laws and regulations for gig workers in India have been a topic of concern in recent years. The Code on Wages, 2019 provides for a universal minimum wage and floor wage to be provided to all organized and unorganized sectors, including gig workers (Government of India, 2019).

The Code on Social Security, 2020 recognizes gig workers as a new occupational category, making them eligible for benefits such as maternity benefits, life and disability cover, old age protection, provident fund, and employment injury benefits (Government of India, 2020). However, eligibility does not ensure the guarantee of these benefits to workers. This issue has been highlighted by various researchers and organizations.

The enactment of the Code on Social Security, 2020 has made understanding the scope and ambit of social security laws easier by consolidating the pre-existing laws (Government of India, 2020). The Code also defined various terms like gig workers and platform workers, which were not previously defined. The Code is expected to increase employment opportunities by engaging workers on a temporary basis and providing them with social security.

The NITI Aayog report titled "India's Booming Gig and Platform Economy" provides a comprehensive and methodical approach to estimating the current size of the gig economy and its potential for employment creation (NITI Aayog, 2022). The report examines the benefits and

challenges of the gig and platform economy and suggests international best practices for social security programs. The objective of the study is to understand the significance of the gig economy in terms of employment generation and suggest measures to encourage employment in the sector.

Chaudhary (2021) explored women's participation and opportunities for work in the gig economy and found that the participation of women in the Labour Force Participation Rate (LFPR) is very low, and there is a significant gap that exists in India.

Pal (2021) raised the issue of the rising popularity of the gig economy and its advantages and disadvantages in both global and Indian contexts. The study discussed the recent initiatives taken by the Central Government of India to regulate the gig economy.

Mukherjee and Sujatha (2020) examined the process of construction of professional identity over organizational identity by independent workers and understood the impact of learning agility on professional identity while engaging in the gig economy.

Rukhsar (2019) analyzed employees' awareness and perception towards the gig system. The authors also looked at the problems faced and suggested potential solutions. They found that the gig system doesn't restrict talent by setting any kind of limitations and allows for better networking in and out of the organization.

In Banwari's (2018) study, the trend of Gig Economy in India was examined, which is rapidly increasing in every sector with the help of technological platforms. The author highlighted the potential benefits and challenges of this economy and emphasized that collaboration between the government and educational institutes can convert these challenges into opportunities. Caza's (2020) study focused on the prevalence of gig work in management education and highlighted three broad areas for future investigation: how the gig economy may influence students, faculties, and universities.

Sargeant's (2017) study provided insight into the advancement of the Gig Economy and its impact on the labor market due to the expansion of contingent work. The study analyzed the size and status of the Gig Economy and also examined the issues raised by lawsuits related to the employment status of workers employed in this developing economy.

Dokko et al. (2015) attempted to identify the opportunities and challenges of non-traditional and contingent employment relationships under the development of the Gig Economy in the United States (U.S.). The study provided a framework for understanding the impact of this emerging economy on workers and their employers.

Methodology

The study employed a quantitative research design using a survey questionnaire to collect data from gig workers in Pune. The survey was administered to a sample of 200 gig workers who were selected through convenience sampling. The questionnaire included questions on demographics, work experience, income, job satisfaction, and challenges faced by gig workers in Pune.

Results

According to the survey's findings, gig workers in Pune encounter a variety of difficulties, such as poor pay, lengthy workweeks, a lack of job stability, and the lack of access to social protection.

The survey found that approximately 75% of respondents claimed to make less than Rs. 15,000 per month. It was also found that 44% respondents worked for more than 40 hours per week, and 32% reported working more than 50 hours per week.

Only 24% of the workers had access to any type of social safety, such as health insurance or retirement plans.

Lastly, it was found that just 38% of Pune's gig workers said they were satisfied with their jobs, according to the survey's final finding.

Discussion and Policy Implications

The results of this study have significant policy repercussions for raising the socioeconomic standing and working conditions of gig workers in Pune.

In Pune, gig workers must first be paid a fair salary that is appropriate for the labour they perform. Setting a minimum salary for gig labour or pressuring platform providers to pay gig employees fairly could accomplish this.

Second, the amount of hours per week that gig workers are expected to work needs to be restricted. This can be achieved by setting a cap on the number of hours gig workers can work each week or by pressuring platform providers to reduce the amount of time that gig workers are required to work.

Thirdly, social safety programmes like health insurance and retirement plans must be made available to gig workers in Pune. This could be achieved by urging platform firms to offer these benefits to gig workers or by creating a social protection programme for gig workers under the direction of the government.

In order to ensure that gig workers in Pune are happy with their jobs, the working conditions must be improved. This might be accomplished by pressuring platform businesses to offer gig employees a secure and comfortable working environment or by setting up a grievance resolution process that would allow gig workers to voice any problems or complaints they may have with their jobs.

Limitations

Notwithstanding the significance of the research's conclusions and their implications for policy, there are a number of limitations of this study that need to be recognized.

First off, this study's sample size was rather small, with only 200 gig workers in Pune. Although every attempt was made to ensure that the sample was representative of the city's overall gig worker population, it is probable that the results cannot be applied to all gig workers in Pune.

Second, the study used self-reported data that could be biased and inaccurate. For instance, in order to project a more positive image of oneself, gig workers may have over reported their hours worked or underreported their pay.

Third, only gig workers who use digital platforms were included in the study. As a result, the findings might not apply to gig workers who do not look for employment online.

Conclusion

Many people in the urban areas, including Pune have begun to rely heavily on the gig economy as a source of income. Yet, because gig work is unpredictable, many gig workers in Pune have little access to social safety or labour rights, making them exposed to economic shocks.

The difficulties that Pune's gig workers experience have been brought to light by this study, including their poor pay, lengthy workweeks, precarious employment, and restricted access to social safety nets. The results of this study have significant policy ramifications for enhancing the socioeconomic standing and working conditions of gig workers in Pune.

It is crucial for authorities to intervene to solve the issues encountered by gig workers in Pune in order to guarantee that they may work acceptable hours, earn a fair income, and have access to social security. By doing this, we can make sure that gigs in Pune are a viable and fair type of employment for everyone.

Future Directions

The limitations of this study should be addressed, and future research should build on its conclusions. The effect of gig labour on the mental health and wellness of gig workers in Pune is one topic of research that may be investigated further. Investigating the prevalence of stress, anxiety, and

depression among gig workers as well as the elements that influence these mental health outcomes would be intriguing.

The role of platform firms in influencing the working conditions and socioeconomic status of gig workers in Pune is another subject of research that might be investigated further. Researchers can better understand the elements that contribute to the difficulties faced by gig workers by looking at the policies and practices of platform businesses.

Also, future studies can look into the possibility of coordinated action among Pune's gig workers. Gig workers may be able to advocate for improved working conditions and labour rights and have more negotiating leverage with platform businesses if they band together and organize.

References

1. Chaudhary, R. (2020). India's Emerging Gig Economy : Shaping the Future of Work for Women. 50–57
2. Boar, A., Bastida, R., & Marimon, F. (2020). A systematic literature review. Relationships between the sharing economy, sustainability and sustainable development goals. *Sustainability (Switzerland)*, 12(17) <https://doi.org/10.3390/SU12176744>
3. Caza, A. (2020). The Gig Economy's Implications for Management Education. *Journal of Management Education*, 44(5), 594–604. <https://doi.org/10.1177/1052562920934150>
4. Ly, B. (2020, December 11). Employment in the Gig Economy. On Research. Retrieved September 15, 2022, from https://www.academia.edu/44680356/Employment_in_the_GIG_Economy
5. Healy, J., Nicholson, D., & Pekarek, A. (2017). Should we take the gig economy seriously? *Labour & Industry: A Journal of the Social and Economic Relations of Work*, 27(3), 232–248. <https://doi.org/10.1080/10301763.2017.1377048>
6. Veluchamy, R., Reddy, P., Pillai, R., & Singh, R. (2021). A Study on Work Life Integration of GIG Workers. *An Anthology of Multi-Functional Perspectives in Business and Management Research*, 1(Volume 1), 23–32.
7. Banik, N., & Padalkar, M. (2021). The spread of the gig economy: Trends and effects. *Foresight and STI Governance*, 15(1), 19–29. <https://doi.org/10.17323/2500-2597.2021.1.19.29>
8. Banwari, Vijeta. (2018). Gig Economy: Opportunity and Challenges in India. 5(11), 413–420
9. Chaturvedi, P., Registrar, D., Rntu, A., & Nihalchandani, T. (2022). Issue 6 www.jetir.org (ISSN-2349-5162). JETIR2206029 *Journal of Emerging Technologies and Innovative Research*, <https://www.jetir.org/papers/JETIR2206029.pdf>
10. Rukhsar, Umaima (2019). A Study on Perception Of Employees Towards Gig System: 4,5349–5368.
11. Sujatha, D. V. M. & D. R. (n.d.). "Identity in a Gig Economy", Does Learning Agility Matter? Talent Management Consultant & Founder Me Green India, Former VP-HR, Research Professor of HR & Entrepreneurship, Entrepreneurship Coach, Amity Business School, Page No : 3610. *Mukt Shabd Journal-Mukt Shabd Journal* ISSN NO : 2347-3150, IX (Vi), 3610–3632
12. Pal, B. (2021). Rising Popularity in Gig Economy: A Case Study from India. *International Journal of Religious and Cultural Studies*, 3(2), 203–208. <https://doi.org/10.34199/ijracs.2021.09.08>
13. Curtis, S. K., & Mont, O. (2020). Sharing economy business models for sustainability. *Journal of Cleaner Production*, 266, 121519. <https://doi.org/10.1016/j.jclepro.2020.121519>

14. https://www.niti.gov.in/sites/default/files/2022-06/25th_June_Final_Report_27062022.pdf
15. <https://iwwage.org/wp-content/uploads/2020/02/Labour-Practises-in-the-emerging-gigeconomy-in-India.pdf>
16. <https://media-publications.bcg.com/India-Gig-Economy-Report.pdf>



**SARDAR PATEL INSTITUTE OF
ECONOMIC AND SOCIAL RESEARCH**

anvesak

A bi-annual journal

CERTIFICATE OF PUBLICATION

This is to certify that the paper entitled

**BANKING SYSTEM TRANSITION FROM A
COMPARATIVELY CLOSED ECONOMY TO
A MARKET ECONOMY**

Authored by

Milind Patil, Dr. Gulnawaz Usmani

UGC

University Grants Commission

Approved Journal

vol. 53 No.01

in

Anvesak A bi-annual Journal

UGC Care Group - 1

ISSN: 0378-4568

January-June 2023

Impact Factor: 6.20



A bi-lingual journal

BANKING SYSTEM TRANSITION FROM A COMPARATIVELY CLOSED ECONOMY TO A MARKET ECONOMY

Milind Patil

Research Scholar, Department of Economics, AKI's Poona College of Arts, Science & Commerce, Camp, Pune.

Dr. Gulnawaz Usmani

Assistant Professor, Department of Economics, AKI's Poona College of Arts, Science & Commerce, Camp, Pune.

Abstract

Following the spate of financial crises in the 1990s, many observers have opined that the need to depoliticize exchange rate movements along with the frequency with which “soft pegs” have been susceptible to speculative attacks in this era of escalating global capital flows necessitates that developing countries adopt corner solutions to exchange rates arrangements. In other words, according to many observers, the exchange rate option for developing countries boils down to one between flexibility, on the one hand, and credible pegging, on the other. Countries have, however, been advised to steer clear of arrangements that lie anywhere between these polar extremes (i.e., those in the “middle”) as they were viewed as inherently unstable. Subsequently, the East Asian crisis in 1997 led to a heightened appreciation of the importance of a strong banking system, not just for efficient financial intermediation but also as an essential condition for macroeconomic stability. Recognizing this, the government appointed a Committee on Banking Sector Reforms to review the progress of reforms in banking and to consider further steps to strengthen the banking system in light of changes taking place in international financial markets and the experience of other developing countries. The two reports provided a road map that has guided the broad direction of reforms in this sector. This paper attempts to clarify some of the issues at hand, and in particular, about the central banking transition from a comparatively closed economy to market economy. The paper also estimates a Taylor type Monetary Policy Rule for India.

Key Words: RBI, developing countries, Open Economy, Closed Economy, Flexibility, Exchange rate

A moment comes, which comes but rarely in history, when we step out from the old to the new, when an age ends, and when the soul of a nation, long suppressed, finds utterance.

- Jawaharlal Nehru

Introduction

Central bank has been in existence in one form or the other since the second half of the 17th century. Over the years these have passed through various phases of evolution and have come up to a stage where they have assumed greater responsibilities ranging from core central banking functions such as monetary policy formulation and currency management to development and regulation of overall financial structure.

In India the reserve bank of India (RBI) started functioning as the central bank since April 01, 1935 after being established by legislation in 1934 through reserve bank of India act 1934. The tasks of the RBI have been aptly described in the preamble to the RBI act as "to regulate issue of bank notes and keeping of reserves with a view to securing monetary stability in India and generally to operate the currency and credit system of the country to its advantage....." the preamble clearly lays out that the RBI shall perform central banking functions viz.,

(a) Issue of bank notes and maintenance of reserves;

(b) Securing monetary stability; and

(c) Operating currency and credit system to the advantages of the country.

India's commercial banking system in 1991 had many of the problems typical of unreformed banking systems in many developing countries. There was extensive financial repression, reflected in detailed controls on interest rates, and large pre-emption of bank resources to finance the government deficit through the imposition of high statutory liquidity ratio (SLR), which prescribed investment in government securities at low interest rates. The system was also dominated by public sector banks, which accounted for 90 percent of total banking sector assets, reflecting the impact of two rounds of nationalization of private sector banks above a certain size, first in 1969 and again in 1983. These banks were nationalized because of the perception that it was necessary to impose social control over banking to give it a developmental thrust, with a special emphasis on extending banking in rural areas. The system suffered from inadequate prudential regulations, and non-transparent accounting practices. Supervision by the Reserve Bank of India (RBI) was also weak. The 1991 balance of payments crisis led to India's 'plunge into structural reforms'. Structural adjustment programs and loans were arranged through the International Monetary Fund (IMF) and the World Bank. The Indian Government was forced to review its trade policies to allow more foreign investment and reduce trade restrictions so that India's economy could be restored to its former level. Import tariffs underwent significant reductions and import/export licensing system procedures were simplified. The opening up of capital markets to include more foreign participation has allowed Australia's entrance into otherwise untapped markets.

Review of Literature

Ghosh, T. et.al, In their paper authors have emphasized the need to bring monetary aggregates back into the exchange rate models, but with better measures of money than the simple-sum accounting measures having no foundations in microeconomic aggregation theory. The following contributions are relevant. Ireland (2001) finds empirical support for including money growth in an interest rule for policy. In Ireland's model, money plays an informational rather than a causal role by helping to forecast future nominal interest rate. Other papers emphasizing the "information content" of monetary aggregates in predicting inflation and output include **Masuch et al. and Bruggeman et al. (2005)**.

Cavoli, T., & Rajan, R. S. studied that there has been a great deal of discussion of whether the Reserve Bank of India (RBI) should adopt an inflation targeting arrangement. This debate has been further fuelled by the release of the Raghuram Rajan report of the Committee on Financial Sector Reforms (CFSR) which recommended that the Reserve Bank of India (RBI) adopt an inflation targeting arrangement. However, some of the popular discussion on the issue appears to be rather confused and insufficiently informed about the details of an inflation targeting arrangement. This paper attempts to clarify some of the issues at hand, and in particular, the implications of such an arrangement for exchange rate management. The paper also estimates a Taylor type Monetary Policy Rule for India.

A strong and resilient banking system is considered a prerequisite for the economic growth and financial stability. Regulations are generally intended to minimise the risk of bank failures and strengthen the financial stability by controlling the behaviour of financial sector participants and building financial buffers. Regulations could take the form of macro-prudential or macroprudential regulations and could be implemented by pricing or structural mechanisms. However, notwithstanding the continued experimentation with the regulations, the banking crises have been almost a recurrent phenomenon in the modern financial history. As a reaction to the successive financial crises, globally, the financial stability is seen as the primary goal of regulations. **Srivastava, D. A.** This book is the first major exploration of Indian political economy using a constructivist approach. Arguing that India's open-economy policy was made, justified, and continued on the basis of the idea of openness more than its tangible effect, the book explains what sustained the idea of openness, what philosophy, interpretations of history, and international context gave it support, justification, and persuasive force. **Alamgir, J.**

Another author studied growth of the Indian banking sector after the liberalization and deregulated environment has brought extensive transformation in the banking industry. The remarkable development of technology and the wide spread use of information technology has brought this paradigm change. For the banking sector, the technological advancements have appeared to be a strategic source for attaining greater level of competence, organized operations, increased efficiency and productivity. From the customer point of view, it is the apprehension of 'Anytime, Anyway and Anywhere' banking vision. **S. B., Gupta et.al.**

Sharma, K. C. in his book modern banking in India stated how today, banks have become a part and parcel of our life. There was a time when, the dwellers of city alone could enjoy their services. Now banks offer access to even a common man and their activities extend to areas hitherto untouched. Apart from their traditional business-oriented functions, they have now come out to fulfil national responsibilities. Banks cater to the needs of agriculturists, industrialists, traders and to all the other sections of the society. Thus, they accelerate the economic growth of a country and steer the wheels of the economy towards its goal of "self-reliance in all fields". It naturally arouses our interest in knowing more about the 'bank' and the various men and activities connected with it. **Ozili, P. K.** in his article explores the eRupee or digital rupee central bank digital currency in India. It explores the benefits and issues surrounding the central bank digital currency in India. The study found that Indian people who were interested in 'cryptocurrency' information were also interested in 'central bank digital currency' information. The study also showed that the introduction of CBDC has potential benefits such as reduced dependency on cash, higher seigniorage due to lower transaction costs and reduced settlement risk. However, the India CBDC has associated risks that need to be carefully evaluated against the potential benefits. The introduction of a digital rupee or CBDC in India will require legal and regulatory changes to make the phased CBDC implementation possible.

Objectives

1. To observe transition of Indian economy from closed to open
2. To study the Indian banking systems in both closed and open economy
3. To examine the current financial condition of Indian Economy
4. To overview banking sectors reform after 1991 economic crisis

Methodology

Type of Research: Observational and Descriptive.

Research Design: The research data will be collected as follows:

The data will be collected from secondary sources.

Some of the sources for secondary data will be Reserve bank of India (RBI), World Bank, various researches on the mentioned topic by reviewing literature.

Independence Of Banking system to Adapt, Reorient and Face New Challenges

Transition from a Comparatively closed economy to a market economy has made it obligatory on the part of the reserve bank of India to remain focused and tackle dilemmas and challenges which are very particular to emerging market economy because of its heterogeneous economic structure. Independence of central banking from government controls is another debatable issue in emerging economies. Today, the dynamism of the economic structure and financial system has put additional responsibility on the central banks in emerging economies to adapt, reorient and face new challenges. in India, the RBI is turning these challenges into opportunities and marching ahead with its mandate in the service of the nation.

Although all these three functions are equally important yet the most important objective of the RBI over the years has been ensuring monetary stability. The term monetary stability can easily be understood as maintaining parity. **Ghosh, T. et.al (2016).**

Between price and incomes levels so as to ensure a synchronous rise in price vis-à-vis income levels. In common parlance, the same is also understood as ensuring price stability. While the main focus of the RBI has remained 'price stability', the other functions have worked as corollaries to this main function of monetary management.

Managing Change from a Closed to an Open Economy

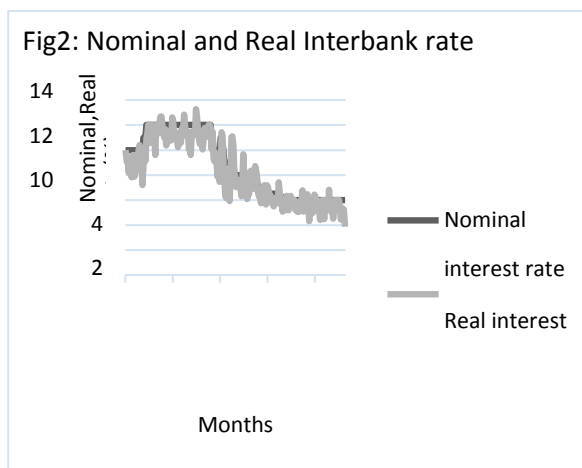
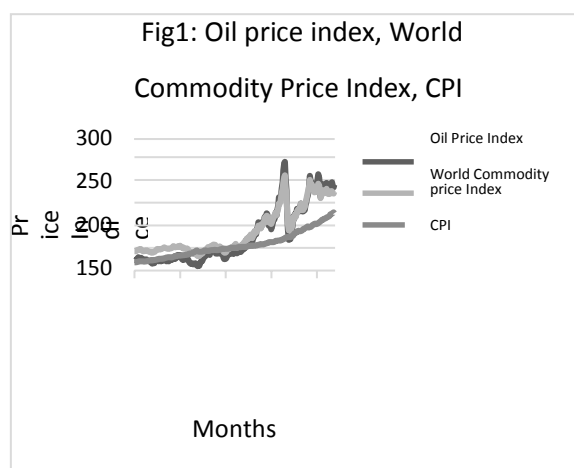
The Indian economy has responded vigorously to a program of stabilisation and reform measures started in 1992. The Indian Government took drastic action including devaluation, the imposition of higher interest rates, fiscal and monetary restraint and import compression. In succeeding budgets long term measures were introduced which removed the protection for Indian industry and commerce from international competition. The reforms that were introduced are addressed in Chapter 3 of the report. An indication of the success of these reforms is given by the change in India's current account deficit. In 1991 it had risen to 3.3 percent of Gross Domestic Product (GDP); by 1993 it had fallen to 1.8 percent, and by 1995 to 0.6 percent. **Masuch et al. (2003) and Bruggeman et al. (2005)**. Professor Mayer stated that the trade and tariff frameworks that were set up to protect the Indian economy have begun to be wound back, but that the process is occurring 'layer by layer, strand by strand; it is not a big bang sort of thing'. The Committee understands that the number of tariff bands is high, some ranging from 0 to 260 percent. From 1991 until it was voted out of power in May 1996, Prime Minister Narasimha Rao's Congress Government developed and implemented a strategy which aimed to transform India's economy from an inward-looking and protectionist one, to one fully integrated in the world trading system. **Masuch et al. (2003) and Bruggeman et al. (2005)**.

Emerging Market Economy (Eme) & Environmental Dynamism

However, phenomenal changes that have taken place in all spheres of economy, especially during the post-liberalization era, have necessitated dynamism in the central banking functions. Demands of an emerging market economy (EME) like India, are far more different than that those of a closed economy and hence, there is a need for central banks to understand the environmental dynamism and evolve strategies to come up to the expectations of the new economy. As a matter of fact, the working than traditional central banking functions. The bank has been transacting the government's business and promoting financial and economic development without jeopardizing price stability. It has helped to set up a number of financial institutions such as IDBI, UTI, NABARD and DFHI besides a number of research institutions. These institutions have been hived off from the parent body over time and they have gone a long way in developing the financial system of india. Yet, the need for continuous efforts aimed at expansion of the dictum of price stability to the doctrine of financial stability cannot be overemphasized. **Ghosh, T. et.al (2016)**

The Indian Economy at a Glance

The following figures provide a brief overview of the Indian economy since 1992.



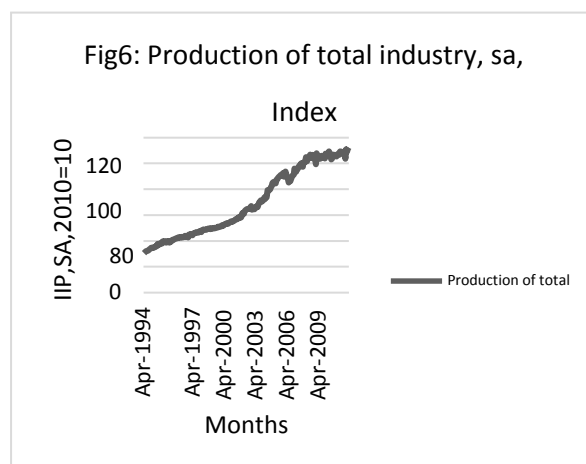
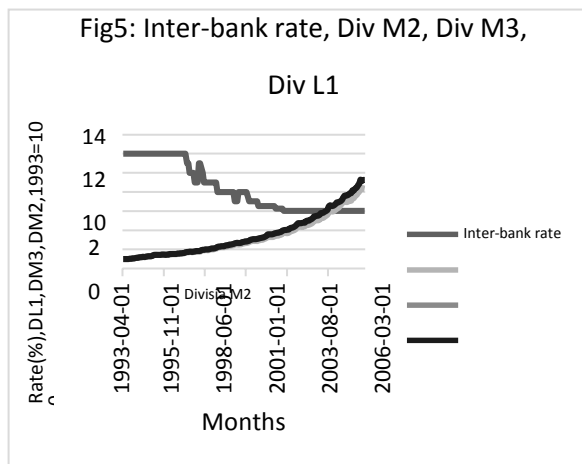
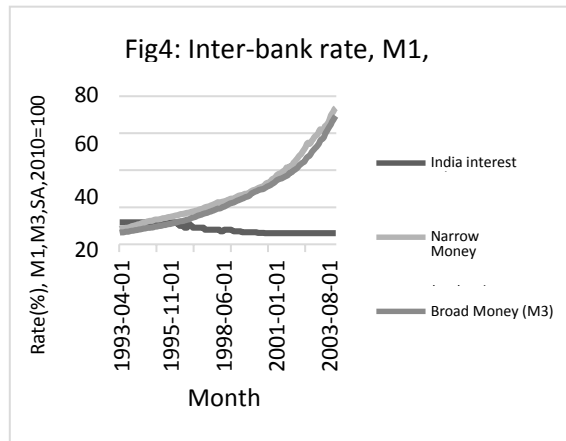
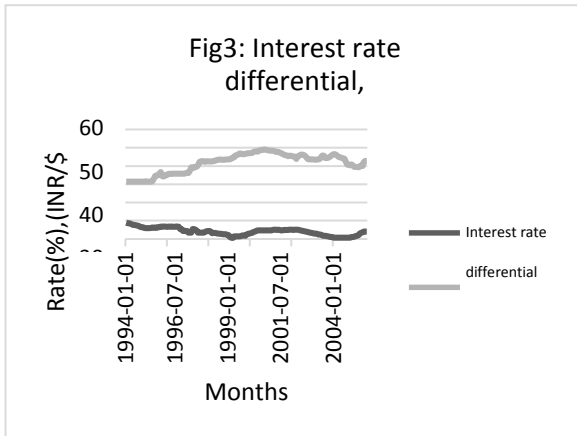


Figure 1 shows the Indian economy experienced very high inflation during the last 24 years. The CPI (consumer price index) between the first quarter of 1992 and the last quarter of 2013 rose by 384 percent. The average was a 17 percent price rise. However, from the first quarter of 1992 to the first quarter of 2000, CPI rose by 89%. On an average, there was a 9 percent price rise every year during that time period. **Alamgir, J. (2008).**

Figure 2 shows that loose monetary stance was a dominant feature of the economy between 1992 and 1997. **Alamgir, J. (2008).**

Figure 3 displays the interest rate differential between India and U.S. and the exchange rate of the India rupee relative to the US dollar. The figure suggests that the movements of the nominal exchange rate appear to have followed the interest rate differential with a lag.

Figure 4 displays the accelerated growth in the money supply for both M1 and M3 during a period of loosening of inter-bank rates. **Alamgir, J. (2008).**

Figure 5 displays the liquidity of the Indian economy using the theoretically grounded Division monetary aggregates. Division reflects much liquidity injection into the economy, but not as much as the simple-sum monetary aggregates would imply. **Alamgir, J. (2008).**

Figure 6 displays the production of total industry (IIP) for India. The period of highest industrial growth was between 2002 and 2007, after which the growth slowed dramatically. **Alamgir, J. (2008).**

Price Stability to financial stability

Price stability though equally important yet most of the times remains a short-sighted goal. A narrow focus of the monetary policy on price stability in the short-term may pose risks to price stability in the are overlooked. It is quite possible to achieve price stability for some time even in a turbulent financial

longer-run if the potential consequences of financial instability for longer-term price developments system through policy manipulations. It is just like taking pain killers for immediate relief without cure. The goal of financial stability, on the other hand, brings along with its policy prescription meant for curing the evils of the system and making it viable and self-sustaining. A financially stable system must be able to assess and mitigate risks take proactive actions and possess adequate shock- absorbers to react and bounce back after vulnerable periods. Financial stability is the single most important thing from the macroeconomic view as it deals with issue like contagion and systems and systemic risks which can lead to most violent upheavals and hence needs to be monitored continuously. While such monitoring is essential, practically it is very difficult due to the fact that unlike price stability it cannot be easily quantified and measured by a few indicators. **Srivastava, D. A. (2018)**

Holistic And Consciously Coordinated Strategy

As a consequence, maintenance of financial stability requires a holistic and consciously coordinated strategy aimed at development and deepening of the financial system. Improving allocating efficiency of the system and facilitating inter-temporal allocation of resources from savers to ultimate users is also essential. Vulnerability of capital flows in emerging market economies has put additional responsibility on payment and settlement systems to remain robust and prevent systemic on risks. Sine qua non for financial stability in a dynamic scenario. **Sharma, K. C. (2007)**

Dilemmas, challenges and opportunities

Transition from a comparatively closed economy to market economy has made it obligatory on the part of the RBI to remain focused and tackle dilemmas and challenges which are very particular to the EME. As a matter of facts, carefully crafted policies are needed for an EME because of its heterogeneous economic structure. Today, the Indian economy presents a dichotomous economic structure; one modern, dynamic and growing rapidly and the other traditional slow paced with old technologies. The Requirements of one structure is entirely different from those of the other. **Cavoli, T., & Rajan, R. S. (2008)** The problem that most of the things are in a transition phase and that too with different paces, makes the job of the central bank more complex and difficult. While some sectors demand and liberal and free environment, at the same time there are other which need to be protected and nurtured. Therefore, making a judicious mix of central banking policies of developed and developing economic is a challenge which the RBI faces today. Specifically speaking, such dilemmas arise out of the following Issues:

- Debt management and monetary management.
- E-money and systemic risk management.
- Liberalization and global imbalances.
- Global alignment and domestic financial inclusion.
- Central banking independence and economic growth.
- Credibility and constructive ambiguity.

Formulation And Conduct of The Monetary Policy

Although not exactly a central banking function, the RBI also works as a debt manager of central and state governments under sections 17(11)(e),21(2),21(A) of the RBI act-1934. It manages issuance, redemption, servicing, etc, of domestic loans which are raised by the governments as per the constitutional provisions under articles 292 and 293 for the fiscal management. Such an activity creates a dilemma as objectives of debt management sometimes come in direct conflict with those of monetary management. The objectives of development management are cost minimization., maturity elongation and smooth rollover. At the same time, formulation and conduct of the monetary policy is also closely related with liquidity and interest rate management in the economy.

Avoiding crowding out of private investments due to heavy government borrowings also becomes a major concern. Moreover, since banks and financial institutions are the principal investors in the government securities, managing low-cost borrowings for government results into poor bottom lines for the financial sector. Monetary management by the central bank, therefore, becomes a tight-rope walk which at times may result in compromise in the monetary management objectives. **Cavoli, T., & Rajan, R. S. (2008)**

Broad Approach to Reform

The strategy for banking reforms was broadly similar to that followed in other countries, but with some important differences. It was similar to the extent that it focused on imposing prudential norms and improving regulatory supervision to meet Basel I standards (standards that were formulated by the committee of the Bank of International Settlement, or BIS, based in Basel, Switzerland), and it aimed at increasing competition to promote greater efficiency. However, there were two important differences compared with reforms in other countries. First, the reforms in banking were much more gradualist than in most countries, a course of action that was in line with the general strategy of reforms in India, made possible by the fact that the reforms were not introduced in the midst of a banking sector crisis, which might have entailed greater urgency. Second, unlike the case in many other countries, there was never any intention to privatize public sector banks. It was clearly recognized that competition was desirable, and this implied that both private sector banks and foreign banks should be allowed to expand their market share if they could. However, the government also declared its intention to strengthen public sector banks and enable them to meet competition. **Srivastava, D. A. (2018)**

There was also a great deal of progress in introducing prudential norms for income recognition, asset classification, and capital adequacy in a phased manner. As a consequence of this gradualist process, income recognition norms and capital adequacy norms have been fully aligned with Basel I standards, while asset recognition norms, though still falling short of international best practice, are now close to existing international standards.

Banking System Performance

The impact of the reforms on the efficiency of the banking system in performing its twin roles of financial intermediation and resource allocation is not easy to evaluate. As far as the scale of bank intermediation is concerned, the ratio of total credit extended by the banking system to India's gross domestic product has increased, but it is still relatively low compared to countries such as China or some of the other East Asian countries. The ratio in India increased from 51.5 percent in 1990 to 53.4 percent in 2000, whereas in China it increased from 90 percent to 132.7 percent in the same period. The figures over the same period are also much higher for Malaysia (75.7% and 143.4%) and Thailand (91.1% and 121.7%), though many Latin American countries have figures closer to those of India.

There is evidence of significant improvement in several dimensions in recent years. Gross nonperforming assets (NPAs) as a percentage of total advances have fallen from 15.7 percent in 1996–1997 to 7.3 percent in 2003–2004. Gross NPAs as a percent of total assets are much lower because Indian banks typically have a large proportion of their assets in sovereign debt; this ratio has also declined from 7 percent in 1996–1997 to 4 percent in 2002–2003. More importantly, the financial strength of the banks is actually better than it appears from these ratios because Indian banks do not write off assets, even though large provisions have been made. Net nonperforming assets, calculated after taking account of provisioning, are 3 percent of total advances and only around 2 percent of total assets. There has been a general improvement in other financial indicators, such as net profit as a percentage of total assets, interest spread as a percentage of assets, and operating expenses as a percentage of total assets, for public sector banks, old private sector banks, new private sector banks, and foreign banks. The financial strength of the banks, as measured by the capital to risk adjusted assets ratio (CRAR), shows distinct improvement in the postreform period. The required CRAR was

increased in phases, to 8 percent at first (which is the Basel I minimum) and then to 9 percent in 1999–2000. Initially, banks with insufficient capital had to be capitalized by the injection of government equity from the budget, but subsequently several banks were able to raise capital from the market, and this, combined with plowing back of profits, led to a substantial improvement in capital adequacy. At the end of March 2003, out of the 93 commercial banks operating in India, 91 were above 9 percent and as many as 87 were above 10 percent, compared with only 54 out of 92 banks above 9 percent and 42 above 10 percent at the end of March 1996. **Srivastava, D. A. (2018)**

It is noteworthy that the Indian banking system did not suffer from any contagion effect in the aftermath of the East Asian crisis. However, this is not so much due to the improvements brought about after 1991, as the fact that the capital account was not fully open. Banks were not allowed to undertake excessive foreign currency exposure, and external borrowing (especially short-term borrowing) was strictly controlled. This cautious policy helped insulate India from the severe reversals of external flows witnessed in many emerging market countries in the 1990s. **Masuch et al. (2003) and Bruggeman et al. (2005).**

Decontrol of Interest Rates and Credit

There has been a significant liberalization of interest rate and credit controls on commercial banks. Earlier, there were detailed restrictions on interest rates that could be paid on different types of deposits and rates that were charged to various categories of customers. These have been extensively liberalized. On the deposit side, interest rates paid on term deposits have been decontrolled, except that the RBI prescribes a maximum interest rate on short-term (15-day) deposits and also prescribes the interest rate on savings deposits. On the lending side, the detailed structure of interest rates prescribed for different types of borrowers and for different sizes of loans has been abolished; the RBI prescribes only the interest rate to be paid under the differential rate of interest scheme a very small window for loans to individuals below the poverty line. For the rest, individual banks fix lending rates with reference to the prime lending rate fixed by the bank. The reforms also abolished the requirement that banks needed to obtain RBI approval for individual credit limits fixed for large customers. With these changes, decisions on the cost of credit and the volume of credit to be extended have been left to bank management, subject to internal guidelines and procedures for credit approval and general prudential limits on single borrower and single project exposure. **Cavoli, T., & Rajan, R. S. (2008)**

Directed Credit

Reducing directed credit requirements is a common feature of banking reforms, and this was the case in India as well. A major directed credit requirement was constituted by the high levels of the SLR, which preempted bank resources to finance the government deficit at low interest rates. Preemption of credit by the government also occurred indirectly because the RBI followed a practice of automatically issuing ad hoc Treasury bills to meet any shortfalls in the government's balances with the RBI. Since this implied a mechanical transmission of fiscal expansion to the monetary side, it was offset by imposing a high cash reserve ratio (CRR) in the commercial banks, thus effectively crowding out private sector credit.

At one stage, prior to the reforms, the combined effect of the high CRR and the SLR was such that only 35 percent of the increment in bank deposits was actually available for commercial advances, the rest being either impounded by the RBI in the form of cash reserve deposits or absorbed by the government. The practice of automatic monetization was abandoned in 1994, and both the CRR and the SLR were reduced over time from 15 percent and 38.5 percent, respectively, before the reforms to 5 percent and 25 percent by 2005. The fiscal deficit is now financed through the auction of government securities conducted by the RBI, and in that sense, the interest rate on government borrowing is market-determined. However, it is interesting to note that, despite the reduction in the SLR from 38.5 percent to 25 percent, the proportion of government securities held by the banks to their total assets has actually increased from 30.4 percent at the end of March 1994 to 34.5 percent at the end of March 2004. This has occurred because of the combined effect of the inability to reduce the

fiscal deficit—a key weakness of the reforms to date—and the fact that the prudential norms give sovereign debt a very low risk weight. In other words, while statutory preemption of bank resources was steadily reduced in the 1990s, the banks' appetite for government debt has remained high because the prudential norms contain a built-in regulatory bias in favor of government debt in preference to commercial credit. **Cavoli, T., & Rajan, R. S. (2008)**

The other major form of directed credit was the requirement that 40 percent of commercial credit has to be extended to the priority sector, which includes agriculture, small-scale industry, small transport operators, artisans, and so on. It applies to Indian commercial banks but not to foreign banks because the latter do not operate in rural areas and therefore cannot engage in agricultural lending. In their case, the requirement is that 15 percent of advances must be for exports and for the small-scale sector. These provisions have not been altered by the reforms. However, although the priority sector target for Indian banks has not been changed, the provision has been liberalized indirectly to some extent by definitional changes that expand the range of borrowers that are eligible. It is also worth noting that while banks are subject to sectoral direction of credit, they are not required to lend to particular borrowers; the credit decision of lending to a particular borrower is left to the bank on the basis of normal credit-worthiness analysis.

Banking System Performance

The impact of the reforms on the efficiency of the banking system in performing its twin roles of financial intermediation and resource allocation is not easy to evaluate. As far as the scale of bank intermediation is concerned, the ratio of total credit extended by the banking system to India's gross domestic product has increased, but it is still relatively low compared to countries such as China or some of the other East Asian countries. The ratio in India increased from 51.5 percent in 1990 to 53.4 percent in 2000, whereas in China it increased from 90 percent to 132.7 percent in the same period. The figures over the same period are also much higher for Malaysia (75.7% and 143.4%) and Thailand (91.1% and 121.7%), though many Latin American countries have figures closer to those of India.

There is evidence of significant improvement in several dimensions in recent years. Gross nonperforming assets (NPAs) as a percentage of total advances have fallen from 15.7 percent in 1996–1997 to 7.3 percent in 2003–2004. Gross NPAs as a percent of total assets are much lower because Indian banks typically have a large proportion of their assets in sovereign debt; this ratio has also declined from 7 percent in 1996–1997 to 4 percent in 2002–2003. More importantly, the financial strength of the banks is actually better than it appears from these ratios because Indian banks do not write off assets, even though large provisions have been made. Net nonperforming assets, calculated after taking account of provisioning, are 3 percent of total advances and only around 2 percent of total assets. There has been a general improvement in other financial indicators, such as net profit as a percentage of total assets, interest spread as a percentage of assets, and operating expenses as a percentage of total assets, for public sector banks, old private sector banks, new private sector banks, and foreign banks. The financial strength of the banks, as measured by the capital to risk adjusted assets ratio (CRAR), shows distinct improvement in the postreform period. The required CRAR was increased in phases, to 8 percent at first (which is the Basel I minimum) and then to 9 percent in 1999–2000. Initially, banks with insufficient capital had to be capitalized by the injection of government equity from the budget, but subsequently several banks were able to raise capital from the market, and this, combined with plowing back of profits, led to a substantial improvement in capital adequacy. **Sharma, K. C. (2007)** At the end of March 2003, out of the 93 commercial banks operating in India, 91 were above 9 percent and as many as 87 were above 10 percent, compared with only 54 out of 92 banks above 9 percent and 42 above 10 percent at the end of March 1996.

It is noteworthy that the Indian banking system did not suffer from any contagion effect in the aftermath of the East Asian crisis. However, this is not so much due to the improvements brought about after 1991, as the fact that the capital account was not fully open. Banks were not allowed to undertake excessive foreign currency exposure, and external borrowing (especially short-term

borrowing) was strictly controlled. This cautious policy helped insulate India from the severe reversals of external flows witnessed in many emerging market countries in the 1990s.

E-Money and Minimization of Paper-Based Transaction

Thrust towards expansion of E-Money and minimization of paper-based transaction though a welcomes step on the part of the RBI, yet the issue of assessing, mitigating and managing systemic risks has also gained currency in recent times. Establishing a robust payment and settlement system in electronics environment is a big challenge and the apex bank will have to live up to the challenges of technological revolution. **Ozili, P. K. (2022)**

Financial Integration

Liberalization has resulted in financial integration to an extent in the economic scenario and the events of one economy instantaneously influence developments in another. However, huge current account deficit of the US and consequents surpluses in Japan and the gulf countries have created global imbalances which may adversely affect some systemically important currencies, especially the US dollar. Of late, it is being argued that the US consumer cannot pull the global demand for a long time as the US current account deficit may become unsustainable, although the Indian economy is insulated to a great extend due to restricted capital account, yet overflowing US dollars through FIIs is a cause of concern. One-way movement of foreign currency may lead to destabilization. However, these things are bound to happen because the world is not flat and increase in the degree of financial integration can further catalyze disparities. Hence, the only remedy that remains is to devices suitable policies, strategies and tactics to tackle such delicate issues, this is a challenge which is to be turned into an opportunity for india to make a mark at the world stage. **Ozili, P. K. (2022)**

Global banking standards and domestic financial inclusion.

Another related issue is the simultaneous fulfilment of the requirement of adopting global banking standards and domestic financial inclusion. The Indian scenario is quite unique due to the fact that banking is still a luxury for a vast chunk of population and we are talking about achieving global standards of banking in terms of technology as well as regulatory norms due to global alignment of the banking industry. Both these objectives are important and require substantial resource allocation. A judicious and balanced strategy is needed to achieve the objective of taking the banking to every nook and corner of the nation and simultaneously achieve global standards without escalating and passing the cost to the common customer. This is again a big challenge and opportunity for the central bank. **Ozili, P. K. (2022)**

Independence of central banking from government controls is another debatable issue in emerging economies. This involves operational as well as financial independence. Although the case for a strong and independent central bank has a firm footing. Yet the extent of independence hinges upon its trade-off with fiscal issues of a developing and transforming economy.

Conclusion and policy implications

The issue of transparency in central banking functions has gained currency in recent times.

Theoretically speaking, as the economy grows and matures the central bank should also become more predictable. However, it is quite difficult to say that the Indian economy and financial system in particular have gained such a depth and maturity; probably it will take some more time to reach the stage of a fully developed financial system. Hence, constructive ambiguity in central banking shall remain a major tool. Being constructively ambiguous and maintaining credibility is indeed an uphill task in which the RBI has been highly successful. The ability of the RBI to surprise the market and move ahead of it while keeping it on the desired path in today's dynamic environment shall be put test in the ensuing time.

Today, the dynamism of the economic structure and financial system has put additional responsibility on the central banks in emerging economies to adapt, reorient and face new challenges. In India, the RBI is turning these challenges into opportunities and marching ahead with its mandate in the service of the nation.

Pro-openness policy makers have been successful on the first count. Even left-leaning parties now provide broad support for the continuity of open-economy policies. Such broad-based support would not have been possible without the imagery of empowerment, loss and global destiny employed consistently by the policymakers. All nationalist appeals are based on some concept of strengthening the nation. The idea of globalism encompasses that appeal and goes farther beyond, not only by showing congruence with the “Indian” identity derived through anticolonial struggles but also by bringing together politically diverse interests under its ideological and rhetorical orbit on economic matters. While various political platforms questioned specific policy measures, virtually none questioned the need for greater global visibility. As the broad idea to frame India’s open-economy policies, globalism has proven to be an extremely useful vehicle to market open-door policies to the domestic constituency.

Limitations and Future Research Directions

Inadequate regulations or failure of regulations to keep pace with financial innovations could have been reasons for financial crises during 1991 in India, but equally critical contributing factors for financial distress have been inadequate internal control, false assumptions about market and liquidity, and lack of due diligence processes. It is obvious, therefore, that the regulations may strengthen but cannot substitute the internal controls and risk management framework at the level of the financial institution. Hence, at the micro level, while it is imperative for the institutions to put in place a comprehensive risk management system, the regulator also needs to ensure that there is adequate risk ownership in the institution at a sufficiently senior position. The key to success is to have a proper balance of macro-prudential and micro-prudential regulations adequately aligned with the nature and culture of financial market behaviour. While traditionally, the securities regulations were backwards looking and rule based and insurance regulations were not highly capital-centric in contrast to the forward-looking capital-intensive macro-prudential banking regulations, now a greater convergence is seen in the regulatory approaches. Financial stability and some elements of macro-prudential focus have now become a common denominator for all the regulators. Another important aspect is an effective supervision because first, it is not possible to forecast and document every likely incidence of risk in the regulatory norms and second, holding buffers against every possible eventuality could stifle the growth and could make the financial institutions inefficient. A forward-looking and vigilant supervisory mechanism could sense early signs of distress, distortions and imbalances and raise a red flag for timely action. However, developing a larger eco-system of effective 360-degree supervision through information dissemination should be the ultimate goal of the supervisory process. It is a challenge is to incentivise the financial market participants to join the regulators in pursuit of effective risk optimisation and strengthening of the 10 financial stabilities. Collaboration and coordination are needed between the regulators and the regulated entities for achieving the common good of a stable and efficient financial system. The one can further monitor and evaluate the financial stabilities in economy in the coming period of time and can always compare it timely with the situation of Indian economy during 90’s.

References

1. **Barnett, W. A., Bhadury, S. S., & Ghosh, T. (2016).** *An SVAR approach to evaluation of monetary policy in India: Solution to the exchange rate puzzles in an open economy.* *Open Economies Review*, 27(5), 871-893.
2. **Cavoli, T., & Rajan, R. S. (2008).** Open economy inflation targeting arrangements and monetary policy rules: Application to India. *Indian Growth and Development Review*.

3. **Srivastava, D. A. (2018).** Financial Crises and the Prudential Regulations: Theory, Practice and the Way Forward. *The Indian Banker, Indian Bank Association, ISSN, 2349-7483.*
4. **Verma, S. B., Gupta, S. K., & Sharma, M. K. (Eds.). (2007).** *E-Banking and development of banks.* Deep & Deep Publications.
5. **Toor, N. S. (2015).** *Handbook of banking information.* Skylark Publications.
6. **Sharma, K. C. (2007).** *Modern Banking in India.* Deep and Deep Publications.
7. **Ozili, P. K. (2022).** Central bank digital currency in India: the case for a digital rupee. *Technical Paper Series.*
8. **Alamgir, J. (2008).** *India's open-economy policy: Globalism, rivalry, continuity.* Routledge.
9. www.rbi.org.in

A STUDY OF PROGRAMS OF SEBI AND ITS IMPACT ON RETAIL INDIVIDUAL INVESTORS OF MAHARASHTRA

Mr. Syed Nayeem Syed Yusuf

Research Scholar, Department of Economics, AKI's Poona College of Arts, Science and Commerce,
Camp, Pune

Dr. Gulnawaz Usmani

(Research Guide), Assistant Professor, Department of Economics, AKI's Poona College of Arts,
Science and Commerce, Camp, Pune

Abstract

The individual investor plays an important role in the stock market because a big share of their savings are invested in the country. India's stock market is now dominated by individual investors. Individual investors now form nearly 45% of trading turnover on the Indian stock exchange. An individual investors in the stock market are at high risk because they tend to look at the higher possible returns from their investment without adequate knowledge of market risks. Trading in complex products without sufficient information may make investors, especially first time investors prone to losses and consequently dent confidence of investors in the stock market. Investor education is important for every investor in making better assessment of suitability of the investment advice, investment products and services. Research study analyses the response of retail individual investors towards programmes of SEBI. Whether those who have attended programmes of SEBI have any future intention to directly invest in the Indian stock market. Research study also analyses the extent to which programs of SEBI have a positive impact on investment behaviour of existing retail individual investors of the Indian stock market. Study found positive response from retail individual investors towards programmes of SEBI.

Keyword: Retail Individual Investor (RIIs), Capital Market, Equity, Share SEBI, Investor Awareness Programs, SMARTs, National Stock Exchange (NSE), Securities Market

1. Introduction

The capital market, by definition, is the market for long term capital or funds. It is a market for buying and selling of equity, debt-debentures & bonds and other securities. Generally, capital market deals with long term securities that have a maturity period of more than one year. Capital market plays an important role in mobilizing long term savings for financing long term investments.

Capital market brings together suppliers of capital and users of the capital. It provides required funds to industries and governments to meet their long-term capital requirements.

India's stock market is now dominated by individual investors. Individual investors now form nearly 45% of trading turnover on the Indian stock exchange. As per the data from National Stock Exchange (NSE), Individual investors have increased from 33% market share since 2016, to 45% in 2021. However, trading in complex products without sufficient information may make investors, especially first time investors prone to losses and consequently dent confidence of investors in the stock market. Information asymmetry makes informed choices more and more difficult for the Retail Individual Investors.

There arises the need for investor education which is necessary for making sound financial decisions and achieving individual financial wellbeing. Investor education is important for every investor in making better assessment of suitability of the investment advice, investment products and services. Investor education is required for not only guiding investors in making investment decisions for their

financial wellbeing but also for investor protection. In other words Investor education and awareness initiatives help in encouraging the individuals' participation in the securities market.

Securities exchange board of India (SEBI) is the regulatory body for securities market. It has been established to protect the interest of investors in the securities market. SEBI is one of the most active regulatory bodies in terms of financial education and literacy in India. SEBI's Investor Education and awareness programs promote confidence among investors by enhancing their knowledge, skills and capability so that investors in the securities market appropriately understand risks like financial risks and opportunities. SEBI's programs help investors in making informed choices and also in avoiding fraudulent investment schemes.

2. SEBI's Programs

With the objective of spreading investor education and awareness, SEBI has been undertaking following activities on all India basis:

A. Investor Awareness Programs

SEBI has been conducting various investor awareness programs for creating awareness about the securities market. These programs are conducted by SEBI jointly with market infrastructure institutions (MIIs) such as stock exchanges, depositories, SEBI recognized investor associations etc.

i. *Regional Seminars / Webinars in Association with Market Infrastructure Institutions:* Since the inception of the regional seminar initiative in 2010, over 2,000 regional seminars had been conducted by SEBI in association with MIIs. Over two lakhs participants have benefited from such Regional Seminars / Webinars. (SEBI, 2020-21)

Table 8.1: Regional Seminars/ Webinars in Association with Market Infrastructure Institutions (MIIs)

Particulars	2020-21	2021-22
Total regional seminars conducted	652	642
Number of participants in regional seminars	79,583	53,463

During 2021-22, SEBI in association with MIIs, conducted 642 regional seminars across the country. These seminars were attended by 53,463 participants.

ii. *Investor Awareness Programs by SEBI Recognized Investor Associations:* Since the beginning of this initiative, SEBI recognized investor associations had conducted nearly 1600 programs/workshops.

B. Dedicated Investor Website: There is a dedicated website <http://investor.sebi.gov.in> which is maintained by SEBI for the benefit of investors.

C. Visit to SEBI: Under 'Visit to SEBI' initiative groups of students from colleges and professional institutes visit different offices of SEBI. These sessions cover various topics like basic concepts of securities market, new developments in securities market etc. Since the beginning of this initiative, 3,423 'Visit to SEBI' programmes have been conducted covering more than 1.53 lakh participants. (SEBI, 2020-21)

D. Financial Education Activities and Workshops Conducted by SEBI – Trained

Resource Persons: Since the inception of the program, these Resource Persons (RPs) have conducted 1, 06,707 financial education workshops/ webinars which cover more than 55 lakhs participants, across all the States and Union Territories of India.

Securities Market Trainers Program (SMARTs): During 2020-21, SMARTs was introduced for enhancing investor education activities of SEBI. (SEBI, 2020-21). The primary objective of SMARTs program is to strengthen the investor education mechanism of SEBI.

There is increasing interest among investors in the securities market. SMARTs is an important initiative of SEBI in the right direction. With the remarkable increase in first time investors there is a greater need to increase the outreach of investor education programmes so that investors understand the securities market better and make informed investment decisions.

SMARTs are expected to conduct Investor Awareness Programs for existing and prospective investors in the securities markets. SMARTs will cover different aspects of the securities markets such as introduction to securities markets, KYC, IPO, mutual funds, grievance redressal etc.

SMARTs Program will be in various regional languages, in addition to Hindi and English.

During 2021-22, SMARTs have conducted 1,797 investor awareness programmes which covered over 1.8 lakh participants. Since its inception in 2020, SMARTs have conducted 2,084 such investor awareness programmes covering over 1.96 lakh participants.

Objectives of SEBI's Investor Education and awareness programs are to make the existing and prospective Retail Individual Investors of Indian Stock Market:

1. Aware of the (financial) risks
2. understand the balance of risk and reward involved in investment products and their costs;
3. recognise that market fluctuations are normal
4. Know who to trust to provide unbiased, objective advice.
5. Better equipped to recognise and avoid fraud and scams.
6. Help investors, detect and avoid suspected fraudulent activity.

SEBI's programs have the potential to help improve financial outcomes for retail investors. Some key benefits of SEBI's programs include more informed investment decision-making, better financial planning, greater confidence and higher participation in the securities markets and increased awareness of investor rights and responsibilities.

The research study examines to what extent expected outcomes of SEBI's Investor Education and awareness programs have been achieved.

3. Review of Literature

An analysis of the literature states that various investor protection and educational measures taken by different financial institutions have yielded positive results but not at the desired level. Investor education acts as an important determinant of investors' investment decisions in different investment products. Empirical research studies indicate association of financial education with financial behaviours of individuals.

Kadariya et al. (2012) this study identified the level of equity investors' access to market information. It revealed that there was a positive relationship between investor awareness and level of investment.

Hathaway and Khatiwada (2008) stated that financial education, financial knowledge and financial behaviour are all interrelated. Financial education leads to greater financial knowledge which in turn leads to better financial behaviour and outcome.

Jawaharlal (1995) conducted a research involving 250 respondents. The result showed a positive relationship between the investors' education programmes and the financial behaviour of the respondents. It was found that the Investors "make informed choices when provided with adequate and reliable information. Such respondents were also found to have a better standard of living.

Barnard (2009), discussed the right kind of education to investors, and was of the view that millions of dollars each year are spent on investor education. However, many educational programmes are targeted at potential Investors, but the effectiveness of these programmes is the biggest issue.

Bandgar and P.K. (2010), based on their study in Bombay city (India) concluded that those middle-class families were found to be adequately financially literate but still, there is scarcity in skilfulness, understanding, and expertise in financial matters.

Arun Lawrence and Dr. Zajo Joseph (2013) in their study entitled “Factors leading stock investment: An Empirical Examination” had concluded that friends and media play a key role in influencing the investors share trading decisions.

M. Kannadhasan (2006) in his article titled "*Risk Appetite and Attitudes of Retail Investors with Special Reference to Capital Market*" - points out that the Retail Investors' financial decisions are not always guided by due consideration. Their decisions are also often inconsistent.

C. Kavitha (2015)- In this research C. Kavitha tried to find out reasons for few issues like less participation in National Stock Exchange (NSE) by local investors, the widespread ignorance about financial assets and the continuous purchase of stocks with no information known about them by most people in the country. Results of the study showed that there was a significant relationship between the investors' attitudes and stock market investments. As the more positive attitude improvement strategies was introduced, the more it was easy for local investors to invest in stock market

Apart from the above studies, many other studies have been conducted on different aspects of retail individual investors like their education level, investors education and awareness programs of different financial institutions, investment behaviour etc. Such studies among others include Shanmugham (2000), Rajarajan (2003), Srinivasan et.al (2010), Jagwani (2012), Ajmi Jy. A. (2008), Bandgar P.K, (2006), Durga Rao and Chalam and Murty (2013).

Gap Indicated By Literature Review

The literature survey reveals that though many studies have been done on different aspects of retail investors and on investor protection measures taken by different financial institutions, there is a need to conduct a specific study on the SEBI's programs with respect to *Awareness, Response and Impact* of such programs among retail Individual Investors of Indian Stock Market.

Considering the remarkable increase in first time investors in the stock market there is a greater need to assess the *Awareness, Response and Impact* of SEBI's programs on retail Individual Investors of the Indian Stock Market.

4. Importance of Research

SEBI as the securities market regulator plays a leading role in investor education which is necessary for making sound financial decisions and achieving individual financial wellbeing. Investor education is important for every investor in making better assessment of suitability of the investment advice, investment products and services. Investor education is required for not only guiding investors in making investment decisions for their financial wellbeing but also for investor protection.

The effectiveness of SEBI's programs in enhancing investor's knowledge, skills and confidence has not been studied to the desired extent. Investors should have proper knowledge and understanding of the various concepts related to the stock market. Research study will assess the impact of SEBI's programs retail individual investors to ascertain whether SEBI has succeeded in achieving its intended objectives of such programs. Study will also examine the challenges faced by existing and prospective retail individual investors in attending the SEBI's programs. And what response (positive/negative) they have regarding these programs so that SEBI may take corrective measures to make its programs more investor friendly, more responsive and more effective in addressing the needs and requirements of retail individual investors.

The study also examines whether SEBI's programs really help in enhancing the knowledge, skills and confidence of retail individual investors of the Indian Stock Market. The study also examines whether SEBI's programs help the public to appropriately understand securities market risks, including financial risks and opportunities.

5. Objectives

1. To examine programs of SEBI and response of individual investors towards SEBI's programs.
2. To analyse the intention of individual investors to directly invest in the Indian stock market after attending programs of SEBI.
3. To examine the impact of programs of SEBI on investment behaviour of retail individual investors of the Indian stock market.

6. Hypotheses

1. Programmes of SEBI do not get any response from individual investors.
2. There is no relation between individuals who have attended programs of SEBI and their intention to invest in the stock market.
3. There is no positive impact of SEBI's programs on investment behaviour of individual investors of the Indian stock market.

7. Research Methodology

The research study is based on both primary and secondary data. The primary data was collected with the help of questionnaire and interviews of the retail individual investors who have attended SEBI's investor education programme. Secondary data was collected from published and unpublished documents and reports of SEBI, BSE, NSE, NSDL, CDSL CMIE, NISM, NCFE and RBI and other related periodicals and journals.

India's stock market is now dominated by individual investors. Individual investors now form nearly 45% of trading turnover on the Indian stock exchange. As per the data from National Stock Exchange (NSE), Individual investors have increased from 33% market share since 2016, to 45% in 2021.

Since the outbreak of the pandemic, there has been an unprecedented increase in demat accounts opened at CDSL and NSDL depositories. The number of demat accounts of individuals has increased by 1.4 times in NSDL and by 3.2 times in CDSL during the period from January 2020 to March 2022. At the end of December 2022, 3.03 crore demat accounts were registered with NSDL and 7.78 crore with CDSL.

This trend was further supplemented by increasing participation by retail individual investors in trading on stock exchanges like NSE & BSE. Further, new investors registering on exchange were not restricted to only metros or big cities. Participation of individual investors is on the rise even from the small towns.

There are several factors which are responsible for increase in investors' participation like absence of alternative investment avenues, and growing awareness amongst the general public, simplification of KYC registration process, effective use of digital technology & initiatives in opening accounts online and enhanced availability of investment information on digital modes.

The research is based on a survey of randomly selected 100 individual investors of Pune city. The survey instrument was a well-structured questionnaire. Clustering method was used to classify investors into different segments/groups based on their pre-investment and post-investment behaviour.

Evaluation of responses of individual investors to the investor education efforts taken by Securities and Exchange Board of India (SEBI).

The respondents from Pune city were asked to respond to 4 questions to study the responses towards investor education efforts taken by SEBI. Following Table 1 shows the response.

Table 1: Responses to Investor Education Programs

Investor Education Variables	Response		
	Yes	No	Total
Was investor education programs sponsored by SEBI useful in enhancing your investment knowledge and decision making?	92	8	100
Have you read the investor education material posted by SEBI?	32	68	
Have you started investing in the Indian stock market before attending programs of SEBI?	64	36	100
Is there any positive impact of SEBI's programs on your investment behaviour?	73	27	100

Analysis of the table reveals that 92 % of the respondents found education programs sponsored by SEBI useful in enhancing your investment knowledge and decision making, while only 32 % have read the investor education materials posted in the web sites. Study found that as many as 64 % respondents started investing in the Indian stock market even before attending programs of SEBI. And 73 % respondents who have attended the investor awareness program have found that the program has had a positive impact on their investment behaviour.

8. Scope of Research

The Research will be restricted to the programs of SEBI. It will examine the Awareness, Response and Impact of programs of SEBI on retail individual investors. The study will be related to the Indian Stock Market and the area of study will be the Pune city, state of Maharashtra.

Conclusion

It can be concluded that investor education programs sponsored by SEBI has positive response among the respondent individual investors. A good majority who have attended the investor awareness programs have benefited from it. SEBI has been continuously working in the right direction to reach every existing and potential individual investor so that investors in the securities market appropriately understand risks like financial risks and opportunities. SEBI's efforts are giving positive results and still a lot needs to be done to enable investors to make informed choices and also avoid fraudulent investment schemes.

Suggestion

It is found that only a small percentage of individual investors participate in the SEBI's investor awareness program. Large majority of the individual investors get information and knowledge from other sources which may not be authentic and accurate and even sometimes misguided.

In such a scenario it is the responsibility of SEBI to reach every existing and potential individual investor of the country by expanding the area and increasing the frequency of such programs. More and more programs should be organized by SEBI in regional languages. Most of the first time investors are not aware of the SEBI's programs so adequate publicity should be given to such programs so that they also make informed choices and avoid investment risks.

References

1. Barnard Jayne W. (2009), "Deception, Decisions and Investor Education", Elder Law Journal, September, pp. 201-237.
2. Bhandari Ravi Baijulal (2017) A Study of Investors Awareness and Selection of Different Financial Investment Avenues for the Investor of Pune City

3. Chatterjee, S.(2015).False Confidence, Stock Market Participation, and Wealth Accumulation of Households: An Examination. *SSRN Electronic Journal*. doi:10.2139/ssrn.2566622.
4. Chhabra Ashmi (2018). A Study on Impact of Investor Education Programmes on the Behaviour of Investors (With Special Reference To Rajasthan)
6. Fox, J., Bartholomae, S., & Lee, J. (2005). Building the case for financial education. *Journal of consumer affairs*, 39(1), 195-214.
7. Hastings, J. S., Madrian, B. C., & Skimmyhorn, W. L. (2013). Financial literacy, financial education, and economic outcomes.
8. Hathaway, I., & Khatiwada, S. (2008). Do financial education programs work?
9. Jagwani, Bhagwan (2012), Relationship between foreign equity ownership and firm performance, *Indian Journal of Finance*, Vol. 6, No.7, pp. 27-33, July.
10. Jariwala Harsha Vijaykumar (2013). To Study the Level of Financial Literacy and Its Impact on Investment Decision An In Depth Analysis Of Investors In Gujarat State
11. Jawaharlal (1995). Assessment of Financial Education, India. *Assessment*, 3(13)
12. Kadariya, S., Subedi, P. P., Joshi, B. and Nyaupane, R. P. (2012). Investor Awareness and Investment on Equity in Nepalese Capital Market. *Banking Journal*. 2(1): 1-
13. Kavitha, C. (2015). Investors Attitudes towards Stock Market Investment. *International Journal of scientific research and management*, Vol.3 (7), 3356-3362.
14. Mandell, L., & Klein, L. S. (2009). The impact of financial literacy education on subsequent financial behavior.
15. Sahu Bhavana (2016). Analysis of the impact of investor protection measures by SEBI on retail investors
16. Shanmugham, R. (2000), "Factors Influencing Investment Decisions Indian Capital Markets – Trends and Dimensions (ed.)", Tata McGraw-Hill Publishing Company Limited, New Delhi.
17. Singh Saurab (2009). Social Science Research Network - Tomorrow's Research Today. *Investors' Behaviour at Indian Capital Markets*.
18. Srinivasan P, Kalaivani M and Sham Bhat K (2010), Foreign Institutional Investment And stock market returns in India: Before and During Global financial Crisis, *The IUP journal of Behavioral Finance*, Vol. 7, No. 1 & 2, pp. 59-75, March
19. Van Rooij, M., Lusardi, A., & Alessie, R. (2011). Financial literacy and stock market participation. *Journal of Financial Economics*, 101(2), 449-472.

Webliography:

1. BSE Limited / Bombay Stock Exchange (BSE) <https://www.bseindia.com/>
2. Central Depository Services Ltd (CDSL) <https://www.cdslindia.com/>
3. National Centre for Financial Education. (2020-25) National Strategy for Financial Education. Retrieved from https://www.ncfe.org.in/images/pdfs/reports/NSFE_20-25_ENG.pdf. Accessed on August 9, 2022
4. National Securities Depository Limited (NSDL) <https://www.nsdl.co.in/>
5. National Stock Exchange of India Limited (NSE) <https://www.nseindia.com/>
6. Securities and Exchange Board of India (SEBI). Annual Report 2020-21

7. [https://www.sebi.gov.in/reports-and-statistics/publications/aug-2021/annual-report-20 20-21_51610.html](https://www.sebi.gov.in/reports-and-statistics/publications/aug-2021/annual-report-20-21_51610.html)
8. SEBI Bulletin - January 2023 https://www.sebi.gov.in/reports-and-statistics/publications/feb-2023/sebi-bulletin-january-2023_68347.html



**SARDAR PATEL INSTITUTE OF
ECONOMIC AND SOCIAL RESEARCH**

anvesak

A bi-annual journal

CERTIFICATE OF PUBLICATION

This is to certify that the paper entitled

**BANKING SYSTEM TRANSITION FROM A
COMPARATIVELY CLOSED ECONOMY TO
A MARKET ECONOMY**

Authored by

Milind Patil, Dr. Gulnawaz Usmani

UGC

University Grants Commission

Approved Journal

vol. 53 No.01

in

Anvesak A bi-annual Journal

UGC Care Group - 1

ISSN: 0378-4568

January-June 2023

Impact Factor: 6.20



A bi-lingual journal

BANKING SYSTEM TRANSITION FROM A COMPARATIVELY CLOSED ECONOMY TO A MARKET ECONOMY

Milind Patil

Research Scholar, Department of Economics, AKI's Poona College of Arts, Science & Commerce, Camp, Pune.

Dr. Gulnawaz Usmani

Assistant Professor, Department of Economics, AKI's Poona College of Arts, Science & Commerce, Camp, Pune.

Abstract

Following the spate of financial crises in the 1990s, many observers have opined that the need to depoliticize exchange rate movements along with the frequency with which “soft pegs” have been susceptible to speculative attacks in this era of escalating global capital flows necessitates that developing countries adopt corner solutions to exchange rates arrangements. In other words, according to many observers, the exchange rate option for developing countries boils down to one between flexibility, on the one hand, and credible pegging, on the other. Countries have, however, been advised to steer clear of arrangements that lie anywhere between these polar extremes (i.e., those in the “middle”) as they were viewed as inherently unstable. Subsequently, the East Asian crisis in 1997 led to a heightened appreciation of the importance of a strong banking system, not just for efficient financial intermediation but also as an essential condition for macroeconomic stability. Recognizing this, the government appointed a Committee on Banking Sector Reforms to review the progress of reforms in banking and to consider further steps to strengthen the banking system in light of changes taking place in international financial markets and the experience of other developing countries. The two reports provided a road map that has guided the broad direction of reforms in this sector. This paper attempts to clarify some of the issues at hand, and in particular, about the central banking transition from a comparatively closed economy to market economy. The paper also estimates a Taylor type Monetary Policy Rule for India.

Key Words: RBI, developing countries, Open Economy, Closed Economy, Flexibility, Exchange rate

A moment comes, which comes but rarely in history, when we step out from the old to the new, when an age ends, and when the soul of a nation, long suppressed, finds utterance.

- Jawaharlal Nehru

Introduction

Central bank has been in existence in one form or the other since the second half of the 17th century. Over the years these have passed through various phases of evolution and have come up to a stage where they have assumed greater responsibilities ranging from core central banking functions such as monetary policy formulation and currency management to development and regulation of overall financial structure.

In India the reserve bank of India (RBI) started functioning as the central bank since April 01, 1935 after being established by legislation in 1934 through reserve bank of India act 1934. The tasks of the RBI have been aptly described in the preamble to the RBI act as "to regulate issue of bank notes and keeping of reserves with a view to securing monetary stability in India and generally to operate the currency and credit system of the country to its advantage....." the preamble clearly lays out that the RBI shall perform central banking functions viz.,

(a) Issue of bank notes and maintenance of reserves;

(b) Securing monetary stability; and

(c) Operating currency and credit system to the advantages of the country.

India's commercial banking system in 1991 had many of the problems typical of unreformed banking systems in many developing countries. There was extensive financial repression, reflected in detailed controls on interest rates, and large pre-emption of bank resources to finance the government deficit through the imposition of high statutory liquidity ratio (SLR), which prescribed investment in government securities at low interest rates. The system was also dominated by public sector banks, which accounted for 90 percent of total banking sector assets, reflecting the impact of two rounds of nationalization of private sector banks above a certain size, first in 1969 and again in 1983. These banks were nationalized because of the perception that it was necessary to impose social control over banking to give it a developmental thrust, with a special emphasis on extending banking in rural areas. The system suffered from inadequate prudential regulations, and non-transparent accounting practices. Supervision by the Reserve Bank of India (RBI) was also weak. The 1991 balance of payments crisis led to India's 'plunge into structural reforms'. Structural adjustment programs and loans were arranged through the International Monetary Fund (IMF) and the World Bank. The Indian Government was forced to review its trade policies to allow more foreign investment and reduce trade restrictions so that India's economy could be restored to its former level. Import tariffs underwent significant reductions and import/export licensing system procedures were simplified. The opening up of capital markets to include more foreign participation has allowed Australia's entrance into otherwise untapped markets.

Review of Literature

Ghosh, T. et.al, In their paper authors have emphasized the need to bring monetary aggregates back into the exchange rate models, but with better measures of money than the simple-sum accounting measures having no foundations in microeconomic aggregation theory. The following contributions are relevant. Ireland (2001) finds empirical support for including money growth in an interest rule for policy. In Ireland's model, money plays an informational rather than a causal role by helping to forecast future nominal interest rate. Other papers emphasizing the "information content" of monetary aggregates in predicting inflation and output include **Masuch et al. and Bruggeman et al. (2005)**.

Cavoli, T., & Rajan, R. S. studied that there has been a great deal of discussion of whether the Reserve Bank of India (RBI) should adopt an inflation targeting arrangement. This debate has been further fuelled by the release of the Raghuram Rajan report of the Committee on Financial Sector Reforms (CFSR) which recommended that the Reserve Bank of India (RBI) adopt an inflation targeting arrangement. However, some of the popular discussion on the issue appears to be rather confused and insufficiently informed about the details of an inflation targeting arrangement. This paper attempts to clarify some of the issues at hand, and in particular, the implications of such an arrangement for exchange rate management. The paper also estimates a Taylor type Monetary Policy Rule for India.

A strong and resilient banking system is considered a prerequisite for the economic growth and financial stability. Regulations are generally intended to minimise the risk of bank failures and strengthen the financial stability by controlling the behaviour of financial sector participants and building financial buffers. Regulations could take the form of macro-prudential or macroprudential regulations and could be implemented by pricing or structural mechanisms. However, notwithstanding the continued experimentation with the regulations, the banking crises have been almost a recurrent phenomenon in the modern financial history. As a reaction to the successive financial crises, globally, the financial stability is seen as the primary goal of regulations. **Srivastava, D. A.** This book is the first major exploration of Indian political economy using a constructivist approach. Arguing that India's open-economy policy was made, justified, and continued on the basis of the idea of openness more than its tangible effect, the book explains what sustained the idea of openness, what philosophy, interpretations of history, and international context gave it support, justification, and persuasive force. **Alamgir, J.**

Another author studied growth of the Indian banking sector after the liberalization and deregulated environment has brought extensive transformation in the banking industry. The remarkable development of technology and the wide spread use of information technology has brought this paradigm change. For the banking sector, the technological advancements have appeared to be a strategic source for attaining greater level of competence, organized operations, increased efficiency and productivity. From the customer point of view, it is the apprehension of 'Anytime, Anyway and Anywhere' banking vision. **S. B., Gupta et.al.**

Sharma, K. C. in his book modern banking in India stated how today, banks have become a part and parcel of our life. There was a time when, the dwellers of city alone could enjoy their services. Now banks offer access to even a common man and their activities extend to areas hitherto untouched. Apart from their traditional business-oriented functions, they have now come out to fulfil national responsibilities. Banks cater to the needs of agriculturists, industrialists, traders and to all the other sections of the society. Thus, they accelerate the economic growth of a country and steer the wheels of the economy towards its goal of "self-reliance in all fields". It naturally arouses our interest in knowing more about the 'bank' and the various men and activities connected with it. **Ozili, P. K.** in his article explores the eRupee or digital rupee central bank digital currency in India. It explores the benefits and issues surrounding the central bank digital currency in India. The study found that Indian people who were interested in 'cryptocurrency' information were also interested in 'central bank digital currency' information. The study also showed that the introduction of CBDC has potential benefits such as reduced dependency on cash, higher seigniorage due to lower transaction costs and reduced settlement risk. However, the India CBDC has associated risks that need to be carefully evaluated against the potential benefits. The introduction of a digital rupee or CBDC in India will require legal and regulatory changes to make the phased CBDC implementation possible.

Objectives

1. To observe transition of Indian economy from closed to open
2. To study the Indian banking systems in both closed and open economy
3. To examine the current financial condition of Indian Economy
4. To overview banking sectors reform after 1991 economic crisis

Methodology

Type of Research: Observational and Descriptive.

Research Design: The research data will be collected as follows:

The data will be collected from secondary sources.

Some of the sources for secondary data will be Reserve bank of India (RBI), World Bank, various researches on the mentioned topic by reviewing literature.

Independence Of Banking system to Adapt, Reorient and Face New Challenges

Transition from a Comparatively closed economy to a market economy has made it obligatory on the part of the reserve bank of India to remain focused and tackle dilemmas and challenges which are very particular to emerging market economy because of its heterogeneous economic structure. Independence of central banking from government controls is another debatable issue in emerging economies. Today, the dynamism of the economic structure and financial system has put additional responsibility on the central banks in emerging economies to adapt, reorient and face new challenges. in India, the RBI is turning these challenges into opportunities and marching ahead with its mandate in the service of the nation.

Although all these three functions are equally important yet the most important objective of the RBI over the years has been ensuring monetary stability. The term monetary stability can easily be understood as maintaining parity. **Ghosh, T. et.al (2016).**

Between price and incomes levels so as to ensure a synchronous rise in price vis-à-vis income levels. In common parlance, the same is also understood as ensuring price stability. While the main focus of the RBI has remained 'price stability', the other functions have worked as corollaries to this main function of monetary management.

Managing Change from a Closed to an Open Economy

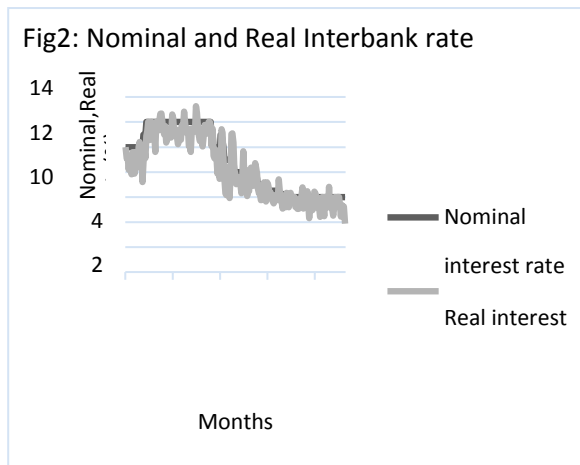
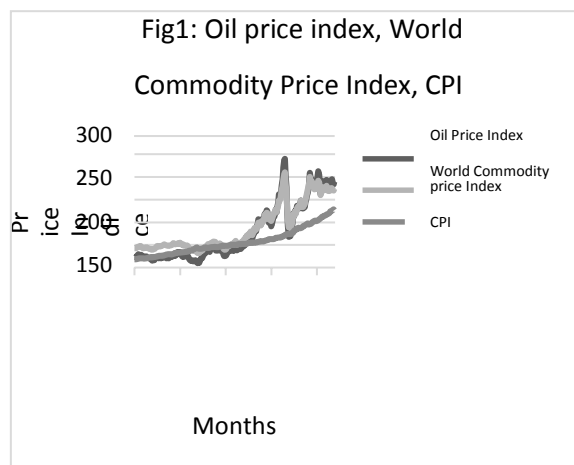
The Indian economy has responded vigorously to a program of stabilisation and reform measures started in 1992. The Indian Government took drastic action including devaluation, the imposition of higher interest rates, fiscal and monetary restraint and import compression. In succeeding budgets long term measures were introduced which removed the protection for Indian industry and commerce from international competition. The reforms that were introduced are addressed in Chapter 3 of the report. An indication of the success of these reforms is given by the change in India's current account deficit. In 1991 it had risen to 3.3 percent of Gross Domestic Product (GDP); by 1993 it had fallen to 1.8 percent, and by 1995 to 0.6 percent. **Masuch et al. (2003) and Bruggeman et al. (2005)**. Professor Mayer stated that the trade and tariff frameworks that were set up to protect the Indian economy have begun to be wound back, but that the process is occurring 'layer by layer, strand by strand; it is not a big bang sort of thing'. The Committee understands that the number of tariff bands is high, some ranging from 0 to 260 percent. From 1991 until it was voted out of power in May 1996, Prime Minister Narasimha Rao's Congress Government developed and implemented a strategy which aimed to transform India's economy from an inward-looking and protectionist one, to one fully integrated in the world trading system. **Masuch et al. (2003) and Bruggeman et al. (2005)**.

Emerging Market Economy (Eme) & Environmental Dynamism

However, phenomenal changes that have taken place in all spheres of economy, especially during the post-liberalization era, have necessitated dynamism in the central banking functions. Demands of an emerging market economy (EME) like India, are far more different than that those of a closed economy and hence, there is a need for central banks to understand the environmental dynamism and evolve strategies to come up to the expectations of the new economy. As a matter of fact, the working than traditional central banking functions. The bank has been transacting the government's business and promoting financial and economic development without jeopardizing price stability. It has helped to set up a number of financial institutions such as IDBI, UTI, NABARD and DFHI besides a number of research institutions. These institutions have been hived off from the parent body over time and they have gone a long way in developing the financial system of india. Yet, the need for continuous efforts aimed at expansion of the dictum of price stability to the doctrine of financial stability cannot be overemphasized. **Ghosh, T. et.al (2016)**

The Indian Economy at a Glance

The following figures provide a brief overview of the Indian economy since 1992.



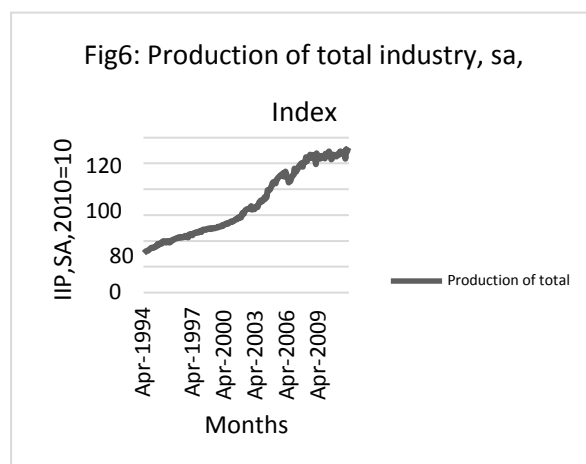
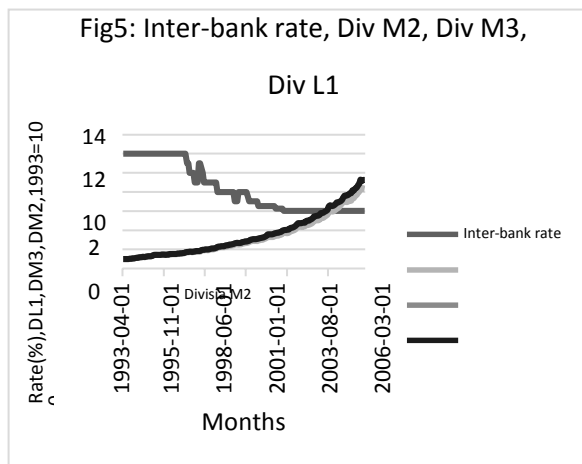
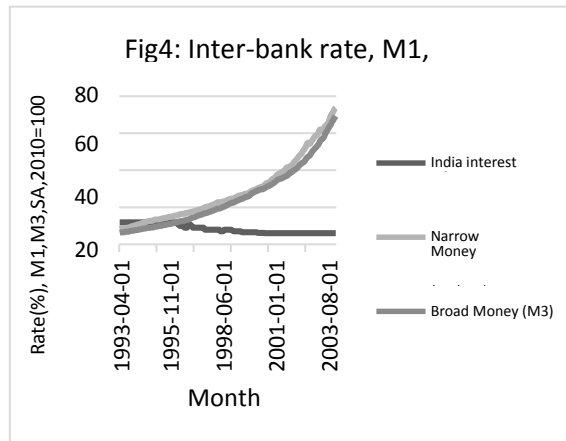
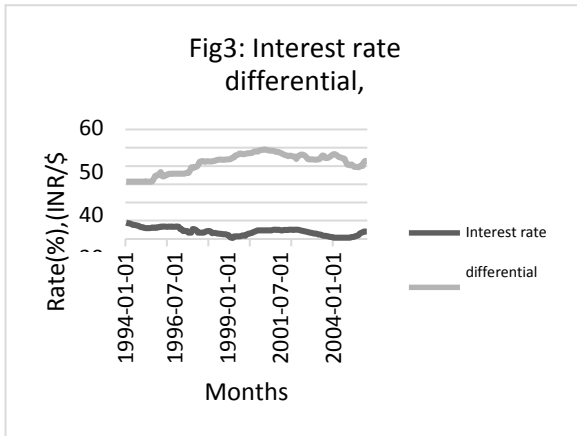


Figure 1 shows the Indian economy experienced very high inflation during the last 24 years. The CPI (consumer price index) between the first quarter of 1992 and the last quarter of 2013 rose by 384 percent. The average was a 17 percent price rise. However, from the first quarter of 1992 to the first quarter of 2000, CPI rose by 89%. On an average, there was a 9 percent price rise every year during that time period. **Alamgir, J. (2008).**

Figure 2 shows that loose monetary stance was a dominant feature of the economy between 1992 and 1997. **Alamgir, J. (2008).**

Figure 3 displays the interest rate differential between India and U.S. and the exchange rate of the India rupee relative to the US dollar. The figure suggests that the movements of the nominal exchange rate appear to have followed the interest rate differential with a lag.

Figure 4 displays the accelerated growth in the money supply for both M1 and M3 during a period of loosening of inter-bank rates. **Alamgir, J. (2008).**

Figure 5 displays the liquidity of the Indian economy using the theoretically grounded Division monetary aggregates. Division reflects much liquidity injection into the economy, but not as much as the simple-sum monetary aggregates would imply. **Alamgir, J. (2008).**

Figure 6 displays the production of total industry (IIP) for India. The period of highest industrial growth was between 2002 and 2007, after which the growth slowed dramatically. **Alamgir, J. (2008).**

Price Stability to financial stability

Price stability though equally important yet most of the times remains a short-sighted goal. A narrow focus of the monetary policy on price stability in the short-term may pose risks to price stability in the are overlooked. It is quite possible to achieve price stability for some time even in a turbulent financial

longer-run if the potential consequences of financial instability for longer-term price developments system through policy manipulations. It is just like taking pain killers for immediate relief without cure. The goal of financial stability, on the other hand, brings along with its policy prescription meant for curing the evils of the system and making it viable and self-sustaining. A financially stable system must be able to assess and mitigate risks take proactive actions and possess adequate shock- absorbers to react and bounce back after vulnerable periods. Financial stability is the single most important thing from the macroeconomic view as it deals with issue like contagion and systems and systemic risks which can lead to most violent upheavals and hence needs to be monitored continuously. While such monitoring is essential, practically it is very difficult due to the fact that unlike price stability it cannot be easily quantified and measured by a few indicators. **Srivastava, D. A. (2018)**

Holistic And Consciously Coordinated Strategy

As a consequence, maintenance of financial stability requires a holistic and consciously coordinated strategy aimed at development and deepening of the financial system. Improving allocating efficiency of the system and facilitating inter-temporal allocation of resources from savers to ultimate users is also essential. Vulnerability of capital flows in emerging market economies has put additional responsibility on payment and settlement systems to remain robust and prevent systemic on risks. Sine qua non for financial stability in a dynamic scenario. **Sharma, K. C. (2007)**

Dilemmas, challenges and opportunities

Transition from a comparatively closed economy to market economy has made it obligatory on the part of the RBI to remain focused and tackle dilemmas and challenges which are very particular to the EME. As a matter of facts, carefully crafted policies are needed for an EME because of its heterogeneous economic structure. Today, the Indian economy presents a dichotomous economic structure; one modern, dynamic and growing rapidly and the other traditional slow paced with old technologies. The Requirements of one structure is entirely different from those of the other. **Cavoli, T., & Rajan, R. S. (2008)** The problem that most of the things are in a transition phase and that too with different paces, makes the job of the central bank more complex and difficult. While some sectors demand and liberal and free environment, at the same time there are other which need to be protected and nurtured. Therefore, making a judicious mix of central banking policies of developed and developing economic is a challenge which the RBI faces today. Specifically speaking, such dilemmas arise out of the following Issues:

- Debt management and monetary management.
- E-money and systemic risk management.
- Liberalization and global imbalances.
- Global alignment and domestic financial inclusion.
- Central banking independence and economic growth.
- Credibility and constructive ambiguity.

Formulation And Conduct of The Monetary Policy

Although not exactly a central banking function, the RBI also works as a debt manager of central and state governments under sections 17(11)(e),21(2),21(A) of the RBI act-1934. It manages issuance, redemption, servicing, etc, of domestic loans which are raised by the governments as per the constitutional provisions under articles 292 and 293 for the fiscal management. Such an activity creates a dilemma as objectives of debt management sometimes come in direct conflict with those of monetary management. The objectives of development management are cost minimization., maturity elongation and smooth rollover. At the same time, formulation and conduct of the monetary policy is also closely related with liquidity and interest rate management in the economy.

Avoiding crowding out of private investments due to heavy government borrowings also becomes a major concern. Moreover, since banks and financial institutions are the principal investors in the government securities, managing low-cost borrowings for government results into poor bottom lines for the financial sector. Monetary management by the central bank, therefore, becomes a tight-rope walk which at times may result in compromise in the monetary management objectives. **Cavoli, T., & Rajan, R. S. (2008)**

Broad Approach to Reform

The strategy for banking reforms was broadly similar to that followed in other countries, but with some important differences. It was similar to the extent that it focused on imposing prudential norms and improving regulatory supervision to meet Basel I standards (standards that were formulated by the committee of the Bank of International Settlement, or BIS, based in Basel, Switzerland), and it aimed at increasing competition to promote greater efficiency. However, there were two important differences compared with reforms in other countries. First, the reforms in banking were much more gradualist than in most countries, a course of action that was in line with the general strategy of reforms in India, made possible by the fact that the reforms were not introduced in the midst of a banking sector crisis, which might have entailed greater urgency. Second, unlike the case in many other countries, there was never any intention to privatize public sector banks. It was clearly recognized that competition was desirable, and this implied that both private sector banks and foreign banks should be allowed to expand their market share if they could. However, the government also declared its intention to strengthen public sector banks and enable them to meet competition. **Srivastava, D. A. (2018)**

There was also a great deal of progress in introducing prudential norms for income recognition, asset classification, and capital adequacy in a phased manner. As a consequence of this gradualist process, income recognition norms and capital adequacy norms have been fully aligned with Basel I standards, while asset recognition norms, though still falling short of international best practice, are now close to existing international standards.

Banking System Performance

The impact of the reforms on the efficiency of the banking system in performing its twin roles of financial intermediation and resource allocation is not easy to evaluate. As far as the scale of bank intermediation is concerned, the ratio of total credit extended by the banking system to India's gross domestic product has increased, but it is still relatively low compared to countries such as China or some of the other East Asian countries. The ratio in India increased from 51.5 percent in 1990 to 53.4 percent in 2000, whereas in China it increased from 90 percent to 132.7 percent in the same period. The figures over the same period are also much higher for Malaysia (75.7% and 143.4%) and Thailand (91.1% and 121.7%), though many Latin American countries have figures closer to those of India.

There is evidence of significant improvement in several dimensions in recent years. Gross nonperforming assets (NPAs) as a percentage of total advances have fallen from 15.7 percent in 1996–1997 to 7.3 percent in 2003–2004. Gross NPAs as a percent of total assets are much lower because Indian banks typically have a large proportion of their assets in sovereign debt; this ratio has also declined from 7 percent in 1996–1997 to 4 percent in 2002–2003. More importantly, the financial strength of the banks is actually better than it appears from these ratios because Indian banks do not write off assets, even though large provisions have been made. Net nonperforming assets, calculated after taking account of provisioning, are 3 percent of total advances and only around 2 percent of total assets. There has been a general improvement in other financial indicators, such as net profit as a percentage of total assets, interest spread as a percentage of assets, and operating expenses as a percentage of total assets, for public sector banks, old private sector banks, new private sector banks, and foreign banks. The financial strength of the banks, as measured by the capital to risk adjusted assets ratio (CRAR), shows distinct improvement in the postreform period. The required CRAR was

increased in phases, to 8 percent at first (which is the Basel I minimum) and then to 9 percent in 1999–2000. Initially, banks with insufficient capital had to be capitalized by the injection of government equity from the budget, but subsequently several banks were able to raise capital from the market, and this, combined with plowing back of profits, led to a substantial improvement in capital adequacy. At the end of March 2003, out of the 93 commercial banks operating in India, 91 were above 9 percent and as many as 87 were above 10 percent, compared with only 54 out of 92 banks above 9 percent and 42 above 10 percent at the end of March 1996. **Srivastava, D. A. (2018)**

It is noteworthy that the Indian banking system did not suffer from any contagion effect in the aftermath of the East Asian crisis. However, this is not so much due to the improvements brought about after 1991, as the fact that the capital account was not fully open. Banks were not allowed to undertake excessive foreign currency exposure, and external borrowing (especially short-term borrowing) was strictly controlled. This cautious policy helped insulate India from the severe reversals of external flows witnessed in many emerging market countries in the 1990s. **Masuch et al. (2003) and Bruggeman et al. (2005).**

Decontrol of Interest Rates and Credit

There has been a significant liberalization of interest rate and credit controls on commercial banks. Earlier, there were detailed restrictions on interest rates that could be paid on different types of deposits and rates that were charged to various categories of customers. These have been extensively liberalized. On the deposit side, interest rates paid on term deposits have been decontrolled, except that the RBI prescribes a maximum interest rate on short-term (15-day) deposits and also prescribes the interest rate on savings deposits. On the lending side, the detailed structure of interest rates prescribed for different types of borrowers and for different sizes of loans has been abolished; the RBI prescribes only the interest rate to be paid under the differential rate of interest scheme a very small window for loans to individuals below the poverty line. For the rest, individual banks fix lending rates with reference to the prime lending rate fixed by the bank. The reforms also abolished the requirement that banks needed to obtain RBI approval for individual credit limits fixed for large customers. With these changes, decisions on the cost of credit and the volume of credit to be extended have been left to bank management, subject to internal guidelines and procedures for credit approval and general prudential limits on single borrower and single project exposure. **Cavoli, T., & Rajan, R. S. (2008)**

Directed Credit

Reducing directed credit requirements is a common feature of banking reforms, and this was the case in India as well. A major directed credit requirement was constituted by the high levels of the SLR, which preempted bank resources to finance the government deficit at low interest rates. Preemption of credit by the government also occurred indirectly because the RBI followed a practice of automatically issuing ad hoc Treasury bills to meet any shortfalls in the government's balances with the RBI. Since this implied a mechanical transmission of fiscal expansion to the monetary side, it was offset by imposing a high cash reserve ratio (CRR) in the commercial banks, thus effectively crowding out private sector credit.

At one stage, prior to the reforms, the combined effect of the high CRR and the SLR was such that only 35 percent of the increment in bank deposits was actually available for commercial advances, the rest being either impounded by the RBI in the form of cash reserve deposits or absorbed by the government. The practice of automatic monetization was abandoned in 1994, and both the CRR and the SLR were reduced over time from 15 percent and 38.5 percent, respectively, before the reforms to 5 percent and 25 percent by 2005. The fiscal deficit is now financed through the auction of government securities conducted by the RBI, and in that sense, the interest rate on government borrowing is market-determined. However, it is interesting to note that, despite the reduction in the SLR from 38.5 percent to 25 percent, the proportion of government securities held by the banks to their total assets has actually increased from 30.4 percent at the end of March 1994 to 34.5 percent at the end of March 2004. This has occurred because of the combined effect of the inability to reduce the

fiscal deficit—a key weakness of the reforms to date—and the fact that the prudential norms give sovereign debt a very low risk weight. In other words, while statutory preemption of bank resources was steadily reduced in the 1990s, the banks' appetite for government debt has remained high because the prudential norms contain a built-in regulatory bias in favor of government debt in preference to commercial credit. **Cavoli, T., & Rajan, R. S. (2008)**

The other major form of directed credit was the requirement that 40 percent of commercial credit has to be extended to the priority sector, which includes agriculture, small-scale industry, small transport operators, artisans, and so on. It applies to Indian commercial banks but not to foreign banks because the latter do not operate in rural areas and therefore cannot engage in agricultural lending. In their case, the requirement is that 15 percent of advances must be for exports and for the small-scale sector. These provisions have not been altered by the reforms. However, although the priority sector target for Indian banks has not been changed, the provision has been liberalized indirectly to some extent by definitional changes that expand the range of borrowers that are eligible. It is also worth noting that while banks are subject to sectoral direction of credit, they are not required to lend to particular borrowers; the credit decision of lending to a particular borrower is left to the bank on the basis of normal credit-worthiness analysis.

Banking System Performance

The impact of the reforms on the efficiency of the banking system in performing its twin roles of financial intermediation and resource allocation is not easy to evaluate. As far as the scale of bank intermediation is concerned, the ratio of total credit extended by the banking system to India's gross domestic product has increased, but it is still relatively low compared to countries such as China or some of the other East Asian countries. The ratio in India increased from 51.5 percent in 1990 to 53.4 percent in 2000, whereas in China it increased from 90 percent to 132.7 percent in the same period. The figures over the same period are also much higher for Malaysia (75.7% and 143.4%) and Thailand (91.1% and 121.7%), though many Latin American countries have figures closer to those of India.

There is evidence of significant improvement in several dimensions in recent years. Gross nonperforming assets (NPAs) as a percentage of total advances have fallen from 15.7 percent in 1996–1997 to 7.3 percent in 2003–2004. Gross NPAs as a percent of total assets are much lower because Indian banks typically have a large proportion of their assets in sovereign debt; this ratio has also declined from 7 percent in 1996–1997 to 4 percent in 2002–2003. More importantly, the financial strength of the banks is actually better than it appears from these ratios because Indian banks do not write off assets, even though large provisions have been made. Net nonperforming assets, calculated after taking account of provisioning, are 3 percent of total advances and only around 2 percent of total assets. There has been a general improvement in other financial indicators, such as net profit as a percentage of total assets, interest spread as a percentage of assets, and operating expenses as a percentage of total assets, for public sector banks, old private sector banks, new private sector banks, and foreign banks. The financial strength of the banks, as measured by the capital to risk adjusted assets ratio (CRAR), shows distinct improvement in the postreform period. The required CRAR was increased in phases, to 8 percent at first (which is the Basel I minimum) and then to 9 percent in 1999–2000. Initially, banks with insufficient capital had to be capitalized by the injection of government equity from the budget, but subsequently several banks were able to raise capital from the market, and this, combined with plowing back of profits, led to a substantial improvement in capital adequacy. **Sharma, K. C. (2007)** At the end of March 2003, out of the 93 commercial banks operating in India, 91 were above 9 percent and as many as 87 were above 10 percent, compared with only 54 out of 92 banks above 9 percent and 42 above 10 percent at the end of March 1996.

It is noteworthy that the Indian banking system did not suffer from any contagion effect in the aftermath of the East Asian crisis. However, this is not so much due to the improvements brought about after 1991, as the fact that the capital account was not fully open. Banks were not allowed to undertake excessive foreign currency exposure, and external borrowing (especially short-term

borrowing) was strictly controlled. This cautious policy helped insulate India from the severe reversals of external flows witnessed in many emerging market countries in the 1990s.

E-Money and Minimization of Paper-Based Transaction

Thrust towards expansion of E-Money and minimization of paper-based transaction though a welcomes step on the part of the RBI, yet the issue of assessing, mitigating and managing systemic risks has also gained currency in recent times. Establishing a robust payment and settlement system in electronics environment is a big challenge and the apex bank will have to live up to the challenges of technological revolution. **Ozili, P. K. (2022)**

Financial Integration

Liberalization has resulted in financial integration to an extent in the economic scenario and the events of one economy instantaneously influence developments in another. However, huge current account deficit of the US and consequents surpluses in Japan and the gulf countries have created global imbalances which may adversely affect some systemically important currencies, especially the US dollar. Of late, it is being argued that the US consumer cannot pull the global demand for a long time as the US current account deficit may become unsustainable, although the Indian economy is insulated to a great extend due to restricted capital account, yet overflowing US dollars through FIIs is a cause of concern. One-way movement of foreign currency may lead to destabilization. However, these things are bound to happen because the world is not flat and increase in the degree of financial integration can further catalyze disparities. Hence, the only remedy that remains is to devices suitable policies, strategies and tactics to tackle such delicate issues, this is a challenge which is to be turned into an opportunity for india to make a mark at the world stage. **Ozili, P. K. (2022)**

Global banking standards and domestic financial inclusion.

Another related issue is the simultaneous fulfilment of the requirement of adopting global banking standards and domestic financial inclusion. The Indian scenario is quite unique due to the fact that banking is still a luxury for a vast chunk of population and we are talking about achieving global standards of banking in terms of technology as well as regulatory norms due to global alignment of the banking industry. Both these objectives are important and require substantial resource allocation. A judicious and balanced strategy is needed to achieve the objective of taking the banking to every nook and corner of the nation and simultaneously achieve global standards without escalating and passing the cost to the common customer. This is again a big challenge and opportunity for the central bank. **Ozili, P. K. (2022)**

Independence of central banking from government controls is another debatable issue in emerging economies. This involves operational as well as financial independence. Although the case for a strong and independent central bank has a firm footing. Yet the extent of independence hinges upon its trade-off with fiscal issues of a developing and transforming economy.

Conclusion and policy implications

The issue of transparency in central banking functions has gained currency in recent times.

Theoretically speaking, as the economy grows and matures the central bank should also become more predictable. However, it is quite difficult to say that the Indian economy and financial system in particular have gained such a depth and maturity; probably it will take some more time to reach the stage of a fully developed financial system. Hence, constructive ambiguity in central banking shall remain a major tool. Being constructively ambiguous and maintaining credibility is indeed an uphill task in which the RBI has been highly successful. The ability of the RBI to surprise the market and move ahead of it while keeping it on the desired path in today's dynamic environment shall be put test in the ensuing time.

Today, the dynamism of the economic structure and financial system has put additional responsibility on the central banks in emerging economies to adapt, reorient and face new challenges. In India, the RBI is turning these challenges into opportunities and marching ahead with its mandate in the service of the nation.

Pro-openness policy makers have been successful on the first count. Even left-leaning parties now provide broad support for the continuity of open-economy policies. Such broad-based support would not have been possible without the imagery of empowerment, loss and global destiny employed consistently by the policymakers. All nationalist appeals are based on some concept of strengthening the nation. The idea of globalism encompasses that appeal and goes farther beyond, not only by showing congruence with the “Indian” identity derived through anticolonial struggles but also by bringing together politically diverse interests under its ideological and rhetorical orbit on economic matters. While various political platforms questioned specific policy measures, virtually none questioned the need for greater global visibility. As the broad idea to frame India’s open-economy policies, globalism has proven to be an extremely useful vehicle to market open-door policies to the domestic constituency.

Limitations and Future Research Directions

Inadequate regulations or failure of regulations to keep pace with financial innovations could have been reasons for financial crises during 1991 in India, but equally critical contributing factors for financial distress have been inadequate internal control, false assumptions about market and liquidity, and lack of due diligence processes. It is obvious, therefore, that the regulations may strengthen but cannot substitute the internal controls and risk management framework at the level of the financial institution. Hence, at the micro level, while it is imperative for the institutions to put in place a comprehensive risk management system, the regulator also needs to ensure that there is adequate risk ownership in the institution at a sufficiently senior position. The key to success is to have a proper balance of macro-prudential and micro-prudential regulations adequately aligned with the nature and culture of financial market behaviour. While traditionally, the securities regulations were backwards looking and rule based and insurance regulations were not highly capital-centric in contrast to the forward-looking capital-intensive macro-prudential banking regulations, now a greater convergence is seen in the regulatory approaches. Financial stability and some elements of macro-prudential focus have now become a common denominator for all the regulators. Another important aspect is an effective supervision because first, it is not possible to forecast and document every likely incidence of risk in the regulatory norms and second, holding buffers against every possible eventuality could stifle the growth and could make the financial institutions inefficient. A forward-looking and vigilant supervisory mechanism could sense early signs of distress, distortions and imbalances and raise a red flag for timely action. However, developing a larger eco-system of effective 360-degree supervision through information dissemination should be the ultimate goal of the supervisory process. It is a challenge is to incentivise the financial market participants to join the regulators in pursuit of effective risk optimisation and strengthening of the 10 financial stabilities. Collaboration and coordination are needed between the regulators and the regulated entities for achieving the common good of a stable and efficient financial system. The one can further monitor and evaluate the financial stabilities in economy in the coming period of time and can always compare it timely with the situation of Indian economy during 90’s.

References

1. **Barnett, W. A., Bhadury, S. S., & Ghosh, T. (2016).** *An SVAR approach to evaluation of monetary policy in India: Solution to the exchange rate puzzles in an open economy.* *Open Economies Review*, 27(5), 871-893.
2. **Cavoli, T., & Rajan, R. S. (2008).** Open economy inflation targeting arrangements and monetary policy rules: Application to India. *Indian Growth and Development Review*.

3. **Srivastava, D. A. (2018).** Financial Crises and the Prudential Regulations: Theory, Practice and the Way Forward. *The Indian Banker, Indian Bank Association, ISSN, 2349-7483.*
4. **Verma, S. B., Gupta, S. K., & Sharma, M. K. (Eds.). (2007).** *E-Banking and development of banks.* Deep & Deep Publications.
5. **Toor, N. S. (2015).** *Handbook of banking information.* Skylark Publications.
6. **Sharma, K. C. (2007).** *Modern Banking in India.* Deep and Deep Publications.
7. **Ozili, P. K. (2022).** Central bank digital currency in India: the case for a digital rupee. *Technical Paper Series.*
8. **Alamgir, J. (2008).** *India's open-economy policy: Globalism, rivalry, continuity.* Routledge.
9. www.rbi.org.in

anvesak

A biannual Journal

2023



**Sardar Patel Institute of
Economic and Social Research**

CONTENTS

1.	A STUDY ON WORKING WOMEN BEHAVIOR PERTAINING TO ONLINE	Kashifa, S.R. Inamdar, Shaikh Farzana Valluddin, V.I. Shaikh, Anand	1-5
2.	ENVIRONMENTAL CONCERNS AND SUSTAINABLE DEVELOPMENT: ISSUES AND CHALLENGES FOR INDIA	Ms. Zeenat B. Merchant	6-10
3.	STUDY OF PROGRESSIVE INVESTORS' IMPACT ON RETAIL INDIVIDUAL INVESTORS OF MAHARASHTRA	Dr. Gulnawaz Usmani	11-18
4.	A STUDY OF GROWTH IN REAL ESTATE MARKET IN INDIA	Dr. Aqueel Ahmed Mohammed Ibrahim Shaikh, Dr. Rahul Prabhakar More	19-22
5.	THE ROLE OF DIGITAL MARKETING FOR CREATING MULTICHANNEL MARKETING STRATEGY TO DRIVE BUSINESS GOALS	Dr. Shahjahan Shaikh	23-29
6.	YOUTUBE VLOGGERS IMPACTING PURCHASE INTENTIONS & BRAND PREFERENCE OF YOUNG SUBSCRIBERS OF YOUTUBE CHANNELS	Ms. Anisa A. Khan, Prin. Prof. Shaifa Bootwala	30-37
7.	GEOPOLITICS OF INDIA	Mr. Malegaonkar Md. Alisab	38-44
8.	GIG WORKERS IN PUNE: OPPORTUNITIES AND CHALLENGES	Mr. Saquib Ali Shahid Ali Khan, Dr. M. Shahid Jamal Ansari	45-49
9.	A STUDY ON STRATEGIC HUMAN RESOURCE MANAGEMENT: A HUMAN CAPITAL PERSPECTIVE	Ms. Shaikh Shirin Naaz, Dr. M.G. Mulla	50-55
10.	UNDERSTANDING INVESTMENT BEHAVIOR OF INDIVIDUALS: REVIEW OF FOREIGN STUDIES	Dr. Paresh P. Bora	56-60
11.	PROBLEMS IN ORAL ENGLISH COMMUNICATION FACED BY F.Y.B.COM STUDENTS OF SAVITRIBAI PHULE PUNE UNIVERSITY WITH SPECIAL REFERENCE TO ABEDA INAMDAR SENIOR COLLEGE	Ms. Nikita. A. Pandhare	61-65
12.	AN EMPIRICAL STUDY ON MARKETING STRATEGY USED BY SNACKS MANUFACTURERS TO SUSTAIN IN INDIAN MARKET	Dr. Lavkush Singh, Dr. M.G. Mulla	66-78
13.	A STUDY OF EMPLOYMENT IN INDIA IN LIGHT OF ARTIFICIAL INTELLIGENCE	CMA Aziz Ahmed Chishti	79-84
14.	AN ANALYSIS OF FINANCIAL PERFORMANCE OF SELECTED NBFCS IN INDIA	Miss. Naziya Riyaz Maldar, Mr. Umer Mohi U Din Wasil	85-90

Volume 96, No. 01(II), 2023

(New Series)

ISSN : 0972-0766



(Established in 1804)

**JOURNAL
OF THE
ASIATIC SOCIETY OF MUMBAI**
(A UGC - CARE Listed Journal)

Editors

Parineets Deshpande

Ambarish Khare

Published by

The Asiatic Society of Mumbai

Town Hall, Mumbai- 400 001.

Maharashtra State (INDIA)

2023

THE POLITICS OF MULTICULTURALISM

Malegaonkar Md Alisab

85-88

SELF-RIGHTEOUSNESS OF SUPERPOWER

Yash V. Pawar

90-92

भारतातीय राजकारणात प्रसारमाध्यमांची भूमिका आणि प्रसारमाध्यमांचे राजकारण

93-95

डॉ. नारायण मधुकर राजुरवार

DISCOVERING THE LIVES OF CHHARAS IN AHMEDABAD THROUGH THE LENS OF BUDHAN THEATRE

96-100

Ms. Swaroop A. Waghmare

AN APPROACH TO UNDERSTAND NARRATIVE ANALYSIS

101-107

Dr. Shafiya Shaikh

AN ANALYTICAL STUDY OF THE RELATIONSHIP BETWEEN VARIOUS ELEMENTS OF SOCIAL MEDIA PROMOTION AND PRESCRIPTION GENERATION BY THE DOCTORS

108-112

Dr Hanif M. Lakdawala

SUBSTANCE USE, ABUSE AND ADDICTION: S.O.S

113-117

Ms. Zeenat Merchant

PROSPECTS AND CHALLENGES OF MULTILINGUAL-HYBRID EDUCATION UNDER NEP 2020

118-123

Savita Gautam and Abdus Samad

AN ANALYSIS ON FEMINIZATION OF POVERTY IN INDIA

124-127

Dr. Sunita Adhuv

ROLE OF NARRATIVES IN LEGAL INTERPRETATIONS AND ADVOCACY

128-131

Kunal Vinod Sonawani

Ek Bharat... Shreshtha Bharat...
**SDVP's Quarterly Journal of
Social Science Deliberations**

Quarterly Journal of Social Sciences

Volume I ■ April-May-June 2023 ■ No. 4

Editor : Dr. Sharad Vasudev Khare

- A. Editorial - India's Vaishwik leap : G -20
Understanding Dr. Amarty Sen. 02
- B. Articles
1. Indian Epistemology :
A philosophical perspective. - Dr. Mrs. Shubhada Joshi 05
2. Commendable contribution
of Christians to Bharat. - Dr. Sharad Khare 24
3. **People, Pawns and Politics** : A Study of Salman
Rushdie's Midnight's Children, Nayantara Sahgal's
Rich Like US, Rohinton Mistry's A Fine Balance,
Upamanyu Chatterjee's English, August and
Kiran Desai's The Inheritance of Loss. **Dr. Ashiwini Purude** 42
4. "The State" under Article 12 of the Constitution of
India and Contemporary Challenges Dr. Priya Chopde 53
5. भारतीय लढावू विमान "तेजस" काशीनाथ देवधर 61
- C. Book Review
The India Way - S. Jayshankar परिचायक डॉ. शरद कुंटे 90

Samshodhan Dnyan Vichar Pratisthan's
Dr. Shripati Shastri Research Institute of Social Sciences

(BPT Act No. 1950 Pune-No. F844 and SR Act 1866 No. MAH /1036/Pune/1975)
C/O. Sahanishtha Society, Sahakarnagar, Parvati, Pune 411009 Ph. : 020-24230345 E-mail ID : kharesharadv@gmail.com
RNI Regn. No. : MAHBIL / 2022 / 82115

Sr No	Content	Page No.
A	Editorial India's 'Vaishwik' leap : G-20 Understanding Dr. Amartya Sen.	02
B. Articles		
1.	Indian Epistemology : A Philosophical perspective. Dr. Mrs. Shubhada Joshi	05
2.	Commendable contribution of Christians to the Nation. Dr. Sharad Khare	24
3.	People, Pawns and Politics : A Study of Salman Rushdie's Midnight's Children, Nayantara Sahgal's Rich Like US, Rohinton Mistry's A Fine Balance, Upamanyu Chatterjee's English, August and Kiran Desai's The Inheritance of Loss. Dr. Ashiwini Purude	42
4.	"The State" under Article 12 of the Constitution of India and Contemporary Challenges Dr. Priya Chopde	53
5.	भारतीय लढावू विमान तेजस काशीनाथ देवधर	61
C. Book Review		
	The India Way - S. Jayshankar परिचायक डॉ. शरद कुंटे	68

**People, Power and Politics : A Study of
 Salman Rushdie's Midnight's Children,
 Neelam Kishore's Rich Like Us, Rohinton
 Mistry's A Fine Balance, Upanmanyu
 Chatterjee's English, August and Kiran
 Desai's The Inheritance of Loss.**

Dr. Arshad Hussain

The present study is about 'People, Power and Politics' in a regional form a common urban background and is used by a few to the entire system. The study portrays the phenomenon of the nature of the common man although he is poor, and his dependence of the common man through his right of social justice and his right to work through his right of social justice. The study examines the role of the common man in a suppressed society, particularly the case of the common man in a suppressed society. The study begins with a common man suffering in a society who tries to become a man under every government system whether it is monarchy or democracy.

People suffer due to the political events and human life system is an indispensable part of human life. The novel shows for the purpose of analysis of the study are Salman Rushdie's *Midnight's Children* (1980), Mistry's *Salvagor's Rich like us* (1987), Upanmanyu Chatterjee's *English* (1996), Kiran Desai's *The Inheritance of Loss* (2006), August (2006) and Kiran Desai's *The Inheritance of Loss* (2006) which deal with political themes. The novels are concerned with the impact of politics on human lives.

The study portrays the sufferings and exploitation of the masses at various levels i.e. physical, economic, social and psychological. The time span of the selected novels is indeed the late 19th to early 19th centuries which cover the major political and social events like national liberation wars with Pakistan, China and Bangladesh, assassination of Mahatma Gandhi, Naxalite movement in the North-Eastern part functioning of bureaucracy and illegal immigration.

Arshad Hussain (Ph.D.), Former College of Arts, Science & Commerce, U.S.A.

Comparative study brought in Pakistan and the problems of political and social problems and depressing experiences which had led to the state of things, laws and spirit in various ways. The study had been developed with the creation of regional studies. The study focuses on the political events after the end of the 19th and its effects on the masses. This time span is chosen for the study as it signifies the end of the political era which was a generation of rulers who were freedom fighters who were the next generation of rulers. Nehru's death had ended an era in which politics played a role for the dynastic rule in urban democracy. Along with a limited time span, the research geographically covers the three continents Asia, America and Europe and early deals with Mumbai, Bangladesh, Pakistan, Madras, Karnataka, Delhi and the rural interiors of India. This wide geographical scope shows how people suffer universally and are affected by the political system.

The special contribution of the study is that it has applied various relevant Constitutional provisions to the selected works of literature and has analyzed the effects of the alteration of democratic process and provisions.

The study has put forth the methodology for the analysis of the selected novels which is using the relevant Constitutional provisions as a framework. For this purpose, the Constitutional provisions and laws like the Directive Principles, Fundamental rights and duties, provisions of bureaucracy, provisions for the North Eastern states and special provisions for Scheduled Castes and Tribes were used.

As the study has dealt with the theme of how politics makes a part of innocent people, it also measures the abuse of the system in the hands of politicians which has tormented the masses. It shows the disparity between theory and practice. The benefit of the few is taken care of rather than the common welfare of the masses.

...the state's ... the ...

...the ... the ...

...the ... the ...

...the ... the ...

...the ... the ...

...the ... the ...

...the ... the ...

...the ... the ...

...the ... the ...

...the ... the ...

...the ... the ...

The research shows that the very nature of the... (text is extremely faint and difficult to read)

... (text is extremely faint and difficult to read)

... (text is extremely faint and difficult to read)

For the analysis of this novel, the researcher has used the... (text is extremely faint and difficult to read)

... (text is extremely faint and difficult to read)

The last novel of the study is Kiran Desai's 'The Inheritance of... (text is extremely faint and difficult to read)

Though the GNLF has represented the oppressed Indian... (text is extremely faint and difficult to read)

The study has shown the consequences of the 1951 act which is a result of a... the study has shown the consequences of the 1951 act which is a result of a... the study has shown the consequences of the 1951 act which is a result of a...

The study has shown the consequences of the 1951 act which is a result of a... the study has shown the consequences of the 1951 act which is a result of a... the study has shown the consequences of the 1951 act which is a result of a...

The study has shown the consequences of the 1951 act which is a result of a... the study has shown the consequences of the 1951 act which is a result of a... the study has shown the consequences of the 1951 act which is a result of a...

The study has shown the consequences of the 1951 act which is a result of a... the study has shown the consequences of the 1951 act which is a result of a... the study has shown the consequences of the 1951 act which is a result of a...

The study has shown the consequences of the 1951 act which is a result of a... the study has shown the consequences of the 1951 act which is a result of a... the study has shown the consequences of the 1951 act which is a result of a...

The study has shown the consequences of the 1951 act which is a result of a... the study has shown the consequences of the 1951 act which is a result of a... the study has shown the consequences of the 1951 act which is a result of a...

The study has shown the consequences of the 1951 act which is a result of a... the study has shown the consequences of the 1951 act which is a result of a... the study has shown the consequences of the 1951 act which is a result of a...

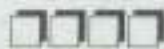
The study has shown the consequences of the 1951 act which is a result of a... the study has shown the consequences of the 1951 act which is a result of a... the study has shown the consequences of the 1951 act which is a result of a...

foreign aggression etc. This capacity to rise again after a setback has kept the Indian society breathing inspite of constant attacks for over two thousand years. This is because of the psychological toughness as well as the flexibility on the part of the society. Also the strong will of the people has led to the survival of democracy enduring several setbacks endangering its existence.

One finds politics has been governing the lives of people irrespective of caste, class, religion or gender. Everyone has been suffering due to politics and at the same time is a part and parcel of politics.

The political system is always instable since no man made system can be perfect as the political framework needs to change to suit the growing and varying needs of the people. After all people are at the centre of governance. The flexibility of the political system with welfare of the people at its centre can only ensure the survival of a healthy and vibrant democracy.

(This is the synopsis of the PhD thesis submitted to the S. P. Pune University.)





CONVICT EDUCATIONAL RESEARCH & REVIEW GROUP (MIT SOBEDC - Special Issue)

MAEER's MIT
SAINT DNYANESHWAR B.ED. COLLEGE, ALANDI, PUNE
INTERNATIONAL CONFERENCE
ON



वसुधैव कुटुम्बकम्

ONE WORLD | ONE FAMILY

In Collaboration with

Under Erasmus + CBHE Project AURORA
Dept. of International Centre, SPPU Pune



Editor

Prof. Swati Karad Chate

Trustee & Secretary General,
MAEER's MIT Group of Institutions, Pune, Bharat

Convener

Dr. Surendra Herkal

Principal, MIT S.D. B.Ed. College,
Alandi (D), Pune

Co-Convener

Mr. Sanjay Shinde

Asst. Prof., MIT S.D. B.Ed. College,
Alandi (D), Pune

Date : 4th February 2023 | **Time** : 10.30 am to 5.30 pm

Venue : Seminar Hall, MITACSC, Alandi Devachi, Pune

SKNCOET EDUCATIONAL RESEARCH & REVIEW (SERR)

ISSN 2455-6173

International Conference

on

“Vasudhaiva Kutumbkam”

(One World One Family)

(04th February, 2023)

In Collaboration with

Under Erasmus + CBHE Project AURORA
Department of International Centre, Pune

EDITOR

Prof. Swati Karad Chate

CO-EDITOR

Prin. Dr. Surendra Herkal

Asst. Prof. Sanjay Shinde

50	Dr. Anurag Shinde & Dr. Sumanth Sankar	MAJEE'S, MIT Savitri Dnyaneshwar B.Ed. College, Alandi, Dombivli, Pune	My Dream World Having Vasudhaiva Kutumbakam		
51	Dr. Vikas Tapaswale	MAJEE'S, MIT Savitri Dnyaneshwar B.Ed. College, Alandi, Dombivli, Pune	"A Study of Attitude of Secondary School Students towards Disaster Management in relation with One World - One Family approach."		
52	Dr. Vijay Patil	"Kavya Shikshant Ganatha VS S.B College of Education, Barampore"	The Earth is not one country and Marketed as Citizens		
53	Dr. Ravi Ganga Satish	Ganathi College of Education, Dombali Pravara, Tal: Rahuri, Dist. Ahmednagar Savitribai Phule Pune University, Maharashtra, India.	Universal Brotherhood and Spirituality in Education for Peace and good mental health		
54	Dr. Tejas Chhabildas Patil	MVP Samaj's KRT Arts, BHM Commerce and AM Science (KTHM) College, Nandik	Bharat to Hindustan via India: A Confluence of Vasudhaiva Kutumbakam		
55	Dr. Sagar Kakade	"Dr. Sagar Kishanrao Kakade(975866161 (Shradhachandraji) Pawar College of Education Koregaon Bhima Tal Shirur Dist. Pune"	To study the effect of project manual regarding Vasudhaiva Kutumbakam at secondary level		
56	Asst.Prof. Shinde Santosh J.	"Sinhgad Technical Education Society's, Smt. Kashibai Navale College of Education and Training (B.Ed), Kusgaon (BK), Lonavala"	"Vasudhaiva Kutumbakam- Vasudhaiva Kutumbakam Shloka with Hindi and English Meaning & Principles"		
57	Dr. Ashwini Manik Purade	AKT's Pooja College of Arts, Science and Commerce, Camp, Pune.	DEPICTION OF THE DARK SIDE OF 'VASUDHAIVA KUTUMBAKAM' IN KIRAN DESAI'S THE INHERITANCE OF LOSS		5
58	Dr. Hejal P. Barot	SNDT College of Arts and SCB College of Commerce and Science for women, SNDTWU, Mumbai-400020	सुखे नो भेदः कः सुखे नो भेदः सुखे नो भेदः		5

DEPICTION OF THE DARK SIDE OF 'VASUDHAIVA KUTUMBAKAM' IN KIRAN DESAI'S *THE INHERITANCE OF LOSS*

Dr. Ashwini Manoj Parale

AKDY Prans College of Arts, Science and Commerce, Camp, Pune

Abstract:

The Inheritance of Loss is a story of the four individuals being turned into pawns due to political turmoil, Sai, Gyan, Biju and the Cook, Pannaial. Through the character of Biju, son of the Cook, Kiran Desai illustrates one of the major themes of the novel that is how globalization has brought in new immigrant culture. The novel analyses how in the post-colonial era, people from colonized countries face terrible hardships in America which is a land of liberty. To fulfill the desire of his father, Biju, using fake documents and false recommendations, goes to America for a better livelihood. He works in various restaurants such as Gandhi Cafe, the Green and Indian Diner, the Baby Bistro, Le Colonial, the Queen of Tarts, and Freddy's Wok etc. Though he works for long hours, he is given only a meager salary and has to bear with terrible insults and ill-treatment. In almost all the restaurants where he works as a Cook, Biju finds to his shock that workers from third-world countries, and especially from the East are given only the lowest positions. As a rootless person and illegal immigrant, he has to move from one restaurant to another in search of a better job and better salary. Kiran Desai also analyzes in the novel how the problems of the legal immigrants are different from those of the illegal immigrants. The illegal immigrants have to live an underground life and are constantly on the run from the police. In fact there is a lot of corruption and indiscipline involved in the process of procuring visa. This leads to the problems of illegal immigrants. While remaining rooted to his father's love and cultural traditions, Biju now realizes that his dream of America is quite different from the places where he has worked and stayed.

Keywords:

Globalization, Biju, immigration, US, cultural alienation

Introduction:

The Inheritance of Loss is the second novel by Kiran Desai published in 2006. It won a number of awards including the Man Booker Prize for that year and the National Book Critics Circle Fiction Award in 2007. It is a literary masterpiece in its description, characterization and depiction of human emotions. It is a story of the four individuals being turned into pawns due to political turmoil, Sai, Gyan, Biju and the Cook, Pannaial. The novel has two strands of narratives: the one dealing with the sociopolitical problems of the people of Kalimpong and the other depicting the painful and alienated existence of the Indian diaspora in New York. Through the character of Biju, son of the Cook, Kiran Desai illustrates one of the major themes of the novel that is how globalization has brought in new immigrant culture.

Review of Literature:

Though Indian culture believes in the concept of 'Vasudhaiva Kutumbakam,' it is hardly followed in the western countries where people are commercial minded. We also believe in 'Athithi Devo Bhava' which imbibes the values of being a good host and respect our guests from the bottom of our hearts. These values are missing in the so called progressive first world countries. This aspect is hardly explored in research in literature of Indian English Writings. This paper highlights the farce of 'Vasudhaiva Kutumbakam,' in their culture.

Objectives of the Study

1. To show how the all-inclusive concept of 'Vasudhaiva Kutumbakam' is missing in the western world with special reference to US.

Though it is highlighted that globalization is the other name of 'transnationalism', it implies that workers to be found in one's behavioural patterns.

...in the post-colonial era, people from colonized countries find certain advantages in America which is a land of liberty. While discussing Desai's treatment of the theme of immigration in the novel, the author points out: "Desai portrays migration as a universal, multifaceted experience, involving a host of emotions of myth and fatalism. Almost fifty years after the judge went to England, Biju, the Cook's son, finds himself working as an illegal immigrant in New York."

...Desai depicts Biju's struggles and pathetic survival as an illegal immigrant in New York - "a city without sunlight" and with "buildings going up like jungle creepers starved for light." To fulfil the desire of his father, Biju, using fake documents and false recommendations, goes to America for a better livelihood. He works in various restaurants such as Gandhi Cafe, the Stars and Stripes Diner, the Baby Bistro, Le Colonial, the Queen of Queens, and Freddy's Wok etc. Though he works for long hours, he is given only a meager salary and has to bear with terrible insults and ill-treatment. Like the judge, who has suffered a lot at the hands of the Whites, Biju is humiliated and marginalized due to racial prejudice. The owner's wife at Piroccchia's Italian restaurant complains to her husband that Biju is smelly. She tells him that she prefers Europeans to Indians or Yugoslavians. At least they might have something in common with them like religion or skin colour. Unable to endure the resentment of the owner, Biju has to quit the place and go in search of jobs in other places. In almost all the restaurants where he works as a Cook, Biju finds to his shock that workers from third-world countries and especially from the East are given only the lowest positions. As a rootless person and illegal worker, he has to move from one restaurant to another in search of a better job and better salary. He finds that even legal immigrants who have come to America without proper documents have to suffer from alienation.

...Desai also analyzes in the novel how the problems of the legal immigrants are different from those of the illegal immigrants. The illegal immigrants have to live an underground life and are constantly on the run from the police. In fact there is a lot of corruption and indiscipline involved in the process of procuring visa. This leads to the problem of illegal immigrants. Knowing the precarious conditions of these immigrants, the owners of restaurants extract a lot of work from them and give them very low wages because they know that the workers have no legal rights to claim a better salary.

Biju and his fellow illegal immigrants have to change their jobs often because of the exploitative nature of the employers and the unhygienic conditions in the places. While remaining rooted to his father's love and cultural traditions, Biju now realizes that his dream of America is quite different from the places where he has worked and stayed. In the restaurants after his hard work, he has to sleep in unhygienic basements during night time. The workers are allotted space to sleep in the restaurants according to their racial origins. At Baby Bistro Restaurant, the French are asked to sleep above the restaurant "but below in the kitchen it was Mexican and Indian. And when a Pakistani was hired, it was Mexican, Indian, Pakistani." Biju undergoes a true colonial experience at Le Colonial Restaurant: "On the top rich colonial, and down below, poor native, Colombian, Tunisian, Ecuadorian, Gambian." At the Stars and Stripes Dinner Restaurant "All American flag on top, all Guatemalan flag below. Plus one Indian flag when Biju arrived."

Though he finds his job disgusting and humiliating, he has the hope of getting a Green Card. He knows to live in America permanently one should possess a Green Card. Even to leave America one must have one. "He watched the legalized foreigners with envy as they shopped at discount baggage stores for the miraculous, expandable

third-world culture. Thus, of course, there were those who lived and died illegal in America and their families, six for ten years, twenty, thirty, never again." Not knowing the conditions in which he had to live in America, his father writes to him: "Stay there as long as you can. Stay there. Make money. Don't come back here."

Findings

Social and cultural alienation, rootlessness, frustration and his longing for his father finally drive Biju to America for India. Through the story of Biju, Kiran Desai provides the reader with the daily life of a globalisation when she describes the customer-receiving areas of an up market restaurant flying an authentic French flag, while in the kitchen the flags are Indian and Honduran. Though Biju lives in New York, he has the time to see the country, lives in poverty where he has to sleep in shifts, or on the floor of the restaurant and even has to serve beef which he detests. When people come to US for the first time and are there to make a living, like Biju they are willing to undergo any torment to make ends meet. The novel tells us that Biju is a pawn as an illegal immigrant and also a pawn at the hands of George Bernard Shaw. The novel tells us that Biju is a pawn who lost him when he returns to India and he suffers as a common man. He is unhappy with the opportunities in India and escapes in search of better prospects.

Conclusion:

Thus, all the characters are suffering from the inheritance of the loss as goes the title of the novel. The author's appreciation of this masterpiece of Kiran Desai is no exaggeration: "Welcome proof that in our encounter with the English language continues to give birth to new children, endowed with lavish gifts." Though the advanced version of 'Vasudhaiva Kutumbakam,' alias 'globalization' claims to have brought the world together, it underlines the non-existent ideal of love, brotherhood and compassion for the world. It is more of a Utopian concept with reference to the western world. Man was always and will be selfish. As George Bernard Shaw rightly calls patriotism as 'Extended Selfishness.' The western world finds the concept in 'Vasudhaiva Kutumbakam,' meaningless and a misfit to their culture. It is easy to say that we follow and believe in 'Vasudhaiva Kutumbakam,' but difficult to implement when it comes to foreign nationalists. This is proven through the example of Biju and his hard struggle for survival in the US.

References

1. Sawhney, Hirsh. "In the Wide World". Rev. of *The Inheritance of Loss*. The Times Literary Supplement, No. 5399, (Sep 22 2006): 22. Print.
2. Desai, Kiran. *The Inheritance of Loss*. US: Atlantic Monthly Press, 2006. 189.
3. <http://www.powells.com/biblio-0802142818>.

Identity Crises in the Work of Jennet Winterson's Novels

¹Sabah Ismael Ahmed, ²Shirin Rashid Shaikh

¹Research Scholar, AbedaInamdar Senior College, Camp, Pune-411001

²Assistant Professor of English, AnjumanKhairul Islam Poona College, 647 Camp New
Modikhana, Pune-411001

Abstract

The characters in the works of Jennet Winterson's "Oranges are Not the Only Fruit" and "The Passion" are investigated in this paper for their "identity" issues. The essay seeks answers by examining accounts of conflict theory, childhood memories, the importance of unconsciousness, and libido drives, which are reflected in Winterson's mental, gender, and sexual identity inadequacies. The debate revolves around the concept of the true self and the effort to undermine one's self-image, which is hampered by both personal indeterminacy and adherence to orthodox society's norms. The aim of literary study of selected examples is to determine whether it is possible to define one's own identity in the face of past influences.

Keywords: Jeanette Winterson, Identity Crisis, The Passion, Oranges Are Not The Only Fruit.

Introduction

Jeanette Winterson's books also address the theme of lost identity, which is prompted by the author's own personal experience. Winterson struggled as a lesbian and adoptive child with antagonistic family members, a prejudiced culture, and, most notably, with her own self, who on the one hand sought to adhere to imposed expectations while on the other wished to obey personal wishes. Identity crises may be triggered by social, religious, or sexual factors, as shown by Winterson's works. "Oranges" is a bridge between harsh realism and a calming imagination, as it depicts Winterson's own psychiatric state, her issues of self-acceptance and social rejection. It may be argued that "Oranges" was written to distort truth and exorcise past ghosts. The fact that it is narrowly linked to the theme of identity in the novel "The Passion".

Despite their superficial differences, all of these books have one thing in common: a central plot built on confusion, quest, and identification. It can also be remembered that the author of this paper intentionally approaches Winterson's fiction and non-fiction in the same way in order to demonstrate the fine line between the two, their interdependence, and interrelationship, as well as to demonstrate how powerful the effect of Winterson's personal experiences was on the development of Oranges and The Passion. The examination of the above books would allow a more in-depth examination of the process of shaping one's own personality in the face of persistent conflict between inner drives and external expectations.

The issue of identity is inextricably linked to human existence. The process of identifying and moulding one's own personality is critical in learning "who am I?" for one cannot work adequately in life without knowing oneself. While many people have no trouble identifying their own identities, a significant amount of people have difficulty answering the question above. Jeanette Winterson's writings stress the complex journey of self-discovery, recognition, and reconciliation, which is often followed by an unjust battle with culture, families, and interpersonal tensions. The author of this essay draws attention to the problem's ambiguity by portraying identity as multiple, unorthodox, and unclear. Winterson declares that the path to discovering one's true self is long, and that any mirror

you gaze into is a magical mirror of its own sort, when you expect to see a more accurate image of yourself.

Winterson travels to places fraught with controversy and the unknown, crossing borders and trespassing on holy ground. Her works are filled with a tangle of unpredictable occurrences, idiosyncrasies, and peculiarities as a result of multiple remedies, hybridities, and the multiplicity of personalities that have fused to create a labyrinth of unexpected events, idiosyncrasies, and peculiarities. Winterson's primary research field is gender, religious, and sexual orientation, but she focuses on a broad variety of subjects and juggles with various notions such as mystic realism, intersexuality, the grotesque, and fragmentation. The writer's desire for inclusion sparks a conversation around diversity and freedom of choice, which is often suppressed by society's prejudiced speech. Winterson's inability to recognize her own personality is well known; as a result, her novels are steeped in reality and sincerity, which appear to resonate more than most other social philosophies.

Decoding the Identity Crises

Winterson, as a novelist, has the ability to escape authoritarian reality by escapism into the realms of imagination. *Oranges Are Not The Only Fruit* is a novel posing as a diary (Onega, Jeanette 18), a vent for the author's past memories and hidden impulses. The semiautobiographical book is a deliberate act of overcoming one's own shortcomings and fears.

Winterson breaks herself off from self- and socially enforced expectations by fiction, allowing her to be free of mental subjugation and endless stress over her incompatibility, first as an adopted child and later as a homosexual in a homogeneous culture. She writes the outline of her own life in *Oranges*, which she cleverly hides behind fairy tales and fantasy worlds. Winterson introduces a heroine who seems to be her alter ego – a teenager who not only shares the writer's name but also "must negotiate both the external and internal worlds by banging first the wall, then her own chest, as seminal for... the emerging self." The external, cultural world, cultural norms, and gender roles of both families and culture as a whole are metaphorically correlated with walls and pollution" (Makinen, 2005). According to *Oranges*, Evangelical culture and, in particular, a woman, or rather, women, had the strongest impact on shaping young Jeanette's character, attitudes, and values. First, Jeanette's biological mother's abandonment instilled in her a sense of remorse and alienation, as well as the dilemma "why has it happened to me?" With the absence of her biological parents, the heroine is cut off from her origins and past, and therefore loses a piece of her identity. Second, she must deal with her adoptive mother's high hopes and religious commitment. For a long time, Jeanette's fear of being rejected by Winterson has prevented her from admitting her homosexuality. To avoid being totally alienated and disconnected from the nearest culture, she is compelled to ignore her own impulses (Freud, Poza 150). Nonetheless, the protagonist is unable to cope with her feelings for another woman, particularly because she lacks support from her conservative mother.

Winterson agrees that the formation of *Oranges* was not an experiment or a whim, but rather the product of a strong wind blowing downstream. It was as though the novel had already been completed (Winterson, *Oranges* xii). We can deduce from this that the plot of the novel is an imitation of Winterson's own fears and anxieties, which have never been unveiled due to a sense of inconsistency in her own conception of identity and the aspirations of her group. The ability to explore fact by sharing her storey from the viewpoint of an unwelcome child and a lesbian, which for an uninitiated reader is nothing more than a work of fiction, helped Winterson to not only discover but also embrace her true self.

Winterson's investigation into sexual identities continues, this time focusing on traditional attitudes to the female body and gender stereotypes. In her other novel, "The Passion," which re-establishes and re-defines the representation of women, identity dialogue is interwoven. About the fact that love is the central theme of *The Passion*, this passage would focus on Villanelle's many personalities. It's important to note, however, that the concepts of love and identity are inextricably linked, and it's impossible to study one without examining the other.

The multidimensional of self-alluded to in 'Front' is perfectly embodied in Villanelle, who, depending on the situation, juggles her personalities and alters her physical identity by donning different masks. Her anatomy, as her gender, blurs the lines between binary opposites. She is a conflation of a man and a woman, a person and an animal, and the double identity is encoded in her body and sexual orientation (Front, 2009). Villanelle, despite being a female, is distinguished by webbed feet reserved for Venetian boatmen. Since webbed feet are just a masculine characteristic, they can be considered a sign of phallus and strength (AsensioArostegui, 2000). This distinctive trait, which can be considered a freak of nature, has both social and political overtones. Villanelle thus transcends physicality and sex divisions. Due to its French origins, Villanelle's entire figure is diffused, including her corporality, ethnicity, sexual orientation, and even her name, which introduces uncertainty and confusion: you are a Venetian, but you wear your name as a mask (Winterson, *The Passion* 54). The idea that Villanelle "gains... the power to choose gender" as a result of her physical transformation is particularly relevant to our investigation (Front 103). She has two faces and two names, allowing her to deceive people about her true identity. Villanelle cleverly switches outfits and dons different masks, claiming that dressing up as a child is part of the fun (Winterson, *The Passion* 54). Her dresses serve as a form of concealment and security, while her body establishes inconsistencies and dichotomies that, when combined, form an androgynous, hermaphroditic, and bisexual unity. Villanelle's nature's duality reshapes her personality, and is torn between femininity and masculinity. She has several affairs while disguised as a child, both with men who are enchanted by the voluptuous particle of Villanelle's delicacy and with women who are drawn to her mystery.

The life of the Venetian girl is divided into parts, and it takes place through various temporalities and parallel poles of posing and candour, lust and attraction, homo- and heterosexuality. Villanelle seems to enjoy tempting Casino patrons who are enthralled by her allure, but she must eventually choose which of her many lives she wants to pursue and which of herself is the true one. The girl tries to recover her name, which is masked by piles of clothes, mazes of masks, false faces, and drawn smiles: And who was I? Was this breeches-and-boots version of myself any less authentic than my garters? (Winterson, *The Passion* 65–66). The character is mature enough at the end of *The Passion* to develop her own persona and avoid dissimulating: "I don't dress up any longer."

We would have thought that, given Villanelle's diverse identities, the heroine couldn't be rescued from identity disintegration; yet, Villanelle's identity is reshuffled like a deck of cards before it eventually finds its centre. As mentioned at the outset of this essay, Villanelle's plight is not entirely dissimilar to that of Jeanette Winterson or the heroine of *Oranges*.

Conclusions

On the basis of Jeanette Winterson's childhood memoirs and her memories as a gay individual with parallels to Freud's ideas, Winterson's "Oranges Are Not The Only Fruit," and her multi faceted novel "The Passion," this paper aimed to explore the development of one's own identity. The sense of incongruity has its origins in the child's own view of oneself, which may lead to complacency or a self-destructive thought path. Furthermore, sexual heterodoxy creates contradictions between an

individual's inner drives and traditional social norms, obstructing identity growth. It is important to note that when social alienation and gender inadequacy are combined, as in the case of Winterson and her fictional characters, psychiatric disorders and a never-ending battle with oneself occur. Altering and rewriting reality, as Winterson points out, allows the repressed identity or id to emerge and initiates identity formation. It is possible to assume that reconciling with the past and crossing social borders will resolve the tension between antithetical self.

References

- Asensio Aróstegui, Mariadel Mar. (2000) "History as Discourse in Jeanette Winterson's *The Passion: The Politics of Alterity*." *Journal of English Studies* 2: 7-18.
- Front, Sonia (2009). *Transgressing Boundaries in Jeanette Winterson's Fiction*. Frankfurt: Peter Lang, 2009.
- Freud, Sigmund. (2016) *Creative Writers and Day-Dreaming*. Web. <<http://www.kleal.com/AP12%20member%20area%20pd2%202013/Fre2f>>
- Makinen, Merja. (2005) *The Novels of Jeanette Winterson*. Houndmills: Palgrave Macmillan.
- Winterson, Jeanette (1988). *The Passion*. New York: Grove Press.
- Winterson, Jeanette (2001). *Oranges are not the Only Fruit*. London: Vintage.

DECONSTRUCTING GENDER AND IDENTITY IN JEANETTE WINTERSON'S FICTION: A POSTMODERN FEMINIST READING

¹Sabah Ismael Ahmed, ²Shirin Rashid Shaikh

¹Research Scholar, Abedalnamdar Senior College, Camp, Pune-411001

²Assistant Professor of English, AnjumanKhairul Islam Poona College, 647 Camp New
Modikhana, Pune-411001

Abstract:

This research paper provides a critical analysis of postmodern feminism in the selected novels of Jeanette Winterson. The study focuses on four of Winterson's works: "Oranges are not the Only Fruit", "Written on the Body", "The Passion", and "The Powerbook". The paper explores how Winterson's literary techniques, themes, and characters challenge essentialist assumptions about gender and identity, and emphasize the fluidity of desire and power. It also highlights the role of language and storytelling in shaping our perceptions of ourselves and others. The study draws on key feminist theorists, including Julia Kristeva, Hélène Cixous, Judith Butler, Michel Foucault, Luce Irigaray, and Donna Haraway. The research concludes that Winterson's novels make a significant contribution to postmodern feminist literature by challenging traditional gender norms and exploring the fluidity of identity. The paper emphasizes the power of language and storytelling to shape our perceptions of ourselves and others, highlighting the potential for literature to challenge and subvert dominant cultural narratives.

Key words: Postmodern feminism, Jeanette Winterson, gender, identity.

Introduction:

Introduction:

Postmodern feminism is an interdisciplinary theory that emerged in the late 20th century, challenging the essentialist assumptions of traditional feminism and emphasizing the role of language, discourse, and power in shaping gender identities and feminist politics. Jeanette Winterson, a contemporary British writer, has been recognized as a prominent voice in postmodern feminism, challenging conventional gender norms and exploring the fluidity of identity in her fiction. This paper aims to decode postmodern feminism in the selected novels of Jeanette Winterson, using a critical analysis of her literary techniques, themes, and characters.

This research paper employs a critical analysis of the selected novels of Jeanette Winterson to decode postmodern feminism in her works. The methodology involves close reading and textual analysis of her literary techniques, themes, and characters, with a focus on the ways in which they challenge traditional gender norms and explore the fluidity of identity. The paper also draws on postmodern feminist theory and literary criticism to contextualize Winterson's works and provide a theoretical framework for the analysis.

The paper draws on the works of several key feminist theorists to support its analysis of Jeanette Winterson's novels. These theorists have made significant contributions to feminist literary theory, postmodern feminism, and gender studies. Julia Kristeva's work explores the relationship between language and the formation of subjectivity, while Hélène Cixous's work explores the relationship between writing, sexuality, and gender. Judith Butler's work challenges the idea that gender is a fixed, biological category, and Michel Foucault's work explores the relationship between power and knowledge. Luce Irigaray's work explores the relationship between language, gender, and sexuality, and Donna Haraway's work explores the relationship between technology, gender, and identity.

Analysis:

Jeanette Winterson's novels are characterized by their postmodernist style and feminist themes. Through her literary techniques, themes, and characters, Winterson challenges traditional gender norms and explores the fluidity of identity. This section of the paper will analyze Winterson's novels in more detail to highlight these themes and techniques.

Oranges Are Not the Only Fruit:

Oranges Are Not the Only Fruit is Winterson's debut novel and is based on her own life experiences. The novel follows the protagonist, Jeanette, as she grows up in a strict religious community and struggles with her own sexuality. Winterson challenges traditional gender norms in the novel by depicting Jeanette as a young girl who rejects traditional gender roles and pursues her own desires. Jeanette's relationship with her girlfriend Melanie challenges the heteronormative expectations of her community and highlights the fluidity of sexuality and desire. Winterson also explores the theme of agency in the novel, emphasizing the need for women to take control of their own lives and challenge oppressive social structures.

Sexing the Cherry:

Sexing the Cherry is a postmodern novel that features multiple narrators, intertextual references, and metafictional elements. The novel explores themes of gender, sexuality, and power by blurring the boundaries between reality and fiction. Winterson challenges essentialist assumptions about gender by depicting a genderless narrator who embodies both male and female traits. The narrator is also a time traveler who visits different periods and cultures, highlighting the constructed nature of historical narratives and gender roles. The novel features female characters who challenge patriarchal norms and seek to redefine their identities. The protagonist, Dog Woman, is a fierce and independent character who defies the traditional gender roles of her society. Dog Woman embodies both male and female traits, challenging essentialist assumptions about gender.

Written on the Body:

Written on the Body is a novel that features a genderless narrator who falls in love with a married woman. The novel explores the fluidity of desire and identity by challenging essentialist assumptions about gender and sexuality. The narrator's genderless identity emphasizes the constructed nature of gender and the potential for fluidity and change. The novel also highlights the role of language and storytelling in shaping our perceptions of ourselves and others. The narrator uses language to describe the object of their desire, challenging the reader's assumptions about the gender of the narrator and the object of desire.

The Passion:

The Passion is a novel that features a female protagonist who defies conventional gender norms and seeks to redefine her identity. The protagonist, Henri, is a soldier in Napoleon's army who falls in love with a cross-dressing Venetian woman named Villanelle. Henri's love for Villanelle challenges traditional gender roles and highlights the fluidity of desire and identity. The novel also explores the theme of power and its relationship to gender and sexuality. Villanelle is a powerful character who challenges the male-dominated power structures of her society by subverting traditional gender roles.

The PowerBook:

The PowerBook is a postmodern novel that features multiple narrators, intertextual references, and metafictional elements. The novel explores themes of identity, desire, and power by blurring the boundaries between reality and fiction. The novel challenges essentialist assumptions about gender and sexuality by featuring a genderless narrator who embodies both male and female traits. The novel also features female characters who challenge patriarchal norms and seek to redefine their identities.

The novel also highlights the role of storytelling in shaping our perceptions of ourselves and others. The novel's multiple narrators and intertextual references emphasize the constructed nature of identity and the potential for fluidity and change. The novel also explores the relationship between power and desire.

One of the key themes that emerges from the analysis is the idea of the "unstable self" and the challenge to fixed identity categories. Winterson's novels, particularly *Written on the Body* and *The PowerBook*, challenge the idea of a stable and fixed gender identity, and instead present a fluid and multiple sense of self. This is in line with postmodern feminist theory, which emphasizes the importance of recognizing the diversity and complexity of identity categories and the need to challenge traditional binaries and hierarchies.

Another important theme that emerges from the analysis is the idea of agency and empowerment. Winterson's novels, particularly *Oranges Are Not the Only Fruit* and *The Passion*, present female characters who challenge patriarchal norms and assert their own agency and desire. This is in line with feminist theory, which emphasizes the need for women to take control of their own lives and challenge oppressive social structures.

Conclusions:

The conclusion of this research paper emphasizes the significant contribution of Jeanette Winterson's novels to postmodern feminist literature. The conclusion highlights how her literary techniques, themes, and characters challenge essentialist assumptions about gender and identity and explore the fluidity of desire and power. It also emphasizes the role of language and storytelling in shaping our perceptions of ourselves and others.

The conclusion highlights the way in which Winterson's works challenge traditional gender norms, particularly in relation to gender binaries and stereotypes. The conclusion also emphasizes the fluidity of identity, explored in all of the novels discussed.

Additionally, this research paper highlights the importance of postmodern feminist theory in analyzing and contextualizing Winterson's works. By drawing on the insights of key feminist theorists such as Julia Kristeva, Hélène Cixous, Judith Butler, Michel Foucault, Luce Irigaray, and Donna Haraway, this paper offers a nuanced analysis of Winterson's novels and situates them within the broader context of feminist theory.

The analysis of Winterson's novels in this paper reveals a number of recurring themes, including the fluidity of identity, the challenge to traditional gender norms, and the power of language and storytelling. These themes are in line with postmodern feminist theory, which emphasizes the constructed and contingent nature of identity and the importance of language and discourse in shaping our perceptions of ourselves and others. Winterson's novels, in particular, challenge essentialist assumptions about gender and identity, presenting a fluid and multiple sense of self.

The conclusion of this research paper underscores the value of Winterson's contributions to postmodern feminist literature, highlighting the ways in which her works challenge traditional gender norms and explore the fluidity of identity. It also emphasizes the importance of postmodern feminist theory in analyzing and contextualizing Winterson's novels, as well as the potential for literature to challenge and shape our perceptions of ourselves and others.

Overall, this research paper offers a comprehensive analysis of postmodern feminism in the selected novels of Jeanette Winterson, drawing on key feminist theorists to provide a theoretical framework for the analysis. Through its critical analysis of Winterson's literary techniques, themes, and characters, this paper demonstrates the significant contribution of Winterson's works to postmodern feminist literature and the ongoing relevance of postmodern feminist theory in the study of gender and identity.

References:

- Butler, J. (1990). Gender trouble: Feminism and the subversion of identity. Routledge.*
- Cixous, H. (1976). The laugh of the Medusa. Signs, 1(4), 875-893.*
- Foucault, M. (1977). Discipline and punish: The birth of the prison. Vintage Books.*
- Haraway, D. J. (1991). A cyborg manifesto: Science, technology, and socialist-feminism in the late twentieth century. In Simians, cyborgs and women: The reinvention of nature (pp. 149-181). Routledge.*
- Irigaray, L. (1985). This sex which is not one. Cornell University Press.*
- Kristeva, J. (1982). Powers of horror: An essay on abjection. Columbia University Press.*
- Winterson, J. (1985). Oranges are not the only fruit. Bloomsbury.*
- Winterson, J. (1992). Written on the body. Vintage Books.*
- Winterson, J. (1999). The passion. Vintage Books.*
- Winterson, J. (2000). The powerbook. Vintage Books.*



Journal of Education
Rabindra Bharati University

ISSN: 0972-7175
A Peer Reviewed Journal

CERTIFICATE OF PUBLICATION

A COMPARATIVE STUDY OF POLITENESS & COOPERATIVE PRINCIPLES IN
THE LAST YANKEE & FINAL SOLUTION

Authored By

Dr. Shirin R Shaikh

Professor, Poona College of Arts, Science & Commerce, Pune.

Published in

Journal of Education: Rabindra Bharati University

ISSN : 0972-7175

Impact Factor: 5.8

Vol.: XXVI, No. :1, 2023

UGC CARE, Peer Reviewed and Refereed Journal



Journal of Education

Volume 96, No. 01(II), 2023
(New Series)
ISSN : 0972-0766



(Established in 1804)

**JOURNAL
OF THE
ASIATIC SOCIETY OF MUMBAI**
(A UGC - CARE Listed Journal)

Editors
Parineets Deshpande
Ambarish Khare

Published by
The Asiatic Society of Mumbai
Town Hall, Mumbai- 400 001.
Maharashtra State (INDIA)
2023

**Volume 96 for 2023
(New Series)
ISSN : 0972-0766**

**JOURNAL
OF THE
ASIATIC SOCIETY OF MUMBAI**

**Editors
Parineets Deshpande
Ambarish Khare**

**Published by
The Asiatic Society of Mumbai
Town Hall, Mumbai- 400 001.
Maharashtra State (INDIA)**

2023

**London Agents
ARTHUR PROBSTHAIN
41, Great Russell Street, London, WCB, 3PL**

CONTENTS

Articles

1	A STUDY OF CHARACTERS, LANGUAGE & SOCIAL CLASS IN BERNARD SHAW'S PYGMALION	Dr. Abdul Saleem	1
2	FAMILY FOCUSED PSYCHOTHERAPEUTIC INTERVENTIONS TO ENHANCE PARENTCHILD RELATIONSHIP AMONG ADOLESCENT	Dr. Freda Cota Pereira	9
3	HUMAN RIGHTS AND WOMEN EMPOWERMENT: ISSUES AND PERSPECTIVES SPECIAL REFERENCE TO AGARTALA MUNICIPAL AREA	Mr. Kalipadha Debnath	16
4	A BRIEF CASE STUDY OF HIMALAYA DRUG COMPANY'S CLOSED DIVISION IN JALGAON DISTRICT OF MAHARASHTRA	Dr. Khalid Arshad & Dr. Aftab Alam	21
5	DETERMINING FACTORS OF INCOME OF THE FEMALE HEADED HOUSEHOLDS OF THE IN MULLAITIVU DISTRICT OF SRI LANKA	Gnanasubramaniam Gnanachandran & Dr.J.A.Arul Chellakumar	27
6	IMPACT OF MIGRATION: A CRITICAL ANALYSIS	Dr. Mukhtar Shaikh	35
7	THE ANGLO FRENCH SAGA: WAR AND DIPLOMACY IN 17TH AND 18TH CENTURY	Dr Zoheb Hasan	40
8	THE COST OF MATERIALISTIC LIFESTYLE, MONEY, MIND AND MORALITY	Zameer Salim Sayyed	45
9	KAMALA DAS: THE VOICE OF THE SUBALTERN	Dr. Vinita Basantani & Ms. Zeenat B.Merchant	49
10	COMPARATIVE ANALYSIS OF THE GLOBAL INNOVATION CAPACITY: A STUDY ON BRICS COUNTRIES	Ms. Lizette D'Costa	52
11	INNOVATIVE DEVELOPMENT IN ECONOMIC WITH RESPECT TO MACRO ECONOMICS	Dr. Thombre Kailas Arjunrao	60
12	A STUDY ON CULTURE AND HERITAGE OF INDIA.	Imran Hussain	64
13	QUALITY OF WORK-LIFE IN BANKING SECTOR	Nishi Shah, Dr. Divya Jain, Miti Suchak & Charvi Joshi	68



THE COST OF MATERIALISTIC LIFESTYLE: MONEY, MIND AND MORALITY

Zameer Salim Sayyed

Assistant Professor of English, Poona College of Arts, Science and Commerce Camp, Pune - 411 001

Abstract:

Wealth accumulation and wealth creation are human-specific activities as all human beings and only human beings act and interact in the context and constraints of their economic standing in the society and culture. The majority, if not all, are seduced to think that to be well, one first has to be well-off. A good life begins arguably, according to many of us, after considerable success in having more money and/or having more than others. Such a materialistic outlook and the ensuing selfishness have no longer remained moral problems but are being seen as major pursuits of life. There are many reasons behind this upheaval, but the most pressing one is the desire to live life according to the standards set by our 'reel' and real society, not by the ideals set by our inward spirit. The present paper aims to probe this human desire of amassing riches 'mindlessly'. The story 'The Fisherman and the Businessman' attributed to Paulo Coelho (b. 1947), a Brazilian writer and lyricist famous worldwide for his novel 'The Alchemist', is taken up for study and analysis to validate the arguments made in the paper.

Keywords:

Materialism, Existential Vacuum, Ethical Criticism, Moral Values

Introduction:

Materialism refers to a societal trend where the pursuit of material possessions and wealth has become the primary goal of many individuals. This tendency is fuelled by the consumerist culture that pervades modern society, where people are bombarded with advertisements and messages that encourage them to acquire more and more goods (Richins; Oprea, Buijzen and Valkenburg). The following observation is very poignant in this case:

"Newspaper headlines exalt the local lottery winner. Get-rich-quick books climb to the tops of best-seller lists. Multicolour ads flash on Web pages. Celebrities on television hawk everything from sport utility vehicles to mascara. Although they differ in form, each of these messages essentially proclaims "Happiness can be found at the mall, on the Internet, or in the catalogue." (Kasser p. 1)

While there is nothing inherently wrong with wanting to improve one's quality of life or to possess material objects, materialistic aspirations extended to the level of toxicity can have negative consequences for both individuals and society as a whole.

A materialistic lifestyle is characterized by a strong focus on accumulating material possessions and wealth as a measure of success and happiness. In this type of lifestyle, the pursuit of money, status, and material goods takes priority over other aspects of life, such as relationships, personal growth, and well-being. Individuals who adhere to a materialistic lifestyle often measure their self-worth and the worth of others based on their possessions and financial standing (Kasser). However, while material possessions can provide temporary satisfaction and pleasure, they do not necessarily lead to long-term happiness or fulfilment. There is a growing body of study that suggests that people whose values are centred on the accumulation of riches or material items are at a higher risk of dissatisfaction, including anxiety, depression, low self-esteem, and relationship issues - regardless of age, income, or culture. (Burroughs and Rindfleisch; Kasser).

Outline of the Story in Question:

In the story *The Fisherman and The Businessman*, a businessman advises a fisherman to work hard catch more fish, and reinvest his profits to grow his business. The fisherman, however, is content with

¹ <https://paulocoelho.blog.com/2015/09/04/the-fisherman-and-the-businessman/#:~:text=Author%3A%20Paulo%20Coelho&text=The%20businessman%20was%20impressed%20and%20%E2%80%9CThe%20businessman%20was%20astonished.> Accessed it on 27th of March 2023.

has simple life, spending time with his family, and enjoying the company of his friends. The businessman fails to understand that the fisherman's approach to life is not about laziness, but rather about prioritizing what truly matters in life.

An Intervention:

A businessman in a small village having no business of his own (!) so sitting idly by the beach seems to be a clarion call about the "existential vacuum" (Frankl) the modern society has been undergoing since the emergence of capitalism. Being one of the major characters in the story, the reader knows nothing about where he comes from, why he is at the shore, or whether he is at shore by chance. Besides his "PhD in Business Management" degree, the reader knows nothing about his business – forget about whether he is a successful businessman or not. He halts a fisherman at shore who is on his way back home after catching "quite a big fish". The businessman was quite "impressed" by the fisherman's "big" gain in a "short while", a very interesting and insightful information about the character of the fisherman. The fisherman is skilled at his work and is satisfied with the life he lives. He says:

"I usually wake up early in the morning, go out to sea and catch a few fish, then go back and play with my kids. In the afternoon, I take a nap with my wife, and evening comes, I join my buddies in the village for a drink — we play guitar, sing and dance throughout the night."

The fisherman is content with having enough food to feed his family and friends and time to enjoy life in company of his loved ones. The businessman pays no heed to the fisherman's joys, not a surprising thing for people with strong materialistic tendencies as the ability or willingness to consider the point of view of such money-minded people decreases degree by degree due to excessive materialistic outlook. (Kasser p. 69-72).

Wondering at why the fisherman does not "stay longer at sea and catch more", the businessman readily extends his "help" to the fisherman, though the fisherman asked for none. Such a *help* from a businessman in the age of capitalism can never be assumed in terms of *cooperation* but in terms of *getting ahead as a businessman*. He suggests him to spend *more* time at sea, fishing more so to have *more* in life by growing his fishing job into a business empire with a headquarter set up in a city along with several branches at various localities distributing fishes. After listening to this plan of the businessman, the fisherman asks a simple question: "And after that?". The businessman says:

"After that, you can finally retire, you can move to a house by the fishing village, wake up early in the morning, catch a few fish, then return home to play with kids, have a nice afternoon nap with your wife, and when evening comes, you can join your buddies for a drink, play the guitar, sing and dance throughout the night!"

The businessman ends up telling him to aim the life the fisherman was always already living. So, the plan was to make the fisherman postpone living his life "meaningfully". And this sounds alarming today when we reconsider the matter of materialistic life: Are we trained to be dissatisfied with what we have now? The loss of meaning in modern society has allowed the tools of reason and science to be deployed in a pitiless and cynical manner against humanity.

The need to have more than one currently has is arguably triggered by people surrounding us physically and virtually. Craving for 'stuffs' which are expensive, brands, status-symbols, and image-builders is activated and accelerated also by (pseudo)realities of media. Consequently, one can never have more as there are always others having more. Thus, one's struggles for money-acquisition do not stop even after rising above poverty levels of income. Having more money is associated with fame and recognition. Getting fame and recognition is a hallmark of success. So, the passion for being successful makes us run faster, work harder, and carry overload at the expense of freedom, interpersonal relationships, and spiritual bliss.

In the story, the businessman suggests the fisherman to increase his "buying power" by expending his time, energy, and talent on fishing more, possibly by being away or absent for more time from people he loves. This assignment of fishing more and thereby having more in life – a disease called "affluenza" – may have caused him to feel insecure in terms of living his life and loving his people. So, the moral



of the story in question is that material success and wealth are not the only measures of a meaningful and fulfilling life. It reminds us to take time to appreciate life's simple pleasures, to spend time with loved ones, and to prioritize our values and passions. Ultimately, it is up to each individual to decide what is most important in life and to pursue it with intention and purpose. "Socrates died so we could think".

Conclusion:

Money in itself has no intrinsic morality. It is a piece of paper, a piece of gold, a series of digits on an electronic account. It is our level of desire for money and what we do with it that determines the morality of money. According to the New York Times personal finance columnist MP Dunleavy, the key to living a life of actual prosperity is reallocating your assets to match your realistic needs (Dunleavy). Every nation has plenty of resources to keep its people housed, fed and mobile, but the people are let to suffer economic injustice as if we can not save anything except money. We do not have money to feed the poor, but we have money to fund a war. Unless an "ethical perspective" is adopted in deciding the measure of a financially successful life and monitoring our lifestyle, desires to have more and more material goods in life will put a heavy burden on our sense of contentment. In this light of the argument, it is a truism that "Materialism causes unhappiness, and unhappiness causes materialism". People who prioritize material possessions and wealth are less happy and more anxious than those who focus on non-materialistic values like personal growth, community involvement, and spirituality. Materialism has been linked to a range of negative psychological outcomes, including lower self-esteem, higher rates of depression and anxiety, and increased feelings of social isolation. Materialistic individuals tend to spend more money than they can afford, often in an attempt to keep up with others or to acquire more status symbols. This can lead to financial problems, such as credit card debt, and can cause stress and strain on personal relationships. The pursuit of material possessions often results in increased consumption, which can have negative environmental consequences, such as resource depletion, pollution, and climate change. Materialism is closely linked to social status and inequality. The pursuit of wealth and status often results in the widening gap between the rich and the poor, which can lead to social unrest and conflict. This culture can be harmful as it promotes the idea that happiness and success can be achieved through the acquisition of material possessions, rather than through meaningful experiences, relationships, and personal growth. To sum up, the adverse effects of materialistic lifestyle are vast and complex. By prioritizing non-materialistic values, such as personal growth, community involvement, and spiritual fulfilment, we can create a more sustainable and fulfilling society. In his speech *Beyond Vietnam: A Time to Break the Silence* (1967), Martin Luther King Jr. appeals to his audience which is still relevant and awaiting *materialisation*:

"We must rapidly begin the shift from a thing-oriented society to a person-oriented society, where machines and computers, profit motives and property rights, are considered more important than people, the giant triplets of racism, extreme materialism and militarism are incapable of being conquered."

Bibliography:

- Burroughs, James E. and Aric Rindfleisch. "Materialism and Well-Being: A Conflicting Values Perspective." *Journal of Consumer Research* 29.3 (2002): 348-370. 28 3 2023 <<https://academic.oup.com/jcr/article-abstract/29/3/348/1800916>>.
- Dunleavy, MP. *Money Can Buy Happiness*. Broadway, 2007.
- Frankl, Victor. *Man's Search for Meaning: An Introduction to Logotherapy*. Boston, Massachusetts: Beacon Press, 1959.
- Kasser, Tim. *The High Price of Materialism*. Massachusetts, London, England: The MIT Press, 2002.
- Oprea, Suzanna J., Moniek Buijzen and Patti M. Valkenburg. "Lower Life Satisfaction Related to Materialism in Children Frequently Exposed to Advertising." *Pediatrics* 130.3 (2012): 28 1 2023. <<https://ncbi.nlm.nih.gov/pubmed/22908113>>.



- Richins, Marsha L. "Media, Materialism, and Human Happiness." *ACR North American Advances* (1987). 28 3 2023. <<http://acrwebsite.org/search/view-conference-proceedings.aspx?id=6720>>.
- Scott, Kristin. *Terminal materialism vs. instrumental materialism: Can materialism be beneficial?* 2009. 28 3 2023. <<https://shareok.org/handle/11244/6820>>.



Shodh-Rityu त्रिमासी शोध-पत्रिका
PEER Reviewed & Refereed JOURNAL

ISSUE-29 VOLUME-I ISSN-2454-6283 July-sept.-2022
IMPACT FACTOR - (IIJIF-7.312) SJIF-6.763, IIFS-4.125,

AN INTERNATIONAL MULTI-DISCIPLINARY RESEARCH JOURNAL

सम्पादक
डॉ. सुनील जाधव, चंद्रपूर
9405384672

सहायकी सम्पादक
अनिल जाधव, मुंबई

पत्राचार हेतु पता-
महालगा ब्रह्म हठसिंग सोसायटी, हनुमान गढ़ समन वं सानने, चंद्रपूर-431005

प्रकाशन/प्रकाशक
डॉ.सुनील जाधव
नव साहित्यकार
पब्लिकेशन, नांदेड-महाराष्ट्र

मुद्रण/ मुद्रक
तन्मय प्रिंटर्स,नांदेड
डॉ.सुनील जाधव,नांदेड

मेल पता shodhrityu78@yahoo.com

वेबसाइट www.shodhrityu.com

'शोध-ऋतु' तिमाही पत्रिका में आलेख लेखक निम्न बिन्दुओं पर अवश्य ध्यान दें।

फॉन्ट-कृति देव 10 बड फाइल में ही सामग्री स्वीकृत की जायेगी।

आलेख पेज की मर्यादा चार पेज होगी।

आलेख विशेषज्ञों द्वारा चयन किये जायेंगे।

चयनित आलेख को सूचना मेल द्वारा आलेख लेखक को दी जायेगी।

चयनित आलेख के लिए 1000रु प्रोसेसिंग शुल्क लिया जायेगा।

लेखक मौलिक शोधपरक एवं वैचारिक आलेख ही भेजे।

कॉटर्स एप-9405384672

बैंक विवरण

NAME	SUNIL GULABSING JADHAV
BANK	BANK OF MAHARASHTRA, WORKSHOP CORNER, NANDED, MAHARASHTRA
ACCOUNT NO.	2015 8925 290
IFSC CODE	MAHB0000720

 PhonePe

ACCEPTED HERE

Scan & Pay Using PhonePe App



or Pay to Mobile Number using PhonePe App

9405384672

Sunil Jadhav

अनुक्रमिका

1. डॉ. प्रदीप सक्सेना 'उजाला' कृत 'मन दर्पण' : एक अवलोकन	6
— सुनीता शरिया	6
2. हिन्दी साहित्य में तृतीय लिंगी का स्वरूप	8
— प्रो. डॉ. राजीव कुमार	8
3. Population Control Law in India: An Overview	10
— Prof. (Dr.) Ashok Kumar Rai	10
4. भारत में स्थानीय शासन में महिलाओं की भागीदारी एवं स्वशासन में महिलाओं के लिये चुनौती	13
— सतीश बन्द	13
5. काल साहित्य की अन्वयण: भारतीय एवं पाश्चात्य विद्वानों द्वारा	16
— 'कविता उषाग्र' 'डॉ. सर्वेश कुमार मिश्र'	16
6. शैलीकरण : मीडिया और साहित्य	18
— डा. गुलाब खोड	18
7. अनुवाद विज्ञान	19
— प्रो. अश्वनी कुमार	19
8. विन्सेट शाही की निधक दृष्टि 'राम कथा : एक पुनर्पाठ' के संदर्भ में	22
— ममता कालड़ा	22
9. दलित साहित्य	26
— डॉ. विजय पाल	26
10. जया जादवानी के कथा साहित्य में नारी पीड़ा	28
— 'कु. लक्ष्मीलया बबुराज पृथ्वीराज' 'डॉ. शेख मोहम्मद शाकिर शेख बशीर'	28
11. 'सदाचार का ताबीज' कहानी में भ्रष्टाचार	30
— डॉ. विष्णु ठरुपन	30
12. रेनु के कहानियों में शिल्प	32
— सुप्राता कुमारी सिंह	32
13. आपका बंटी उपन्यास में मनोवैज्ञानिकता	35
— डा. मनीषा ठक्कर	35
14. उर्दू जनजातियों का लोकगीत में निहित जीवन दर्शन	38
— चाँदनी कुमारी	38
15. सर्वेश्वर दयाल सक्सेना के नाटकों में बहती मानवीयता की सदानौरा	39
— डॉ. शशिनी जोस	39
16. निबंधकार दिनकर का शिक्षा दर्शन	43
— आरती कुमारी	43
17. दलित समस्या का आर्थिक-सामाजिक-सांस्कृतिक संदर्भ	44

साथ अभिव्यक्त किया और तथाकथित सत्य समाज को सवाल के घेरे में लाकर खड़ा कर दिया। मोहनदास नैमितराय की 'अपने-अपने पिता' दलित साहित्य की प्रथम आत्मकथा है। ओम्प्रकाश वाल्मीकि की आत्मकथा 'जूटन' भी बहुत महत्वपूर्ण कृति है। रवीराज सिंह बेचैन की आत्मकथा 'मेरा बचपन मेरे कंधों पर' एक दलित बाल-मजदूर की संघर्षमय यात्रा का साहित्यिक विवरण समाज के सामने प्रस्तुत करता है। सूरजपाल चौहान की आत्मकथा 'संतान' और त्रिस्तुत, डॉ.धर्मवीर की आत्मकथा 'मेरी पत्नी और भंडिया' सामाजिक सन्दर्भों को पारिवारिक समस्याओं के रूप में उजागर करती हैं। डॉ. तुलसीराम की मुदंहिया और मणिकर्णिका, कौसल्या बैसंत्री की 'टोहरा अभिशाप', डॉ. सुशीला टांकनौर की 'शिकंजे का दर्द' और माता प्रसाद की 'झोपड़ी से राजमदन' अन्य महत्वपूर्ण आत्मकथाएँ हैं।

दलित साहित्य में नाटक और आलोचनात्मक पुस्तकों की भी कमी नहीं है। माता प्रसाद ने समाज के यथार्थ को अपने नाटकों का विषय बनाया है। आलोचना के क्षेत्र में ओम प्रकाश वाल्मीकि, डॉ. धर्मवीर, रवीराज सिंह बेचैन, डॉ.तेज सिंह, जय प्रकाश कर्दन, एन.सिंह, कवत भारती, डॉ. कालीधरण स्नेही, डॉ. विष्णु सर्वदे, डॉ. रामचंद्र, डॉ.अजमेर सिंह काजल, डॉ.नामदेव विमल शोरात, पूनम सिंह, रजनी दिमोदिया, विनीता रानी, रजनी शिलक, अनिता भारती, सूरज बहल आदि का नाम लिया जा सकता है।

सन्दर्भ-(1)शर्म, रामचंद्र, मानक हिंदी कोष, खंड-3, प.36 (2)बाहरी,हरदेव,राजपाल हिंदी शब्दकोश,प.386 (3)वाल्मीकि, ओम्प्रकाश, दलित साहित्य का सौन्दर्यशास्त्र,प.14 (4)बेचैन, रवीराज सिंह उषा सदी के हिंदी कथा साहित्य में दलित विमर्श,प.21 (5)कमलेश्वर(सं)साहित्य,सामान्यतर कहानी विशेषांक-7,दलित साहित्य (मराठी)अंक अप्रैल 1975,ले.प्र.श्री नेरकर,प.74 (6)मेघवाल,कुसुम-हिंदी उपन्यासों में दलित वर्ग,प.1 (7)सिंह डॉ. एन.-सुमनलिपि,साक्षात्कार,अक्टूबर-नवम्बर,1993,प.35 (8)धर्मवीर,डॉ.-दलित चिन्तन का विकास,जमिन्शा चिन्तन से इतिहास चिन्तन की ओर,प.18 (9)बेचैन,रवीराज सिंह,वीधे,देवेन्द्र-चिन्तन की परम्परा और दलित साहित्य,प.83 (10)वही,प.84 (11)बेचैन,रवीराज सिंह,वीधे,देवेन्द्र-चिन्तन की परम्परा और दलित साहित्य,प.85 (12)सुमनक्षर,सोहनपाल-दलित साहित्य,प.10 (13)मदन,गुरु प्रसाद-बाबा साहब से पहले स्वामी अछूतानन्द हरिहर,पत्रिका-बहुरि नहीं आया, अप्रैल-सितम्बर 2012,प.29

10.जया जादवानी के कथा साहित्य में नारी पीढ़ा

-**डॉ. तुलसीराम बाबुराव पृथ्वीराज, डॉ.रोस मोहम्मद शाकिर शंख शर्मा**

शोधार्थी, एम्.ए.बी.एड. एम.फिल.
मार्गदर्शक, पुना कॉलेज, हिंदी विभाग, अहमद-पुणे

संसार में यदि नारी नहीं होती तो सभ्यता और संस्कृति ही नहीं होती। नारी ने अपने विविध रूपों में पुरुष को प्रोत्साहन, संघर्ष और शक्ति दी है। यह समाज में पुरुष के लिए कभी जन्मदात्री, पोषणकर्त्री माता के रूप में आती है तो कभी स्नेह की भावना से प्रभावित करनेवाली भगिनी के रूप में लक्षित होती है। अतः समाज में नारी के माता, पत्नी, भगिनी, पुत्री, सखी, सौमित्रा, पारिवारिक, तपस्विनी आदि अनेकानेक रूप हैं। लेकिन इसी नारी पर भारत में सदियों से अत्याचार, अत्याचार होता आ रहा है। 'प्राचीन काल से समाज में उस पर लज्जा, मर्यादा, विनयशीलता, कोमलता, त्याग, समर्पण आदि गुण थोप दिए हैं और दुर्बल, अवल नारी कलर दं दिया।' 'बेद सौ वर्षों के बाद अंग्रेजों से छुटकारा पाने के बाद भारत वर्ष ने स्वतंत्रता की राँस ली। नारी संघर्ष में पहले चूल्हा-चौका और बन्ना इन्हें सँभलते हुए औरत को घर की सौकर के बाहर जाना बना था। लेकिन म्हात्मन ज्योतिबा फुले तथा उनकी अर्धशिषी ब्रह्मिणीपोती शक्तिश्रीबाई चूले जैसे महान समाज सुधारकों की वजह से औरत को पढ़ने-लिखने का सुनहरा मौक़ा मिला। उन्होंने कहा 'जब तक स्त्रियों को शिक्षित नहीं किया जाएगा, तब तक भारत जैसा विशाल देश का एक भी घर नहीं सुधरेगा।' शिक्षा ने नारी को अपने पैरों पर खड़ा कर कामकाजी बनाकर उसके व्यक्तित्व को निखारने का प्रयास किया। स्त्री ने स्वयं गुलाम रहना चाहती है और न ही पुरुष को गुलाम बनाना चाहती है, यह सिर्फ़ चाहती है मानवीय अधिकार। 'जिस दिन यह समाज स्त्री शरीर का नहीं, शरीर के अंग प्रवर्ण का नहीं, स्त्री की मेधा और श्रम का मूल्य देना सीख जाएगा, सिर्फ़ उसी दिन स्त्री 'मनुष्य' के रूप में स्वीकृत होगी।'

नारी विमर्श :- विकास की राह पर निरंतर अग्रसर होती स्त्री हमेशा से ही विमर्श के खंड में ही रही है। स्त्री विमर्श और कुछ नहीं, अपनी अस्मिता की पहचान 'स्व' की चिंता, अस्तित्व बाँप और अधिकार को जताने और स्वतंत्रता का विचार चिंतन है। जहाँ 'मैं' की चिंता का एहसास है। समझना चाहिए कि यहाँ से 'स्त्री विमर्श' की शुरुवात है। भारतीय हिंदी कोश के अनुसार विमर्श 'पाने 'समीक्षा, परीक्षण, ज्ञान, तर्क, विवेचन, तर्क करनेवाला, उद्घेद, शंभ, विचारणा, व्याकुलता।' स्त्री विमर्श अपने समय और

समज में नारी जीवन की वान्तविकता तथा संभावनाओं की तलाश करनेवाली दृष्टी है। जब भारता की अपेक्षा बुद्धि की कसौटी पर, विभक्ता की अपेक्षा समता की कसौटी पर, परंपरा की अपेक्षा आधुनिकता की कसौटी पर, संस्कृति की अपेक्षा कार्य शांति की कसौटी पर और लिंगालम्बक की अपेक्षा गुणात्मक कसौटी पर व्यक्ति के मूल्यांकन का सुत्रपात होगा तभी स्त्री विमर्श के चिंतन को बल मिलेगा। नासिरा शर्मा नारी विमर्श पर टिपण्णी करते हुए कहती हैं, 'नारी-विमर्श द्वारा साक्षात्कारों से बने आ रहे अंकुश की जंजीरों को तोड़ा जाता है, जो औसत की जवान और जज्बात को बंधे हुए हैं।'⁹

विश्व प्रवेश :- रामचंद्र वर्मा अपने कोश में पीढ़ा की व्याख्या करते हुए लिखते हैं- 'प्राणियों को दूषित या व्यथित करनेवाली यह अग्नि-अनुभूति जो किसी प्रकार का मानसिक या शारीरिक आघात करने, कष्ट पहुँचाने या हानि होने पर उत्पन्न होती है और उसे बहुत ही मिन चिंतित और विकृत रखती है।'¹⁰ समकालीन हिंदी कथा साहित्य में जब जादवानी एक महत्वपूर्ण उपरीभूति है। उसका लेखन संक्रमणशील युग का लेखन है। अपने विचारों में आधुनिकता के कारण जया जादवानी जी समकालीन रचनाओं में अग्रणी हैं। जया जादवानी की कहानियाँ स्त्री मन की पीड़ा, उसके संघर्ष की वान्तविकता की तस्वीर हमारे सामने रखती हैं। जया जादवानी की कहानियाँ नारी-केंद्रित कहे तो कोई अतिशयोक्ति नहीं होगी। जया जादवानी का कहानी संग्रह 'अंधर के प्राणियों में कोई सपना धँपता है' कहानियाँ नारी की घना, पीड़ा, संघर्ष, पारिवारिक समस्याओं की अभिव्यक्ति देती है। मनुष्य एक सामाजिक प्राणी है। समाज में रहकर ही उसकी सभी जरूरतें पूर्ण होती हैं। उसका जीवन संसार में घुसना ही है और इसी संसार में समाज भी होता है। पुरुषों ने अपने आपको इस संसार का स्वामी माना है। वह स्वामी बनकर अपने स्वमित के तहत अपने आपको इस संसार का अकेला उपभोक्ता मानने लगता है। उसकी यह वृत्ति उसकी अर्धांगिनी स्त्री को इस संसार या अपने वैवाहिक जीवन से उदासीन बनाती जा रही है। 'क्यामत का दिन उषा कन्न से बाहर' की नायिका मिसोज नागपाल अपने वैवाहिक कार्यान्वयन से परेशान है। उसका जीवन केवल पंचकत बन गये है। नायिका के पति ने उसे एक कार भी दी है, जिसकी बाधी उसके पति के पास ही रहती थी। पति ने यह कार उसे उन दो सेवकों के लिए दान में दी थी, जिन्हें हर चौबीस घंटे वह बड़ी करमाबदारी से निभाती है। नायिका अपना जीवन पति के दबाव, पूर्ण, तिरस्कार, उर, संकोच में बीता रही थी। अब वह अपना जीवन स्वच्छंदता से गुजारना चाहती थी। इसी इच्छा को लिए वह घर

से बाग निकलती है। पति के रोकने पर वह पति के एक करारा धमक रसीद देती है। कार को जोरदार त्रात जनाकर भाग जाती है। पति विद्यता है, 'चोकीदार पकड़ो इसे'।

'पलश का फूल' कहानी की नायिका अपने मन की इच्छाएँ पति को बताती है, उसे बा-बार गलाती है कि वह उसे समझे, उसका सहवर बने। उसके साथ अपना अलग घर बनाए किंतु पति को नायिका की इच्छा एक आँख नहीं भोंति। कहानी की नायिका पति तथा परिवारवालों के प्रति उदासीन हो जाती है। 'पलश का फूल' की नायिका अपूर्वा पढ़ी-लिखी, स्वाभिमानी और महत्वकांक्षी स्त्री है। वह अपने निर्णय स्वयं लेती है। अपने पिता के नर्जों के खिलाफ जाकर तीन बच्चों के पिता एक विदुर रोहित से शादी के बंधन में बंध जाती है। किंतु समुदाय में उसे अपेक्षा का शिकार होना पड़ता है। घरवाले उसका तिरस्कार करते हैं। अपूर्वा लगभग पौध सालों तक घरवालों के नफरत को झेलती है। रोहित के बच्चे भी उसे माँ का अधिकार नहीं देते। वह इस बर्ताव से झूझती जाती है। अपूर्वा को घर की बेलाग रिश्ते और धा के सदस्यों में कोई कर्क करना मुश्किल नहीं लगता। इस पारिवारिक समस्या से परेशान अपूर्वा पति रोहित को गुस्से में कहती है, 'तुम मेरे सपनों के पुत्र नहीं हो, पुरुष तो वह होता है, जो कुछ दे, कुछ ले, तुम तो न कुछ दे सकते हो और न ले सकते हो। तुम्हारा न लेना मेरी बदनामी ही हो सकती है, न देना मेरी हार नहीं।' 'प्राचीन भारतीय परंपरा में कहा जाता है कि स्त्री का स्थान समाज में सर्वोपरि था। स्त्री प्रधान समाज व्यवस्था की स्थिति शायद ही वैदिक परंपरा से पूर्व ही हो, परंतु जब वे वैदिक परंपरा का परिधातन समाज में हुआ है, तब से लेकर अब तक स्त्री की स्थिति को देखने से पता चलता है कि वह बार-बार अपने ही जीवन साथी से उली चर्च है।

'परिदृश्य' कहानी की नायिका मिसोज गौयल अपने पति के व्यवहार से अब ऊब गई है। रोज छोटी-छोटी बातों को लेकर उसका पति उसे अपमानित करता है। नायिका धरेलू जिम्मेदारियों निभाने में इतनी व्यस्त रहती है कि उसे खुद के लिए एक पल का भी समय नहीं मिलता। पति की आज्ञा का पालन करना उसका परम कर्तव्य हो गया है। खाना तैयार करना, पानी गरम करना, कमीज के बटन लगाना, बच्चों को, पति को टिफिन देना, बच्चों को स्कूल छोड़ना, डॉक्टर के पास ले जाना, पति का ब्रीफकेस तैयार करना आदि काम से उसे कूरस्त नहीं मिलती। इतना काम करने के बावजूद भी उसका पति उसे डाँटता हुआ कहता है, 'ये रोक्य इतनी बंधी क्यों है? क्या करती रहती हो तुम सारा दिन घर पर? कुछ नहीं होता तुमसे?' उसका जीवन

यंत्रण बन जाता है। कुछ नशापान न होने के कारण वैवाहिक जीवन के प्रति वह उदासीन हो जाती है। इसी घुटन से पीड़ित होकर उसमें एक प्रकार की जड़ता आ जाती है। जसा जादवानी जी ने ऐसी नरियों की व्यथा का चित्रण किया है जिनके पति निष्ठुर हैं। जो कुछ सम्भाल नहीं करते। मेलना की कन्या शराब में उतरते हैं। जसा जादवानी जी ने अपनी कहानी 'ये रात कितनी लम्बी है' की नारी की विधवाता, उसके दर्द को प्रस्तुत की है। जो बेकार पति का निर्वाह करती है। नायिका का पति दिन भर घर में टी. वी. के सामने बैठकर शराब पीता है। घर की जिम्मेदारियों, समस्याओं से भागत रहता है। वह अपने कर्तव्य को त्यागकर पानी की कन्या पर अपना जीवन गुजारना चाहता है। अकेले ही परिवार की जिम्मेदारियों को निभाते-निभाते नायिका इन और नन दोनों से पराजित हो जाती है। पति के इस व्यवहार से वह वैवाहिक जीवन के प्रति उदास तथा दुखी हो जाती है।

निर्धर :- जसा जादवानी जी की कहानियों के केंद्र में मध्यमवर्गीय नारी है, जो पारिवारिक समस्याओं से पीड़ित तथा उदासीन है। उन्होंने नारी का इमन, शोचन, स्त्री स्वतंत्रता की भावना आदि दृष्टि से उसके विविध समस्याओं को समाज के सामने रखने का प्रयास किया है। नारी के अंतर्गत अतृप्ति, घुटन, पैदा एकाकीपन की त्रासदी को बर्ताया है। यह नारियां किनी ना किनी ना किनी त्रासदी की शिकार बनें हुई हैं। उपर्युक्त उदाहरणों के आधार पर हम यह कह सकते हैं कि आज भी स्त्रियों की समस्याएँ कम नहीं हुई हैं। कर्क इतना ही है कि उनका स्वरूप बदल गया है।

संदर्भ संकेत :- (1) राष्ट्रवाणी दैनिक, नवंबर-दिसंबर 2010, नगरमोदे अजित, पृष्ठ 47(2) क्रांतिज्योति साप्ताहिक, जिया लाल आर्य, वाणी प्रकाशन, नई दिल्ली, प्रथम संस्करण 2018, पृष्ठ 40(3) औरत के हक में, तसलीमा नसरीन, वाणी प्रकाशन, नई दिल्ली, पृष्ठ संख्या 69 (4) भारतीय हिंदी कोश, दक्षिण भारत हिंदी प्रचार सभा, सहाय, प्रथम संस्करण, अगस्त 1956, पृष्ठ 84(5) औरत के लिए औरत, नासिरा शर्मा, सामाजिक प्रकाशन 2003, नई दिल्ली, पृष्ठ 32(6) मानक हिंदी कोश, रामचंद्र वर्मा, खण्ड 3, पृष्ठ 518(7) अंधेरे के पक्षियों में कोई सपना कौपल है, जसा जादवानी, वाणी प्रकाशन, प्रथम संस्करण 2002, नई दिल्ली, पृष्ठ(8)वारी, पृष्ठ 18(9)वही, पृष्ठ 53

1. 'सदाचार का तथैव' कहानी के आधार

- डॉ. विष्णु शंकर

सहायक प्राध्यापक, हिन्दी विभाग,
पद्मनभ संस्कृत विश्वविद्यालय, पद्मनूर कन्नूर जिल्ला, केरल

हिन्दी साहित्य में सदाचार का चर्चा परसाई का साहित्य में परापूर्व अपनी अर्थ शैली को लेकर हुआ है। पिछले कई सालों से उनके जन्मदिन के साहित्यिक प्रोग्रामों की रचनाओं पर कई साहित्यिक कार्यक्रम आयोजित करते रहते हैं। उनकी जन्मशताब्दी भी बहुत निकट है। इसलि सदाचार ही उनका साहित्य सर्वांशों के केंद्र में आया है। हिन्दी साहित्य में व्यंग्य का प्रयोग के रूप में प्रतिष्ठित करने में उनका योगदान अत्यंत महत्वपूर्ण है। परसाई पूरे हिन्दी साहित्य में व्यंग्य सम्राट के रूप में विख्यात हुए। हिन्दी साहित्य में भारतीय युग से ही व्यंग्य का प्रयोग हुआ लेकिन साहित्य में व्यंग्य को प्रतिष्ठित करने का श्रेय परसाई को ही जाता है। उन्होंने अपनी स्वतः सिद्ध शैली में प्रभावशाली व्यंग्य का प्रयोग किया तथा शैली मात्र से एक विधा के रूप में प्रतिष्ठा की। स्वयं में कहा जाए तो भारतीय और विदेशी युगों में व्यंग्य के प्रयोग में सबसे ज्यादा सफलता परसाई ने ही पाई।

सामाजिक कृत्रिमता, लोकांतर में व्यंग्य उदघर्षनों को सुधारने के लिए व्यंग्य के माध्यम से व्यंग्य को अपनाया। उनके ही शब्दों में 'व्यंग्य जीवन से सकारात्मक करता है जीवन को अलगाव करता है। विसंश्रितियों, विधवाओं और बाधों का निवारण करता है। यह बता रही है, मैं कह रहा हूँ कि जीवन के लोकांतर में ही निष्ठा होती है। जितनी गंभीर रचनाकार साहित्यिक उदघर्षन यह जीवन के प्रति दृष्टि का अनुभव करता है, उतना ही सतर्कता से बाध भी जन्मानस बाध नहीं हुआ। स्वतंत्रता के क हस्तारण के लिए गये थे। सतर्क में अंधों का स्वयं को भ्रमों में गिराने का। उन लोगों ने लोकांतर के सभी खानों का फाँदा उड़ाया। व्यंग्य उन मसक बन गया। लोकांतर में तैनी संन किया। कार्यपालिका, न्यायपालिका अंतर्गत। परसाई जी इसका सुझाव देने के लिए तैयार न था। व्यंग्य के माध्यम से सत्ताधारियों को लोकांतर को एक-एक करके उखाड़ना के समर्थ प्रस्तुत किया। राजनीतिक गण, अफसाना, उपन्यास, पुस्तिका जैसे सरकार और व्यंग्य को बोधा देनेवाले सभी वर्गों में व्यंग्य के कलम के शिकार हुए। परसाई सदाचार को वर्तमान भारतीय लोकांतर को सबसे बड़ी चुनौती मानते हैं। अवसर पर सदाचार को लोकांतर विचार करना जरूरी है। अंधों को सदाचार के लिए 'कारण' का प्रयोग होता है। लेकिन भाषा के कठिनाई से इसकी व्यवस्था नहीं। इसका सामान्य अर्थ 'नैतिकता का हाथ सामान्य स्तर से नीचे गिरना, स्थिति का विवरण आदि है।' 2 प्रतिष्ठ समाज शास्त्री देविद शैलम ने करकल शब्द की व्याख्या इस प्रकार



30.हिंदी एवं मराठी कथा साहित्य में आदिवासी विमर्श**-¹सौ.आरती पराग देशपांडे ²डॉ.शेख मोहम्मद शाकिर शेख****बशीर**

¹शोधार्थी—प्रा.रामकृष्ण मोरे कला, वाणिज्य एवं विज्ञान महाविद्यालय, आकुर्डी, पुणे. ²सहयोगी प्राध्यापक, पुना साइंस, आर्ट्स एवं कॉमर्स महाविद्यालय, कॅम्प, पुणे.

साहित्य का मूलभूत सरोकर जीवन से है। इससे विमुख होकर उसका कोई अस्तित्व नहीं, अब कोई रचना अपने समय और समाज की संवेदना की प्रस्तुत करती है। तब वह प्रासंगिक बनती है। 20 वीं शताब्दी में विमर्शों को आधार बनाकर समाज-शास्त्रीय रचनात्मक आग्रह जब से बढ़े हैं तब से सबसे पिछड़े तबकों को केन्द्र में रखकर साहित्यिक विमर्श या परिचर्चा का दौर शुरु हुआ। जैसा की विदित है साहित्य समाज का दर्पण है और इस दर्पण में अनेकों विमर्शों की छवि उनके स्वरूप देखने को मिलते हैं सवाल यह उठता है कि क्या? इस दर्पण में समता, अखण्डता, समभाव, सहजता, एकता की स्पष्ट छवि देखी जा सकती है। और इन्हीं प्रश्नों के हल खोजने के लिए समय-समय पर साहित्य के माध्यम से इन विषयों को केंद्र में रखकर समीक्षक, आलोचक, कथाकार बड़े पैमाने "विमर्श" के जरिए लोक चेतना जाग्रित करने का महत् कार्य करते हैं।

आधुनिक साहित्य में वर्तमान में 'विमर्शों' के प्रधान केंद्र पर आदिवासी लेखन, आदिवासियत और उनका साहित्य जोरों पर हैं। भले ही हिंदी साहित्य में यह नया विमर्श न हो पर अन्य भाषाओं के साहित्य में नव विमर्श हो सकता यही प्रयास हिंदी एवं मराठी कथा साहित्य में आदिवासी विमर्श की रेखांकित करने का प्रयास है। आदिवासी समाज या उनके जीवन के बारे में किया

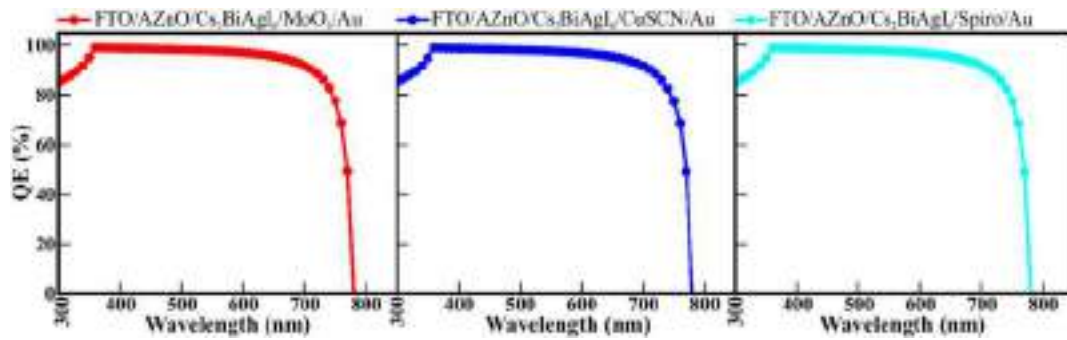


Figure 8. Quantum efficiency curves for the $\text{Cs}_2\text{BiAgI}_6$ -based double perovskite solar cells comprising various HTLs (MoO_3 / CuSCN / Spiro-OMeTAD).

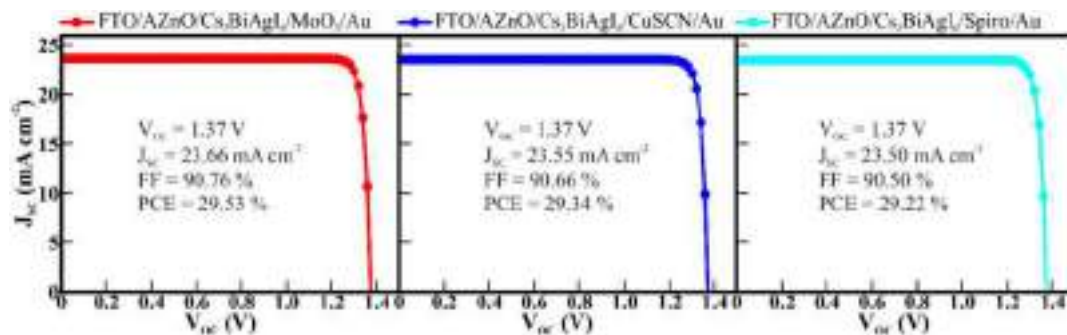


Figure 9. J - V curves for the $\text{Cs}_2\text{BiAgI}_6$ -based double perovskite solar cells comprising various HTLs (MoO_3 / CuSCN / Spiro-OMeTAD).

efficiency or quantum efficiency. The quantum efficiency of the $\text{Cs}_2\text{BiAgI}_6$ -based double perovskite solar cells is shown in **Figure 8**. $\text{Cs}_2\text{BiAgI}_6$ -based double perovskite solar cells with different HTLs showed a broad absorption in the complete visible range (400–800 nm). Further, the J - V curves of $\text{Cs}_2\text{BiAgI}_6$ -based double perovskite solar cells with different HTLs are shown in **Figure 9**. The optimum solar cell parameters evaluated for all $\text{Cs}_2\text{BiAgI}_6$ -based solar cells show high efficiency of $\approx 29\%$. The solar cells show V_{OC} , J_{SC} , and FF in the range of ≈ 1.37 V, ≈ 23 mA cm^{-2} , and $\approx 90\%$, respectively.

4. Conclusion

In conclusion, the theoretical potential of the $\text{Cs}_2\text{BiAgI}_6$ double perovskite light harvester is evaluated using the SCAPS-1D software package. $\text{Cs}_2\text{BiAgI}_6$ light harvesters are environmentally benign and render long-term stability. The high-efficiency solar cells are optimized based on the AZnO ETL and three different HTLs. Solar cells based on all three HTLs at optimized conditions delivered PCEs $\approx 29\%$. Compared to all the physical parameters varied in the optimization, the thickness and bulk defect density of the $\text{Cs}_2\text{BiAgI}_6$ double perovskite light harvester had the highest control over performance. The cheap and economical carbon electrodes could deliver a PCE of $\approx 29\%$ in the modeled $\text{Cs}_2\text{BiAgI}_6$ -based double perovskite solar cells. Further, even when the operating temperature shoots up to 400 K, the $\text{Cs}_2\text{BiAgI}_6$ -based double perovskite solar cells delivered a PCE of $\approx 26\%$. Therefore, while experimentally fabricating

$\text{Cs}_2\text{BiAgI}_6$ double perovskite solar cells, it should be noted that $\text{Cs}_2\text{BiAgI}_6$ perovskite is unstable. Hence, it is imperative to produce films with very low bulk defect density and prefer a practical rear contact. The present preliminary analysis accurately illustrates the factors which govern the PCE of $\text{Cs}_2\text{BiAgI}_6$ solar cells. The procedure employed in this assessment can provide guidelines for experimental implementation and be further expanded to examine additional light harvesters for optoelectronic applications.

Acknowledgements

The authors would like to thank Mr. Marc Burgelman, the Electronics and Information Systems (ELIS), University of Ghent, Belgium, for providing them free access to the SCAPS 1D simulation tool on request. V.M., E.C., M.S., and S.S. thank Prof. Rupesh S. Devan, Department of Metallurgy Engineering and Materials Science, Indian Institute of Technology Indore, for providing infrastructure.

Conflict of Interest

The authors declare no conflict of interest.

Data Availability Statement

The data that support the findings of this study are available from the corresponding author upon reasonable request.

Keywords

Cs₂BiAgI₆ double perovskite, lead-free, 1D Solar Cell Capacitance Simulator (SCAPS-1D), simulation, solar cells

Received: September 15, 2022

Revised: November 3, 2022

Published online:






- [1] T. Baikie, Y. Fang, J. M. Kadro, M. Schreyer, F. Wei, S. G. Mhaisalkar, M. Graetzel, T. J. White, *J. Mater. Chem. A* **2013**, *1*, 5628.
- [2] M. M. Lee, J. Teuscher, T. Miyasaka, T. N. Murakami, H. J. Snaith, *Science* **2012**, *338*, 643.
- [3] H. S. Jung, N.-G. Park, *Small* **2015**, *11*, 10.
- [4] V. Manjunath, S. Bimli, P. Shaikh, S. Ogale, R. S. Devan, *J. Mater. Chem. C* **2022**, *10*, 15725.
- [5] J. Jeong, M. Kim, J. Seo, H. Z. Lu, P. Ahlawat, A. Mishra, Y. G. Yang, M. A. Hope, F. T. Eickemeyer, M. Kim, Y. J. Yoon, I. W. Choi, B. P. Darwich, S. J. Choi, Y. Jo, J. H. Lee, B. Walker, S. M. Zakeeruddin, L. Emsley, U. Rothlisberger, A. Hagfeldt, D. S. Kim, M. Gratzel, J. Y. Kim, *Nature* **2021**, *592*, 381.
- [6] S. Chand Yadav, A. Srivastava, V. Manjunath, A. Kanwade, R. S. Devan, P. M. Shirage, *Mater. Today Phys.* **2022**, *26*, 100731.
- [7] H. Kim, K. A. Huynh, S. Y. Kim, Q. V. Le, H. W. Jang, *Phys. Status Solidi RRL* **2020**, *14*, 1900435.
- [8] M. M. Tavakoli, Z. Fazel, R. Tavakoli, S. Akin, S. Satapathi, D. Prochowicz, P. Yadav, *Sol. RRL* **2022**, *6*, 2200106.
- [9] V. Manjunath, P. K. Mishra, R. Dobhal, S. Birli, P. M. Shirage, S. Sen, P. A. Shaikh, R. S. Devan, *ACS Appl. Electron. Mater.* **2021**, *3*, 4548.
- [10] S. Ma, Y. Bai, H. Wang, H. C. Zai, J. F. Wu, L. Li, S. S. Xiang, N. Liu, L. Liu, C. Zhu, G. L. Liu, X. X. Niu, H. N. Chen, H. P. Zhou, Y. J. Li, Q. Chen, *Adv. Energy Mater.* **2020**, *10*, 1902472.
- [11] A. H. Slavney, T. Hu, A. M. Lindenberg, H. I. Karunadasa, *J. Am. Chem. Soc.* **2016**, *138*, 2138.
- [12] S. C. Yadav, V. Manjunath, A. Srivastava, R. S. Devan, P. M. Shirage, *Opt. Mater.* **2022**, *132*, 112676.
- [13] Z. W. Xiao, W. W. Meng, J. B. Wang, Y. F. Yan, *Chemsuschem* **2016**, *9*, 2628.
- [14] X. B. Kong, Y. Q. Wu, F. Xu, S. K. Yang, B. Q. Cao, *Phys. Status Solidi RRL* **2021**, *15*, 2100134.
- [15] Q. H. Chen, K. M. Deng, Y. Shen, L. Li, *Infomat* **2022**, *4*, e12303.
- [16] J. N. Li, X. H. Meng, Z. H. Wu, Y. Y. Duan, R. X. Guo, W. D. Xiao, Y. S. Zhang, Y. K. Li, Y. L. Shen, W. Zhang, G. S. Shao, *Adv. Funct. Mater.* **2022**, *32*, 2112991.
- [17] K. Z. Du, W. W. Meng, X. M. Wang, Y. F. Yan, D. B. Mitzi, *Angew. Chem., Int. Ed.* **2017**, *56*, 8158.
- [18] A. H. Slavney, L. Leppert, D. Bartesaghi, A. Gold-Parker, M. F. Toney, T. J. Savenije, J. B. Neaton, H. I. Karunadasa, *J. Am. Chem. Soc.* **2017**, *139*, 5015.
- [19] Q. Li, Y. G. Wang, W. C. Pan, W. G. Yang, B. Zou, J. Tang, Z. W. Quan, *Angew. Chem., Int. Ed.* **2017**, *56*, 15969.
- [20] X. G. Zhao, D. Yang, J. C. Ren, Y. Sun, Z. Xiao, L. Zhang, *Joule* **2018**, *2*, 1662.
- [21] M. R. Filip, S. Hillman, A. A. Haghighirad, H. J. Snaith, F. Giustino, *J. Phys. Chem. Lett.* **2016**, *7*, 2579.
- [22] X. Y. Zhao, H. P. Shen, Y. Zhang, X. Li, X. C. Zhao, M. Q. Tai, J. F. Li, J. B. Li, X. Li, H. Lin, *ACS Appl. Mater. Interfaces* **2016**, *8*, 7826.
- [23] J. Kruszynska, J. Ostapko, V. Ozkaya, B. Surucu, O. Szawcow, K. Nikiforow, M. Holdynski, M. M. Tavakoli, P. Yadav, M. Kot, G. P. Kolodziej, M. Wlazlo, S. Satapathi, S. Akin, D. Prochowicz, *Adv. Mater. Interfaces* **2022**, *9*, 2200575.
- [24] S. Mandati, K. R. Dileep, G. Veerappan, E. Ramasamy, *Solar Energy* **2022**, *240*, 258.
- [25] S. Maniarasu, M. K. Rajbhar, R. K. Dileep, E. Ramasamy, G. Veerappan, *Mater. Lett.* **2019**, *245*, 226.
- [26] S. Seo, K. Akino, J. S. Nam, A. Shawky, H. S. Lin, H. Nagaya, E. I. Kauppinen, R. Xiang, Y. Matsuo, I. Jeon, S. Maruyama, *Adv. Mater. Interfaces* **2022**, *9*, 2101515.
- [27] V. Manjunath, S. Bimli, K. H. Parmar, P. M. Shirage, R. S. Devan, *Sol. Energy* **2019**, *193*, 387.
- [28] V. Karthikeyan, S. Maniarasu, V. Manjunath, E. Ramasamy, G. Veerappan, *Sol. Energy* **2017**, *147*, 202.
- [29] V. Manjunath, Y. K. Reddy, S. Bimli, R. J. Choudhary, R. S. Devan, *Mater. Today Commun.* **2022**, *32*, 104061.
- [30] M. Alla, V. Manjunath, N. Chawki, D. Singh, S. C. Yadav, M. Rouchdi, F. Boubker, *Opt. Mater.* **2022**, *124*, 112044.
- [31] M. Mottakin, K. Sobayel, R. C. Ismail, M. Shahiduzzaman, G. Muhammad, M. A. Ibrahim, M. Akhtaruzzaman, E. S. Hossain, *Phys. Status Solidi RRL* **2022**, *16*, 2200216.
- [32] M. Alla, S. Bimli, V. Manjunath, M. Samtham, A. Kasaudhan, E. Choudhary, M. Rouchdi, F. Boubker, *Mater. Technol.* **2022**, *37*, 2963.
- [33] D. K. Sarkar, A. K. M. Hasan, M. Mottakin, V. Selvanathan, K. Sobayel, M. A. Islam, G. Muhammad, M. Aminuzzaman, M. Shahiduzzaman, K. Sopian, M. Akhtaruzzaman, *Sol. Energy* **2022**, *243*, 215.
- [34] K. Sobayel, M. Shahinuzzaman, N. Amin, M. R. Karim, M. A. Dar, R. Gul, M. A. Alghoul, K. Sopian, A. K. M. Hasan, M. Akhtaruzzaman, *Sol. Energy* **2020**, *207*, 479.
- [35] Y. K. Reddy, V. Manjunath, S. Bimli, R. S. Devan, *Sol. Energy* **2022**, *244*, 75.
- [36] I. Mesquita, L. Andrade, A. Mendes, *Chemsuschem* **2019**, *12*, 2186.
- [37] F. Haque, M. Mativenga, *Phys. Status Solidi RRL* **2021**, *15*, 2100211.
- [38] A. Ait Abdelkadir, E. Oublal, M. Sahal, A. Gibaud, *Results Opt.* **2022**, *8*, 100257.
- [39] S. Srivastava, A. K. Singh, P. Kumar, B. Pradhan, *J. Appl. Phys.* **2022**, *131*, 175001.
- [40] S. Ahmed, F. Jannat, M. A. K. Khan, M. A. Alim, *Optik* **2021**, *225*, 165765.

REVIEW



Cite this: *J. Mater. Chem. C*, 2022, 10, 15725

Understanding the role of inorganic carrier transport layer materials and interfaces in emerging perovskite solar cells

Vishesh Manjunath,  †^a Santosh Bimli,  †^a Parvez A. Shaikh,  ^{ab}
Satishchandra B. Ogale  *^{cd} and Rupesh S. Devan  *^a

In the last decade, organic–inorganic hybrid and metal halide perovskite materials have shown tremendous tunability properties and capacity to harvest solar energy efficiently via conceptually new solar cell architectures. Presently, third-generation thin-film solar cells employing perovskite light absorbers produce a power conversion efficiency of ~25%, which is attributed to their exceptionally unique and device-worthy optoelectronic properties. Although the perovskite light absorbers play a main role in the harvesting process, the corresponding device architectures must contain other backing layers such as electron and hole transport layers, which are crucial for the efficient and stable electronic functioning of the solar cell. Thus, understanding the functional significance of these transport layers and synergistically optimizing them with respect to the perovskite light absorbers is highly significant for further developments in this arena. Therefore, this review focuses and critically analyses the electron and hole transport layers used in perovskite solar cells, highlighting their functional significance and critical role. Their functionality basically originates from their crystal structure, chemistry, electronic and optical properties, and compatibility with the corresponding synthesis protocols of perovskites. Overall, this work aims at developing a comparative analysis and enhanced understanding of the transport of photogenerated charges across the active interfaces in the perovskite solar cells.

Received 11th July 2022,
Accepted 5th September 2022

DOI: 10.1039/d2tc02911a

rsc.li/materials-c

^a Department of Metallurgy Engineering and Materials Science, Indian Institute of Technology Indore, Khandwa Road, Simrol, 453552, India. E-mail: rupesh@iiti.ac.in

^b Department of Physics, AKI's Poona College of Arts, Science and Commerce, Pune, Maharashtra, 411001, India

^c Department of Physics and Centre for Energy Science, Indian Institute of Science Education and Research, Pune 411008, India. E-mail: satishogale@iiserpune.ac.in

^d Research Institute for Sustainable Energy (RISE), TCG Centres for Research and Education in Science and Technology (TCG-CREST), Kolkata 700091, India.

E-mail: satish.ogale@tcgcrest.org

† Authors share equal authorship.



Vishesh Manjunath

Vishesh Manjunath received his Master's Degree (2016) in Nanotechnology from VIT University, Vellore, India. In 2017, he joined Dr Rupesh's research group for a PhD program in the Department of Metallurgy Engineering and Materials Science at the Indian Institute of Technology Indore, India. His research interests include photovoltaics, thin-film technology, green hydrogen generation, visible and ultraviolet light sensors and the fabrication of optoelectronic devices.



Santosh Bimli

Santosh Bimli received his Master's Degree (2019) in Material Science Engineering from the Indian Institute of Technology Indore, India. In 2019, he joined Dr Rupesh's research group for a PhD program in the Department of Metallurgy Engineering and Materials Science at the Indian Institute of Technology Indore, India. His research interests include developing nanostructures for optoelectronic applications like Hybrid thin film solar cells, resistive switching devices, photodetector, and magneto-optics.

1. Introduction

Renewable energy has shown great promise to combat the emerging energy demand globally, with its contribution to the energy sector increasing fairly rapidly.¹ Among the renewable energy resources and their harvesting approaches, solar energy conversion into electrical energy has shown excellent promise towards sustainable development.² Solar cells are devices that convert incoming light energy into usable electrical energy. Although a myriad of efforts has been undertaken in the past 50 years to achieve a high power conversion efficiency (PCE) through different solar cell designs and architectures, a knowledge gap still persists in the comprehensive understanding of how different material interfaces can affect the overall advancement of solar cell technology.³



Parvez A. Shaikh

Dr Parvez Shaikh is currently a SERB-TARE Fellow in Dr Rupesh's group at the Indian Institute of Technology Indore, India, and working (since 2017) as an Assistant Professor of PHYSICS at AKI's Poona College of Arts, Science & Commerce, Pune, India. He has worked as a Post-Doctoral Fellow at King Abdullah University of Science and Technology (KAUST), Kingdom of Saudi Arabia (2014–2017). He was also CSIR-Research Associate (2011–2014) at the National Chemical Laboratory (NCL) Pune, India. His research interests are hybrid optoelectronic materials, solar cells, and devices for energy conversion.

Silicon-based solar cells are one of the earliest solar cells making use of crystalline silicon with a bandgap of 1.11 eV, which is well-positioned in the optimum range for broadband light absorption. At present, first-generation silicon solar cells continue to dominate this field, with significant progress being made towards a high photovoltaic conversion efficiency (PCE) due to the developed purification and fabrication technology and earth abundance of the required materials.⁴ Recently, the greater supply than demand has also reduced the costs of other materials, and thus the corresponding improved yields have reduced the projected price of photovoltaic technology.⁵ Moreover, over the years, various materials such as amorphous-Si, GaAs, CdTe/Se, PbSe/S, CIGS, and CZTS have been successfully deposited and optimized into thin films with required thickness and quality and are used as absorbers in second-generation solar cells to further address and combat related problems.^{6–11} The advantages of these second-generation solar cells include their low production cost, flexibility, and light weightness.¹²

During the last few decades, third-generation solar cells based on nanocrystals, polymers, sensitized dyes, organic-inorganic and inorganic halide perovskites have shown tremendous progress bringing a high degree of novelty and versatility in both the design of new materials and solar cell architectures.^{13–16} Specifically, the emerging perovskite solar cells (PSCs) have gained enormous interest in the last decade with the corresponding conversion efficiency (~25%) competing with their first-generation silicon counterparts.¹⁷ Also, the newly introduced perovskite/Si tandem cells have already delivered a remarkable efficiency of 29.5% (refer to the NREL website for more details).

Hybrid perovskites are molecularly assembled organic-inorganic compounds that absorb incoming light energy efficiently across a significant portion of the solar spectrum. They can be highly tuned to generate various desirable optical and



Satishchandra B. Ogale

Research Scientist at the University of Maryland, College Park (1996–2006). He has performed research for many years on advanced functional materials for energy applications which includes hybrid perovskite and solar cells, green energy and energy storage devices, photocatalytic water splitting and CO₂ reduction.

Prof. (Dr) Satishchandra Ogale is currently a Professor Emeritus, IISER Pune and Director, Research Institute for Sustainable Energy (RISE), Salt Lake, Kolkata, India. Previously he was a Raja Ramanna Fellow of the Department of Atomic Energy (2019–20), Professor of Physics at IISER Pune (2015–18), Academy of Scientific and Innovative Research (AcSIR, CSIR), New Delhi (2006–15), and Pune University (1980–96). He was also a Visiting Professor and Senior



Rupesh S. Devan

architectures and hybrid materials for applications in supercapattery, solar cells, photodetectors, green hydrogen generation, and water remediation.

Dr Rupesh Devan is currently an Associate Professor in the Department of Metallurgy Engineering and Materials Science at the Indian Institute of Technology Indore, India. Before receiving the INSPIRE Faculty Award (2014) from the Department of Science and Technology (DST) India, he worked as a Post-Doctoral Fellow at National Dong Hwa University, Taiwan (2007–2013). His research areas include developing nano-hetero-

optoelectronic properties. These organo-inorganic perovskite materials form the ABX_3 structure, where A represents an organic cation ($CH_3NH_3^+$, Cs^+ , etc.), B represents a divalent metal (Pb^{2+} , Sn^{2+} , etc.) and X is a halogen (Cl^- , I^- , and Br^-). The size of these three ions is strictly confined by the tolerance factor (t) for a stable perovskite structure.¹⁸ Moreover, the perovskite light absorbers possess a high absorption coefficient in the visible region (~ 350 to 800 nm), high extinction coefficient ($\sim 10^4$ cm^{-1} at 550 nm), long charge diffusion lengths, and ease of processing, which have led to the fabrication of low-cost PSCs at room temperature consuming a lower amount of material.¹⁹ These intrinsic properties of perovskite light absorbers can be tailored to meet the requirements by merely substituting the ions in perovskite materials.²⁰ However, compared to the perovskite light absorbers, the transport layers are equally important in the solar cell design to render high efficiency and stability.

Two different carrier-selective transport layers are required to achieve effective carrier extraction at both external terminals. These transport layers preferably perform selective charge carrier extraction (*i.e.*, n-type or p-type) by blocking the transport of the other (*i.e.*, p-type or n-type). The deposition of a p or n type transport layer on the light exposure side of the solar cell first, followed by an intrinsic layer results in the device configuration of the conventional negative–intrinsic–positive (n–i–p) and inverted positive–intrinsic–negative (p–i–n). Theoretically, both the (n–i–p) and (p–i–n) device architectures should give the same efficiency, but they differ due to their optical properties, transmittance in the UV-Vis-NIR region, material compatibility, and formation of an ohmic contact with the transparent side of the electrode. Additionally, the investigation of an inverted (p–i–n) architecture that alters optical behaviour was reported in the literature.²¹ Generally, the recombination process involves both types of carriers present within the proximity of the charge diffusion pathway, where the extraction of particular types of charge carriers at different ends will reduce their recombination. However, various other qualities such as high conductivity for selected carrier types, reduction of the unfavourable effect at the interfaces, closely matching mobilities of the charge carriers across the interface and tuning of the bandgap for smooth charge transfer of the interfacial charge carrier-type selective transport layers contribute to the realization of high efficiency in PSCs.

In this review, we critically discuss and compare different possible inorganic transport layers (electrons and holes) mainly used for the PSCs. The functionalities, properties, and requirements of these transport layers to achieve efficient PSCs are the main focus. We primarily present, analyse, and discuss the developments pertaining to highly efficient inorganic electron transport layers (ETLs) composed of TiO_2 , SnO_2 , ZnO , and ternary metal oxides and hole transport layers (HTLs) composed of NiO_x , VO_x , CoO_x , CuO , CuI , and $CuSCN$. Further, the effect of the physical, chemical, and photoelectrical properties of these widely used inorganic transport layers on the performance of PSCs is discussed in depth. Finally, we also include a brief section on the most extensively used organic transport layers towards the end of this review article.

2. Importance of transport layers

The transport layers in PSCs perform specific functions similar to that in dye-sensitized solar cells (DSSCs) (Fig. 1). However, the term ‘division of labour’ has been widely used to understand the functionalities of each component in PSCs,²² which include (i) perovskite light absorber: absorbs the majority of the solar spectrum and creates electron–hole pairs, (ii) transport layers: selectively dissociate the excitons generated in the light absorber, and (iii) electrodes: establish an electronic high-quality interface between the device and the external circuit with minimal resistance. Accordingly, the systematic synchronization of these basic components in terms of optical, chemical, structural, and electronic properties leads to a high performance in PSCs. The range of coverage, uniformity, and thickness of the transport layers depend on the employed coating technique. Notably, the interface at the transport layer/perovskite absorber plays a crucial role in the overall device performance. Depending on the structure of the employed transport layers, PSCs are classified into planar and mesoporous device architectures (Fig. 2). Theoretically, the device architecture with a larger charge diffusion length (L_d) than the thickness of the perovskite absorber (t) (*i.e.*, $L_d > t$) is identified as a planar device architecture, which is the opposite in the mesoscopic device architecture (*i.e.*, $L_d < t$). This structure is further divided into two configurations, namely,

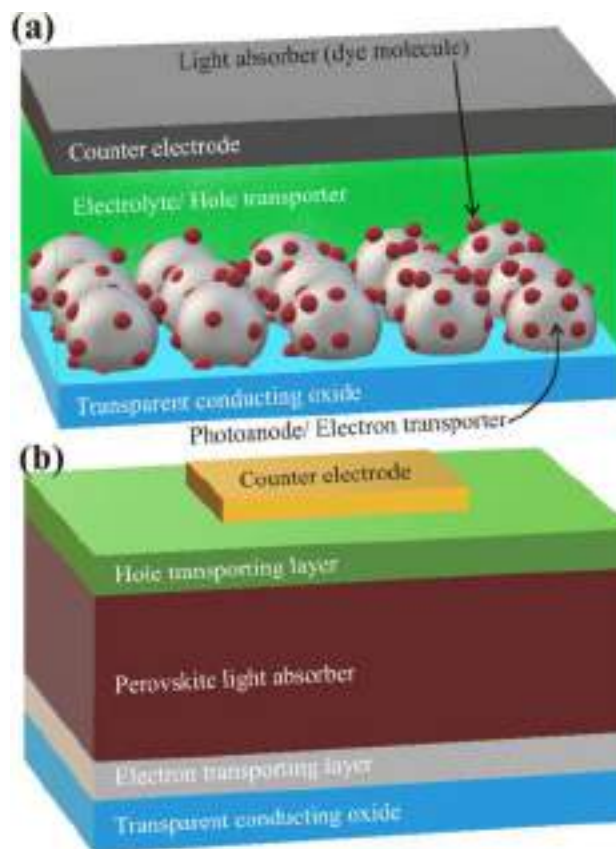


Fig. 1 Schematic representation of (a) dye-sensitized solar cell (*i.e.*, DSSC) and (b) perovskite solar cells (*i.e.*, PSC).

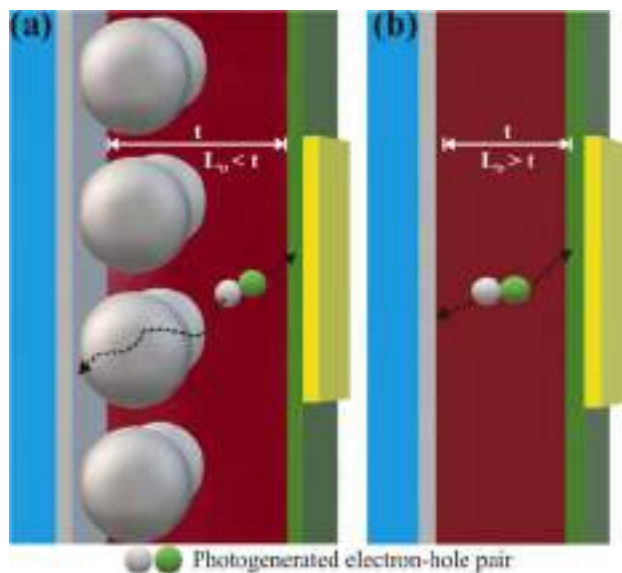


Fig. 2 Schematic of (a) mesoporous and (b) planar PSC.

regular planar with negative intrinsic positive (n-i-p) and inverted planar with positive intrinsic negative (p-i-n), to facilitate excellent optical transparency in the transport layer and allow maximum light illumination on the perovskite-like absorber.²³ Alternatively, the mesoporous structure demonstrates a large effective interface between the transport layer and perovskite, facilitating dissociation of the generated excitons, but lacks charge collection efficiency due to the grain boundary-assisted recombination.²⁴ The transport layers are found to guide the growth of the perovskite absorber, but the lattice mismatch between the perovskite and transport layers alters the charge transport. Also, chemical compatibility aspects such as stability and reactivity of the transport layer with the perovskite layer are equally important. Moreover, the transport layers optically protect the perovskite absorber from high-energy UV radiation, enhancing the device stability. Leijtens *et al.*²⁵ observed higher stability in mesoscopic PSCs sensitized with metal oxide than non-sensitized PSCs. The surface-adsorbed oxygen states of metal oxides possess deep trap sites for the injected electrons upon continuous exposure to the UV spectrum and may leak into the hole transport material. Furthermore, the presence of defects, interstitials, and impurities in the transport layer, and thereby at its interface with perovskite, strongly influences the charge mobility, transport, and recombination. The oxygen vacancies and interstitial atoms at the interface are known to create shallow or deep levels near the band edge, which form recombination centres.²⁶ Therefore, the selection of defect tolerant interfaces is a prerequisite for smooth charge transfer and to avoid charge recombination. The charge mobilities of the transport layers, when closely matched with the perovskite light absorber, drastically reduce the charge accumulation at the transport layer/perovskite interface and enhance the collection efficiency. Therefore, engineering of the transport layers by doping, faceting, or growing heterostructures is required to address these charge recombination issues.^{27–31} Although a

wide range of transport layers has been employed to efficiently transport electrons from the perovskite absorbers to the contacts, the bandgap and band alignment of the transport layers with perovskite light absorbers are fundamental prerequisites for the fabrication of a working device. Usually, wide bandgap semiconductors are employed to allow the maximum visible spectrum illumination on the perovskite films. Band alignment or band edge alignment guides the electrons through the transport layers to reduce the leakage of excited charges in the opposite direction. Besides these functionalities, the ease of processing, use of earth abundant materials, chemical stability, stability under light illumination, non-toxicity, and feasibility of real-time operation are the main concerns to realize the commercial availability of PSCs. Usually, the high processing temperature of metal oxides restricts the use of plastic substrates in PSCs. Overall, in the continuing search for ideal transport layers, different material systems with a wide range of approaches are discussed in the present review.

3. Role of interface and carrier transport in PSCs

3.1 Interfaces

When the perovskite layer absorbs light, the photo-generated charge carriers drift towards the respective interfaces (perovskite/ETL or perovskite/HTL) under the influence of the built-in electric field, where an ultrafast charge extraction process takes place. The efficient charge extraction depends on smooth charge transport through the interface, which is hindered by peculiar features related to the interface such as the surface energy of the two constituent layers, energy level alignment at the interface, interfacial layer, defects, mobile ions, trap states, charge recombination, and charge accumulation. These obstructions result in the recombination of charges, hysteresis effect, and light soaking in PSCs. Consequently, the precise control of these issues (discussed here and shown in Fig. 3) strongly influences the performance and stability of PSCs, which is discussed in detail in this review.

The understanding and investigation of the reasons for the recombination process in the perovskite layer and at the interface are imperative not only to control it but also to narrow the interface engineering schemes, which can be done with the help of a differential equation expressed as follows:

$$\frac{dp(t)}{dt} = -r_3p^3 - r_2p^2 - r_1p \quad (1)$$

where p is the photo-induced charge carrier density, and r_1 , r_2 and r_3 are trap-assisted (mono-molecular), interfacial (bi-molecular), and auger recombination rate constants, respectively. The latter is negligible due to the wide bandgap nature of perovskite materials. The charge recombination in the perovskite is also significantly less for highly crystalline perovskite films. The dominant recombination is mainly due to the second-order, *i.e.*, interfacial (bimolecular), recombination arising from (i) structural defects in the perovskite layer emanating

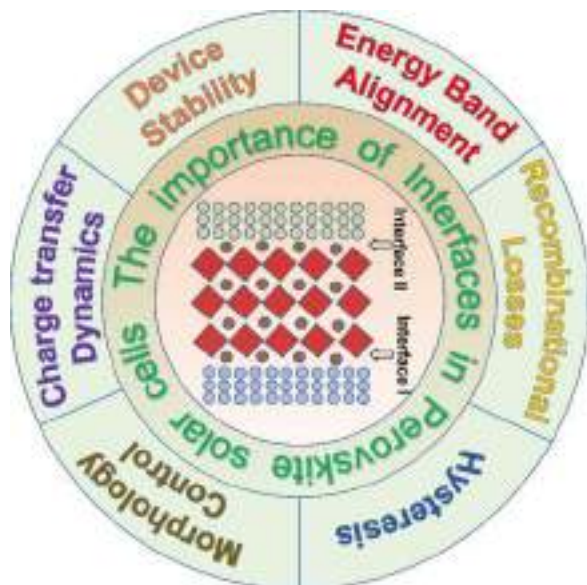


Fig. 3 Schematic illustrating the importance of interfaces in PSCs.

from the lattice mismatch and thermal vibration, (ii) energy offset between the perovskite and transport layers, (iii) surface defects present in the transport materials such as ZnO and SnO₂ (ETL) and NiO (HTL), and (iv) difference in the charge carrier mobility of perovskite and transport layers.³²

The charge dynamics, including extraction, transfer, and recombination of charge carriers, happens at the interface. Charge extraction is a very fast process and takes a few hundred picoseconds, which is significantly less than the lifetime of the charge carriers (around a few nanoseconds). Although the charge extraction process is hindered by the presence of PbI₂ at the surface of the perovskite, surface modification has become a prime requirement.^{33,34} Furthermore, the hole traps resulting from the under-coordinated halide anions on the crystalline surface of MAPbI₃ thin films can induce significant charge accumulation at the perovskite/HTL interface.³⁵ These trap states existing at the interface can be eliminated by interface engineering to reduce the recombination rate and improve the charge transfer. Also, it has been perceived that the passivation of trap states can eradicate the hysteresis anomaly. Another obstruction for efficient charge extraction is the migration of ions present in the perovskite (MA⁺, Pb²⁺, and I⁻) towards the interface, which can also affect the device performance. These ions have low activation barriers and ionic diffusion coefficients to move within the perovskite, especially when the device is exposed to light illumination.³⁶

Another important feature is the energy level alignment at the interface, which is essential for smooth charge transportation. Generally, a band offset of ~0.2 eV is required for efficient charge transfer at the perovskite/ETL interface. Further, the appropriate tailoring in the energy level alignment allows smooth charge transportation, which results in a higher short circuit current density (J_{sc}) and fill factor (FF). Also, an increase in the open circuit voltage (V_{oc}) can be achieved by optimum tailoring of the band alignment.³⁷

Different approaches for interface engineering, including screening of alternative transport materials with different morphologies and surface modification to alter the charge carrier dynamics, have been attempted to improve the device performance, mainly V_{oc} , J_{sc} , and FF. Furthermore, the use of a mesoporous layer can affect the ion migration, producing a lower accumulation of charge carriers at the interface. The use of doped and composite transport materials, transport layer with different morphologies (one-dimensional and three-dimensional), and bi-layered mesoporous scaffolds can alter the mobility and band alignment of the transport layer, which will improve the device performance and stability. Additionally, different surface modifications and surface passivation techniques can and have been used to optimize the interface.

3.2 Charge carrier dynamics

The two main carrier characteristics of the transport layers that influence the performance of PSCs are mobility (μ) and conductivity (σ). The mobility of the carriers in the perovskite should be well-matched to that of the transport layers, *i.e.*, the mobility of carriers in the transport layers should be greater than or equal to that of the perovskite absorbers for smooth extraction from the perovskite absorber at the interface of the perovskite and transport layer. Conversely, charge accumulation occurs at the perovskite/transport layer interface when the mobility of the carriers in the transport layers is lower than that in the perovskite light absorbers, leading to interfacial recombination. Practically, the carrier mobility of a material depends on its processing methods, microstructures, morphology, and defect characteristics. The electron mobility in a semiconductor can be expressed as follows:

$$\mu = \frac{\tau}{m^*} \quad (2)$$

where μ , m^* and τ are the charge mobility (cm² V⁻¹ s⁻¹), effective mass, and characteristic time (s) of the charges in the transport layers, respectively.

Further, the charge conductivity of the transport layer should be comparable to that of the perovskite absorber to ensure lower charge recombination in the transport and achieve better performances in PSCs. The electrical conduction in a semiconductor is given by the following equation:

$$\sigma = nDE \quad (3)$$

where σ is the electrical conductivity (S m⁻¹), n is the free charge concentration based on the Boltzmann relation, D is the diffusion coefficient of charges, and E is the electric field (V m⁻¹). Thus, considering Einstein's equation, the electrical conductivities of the transport layers can be increased by either increasing the charge mobility (μ_e and μ_h for ETLs and HTLs, respectively) or concentration of free charges (n_e and n_h for ETLs and HTLs, respectively). Furthermore, the conductivity and mobility of the transport layers largely influence the series and shunt resistance of PSCs. Various reports suggest that the inclusion of low mobility transport layers at perovskite/transport layer interface results in dominant trap-assisted

recombination losses, delivering poor device performances. Therefore, various research groups have used the doping strategy to enhance the carrier mobility in the transport layers, but doping results in other unfavourable issues such as parasitic absorption, dopant diffusion, and doping-induced degradation pathways. In addition, the concentration of dopants required to enhance the mobility in the semiconducting transport layers depends on their thickness and creates ambiguity in ascertaining the exact dopant that can work and its concentration. Le-Corre *et al.*³⁸ reported an alternative strategy to doping and found a different transport layer (with high mobility), namely, optimizing the thickness of the transport layers, which directly affected the fill factor (FF) of the PSCs. Further, to reduce the recombination of photogenerated charge carriers in the perovskite light absorbers, the mobility of electrons (μ_e) and holes (μ_h) should be balanced, *i.e.*, the ratio of μ_e and μ_h should be equal to one. Thus, Chen *et al.*³⁹ used the space-charge-limited current (SCLC) method and demonstrated the importance of choosing and grading the transport layers to achieve a μ_e and μ_h ratio of 1, which enhanced the performance of PSCs.

In general, the carrier transport in the perovskite layer is discussed based on the ideal space charge region, but some studies have reported changes in the semiconducting state (p, i, or n) of the perovskite absorber depending on its ionic composition. Subsequently, Byeon *et al.*⁴⁰ introduced the concept of dominant p–n junction depending on the type of ETL used. Electron-beam-induced current measurement (EBIC) and Kelvin probe force microscopy (KPFM) were used to analyse the electric field and charge densities. The EBIC measurements for devices based on a TiO_2 ETL showed a strong EBIC signal at the TiO_2 /perovskite interface, unlike PSCs with a C_{60} ETL, showing a strong EBIC signal at the perovskite/spiro interface, as shown in Fig. 4. Specifically, the generated charges dissociate at the dominant junction with a strong built-in potential and are transferred to the corresponding transport layers. Further, the E-field inside the junction was measured by local contact potential differences (CPDs) with cross-sectional KPFM measurements. A strong E-field was observed at the TiO_2 /perovskite interface for the TiO_2 -based device, while the uniform distribution of a weak E-field was noticed at the MAPbI_3 /spiro-MeOTAD interface and in the MAPbI_3 layer. On the contrary, a strong

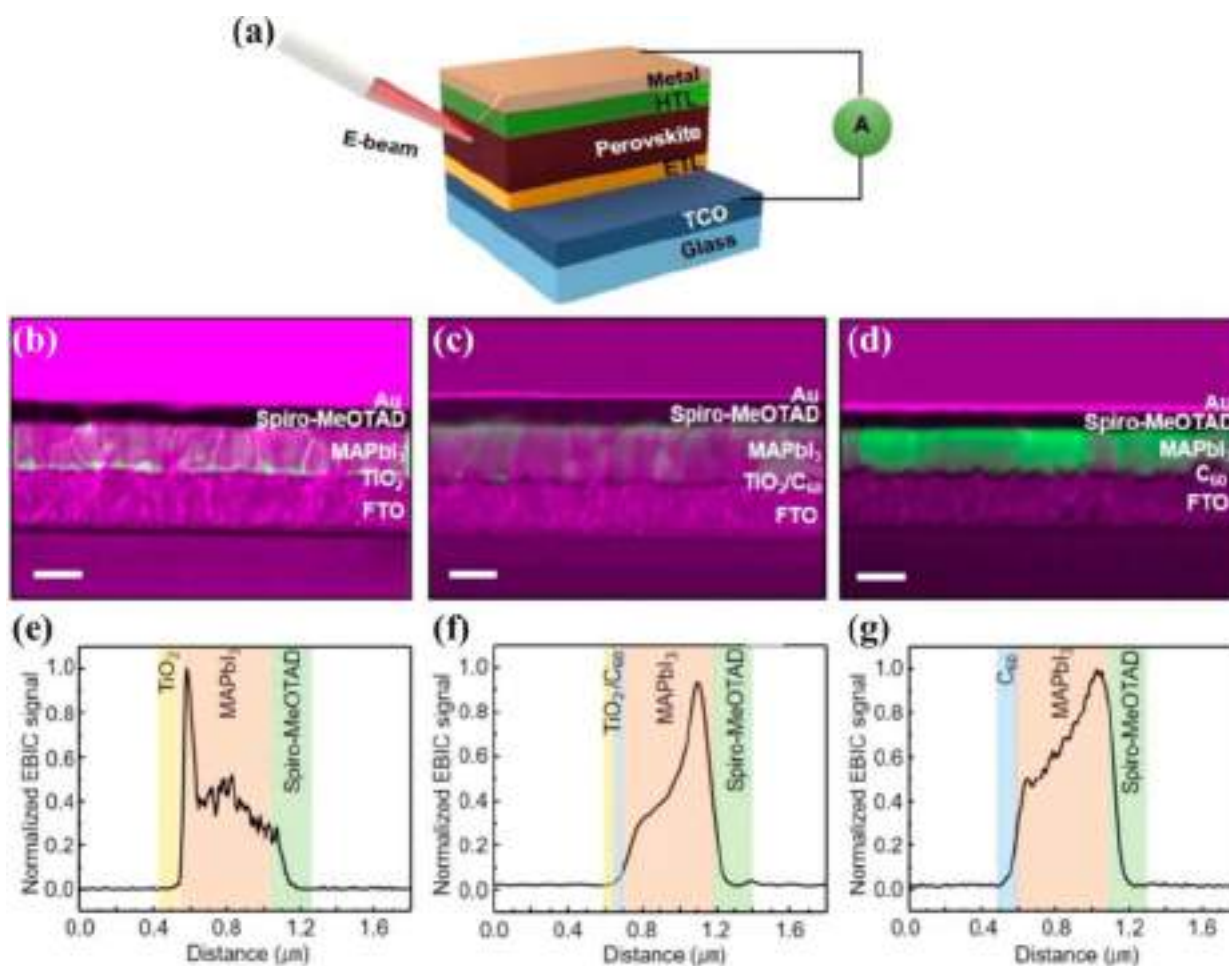


Fig. 4 (a) Schematics of electron-beam-induced current measurement setup. (b–d) Cross-sectional SEM images representing the EBIC signal in a bright green color and (e–g) their line profiles perpendicular to layers of TiO_2 , $\text{TiO}_2/\text{C}_{60}$, and C_{60} , respectively. The scale bars in SEM images are 500 nm.⁴⁰ Reprinted with permission from (ACS Energy Lett., 2020, 5, 2580–2589). Copyright (2020), the American Chemical Society.

E-field developed at the MAPbI₃/spiro-MeOTAD interface instead of the C₆₀/MAPbI₃ interface in the C₆₀-based device. This again corroborates that the choice of ETL decides the location to form the dominant p–n junction. The carrier density profiles obtained showed that holes were extensively amassed at the TiO₂ interface, and therefore, the net charge of the perovskite layer was also positive for the TiO₂-based device. However, the C₆₀-based device mainly showed electron accumulation at the spiro-MeOTAD interface rather than C₆₀ (Fig. 5). The net charge of the entire perovskite layer was negative in the device comprised of C₆₀ than that of TiO₂. Thus, the actual devices were not an ideal p–i–n solar cell, indicating a localized E-field at the specific interface with distinct transport layers.

This further emphasizes the choice of transport layers as a key factor in controlling the carrier dynamics in the PSCs.

The semiconducting transport layers are vital components of high-performing PSCs, but these metal oxide transport layers usually possess inherent trap states. The UV active trap states in the semiconducting transport layers act as recombination centres, which directly impact the FF and short circuit current densities (J_{SC}) of the PSCs. Further, the recombination centres formed at the interface of the transport layer and perovskite absorber give rise to hysteresis in PSCs. Nimens *et al.*⁴¹ emphasized that the fabrication method used to deposit the transport layers directly determines the trap density at the transport layer/perovskite interface. Further, besides the morphology of

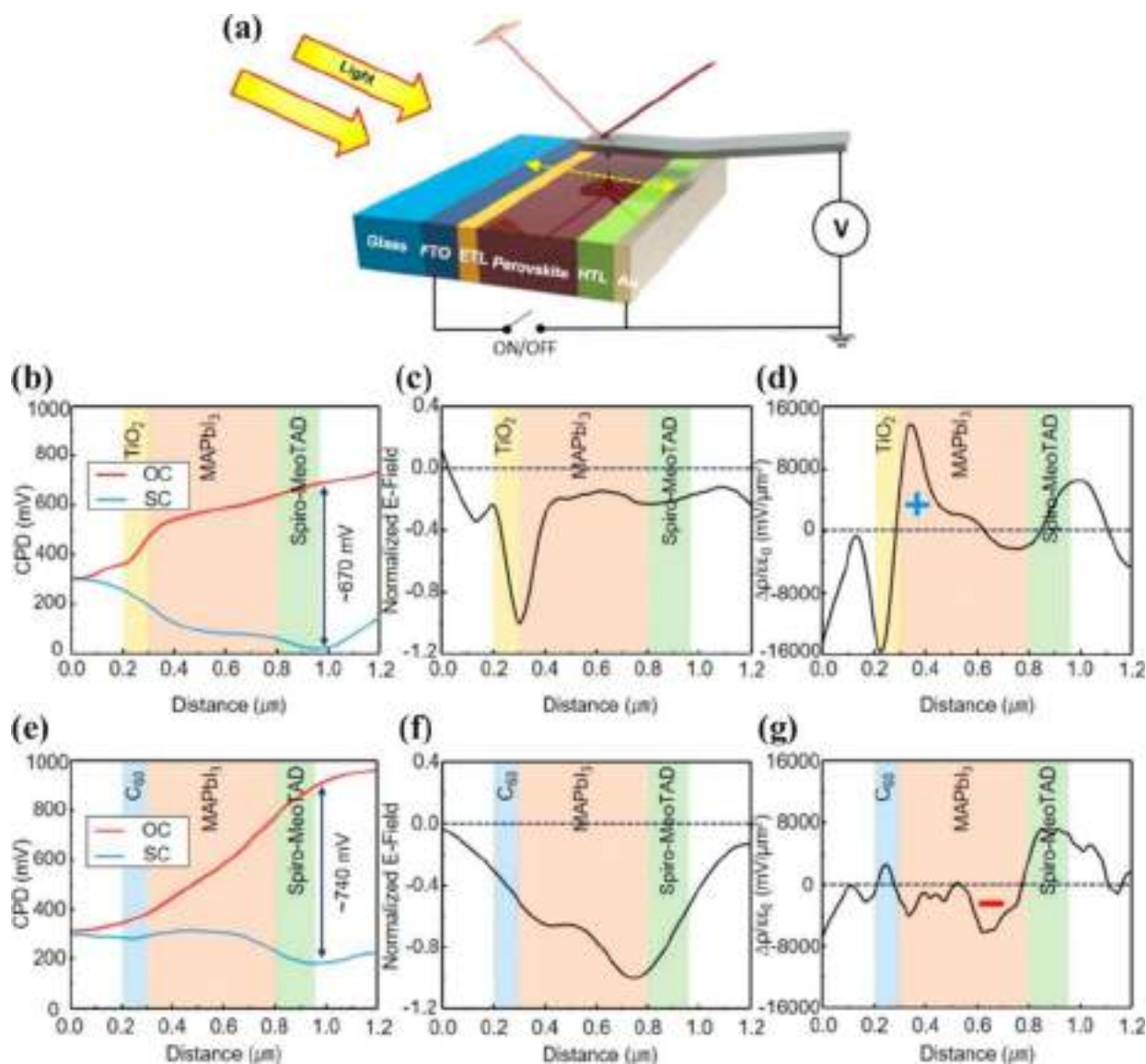


Fig. 5 (a) Schematic of cross-sectional Kelvin probe force microscopy measurement scheme. (b and e) Distribution of contact potential differences in OC (red line) and SC (blue line) condition and (c and f) normalized E-field distribution and OC conditions under illumination and (d and g) charge density profile evaluated from photo-potential difference between $V_{OC} - V_{SC}$ of TiO₂- and C₆₀-based PSCs, respectively. The arrows in (b) and (e) indicate the built-up V_{OC} . (OC: open circuit, SC: short circuit, V_{OC} : open circuit voltage, and V_{SC} : short circuit voltages).⁴⁰ Reprinted with permission from (ACS Energy Lett., 2020, 5, 2580–2589). Copyright (2020), the American Chemical Society.

the transport layers or the perovskite absorber films, the trap density obtained due to the fabrication process of the transport layer greatly controls the performance of PSCs.

Overall, the charge transfer dynamics compete at different timescales. The lifetime of photogenerated carriers in polycrystalline perovskite films ranges from 10–100 ns. With driving forces such as concentration gradient and built-in potential, the photogenerated carriers diffuse to the transport layer/perovskite interface and are selectively separated in a timescale of ~ 10 ns. Subsequently, the free carriers get collected through the transport layers at a typical timescale of ~ 10 μ s. In the transport layers, before the carriers reach the electrode, the interfacial recombination competes with the carrier transport at the typical timescale of 1–1000 μ s depending on the concentration of interfacial traps arising from their synthesis protocol, resulting in photocurrent and photovoltage loss.^{42–44} Thus, by ensuring that the transport layers possess less traps at the transport layer/perovskite interface, the photovoltaic performance of PSCs can be significantly enhanced.

3.3 Density of states

The density of states (DOS) can help understand the distribution of the number of electron states per unit volume in the electronic band structure, which determines the optical properties and the V_{OC} of solar cells.^{45,46} Interestingly, the atomic and electronic structure at the interface is the result of the combined effects of the surface structures of the independent constituent layers, giving rise to the solitary electronic structure,

while forming the interface. Particularly, at the interface of the perovskite/transport layer, the atomic and electronic structure plays a pivotal role by affecting the lifetime and mobility of charge carriers.⁴⁷ Furthermore, the conduction band minimum and valence band maximum (mostly inorganic semiconductors) are analogous to the highest occupied molecular orbital (HOMO) and the lowest unoccupied molecular orbital (LUMO) (mostly organic/polymer semiconductors). Fig. 6(a) shows the electronic structure, which is comprised of the vacuum energy level (E_{vac}), work function (WF), Fermi energy (E_f), bandgap (E_g), electron affinity (EA), and ionization energy (IE) for all organic/inorganic semiconductors. The position of these energy levels and their alignment at the junction plays a key role in the overall performance of electronic devices.⁴⁸

The vacuum energy level is the energy of a stationary electron with zero kinetic energy located outside the surface of the material. The work function is the energy difference between the vacuum level and Fermi level ($WF = E_{vac} - E_f$), which depicts the energy barrier that restricts an electron from escaping the material. The Fermi energy represents the value at absolute zero temperature. The ionization energy (IE) refers to the energy difference between the vacuum level and valence band (VB) and depicts the minimum energy necessary to eliminate the electrons from the VB. Reciprocally, the energy gained by dropping an electron from the vacuum level to the conduction band (CB) is known as the electron affinity (EA) of the semiconductors. The distribution of DOS in the energy band can be better understood by splitting semiconductors into

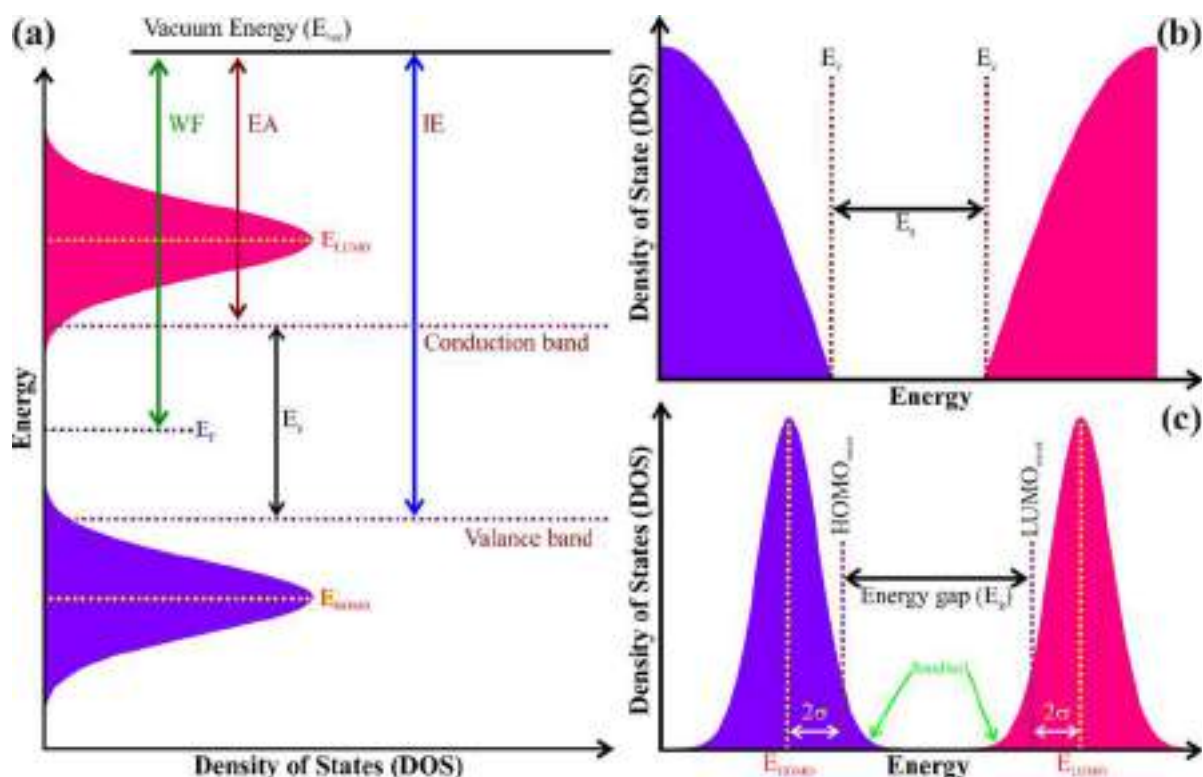


Fig. 6 Schematic of the electronic structure for (a) all organic/inorganic, (b) ordered (or crystalline), and (c) amorphous (or disordered) semiconductors.

two categories, *i.e.*, ordered (single crystals and polycrystalline thin films) and disordered (amorphous materials) systems. In the case of ordered semiconductors, the localised charge carriers are at the band edges, and it shows a parabolic shape distribution of the DOS at the band edges, which can be represented as follows:⁴⁹

$$g_c(E) \propto \sqrt{E - E_c} \quad (4)$$

$$g_v(E) \propto \sqrt{E_v - E} \quad (5)$$

where E_c and E_v are the conduction and valence band edges, respectively. This infers that there are no gap states in the forbidden gap of the semiconductor or the DOS is reduced to zero in the energy gap $E_v < E < E_c$. This results in the formation of sharp conduction and valence band edges, as shown in Fig. 6(b).⁵⁰

In the case of disordered semiconductors such as amorphous and most organic semiconductors, the charge carriers have a poor degree of localization.⁵¹ The weak localization at the band edges results in extended states, which progressively change to localized states, leading to the outgrowth of an extended state tail in the energy gap.^{50,51} Therefore, the DOS is more appropriately described by the Gaussian or exponential distribution. Further, the Gaussian disorder model (GDM) was proposed to understand the charge carrier transport in disordered organic semiconductors, which gives the Gaussian density-of-state function, $g(E)$, as follows:

$$g(E) = \frac{N_0}{\sqrt{2\pi}\sigma} \exp\left\{-\frac{E^2}{2\sigma^2}\right\} \quad (6)$$

where N_0 is the density of states per unit volume, which is generally considered the density of the molecule, and σ is the width of the distribution. The extended states tailing from the

Gaussian-distributed DOS are incapable of accurately defining clear bandgap and sharp band edges. Therefore, the energy gap is defined as the energy difference between HOMO_{onset} and LUMO_{onset} (Fig. 6(c)). Further details on determining the bandgap of disordered semiconductors can be found in previous studies.^{50,52,53}

In PSCs, to locate the band edges at the interface, Chatterjee *et al.* used scanning tunneling microscopy, *i.e.*, they recorded the tunneling current *versus* tip voltage of ultra-thin films of layers of PSCs subsequently coated over n-type silicon substrates. The differential conductance (dI/dV) of the thin films was calculated from the obtained data, which corresponds to the DOS. The spectra in Fig. 7 show the positive and negative voltages, denoted as the CB and VB levels, respectively, obtained with respect to the Fermi level. Further, the difference in the valence and conduction band levels (transport gap) is slightly lower than the optical bandgap due to trap states, which contributes to the tunneling current.⁵⁴ Moreover, the surface oxide states of the transport layer nanoparticles can be modified by ligands (silanes or thiols), which can alter the valence and conduction band edge levels by altering the density of states.⁵⁵

Photoelectron yield spectroscopy (PYS) can also be further used to determine the work function of the transport layers. Teo *et al.* tailored the work function of an NiO_x layer with lanthanum doping, which could alter the density of states owing to changes in the valence and conduction band levels.⁵⁶ It should also be noted that the lattice mismatch at the transport layer/perovskite influences the charge dynamics. Hu *et al.*⁵⁷ conducted a first-principles study on the SnO₂/CsPbI₂Br heterojunction and showed that the SnO₂(110) surface is well-matched with the CsPbI₂Br (100) surface due to their mismatch of 6.4%. The DOS at the interface was different from that in the bulk

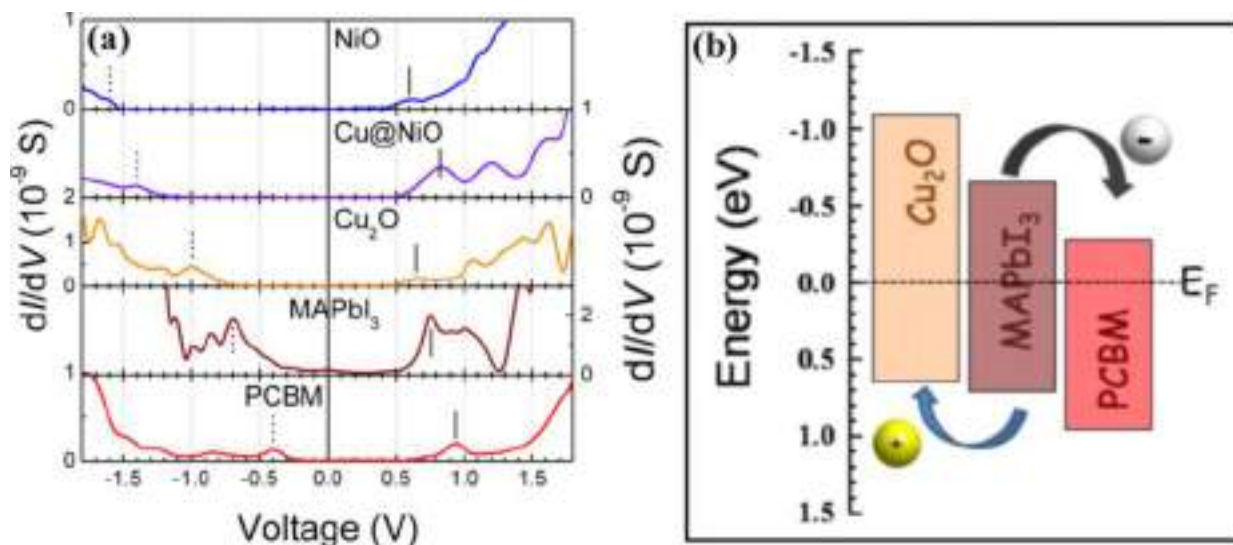


Fig. 7 (a) Differential conductance (dI/dV) plots of NiO, Cu@NiO, Cu₂O, MAPbI₃, and PCBM thin films. VB and CB edges of the materials and HOMO and LUMO levels of PCBM with respect to the Fermi energy are marked with vertical continuous and broken straight bars in the positive and negative voltage regions, respectively. (b) Schematic energy level diagram of Cu₂O/MAPbI₃/PCBM heterojunction. The dashed line represents the Fermi energy after contact.⁵⁴ Reprinted with permission from (*J. Phys. Chem. C*, 2016, **120**, 1428–1437). Copyright (2016), the American Chemical Society.

because of the corresponding variation in electronic states at the interface. Therefore, it should be noted that the DOS in PSCs depends on not only the bulk of the subsequent layers but also the interface; however, it can be tuned by controlled doping to adjust the band offsets and achieve a high V_{OC} .

4. Electron transport layer (ETL)

The bandgap and band alignment of the ETLs control and guide the electron transfer at the ETL/perovskite interface. ETLs, in the form of wide bandgap n-type semiconductors transparent to visible light, absorb in the UV wavelength range.⁵⁸ Moreover, they allow full visible radiance to strike the perovskite absorber, but this may not be true in inverted device architectures where light strikes through the hole transport layer (HTL) and transparent conducting substrates.⁵⁹ Typically, the bandgap values of the ETLs are higher than the perovskite absorbers utilized to fabricate PSCs. Therefore, the CB edge of the ETL should be at a lower potential than that of the perovskite absorber to guide the electrons through the ETL and reduce the leakage of excited charges in the opposite direction. In the n-type structure, the Fermi levels of the ETLs are close to the CB; hence, the probability of the VB electron movement from the perovskite to ETL is close to zero, and hence negligible (Fig. 8). Therefore, variety of ETLs has been explored to control the recombination process and accelerate the charge carrier recombination dynamics in search of efficient and stable photovoltaic performances. In this section, we discuss the important characteristics of various inorganic ETLs and their outstanding development in delivering excellent PCEs when combined with perovskite absorbers.

4.1. Inorganic ETLs

Inorganic ETLs, which are engineered into nanostructures for exploiting the nano-regime physical properties, increase the

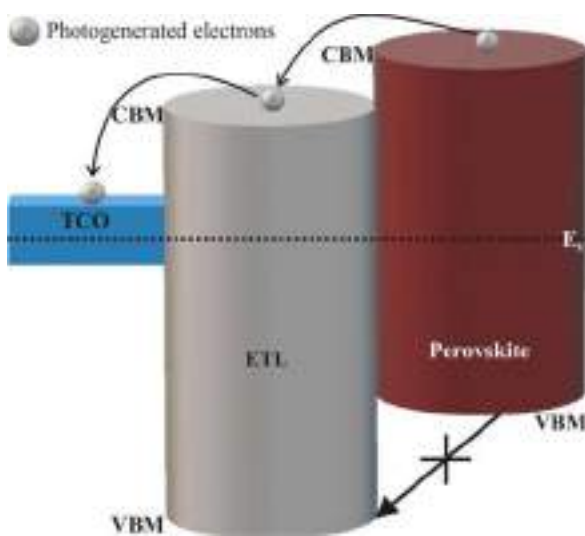


Fig. 8 Schematic depicting the path of a photogenerated electron from the perovskite light absorber to the external circuit. (CBM: conduction band minimum and VBM: valence band maximum.)

junction interface. Therefore, oxides of various metals such as titanium (Ti), tin (Sn), zinc (Zn), tungsten (W), barium (Ba), strontium (Sr), aluminium (Al), iron (Fe), and indium (In) have been explored for their performance as ETLs in PSCs.^{60–64} The band structures of several persuasive inorganic ETLs are summarized in Fig. 9. The appearance of inorganic ETLs in various crystalline polymorphs and their ability to tailor the charge transfer dynamics are of special interest to the PV community. The objective is to look for cost-effective inorganic ETLs processible under ambient conditions. Furthermore, the ETLs can act as a prominent template for the overlaying perovskite layer in PSCs after engineering their phases and crystallinity. The synthesis, characterization, and significance of a few critical inorganic ETLs employed in PSCs are thoroughly discussed in this section.

4.1.1. Titanium dioxide (TiO₂). TiO₂ is one of the fascinating electron transport materials widely used in the fabrication of PSCs due to its low processing cost, chemical stability, and non-toxic nature. Titanium oxide has several allotropic forms categorized as TiO₂ and Ti_nO_{2n–1} with different crystal structures, namely, monoclinic, triclinic, tetragonal, orthorhombic, rhombohedral, and hexagonal.^{65,66} However, its most well-known forms are anatase (tetragonal structure, $I4_1/amd$ space group), brookite (orthorhombic structure, $Pbca$ space group), and rutile (tetragonal structure, $P4_2/mnm$ space group), which are composed of a TiO₆ octahedral network through shared oxygen at the corners. The TiO₆ octahedra share both the corners and the edges to form the rutile and brookite-type crystal structures, but the sharing of only edges results in the formation of an anatase crystal structure. The chains of the edge-shared distorted TiO₆ octahedra run parallel to the *c*-axis and deliver the brookite phase. These distinct crystalline forms influence the electronic and electrochemical properties of TiO₂ nanostructures,^{67–72} and hence play a crucial role in the performance of PSCs. In the nanocrystalline form, the anatase, brookite, and rutile phases are the most thermodynamically stable at crystalline dimensions of ≤ 11 nm, between 11 to 35 nm, and ≥ 35 nm, respectively.⁷³ Nevertheless, the synthesis of the brookite phase is most challenging because of its metastable nature.^{74,75} Owing to the ease of processing of the anatase and rutile phases, they are more widely utilized than the brookite phase in solar cells.^{76–78}

The wide adaptability of TiO₂ as photoanodes in DSSCs has promoted it as an interesting ETL material in PSCs.^{79,80} TiO₂, which is an n-type wide bandgap semiconductor (*i.e.*, $E_g = 3.2$ eV with CB edge level at -4.2 eV and VB edge level at -7.0 eV), is one of the most transparent materials to visible light and offers electronically favourable band edge alignment with most of the known perovskite absorbers. Usually, a compact TiO₂ film is used as the hole-blocking layer in PSCs. Various thin film growth techniques, namely, spin coating,⁸¹ aerogel-assisted coating,⁸² electrospinning,⁸³ sputtering,⁸⁴ atomic layer deposition (ALD),⁸⁵ hydrothermal growth,^{86,87} spray coating,⁸⁸ and template-based synthesis,⁸² have been employed for the synthesis of good-quality TiO₂ transport layers. However, hydrothermal synthesis is an attractive process for obtaining hierarchical nanostructures such as nano-dendrites,

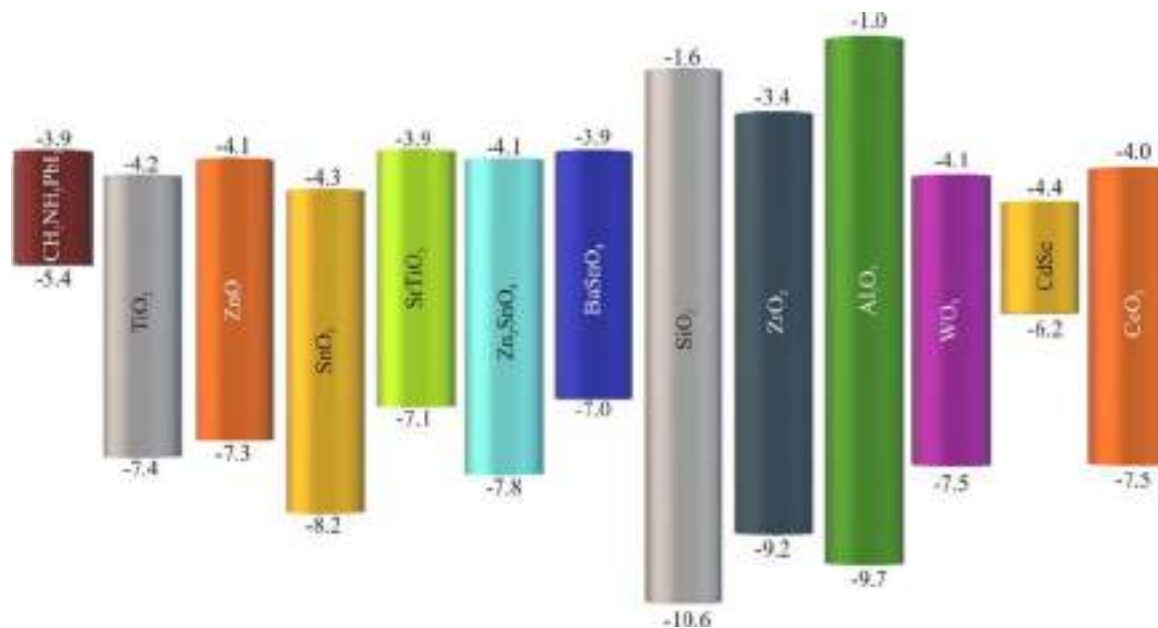


Fig. 9 Schematic showing the band structures and the band alignment of various inorganic ETLs with a perovskite absorber.

which offer dual functions of significant light trapping and efficient electron collection (Fig. 10).⁸⁹ The 3D morphology efficiently extracts the photoelectrons from the perovskite absorber (*i.e.*, MAPbI₃) and reduces the electron transport length in the matrix to surmount the obstacle of short electron diffusion length. Further, finite difference time domain (FDTD) simulations revealed that the electron transport pathway in PSCs consisting of branched nano-dendrites assists in the photoelectron collection near the spiro-MeOTAD layer due to absorption of long-wavelength light. Moreover, the surface passivation of the 1D TiO₂ nanorods by atomically deposited TiO₂ nanoparticles offers excellent charge separation, controlling the back-flow reaction of the electrons excited from the perovskite absorber. This facilitates a low recombination rate with a conversion efficiency of 13.45%.⁹⁰ The secondary oxidation treatments at higher temperatures always contribute to the presence of defects/impurities (*i.e.*, residual carbon) and changing the band alignment at the interface. The impurities serve as unproductive quenching sites or charge recombination centres, effectively trapping the photogenerated electrons at the interface of the TiO₂ ETL and perovskite absorber, thereby curtailing the dramatically injected electron yield. However, the formation of defects or impurities was eliminated *via* UV-O₃ treatment without compromising the density of oxygen vacancies to gain competitive efficiency from the amorphous ALD-grown TiO₂ (*i.e.*, 9.97%) and compact TiO₂ (*i.e.*, 16.9%) ETLs.^{91,92} Moreover, the uneven blocking layer of TiO₂ nanoparticles between the valleys and plateaus of F-doped SnO₂ induced unidentical electron transportation, and thereby the poor charge collection reduced the performance of the corresponding PSCs.⁹³

Dharani *et al.*⁹⁴ introduced electrospun TiO₂ nanofibers as a photoanode, enabling a greater loading of perovskite materials and also lowering the trap-assisted recombination. Despite the

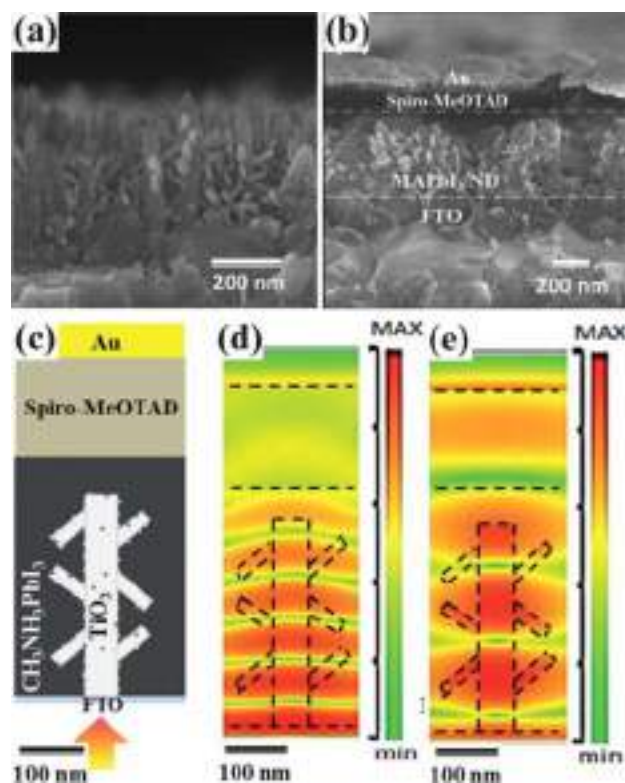


Fig. 10 Cross-sectional SEM images of (a) TiO₂ nanodendrites and (b) solar cell architecture comprised of TiO₂ nanodendrites. (c) Schematic of the FDTD simulation cells for perovskite–TiO₂ nanodendrites. FDTD-simulated EM energy density distribution in PSC after continuous electromagnetic waves passing through the perovskite–TiO₂ nanodendrites with wavelengths of (d) 450 nm and (e) 650 nm.⁸⁹

more open structure and porous arrangement of the nanofibers, the poor PbI₂ conversion in CH₃NH₃PbI₃ was reported to

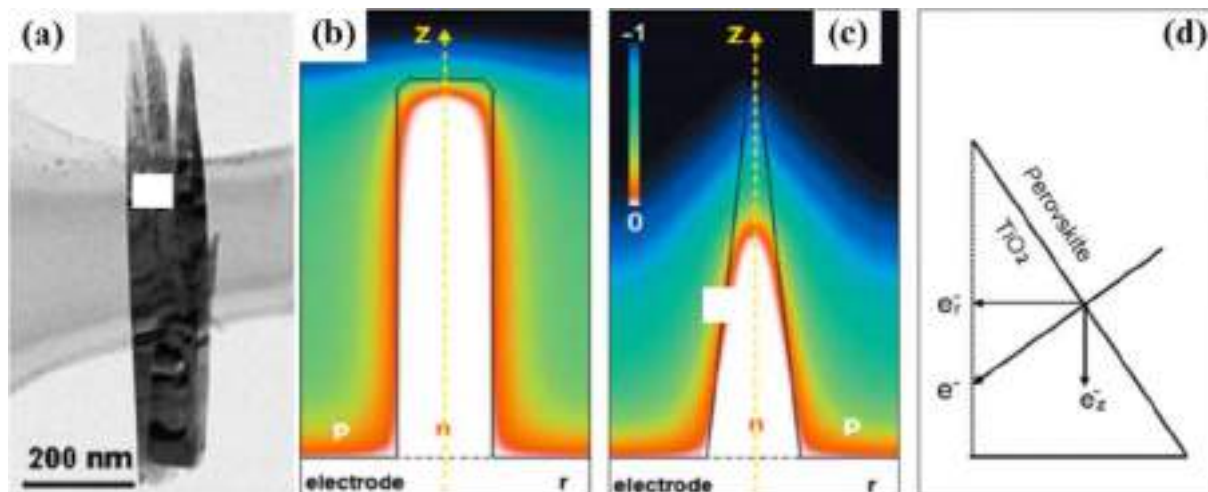


Fig. 11 (a) Low-magnification TEM image of TiO_2 nanocones. Electric potential contours for n-type (b) nanorod and (c) nanocone in the p-type matrix and (d) scheme of electron injection from perovskite to TiO_2 and transport within TiO_2 . Note: e_r^- represents electron injection along the radial direction and e_z^- along the axial direction.⁹⁶ Reprinted with permission from (*Nano Energy*, 2015, **11**, 409–418). Copyright (2015), Elsevier.

impede the device efficiency.⁹⁵ The tapered nanocones of rutile TiO_2 oriented in the [002] direction exhibited superior efficiency than nanorods, irrespective of the variation in their length (Fig. 11).⁹⁶ The suppressed charge recombination due to the faster electron injection rate of the TiO_2 nanocones was beneficial for the charge separation at their interfaces with $\text{CH}_3\text{NH}_3\text{PbI}_3$, resulting in an enhancement in the efficiency. The two possible factors responsible for the faster electron transfer from the perovskite to nanocones are as follows: (i) larger surface to volume ratio of the nanocones improving the charge separation and (ii) decreased distribution of electrostatic potential for p–n junction, generating an electric field along the axial direction, which enabled enhanced electron transportation, while minimizing its trapping. Specifically, the driving force for the injection of electrons into the TiO_2 nanocone ETL and transport along the axial direction for the nanocone/perovskite systems was absent in the nanorods (Fig. 11(d)), which led to faster electron transfer from the perovskite to TiO_2 nanocones, suppressing the charge recombination. Likewise, highly ordered anti-reflecting titania nanotubes served as nanocontainers and ETL in $\text{CH}_3\text{NH}_3\text{PbI}_3$ PSCs and facilitated efficient charge collection/extraction, delivering an efficiency of 14.8% despite the relatively lower loading of $\text{CH}_3\text{NH}_3\text{PbI}_3$.⁶⁰

It was shown by Xiao *et al.*⁹⁷ that nanoporous submicron TiO_2 spheres with high specific surface area ensure higher light scattering effect and better contact with the perovskite through infiltration, which caused higher light absorption and faster charge transport, respectively, delivering excellent stability against atmospheric moisture when the PSCs with 14.3% efficiency were exposed to the air. Similarly, the smaller leakage current and reduced transport resistance of opal-like mesoscopic TiO_2 ensued a high (18.2%) efficiency.⁹⁸ Further, as shown by Thambidurai *et al.*,⁹⁹ interface modification of a mesoporous TiO_2 ETL by $(\text{OH})_2$ uplifted the conduction band of TiO_2 , leading to better energy level alignment with the

perovskite, thereby enhancing the optical absorption, reducing the carrier recombination, and rendering excellent electron transportation. Together, they led to a high PCE of 17.5%. The passivation of the perovskite/ TiO_2 interface using poly(vinylcarbazole) (PVCz) and PCBM is a versatile and rational method to gain a PCE of around 21.1%. The PVCz-assisted homogeneous dispersion of PCBM in the mesoporous TiO_2 layer also prevented elution after the formation of the perovskite layer. The interface modification induced efficient charge transport to the TiO_2 ETL and efficiently reduced the carrier recombination at the ETL/perovskite interface.¹⁰⁰ Moreover, the introduction of a sodium sulfate (Na_2SO_4) passivation layer at the interface of the TiO_2 ETL and perovskite delivered an efficiency of 18.75%.¹⁰¹

Recently, Wang *et al.*¹⁰² introduced the interface modification of TiO_2 /perovskite by CsAc to reduce the interface defect density and the related carrier recombination. Even though the CsAc improved the affinity of the perovskite precursor to form a compact and highly crystalline perovskite layer by decreasing the Gibbs free energy for heterogeneous nucleation, the carbon as an HTL may have restricted the efficiency to 13.8%. Likewise, a robust and simple acid-treatment strategy was introduced to produce an amorphous TiO_2 buffer layer above the anatase TiO_2 surface as an ETL.¹⁰³ The acid treatment weakened the bonding of the zigzag octahedral chains in TiO_2 and formed an amorphous buffer layer by shortening the staggered octahedron chains. This led to the formation of oxygen vacancies in the amorphous TiO_2 ETL, and hence increased electron density, efficiently transferring electrons from the perovskite to ETL layer. Modification of the interlayer between the TiO_2 and perovskite layers by introducing air-stable n-type DMBI-doped PCBM was shown to significantly diminish the energy level offset at the interface, thereby delivering an efficiency of 20.1%.¹⁰⁴

Nanocomposites of TiO_2 have also been explored to ensure the higher performance of PSCs based on them. Indeed, it was found that the PCE of 15% achieved using a TiO_2 /graphene

nanocomposite²⁹ further improved after replacing graphene with single-walled carbon nanotubes (SWCNTs).¹⁰⁵ However, the increased number of recombination sites due to higher loading of SWCNTs adversely affected the performance features. The composite of phosphotungstic acid (PW₁₂) and TiO₂ ETL down-shifted the conduction band edge and led to a well-aligned interface with the perovskite for excellent electron excitation.¹⁰⁶ Besides, metal oxides were also used as a substitute of carbon materials to form nanocomposites with TiO₂, but were found to be relatively inefficient as ETLs due to the inhibited recombination rate offered by impure phase formation.¹⁰⁷ Therefore, Y,¹⁰⁸ Ga,¹⁰⁹ Zr,¹¹⁰ and Ru¹¹¹ doped and Zr/N¹¹² and Er–Yb,¹¹³ co-doped TiO₂ nanostructures have also been explored as ETLs to achieve longer carrier lifetimes and higher charge density at the ETL/perovskite interface. Moreover, hydrogen¹¹⁴ and cadmium¹¹⁵ have been utilized to alter the recombination resistance and charge carrier density of TiO₂ to further increase the collection efficiency. An Nb-doped TiO₂ ETL covered with an over-layer of TiO₂ nanorods was shown to reduce the interface transport resistance and capacitance, thereby delivering an efficiency of 18.88% due to electron injection from the CB of perovskite to Nb–TiO₂.¹¹⁶

Sung *et al.*¹¹⁷ doped a TiO₂ ETL with Na₂S in search of interface defect passivation and improved conductivity. The Na cations and S anions were observed to improve the conductivity and change the wettability of the TiO₂ layers, respectively. This was noted to improve the crystallinity of the perovskite layers and passivate defects at the ETL/perovskite interface. Recently, various anions of TFSI[−], Cl[−], F[−], and CO₃^{2−} of Li salts have been explored as ETLs for PSCs.¹¹⁸ The first three anions of Li salts remain doped in TiO₂ to improve the electrical properties by one-order enhancement in electron mobility and reduced electron trap density of Li-doped TiO₂ ETLs. Conversely, the stronger chemical bonding between Li₂CO₃ and TiO₂ exhibits the deepest conduction band and delivers the maximum efficiency of over 25%. The high temperature firing at ~450 °C required to gain the crystalline phase of pristine or doped TiO₂ nanostructures restricts the processing of the ETLs over plastic substrates. Alternatively, low-temperature processing to protect the plastic substrate, while gaining the desired crystalline phase of TiO₂ has been attempted to fabricate flexible PSCs. The plasma-enhanced atomic layer deposition of a compact TiO₂ layer at 80 °C on ITO-coated PEN flexible substrates¹¹⁹ and E-beam evaporation of TiO₂ on PET substrates¹²⁰ have been found to be effective to fabricate wearable power devices, achieving a PCE of 13%. However, physical deposition methods, such as ALD,¹¹⁹ e-beam evaporation¹²⁰ and sputtering,¹²¹ are complex and demand high energy consumption to create a vacuum. Therefore, the use of solution methods such as spin coating¹²² and solution dispersion¹²³ on flexible substrates was also attempted, but the PCE was limited to 10%. Consequently, further optimization of the solution-based processes at low temperature to gain dense and compact TiO₂ ETLs is essential to improve the PCE.

4.1.2. Tin oxide (SnO₂). Tin oxide can be synthesized in various chemical forms (*i.e.*, SnO₂, SnO, Sn₂O₃, and Sn₃O₄) and

crystalline phase forms (*i.e.*, orthorhombic, tetragonal, cubic, and triclinic crystals).⁶⁵ Most importantly, being chemically stable, UV-resistant, and low-temperature processible (<200 °C), SnO₂ also supports high bulk electron mobility (*i.e.*, 240 cm² V^{−1} s^{−1}), wide bandgap (*i.e.*, 3.6–4.0 eV), and visible transparency.¹²⁴ Thus, considering its higher charge mobility and extended UV stability, it can potentially dethrone the lower charge mobility ETLs such as TiO₂. Recently, SnO₂ nanocrystalline films have been identified as both technically viable ETLs and antireflection films.¹²⁵ Various synthetic techniques such as ALD,¹²⁶ chemical bath deposition,¹²⁷ electrochemical deposition,¹²⁸ pulsed laser deposition (PLD),¹²⁹ e-beam evaporation,¹³⁰ and spray coating^{131,132} have also been used to synthesize compact, uniform, and well-defined morphologies of SnO₂ ETLs. However, the solution processing of salts such as SnCl₂, SnCl₄, SnCl₂·2H₂O, and SnCl₄·5H₂O, followed by thermal decomposition,¹²⁵ is the most widely employed technique due to its easy scalability as an industrial tool to render well-defined morphologies of ETLs for PSCs. Moreover, the uniform layers of SnO₂ nanoparticles easily realized by an automated spray coating technique at lower processing temperature over 15 cm² active area was shown to deliver an improved charge-lifetime at the ETL/perovskite interface and stable performance under self-life test for 1000 h.¹³²

A thin layer of SnO₂ nanoparticles as the ETL delivered an efficiency of 21% in planar-structure PSCs,¹³³ but the development of PbI₂, a p-type material at the interface, led to a higher hole transfer rate than electron transfer rate. The reduced barrier at the perovskite/spiro-OMeTAD interface and passivation of the surface or grain boundary defects by PbI₂ were found to control the device performance. Moreover, SnO₂ was also studied with ZnO nanostructures to improve the PCE performance, where a hollow domed SnO₂ nanotube array was grown over ZnO nanorods as a sacrificial template (Fig. 12), but the PCE was still restricted to 12.1%, which could be due to sluggish electron transport from the hierarchical thicker shell layer of SnO₂ nanotubes, providing pinholes.¹³⁴ The pinholes caused surface current leakage and compromised the charge recombination processes at the interface. Therefore, the preparation of a smooth and compact bilayer structure of SnO₂ nanoparticles by filling the pin-holes reduced the oxygen-deficient regions, improved crystallinity, and downsized the dislocations, facilitating its efficacy as an ETL for PSCs. Indeed, the bilayer SnO₂ structure delivered a PCE of 16.84% due to the lowered electron trap density, enormously reduced contact resistance, and charge accumulation at the ETL/perovskite interface.¹³⁵

Surface treatments with aqueous solutions of salts such as TiCl₄ have been explored to significantly retard the recombination process of SnO₂.¹³⁶ However, the inclusion of conducting materials in SnO₂ ETLs provides a better interface with the perovskite and control over the recombination process, and thus more attractive in the search for improved PCEs. The addition of a small amount of graphene quantum dots was shown to enrich the electronic properties of SnO₂, thereby aiding the delivery of a steady-state PCE of 20.23% with very little hysteresis *via* controlled electron transfer from graphene.¹³⁷

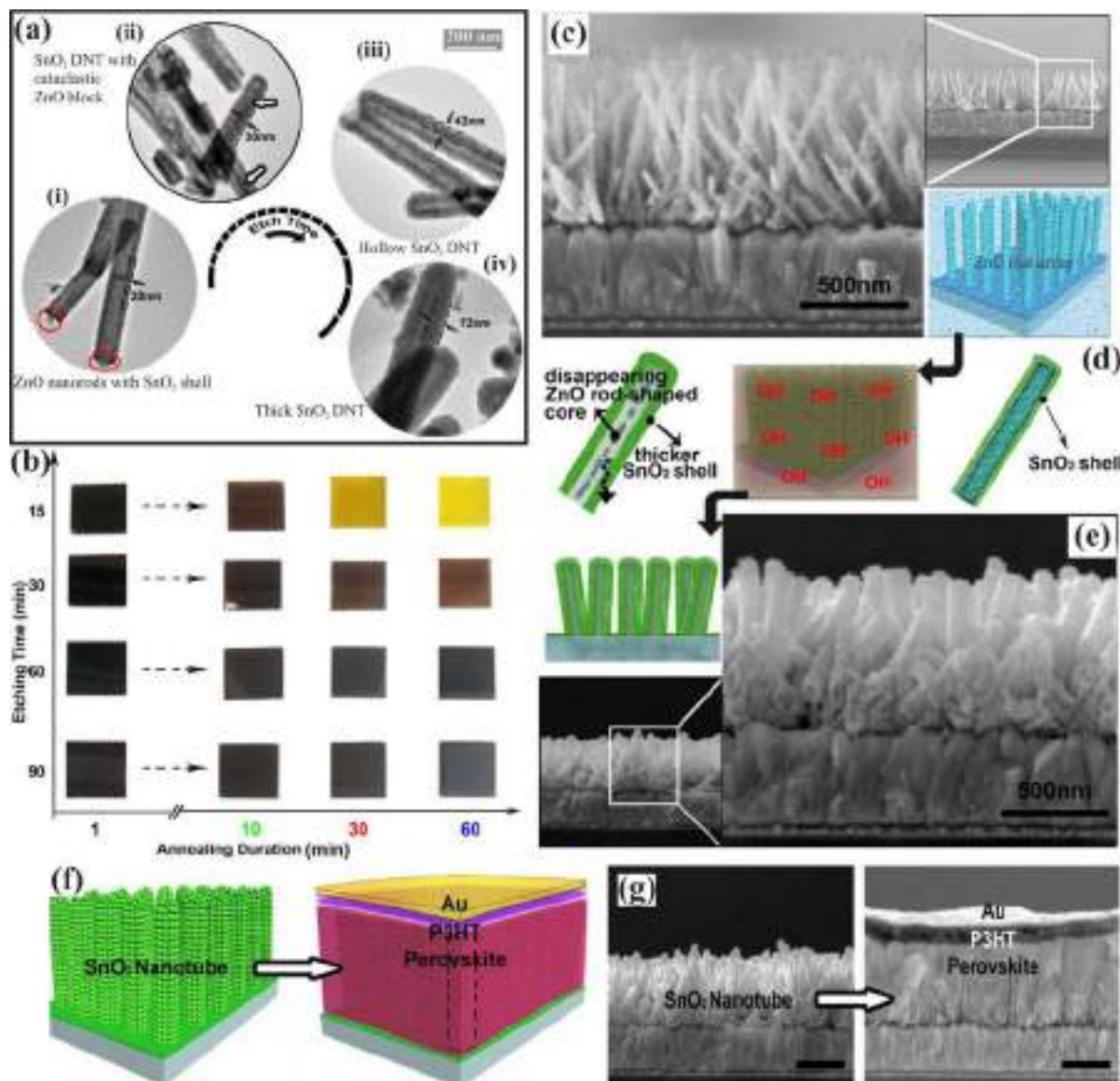


Fig. 12 (a) TEM images of time-dependent growth of SnO₂-DNTs under reaction time of (i) 15, (ii) 30, (iii) 60, and (iv) 90 min. (b) Spin-coated perovskite films over SnO₂-DNT/FTO/glass substrates at different reaction times. Schematic growth mechanism of (c) ZnO nanorods covered with discontinuous SnO₂ nanoparticles. (d) OH⁻ ions as by-product of SnO₂ can etch the ZnO nanorods, and (e) SnO₂-DNT@ZnO nanorods. (f) Fabrication scheme of PSCs and (g) corresponding cross section of SnO₂-DNTs and SnO₂-DNT/perovskite/P3HT/Au device. The scale in black indicates 500 nm.¹³⁴ Reprinted with permission from (*Chem. Eng. J.*, 2017, **325**, 378–385). Copyright (2017), Elsevier.

The photogenerated electrons from graphene effectively fill the electron traps and improve the electron density in the conduction band (CB) of SnO₂, which collectively accounts for the reduced work function and improved conductivity of SnO₂. The reduced electron trap density and increased conductivity of the ETLs facilitated an enhancement in the electron extraction efficiency and reduced recombination at the ETL/perovskite interface. Further, the addition of graphene to mesoporous SnO₂ microspheres resulted in a relatively reduced charge transfer resistance (*i.e.*, faster electron extraction) and larger recombination resistance than the pristine SnO₂, consequently leading to the least interface potential loss and PCE of 17.08%.¹³¹ Likewise, the inclusion of carbon nanotubes substantially increased the

conductivity of the SnO₂ ETL by lowering the defect density, which improved the electron extraction and transport. This reduced the electron accumulation at the ETL/perovskite interface and significantly enhanced the PCE to 20.33%.¹³⁸

Recently, Yoo *et al.*¹³⁹ introduced a holistic approach to improve the performance of PSCs by virtue of charge carrier management. The SnO_x ETL was developed with an ideal film coverage and thickness by tuning the chemical bath deposition protocol. Further, the decoupling of the passivation strategy between the bulk and the interface minimized the bandgap barrier and improved the charge carrier properties. Although control of the pH from most acidic (*i.e.*, 1) to 6 delivered thin uniform films to a distinct nanorod morphology, where the

lower film coverage at the most acidic pH caused interfacial recombination, and the oxygen site defects at $\text{pH} > 3$ reduced the carrier lifetime by increasing the non-radiative recombination. The magic reaction at $\text{pH} 1.5$ exhibited ideal film coverage, morphology, and chemical composition and delivered a certified PCE of 25.2%. A high FF of 84.8% was identified to be responsible for the enhanced PCE, which improved the carrier mobility in the $\text{CH}_3\text{NH}_3\text{PbBr}_3$ active layer and excellent charge collection with the least parasitic losses from shunt/series resistances. Thus, the close association of charge carrier management with the FF and the V_{OC} can direct the improved performances of PSCs to reach the theoretical efficiency limit. Moreover, the resistance gradient across the edge and centre of the thin film influences the free carrier mobility to a considerable extent.¹⁴⁰ Hence, the realization of a uniform film with the controlled agglomeration of grains, which is feasible by adopting the rastering of multiple spray nozzles, can render an excellent ETL for PSCs.

Besides these efforts, doping strategies have been considered to improve the electron charge transfer, lower the charge recombination, and reduce the contact resistance at the SnO_2 /perovskite interface. The downward shift of the CB or Fermi level and enhanced conductivity of the SnO_2 ETL after Li,⁶¹ Mo,¹⁴¹ Mg,¹⁴² Cl,¹⁴³ Er,¹⁴⁴ KF,¹⁴⁵ TaCl_5 ,¹⁴⁶ Zr/F,¹⁴⁷ and NH_4Cl ,¹⁴⁸ doping expedited the injection and transfer of electrons, increased the offsets of the doped ETLs/perovskite layers, and inhibited the charge recombination at the interface. Yang *et al.*¹⁴⁹ explored a Y-doped SnO_2 ETL in search of efficient PSCs. The Y-doping promoted the homogeneous distribution of well-aligned SnO_2 nanosheets, which allowed better infiltration in and contact with the perovskite and improved electron transfer from the perovskite to SnO_2 nanosheet ETL. Moreover, after Y-doping, the uplifted band levels resulted in better energy level alignment and reduced charge recombination at the Y- SnO_2 /perovskite interface. Moreover, the optimized 5 mol% doping of Nb in SnO_2 created better surface coverage with perovskite and yielded a PCE of 20.5% due to the reduced recombination centres and enhanced electron extraction at the interfacial contact.¹⁵⁰ The Cl-capping uplifted the band levels of the SnO_2 nanoparticle ETL and suppressed the non-radiative recombination with faster transfer of charge carriers. Moreover, Cl-capping created a hydrophobic surface for SnO_2 , which reduced the trap density and suppressed the interfacial recombination of charges by dramatically increasing the grain size and crystallinity of the perovskites, delivering the hysteresis-free PCE of 18.1%.¹⁵¹ In another study, nitrogen-doped graphene oxide (NGO) was introduced as an oxidizing agent for SnO_2 to control the oxygen defects. The altered oxidation state from Sn^{2+} to Sn^{4+} reduced the oxygen vacancies in SnO_2 in the composite of NGO- SnO_2 and efficiently extracted the charges and reduced the carrier recombination, thereby delivering a PCE of 16.55%.¹⁵² Likewise, diluted CdS quantum dots improved the carrier mobility of SnO_2 and delivered a PCE of 20.78% by accelerating the charge extraction at the modified interface.¹⁵³

Xia *et al.*¹⁵⁴ introduced the zwitterion sulfamic acid ($^+\text{H}_3\text{N}-\text{SO}_3^-$) between the SnO_2 ETL and the perovskite layer, in which the interfacial chemical bridge formed through the coordination

bond *via* $-\text{SO}_3^-$ anions and electrostatic interactions *via* $-\text{NH}_3^+$, remedying the oxygen vacancies of SnO_2 and passivating the charged defects of the perovskites, respectively. This dipole alignment passivated the interfacial defects and offered barrier-free efficient charge transfer between SnO_2 and perovskites, leading to a PCE of 20.4%. Recently, the bi-directional functionalization *via* $-\text{NH}_2$ groups resulted in a PCE of 20.25%.¹⁵⁵ The chemical interface of $-\text{NH}_2$ groups expedited the charge transfer in the ETL and reduced the trap-state density in the perovskite.

Tu *et al.*¹⁵⁶ introduced the effect of molecular doping in an SnO_2 ETL on the overall performance of PSCs. The triphenylphosphine oxide (TPPO) molecule adopted n-type doping in SnO_2 to realize electron transfer from the $\text{R}_3\text{P}^+-\text{O}^-$ σ bond to the peripheral Sn atoms rather than the atoms directly interacting at the surface, which produced delocalized electrons at the surface, leading to a reduced work function and increased conductivity (Fig. 13). Moreover, the significantly reduced energy barrier (*i.e.*, 0.55 to 0.39 eV) after TPPO doping assisted the electron transfer and faded the charge accumulation at the interface, delivering a PCE of 20.69%. Similarly, graphdiyne doping in SnO_2 was employed to precisely engineer the interface due to heterogeneous perovskite nucleation, reducing the grain boundaries and defect density and leading to favourable C-O σ bond formation and band alignment. Consequently, this reduced the interfacial recombination and delivered a PCE of 20.74%.¹⁵⁷ In the future, molecular doping in the ETL can lead to achieving an excellent efficiency in PSCs, but the strong reducibility and stability under ambient conditions need be inspected thoroughly. Similarly, modulation of the perovskite crystallization process needs to be explored deeply to gain a deeper understanding of the process of realizing highly stable and crystalline perovskite films. Recently, it was shown that a $\text{Ti}_3\text{C}_2\text{T}_x$ quantum dot-modified SnO_2 ETL delivered a steady-state PCE of 23.3% with excellent charge extraction efficiency.¹⁵⁸

4.1.3. Zinc Oxide (ZnO). Zinc oxide, an n-type semiconductor, offers high crystallinity at low processing temperature and favourable band alignment with hybrid perovskite. A direct band-gap of 3.2 eV, electron mobility of $205\text{--}300\text{ cm}^2\text{ V}^{-1}\text{ s}^{-1}$, and electron diffusion co-efficient of $1.7 \times 10^{-4}\text{ cm}^2\text{ s}^{-1}$ are the other major characteristics of ZnO, attracting researchers to explore it as a potential ETL to improve the performance of PSCs.^{159–164} Various methods have been widely explored to process and coat ZnO films under an ambient atmosphere, and each method provides a unique way of controlling the structure, electronic properties, and surface defects,^{165,166} which strongly affect the charge carrier transfer at the ZnO/perovskite interfaces. Furthermore, various morphologies (nanorods, nanosheets, monolayers, and nano-flowers, *etc.*) of ZnO have been explored to improve the charge carrier collection efficiency at this interface. A simple and cost-effective approach to process the ZnO hole-blocking layer is repeated spin coating of a mixed solution of ethanol and zinc acetate as a precursor with intermediate drying to achieve the desired thickness. Son *et al.*¹⁶⁷ introduced the solution-immersion method for the preparation of one-dimensional (1D) ZnO nanorods as an ETL in PSCs, which resulted in fast charge collection efficiency, leading to improved efficiency compared to that of TiO_2

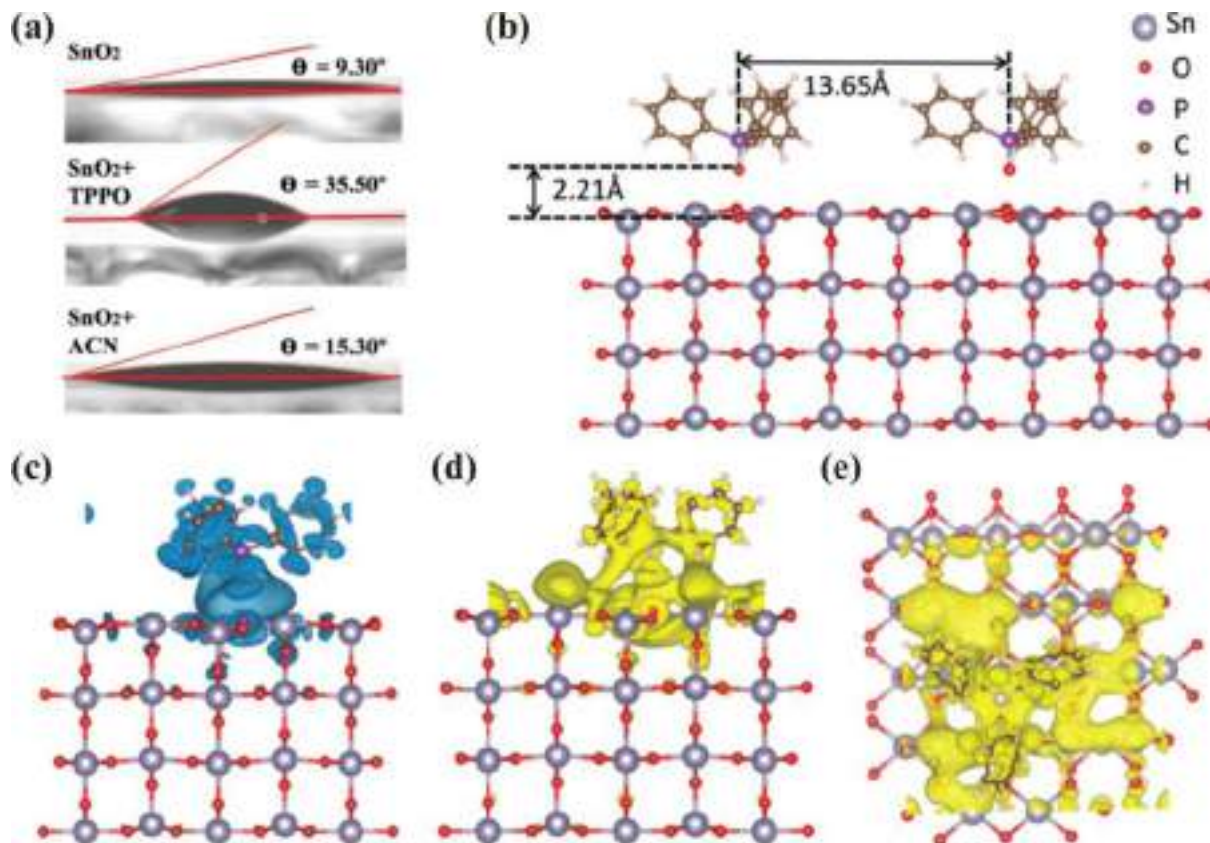


Fig. 13 (a) Surface contact angle of SnO₂, TPPO-doped SnO₂, and acetonitrile treated SnO₂ on ITO substrate; the oxygen atom of TPPO tetrahedral molecule connection with Sn atom leaving other three ends facing upward delivered larger contact angle; (b) the side view of the relaxed model of TPPO absorbed SnO₂(110) surface; charge density difference ($\Delta\rho$) of TPPO on SnO₂(110) surface was evaluated at isovalue of $1.2 \times 10^{-4} \text{ |e| \AA}^{-3}$; (c) blue indicates electron depletion, and (d) yellow indicates electron accumulation; (e) top view of charge density difference ($\Delta\rho$) of TPPO absorbed on SnO₂(110), electron gain is indicated by yellow.¹⁵⁶ Reprinted with permission from (*Adv. Mater.*, 2019, **31**, 1805944). Copyright (2019) John Wiley & Sons.

nanorods as the ETL. The single-crystalline 1D ZnO nanorods offered smooth charge transfer across the ZnO/perovskite interface due to the internal electric field along the *c*-axis, *i.e.*, common growth direction for ZnO nanorods and absence of grain boundaries.¹⁶⁸ The compact and uniform planar ZnO films indeed delivered relatively high-efficiency solar cells.

Tseng *et al.*¹⁶⁹ produced uniform ZnO films using RF sputtering under pure Ar and Ar + O₂ working gas to tune the surface electronic properties, which resulted in downshifting of the band structure, improving the electron injection and rendering an efficiency of $\sim 16\%$ combined with methylammonium lead iodide (*i.e.*, MAPbI). However, given that the high-energy ions used during sputtering damage the substrate and deteriorate the ZnO film quality, ALD has been utilized to obtain high-quality ZnO films.¹⁷⁰ The optimized thickness of 30 nm for ALD-grown ZnO films attained a high V_{OC} (*i.e.*, 0.97 V), FF (*i.e.*, 48%), and J_{SC} (*i.e.*, 14.15 mA cm⁻²) of the PSCs. This study revealed a better excitation dissociation rate at the ZnO/perovskite interface, hinging on the exciton lifetime and photo-induced absorption strength. Nevertheless, an increase in thickness beyond 30 nm caused a high series resistance, and the performance of the PSCs decreased. Besides, the spray coating technique was also explored for the mass production of planar ZnO films over a larger

area.¹⁷¹ Hydrothermally grown 1D hexagonal ZnO nanorods exhibited high charge conduction due to their sparsely populated conduction band and showed a good agreement between the experimentally measured J_{SC} and integrated current density calculated from the external quantum efficiency.¹⁶⁷

The two major drawbacks of ZnO ETLs are the severe charge recombination at the ZnO/perovskite interface due to the high-density of surface defect states and their poor chemical stability due to the presence of hydroxyl groups and organic residue on the surface of ZnO, which deteriorate cell efficiency. Notably, the presence of volatile organic residue on the surface of ZnO enables the penetration of atmospheric water/oxygen at the ZnO/perovskite interface and degrades the perovskite, leading to the operational instability of PSCs.⁴⁴ Thus, this has stimulated researchers to investigate other possibilities of ZnO surface control to overcome the interface stability. The chemical behavior of the ZnO surface, which is basic in nature, is responsible for the deprotonation of the methylammonium cation to form methylamine through an acid–base reaction, which causes the perovskite to undergo thermal decomposition even in the absence of hydroxyl groups and residual organic ligand at the ZnO surface.^{172,173} Density functional theory (DFT) calculations for the geometry optimization of the

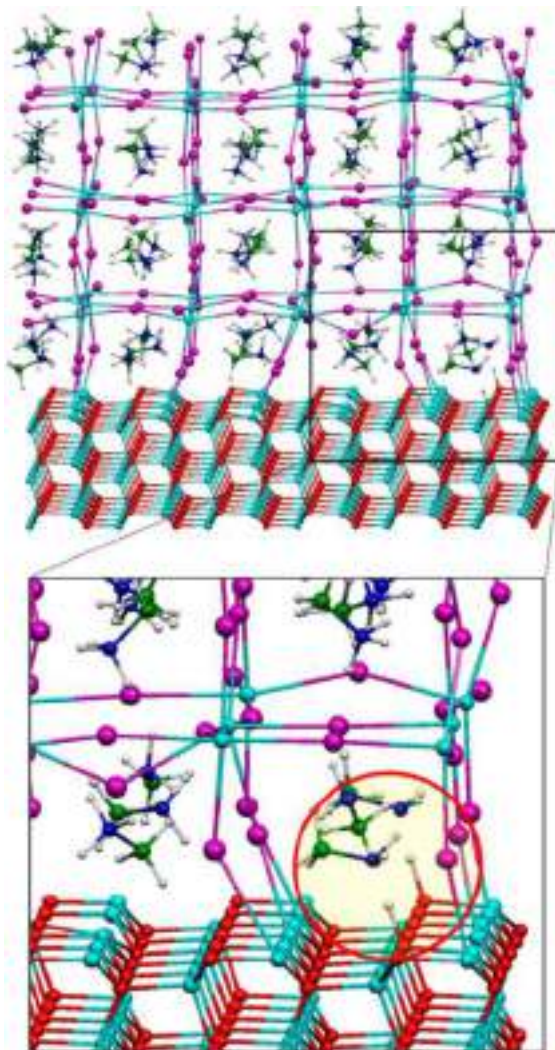


Fig. 14 Optimized geometrical structure of the ZnO ETL and $\text{CH}_3\text{NH}_3\text{PbI}_3$ perovskite (upper panel). The magnified structure of deprotonated methylammonium cations (lower panel) from the portion marked in the upper panel.¹⁷² Reprinted with permission from (*Chem. Mater.*, 2015, **27**, 4229–4236). Copyright (2015), the American Chemical Society.

ZnO/perovskite structure revealed that the deprotonation of the methylammonium ion (Fig. 14) is a constructive guide to develop PSCs capable of withstanding harsh temperature conditions.

Moreover, creative strategies such as doping and surface passivation of ZnO have been effectively used in search of its excellent performance as an ETL in PSCs. Both planar and nanostructured ZnO ETLs were doped with elements such as Mg,^{174–176} Al,^{177–179} I,¹⁸⁰ and Sn¹⁸¹ to develop low defect sites, larger surface area, and rapid electron extraction, which are some of the prerequisites for efficient ETLs. Besides, recently, the ZnO surface was modified with methylammonium chloride (MACl),¹⁸² carbon nanotubes (CNTs),¹⁸³ and ethylene diamine tetraacetic acid (EDTA)¹⁸⁴ to eliminate the deprotonation ability and enhanced stability of the ZnO/perovskite interface was achieved.

Separately, the most widely studied optoelectronic material, aluminium-doped ZnO (*i.e.*, AZO), has been proposed as an ETL and transparent conducting electrode in PSCs, which also improves the thermal stability by decreasing the Lewis acid–base chemical reaction at the ZnO/perovskite interface.¹⁷⁹ A monolayer of Cs and Li-doped ZnO as the ETL in a PSC delivered a PCE of 18%, which is comparable to that of the well-accepted TiO_2 . This is attributed to the increased electron density due to the decrease in trap density by reducing the oxygen vacancies at the ZnO surface.¹⁸⁵ The doping of iodine facilitated the dense growth of ZnO:I nanopillars and led to a matching work function between the ETL and perovskite, which resulted in a PCE of around 18%.¹⁸⁰ The doping of ZnO¹⁷⁴ is a common and effective approach to fine-tune the position of the Fermi level (E_F) and band structure and increase the conductivity to avoid interface charge recombination by achieving an optimized CB edge difference between ZnO and perovskite. Alternatively, the surface passivation strategy helps to enhance the thermal stability during annealing,¹⁸⁶ improve the morphology of the perovskite layer,¹⁸⁷ and reduce the back electron transfer and charge recombination.¹⁶⁸ ZnO ETLs passivated with thin layers of MgO,⁶² TiO_2 ,¹⁸⁶ Zn_2SnO_4 ,¹⁸⁸ Nb_2O_5 ,¹⁸⁷ SnO_2 ,¹⁶⁸ *etc.* were used to limit the degradation of the perovskite absorber due to the surface defects of ZnO at the perovskite/ZnO interface. The well-optimized passivation of ZnO with TiO_2 using the wet chemical approach of layer-by-layer absorption and reaction (LBLAR) method¹⁸⁹ achieved an efficiency of $\sim 13.5\%$ with better long-term stability compared to unpassivated ZnO nanorods (Fig. 15).¹⁸⁶

Overall, the degradation and thermal decomposition of perovskite due to the ZnO surface hinder the long-term stability and outdoor applications of ZnO-based PSC devices. Therefore, more efforts by the broader research community are required to search for novel ways other than passivation that can stop the deprotonation of methylammonium and also provide smooth charge transfer across the ZnO/perovskite interface.

4.1.4. Ternary metal oxides. Ternary metal oxides with the perovskite structures of ABO_3 and A_2BO_4 are gaining more attention than binary metal oxides, given that they allow better tunability of the bandgap, work function, and conductivity by adjusting the relative ratio of cations.^{190–195} BaSnO_3 (BSO) is a wide bandgap (*i.e.*, 3.2 eV) n-type transparent semiconductor with a perovskite structure similar to the photoactive layer. High-temperature processed BSO led to reduced charge recombination and charge transfer resistance at the BSO/perovskite interface, delivering PCEs close to 12%.^{196,197} Additionally, one-dimensional BSO nanorods showed better electron conduction subject to direct pathways and less grain boundaries than nanoparticles.¹⁹⁸ Further, to gain atomic insights into the BSO/perovskite interface, first principal DFT calculations were performed by Guo *et al.*,¹⁹⁹ revealing large interface binding energies, favouring robust interface and charge transfer capability, which were shown to further improve with the doping depth of La in BSO. Moreover, theoretical studies also predicted the easy bandgap tuning of BSO by substituting La²⁰⁰ or Sr²⁰¹ to produce optimal band alignment for improved device

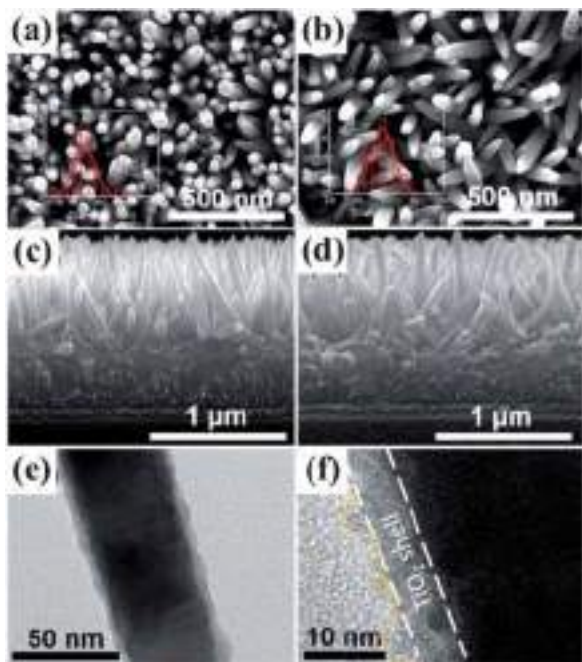


Fig. 15 SEM images of ZnO nanorods (a and c) without and (b and d) with TiO₂ passivation, depicting the top and cross sectional views, respectively. (e) TEM and (f) HRTEM images of ZnO nanorod with TiO₂ passivation. The yellow dashed line in the HRTEM image marks the edge of the ZnO/TiO₂ nanorod.¹⁸⁶

performance. Likewise, La-doping of BSO *via* the superoxide colloidal solution route was shown to yield improved electron mobility and optimal bandgap of BSO, which delivered an efficiency close to ~21% from the PSCs fabricated with a single cation lead triiodide. Recently, Zn doping also led to improved interfacial contact and reduced charge recombination at the interface of BSO.²⁰²

SrTiO₃ (STO), having high electron mobility and a slightly higher conduction band than TiO₂, has also been employed as the ETL for PSCs, giving a PCE of 10%.²⁰³ This striking device performance was ascribed to the STO/perovskite interface with reduced charge recombination due to the high dielectric constant of STO and formation of a uniform photoactive layer with large crystals on STO, allowing complete surface coverage.²⁰⁴ Unfortunately, the high-temperature processing, poor average J_{SC} , and inadequately studied STO/perovskite interface were limitations in the initial stage. However, Neophytou *et al.*²⁰⁵ achieved a PCE of 19% from low temperature (150 °C)-processed STO as the ETL, which was attributed to the better optical transparency, reduced interfacial trap state density, improved electron transport, and efficient charge extraction. Despite the long term stability under UV light illumination, the conduction band edge of STO is unfavourable for the injection of electrons from the perovskite layers. Therefore, tuning of the CB position of STO by Nb doping, together with the removal of SrO phase segregated on the surface of Nb-doped STO, was shown to enable fast charge transfer at the interface, which collectively resulted in the highest PCE of 20.2%.²⁰⁶ In parallel attempts to use STO as the ETL of PSCs, a variety of

nanocomposites such as graphene/STO,²⁰⁷ 3-D self-branching of TiO₂/STO nanoparticles,²⁰³ and Al₂O₃-graphene/STO²⁰⁸ has been employed to achieve the highest PCE of close to 20.6%. Besides, BaTiO₃ (BTO), a ferroelectric material, has also been utilized as the ETL in PSCs owing to its spontaneous polarization, which drives the photo-generation of electrons to improve the transport and charge extraction.²⁰⁹ The use of a mesoporous double layer of BTO/TiO₂²¹⁰ and ultrathin layer of BTO to modify the mesoporous TiO₂-perovskite interface²¹¹ resulted in boosted charge extraction and reduced charge recombination. Also, doped ABO₃ perovskites such as Y-doped SrSnO₃²¹² and La-doped SrSnO₃²¹³ have helped to achieve an efficiency close to 19%.

Ternary metal oxides besides the ABO₃ perovskite structure such as A₂BO₄ and A₂B₃O₈ have been scarcely studied as ETLs in PSCs. Among them, particularly, Zn₂SnO₄ (ZSO) is an up-and-coming alternative to TiO₂ in PSCs due to its comparable conduction band edge, higher electron mobility, much faster charge injection, and high electron diffusion efficiency, as observed by time and frequency-resolved spectroscopy.²¹⁴ Moreover, it provides negligible hysteresis and extraordinary stability with acid/base and polar molecules, and also enhances the crystallization of the perovskite layer. Its refractive index close to FTO permits high transmittance in the visible range. Furthermore, the use of ZSO as an ETL instead of ZnO plays a dual role by improving the crystallization of the perovskite without antisolvent treatment and providing increased stability without encapsulation.²¹⁵ Also, the use of ZSO/ZnO and ZSO/RGO nanocomposites as ETLs has resulted in better transmittance, electrical conductivity, and charge collection efficiency.^{216,217} Amorphous ZSO films with extreme surface uniformity delivered an efficiency close to 20% in the presence of the FAMAPbI₃ perovskite light absorber.⁶³ In an attempt to overcome the differences in charge diffusion lengths between the perovskite and transport layers, a bulk heterojunction (BHJ) of a composite of ZSO nanoparticles and perovskite was also explored as the photoactive layer (Fig. 16). The enhanced charge collection efficiency, improved morphology of the perovskite layer with large crystal size, balanced charge carrier mobility, and reduced trap density of BHJ films helped to achieve an efficiency close to 21%.²¹⁸ Finally, a mesoporous layer of the Zn₂Ti₃O₈ perovskite structure was employed as an ETL in a PSC, resulting in a PCE of 17.2%.²¹⁹

4.1.5. Scaffolding technique. The scaffolding technique has attracted attention due to its ability to exploit the long charge diffusion lengths of the perovskite light absorbers. The dielectric scaffolds offer a higher level of conduction band edge than the perovskite absorbers and prohibit the reverse electron transport from the perovskite, increasing the V_{OC} of PSCs.^{220,221} Moreover, the implementation of insulating scaffolds is possible due to the long-range balanced electron and hole diffusion lengths of organic-inorganic perovskites. A mesoporous metal-oxide scaffold contributed to the electron-hole diffusion length of $\sim > 1 \mu\text{m}$ in a mixed halide (CH₃NH₃PbI_{3-x}Cl_x) and $\sim 100 \text{ nm}$ in triiodide (CH₃NH₃PbI₃) perovskite absorbers.²²² Lee *et al.*²²⁰ demonstrated the use of a mesostructured

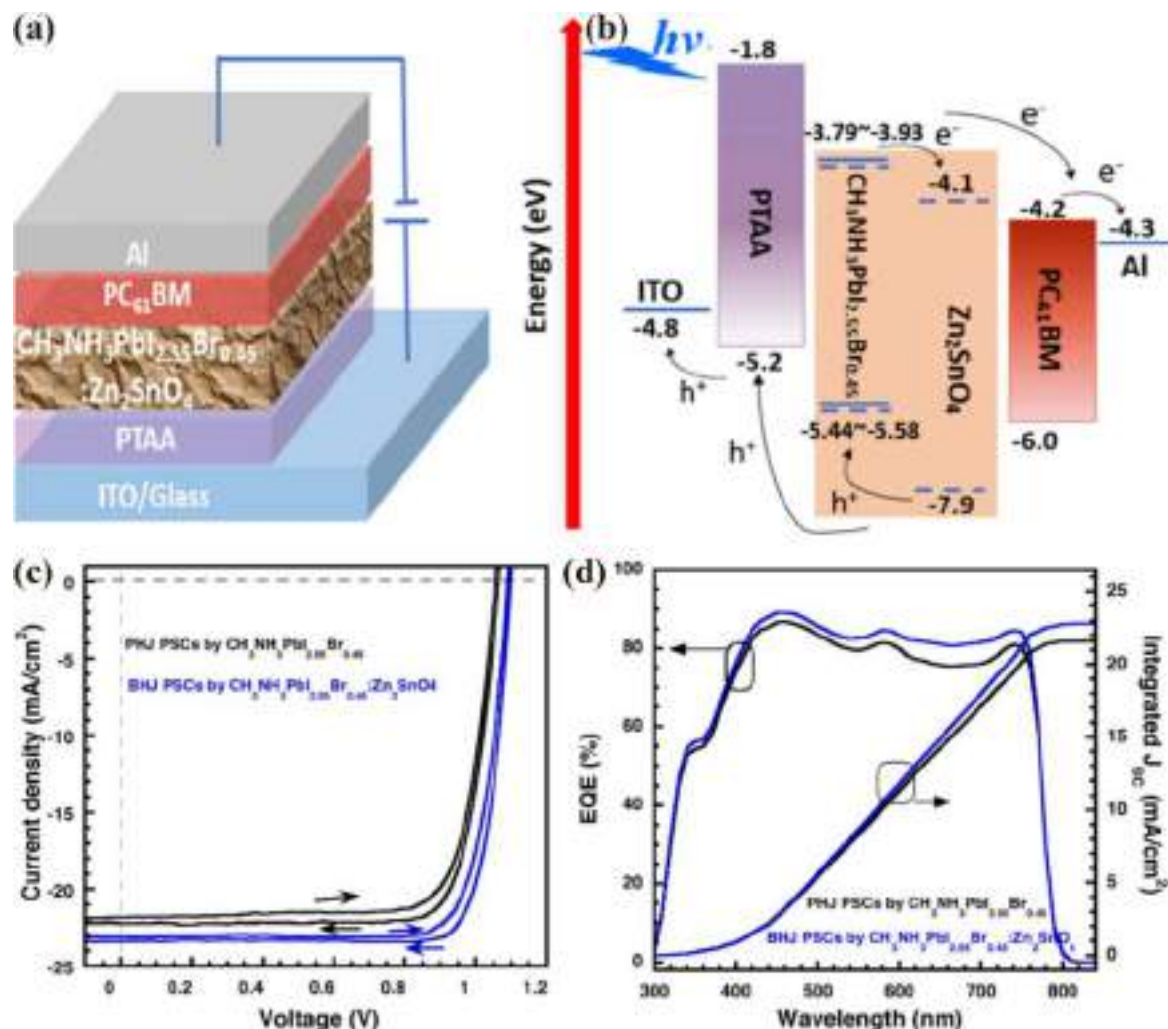


Fig. 16 Schematic of (a) device structure and (b) band diagram of bulk heterojunction (BHJ) PSCs. (c) J - V characteristics and (d) EQE spectra (with integrated J_{sc}) of planar heterojunction (PHJ) and BHJ PSCs, respectively.²¹⁸ Reprinted with permission from (ACS Appl. Mater. Interfaces, 2019, **11**, 34020–34029). Copyright (2019), the American Chemical Society.

insulating scaffold to enhance the light absorption and photon management. The assembly of perovskite absorbers over the mesostructured scaffolds forced the electrons to reside in and be transported through the perovskite, thereby being effective in providing a better PCE. The balance between series and shunt resistances was obtained by a thicker capping layer of less conductive spiro-OMeTAD (*i.e.*, $\sim 10^{-5}$ S cm^{-1}). The self-connected percolating network of scaffolds with a larger surface area infiltrated the perovskite and allowed better charge transport. In these scaffolds, the photo-generated electrons flow through the perovskite absorbers to the front electrodes rather than injecting into the oxide layer, and the holes inject into the organic hole conductor to flow through the back contact.

Bell *et al.*²²³ systematically explored the effect of inorganic scaffolds on the performance of PSCs, which efficiently absorb light, generate charges, and transport electrons/holes with little recombination losses. This approach eliminates the use of discrete hole and electron transport media in interpenetrating composites by introducing an ambipolar material for the

conversion of absorbed photons into collected charges and transport of both electrons and holes. A porous Al_2O_3 scaffold placed between TiO_2 and the perovskite absorber supported the charge separation and transport to deliver a PCE of 12.3%. Moreover, the ultraviolet light instability of TiO_2 , due to the surface oxygen vacancies promoting the degradation of perovskite absorbers, was countered by introducing a mesostructured inert Al_2O_3 scaffold in an organometal tri-halide PSC to form a p-i-n heterojunction with spiro-OMeTAD HTL.²⁵

For the efficient transfer of photogenerated electrons by the inorganic scaffolds, the infiltration of perovskites deep inside the scaffold is an important issue to be investigated. Hwang *et al.*²²⁴ controlled the size of monodispersed SiO_2 nanoparticles and observed an excellent performance at the diameter of 50 nm due to the optimized domain size of the perovskites and stronger optical absorption. The fragmentary infiltration of perovskites in the scaffold with a particle diameter < 50 nm restricted the transport of electrons, whereas the needle-like growth of the perovskite grains over the particles with a size of > 50 nm

decreased the absorption of light due to the complex scattering behaviour, thereby impeding the performance of PSCs. However, the inclusion of SiO₂ nanoparticles in the matrix of TiO₂ formed a mesoporous composite scaffold, which led to an increase in photocurrent by affecting the optical properties of the mesoporous scaffold and altering the ion migration at the perovskite interface, providing a beneficial effect to render a PCE of 16.71%.²²⁵ Zhao *et al.*²²⁶ replaced the Al₂O₃ scaffold with a hygroscopic polyethylene glycol (PEG) scaffold to control the PSC performance in a highly humid environment. Even though the hygroscopic PEG absorbs H₂O and prevents the evolution of PbI₂ (*i.e.*, degradation of perovskite) by forming a compact moisture barrier in the vicinity of the perovskite grains, the PCE did not exceed 15.4% for unknown reasons. Further, scaffold and mesoporous transport layer combinations have been made to enhance the charge transport synergistically and suppress the charge recombination at the perovskite/transport layer interface. In these combinations of scaffolds, the ratio of scaffold to transport layer nanoparticles is controlled to optimize the transport processes.²²⁷ The TiO₂ ETL quickly transfers the electrons through a wide interface with the perovskite, but the insulating Al₂O₃ scaffold directs the electrons to transport entirely through the perovskite. Nevertheless, the heterogeneous combination of Al₂O₃ and TiO₂ directs the electrons to take easy pathways either through the ETL or the perovskite (Fig. 17) and renders a good PCE by engineering the difference in charge carrier balance and ion migration. Moreover, a bilayer mesoporous scaffold of TiO₂ and Al₂O₃ was shown to enhance the

air-stability of ambient-processed PSCs with a PCE of 16.84%.²²⁸ The inclusion of the Al₂O₃ scaffold not only protected the infiltrated perovskite from degradation due to moisture attack but also offered stable light transmission, ensuring an adequate yield of photo-generated charge carriers, and mitigated the charge transportation property deterioration.

Kwon *et al.*²²⁹ introduced parallelized nanopillar PSCs using anodized alumina oxide (AAO) as a scaffold. The AAO scaffold provided control over spatial distribution, relative volume fraction, and visible range transparency of the perovskite absorber. The vertically aligned perovskite pillars terminated the shunt currents and modulated the visible transmittance due to the vertical electronic transport and modulated the parasitic scattering because of the uneven deposition of the perovskite. The incorporation of an MoO_x buffer layer and TiO₂ ETL together with the AAO scaffold controlled the ion migration at the perovskite interface and delivered a PCE of 9.6%.

Recently, Xu *et al.*²³⁰ introduced slot-die coating for the mass production of PSCs consisting of a TiO₂ ETL and ZrO₂ scaffolds. Even though the infiltration mechanism in the scaffold was discussed based on the Lucas-Washburn model, further understanding of the coating parameters and their effect on the charge transport at the interface is recommended for the mass production of the PSCs. Quiang *et al.*²³¹ explored an Al₂O₃ scaffold with Li-doped SnO₂ ETL to achieve an enhanced PCE. The Li-doped ETL and scaffold inhibited the charge recombination and prolonged the electron lifetime, but the PCE was restricted to 10.1% due to the unfavourable participation of the grain boundaries and bulk of the materials in the charge transfer process.

Overall, SiO₂,²²⁴ Al₂O₃,²³² AAO and ZrO₂²³³ scaffolds have been explored for the better infiltration of perovskites to gain high PCEs, but most of them delivered efficiencies in the range of 10% to 16%. Furthermore, they do not eliminate the need for a compact hole-blocking layer or ETL to fabricate efficient PSCs. The thickness, roughness, and porosity of the scaffolds need to be considered for controlling the charge transport, diffusion coefficient, and collection efficiency of PSCs.

4.1.6. Other inorganic ETLs. In addition to the well-studied binary metal oxides such as TiO₂, ZnO, and SnO₂, many other metal oxides such as WO_x,²³⁴ CeO_x,²³⁵ In₂O₃,²³⁶ Nb₂O₅,²³⁷ and Fe₂O₃²³⁸ have been explored as ETLs for PSCs. Cerium oxide (CeO_x) offers several benefits including wide bandgap (*i.e.*, 3.5 eV), high dielectric constant ($\epsilon \sim 26$),²³⁹ sufficient optical transparency (refractive index of 2.1–2.7),²⁴⁰ good ionic conductivity ($\sigma = 120 \text{ S cm}^{-1} \text{ K}^{-1}$),²⁴¹ high thermal and chemical stability, ease of processing, low cost, and earth abundance, thereby qualifying as a highly promising ETL material.^{235,242–248} The low-temperature processing of CeO_x ($x = 1.81$ °C at 100 °C) with an inverted architecture and CeO_x ($x = 1.87$ °C at 150 °C) with a planar device architecture resulted in PCEs of 16.1% and 17.4%, respectively.^{235,248} Recently, lower-temperature processed CeO_x (at 80 °C) as an ETL was shown to help realize a PCE of 14.6%.²⁴³ The dense CeO_x layers not only protect the perovskite absorber from moisture but also act as a diffusion barrier to prevent corrosion.²⁴⁸ Additionally, CeO_x nanocrystals

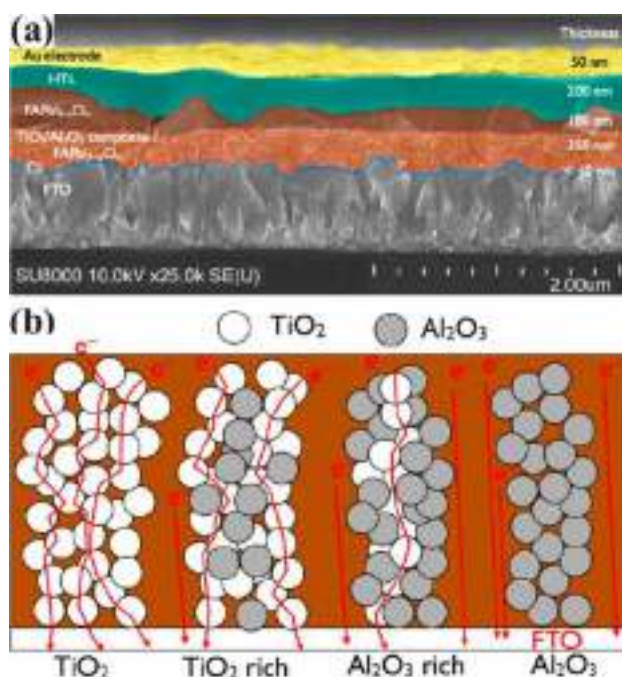


Fig. 17 (a) Device structure composed of mesoscopic Al₂O₃ scaffold, TiO₂ ETL and FAPbI_{3-x}Cl_x perovskite. (b) ELT/scaffold (*i.e.*, TiO₂/Al₂O₃) constitution variation-dependent electron transport mechanism.²²⁷ Reprinted with permission from (*ACS Appl. Mater. Interfaces*, 2016, **8**, 4608–4615). Copyright (2016), the American Chemical Society.

were utilized as a double ETL with PCBM^{242,245} and ZnO²⁴⁶ to achieve the best efficiency values of 17.3% and 19.5%, respectively. The improvement in PCE with double ETLs was possible due to the decreased series resistance for charge extraction.²⁴⁵ CeO_x, when introduced with regular ETLs (ZnO), reduces the work function of the electron transport material (*i.e.*, ETM) and eliminates the interfacial barrier. The rich discrete energy levels of CeO_x also prevent the UV-induced degradation of the perovskite absorber.²⁴⁶

Tungsten oxide (WO_x) is another crucial ETM possessing excellent chemical stability, wide bandgaps (2 to 3 eV),^{249–251} and high electron mobility (10 to 20 cm² V⁻¹ s⁻¹).²⁵² Mahmood *et al.*²⁵³ explored 0D, 1D, and 2D nanostructures of WO₃ as ETLs for PCSs. The 2D WO₃ nanosheets offered good perovskite infiltration and fast carrier charge dynamics, thereby performing well compared to the nanoparticle and nanorod morphologies. However, they suffered from recombination losses at the WO₃/perovskite interface, which had to be controlled by forming WO₃-TiO₂ core-shell structures. Amorphous WO_x offered control over the conductivity and short circuit current, leading to an improved PCE (~15%) at the cost of lower transmittance (80% of TiO₂) and V_{OC} due to the inherent charge recombination.^{234,254} Conversely, a WO_x film introduced with TiO₂ as a bilayer ETL served as an antireflection coating, rendering an enhanced J_{SC}²⁵⁵ and improved non-wettability, which led to better crystallization of the CH₃NH₃PbI₃ perovskite and resulted in a PCE of ~20%.²⁵⁶ The high-temperature processing of amorphous WO_x incorporates defects, and subsequently deteriorates the performance of PCSs. On the contrary, ultra-low temperature (< 50 °C) processing scales down the trap densities and offers high electron mobility, thereby yielding an efficiency of ~20%.⁶⁴

The higher built-in potential achieved by the α-Fe₂O₃ ETL/perovskite interface led to more efficient charge extraction/transport, reduced charge accumulation, and less charge recombination than TiO₂ ETLs.²³⁸ The solution-processed Ni-doped (4%) α-Fe₂O₃ yielded an efficiency of ~11% with the CH₃NH₃PbI₃ perovskite owing to its enhanced electrical conductivity and lowered conduction band minimum, and also exhibited good stability upon exposure to ambient air and high-level UV irradiation.²⁵⁷ The effective approach of doping non-equilibrium Ti⁴⁺ in the lattice of Fe₂O₃ *via* the quenching process reduced the surficial oxygen vacancies and structural defects, which act as deep trap states. These states are responsible for the sluggish electron charge transfer and accumulation of charges at the ETL/perovskite interface, delivering a PCE of 17.8%.²⁵⁸ The quenching approach assisted with a uniform doping distribution and increased doping density in the bulk lattice of Fe₂O₃ by suppressing the segregation of TiO_x on the surface (Fig. 18(a)). Likewise, 1D core-shell nanostructures serve to reduce the absorber instability and increase the mobility and recombination resistance. The core-shell structures of ZnO/SnO₂,¹⁶⁸ Al₂O₃/ZnO,²⁵⁹ WO₃/TiO₂,²⁵³ TiO₂/MgO,²⁶⁰ *etc.* have been explored to gain efficient electron injection and enhancing the recombination resistance at the ETL/perovskite interface. A thin MgO layer (large bandgap of ~8 eV) coating over

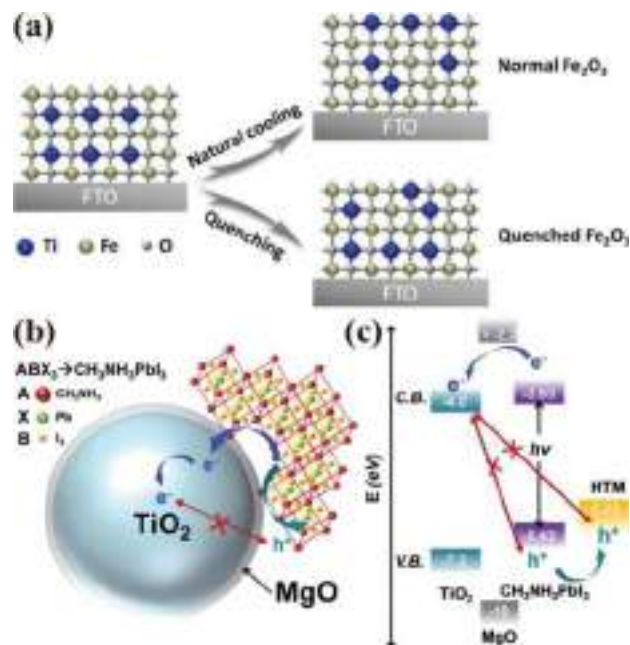


Fig. 18 Schematic representation of (a) mechanism for increased doping density in the bulk and suppressed segregation on the surface of Ti-Fe₂O₃,²⁵⁸ (b) charge transfer mechanism, and (c) band energy diagram of the MgO/TiO₂ core-shell nanoparticle-based PSC.²⁶⁰

mesoporous TiO₂ particles increased the recombination resistance through an effective charge transfer mechanism (Fig. 18(b) and (c)), leading to a better V_{OC} and FF (*i.e.*, 0.89 V and 67.1%) than that of the pristine TiO₂ (*i.e.*, 0.85 V and 71.2%), respectively.

Moreover, the well-optimized In₂O₃, which satisfies the properties required for excellent ETLs such as wide bandgap (*i.e.*, 3.8 eV), high electron mobility ($\mu = 10 \text{ cm}^2 \text{ V}^{-1} \text{ s}^{-1}$),²⁶¹ high transparency, antireflection property, and thermal stability, offer efficient electron extraction and charge transfer, producing a stable efficiency of ~14% for 31 days when In³⁺ was stabilized by inhibiting hydrolysis using acetylacetone.²⁶² The PCE was further improved (*i.e.*, up to 18.12%) by modifying the In₂O₃/perovskite interface with a PCBM interlayer.²⁶¹ The doping with Ce,²⁶³ Zr,²⁶⁴ and Sn²⁶⁵ resulted in higher electron mobility and lower parasitic absorption in the NIR range than that of pristine In₂O₃ and resulted in a PCE of above 20%. Alternatively, Nb₂O₅ is a visibly transparent, air-stable, and water-insoluble material with extensive polymorphism, and its bandgap can be tuned by controlling the stoichiometry and crystallinity.^{266,267} Kogo *et al.*²⁶⁸ first introduced Nb₂O₅ as an effective ETL with mesoporous Al₂O₃ perovskite-based PSCs and observed a higher V_{OC} (1.13 V) than that with TiO₂. However, the room-temperature processed amorphous Nb₂O₅ rendered a PCE of 17% and replaced the crystalline Nb₂O₅ as an ETL in flexible PSCs.²³⁷ However, the direct e-beam-evaporated²⁶⁹ and spin-coated²⁷⁰ pristine Nb₂O₅ were shown to offer smooth charge transfer by reducing the charge resistance and recombination at the interface, producing an efficiency of ~19%. Moreover, 5% Zn doping further assisted in faster charge extraction and reduced charge recombination at the Nb₂O₅ ETL/perovskite

interface.²⁷¹ The Nb₂O₅ passivation over TiO₂ and ZnO was shown to improve the crystallinity of the perovskite overlayer, and thereby the stability of PSCs.^{187,272} Low-temperature processed CdSe,²⁷³ CdS,²⁷⁴ and Bi₂S₃ nanocrystals are also appealing in the foregoing context due to their corresponding smaller interfacial barrier with suppressed charge trapping and smooth charge transfer without accumulation at the interface.²⁷⁵ Besides the above-mentioned developments to enhance the capabilities of inorganic ETLs, plasmonic nanoparticles (such as Au and Ag cores) have also been incorporated in inorganic ETLs to enhance their light absorption even further and reduce the exciton binding energy.^{31,276,277}

Even though several inorganic materials have been demonstrated as alternatives to the most common inorganic ETLs (*i.e.*, TiO₂, ZnO, and SnO₂), various combinations of earth-abundant constituent elements in terms of doping, composites, core-shell structures, *etc.* need to be explored for controlled interfacial reactions, delivering a higher PCE. Additionally, theoretical work on new inorganic ETL materials is essential to understand the electronic and structural properties of the interface, leading the way for a targeted experimental approach.

4.2. Organic ETLs

Organic n-type semiconductors are promising alternatives to metal-oxide-based ETLs due to their good thermal/chemical stability, low-temperature processability, LUMO level matching with the conduction band of the perovskite, *etc.*^{278–280} Additionally, organic ETLs can mend the surface defects by coordination with lead ions and reduce the charge-trap related recombination at the ETL/perovskite interface.²⁷⁸ In contrast, low-temperature processed inorganic ETLs either require high-cost techniques or provide non-uniform film coverage.⁸⁴ Therefore, various researchers have replaced inorganic ETLs with organic counterparts to address these problems. Particularly, fullerene and its derivatives, with excellent electron mobility and ability to passivate the trap state on the surface of the perovskite layer, have shown the promising possibility of utilization as ETMs.²⁷⁹

A [6,6]-phenyl-C₆₁-butyric acid methyl ester (PCBM) derivative of fullerene, a well-studied compound in organic solar cells, has been used in low temperature-processed PSCs as an ETL, which efficiently blocks the holes at the perovskite/PCBM interface because of the higher VB of the perovskite than the HOMO level for PCBM, resulting in a PCE of ~12%.²⁸¹ Furthermore, graphene quantum dot/PCBM nano-composite²⁸² was shown to improve the electrical conductivity compared to pristine PCBM. A blend of polystyrene/PCBM²⁸³ was shown to yield smooth films together with a uniform layer of organic ETL, which helped to enhance the charge collection. Moreover, a blend of organic and inorganic ETLs was also explored to govern the morphology and control the stability of the perovskite absorber and improve the device performance. Zeng *et al.*²⁸⁴ achieved a PCE of ~14% from a composite of CdSe quantum dots with PCBM as the ETL, increasing the built-in potential at the perovskite/ETL interface, which facilitated efficient electron-hole pair separation and enhancement of the photocurrent.

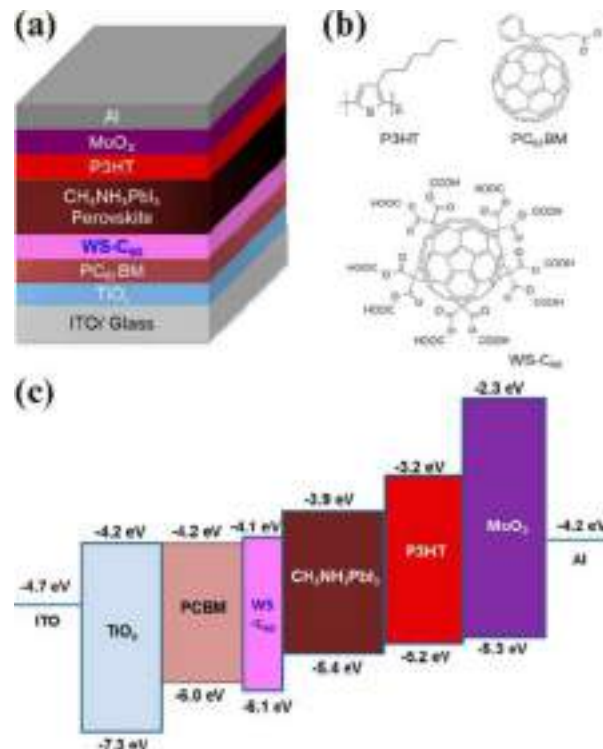


Fig. 19 (a) The device assembly of perovskite hybrid solar cells incorporated with PC₆₁BM the electron extraction layer, (b) molecular structures of PC₆₁BM, water-soluble fullerene derivative (C₆₀-Ac₁₀) and P3HT. (c) LUMO and HOMO energy levels of the materials used in the perovskite hybrid solar cells.²⁸⁵ Reprinted with permission from (*ACS Appl. Mater. Interfaces*, 2015, **7**, 1153–1159). Copyright (2015) American Chemical Society.

Liu *et al.*²⁸⁵ explored thin films of organic PC₆₁BM over inorganic TiO₂ coupled with C₆₀ as the ETL and observed efficient charge extraction at the ETL/perovskite interface (Fig. 19),

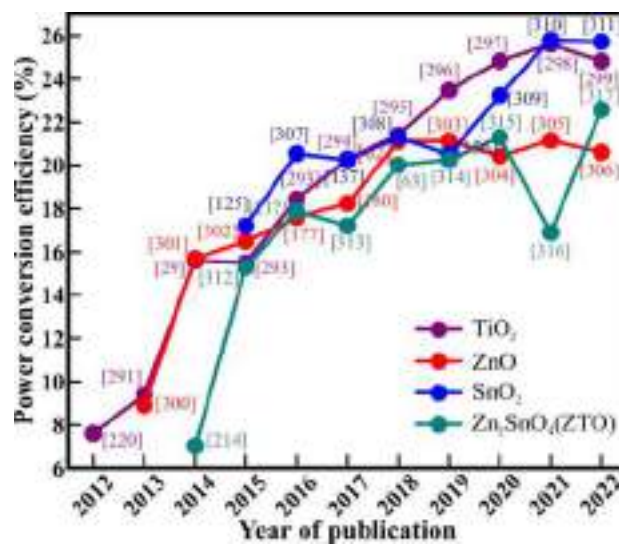


Fig. 20 Comparative study of the influential ETLs developed by year to gain the best maximum efficiency in the last decade (collected from ISI Web of Knowledge up to 15th August 2022).^{296,297,304,309,314,316}

Table 1 A brief summary of inorganic ETLs processed with various synthesis methods and their corresponding device performance parameters

S. no.	Device configuration	Method ^a	V _{oc} (V)	J _{sc} (mA cm ⁻²)	FF	PCE (%)	Year	Ref.
Titanium dioxide (TiO ₂)								
1.	FTO/LD-TiO ₂ /FA _x MA _{1-x} PbI _{3-y} Cl _y /spiro-OMeTAD:Li-TFSI:TBP/Au	CBD	1.174	25.43	0.831	24.81	2022	299
2.	FTO/RbCl:TiO ₂ /CH ₃ NH ₃ PbI ₃ /spiro-OMeTAD/Ag	DC	1.11	23.14	0.807	20.75	2022	318
3.	FTO/Ta:TiO ₂ /Cs _{0.05} (FA _{0.9} MA _{0.1}) _{0.95} PbI _{2.55} Br _{0.45} /spiro-OMeTAD/Au	SPM	1.094	23.94	0.781	20.45	2022	319
4.	FTO/c-TiO ₂ /CH ₃ NH ₃ PbI ₃ /spiro-OMeTAD/Au	SC/MW	1.07	22.18	0.71	17.97	2022	320
5.	FTO/c-TiO ₂ /mp-TiO ₂ /α-FAPbI ₃ /OAI/spiro-OMeTAD/Au	SP	1.189	26.35	0.817	25.6	2021	298
6.	FTO/c-TiO ₂ /Li ₂ CO ₃ -TiO ₂ /CH ₃ NH ₃ PbI ₃ /spiro-OMeTAD/Au	SC	1.171	26.17	0.825	25.28	2021	118
7.	FTO/TiO ₂ /CH ₃ NH ₃ PbI ₃ /spiro-OMeTAD/Ag	ALD	1.06	23.92	0.71	18.05	2021	98
8.	FTO/TiO ₂ /FAPbI ₃ /spiro-OMeTAD/Au	HT/S	1.16	24.56	0.808	22.99	2020	321
9.	FTO/Nb-TiO ₂ /(FA _{0.79} MA _{0.16} Cs _{0.05} Pb(Br _x I _{1-x}) ₃ /spiro-OMeTAD/Au)	SC	1.11	24.7	0.78	21.3	2020	322
10.	FTO/c-TiO ₂ /mp-TiO ₂ /CH ₃ NH ₃ PbI ₃ /spiro-OMeTAD/Ag	HT	1.11	23.42	0.74	19.39	2020	323
11.	ITO/NH ₂ -TiO ₂ NPs/Cs _{0.05} (FA _{0.87} MA _{0.13}) _{0.95} PbI _{2.55} Br _{0.45} /spiro-OMeTAD/Au	SGS	1.20	23.15	0.767	21.33	2019	324
12.	FTO/TiO ₂ -B/(FAPbBr ₃) _{1-x} (MAPbBr ₃) _x /spiro-OMeTAD/Au	SC	1.05	24.94	0.72	18.83	2019	325
13.	FTO/Y-TiO ₂ /CH ₃ NH ₃ PbI _{3-x} Br _x /spiro-OMeTAD/Au	HP	1.04	23.55	0.75	18.32	2019	108
14.	FTO/c-TiO ₂ /m-TiO ₂ NC-NR/Cs _{0.05} (MA _{0.17} FA _{0.83}) _{0.95} Pb(I _{0.83} Br _{0.17}) ₃ /spiro-OMeTAD/Au	HT	1.055	22.95	0.71	17.2	2019	326
15.	FTO/c-TiO ₂ /a-SnO ₂ /Cs _{0.05} MA _{0.15} FA _{0.85} Pb(I _{0.85} Br _{0.15}) ₃ /spiro-OMeTAD/Au	SC	1.169	23.91	0.765	21.4	2018	295
16.	FTO/Nb:TiO ₂ /TiO ₂ NR/CH ₃ NH ₃ PbI _{3-x} Br _x /spiro-OMeTAD/Au	HP	1.03	23.95	0.77	18.88	2018	116
17.	ITO/TiO ₂ -TOPD/PC ₆₀ BM/CH ₃ NH ₃ PbI ₃ /spiro-OMeTAD/Au	SC	1.10	23.11	0.802	20.3	2017	294
18.	FTO/TiO ₂ /FA _x MA _{1-x} PbI _{3-y} Br _y /spiro-OMeTAD/Au	SC	1.075	22.28	0.769	18.43	2016	293
19.	FTO/c-TiO ₂ /TiO ₂ NE/CH ₃ NH ₃ PbI ₃ /spiro-OMeTAD/Ag	CBD	0.985	22.0	0.72	15.71	2016	327
20.	FTO/TiO ₂ /mp-TiO ₂ NF/CH ₃ NH ₃ PbI ₃ /spiro-OMeTAD/Ag	ES	0.98	20.0	0.74	15.5	2015	292
21.	FTO/c-TiO ₂ /CH ₃ NH ₃ PbI _{3-x} Cl _x /P3HT/Ag	ALD	0.979	24.3	0.572	13.60	2015	328
22.	FTO/graphene/TiO ₂ /CH ₃ NH ₃ PbI _{3-x} Cl _x /spiro-OMeTAD/Au	SC	1.05	21.9	0.74	15.6	2014	29
23.	FTO/c-TiO ₂ /m-TiO ₂ /CH ₃ NH ₃ PbI ₃ /spiro-OMeTAD/Au	TO	1.09	21.97	0.63	15.07	2014	84
24.	FTO/r-TiO ₂ NR/MAPbI ₃ /spiro-OMeTAD/Au	SC	0.955	15.6	0.63	9.4	2013	291
25.	FTO/c-TiO ₂ /CH ₃ NH ₃ PbI ₂ Cl/spiro-OMeTAD/Ag	SC	0.80	17.8	0.53	7.6	2012	220
Zinc oxide (ZnO)								
26.	FTO/ZnO/2-TA/Cs _{0.05} (FA _{0.9} MA _{0.1}) _{0.95} PbI _{2.55} Br _{0.45} /spiro-OMeTAD/Au	SC	1.16	22.9	0.775	20.6	2022	306
27.	FTO/AZO/CH ₃ NH ₃ PbI ₃ /spiro-OMeTAD:Li-TFSI:TBP/Au	ALD	1.05	23.16	0.74	18.09	2022	329
28.	FTO/Mg:ZnO/CH ₃ NH ₃ PbI ₃ /spiro-OMeTAD:Li-TFSI:TBP/Au	ES	0.83	25.06	0.65	13.52	2022	330
29.	ITO/ZnO/ZnO-Cl-Phen/FA _{0.9} Cs _{0.1} PbI _{2.7} Br _{0.3} /spiro-OMeTAD/Ag	SC	1.16	22.88	0.797	21.15	2021	305
30.	FTO/ZnO/ZnS/TiO ₂ /spiro-OMeTAD/Au	HT	1.12	24.07	0.77	20.6	2021	331
31.	FTO/ZnO/IBA/CH ₃ NH ₃ PbI ₃ /spiro-OMeTAD/Au	SC	1.12	21.93	0.75	18.84	2020	332
32.	FTO/MLG/ZnO/FA _x MA _{1-x} PbI _{3-y} Br _y /spiro-OMeTAD/Au	SC/LPCVD	1.15	23.42	0.781	21.03	2019	303
33.	FTO/ZnO-MgO-EA ⁺ /TiO ₂ (CsFAMA)Pb(BrI) ₃ /spiro-OMeTAD/Au/graphene	SC	1.12	23.86	0.789	21.08	2018	62
34.	ITO/ZnO-K/CH ₃ NH ₃ PbI ₃ /spiro-OMeTAD/Au	SGS	1.13	23.0	0.771	19.90	2018	333
35.	ITO/c-ZnO/ZnO:1/CH ₃ NH ₃ PbI ₃ /spiro-OMeTAD/Ag	HT	1.13	22.42	0.719	18.24	2017	180
36.	ITO/AZO/CH ₃ NH ₃ PbI ₃ /spiro-OMeTAD/Ag	RFS	1.07	21.5	0.725	17.6	2016	177
37.	ITO/Mg-ZnO/CH ₃ NH ₃ PbI ₃ /spiro-OMeTAD/Ag	SC	1.07	20.6	0.745	16.5	2016	175
39.	PEN/ITO/ZnO/CH ₃ NH ₃ PbI ₃ /PTAA/Au	SP	1.10	18.7	0.75	15.6	2016	334
40.	ITO/PEDOT:PSS/CH ₃ NH ₃ PbI ₃ /ZnO/Ag/Al ₂ O ₃ -PET	ALD	1.02	20.73	0.764	16.5	2015	302
41.	ITO/c-ZnO/CH ₃ NH ₃ PbI ₃ /spiro-OMeTAD/Ag	SC	1.03	20.4	0.749	15.7	2014	301
42.	FTO/c-ZnO/ZnO NR/CH ₃ NH ₃ PbI ₃ /spiro-OMeTAD/Au	HT	0.991	20.08	0.56	11.13	2014	167
43.	FTO/ZnO/CH ₃ NH ₃ PbI ₃ /spiro-OMeTAD/Au	CBD	1.02	16.98	0.511	8.9	2013	300
Tin oxide (SnO ₂)								
44.	FTO/c-TiO ₂ /Paa-QD-SnO ₂ /FA _x MA _{1-x} PbI _{3-y} Cl _y /OAI/spiro-OMeTAD/Au	SC	1.176	26.09	0.838	25.72	2022	311
45.	FTO/SnO ₂ /BA + PEAI/Cs _{0.05} (FA _{0.9} MA _{0.1}) _{0.95} PbI _{2.55} Br _{0.45} /spiro-OMeTAD/MoO ₃ /Ag	SC	1.144	25.16	0.811	23.35	2022	335
46.	FTO/SnO ₂ -LiOH/FA _x MA _{1-x} PbI _{3-y} Br _y /spiro-OMeTAD:Li-TFSI:TBP/Ag	SC	1.15	24.20	0.763	21.31	2022	336
47.	FTO/Cl-SnO ₂ /FA _x MA _{1-x} PbI _{3-y} Br _y /spiro-OMeTAD:Li-TFSI:TBP/Au	SC/DC	1.07	24.25	0.73	18.94	2022	337
48.	FTO/SnO ₂ /FAPbI ₃ :0.38MDACl ₂ /spiro-OMeTAD/Au	SC	1.189	25.74	0.832	25.8	2021	310
49.	FTO/SnO ₂ /MA _{0.15} FA _{0.85} Pb(I _x Cl _{3-y} Br _{1-x-y}) ₃ /spiro-OMeTAD/Au	CBD	1.181	25.14	0.848	25.2	2021	139
50.	FTO/SnO ₂ -K ₂ SO ₄ /Cs _{0.05} (FA _{0.9} MA _{0.1}) _{0.95} PbI _{2.55} Br _{0.45} /spiro-OMeTAD:Li-TFSI:TBP/Ag	SC	1.2	22.89	0.771	21.18	2021	338
51.	FTO/SnO ₂ :CdS QD/CH ₃ NH ₃ PbI ₃ /spiro-OMeTAD/Ag	HT/SC	1.13	23.45	0.78	20.78	2021	153
52.	FTO/SnO ₂ /CH ₃ NH ₃ PbI ₃ /spiro-OMeTAD/Ag	SC	1.14	23.38	0.76	20.24	2021	339
53.	ITO/urea-SnO ₂ /CH ₃ NH ₃ PbI ₃ /spiro-OMeTAD/Au	SC	1.13	23.51	0.76	20.25	2021	155
54.	FTO/SnO ₂ /SnO ₂ :TaCl ₅ /CH ₃ NH ₃ PbI ₃ /spiro-OMeTAD/MoO ₃ /Ag	SC	1.08	22.56	0.75	18.23	2021	146
55.	ITO/SnO ₂ /SnO ₂ -KF/CsPbI ₂ Br/spiro-OMeTAD/MoO ₃ /Ag	SC	1.31	14.79	0.79	15.39	2021	145
56.	FTO/SnO ₂ :Eu/CH ₃ NH ₃ PbI ₃ /spiro-OMeTAD/Au	CBD	1.13	22.61	0.79	20.14	2021	144
57.	FTO/SnO ₂ NR/Cs _{0.05} (MA _{0.15} FA _{0.85}) _{0.95} Pb(I _{0.85} Br _{0.15}) ₃ /spiro-OMeTAD/Au	ET	1.15	23.45	0.78	21.35	2020	340
58.	ITO/SnO ₂ /SA/Cs _{0.05} (FA _{0.85} MA _{0.15}) _{0.95} Pb(I _{0.85} Br _{0.15}) ₃ /spiro-OMeTAD/Au	SC	1.15	22.80	0.78	20.41	2020	154

Table 1 (continued)

S. no.	Device configuration	Method ^a	V _{oc} (V)	J _{sc} (mA cm ⁻²)	FF	PCE (%)	Year	Ref.
59.	ITO/SnO ₂ -CNT/CH ₃ NH ₃ PbI ₃ /spiro-OMeTAD/Au	SC	1.12	23.26	0.782	20.33	2020	138
60.	FTO/SnO ₂ /MgO/CsPbI ₂ Br ₂ /spiro-OMeTAD/Ag	SC	1.36	11.70	0.693	11.04	2020	341
61.	ITO/SnO ₂ /TPPO/Cs _{0.05} (MA _{0.15} FA _{0.85}) _{0.95} Pb(I _{0.85} Br _{0.15}) ₃ /spiro-OMeTAD/Au	SC	1.11	24.3	0.77	20.69	2019	156
62.	ITO/SnO ₂ /TiO ₂ /FA _x MA _{1-x} PbI _{3-y} Br _y /spiro-OMeTAD/Au	SC	1.10	24.2	0.77	20.5	2019	342
63.	FTO/SnO ₂ :NH ₄ Cl/Cs _{0.05} (FA _{0.85} MA _{0.15}) _{0.95} Pb(I _{0.85} Br _{0.15}) ₃ /spiro-OMeTAD/Au	SC	1.19	22.2	0.75	20	2019	143
64.	ITO/SnO ₂ :NGO/Rb _{0.05} (FA _{0.83} MA _{0.17}) _{0.95} Pb(I _{0.83} Br _{0.17}) ₃ /spiro-OMeTAD/Au	SC	1.17	18.87	0.75	16.54	2019	152
65.	ITO/SnO ₂ /C ₉ /CH ₃ NH ₃ PbI ₃ /spiro-OMeTAD/Au	SC	1.12	22.8	0.789	21.3	2018	308
66.	FTO/Mg-SnO ₂ bil/SnO ₂ /CH ₃ NH ₃ PbI ₃ /spiro-OMeTAD/Au	SGS	1.112	22.80	0.758	19.21	2018	343
67.	ITO/SnO ₂ :GQDs/CH ₃ NH ₃ PbI ₃ /spiro-OMeTAD/Au	SC	1.13	23.05	0.778	20.23	2017	137
68.	FTO/SnO ₂ NS/C ₆₀ /CH ₃ NH ₃ PbI ₃ /spiro-OMeTAD/Au	HT	1.039	23.62	0.75	18.31	2017	344
69.	ITO/SnO ₂ /CH ₃ NH ₃ PbI ₃ /spiro-OMeTAD/Ag	ED	1.08	19.75	0.65	13.88	2017	128
70.	ITO/SnO ₂ :(FAPbI ₃) _{0.97} (MAPbI ₃) _{0.03} /spiro-OMeTAD/Au	SC	1.10	25.28	0.731	20.28	2016	307
71.	FTO/SnO ₂ /CH ₃ NH ₃ PbI ₃ /spiro-OMeTAD/Au	SC	1.11	23.27	0.67	17.21	2015	125
Ternary metal oxides								
72.	FTO/LBSO-PFA/Cs _{0.05} FA _{0.81} MA _{0.14} PbI _{2.55} Br _{0.45} /spiro-OMeTAD:Li-TFSI:TBP/Au	laser	1.139	24.10	0.86	23.74	2022	345
73.	FTO/ZSO/FA _x MA _{1-x} PbI _{3-y} Br _y /spiro-OMeTAD:Li-TFSI:TBP/Au	CBD	9.368	3.24	0.745	22.59	2022	317
74.	FTO/c-TiO ₂ /NO-BSO/ZrO ₂ /CH ₃ NH ₃ PbI ₃ /spiro-OMeTAD/Au	SP	0.94	23.04	0.68	14.77	2021	346
75.	FTO/ZSO/CsMAFA/spiro-OMeTAD/Au	CBD	1.14	23.59	0.79	21.3	2020	315
76.	FTO/La-SrSnO ₃ /CH ₃ NH ₃ PbI ₃ /spiro-OMeTAD/Au	SC	1.12	23.3	0.718	18.7	2020	213
77.	FTO/c-ZSO/mp-ZSO/CH ₃ NH ₃ PbI ₃ /spiro-OMeTAD/Au	HT	1.05	24.79	0.704	18.32	2020	347
78.	FTO/La ³⁺ -BaTiO ₃ /TiO ₂ /CH ₃ NH ₃ PbI ₃ /spiro-OMeTAD/Au	HT	0.96	21.5	0.69	14.3	2020	348
79.	FTO/c-ZSO/mp-ZSO/Cs _{0.5} (MA _{0.17} FA _{0.83}) _{0.95} Pb(I _{0.83} Br _{0.17}) ₃ /spiro-OMeTAD/Au	RC	1.06	24.58	0.79	20.1	2019	349
80.	FTO/am-ZSO/SnO ₂ /CH ₃ NH ₃ PbI ₃ /spiro-OMeTAD/Au	PLD	1.12	22.49	0.796	20.04	2019	350
81.	FTO/Y-SrSnO ₃ /CH ₃ NH ₃ PbI ₃ /spiro-OMeTAD/Au	SC	1.14	22.7	0.74	19.0	2019	212
82.	ITO/SrTiO ₃ /CH ₃ NH ₃ PbI ₃ /spiro-OMeTAD/Au	SC	1.143	23.02	0.721	19.0	2019	205
83.	FTO/ZSO/FAMAPbI ₃ /spiro-OMeTAD/Au	SC	1.036	24.72	0.781	20.02	2018	63
84.	FTO/LBSO/CH ₃ NH ₃ PbI ₃ /PTAA/Au	PP/SC	1.12	23.4	0.81	21.2	2017	200
85.	FTO/c-TiO ₂ /ZSO/CH ₃ NH ₃ PbI ₃ /spiro-OMeTAD/Au	HT	1.048	23.71	0.692	17.21	2017	313
86.	FTO/ZnO/ZSO/CH ₃ NH ₃ PbI ₃ /spiro-OMeTAD/Au	SP	1.035	19.71	0.59	12.03	2017	216
87.	FTO/BSO/CH ₃ NH ₃ PbI ₃ /spiro-OMeTAD/Au	PP	0.968	17.45	0.637	10.96	2017	197
88.	FTO/bl-ZSO/rGO-ZSO/(FAPbI ₃) _{0.85} (MAPbBr ₃) _{0.15} /PTAA/Au	ES	1.046	22.50	0.76	17.89	2016	217
89.	FTO/TiO ₂ /BSO/CH ₃ NH ₃ PbI ₃ /spiro-OMeTAD/Au	SC	1.03	16.8	0.71	12.3	2016	196
90.	FTO/TiO ₂ /BaTiO ₃ /CH ₃ NH ₃ PbI ₃ /spiro-OMeTAD/Ag	SC	0.962	19.3	0.67	12.4	2016	210
91.	ITO/ZSO/CH ₃ NH ₃ PbI ₃ /PTAA/Au	SC	1.05	21.6	0.67	15.3	2015	312
92.	FTO/ZSO/CH ₃ NH ₃ PbI ₃ /spiro-MeOTAD/Au	SC	0.84	15.03	0.62	7.02	2014	214
Scaffolds								
93.	FTO/Nb:SrTiO ₃ /SrO/(MAPbI ₃) _x (CsFAMA) _{1-x} /spiro-OMeTAD/Au	ST	1.11	23.9	0.76	20.2	2020	206
94.	ITO/ZrO ₂ /SnO ₂ /CH ₃ NH ₃ PbI _{3-x} Cl _x /spiro-OMeTAD/Ag	SC/UVT	1.068	23.32	0.782	19.48	2020	351
95.	FTO/Nb ₂ O ₅ /Al ₂ O ₃ /CH ₃ NH ₃ PbI _{3-x} Cl _x /spiro-OMeTAD/Au	SC	1.13	12.80	0.72	10.3	2015	268
96.	FTO/TiO ₂ /SiO ₂ /CH ₃ NH ₃ PbI _{3-x} Cl _x /spiro-OMeTAD/Au	SG	1.05	16.4	0.66	11.45	2014	224
97.	FTO/c-TiO ₂ /mp-ZrO ₂ /CH ₃ NH ₃ PbI ₃ /spiro-OMeTAD/Au	SC	1.07	17.3	0.59	10.8	2013	233
98.	FTO/TiO ₂ /Al ₂ O ₃ /Au@SiO ₂ /CH ₃ NH ₃ PbI _{3-x} Cl _x /spiro-OMeTAD/Ag	SC	1.02	16.94	0.64	11.4	2013	31
99.	FTO/c-TiO ₂ /Al ₂ O ₃ /CH ₃ NH ₃ PbI ₂ Cl/spiro-OMeTAD/Ag	SC	0.98	17.8	0.63	10.9	2012	220
Other Inorganic ETLs								
100.	ITO/c-TiO ₂ /CdSe/ZnS QDs/CH ₃ NH ₃ PbI ₃ /spiro-OMeTAD/Au	SC	1.08	22.9	0.73	18.1	2020	352
101.	ITO/a-WO ₃ /SnO ₂ /CH ₃ NH ₃ PbI ₃ /spiro-OMeTAD/Ag	TE	1.11	23.01	0.803	20.52	2019	353
102.	FTO/In ₂ S ₃ /CsPbI ₂ Br ₂ /spiro-OMeTAD:Li-TFSI:TBP/Au	CBD	1.09	7.76	0.659	5.59	2019	354
103.	FTO/TiO ₂ NCS/Nb ₂ O ₅ /CH ₃ NH ₃ PbI ₃ /spiro-OMeTAD/Au	SC	1.04	20.49	0.716	15.25	2018	355
104.	FTO/mp-TiO ₂ -ZnS/CH ₃ NH ₃ PbI ₃ /spiro-OMeTAD/Au	SILAR	1.02	19.05	0.754	14.9	2018	356
105.	FTO/NMT-CdS/CH ₃ NH ₃ PbI ₃ /spiro-OMeTAD/Au	CBD	1.12	19.7	0.74	16.3	2018	357
106.	FTO/CdS/MAPbI ₃ /spiro-OMeTAD/Ag	P-CVD	1.04	20.76	0.68	14.68	2017	358
107.	ITO/WO ₃ /SAMS/CH ₃ NH ₃ PbI ₃ /spiro-OMeTAD/Ag	SC	1.02	21.9	0.665	14.9	2015	359

^a SC = spin coating, P-CVD = plasma-activated chemical vapor deposition, CBD = chemical bath deposition, SILAR = successive ionic layer adsorption and reaction, TE = thermal evaporation, ALD = atomic layer deposition, SP = spray-pyrolysis, RC = reflux condensation, ED = electrochemical deposition, ET = emulsion technique, LPCVD = low pressure chemical vapor deposition, TO = thermal oxidation, HP = hydrolysis pyrolysis, SGS = sol-gel synthesis, HT = hydrothermal, ES = electro-spinning, ST = solvothermal, PP = peroxide-precipitate, UVT = UV treatment, S = spray, and RFS = RF sputtering.

which was stimulated by the higher electrical conductivity of PC₆₁BM. Furthermore, an interlayer of organic molecules between the ETL/metal contact interface was introduced to passivate the defects, reducing the band bending and acting

as a permeation barrier for moisture to enhance the stability.²⁸⁶

The inclusion of additives in PCBM decreases the film roughness and influences the morphology, which increases

the recombination resistance at the perovskite/PCBM interface. Also, these additives ease the exciton dissociation and promote fast charge transport.²⁸⁷ Recently, Xiong *et al.*²⁸⁰ used poly(3-hexylthiophene) (P3HT) as an additive to dope PCBM to avoid aggregation, thereby enhancing the moisture and water resistance. This was shown to result in a retention of 85% of the initial PCE at 20% for 720 h. Similarly, after the modification of the PCBM/perovskite interface with poly(9-vinyl-carbazole) (PVK) doping in PCBM, it showed better anti-UV, moisture, and thermal stability.²⁸⁸ The other non-fullerene-based organic ETLs include naphthalene diimide derivatives, perylene diimide derivatives, azaacene derivatives, indacenodithiophene derivatives, and n-type conjugated polymers, which can be new alternatives to gain a better performance than various modifications of PCBM.²⁸⁹ Non-fullerene-based ETLs have unique advantages such as molecular structure diversity and adjustable frontier molecular orbitals.²⁹⁰ However, a detailed review of organic ETMs is beyond the scope of this review, which can be found in the literature.^{289,290}

Despite the promising properties of organic ETLs, they have only appeared in a small number of reports compared with inorganic ETLs. However, assuming that the superior electrical and optical properties can be harnessed from organic ETMs, a roadway for higher efficiency in PSCs can be visualized. Overall, matching the only energy levels at the ETL/perovskite interface is not sufficient, where matching the electron mobility is a prerequisite to avoid charge accumulation. A detailed study of the interface is required considering the defects on the perovskite surface, chemical reactions, and effect on perovskite morphology due to the presence of the ETL, charge trapping, and charge recombination.

Despite the differences in the electrical properties, synthesis process, and interface effects in the various above-cited materials used as ETLs, numerous ETL systems have delivered high PCEs. ETLs continue to exert a significant influence on the device performance and efficiency even after selecting distinguished perovskite materials as overlayers in PSCs. In the initial stage of research, only ~7% efficiency was observed with the PSCs utilizing oxides of Ti, Zn, Sn, *etc.* to form ETL/perovskite heterostructures. The higher efficiency reported each year for a decade from a variety of ETLs in the most prominent recent reports is shown in Fig. 20. Recently, the efficiency reached ~25% with the advancement of ETLs in interface engineering due to the doping, co-doping, compositing, decoration, *etc.* of ETLs. A brief summary of the inorganic ETLs processed using various synthetic methods and their corresponding device performance parameters are tabulated in Table 1. Thus, future developments of novel ETLs should not only focus on enhancing the power conversion efficiency but must be rationalized based on cost and sustainability.

5. Hole transport layer (HTL)

The HTL is equally essential to transport the acceptors or holes generated in the photoactive perovskite layer to the cathode. The HOMO of the hole transport material (HTM) under

consideration for PSCs is required to be located at a higher level than the valence band edge of the perovskite absorber (Fig. 21). The minimized energy barrier at the perovskite/HTL interface allows easy collection of the photogenerated holes. Moreover, the conductivity of the HTM, which plays a vital role in charge transfer and charge recombination at the perovskite/HTL interface, can be revamped by governing interface energetics and defect densities. Besides, the thermal and chemical stability of HTMs continue to be a concern for the long-term and efficient photovoltaic performance. Thus far, various nanostructured, doped, and passivated HTLs have been explored in PSCs depending on the selected device architecture. In this section, we critically discuss the involvement of various inorganic HTLs in delivering a higher PCE.

5.1. Inorganic HTLS

Inorganic HTLs have gained importance in PSCs due to their ability to be downsized to nanostructures, increasing the junction interface. Given that PSCs are the resultant evolution of sensitized solar cells, though with conceptually newer foundations, redox electrolytes have been replaced with solid-state electrolytes or HTLs in PSCs. However, the expensive solid-state organic spiro-OMeTAD when introduced in PSCs degrades the perovskite absorbers due to the use of hygroscopic dopants. Therefore, the low-cost inorganic HTLs with high chemical/thermal stability and scalability have attracted considerable attention from the scientific and industrial community as a replacement for spiro-OMeTAD. Various inorganic materials based on binary oxides, cyanates, and delafossite such as NiO, VO_x, CoO_x, CuO_x, CuI, CuCSN, and CuGaO₂ have been investigated for their performance as HTLs in PSCs.^{360–363} The band structure positions of selected inorganic HTLs with reference to the perovskite absorber are summarized in Fig. 22. These HTMs are sensibly engineered to alter the charge transfer dynamics and to efficiently extract holes. The significance and optoelectronic properties of these important inorganic HTLs employed in PSCs are discussed in this section.

5.1.1. Nickel oxide (NiO). NiO is one of the most widely studied HTLs for PSCs due to its chemical inertness, low processing cost, and earth-abundant nature. Nickel oxides with molecular formulas of NiO, NiO₂, and Ni₂O₃ can be engineered to obtain cubic, monoclinic, rhombohedral, and hexagonal crystalline phases.^{364–369} Mainly, p-type semiconducting stoichiometric NiO with a wide bandgap of 3.6–4 eV^{65,370,371} and deep valence band edge (*i.e.*, –5.2 to –5.4 eV) provides excellent band alignment with the perovskite light absorber. The higher conduction band positioning of NiO than perovskite materials become advantageous to conduct holes very efficiently and serves as an excellent electron blocking layer.

Docampo *et al.*³⁷² introduced NiO as an HTL in PSCs and gained an efficiency of <1% when utilized with a mixed halide perovskite absorber as the photoactive material. The low efficiency was attributed to the inadequate surface coverage and large number of pinholes in the perovskite films coated over the NiO HTL in the inverted device architecture. The possibility of improving the PCE after controlling the doping density

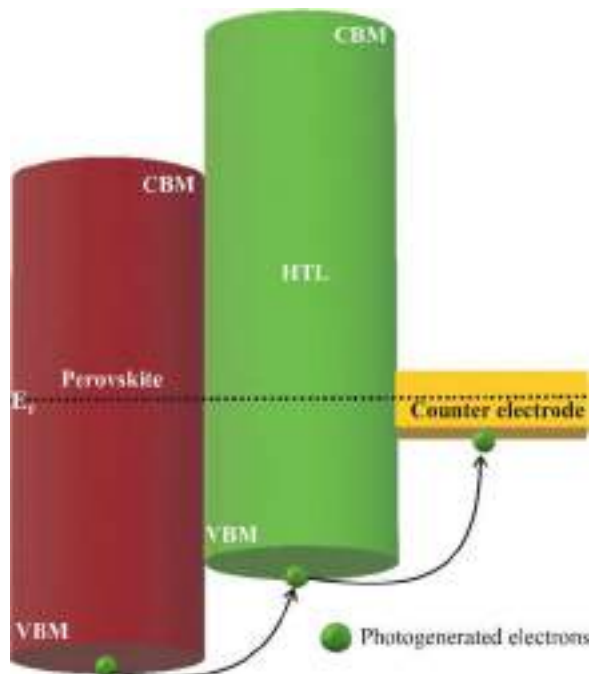


Fig. 21 Schematic displaying the path of the photogenerated hole from the perovskite light absorber to the external circuit. (CBM: conduction band minimum and VBM: valence band maximum.)

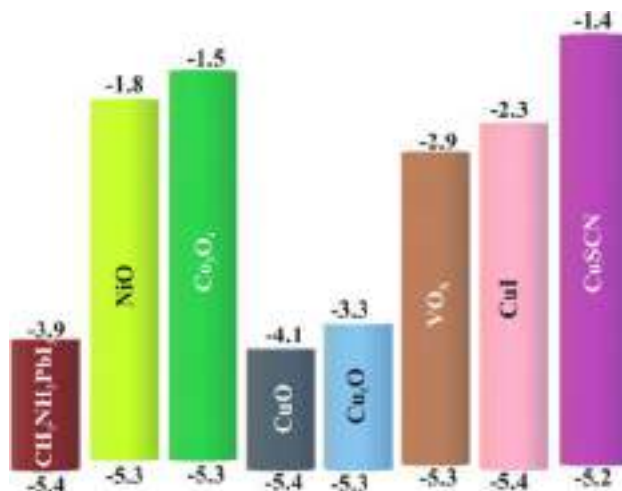


Fig. 22 Schematic of band alignment of various inorganic HTLs with perovskite absorber.

projected NiO as one of the forthcoming worthwhile HTL candidates. Therefore, various growth mechanisms and thin-film technologies have been explored for its synthesis or/and coating of NiO films in the ambient atmosphere, such as sputtering,³⁷³ atomic layer deposition (ALD),³⁷⁴ solvothermal growth,³⁷⁵ sol-gel,³⁷⁶ e-beam evaporation,³⁷⁷ reactive e-beam evaporation,³⁷⁸ atmospheric pressure spatial atomic layer deposition (AP-SALD),³⁷⁹ and thermal evaporation followed by oxidation.³⁸⁰ Among them, repeated spin coating has been observed to be a simple and cost-effective method to gain precise control over the thickness and crystallinity of NiO nanostructures, although the

residual ligands reduce the coverage of the perovskite absorber, and hence the performance of PSCs. Moreover, the thickness of the faceted and corrugated NiO nanocrystalline films controls the hole extraction and transport competence at the HTL/perovskite interface³⁷⁶ because a lower thickness presents a higher leakage current and a higher thickness offers higher series resistance. A precisely controlled ultra-thin NiO film with negligible absorption loss prepared by ALD showed no residuals and pinholes. The extremely thin NiO film with a thickness of 5–7.5 nm, few times the Debye length (*i.e.*, 1–2 nm for NiO), increased the work function and hole concentration by overlapping of the space charge regions. Moreover, high-temperature treatment improved its interfacial properties by reducing the content of hydroxylate NiOOH and reducing the amount of surface defects related to C–N at the HTL/perovskite interface, achieving a PCE of 16.4%.³⁷⁴ Subsequently, Liu *et al.*³⁸¹ utilized a solution-combustion based NiO HTL with the two-step-processed MA_{1–y}FA_yPbI_{3–x}Cl_x perovskite to achieve a PCE 19.4%. Recently, the controlled island-like growth of NiO offered a lower absorption in the visible region, and also increased the effective interface with the perovskite absorber, while governing the shunt resistance.³⁸⁰ Knowing the fact that mesoporous structures provide a better interface between the HTL and perovskite, Yin *et al.*³⁸² explored a mesoporous nanoforest of 1D NiO nanotube morphology. The hierarchical tube morphology offered a continuous conducting pathway for rapid hole extraction and less charge leakage due to the substantially passivated interfacial hole-trapping state density (*i.e.*, $1.274 \times 10^{16} \text{ cm}^{-3}$), which yielded a PCE of 18.77% with quenched Shockley–Read–Hall recombination losses (Fig. 23).

The Ni³⁺ and Ni²⁺ variations govern the defect levels in NiO and inversely alter the conductivity and optical transmittance of the HTL. The spatial localization of the HOMO of the perovskite/HTL system on the NiO layer estimated by adopting the relativistic pseudopotentials and pseudo-atomic orbitals predicted the transfer of holes from the perovskite in close proximity of the NiO surface connected by halogen and lead atoms (Fig. 24).³⁸³ Therefore, precise control of the Ni³⁺/Ni²⁺ ratio by the defect density aligns the VB of the HTL with the perovskite and provides faster hole extraction with lower energy losses, offering a PCE close to 18%.^{377,383,384} Nevertheless, the significantly reduced oxygen vacancies in self-doped Ni₂O₃³⁸⁵ and NiOOH³⁸⁶ yielded a PCE close to 20%, gaining attention as futuristic HTLs to replace NiO. The Ni³⁺ cation sites act as a Lewis electron acceptor and Brønsted proton acceptor by deprotonating cation amines and oxidizing iodide species. Therefore, different amounts of Cu,^{387,388} Y,³⁸⁹ La,⁵⁶ Fe,³⁹⁰ Co,^{391,392} Sr,³⁹³ Ag,³⁹⁴ Na,³⁹⁵ and Zn^{396,397} metals and rare earth elements (*i.e.*, Eu, Yb, Tb, Ce, and Nd)³⁹⁸ were doped to enhance the intrinsic conductivity, charge extraction ability, hole mobility, energy level alignment, and optical transparency of NiO films by reducing the Ni²⁺/Ni³⁺ vacancy formation energy due to their replacement. Even though the segregation of alkaline cations such as Li,³⁹⁹ Cs,⁴⁰⁰ and K^{401,402} on the NiO surface improve the performance of PSCs due to their favourable interaction with perovskite, their time-dependent disparity

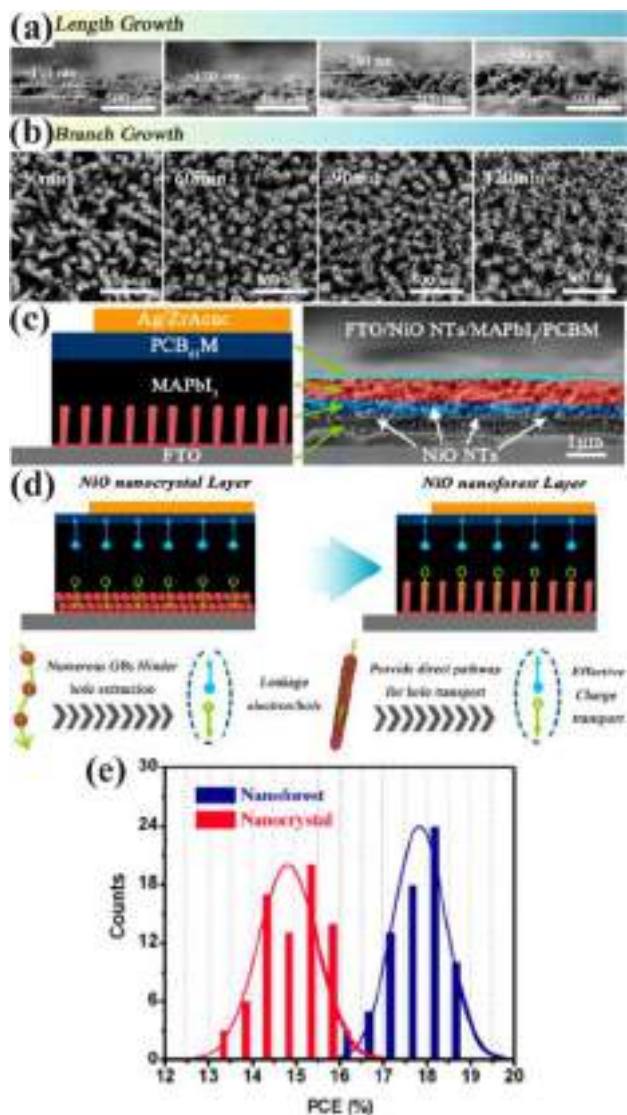


Fig. 23 (a) Cross-sectional and (b) top-view SEM images of the NiO nanotube nanoforest with controlled length and branch growth. Schematic of (c) device architecture and corresponding cross-section SEM image and (d) charge transport in PSCs consisting of NiO nanocrystals and nanoforest HTLs. (e) Comparative PCE distribution of nanocrystal and nanotubes.³⁸² Reprinted with permission from (*ACS Appl. Mater. Interfaces*, 2019, **11**, 44308–44314). Copyright (2019), the American Chemical Society.

in the spatial distribution modifies their performance and stability.

Al doping in the lattice of NiO_x not only enhances the electrical conductivity of the HTL but also improves the crystalline growth of the perovskite absorber, concurrently aligning its energy levels, which dramatically reduces the energetic non-radiative recombination losses and enables quicker hole transportation at the perovskite/HTL interface to deliver a PCE of 20.84%.⁴⁰³ Mg doping has shown to downshift the VB maximum, matching it well with the perovskite and lowering the energy redundancy for hole injection. The reduced energy band offset benefitted the efficient charge collection/transport

and curtailed the hysteresis, yielding a reproducible PCE of 18.5% from an ambient-stable commercial device with an active area of 10 cm × 10 cm.⁴⁰⁴ Interestingly, embedding Au inside an NiO layer to form Au–NiO_x as both an electrode and electrode interlayer for PSCs was attempted to replace the ITO electrode, but difficulties were encountered in the formation of a compact layer, reducing the film thickness to control the transmittance, and loss of photoexcitation energy due to self-recombination of opposite charges at the electrode. This hampered the PSC device performance (*i.e.*, PCE = 10.24%).⁴⁰⁵ The further addition of Cu on the top of Au–NiO film effectively reduced the resistance, but the device delivered a maximum PCE of 11.1% at a 1 nm Cu layer. This was reduced further with an increase in the thickness of Cu (*i.e.*, >1 nm).⁴⁰⁶ UV-ozone irradiation reduced the interface barrier between a Cu-doped NiOOH HTL and MAPbI₃ perovskite by surface dipole formation and also increased the carrier concentration and charge extraction efficiency.⁴⁰⁷ Recently, Zhou *et al.*⁴⁰⁸ improved the electrical conductivity of an NiO_x film by enhancing the Ni³⁺ content after N-doping and achieved a PCE of 17.02%. The reduced Gibbs free energy on the hydrophilic N-doped NiO_x surface led to a higher nucleation density, and thereby larger grain growth of the perovskite absorber with improved interfacial contact and passivation of the trap states in the perovskite layer, thereby suppressing nonradiative recombination.

Cobalt-doping exhibits a synergistic effect and endows the NiO_x film with a further improvement in its performance. As an HTL in PSCs, p-type Co-doping provides low transparency and high conductance, whereas alkali and alkaline co-dopants result in high transparency with low conductivity. It was reported that 10% Li@5% Co co-doping synergistically enhanced the PCE to 20.1% by providing a shorter carrier lifetime of 0.67 μs and a larger recombination lifetime of 5.24 ms, signifying efficient hole/charge transfer/extraction and suppressed charge carrier recombination, respectively.⁴⁰⁹ The synergy between Ag and Li co-dopants with the +1 oxidation states was shown to tailor the optoelectronic properties of NiO. The smallest formation energy of Li and Ag among the related defects created shallower acceptor levels in NiO and enhanced the hole concentration, which effectively optimized the charge extraction/transport and reduced the charge accumulation at the interface, therefore boosting the PCE to 19.24%.⁴¹⁰ Mg²⁺ doping compensates the undesirable positive shift caused in the VB of NiO_x due to the incorporation of Li and promotes the formation of an ohmic contact at the perovskite interface by reducing the barrier height *via* staircase energy level alignment with the MAPbI₃ perovskite.³⁶⁰ However, the inclusion of Co²⁺ in Mg–Li reduced the device performance severely (*i.e.*, PCE = 13.22%) for unknown reasons.⁴¹¹ Besides, polymeric PTAA, DEA, PFBT, and PEAI coatings^{412–415} introduced as an overlayer for the NiO_x HTL effectively modified the interfacial contact and boosted the interfacial charge transfer through gradient band alignment and reduced trap state density. The lone-paired functional groups on the polymer coordination with Ni and Pb ions form a quasi-2D polymeric-perovskite grain, which blocks the electron transport in the HTL and limits the carrier recombination at the interface.

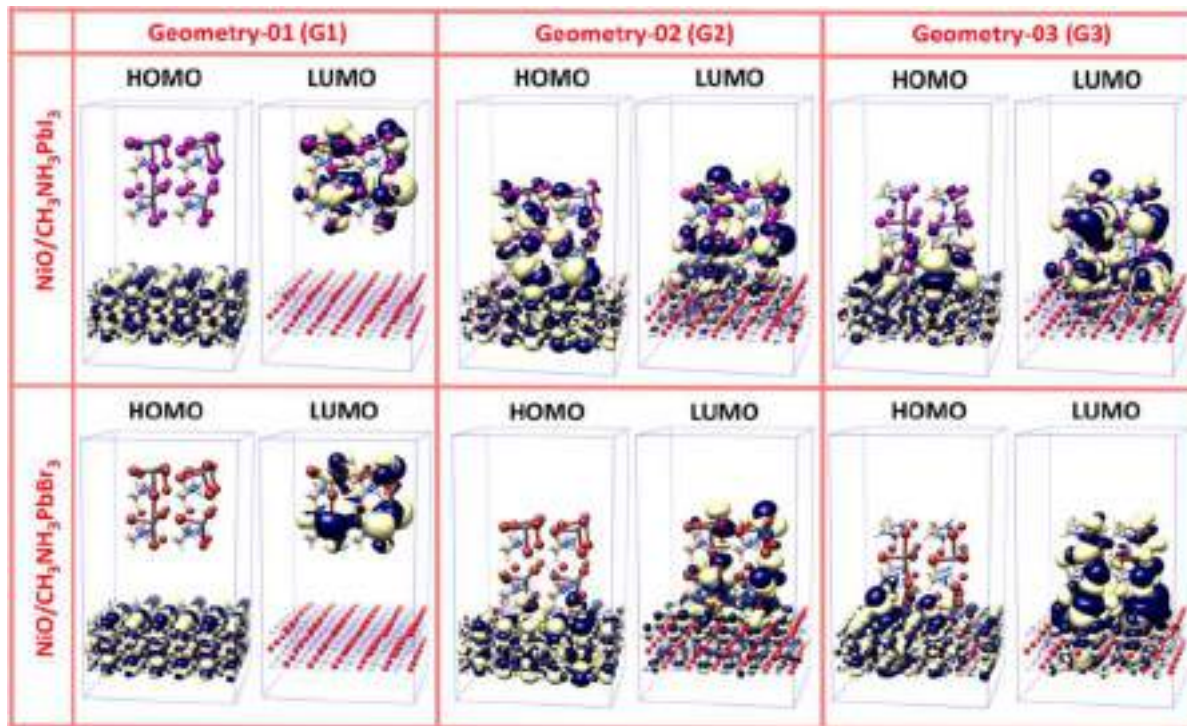


Fig. 24 Optimized structures showing the HOMO (left) and LUMO (right) orbitals for three mutual orientations of an NiO (lower) and perovskite (upper) interfacial region. The geometries G1 refer to the surface separation of ~ 1 nm between the perovskite and NiO, and G2 and G3 indicate the close proximity of < 0.3 nm between the perovskite and NiO, but perovskite contact NiO(100) surface *via* the closest halogen atom and MA ion and halogen atom and lead atoms, respectively. The upper row shows the MAPbI₃, and the lower row represents the MAPbBr₃ perovskite nanoparticles. In the NiO structure, the Ni and O atoms are represented by green and red spheres, respectively. In the perovskite structure, the Br, I, and Pb atoms are identified in brown.⁵⁸⁵ Reprinted with permission from (*ACS Appl. Mater. Interfaces*, 2020, **12**, 11467–11478). Copyright (2020), the American Chemical Society.

5.1.2. Vanadium oxide (VO_x). Vanadium oxides composed of VO₅ square pyramids or distorted VO₆ octahedra with shared oxygen atoms appear in various chemical forms such as VO₂, V₂O₃, V₂O₅, V₃O₅, V₃O₇, V₄O₇, V₅O₉, V₆O₁₁, and V₆O₁₃ of orthorhombic, cubic, triclinic, tetragonal, monoclinic, and rhombohedral crystalline phases.⁶⁵ The existence of valence band levels and conduction band levels at ~ -5.36 eV and ~ -2.94 eV, respectively, and the bandgap of ~ 2.6 eV have projected VO_x as another interesting HTL candidate material for PSCs. The low-temperature synthesis protocols have been shown to incorporate hydroxyl groups in vanadium oxides (*i.e.*, VO_x), and the post-synthesis heat treatment results in oxygen vacancies by establishing V⁵⁺ (*i.e.*, $\sim 65\%$ to 75%) and V⁴⁺ (*i.e.*, $\sim 35\text{--}25\%$) cations,^{416–420} which are prominent trap sites, restricting their use as HTL. Basically, the air-oxidation of VO_x films during their synthesis naturally results in the formation of V₂O₅ on the top surface at the interface between the perovskite absorber and VO_x HTL and controls the device performance by monitoring the band-offset.⁴²¹ The large variation between the V⁵⁺ and V⁴⁺ cations results in the assembly of V₂O_x films with higher roughness and sizable thickness, which typically yield a larger barrier to allow the tunnelling of charges in PSCs.⁴¹⁹ Therefore, a thin layer of hydrated V₂O₅ (*i.e.*, VO_x) has been explored as an alternative HTL to overcome the catastrophic electrical and structural inhomogeneities in the

frequently explored PEDOT:PSS hole extraction layer, which adversely affect the device lifetime. Moreover, a compact layer of thermally stable VO_x nanoparticles not only enhanced the light-harvesting but also delivered extremely high transmittance (*i.e.*, 95–98%), higher quenching efficiency, and reduced internal resistance, which facilitated efficient charge transportation, offering a PCE close to 14%.^{417,418} Likewise, it also assisted in improving the stability of gradient hetero-junction-based PSCs exposed to solar radiation in N₂ (*i.e.*, 15.8% PCE for 750 h) and ambient (14.1% PCE for 175 h) environments.⁴¹⁶

The V₂O_x additive, as an interface modification layer, is a good hole extraction layer, and thus has been utilized to improve the quality of perovskite light absorbers (*i.e.*, CH₃NH₃PbI_{3-x}Cl_x).^{420,422} The hydrogen bonds and dangling bonds in the hydrated V₂O_x additive produce larger perovskite grains. The optimized amount of additive produces a dense perovskite film of larger grains, which play a crucial role in reducing the trap charge density to improve the current injection, thereby concurrently limiting the leakage current. Although these modifications are performed to overcome the high recombination rate at the V₂O_x/perovskite interface, they also mitigate the migration of iodide ions into the crystal boundaries and retain a stable device performance beyond 1000 h. Besides, an ambient atmosphere-processed VO_x interlayer in an unencapsulated n-i-p device showed excellent PCE retention (*i.e.*, 71% of initial value) after

illumination at the high temperature of 70 °C for 1100 h,⁴²³ but the slow ingress of oxygen and water in the unencapsulated device degraded the perovskite layer, despite a barrier layer being imposed to reduce the rate of vanadium ion diffusion. Therefore, the VO_x thin film was further passivated with an aminopropanoic acid (APPA) interfacial layer to control the effect of oxygen vacancies on the charge recombination at the perovskite/VO_x HTL interface, which also enriched the perovskite crystallinity, reducing the content of charge-trapping pinholes.⁴²⁴

A copper phthalocyanine (CuPc)⁴²⁵ and thermally crosslinked triarylamine-based X-DVTPD⁴²⁶ buffer layer was introduced in the VO_x matrix to resist the incorporation of moisture and realize excellent interfacial energy level alignment. The synergistic bilayer HTL was shown to reduce the charge carrier recombination, enhancing the charge extraction at the interface. Furthermore, VO_x was also introduced over poly(triarylamine) to induce hydrophilicity to grow a high-quality perovskite absorber layer, thereby improving the PCE (*i.e.*, 18.9%).⁴²⁷ A thin overlayer of VO_x was shown to suppress the trap-assisted recombination, significantly improving the charge extraction and transport at the interface. However, owing to the limited improvement in

PCE to 19%, subsequent efforts were focused on increasing the conductivity of pristine VO_x by doping rather than *via* additives or complex bilayer formation.

The improved conductivity of VO_x (*i.e.*, $1.05 \times 10^{-3} \text{ S m}^{-1}$) and interfacial adhesion with the MAPbI₃ perovskite layer after Cs doping resulted in a 30% enhancement in the device efficiency.⁴²⁸ On the contrary, when dispersed in carbon, VO_x facilitates the charge transfer at the perovskite/carbon interface due to the high work function without compromising the conductivity of carbon.⁴²⁹ Recently, PSCs with a top hybrid HTL comprised of VO_x incorporated p-type polytriarylamine (PTAA) polymer reached an efficiency of 20.1% and exhibited negligible degradation after 4500 h of light soaking due to the higher tolerance of VO_x towards the perovskite absorber (Fig. 25).⁴³⁰ The donor-acceptor interactions between the electron-deficient VO_x and electron-rich amine-centers of polymer enable the impeccable fusion of VO_x and PTAA layers, which provide improved charge transport, possibly similar to doping effects. The post-treatment strategy of vanadium oxides offers great flexibility to tailor the cation distribution, and hence the energy level alignment. The UV post-treatment of a few-atomic layer thick ($\sim 1 \text{ nm}$) pristine VO_x HTL film was shown to increase the

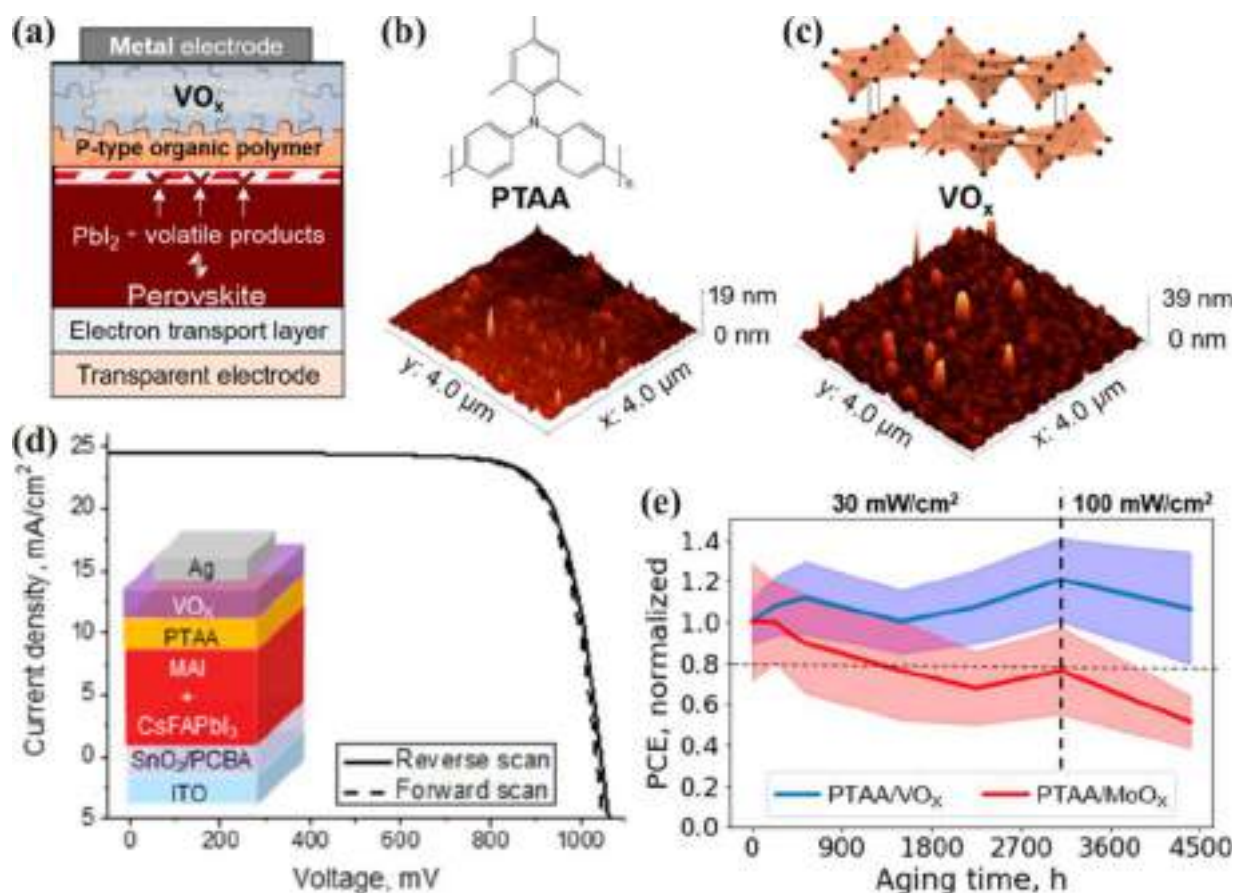


Fig. 25 (a) Schematic of n-i-p PSCs consisting of a hybrid HTL of PTAA and VO_x with lower gas permeability and better barrier properties than the volatile perovskite decomposition products. Molecular structure, linked pyramid-based structure and topography of (b) spin-coated p-type PTAA thin film and (c) evaporated 30 nm-thick VO_x film on glass. (d) *I*-*V* characteristics of PSC consisting of VO_x in bilayer hybrid HTL. (e) Stability of PSCs with bilayer hybrid HTLs under illumination.⁴³⁰ Reprinted with permission from (*J. Phys. Chem. Lett.*, 2020, **11**, 5563–5568). Copyright (2020), the American Chemical Society.

oxidation states from V^{4+} to V^{5+} , drawing the Fermi level close to the valence band, thereby enabling the hole quenching pathway for the transportation of holes to improve the device efficiency.⁴³¹ Even though VO_x has shown promise towards efficient and stable PSCs, further investigation of morphology controlled VO_x nanostructures, doped VO_x , and composites with other promising materials are required to explore as it as an HTL for reaching a milestone efficiency and the cost-effective mass production of PSCs.

The use of an ALD V_2O_5 buffer layer a barrier layer was shown to improve the long-term thermal stability of PSCs.⁴³² Indeed, a precisely controlled stoichiometric V_2O_5 HTL enhanced the PCE from 13.26% to 18.03% when interfaced with PEDOT:PSS under ambient conditions.^{433–435} V_2O_5 curbs the formation of oxygen defects and also ensures hole transfer from the perovskite absorber ($CH_3NH_3PbI_3$) to V_2O_5 HTL by forming an excellent ohmic contact.⁴³⁶ Moreover, filling the pinholes of PEDOT:PSS by incorporating V_2O_5 nanoparticles improved the carrier mobility and increased the surface energy by exposing more PEDOT chains to the interface with the perovskite absorber.⁴³⁷ Further, V_2O_5 combined with nickel phthalocyanine (NiPc) effectively extracted holes from the perovskite by mediating the VB of both and rendered a 63% enhancement in the PCE (*i.e.*, 19.4%).⁴³⁸ Basically, the VB of pristine V_2O_5 forms an electronically barrier-free cascading contact for hole transportation and extraction across the interface.

5.1.3. Cobalt oxide (CoO_x). Cobalt oxide is another HTM attracting attention due to its hole-quenching capability and low processing cost. Cobalt oxides with the molecular formulas CoO , Co_3O_4 , and Co_2O_3 can be obtained in cubic and hexagonal spinel crystalline phases with a wide bandgap in the range of 1.3 to 2.4 eV.⁴³⁹ The much shorter hole extraction time of CoO_x (2.8 ns) relative to NiO_x (22.8 ns) and CuO_x (208.5 ns) has projected Co-oxides as possible competitor materials to other inorganic HTLs.⁴⁴⁰ In 2016, Shalan *et al.*⁴⁴⁰ introduced ultrathin CoO_x films as an HTL in inverted PSCs, which was obtained *via* a simple spin-coating technique followed by high-temperature processing (400 °C). Besides the excellent light harvesting capability, it was mainly the phenomenal charge separation ability of the highly transparent CoO_x (*i.e.*, 15 nm thick) achieved a PCE of 14.5% even with a single-cation single-halide perovskite. Despite the fact that an ultrathin HTL minimizes the incident photon loss induced by Co ion absorption and curtails the carrier losses by shortening the transport path, the introduction of a metal ion in the CoO_x lattice changes the conductivity of CoO_x and energy-level mismatch with the perovskite. The deeper VB position of CoO_x (~5.46 eV) than the HOMO of $CH_3NH_3PbI_3$ (−5.4 eV) hinders the hole transport and causes severe recombination. However, the incorporation of Cu in CoO_x uplifts the VB (−5.34 eV), without altering the CB edge (−3.2 eV), which is maintained much higher than that of $CH_3NH_3PbI_3$ (−3.9 eV). This severely reduces the carrier transfer loss at the interface and energetically favours the electron injection.⁴⁴¹

Spinel Co_3O_4 with octahedral Co^{3+} is significantly tolerant to structural distortion or disorder, and hence excellent hole

transport materials for PSCs. Co_3O_4 assists with the issues of carrier transport and recombination process at the carbon/perovskite interface in carbon-based PSCs by reducing the charger transfer resistance from perovskite and suppressing interfacial recombination. Moreover, the interfacial layer of Co_3O_4 significantly promotes the separation and extraction of photo-generated carriers, as well as the hydration of perovskites, thereby providing a steady performance under ambient and light soaking conditions.^{442,443} Low-valency doping reduces the density of defect states and enhances the hole mobility of Co_3O_4 by introducing acceptor energy levels on both the Co^{2+} and Co^{3+} sites of Co_3O_4 . Therefore, Li^+ doping in the lattice of Co_3O_4 improves the light absorption and boosts the hole mobility by forming an Li-enriched $LiCoO_2$ overlayer, which facilitates efficient hole transportation at the $Li-Co_3O_4$ /perovskite interface, delivering a PCE of ~14%.⁴⁴⁴ However, the super-hydrophilicity induced in $LiCoO_2$ after UV/ozone treatment led to the formation of a highly dense $MAPbI_3$ film with an excellent interface, which was shown to enhance the PCE to 19%.⁴⁴⁵

Recently, the co-doping of Zn^{2+} in $LiCoO_2$ improved its conductivity and enormously enhanced its hole mobility, which caused a 4-fold enhancement in the PCE compared to that of the pristine Co-oxide HTL.⁴⁴⁶ The rock-salt CoO with octahedral high-spin Co^{2+} is another HTM from the CoO_x family that has the potential to improve the PCE. Recently, a CoO film was treated with pyridine to control the adverse effect of oleylamine molecules present on the CoO film on the growth of the perovskite film, and thereby the performance of PSCs. The ligand exchange process by pyridine not only improved the conductivity by influencing the defect states in CoO but also altered the HTL/perovskite interface for excellent charge extraction, showing a 5-fold improvement in the PCE.⁴⁴⁷ Recently, the decoration of CoO nanoplates in a discontinuous manner to fill the boundaries of crystalline perovskite grains yielded the highest PCE of 20.72% by improving the charge-transfer kinetics and hole extraction ability (Fig. 26).⁴⁴⁸ The uncovered perovskite grains assured uninterrupted hole transport from the perovskite to spiro-OMeTAD HTL; moreover, the CoO nanoplates residing at the perovskite grain boundaries (where defect sates exist) reduced the trap state density ($3.773 \times 10^{15} \text{ cm}^{-3}$), suppressing the charge recombination. Overall, the best PCE is still to be realized from PSCs utilizing Co-oxide HTLs. In the future, the choice of precursor and reaction kinetics should be considered to obtain the best-quality nanostructures of Co-oxide HTLs to ensure maximum hole quenching and improved efficiency. Therefore, the research direction should be focused on improving the conductivity and mobility of CoO by proper choice of doping and the film quality by tuning the processing method to boost the interface between CoO -perovskite to reduce the recombination loss.

5.1.4. Copper oxide (CuO_x). The earth abundance oxides of copper with molecular formulas of CuO (cupric oxide), Cu_2O (cuprous oxide), and Cu_4O_3 (paramelaconite, thermodynamically unstable) can be realized in cubic, monoclinic, and tetragonal structures, respectively.^{449,450} Cu-oxides are primarily

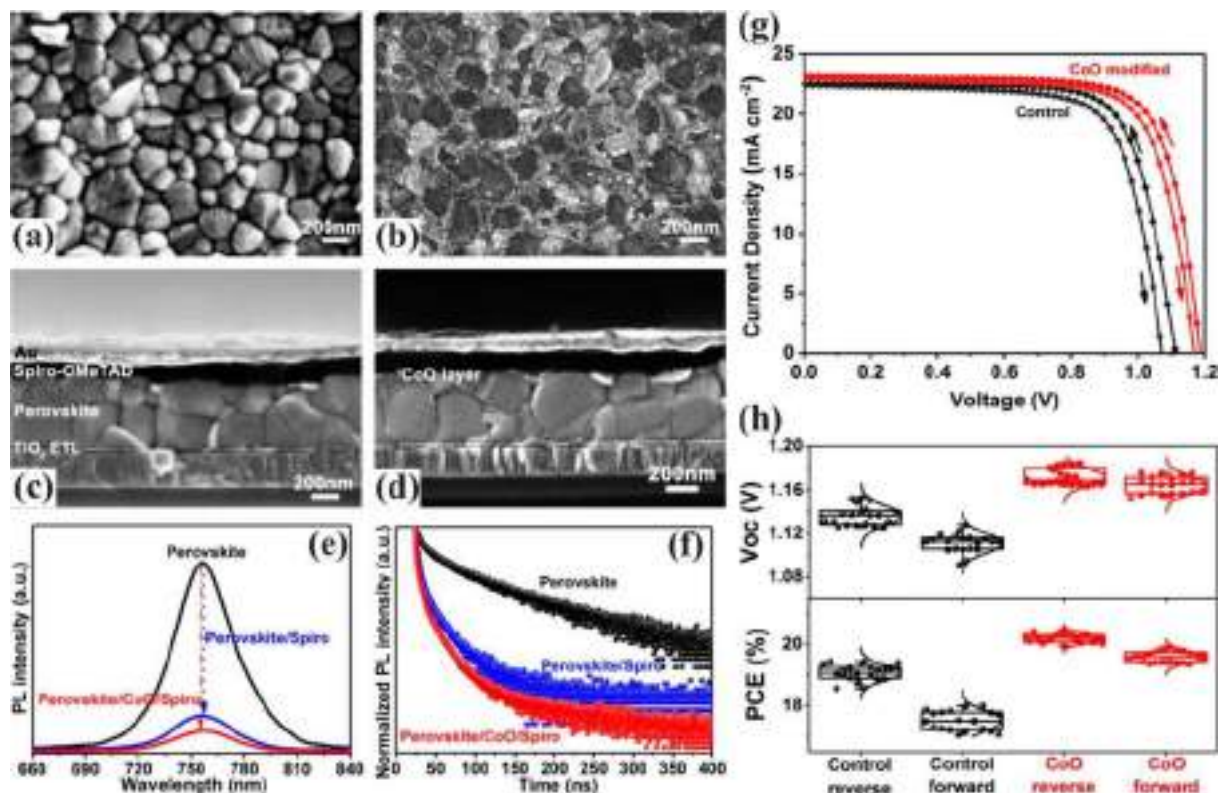


Fig. 26 Top-view SEM images of the perovskite layer (a) without and (b) with CoO nanoplate HTL, and their respective cross-sectional views (c) without and (d) with CoO nanoplate HTL. (e) PL and (f) TRPL spectra of the CoO nanoplate HTL. (g) J - V curves of the PSCs with and without CoO nanoplate HTL and (h) V_{OC} and PCE obtained by forward and reverse scan of 20 of these PSCs. The control was a PSC without CoO nanoplates.⁴⁴⁸ Reprinted with permission from *ACS Appl. Mater. Interfaces*, 2019, **11**, 32159–32168). Copyright (2019), the American Chemical Society.

utilized as buffer layers for the stable encapsulation of PSCs to maintain efficiency in adverse environmental conditions.⁴⁵¹ The two-orders of magnitude higher mobility of pristine and modified Cu-oxides (*i.e.*, $\sim 256 \text{ cm}^2 \text{ V}^{-1} \text{ s}^{-1}$) than NiO (*i.e.*, $2.8 \text{ cm}^2 \text{ V}^{-1} \text{ s}^{-1}$) makes them an excellent choice as HTLs. Most importantly, the best-performing PSCs using copper oxide are prepared with ultrathin films of CuO_x , but the ultra-thin nature of the film restricted the analysis of its crystallographic data for tailoring its interfacial properties. Therefore, X-ray photoelectron spectroscopy (XPS) studies have been given importance to understand the properties of the surface facing the interface. The existence of a Cu^+ content in the range of 63–68% (*i.e.*, 37–32% of Cu^{2+}) confirmed the presence of both Cu_2O and CuO phases in CuO_x .^{452,453} Nevertheless, the $\text{Cu}^+/\text{Cu}^{2+}$ ratio was controlled *via* the self-oxidation of independently prepared Cu_2O and CuO thin layers to govern the channels for charger carrier transport by lattice matching, and thereby the solar device efficiency.⁴⁵⁴ The equal existence of Cu^+ and Cu^{2+} delivered a Cu_4O_3 phase with a bandgap of $< 1.6 \text{ eV}$,^{449,455} which is lower for blocking the conduction electrons, and hence not explored much. However, the Cu_2O and CuO forms exhibit bandgaps (E_g) in the range of ~ 2.1 to 1.6 eV , with an approximately similar VB level of -5.4 eV , satisfying the primary requirement as HTLs in PSCs.

The conversion of spin-coated CuI into Cu_2O and CuO under controlled thermal treatment delivered a PCE close to 13% and

created excitement among the scientific community exploring solar materials.³⁶¹ The mixture of $\text{Cu}^{2+}/\text{Cu}^+$ with a ratio of 3 : 1 produced a PCE of 17.4% by improving the hole extraction and charge dissociation at the $\text{CuO}_x/\text{MAPbI}_3$ interface in the presence of a buffer layer.⁴⁵² Further, in search of improved efficiency, Chen *et al.*⁴⁵⁶ transformed complex $\text{CuO-Cu}_2\text{O}$ uneven morphologies into stable CuO nanoparticles of uniform dimension, but this complex $\text{CuO-Cu}_2\text{O}$ structure delivered a maximum PCE of only $\sim 8\%$ for unknown reasons. Therefore, various synthesis techniques such as electrostatic spray deposition,⁴⁵⁷ magnetron sputtering,⁴⁵⁶ solvothermal method,⁴⁵⁸ SILAR,⁵⁴ ion beam sputtering,⁴⁵⁹ thermal oxidation,⁴⁵³ spin-coating,⁴⁵² chemical vapor deposition,⁴⁵¹ and electrospinning⁴⁶⁰ have been examined to control the Cu-oxide film thickness and its interface with the perovskite absorber layer, influencing the efficiency of PSCs. The CuO_x employed in place of PEDOT:PSS HTL exhibited a stable and higher PCE (17.1%) than that of the pure Cu_2O and CuO HTLs.^{453,461} Recently, it has been shown that a highly crystalline perovskite overlayer on CuO_x quantum dots reduced the charge trap state density, leading to a higher carrier transfer efficiency and reduced charge recombination, delivering a PCE of 19.91%.⁴⁶² However, CuO_x suffers from a low transmittance in the visible range, and its further improvement by reducing thickness compromises the optical losses.

The nanoparticle-based interface modification concept provides a series of benefits in PSCs. Monodispersed CuO

nanoparticles (5–10 nm) improve the light manipulation, suppress parasitic interfacial resistance, and induce higher hole-extraction ability, resulting in a V_{OC} of 1.09 V and an efficiency of 15.3%.⁴⁵⁸ However, CuO nanowires introduced as an anode buffer layer in the inverted planar device structure yielded a PCE of 16.35%, which originated from the higher hole mobility (or improved conductivity) of the HTL and its larger interfacial area with perovskite. Even though the diameter of nanowires plays a central role in improving the charge extraction ability, unoptimized overlapping of the nanowires increases the hole transport distance and declines the crystallinity of the perovskite layer, thereby reducing the performance of PSCs.⁴⁶⁰ Further, Ag nanoparticle doping in CuO nanowires increases the light trapping and suppresses the charge recombination rate, but their high cavity mobility reduces the PCE (*i.e.*, ~11%).⁴⁶³ Besides, a reactively sputtered CuO thin film barely accompanied with Cu_2O , under controlled annealing conditions, had shown the highest efficiency of 22.56% due to the increased exciton-assisted band-to-band recombination.⁴⁶⁴

The incorporation of Cu_2O in PSCs has been shown to reduce the recombination losses at the interface. Cu_2O forms type II band alignment at both the p–i and i–n interfaces, enabling charge separation and uninterrupted carrier transport from MAPbI₃.⁵⁴ The synergistic effect of Cu_2O nanocubes as the top HTL on the perovskite light absorber ($CH_3NH_3PbI_3$) in a planar n–i–p PSC demonstrated a highly stable PCE of ~17.23% at room temperature without encapsulation.⁴⁶⁵ Further, the heterojunction of Cu_2O with SiO_2 enhanced the PCE to 18.4% by effectively preventing defects and pinholes, and also tailoring the recombination and recollection of charge carriers at the interface with the perovskite absorber.⁴⁶⁶ To further enhance the device performance, surface modification strategies using nonpolar solvents have been explored. Surface modification of Cu_2O quantum dots using silane molecules has been seen to increase the recombination resistance, offering faster and more efficient charge carrier extraction to deliver a PCE of 18.9%.⁴⁶⁷ Moreover, a Cu/ Cu_2O composite layer introduced as a p-type-modified layer between low-mobility hole transport materials and the metal electrode acted as an electron blocking buffer layer and effectively improved the PCE.^{459,468} Cu_2O was also blended with CuSCN to avoid the formation of defects and impurities at the interface due to the reaction of halides migrated from organohalide perovskites into CuSCN.⁴⁶⁹ The existence of Cu_2O nanoparticles resulted in the faster extraction of charges generated in organohalide perovskites by their interaction with CuSCN, thereby rendering a PCE of 19.2% by minimizing the detrimental interfacial degradation.

Device simulations have predicted that Cu_2O has the ability to improve the PCE to over to 25% by tuning the bandgap^{470–472} due to its high mobility despite the complications in its synthesis. However, control over the interface properties has become a key obstacle in this development. Due to the presence of Cu vacancies at the surface or termination in the oxygen planes, the reactive oxygen becomes the recombination centres to trap the conduction electrons. Therefore, the atomistic model developed by Castellanos-Aguila *et al.*⁴⁷³ for the

$Cu_2O(001)$ and MAPbI₃ interface showed that the formation of vacancies in the Cu_2O -terminating planes eliminates the dangling bonds and deep trap states, enabling the PSCs to exhibit excellent photoconversion efficiency (Fig. 27). However, the diverse nanostructure morphologies and doping or co-doping of Cu_2O with promising elements are yet to be fully explored in-depth to understand their effect on the device performance.

5.1.5. Copper iodide (CuI). CuI crystallizes in zinc blende (<390 °C), wurtzite (>390 °C and <440 °C) and rock salt (>440 °C) structures,^{474,475} which is another promising HTL with a wide bandgap (*i.e.*, ~3.1 eV), high hole mobility (*i.e.*, 0.5–2 cm² V⁻¹ s⁻¹), high transparency, good chemical stability, and low production cost. Various solution-based and solid–gas reaction processes have been endorsed as facile methods to synthesize CuI.^{476–480} Systematic modelling based on a combination of DFT-based computational and group-theory methods has illustrated that among the intrinsic point defects, copper vacancies are the most prominent to govern the electronic and transport properties of CuI, resulting in an improvement in the PCE.⁴⁷⁵ Initially, CuI was explored in conventional n–i–p PSCs, and then utilized in inverted planar PSCs to improve the PCE by avoiding iodide formation at the interface. The incorporation of an iodine atom expands the Cu (with lattice constant of 3.59 Å) structure of the film and results in the formation of a compact CuI crystal, removing the pinhole defects. Simultaneously, new species are formed at the interface of perovskite/CuI by loading Cu in the perovskite, resulting in stronger charge-extraction and noticeable short circuit current density.⁴⁸¹ Nevertheless, the redundant iodine acts as an interfacial recombination centre.

Christians *et al.*⁴⁷⁷ introduced CuI as a competitor to spiro-OMeTAD in PSCs, providing 2-orders of magnitude larger electrical conductivity; nevertheless, the high recombination in the CuI-based device restricted the PCE to 6% at a lower V_{OC} , suggesting a strong possibility for the advancement of its performance. Moreover, benefitting from the high transmittance of CuI, with deep valence band, it showed a higher PCE than the acidic and hygroscopic PEDOT:PSS-based PSCs.⁴⁸² The smaller magnitude of charge separation at the perovskite/CuI interface leads to the generation of a smaller local electric field; thereupon, the faster polarization relaxation down-sizes the hysteresis in J – V measurement of CuI based PSCs.⁴⁸³ The larger roughness of a powder-pressed CuI HTL reduced the device performance by severely trapping the charge carriers at the numerous air voids generated deep inside the HTL layer.⁴⁷⁶ The thermally evaporated ~40 nm-thick compact CuI HTL decreased the charge-carrier recombination losses at the interface and exhibited an air-stable PCE of 14.7%.⁴⁸⁴ Later, an air-stable PCE of 16.8% was obtained by optimizing the morphology of the perovskite film coated on the CuI HTL to effectively reduce the energy loss at the interface.⁴⁸⁵ Recently, the use of CuI-decorated Cu nanowires as a hybrid Cu@CuI nanostructure enabled a PCE of 18.4% by efficient charge extraction from the outer CuI layer and rapid charge transfer from the inner Cu wires.⁴⁸⁶ However, the synergistic effect of Na-doped TiO₂ ETL

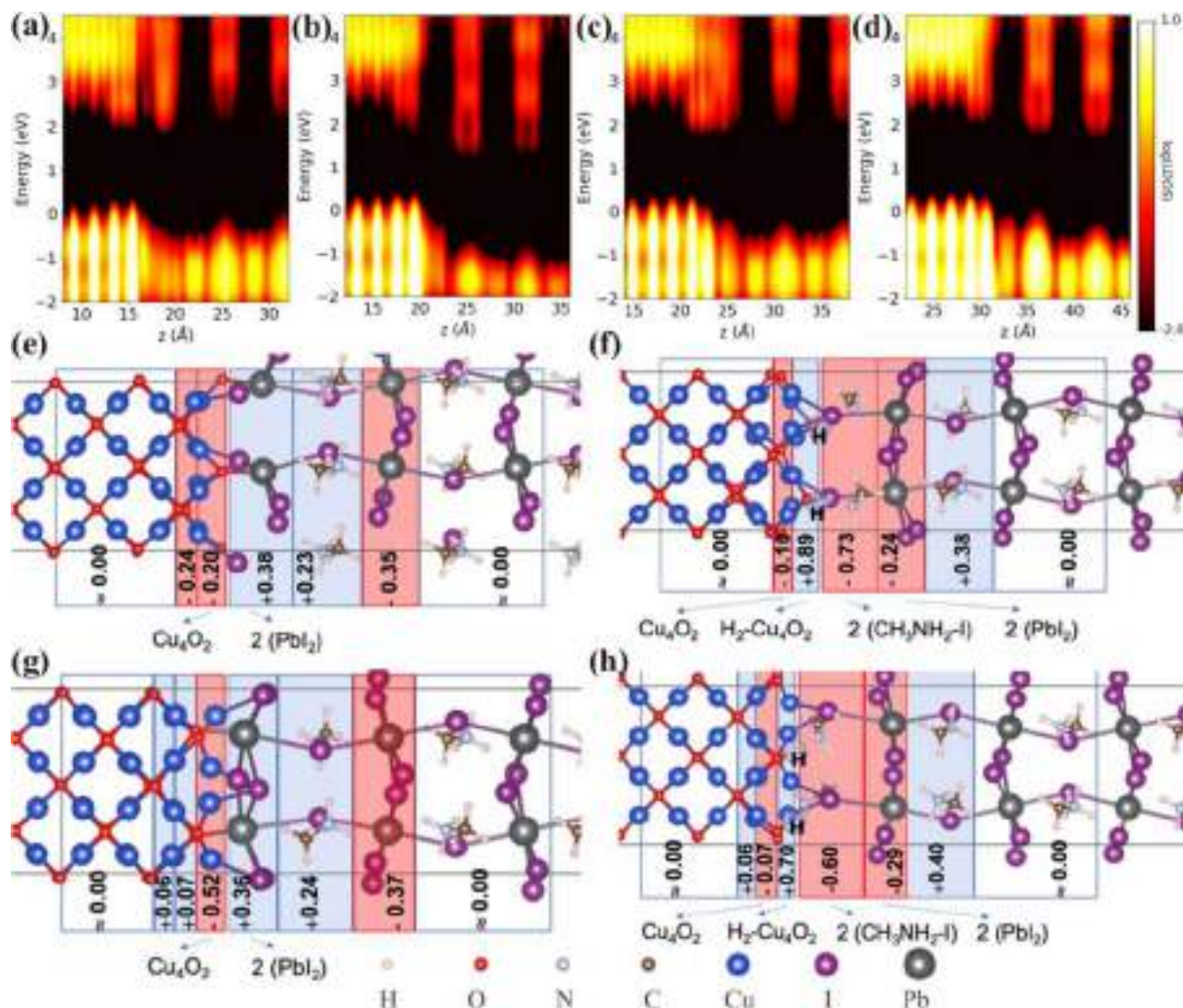


Fig. 27 (a–d) Logarithm of $LDOS \times V_{cell}$ averaged in the xy planes calculated between the MAPI and Cu_2O interface and (e–h) their Bader charges summed by layers for the four interface models: (a and e) O/PbI, (b and f) O/MAI, (c and g) Cu/PbI, and (d and h) Cu/MAI. The interface states are higher in energy than the MAPI CB, allowing electrons to return to MAPI. Therefore, holes can be transferred from MAPI to Cu_2O without being trapped, although they can be attracted and recombine with electrons trapped at the O/PbI and Cu/PbI interfaces.⁴⁷³ Reprinted with permission from *ACS Appl. Mater. Interfaces*, 2020, **12**, 44648–44657. Copyright (2020), the American Chemical Society.

and CuI HTL, where Na-doped TiO_2 enhanced the electron conductivity/mobility and CuI induced a higher recombination resistance, improved charger transport at both interfaces (*i.e.* HTL/perovskite and ETL/perovskite interface) and delivered an efficiency of 17.6%.⁴⁷⁸

Despite its high mobility, the CuI HTL alone forms leakage paths, leading to carrier recombination at the CuI/perovskite interface. Therefore, PEDOT:PSS was introduced as a middle layer for efficient carrier extraction through adequate energy level alignment, making the architecture more efficient with a thicker CuI overlayer.^{479,487} The further addition of CuI as a middle layer between PTAA and perovskite enhanced the charge extraction on both the sides and yielded a PCE of 20.34% by creating enhanced upward band bending (0.35 eV) at the CuI/perovskite interface with a large built-in potential (~ 1.28 V) all over the active layer.⁴⁸⁸ Moreover, CuI is beneficial to reduce the trap-state concentration and parasitic charge

accumulation, limiting the flow of charges through the passivation of other HTLs. Saranin *et al.*⁴⁸⁹ observed that the passivation layer of CuI fills the pinholes and severely reduces the trap states of metal oxide, protecting the perovskite/HTL interface from degradation and providing faster injection and relaxation processes in devices, yielding an impressive PCE of 15.2%.

Byranvand *et al.*⁴⁹⁰ introduced CuI islands on a TiO_2 ETL to pull the electrons at the perovskite/ TiO_2 interface and extract them *via* the dipole moments formed. The higher conduction-band energy level of CuI (*i.e.*, -2.2 eV) than the perovskite prevents the formation of PbI_2 at the interface, facilitating superior electron extraction with a lower trap density, and the smaller Cu^+ and larger I^- ions mimicking PbI_2 (*i.e.*, Pb^{2+} and I^{2-}) inhibit the back-recombination (Fig. 28(a and b)). Although a moderate number of CuI islands improved the PCE (*i.e.*, 19%), a large number of CuI islands reduced it by blocking the electron pathways (Fig. 28(c)). Apparently, the

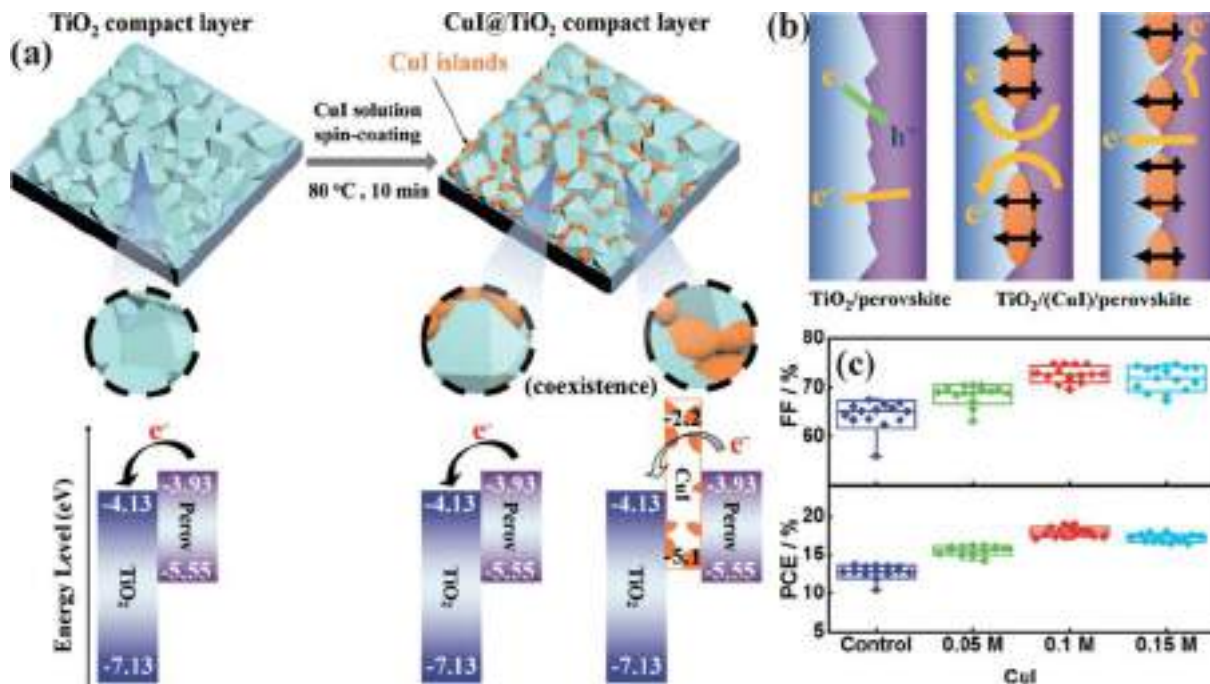


Fig. 28 (a) Schematic of CuI islands formed on TiO₂ compact layer and subsequent deposition of perovskite layer. In CuI-modified TiO₂ (CuI@TiO₂)-based PSCs, electrons move from the perovskites to the exposed TiO₂ surface instead of CuI islands because of its high conduction band energy level. (b) Interfaces with various amounts of CuI islands. (c) FF and PCE of devices with various concentrations of CuI.⁴⁹⁰ Reprinted with permission from (*Adv. Energy Mater.*, 2017, **8**, 1702235). Copyright (2017), John Wiley & Sons.

incorporation of thiourea in CuI (*i.e.*, Cu(Tu)I) operates by accelerating the hole transport and reducing the charge carrier recombination due to the increased depletion width (from 126 to 265 nm) as compared to the traditional CuI. Thus, Cu(Tu)I exhibited a PCE of 19.9% by lowering the trap state energy level and eliminating the potential wells for hole transport at the interface.⁴⁹¹ This is why the doping or passivation strategies for further the modification of CuI endow it with potential to serve as magnificent HTLs for efficient PSCs.

Overall, CuI is one of the best HTMs to produce PCEs in the range of 20% to 26% after combining with TiO₂, CdS, ZnSe, ZnO, ZnOS, *etc.*,^{492,493} but a well-optimized thickness ratio of the ETL, perovskite, and HTL is highly demanded. The interplay of Pb and CuI recovers the (Pb-based) perovskite by the Cu–I chemical drain in the system and increases the CuI contact, and hence the charge carrier transport. CuI-based devices show suppressed hysteresis with a significant light soaking effect. The chemical potential gradient redistributes the I[−] ions from CuI to the perovskite by diffusive movement during aging, which can be tuned by controlling the distribution and morphology of CuI. The ageing instability can be seen in any PSC that undergoes diffusive ion migration towards the interface, but it is relatively less for HTLs like CuI barely accumulating I[−] ions.

5.1.6. Copper thiocyanate (CuSCN). CuSCN is one of the cost-effective hole selective contacts for the emerging organometal halide PSCs. The hole mobility of 0.01–0.1 cm² V^{−1} s^{−1}, HOMO level of −5.3 eV (& E_{CB} = −1.8 eV), and high thermal and chemical stability of CuSCN have gained attention as inorganic

HTLs in PSCs.⁴⁹⁴ CuSCN with an inherently wide bandgap (E_g = ~3.8 eV) transmits in the complete visible spectrum, facilitates photoactive materials to absorb more light, and generates higher photocurrents in solar cells. Ito *et al.*⁴⁹⁵ proposed the use of CuSCN as an HTL in PSCs for the first time to control the degradation of the CH₃NH₃PbI₃ perovskite layer during the light exposure test without encapsulation. Later, various synthesis protocols such as drop-casting,⁴⁹⁶ electrodeposition,^{497,498} spin coating,⁴⁹⁹ and spraying⁵⁰⁰ were developed to obtain CuSCN in an ambient atmosphere with minimum damage to the underlying perovskite absorber, followed by annealing strategies to achieve a higher efficiency. Nevertheless, the texturized grain growth of CuSCN after recrystallization produces poor interaction with the perovskite absorber, thus inducing non-contacting sites as charge recombination centres, thereby reducing the device efficiency. The high-temperature treatment causes the SCN[−] ions to diffuse near the perovskite/HTL interface, resulting in the degradation of the device performance, which can be impeded either by vacuum-assisted thermal treatment⁵⁰¹ or K-SCN post-treatment.⁵⁰²

PSCs employing a CuSCN HTL exhibited a PCE of 13.3%, which degraded faster under elevated temperatures in ambient atmosphere. Therefore, the critical instability caused by the interfacial degradation of the heterojunction of CuSCN and perovskite in a dry N₂ environment was resolved with rudimentary on-cell encapsulation using an additional coating of insulating poly-methyl-methacrylate (PMMA).⁵⁰³ The mesoporous and rough surface of a 600–700 nm-thick CuSCN layer utilized in conventional and mesostructured PCSs attained a maximum

of PCE of 12%.^{496,504} However, a very thin (40 nm) uniform and compact CuSCN film furnished a higher degree of transparency, rendering a PCE of 16%, given that it efficiently generates a higher photocurrent and mitigates the recombination losses at the interface.⁴⁹⁹ The well-aligned junction geometries of the nanostructured arrays substantially increase the light trapping by reducing reflection losses, and also improve the carrier extraction by increasing the interfacial area at the perovskite/HTL interface. However, the hexagonal 3D prism, 2D pyramid, and 1D nanowire-like structures of the CuSCN HTL produced uncontrolled defect density and oversized growth of perovskite, restricting the PCE to <12%.⁵⁰⁵ Importantly, the incorporation of CuSCN in the mesoporous perovskite absorber layer resulted in the formation of a bulk heterojunction, which facilitated faster hole extraction with a resulting PCE of >15%.⁵⁰⁶

The deposition of the CuSCN HTL overlayer causes damage to the perovskite absorber. Therefore, a protective buffer solvent layer of chlorobenzene⁵⁰⁷ and PDMS⁵⁰⁸ was placed over the perovskite before the deposition of CuSCN, which not only hampered the formation and migration of defects but also promoted the crystallization of CuSCN to benefit the charge extraction at the interface (Fig. 29). However, the use of NH₃ (aq) as a substitute to the commonly used diethyl sulfide solvent is seen to reduce the shunting pathways and interfacial current losses, resulting in a PCE of 17.5%.³⁶² Further, a fast solvent removal process facilitates the formation of a compact and conformal CuSCN layer, which serves towards rapid charge extraction and collection. The potential-induced degradation of the CuSCN/Au contact provoked the operational instability of the PSCs with a PCE exceeding 20%. Accordingly, the inclusion of a conductive rGO spacer between CuSCN and Au avoids the electrical potential-induced reaction at their interface, forming an undesirable barrier and exceptionally improving the stability (*i.e.*, >95% of the initial PCE at 60 °C for 1000 h aging).⁵⁰⁹ However, rGO has been seen to fail in improving the hole extraction and electron blocking, which cannot further enhance the PCE. Therefore, the introduction of ultrathin polymers layers of DTB⁵¹⁰ and PTB7⁵¹¹ over CuSCN has gained attention.

These innovative alterations have enhanced the hole extraction efficiency by cascading energy levels and providing environmentally stable PCEs of above 20% for over >1000 h of light illumination. Considering the dissimilarity around the defects structures, multi-component systems have been found to be helpful for the passivation of defects. The interfacial treatment of functional molecules such as Pr-ITC and Ph-DITC has been found to be effective in controlling the perovskite/CuSCN interface, resulting in a PCE of 19.17% PCE with an enhanced V_{OC} .⁵¹²

Recently, Kim *et al.*⁵¹³ introduced CuSCN/P3HT composites to address the instability of PSCs towards high-moisture conditions. The hole-extractive CuSCN, when combined with a p-type conductive polymer, initiated oxidative activities and triggered in-situ p-doping of polymers, thereby improving the interfacial charge transportation and device performance. Alternatively, the coordination strategy, where the coordination bond between CuSCN and ligands (*e.g.*, pyridine derivative) forms a stable intermediate phase, has been found to be exceptionally good for realizing a compact CuSCN HTL by reducing the formation of intermediate adducts and enabling faster recrystallization. Consequently, it facilitated hole extraction and suppressed charge recombination at the interface, resulting in a PCE of 19.2%.⁵¹⁴ Besides, CuSCN is either doped or combined with organic HTLs such as F4TCNQ,⁵¹⁵ PEDOT:PSS,⁵¹⁶ and spiro-OMeTAD⁵¹⁷ to reduce the energy barrier and improve the charge extraction at the interface.

Overall, the theoretically predicted PCE of 25%⁵¹⁸ for the device utilizing CuSCN HTL, where Cu–I and Pb–N bonds form at the interface, inducing more significant electrostatic potential and electron–hole pair excitation, is highly encouraging. However, one should always consider that the molecular (atomic) adsorbates such as iodide and lead present in the perovskite absorber interact with CuSCN at the interface and form the PbI₂ moiety, leading to additional empty states in the bandgap of CuSCN and tailoring the corresponding optoelectronic properties. Therefore, theoretical studies on the passivation of CuSCN and interaction of solvent molecules (DMSO or DMF) with CuSCN need to be thoroughly devoted to the molecular interfacial engineering of CuSCN HTLs for realizing excellent PCEs.

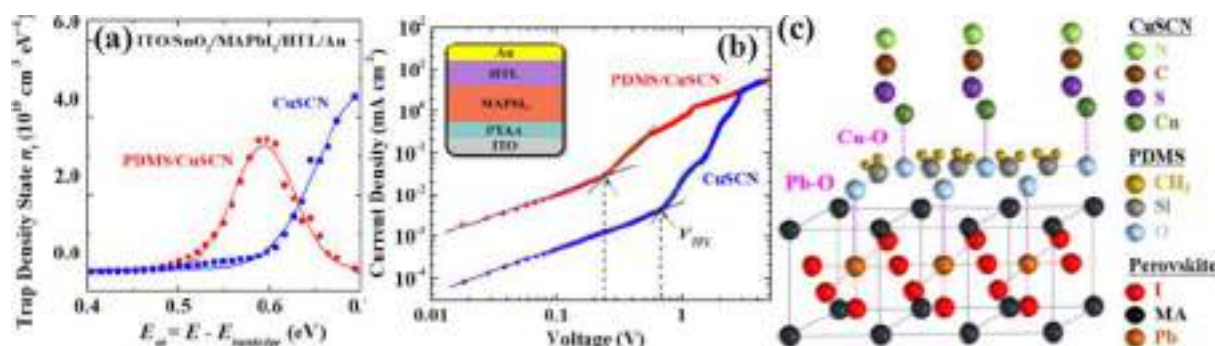


Fig. 29 (a) Trap distribution spectra and (b) J - V characteristics measured in the dark for the MAPbI₃/CuSCN-based PSCs with and without the PDMS interlayer. (c) Schematic of the cross-linking PDMS interlayer. The resistive and defective features of the PSCs are estimated from the curves in (a) fitted with solid lines. The arrows in (b) indicate the trap-filled limit voltages (V_{TFL}).⁵⁰⁸ Reprinted with permission from (*ACS Appl. Mater. Interfaces*, 2019, **11**, 46818–46824). Copyright (2019), the American Chemical Society.

5.1.7. Other inorganic HTLs. Delafossite materials with the general chemical formula of ABO_2 , where A (\equiv Cu), B (\equiv Al, Ga, Cr), and O bear +1, +3, and -2 states, respectively, have also attracted scientific attention to understand their photoactivity. These layers are composed of edge-sharing BO_6 octahedrons linked by triangular sheets of monovalent A^+ ions in the ABO_2 materials and possess high mobility, wide bandgap, and excellent stability. However, limited delafossite materials have been explored as HTLs for PSCs. $CuAlO_2$ (CAO) exhibiting a bandgap of ~ 3.75 eV and hole mobility of ~ 3.6 $cm^2 V^{-1} s^{-1}$ ⁵¹⁹ is one of them. However, CAO, possessing decent optical transparency and thermal/chemical stability, has processing issues due to the need for high-temperature processing to gain pure polycrystalline delafossite form, and the complex Al chemistry prohibits the efficient synthesis of nanostructures. However, its amorphous phase, which provides a band gap of ~ 3.86 eV, has attracted attention due to its nonreactive behaviour with ITO or other HTL materials during deposition. Therefore, Igbari *et al.*⁵²⁰ introduced magnetron-sputtered CAO thin films below a PEDOT:PSS HTL in planar PSCs. The variation in the thickness of the CAO film tailored the energy level alignment and reduced the charge transfer resistance at the HTL/perovskite interface, which yielded an optimized PCE of $\sim 14.52\%$ and stable performance with efficiency retention of 90% over 250 h in the ambient atmosphere without encapsulation. Further, the incorporation of 23% CuO in the uniformly distributed CAO nanoparticles enhanced the electrical conductivity, which further reduced the interfacial charge recombination and induced faster charge collection to render a higher PCE of 16.3%. Recently, PANI introduced during the electro-spray process to form a CAO/polyaniline (PANI) composite film delivered an $\sim 5\%$ larger efficiency for the optimized wt% of CAO (*i.e.*, 0.1%) than pure PANI film.⁵²¹ The addition of PANI improved the interconnectivity between the CAO nanoparticles, enabling the conformal film coating of a CAO HTL, and enhanced the hole conduction into the organic polymer. Nevertheless, the excessive aggregation of CAO induced high surface roughness and increased the series resistance by segregating the CAO and polymer.

$CuCrO_2$ (*i.e.*, CCO) is another delafossite material with a hole mobility of $0.1\text{--}1$ $cm^2 V^{-1} s^{-1}$, valence band maximum of -5.3 eV w.r.t. the vacuum level, and a bandgap of 3.1 eV,⁵¹⁹ which can offer the tuning of the energy levels by altering the phase composition. Low-temperature solution-processed CCO nanocrystals demonstrated a PCE of $\sim 19\%$ as HTLs in PSCs and acted as an excellent UV inhibitor, protecting the perovskite absorber from UV-induced degradation.⁵²² Although DFT analysis proposed the formation of distinct hexagonal 2H (space group $P6_3/mmc$) and rhombohedral 3R (space group $R\bar{3}m$) polytypes of CCO, both are stable and deliver identical optoelectronic properties.⁵²³ Besides the inverted device structure, CCO nanoparticles were utilized with a triple cation perovskite light absorber to form a highly stable n-i-p structure, exhibiting an efficiency of 16%.⁵²⁴ A bigger VB offset does not favour hole transfer, whereas a lower electron affinity favours electron-blocking. Therefore,

Qin *et al.*⁵²⁵ employed different Cu/Cr ratios to modulate the energy levels and phase composition of a CCO film to improve the hole-collection and electron-blocking ability. These Cr-terminated polar CCO films achieved a respectable PCE of 17.19% (Fig. 30).

Yang *et al.*⁵²⁶ introduced an azeotropic-promoted doping approach for CCO to explore cost-effective commercialization aspects. The d-d excitation of the Cr^{3+} cations at the oxygen octahedrons of the delafossite structure causes the low transparency of CCO. The replacement of Cr^{3+} by In^{3+} (*i.e.*, doping) decreases the absorption of d-d and improves the conductivity (*i.e.*, carrier mobility) and transmittance of CCO, which are beneficial for solar-light harvesting and hole transport, and consequently an impressive PCE of 20.54% was achieved. Furthermore, considering the band alteration due to the doping of metallic elements, Mg has also been introduced in CCO. The smaller ionic radius of Mg than Cr overlaps the Cu d-orbitals by reducing the Cu-Cu bond distance, resulting in improved charge mobility and conductivity, which produces an efficiency close to 13%.⁵²⁷

$CuGaO_2$ (*i.e.*, CGO) is also a prominent HTL material with high carrier mobility ($\sim 10^{-1}$ $cm^2 V^{-1} s^{-1}$) and a bandgap of ~ 3.58 eV, furnishing a well-matched energy level with perovskite absorbers.⁵¹⁹ However, the aggregation of CGO results in a larger particle size, which is incapable of enabling the formation of a compact pinhole-free film, hindering its use as an HTL. Therefore, a surfactant such as Pluronic 123 was utilized to synthesize CGO nanoparticles with a diameter of < 10 nm.⁵²⁸ Moreover, the use of CGO with CuSCN improved the PCE to 16% by reducing the trap density of cells.⁵²⁹ Besides the increased efficiency, a bilayer HTL was shown to offer high thermal stability, retaining 80% of the initial efficiency after exposure to a temperature of 85 °C and 85% relative humidity (RH) condition (encapsulated) for 400 h. Furthermore, Zn^{2+} doping (*i.e.*, 5%) enhanced the hole mobility of pristine CGO (*i.e.*, from 3.81×10^{-2} to 1.39×10^{-1} $cm^2 V^{-1} s^{-1}$), which yielded an efficiency of $\sim 20\%$ and high inertness to humidity and temperature.⁵³⁰ Chen *et al.*⁵³¹ reported the development of mesoscopic inverted device structures utilizing compact NiO_x and CGO mesoporous layers. The graded band alignment formed at the HTL with compact NiO_x and mesoporous CGO was shown to enable higher hole extraction, leading to an efficiency of $\sim 19\%$. Further, solution-processed CGO nanoplates were coated on the perovskite absorber to form an n-i-p device structure, effectively lowering the monomolecular Shockley-Read-Hall (SRH) recombination and providing a PCE of $\sim 18\%$.³⁶³ Recently, a 3D hybrid HTL consisting of Cr-doped CGO nanoplates and NiO nanoparticles yielded a PCE of $\sim 20\%$. The nanoplates acted as expressways for hole extraction, whereas the ultrafine NiO nanoparticles modified the surface properties.⁵³²

Besides delafossite materials, various inorganic materials such as CuS, FeS_2 , CuZnS, and CZTS have been investigated for their application as HTLs in PSCs. The use of CuS nanoparticles uniformly deposited on ITO without compromising the roughness and transmittance of the ITO substrate resulted in an

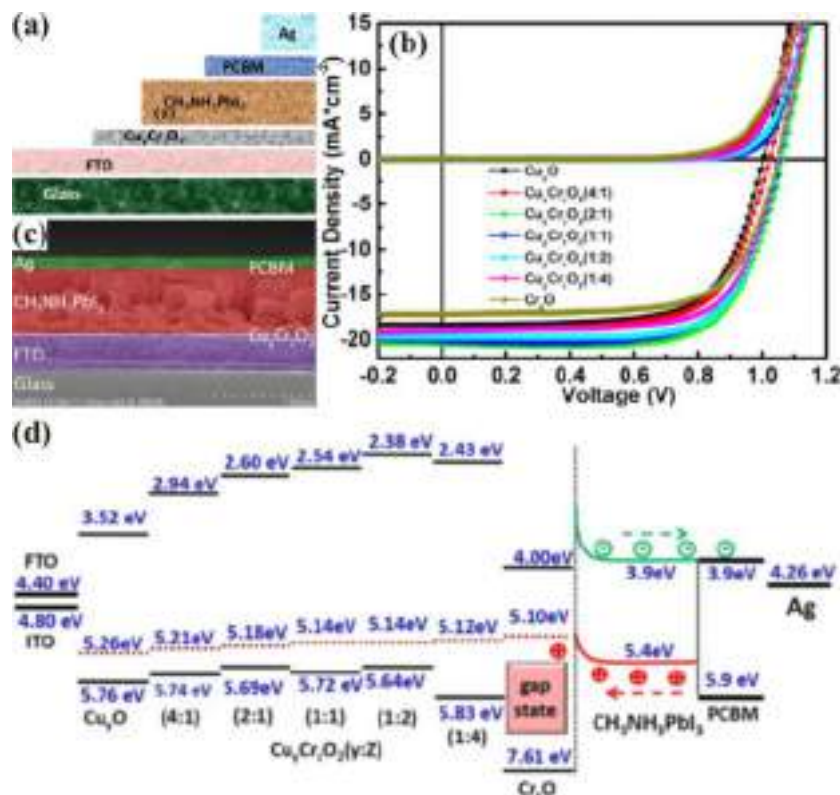


Fig. 30 (a) Schematic, (b) J - V characteristics under illumination, and (c) a cross-sectional SEM image of PSCs consisting of $\text{Cu}_y\text{Cr}_z\text{O}_2$ film. (d) Band energy level diagram of PSCs comprised of $\text{Cu}_y\text{Cr}_z\text{O}_2$ HTL in various volume ratios of $y:z = 1:0, 4:1, 2:1, 1:1, 1:2, 1:4$, and $0:1$.⁵²⁵ Reprinted with permission from (*Solar RRL*, 2017, **1**, 1700058). Copyright (2017), John Wiley & Sons.

efficiency of $\sim 16\%$ with $\text{CH}_3\text{NH}_3\text{PbI}_3$ as the light absorber, although its V_{OC} was limited to ~ 0.8 V due to the considerable offsets in valence band levels at the $\text{CuS}/\text{perovskite}$ interface.⁵³³ High hole mobility CuS nanoparticles have been incorporated in carbon to form a CuS/C composite HTL and improved the hole mobility.⁵³⁴ Moreover, digenite CuZnS nanocrystals were formed by partially replacing Cu with Zn in the covellite CuS structure and tested as HTLs in PSCs. The ternary CuZnS material showcased its potential as an HTL by yielding an efficiency of $\sim 18\%$.⁵³⁵ High-purity kesterite $\text{Cu}_2\text{ZnSnS}_4$ (CZTS) nanocrystals as an inorganic HTM with $\text{CH}_3\text{NH}_3\text{PbI}_3$ perovskite achieved an efficiency of $\sim 15\%$ and remarkable FF of 81% .⁵³⁶ Further, quantum dots of CZTS as HTLs were tested with all-inorganic CsPbBr_3 perovskite absorbers, showing a promising efficiency of $\sim 5\%$.⁵³⁷ The thickness of the light-absorbing CZTS HTLs in inverted PSCs plays a prominent role in controlling the irradiation over the perovskite light absorber.⁵³⁸ Interestingly, numerical simulations have identified the plausible tailorability of the $\text{Cu}_2\text{Zn}(\text{Sn}_{1-x}\text{Ge}_x)\text{S}_4$ bandgap and band offsets at the perovskite/HTL interface through the partial replacement of Sn with Ge (*i.e.*, $x = 0.8$) and predicted a theoretical efficiency of $\sim 20\%$ in combination with $\text{CH}_3\text{NH}_3\text{PbI}_3$ as a light absorber.⁵³⁹ Koo *et al.*⁵⁴⁰ observed an efficiency of $\sim 13\%$ with octadecylamine-capped FeS_2 nanoparticles, preventing moisture attack in the perovskite light absorber, thereby retaining stability for 1000 h. Further, the hole quenching capacity of

iron pyrite FeS_2 is comparable to that of the benchmark spiro-OmeTAD, but its efficiency is not higher to the defect-mediated recombination at the $\text{FeS}_2/\text{perovskite}$ interface, where low-energy photons are left largely unutilized with non-productive recombination events taking place.⁵⁴¹ Although FeS_2 is 300 times cheaper than spiro-OmeTAD, its inefficient hole collection needs to be improved by using a capping ligand. Moreover, a wide bandgap p-type quaternary chalcogenide $\text{Cu}_2\text{BaSnS}_4$ semiconductor having favourable band alignment with a $\text{CH}_3\text{NH}_3\text{PbI}_3$ perovskite light absorber and high carrier mobility ($\sim 10 \text{ cm}^2 \text{ V}^{-1} \text{ s}^{-1}$) was shown to exhibit an efficiency of 10% in inverted PSCs.⁵⁴² Similarly, spinel oxides of Ni , Co , Cu , *etc.* (such as CuCo_2O_4 and NiCo_2O_4) have been explored as HTLs in PSCs due to their high electrical conductivity, high optical transparency in the UV-Vis-NIR region, and well-matched energy levels to the perovskite absorber.^{543,544} The low-temperature solution-processable monodispersed spinel NiCo_2O_4 oxide nanoparticles synthesized *via* a combustion method show high electrical conductivity ($\sim 4 \text{ S cm}^{-1}$) and low roughness (0.56 nm), delivering an efficiency of $\sim 15\%$ for the optimized film thickness of 15 nm with higher transmittance and better charge collection.⁵⁴⁵ Likewise, various doping strategies⁵⁴³ have been explored to investigate the practicality of spinel NiCo_2O_4 as HTLs in PSCs. Thus, besides the traditional inorganic HTLs used in PSCs, various combinations of pristine novel p-type materials need to be tested for their hole quenching capabilities.

5.2. Organic HTLS

Several organic HTMs previously used in DSSCs and organic bulk heterojunction solar cells, which satisfy the requirements of PSCs, have been tested as HTLs to improve the performance. 2,2',7,7'-Tetrakis-(*N,N*-di-4-methoxyphenylamino)-9,9'-spirobifluorene (spiro-OMeTAD) is one of the widely used organic small molecule p-type semiconductors and dominant solid-state HTLs in PSCs. The large bandgap (about 3 eV) with a deep HOMO level of spiro-OMeTAD located at -5.2 eV eases the acceptor transport from most of the perovskite absorbers to the external contact.⁵⁴⁶ Although spiro-OMeTAD has been proven to be the best HTM with good thermal stability owing to its high melting temperature, it suffers from poor conductivity (6×10^{-5} mS cm⁻¹) and hole mobility (2×10^{-4} cm² V⁻¹ s⁻¹).⁵⁴⁷ Thus, different strategies have been employed to deal with these issues, as follows: (a) doping to improve the conductivity together with hole mobility and to expedite the oxidation process; (b) designing novel synthesis processes to improve the film quality, coverage, and avoid pinholes; and (c) controlling the

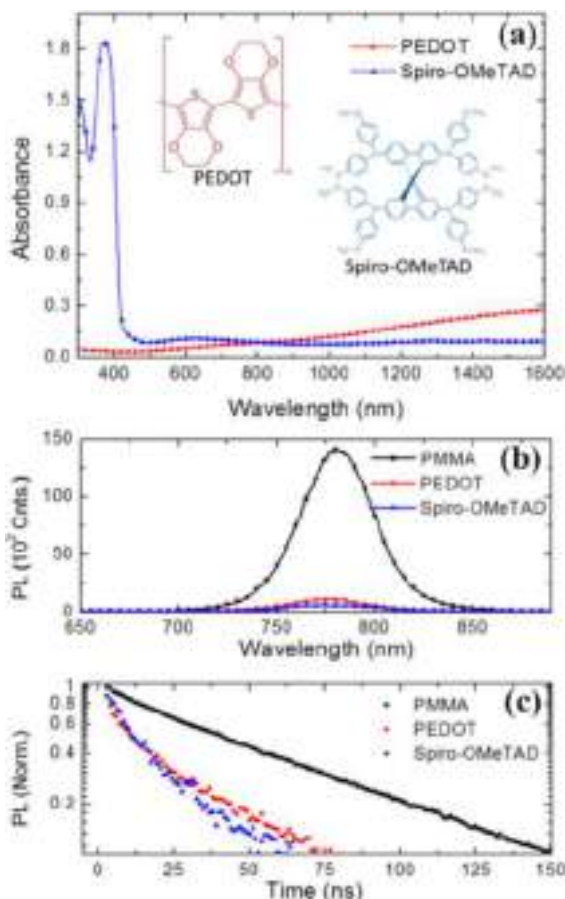


Fig. 31 (a) Absorbance spectra of ~ 230 nm-thick PEDOT films (red circles) and ~ 280 nm-thick spiro-OMeTAD films doped with Li-TFSI (blue triangles) deposited on glass. (b) Steady-state PL spectra and (c) time-resolved PL decay excited at 507 nm of perovskite films coated with PMMA (black squares), PEDOT (red circles), and spiro-OMeTAD (blue triangles), respectively.⁵⁵⁵ Reprinted with permission from (*J. Phys. Chem. Lett.*, 2015, **6**, 1666–1673). Copyright (2015), the American Chemical Society.

defects and hydrophobic nature at the interface. Butyl pyridine (TBP) and lithium salt (LiTFSI) are the most common dopants that increase the hole mobility of spiro-OMeTAD,⁸¹ but PSCs suffer from low stability with the introduction of the hygroscopic lithium. The doping of CuSCN and CuI in spiro-OMeTAD reduced the amount of pinholes and improved its crystallinity, which protected the perovskite absorber from humidity and exhibited an efficiency of $\sim 18\%$.⁵⁴⁸ However, spiro-OMeTAD suffers from complicated synthesis and is ~ 20 times more expensive than gold.⁵⁴⁹ Recently, a mixture of PbS/spiro-OMeTAD and potassium persulfate (KPS)-doped spiro-OMeTAD HTLs exhibited a PCE of above 20%.^{550,551}

Likewise, poly(3,4-ethylene dioxithiophene):poly(styrenesulfonate) (PEDOT:PSS) is a typical choice as an HTL for inverted PSCs (p-i-n type), which shows high optical transparency in the visible region and exhibits the HOMO level of -5.3 eV, matching well with the perovskite. Unfortunately, PEDOT:PSS in its pristine form suffers from low conductivity (10^{-3} S cm⁻¹), poor hole mobility, and hygroscopic and acidic nature.^{552,553} Thus, to overcome these issues, PEDOT:PSS is either treated with a dimethylformamide (DMF)/methanol mixture or annealed with non-polar vapours of toluene, which improves its conductivity, reduces its trap state density, and facilitates smooth charge transfer at the PEDOT:PSS/perovskite interface, resulting in an improved PCE than the pristine HTL.^{553,554} Separately, the development of a PEDOT:PSS toluene-based ink coated over the perovskite absorber in the conventional planar (n-i-p type) device architecture has attracted attention from the scientific and industrial community.⁵⁵⁵ The absorbance of PEDOT films is very low in the UV-visible region, causing less parasitic losses during the second pass through the perovskite layer and resulting in an increased photocurrent with a PCE of 14.5% (Fig. 31). Further, the addition of island-like GeO₂ particles in PEDOT:PSS film served well as growth sites for perovskite absorbers with better crystallinity,⁵⁵⁶ resulting in a PCE of $\sim 15\%$.

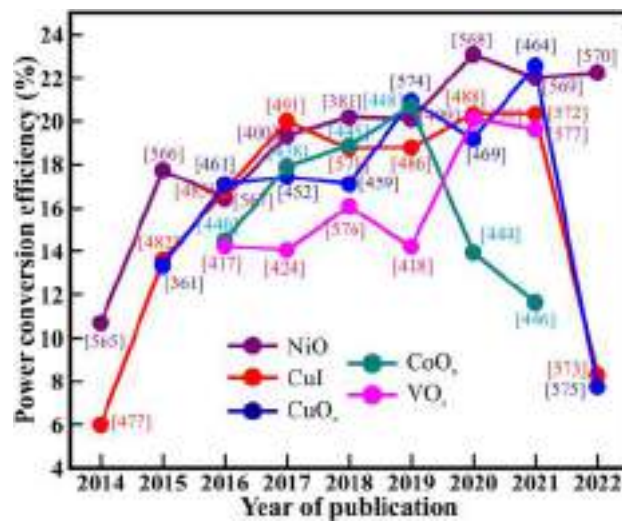


Fig. 32 Comparative study of the influential HTLs developed by year to gain the best maximum efficiency in the last decade (collected from ISI Web of Knowledge up to 31st December 2021).⁵⁷⁴

Table 2 A brief summary of inorganic HTLs processed with various synthesis methods and their corresponding device performance parameters

S. no.	Device configuration	Method ^a	V _{OC} (V)	J _{SC} (mA cm ⁻²)	FF	PCE (%)	Year	Ref.
Nickel oxide (NiO)								
1.	ITO/NiO _x /TPA-BA/PC ₆₁ BM/BCP/Au	SC	1.15	23.36	0.829	22.25	2022	570
2.	FTO/S-NiO/CH ₃ NH ₃ PbI ₃ /PC ₆₁ BM/BCP/Au	SC	1.13	22.56	0.78	19.91	2022	578
3.	ITO/NiO _x /Cs _{0.5} (MA _{0.17} FA _{0.83}) _{0.95} Pb(I _{0.83} Br _{0.17}) ₃ /PS-PAN/PCBM/C ₆₀ /BCP/Cr/Au	SC	1.12	23.51	0.836	22.02	2021	569
4.	ITO/NiO _x /RT-MAPb(I _{1-x} Cl _x) ₃ /PCBM/BCP/Ag	SC	1.16	23.52	0.847	23.07	2020	568
5.	ITO/Al:NiO _x /CH ₃ NH ₃ PbI ₃ /PCBM/am-TiO ₂ /Ag	SC	1.06	24.34	0.813	20.84	2020	403
6.	FTO/c-TiO ₂ /Al ₂ O ₃ /FA _{0.026} MA _{0.974} PbI _{3-y} Cl _y -Cu:NiO/spiro-OMETAD/Au	CP/SC	1.05	24.51	0.805	20.67	2020	388
7.	FTO/Ni ₂ O ₃ /MA _{0.85} FA _{0.15} PbI _{0.9} Cl _{0.1} /PCBM/BCP/Ag	SC	1.06	19.66	0.826	17.89	2020	385
8.	ITO/Li:CO-NiO/MA _{1-y} FA _y PbI _{3-x} Cl _x /PC ₆₁ BM/BCP/Ag	SC	1.09	23.8	0.78	20.1	2019	409
9.	FTO/NiO NCS/mp-NiO/CH ₃ NH ₃ PbI ₃ /PC ₆₁ BM/BCP/Au	ST	1.11	22.20	0.741	18.17	2019	579
10.	FTO/NiO/MA _{1-y} FA _y PbI _{3-x} Cl _x /PCBM/BCP/Ag	C	1.12	23.7	0.76	20.2	2018	381
11.	ITO/Ag:NiO _x /CH ₃ NH ₃ PbI ₃ /PCBM/BCP/Ag	SC	1.08	19.70	0.783	16.86	2018	394
12.	FTO/NiO/CH ₃ NH ₃ PbI ₃ /PCBM/BCP/Ag	RFS	1.05	20.57	0.752	16.29	2018	580
13.	FTO/Cs:NiO _x /CH ₃ NH ₃ PbI ₃ /PCBM/ZrAcac/Ag	SC	1.12	21.77	0.793	19.35	2017	400
14.	FTO/c-TiO ₂ /NiO NTs + CH ₃ NH ₃ PbI ₃ /spiro-OMETAD/Au	ES	1.12	22.7	0.752	19.3	2017	581
15.	FTO/NiMgO _x /CH ₃ NH ₃ PbI ₃ /PCBM/ZnMgO/Al	DCS	1.08	21.3	0.79	18.2	2017	404
16.	ITO/NiO _x /CH ₃ NH ₃ PbI ₃ /PCBM/Ag	SC	1.07	20.58	0.748	16.47	2016	567
17.	ITO/Cu:NiO _x /CH ₃ NH ₃ PbI ₃ /bis-C ₆₀ /Ag	C	1.05	22.23	0.76	17.74	2015	566
18.	ITO/Cu:NiO _x /CH ₃ NH ₃ PbI ₃ /PC ₆₁ BM/C ₆₀ /Ag	CP	1.12	19.17	0.73	15.4	2015	582
19.	ITO/NiO _x /CH ₃ NH ₃ PbI ₃ /PCBM/BCP/Al	RFS	1.00	17.4	0.61	10.7	2014	565
Cobalt oxide (CoO _x)								
20.	ITO/Zn,Li ⁺ :CoO _x /CH ₃ NH ₃ PbI ₃ /PCBM/BCP/Ag	SC	0.93	19.7	0.639	11.64	2021	583
21.	ITO/Li-Co ₃ O ₄ /CH ₃ NH ₃ PbI ₃ /PCBM/ZnO/Ag	SC	1.04	20.66	0.65	13.96	2020	444
22.	FTO/CoO/Cs _{0.05} (MA _{0.17} FA _{0.83}) _{0.95} Pb(I _{0.83} Br _{0.17}) ₃ /PCBM/Ag	LEP	0.99	18.9	0.572	10.1	2020	447
23.	ITO/TiO ₂ /Cs _{0.05} (MA _{0.15} FA _{0.85}) _{0.95} Pb(I _{0.85} Br _{0.15}) ₃ /CoO/spiro-OMETAD/Au	ST	1.18	23.19	0.757	20.70	2019	448
24.	FTO/TiO ₂ /CH ₃ NH ₃ PbI ₃ /ZrO ₂ /Co ₃ O ₄ /C	CP	0.88	23.43	0.64	13.27	2018	442
25.	FTO/Co _{1-y} Cu _y O _x /CH ₃ NH ₃ PbI ₃ /PCBM/Ag	DCS	0.93	17.98	0.599	9.98	2017	441
26.	FTO/Ni:CoO _x /CH ₃ NH ₃ PbI ₃ /PCBM/Ag	DCS	0.99	15.96	0.607	9.63	2017	584
27.	ITO/CoO _x /CH ₃ NH ₃ PbI ₃ /PCBM/Ag	SC	0.95	20.28	0.755	14.5	2016	440
Copper oxide (CuO _x)								
28.	FTO/c-TiO ₂ /mp-TiO ₂ /CH ₃ NH ₃ PbI ₃ /CuO/C	SC	0.83	16.98	0.55	7.75	2022	575
29.	ITO/CuO _x /CH ₃ NH ₃ PbI ₃ /PCBM/Ag	RFS	1.06	27.14	0.786	22.56	2021	464
30.	ITO/NiO _x /CuO _x /CH ₃ NH ₃ PbI ₃ /PCBM/Au	SC	1.12	22.29	0.783	19.91	2021	462
31.	ITO/SnO ₂ /CsFAMA/Cu ₂ O-CuSCN/Au	SC	1.05	23.23	0.784	19.2	2020	469
32.	FTO/Cu ₂ O/CH ₃ NH ₃ PbI ₃ /SiO ₂ /GZO/Ag	RFS	1.12	20.90	0.786	18.4	2020	466
33.	FTO/c-TiO ₂ /mp-TiO ₂ /Cs _{0.05} MA _{0.14} FA _{0.81} PbI _{2.55} Br _{0.45} /Cu ₂ O/Au	SC	1.15	22.2	0.742	18.9	2019	467
34.	FTO/TiO ₂ /CH ₃ NH ₃ PbI ₃ /Cu ₂ O/Au	SC	1.13	22.53	0.673	17.23	2019	465
35.	FTO/TiO ₂ /CH ₃ NH ₃ PbI ₃ /spiro-OMeTAD/Cu ₂ O/Ag	IBS	1.03	22.46	0.741	17.11	2018	459
36.	ITO/CuO _x /CH ₃ NH ₃ PbI ₃ /PC ₆₁ BM/ZnO/Al	SC	1.03	22.42	0.76	17.43	2017	452
37.	ITO/CuO _x /CH ₃ NH ₃ PbI ₃ /C ₆₀ /BCP/Ag	SC	0.99	23.2	0.744	17.1	2016	461
38.	ITO/Cu ₂ O/CH ₃ NH ₃ PbI ₃ /PC ₆₁ BM/Ag	RFS	0.95	17.5	0.662	11.03	2016	453
39.	ITO/Cu ₂ O/CH ₃ NH ₃ PbI ₃ /PC ₆₁ BM/Al	DipC	1.07	16.52	0.755	13.35	2015	361
	ITO/CuO/CH ₃ NH ₃ PbI ₃ /PC ₆₁ BM/Al		1.06	15.82	0.725	12.16		
Vanadium oxide (VO _x)								
40.	ITO/Cs-VO _x /PTAA/CH ₃ NH ₃ PbI ₃ /PCBM/BCP/Ag	SC	1.08	22.47	0.79	19.64	2021	577
41.	ITO/PTAA/VO _x /CH ₃ NH ₃ PbI ₃ /PCBM/C ₆₀ /LiF/Al	SC	1.12	22.65	0.75	18.9	2021	427
42.	ITO/VO _x /CH ₃ NH ₃ PbI ₃ /PCBM/ZnO/Al	RFS	1.00	20.7	0.66	13.66	2021	421
43.	ITO/SnO ₂ /PCBA/CsFAPbI ₃ /MAI/PTAA/VO _x /Ag	TE	1.044	24.6	0.78	20.1	2020	430
44.	ITO/PEDOT:PSS/PEDOT:PSS-VO _x /CH ₃ NH ₃ PbI ₃ /PCBM/C ₆₀ /LiF/Al	SC	1.02	22.98	0.77	18.0	2020	416
45.	ITO/V ₂ O ₅ :PEDOT:PSS/PTB ₇ -Th:PC ₇₁ BM/PDINO/Al	SC	0.80	16.83	0.701	9.44	2020	437
46.	ITO/PEDOT:PSS/VO _x /CH ₃ NH ₃ PbI ₃ /PCBM/C ₆₀ /BCP/Al	SC	0.969	20.3	0.722	14.22	2019	418
47.	FTO/VO _x /CH ₃ NH ₃ PbI ₃ /PCBM/Al	SC	0.99	20.98	0.761	16.06	2018	576
48.	FTO/TiO ₂ /(FAPbI ₃) _{0.85} (MAPbBr ₃) _{0.15} /NiPc-(OBu) ₈ /V ₂ O ₅ /Au	SC	1.07	23.0	0.728	17.9	2017	438
49.	ITO/VO _x /APPA/CH ₃ NH ₃ PbI ₃ /PC ₆₁ BM/BCP/Ag	SC	0.96	19.42	0.752	14.07	2017	424
50.	ITO/VO _x /CH ₃ NH ₃ PbI ₃ /PCBM/Al	SC	0.90	22.29	0.71	14.23	2016	417
Copper iodide (CuI)								
51.	ITO/SnO ₂ /FA _x MA _{1-x} PbI _{3-y} Cl _y /CuI/PDMS/Au	SP	0.795	19.3	0.538	8.3	2022	573
52.	ITO/CuI/CuSCN/CH ₃ NH ₃ PbI ₃ /PCBM/carbon	ED	1.10	20.26	0.78	20.35	2021	572
53.	ITO/PEDOT:PSS/CuI/CH ₃ NH ₃ PbI ₃ /PCBM/BCP/Al	SC	0.977	23.13	0.737	16.65	2021	487
54.	FTO/CuSCN@CuI/CH ₃ NH ₃ PbI ₃ /PC ₆₁ BM/carbon	ED	1.08	18.24	0.79	15.58	2021	585
55.	PTTA/CuI/FA _{0.05} MA _{0.95} PbI ₃ /PCBM/C ₆₀ -N/Ag	SC	1.057	24.8	0.77	20.34	2020	488
56.	FTO/CuI/PEDOT:PSS/(FASnI ₃) _{0.6} (MAPbI ₃) _{0.4} /C ₆₀ /BCP/Cu	SC	0.75	28.5	0.737	15.75	2020	479
57.	ITO/CuI/HaP/PCBM/AZO/Ag	SC	0.99	19.39	0.74	14.21	2020	480

Table 2 (continued)

S. no.	Device configuration	Method ^a	V _{OC} (V)	J _{SC} (mA cm ⁻²)	FF	PCE (%)	Year	Ref.
58.	FTO/Cu@CuI/PCBM/ZnO/Ag	SC	1.06	23.31	0.761	18.80	2019	486
59.	FTO/NiO/CuI/CH ₃ NH ₃ PbI ₃ /PCBM/BCP/Ag	SC	1.07	20.60	0.69	15.26	2019	489
60.	FTO/c-TiO ₂ /mp-TiO ₂ /CH ₃ NH ₃ PbI _{3-x} Cl _x /CuI/Pt-FTO	PPT	0.67	24.23	0.50	8.1	2019	476
61.	ITO/CuI/CH ₃ NH ₃ PbI _{3-x} Cl _x PC ₆₁ BM/PEI/Ag	SC	1.05	20.05	0.69	14.53	2018	571
	ITO/CuI/CuSCN/CH ₃ NH ₃ PbI _{3-x} Cl _x PC ₆₁ BM/PEI/Ag		1.11	22.33	0.76	18.76		
62.	ITO/Cu(Tu)I-CH ₃ NH ₃ PbI _{3-x} Cl _x /C ₆₀ /BCP/Ag	SC	1.12	22.3	0.798	20.0	2017	491
63.	FTO/Na-TiO ₂ /CH ₃ NH ₃ PbI ₃ /CuI	S	1.03	22.78	0.75	17.6	2017	478
64.	FTO/CuI/CH ₃ NH ₃ PbI ₃ /PCBM/PEI/Ag	VI	1.04	20.9	0.68	14.7	2017	484
65.	ITO/CuI/CH ₃ NH ₃ PbI ₃ /C ₆₀ /BCP/Ag	SC	1.01	22.9	0.728	16.8	2016	485
66.	ITO/TiO ₂ /CH ₃ NH ₃ PbI _{3-x} Cl _x /CuI/spiro-OMeTAD/Ag	SC	1.06	21.52	0.73	16.67	2016	548
67.	FTO/TiO ₂ /CH ₃ NH ₃ PbI ₃ /CuI/Au	TE	0.73	32.72	0.31	7.40	2016	481
68.	FTO/CuI/CH ₃ NH ₃ PbI ₃ /PCBM/Al	SC	1.04	21.06	0.62	13.58	2015	482
69.	FTO/c-TiO ₂ /mp-TiO ₂ /CH ₃ NH ₃ PbI ₃ /CuI/Au	DC	0.55	17.8	0.62	6.0	2014	477
Copper thiocyanate (CuSCN)								
70.	FTO/c-TiO ₂ /CH ₃ NH ₃ PbI ₃ /CuSCN/Au	SC	0.981	23.77	0.724	16.89	2022	586
71.	FTO/c-TiO ₂ /CH ₃ NH ₃ PbI ₃ /CuSCN/Au	SC	0.93	17.2	0.63	10.1	2022	587
72.	FTO/TiO ₂ /CsPbI ₃ Br/CsBr/CuSCN/Au	SC	1.05	12.3	0.76	9.96	2022	588
73.	ITO/SnO ₂ /FA _{1-y} MA _y PbBr _{3-x} I _x /CuSCN/DTB/Au	SC	1.15	24.31	0.786	21.7	2020	510
74.	FTO/c-TiO ₂ /mp-TiO ₂ /CH ₃ NH ₃ PbI ₃ /CuSCN/Au	SC	0.83	22.15	0.60	11.02	2020	589
75.	FTO/TiO ₂ /Cs _{0.05} FA _{0.81} MA _{0.14} PbI _{2.55} Br _{0.45} /CuSCN/Au	SBND	1.074	23.17	0.756	18.74	2019	590
76.	FTO/TiO ₂ /CH ₃ NH ₃ PbI _{3-x} Cl _x /PSC-CuSCN/Au	SC	1.068	22.85	0.761	18.57	2019	512
77.	FTO/c-TiO ₂ /mp-TiO ₂ /Cs _{0.05} (MA _{0.17} FA _{0.83}) _{0.95} Pb(I _{0.83} Br _{0.17}) ₃ /CuSCN/ITO	SC	0.978	20.2	0.721	14.2	2019	591
78.	ITO/r-GO/CuSCN/CH ₃ NH ₃ PbI ₃ /PCBM/BCP/Ag	SC	1.031	18.21	0.761	14.28	2018	592
79.	FTO/TiO ₂ /CH ₃ NH ₃ PbI ₃ /CuSCN/Au	S	1.013	23.10	0.731	17.10	2017	500
80.	ITO/3D-CuSCN/CH ₃ NH ₃ PbI ₃ /C ₆₀ /Bphen/Ag	ED	0.92	19.45	0.69	11.89	2017	505
	ITO/2D-CuSCN/CH ₃ NH ₃ PbI ₃ /C ₆₀ /Bphen/Ag		0.82	18.56	0.61	9.19		
Other inorganic HTLs								
81.	ITO/CuBr/CH ₃ NH ₃ PbI ₃ /PCBM/C ₆₀ -N/Ag	SC	1.03	23.15	0.738	17.65	2022	593
82.	FTO/TiO ₂ /Cs _{0.05} (MA _{0.17} FA _{0.83}) _{0.95} Pb(I _{0.83} Br _{0.17}) ₃ /CuIn _{0.75} Ga _{0.25} S ₂ /C	SC	1.08	23.86	0.62	15.93	2020	594
83.	FTO/TiO ₂ /CH ₃ NH ₃ PbI ₃ /Fe ₃ O ₄ /Au	SC	1.13	19.29	0.71	15.42	2020	595
84.	FTO/NiCoO _x /CH ₃ NH ₃ PbI ₃ /PCBM/BCP/Ag	SC	1.08	22.27	0.833	20.03	2019	596
85.	ITO/c-CuCrO ₂ /CH ₃ NH ₃ PbI ₃ /PCBM/BCP/Ag	HT	1.07	21.94	0.81	19.0	2018	522
86.	ITO/LiCoO ₂ /CH ₃ NH ₃ PbI ₃ /C ₆₀ /BCP/Ag	RFS	1.06	22.5	0.8	18.88	2018	445
87.	FTO/c-TiO ₂ /CH ₃ NH ₃ PbI _{3-x} Cl _x /CuGaO ₂ /Au	HT	1.11	21.66	0.77	18.51	2017	363
88.	ITO/CuAlO ₂ /PEDOT:PSS/CH ₃ NH ₃ PbI _{3-x} Cl _x /PCBM/Ag	DCS	0.88	21.98	0.75	14.52	2016	520

^a SC = spin coating, CP = chemical or co-precipitation method, RFS = RF sputtering, DCS = DC sputtering, SP = screen printing, ST = solvothermal, HT = hydrothermal, ED = electrochemical deposition, IBS = ion beam sputtering, ES = electro-spinning, LEP = ligand exchange process, TE = thermal evaporation, SBND = smart bottle neck deposition, DC = drop casting, VI = vapour iodization, PPT = powder press technique, DipC = dip coating, S = spray, and C = combustion.

Furthermore, different doping materials such as WO₃, EMIC (1-ethyl-3-methylimidazolium chloride), CuSCN, and 3-(cyclohexylamino)-2-hydroxy-1-propane sulfonic acid (CAPSO) have been employed to achieve the required electronic and optical properties at the PEDOT:PSS HTL/perovskite interface.^{516,552,557,558}

Poly(3-hexylthiophene) (P3HT) has been recommended as a promising organic HTL due to its larger-area solution processability, excellent optoelectronic properties, good hole mobility (0.1 cm² V⁻¹ s⁻¹),⁵⁵⁹ and hydrophobic surface (contact angle >100°)⁵⁶⁰ compared to other organic HTLs. Recently, Jung *et al.*⁵⁵⁹ employed P3HT as the HTL in PSCs and achieved a PCE of 22.7%, which retained 16% over a large area (25 cm²). The surface treatment of P3HT using a gallium-based ligand, *i.e.*, gallium(III) acetylacetonate (Ga(acac)₃), interacted with the defects on the perovskite layer and modified the P3HT/perovskite interface, resulting in PCE of 24%.⁵⁶¹ Moreover, the comparative performance of spiro-OMeTAD, P3HT and 4-(diethylamino)-benzaldehyde diphenyl-hydrazone (DEH) as the HTL in

PSCs showed a better light absorption for P3HT in the visible region compared to spiro-OMeTAD and DEH; besides, a negligible change in photon conversion efficiency.⁵⁶² In addition, other organic HTLs such as poly[bis(4-phenyl)(2,4,6-trimethylphenyl)-amine] (PTAA),⁵⁶³ polyaniline doped with camphor sulfonic acid (PANI-CSA),⁵⁶⁴ and tetraphenyl benzidine and MeO-triphenylamine (TPB-*n*-MOTPA) have been employed in PSCs as alternative organic HTLs.

Although the overall efficiency of PSCs generally increases with the use of organic HTLs, their high cost, requirement of very high purity, complicated synthesis process in an inert atmosphere, hydrophilic nature of the surface, requirement of surface treatment, and long-term instability continue to be prime concerns. The stability of the devices is reduced drastically due to the use of hygroscopic dopants, which triggers the degradation of the perovskite layer. In the future, these drawbacks need to be targeted to develop effective strategies for easy processing in the ambient atmosphere.

Similar to ETLs, numerous HTLs have delivered high PCEs despite their distinct electrical, optical, and interfacial properties. HTLs have tailored the device performance and efficiency when utilized with different perovskite coating layers in PSCs. The highest efficiencies proclaimed in the most prominent recent reports from a variety of HTLs are shown in Fig. 27. The initial ~6% efficiency reported for PSCs utilizing oxides of Ni, Cu, Co, and V as HTLs to form an HTL/perovskite heterojunction has recently been boosted to ~23% (Fig. 32) with their advancement in terms of doping, co-doping, composite formation, decoration, *etc.* A brief summary of the inorganic HTLs processed with various synthesis methods and their corresponding device performance parameters are provided in Table 2. Therefore, the future development of novel HTLs should be explored, focusing on enhanced PCE and sustainable and cost-effective device designs. Finally, the easy, quick, low cost and low-temperature processing of each of the layers of PSCs is an extremely important and decisive consideration for the commercialization of this technology. Therefore, alternative methods are desirable to explore for the cost-effective processing of various HTLs in the ambient atmosphere. Besides, a significant variation in the device performance can be observed when the devices are tested for a small area and scaled to large-area devices. The uniform interface over a larger area is a major concern, which affects the performance and stability of the device under testing. In this scenario, there is plenty space for investigation and finding new materials and processing methods for HTLs, to bring the commercialization of this technology one step closer.

6. Summary and outlook

The past few years have witnessed the significant role of the transport layers on the performance of PSCs and a notable upshot among the PSC devices. Some of the important features attracting researchers in this area are the cost-effective synthesis procedures, use of solar energy, engineering compatibility of ETLs and HTLs, altering the carrier mobility, band edge alignment, carrier concentration, conductivity, optical transparency, and other optoelectronic properties of the transport layers, effects of trap states, dopant and defects on the device performance, charge transport and recombination at the ETL/perovskite interface, *etc.* Nevertheless, the most essential is the development of ideal transport layers.

Both organic and inorganic PSCs have shown promise to meet future energy demands. Unlike 3D perovskites predominantly suffering from instability, low-dimensional well-oriented perovskites may exhibit enhanced long-term stability. However, other supporting layers utilized with bulk and low-dimensional perovskites can alter the performance and stability of PSCs. Among the layers, the transport layers play a crucial role in maintaining and efficiently separating the photogenerated charge carriers and further boosting the solar efficiency and long-term stability. Engineering compatible transport layers with the perovskite light absorbers is essential given that the

ETLs and HTLs perform peculiar functionalities depending on the adopted device architecture. Therefore, understanding the intrinsic properties of the transport layers, namely, the electronic band edge alignment, optical transparency, charge conductivity, and charge mobility, is fundamental for developing efficient PSCs. Among the plethora of material systems that can be used as transport layers in PSCs, the ideal transport layers should also be cost-effective with easy processing. Consequently, the research trend reveals that well-organized approaches to develop distinct transport layers will complement the improvement in overall solar cell efficiency, but the search for ideal transport layers is a never-ending process.

In this review, we summarized the evolution of the transport layers analogous to the progress of PSCs based on the observations and discussions in the literature. Although the perovskite light absorbers have shown superior optoelectronic properties, the importance of the transport layers in PSCs was explained parallel to the photoanodes and electrolytes used in DSSCs. Additionally, the transport layers are distinguished based on the filled states as n-type (ETL) and p-type (HTL) to gain deeper insight. In the regular n-i-p device structures, besides the band edge and bandgap alignment with the perovskite light absorbers, the ETLs provide a template for perovskite deposition and blocking UV irradiation, which deteriorate the perovskite light absorber. The compatible electron mobilities of the ETL with perovskite absorbers and conductivity of electrons in ETLs have become the detrimental factor in avoiding charge accumulation and charge recombination at the ETL/perovskite interface. The techniques such as nanostructuring, doping, and faceting used to tackle the charge accumulation and recombination were explained w.r.t. the majorly reported inorganic ETLs. The role of cost-effective synthetic procedures used for developing efficient inorganic ETLs and their feasibility in large-scale production were correlated with the PCEs. Furthermore, different inorganic materials reported as ETLs for PSCs were scrutinized depending on their functionalities, synthetic procedures, and electrical and optical properties. The inorganic ETLs initially delivered an efficiency of 3–9%, but reached the milestone of ~26%. Among the ETLs, employing doped TiO₂ ETLs has shown efficiencies of ~25% and created excitement among researchers. However, their application on plastic substrates is limited by their high processing temperature. Furthermore, the ZnO ETLs contribute to the deprotonation of the perovskite light absorbers. Although SnO₂ ETLs have shown chemical stability and high efficiency with low-temperature processing, understanding their trap states will be beneficial to further tailor the properties towards ideal ETLs. Furthermore, ternary metal oxides need to be engineered as ETLs with better controllability over their optoelectronic properties. The scaffolding technique has been used to prevent shunting paths in PSCs, and thereby increase the V_{OC} . The diverse materials and their composites or combinations that can be used as ETLs in PSCs were discussed. Also, the extensively used organic ETLs in PSCs were compared for a comprehensive understanding. Overall, the ETLs have a direct influence on the efficiency of PSCs.

Conversely, there is an urgent need to replace the expensive hygroscopic organic HTLs employed in high-efficiency PSCs to increase their long-term stability and reduce their cost. Therefore, the importance of the HTL depending on the PSC device architecture was discussed in depth. Analogous to ETLs, HTLs perform similar functionalities w.r.t. the transport of photogenerated holes. Thus, the various techniques such as nanostructuring, doping, and forming composites used in PSCs were summarized. Inorganic HTLs such as NiO have achieved efficiency close to 22% in PSCs due to their well-aligned band edges and bandgap with perovskite light absorbers. Similarly, CoO_x as an HTL has shown promise due to its high hole conductivity. The synthetic protocols, nanostructuring, and hole-quenching capabilities of multiple combinations of Cu-based HTLs such as CuO, Cu_2O , CuSCN, and CuI are yet to be explored for a deep understanding. Although there are several reports based on VO_x as an HTL in PSCs, doped and nanostructured VO_x are yet to be explored. Further, the class of materials known as delafossites was briefly presented for their controllability over hole conductivity and ease of processibility. Finally, the most commonly used organic HTLs and their influence on the efficiency and long-term stability of PSCs were compared.

Overall, all the materials reported as transport layers were scrutinized based on their optoelectronic properties, stability, durability, and charge separation at the perovskite interface with the transport layer. Furthermore, in this review, the efficiency of PSCs was comparatively evaluated based on only their transport layers. The ETLs and corresponding HTLs play a significant role in the overall performance of PSCs and *vice versa*. However, to gain better efficiency, the quality of the perovskite light absorber films used and the active device area should be considered during further studies. The systematic investigation of different transport layers and involved material systems interpret that an ideal ETL in the n-i-p device structure should have a band-edged and bandgap alignment with the perovskite light absorbers, should possess compatible electron mobilities and conductivities with the perovskite light absorbers, and should be easily processible at low temperatures with no toxicity at a low-cost. Moreover, the increased effective interface at nanostructured ETL/perovskite (mesoporous structure) can relatively enhance the free-electron transport. Further, the synthesized films should have no pinholes and be easily scaled up with high reproducibility. Conversely, ideal HTLs should perform similar functions as ETLs for hole transport depending on the device architecture.

The outlook for ideal transport layers is presented here.

(a) Tailoring the carrier mobility, band edge levels, and diffusion lengths is a promising approach to achieve ideal ETLs/HTLs.

(b) The physical vapor deposition techniques such as ALD, sputtering, and PLD are feasible for the industrial production of the transport layers. However, one should look for industrially scalable low-temperature processing techniques for the easy and reasonable deposition of ETL/HTL encompassing non-toxic and naturally abundant materials in the ambient

atmosphere. Novel low-temperature processing or synthesis can bring out uniform coating, leading to firm interfaces between different materials, which is necessary to avoid unfavourable effects at interfaces, defect state, and interfacial losses such as light soaking effect and charge recombination.

(c) Precise engineering of the transport layer with minimum lattice mismatch, better chemical stability, excellent light management, and non-hygroscopic nature is mandatory to reduce defects and alterations in the intrinsic property of the perovskite active layer.

(d) The quest should be continued to explore new inorganic transport layers with higher p- and n-type conductivity and compatibility with the perovskite solution process deposition method. Moreover, the decoration, doping, faceting, and composites of promising materials identified as ETL/HTL will assist in electron/hole mobility matching, enhancing the light absorption, and improving the recombination resistance, and therefore, enhance the charge extraction. Hence, various combinations of 3d transition metals, graphene, noble metal nanoparticles, organic molecules, *etc.* should be explored in line with further advancement.

(e) Numerical simulation and first-principles calculations can help to understand the density of states, charge accumulation, flow of charge carriers, defect density, optical transparency, optimized thickness, band edge, and photo/thermal stability of the transport layers, which will open up a new window for efficient charge separation, overcoming the issues of photo-reactivity and interface defects, and improving the sensitivity in the visible spectrum. The additional direction of theoretical work should focus on the intrinsic modification and electronic alterations at the transport layer-perovskite interface where experiments are complicated and require simulation-assisted experiments. Furthermore, theoretical methods such as first-principles calculations, DFT, and *ab initio* calculations are necessary to give directions towards less known families of materials that can be applied as transport layers of PSCs.

(f) The industrial focus is on the preparation of planar ETLs and HTLs using physical/chemical vapor deposition methods due to ease of reproducibility and commercial viabilities. However, mesoporous 3D nanostructures provide a larger surface area and better interface with the perovskite absorber layer, have secured a place in the best efficiency chart, and need to be explored for their utilization in the cost-effective mass production of PSCs.

(g) Among the explored nanostructures such as 0D, 1D, and 2D, 1D ETLs and HTLs provide a larger aspect ratio and deliver excellent light trapping deep inside the perovskite absorber and ensure relatively enhanced charge conduction, and hence enhanced efficiency. However, the large-area production of well-defined 1D nanostructures and their better interface with the perovskite absorber needs to be explored for pilot production.

Overall, the paths for the finest optimization of the device structure and successful commercialization of PSCs entail the complete understanding of the transport layers and the charge extraction mechanism.

Author contributions

All authors contributed to conceptualization and writing of this review article.

Conflicts of interest

There are no conflicts to declare.

Acknowledgements

SBO acknowledges funding support under the UK-India SUN-RISE project. RSD and PAS would like to thank the UGC-DAE CSR, Indore, and SERB-DST, India, for their financial support of this work under grant No. CRS/2021-22/01/428 and TAR/2019/000106, respectively. V. M. and S. B. acknowledges the Institute Fellowship from IIT Indore for doctoral research work.

References

- 1 N. Kannan and D. Vakeesan, *Renewable Sustainable Energy Rev.*, 2016, **62**, 1092–1105.
- 2 E. Kabir, P. Kumar, S. Kumar, A. A. Adelodun and K.-H. Kim, *Renewable Sustainable Energy Rev.*, 2018, **82**, 894–900.
- 3 J. Zheng, C. F. J. Lau, H. Mehrvarz, F.-J. Ma, Y. Jiang, X. Deng, A. Soeriyadi, J. Kim, M. Zhang, L. Hu, X. Cui, D. S. Lee, J. Bing, Y. Cho, C. Chen, M. A. Green, S. Huang and A. W. Y. Ho-Baillie, *Energy Environ. Sci.*, 2018, **11**, 2432–2443.
- 4 C. Battaglia, A. Cuevas and S. De Wolf, *Energy Environ. Sci.*, 2016, **9**, 1552–1576.
- 5 M. A. Green, *Joule*, 2019, **3**, 631–633.
- 6 S. S. Mali, B. M. Patil, C. A. Betty, P. N. Bhosale, Y. W. Oh, S. R. Jadhkar, R. S. Devan, Y. R. Ma and P. S. Patil, *Electrochim. Acta*, 2012, **66**, 216–221.
- 7 S. R. Rondiya, Y. A. Jadhav, A. Zivkovic, S. B. Jathar, G. K. Rahane, R. W. Cross, A. V. Rokade, R. S. Devan, S. Kolekar, R. L. Z. Hoye, H. N. Ghosh, N. H. de Leeuw, S. R. Jadhkar and N. Y. Dzade, *J. Alloys Compd.*, 2022, **890**, 161575.
- 8 T. S. Bhat, A. V. Shinde, R. S. Devan, A. M. Teli, Y. R. Ma, J. H. Kim and P. S. Patil, *Appl. Phys. A: Mater. Sci. Process.*, 2018, **124**, 34.
- 9 S. B. Pawar, J. S. Shaikh, R. S. Devan, Y. R. Ma, D. Haranath, P. N. Bhosale and P. S. Patil, *Appl. Surf. Sci.*, 2011, **258**, 1869–1875.
- 10 S. A. Pawar, R. S. Devan, D. S. Patil, A. V. Moholkar, M. G. Gang, Y. R. Ma, J. H. Kim and P. S. Patil, *Electrochim. Acta*, 2013, **98**, 244–254.
- 11 S. A. Pawar, D. S. Patil, S. K. Patil, D. V. Awale, R. S. Devan, Y. R. Ma, S. S. Kolekar, J. H. Kim and P. S. Patil, *Electrochim. Acta*, 2014, **148**, 310–316.
- 12 D. M. Bagnall and M. Boreland, *Energy Policy*, 2008, **36**, 4390–4396.
- 13 H. W. Hillhouse and M. C. Beard, *Curr. Opin. Colloid Interface Sci.*, 2009, **14**, 245–259.
- 14 F. C. Krebs, *Sol. Energy Mater. Sol. Cells*, 2009, **93**, 394–412.
- 15 S. Shalini, R. Balasundara Prabhu, S. Prasanna, T. K. Mallick and S. Senthilarasu, *Renewable Sustainable Energy Rev.*, 2015, **51**, 1306–1325.
- 16 J.-P. Correa-Baena, A. Abate, M. Saliba, W. Tress, T. Jesper Jacobsson, M. Grätzel and A. Hagfeldt, *Energy Environ. Sci.*, 2017, **10**, 710–727.
- 17 G. Kim, H. Min, K. S. Lee, D. Y. Lee, S. M. Yoon and S. I. Seok, *Science*, 2020, **370**, 108–112.
- 18 M. A. Green, A. Ho-Baillie and H. J. Snaith, *Nat. Photonics*, 2014, **8**, 506–514.
- 19 H. S. Jung and N. G. Park, *Small*, 2015, **11**, 10–25.
- 20 S. Sun, N. T. P. Hartono, Z. D. Ren, F. Oviedo, A. M. Buscemi, M. Layurova, D. X. Chen, T. Ogunfunmi, J. Thapa, S. Ramasamy, C. Settens, B. L. DeCost, A. G. Kusne, Z. Liu, S. I. P. Tian, I. M. Peters, J.-P. Correa-Baena and T. Buonassisi, *Joule*, 2019, **3**, 1437–1451.
- 21 Y. Bai, X. Meng and S. Yang, *Adv. Energy Mater.*, 2018, **8**, 1701883.
- 22 J. Sun, D. K. Zhong and D. R. Gamelin, *Energy Environ. Sci.*, 2010, **3**, 1252–1261.
- 23 S. S. Mali and C. K. Hong, *Nanoscale*, 2016, **8**, 10528–10540.
- 24 A. R. Pascoe, M. J. Yang, N. Kopidakis, K. Zhu, M. O. Reese, G. Rumbles, M. Fekete, N. W. Duffy and Y. B. Cheng, *Nano Energy*, 2016, **22**, 439–452.
- 25 T. Leijtens, G. E. Eperon, S. Pathak, A. Abate, M. M. Lee and H. J. Snaith, *Nat. Commun.*, 2013, **4**, 2885.
- 26 J. Kim, K. S. Kim and C. W. Myung, *npj Comput. Mater.*, 2020, **6**, 100.
- 27 Q. Hu, J. Wu, C. Jiang, T. H. Liu, X. L. Que, R. Zhu and Q. H. Gong, *ACS Nano*, 2014, **8**, 10161–10167.
- 28 A. Yella, L. P. Heiniger, P. Gao, M. K. Nazeeruddin and M. Gratzel, *Nano Lett.*, 2014, **14**, 2591–2596.
- 29 J. T. W. Wang, J. M. Ball, E. M. Barea, A. Abate, J. A. Alexander-Webber, J. Huang, M. Saliba, I. Mora-Sero, J. Bisquert, H. J. Snaith and R. J. Nicholas, *Nano Lett.*, 2014, **14**, 724–730.
- 30 V. Karthikeyan, S. Maniarasu, V. Manjunath, E. Ramasamy and G. Veerappan, *Sol. Energy*, 2017, **147**, 202–208.
- 31 W. Zhang, M. Saliba, S. D. Stranks, Y. Sun, X. Shi, U. Wiesner and H. J. Snaith, *Nano Lett.*, 2013, **13**, 4505–4510.
- 32 A. Fakharuddin, L. Schmidt-Mende, G. Garcia-Belmonte, R. Jose and I. Mora-Sero, *Adv. Energy Mater.*, 2017, **7**, 1700623.
- 33 K.-C. Wang, J.-Y. Jeng, P.-S. Shen, Y.-C. Chang, E. W.-G. Diau, C.-H. Tsai, T.-Y. Chao, H.-C. Hsu, P.-Y. Lin, P. Chen, T.-F. Guo and T.-C. Wen, *Sci. Rep.*, 2014, **4**, 4756.
- 34 V. Manjunath, P. K. Mishra, R. Dobhal, S. Bimli, P. M. Shirage, S. Sen, P. A. Shaikh and R. S. Devan, *ACS Appl. Electron. Mater.*, 2021, **3**, 4548–4557.
- 35 B. Chen, M. Yang, S. Priya and K. Zhu, *J. Phys. Chem. Lett.*, 2016, **7**, 905–917.
- 36 C. Eames, J. M. Frost, P. R. F. Barnes, B. C. O'Regan, A. Walsh and M. S. Islam, *Nat. Commun.*, 2015, **6**, 7497.
- 37 Z. Zhou, S. Pang, Z. Liu, H. Xu and G. Cui, *J. Mater. Chem. A*, 2015, **3**, 19205–19217.

- 38 V. M. Le Corre, M. Stolterfoht, L. Perdígón Toro, M. Feuerstein, C. Wolff, L. Gil-Escrig, H. J. Bolink, D. Neher and L. J. A. Koster, *ACS Appl. Energy Mater.*, 2019, **2**, 6280–6287.
- 39 G.-S. Chen, Y.-C. Chen, C.-T. Lee and H.-Y. Lee, *Sol. Energy*, 2018, **174**, 897–900.
- 40 J. Byeon, J. Kim, J.-Y. Kim, G. Lee, K. Bang, N. Ahn and M. Choi, *ACS Energy Lett.*, 2020, **5**, 2580–2589.
- 41 W. J. Nimens, J. Ogle, A. Caruso, M. Jonely, C. Simon, D. Smilgies, R. Noriega, M. Scarpulla and L. Whittaker-Brooks, *ACS Appl. Energy Mater.*, 2018, **1**, 602–615.
- 42 J. Shi, X. Xu, D. Li and Q. Meng, *Small*, 2015, **11**, 2472–2486.
- 43 J. Shi, Y. Li, Y. Li, D. Li, Y. Luo, H. Wu and Q. Meng, *Joule*, 2018, **2**, 879–901.
- 44 Z. Yang, B. H. Babu, S. Wu, T. Liu, S. Fang, Z. Xiong, L. Han and W. Chen, *Solar RRL*, 2020, **4**, 1900257.
- 45 H.-S. Kim, J. S. Park, H.-K. Jeong, K. S. Son, T. S. Kim, J.-B. Seon, E. Lee, J. G. Chung, D. H. Kim, M. Ryu and S. Y. Lee, *ACS Appl. Mater. Interfaces*, 2012, **4**, 5416–5421.
- 46 N. K. Elumalai and A. Uddin, *Energy Environ. Sci.*, 2016, **9**, 391–410.
- 47 M. F. N. Taufique, R. Khanal, S. Choudhury and S. Banerjee, *J. Chem. Phys.*, 2018, **149**, 164704.
- 48 M. H. Gharahcheshmeh and K. K. Gleason, *Mater. Today Adv.*, 2020, **8**, 100086.
- 49 G. Horowitz, *J. Appl. Phys.*, 2015, **118**, 115502.
- 50 S. Jung, C.-H. Kim, Y. Bonnassieux and G. Horowitz, *J. Phys. D: Appl. Phys.*, 2015, **48**, 395103.
- 51 H. F. Haneef, A. M. Zeidell and O. D. Jurchescu, *J. Mater. Chem. C*, 2020, **8**, 759–787.
- 52 J.-P. Yang, L.-T. Shang, F. Bussolotti, L.-W. Cheng, W.-Q. Wang, X.-H. Zeng, S. Kera, Y.-Q. Li, J.-X. Tang and N. Ueno, *Org. Electron.*, 2017, **48**, 172–178.
- 53 A. D. Scaccabarozzi, A. Basu, F. Aniés, J. Liu, O. Zapata-Arteaga, R. Warren, Y. Firdaus, M. I. Nugraha, Y. Lin, M. Campoy-Quiles, N. Koch, C. Müller, L. Tsetseris, M. Heeney and T. D. Anthopoulos, *Chem. Rev.*, 2022, **122**, 4420–4492.
- 54 S. Chatterjee and A. J. Pal, *J. Phys. Chem. C*, 2016, **120**, 1428–1437.
- 55 R. Chakraborty, H. Bhunia, S. Chatterjee and A. J. Pal, *J. Solid State Chem.*, 2020, **281**, 121021.
- 56 S. Teo, Z. Guo, Z. Xu, C. Zhang, Y. Kamata, S. Hayase and T. Ma, *ChemSusChem*, 2019, **12**, 518–526.
- 57 W. Hu, J. An, F. Si, H. Xue, F. Tang and W. Li, *J. Electron. Mater.*, 2021, **50**, 2129–2136.
- 58 V. Zardetto, B. L. Williams, A. Perrotta, F. Di Giacomo, M. A. Verheijen, R. Andriessen, W. M. M. Kessels and M. Creatore, *Sustainable Energy Fuels*, 2017, **1**, 30–55.
- 59 F. Fu, T. Feurer, T. P. Weiss, S. Pisoni, E. Avancini, C. Andres, S. Buecheler and A. N. Tiwari, *Nat. Energy*, 2016, **2**, 16190.
- 60 P. Qin, M. Paulose, M. I. Dar, T. Moehl, N. Arora, P. Gao, O. K. Varghese, M. Gatzel and M. K. Nazeeruddin, *Small*, 2015, **11**, 5533–5539.
- 61 M. Park, J.-Y. Kim, H. J. Son, C.-H. Lee, S. S. Jang and M. J. Ko, *Nano Energy*, 2016, **26**, 208–215.
- 62 J. Cao, B. Wu, R. Chen, Y. Wu, Y. Hui, B.-W. Mao and N. Zheng, *Adv. Mater.*, 2018, **30**, 1705596.
- 63 K. Jung, J. Lee, C. Im, J. Do, J. Kim, W.-S. Chae and M.-J. Lee, *ACS Energy Lett.*, 2018, **3**, 2410–2417.
- 64 C. Chen, Y. Jiang, Y. Wu, J. Guo, X. Kong, X. Wu, Y. Li, D. Zheng, S. Wu, X. Gao, Z. Hou, G. Zhou, Y. Chen, J.-M. Liu, K. Kempa and J. Gao, *Solar RRL*, 2020, **4**, 1900499.
- 65 R. S. Devan, R. A. Patil, J.-H. Lin and Y.-R. Ma, *Adv. Funct. Mater.*, 2012, **22**, 3326–3370.
- 66 S. S. Mali, C. A. Betty, P. N. Bhosale, R. S. Devan, Y. R. Ma, S. S. Kolekar and P. S. Patil, *CrystEngComm*, 2012, **14**, 1920–1924.
- 67 S. S. Mali, S. K. Desai, S. S. Kalagi, C. A. Betty, P. N. Bhosale, R. S. Devan, Y.-R. R. Ma and P. S. Patil, *Dalton Trans.*, 2012, **41**, 6130–6136.
- 68 R. S. Devan, Y.-R. Ma, R. A. Patil and S.-M. Lukas, *RSC Adv.*, 2016, **6**, 62218–62225.
- 69 P. N. Didwal, P. R. Chikate, P. K. Bankar, M. A. More and R. S. Devan, *J. Mater. Sci.: Mater. Electron.*, 2019, **30**, 2935–2941.
- 70 N. Kitchamsetti, R. S. Kalubarme, P. R. Chikate, C. J. Park, Y. R. Ma, P. M. Shirage and R. S. Devan, *ChemistrySelect*, 2019, **4**, 6620–6626.
- 71 P. N. Didwal, K. S. Pawar, P. R. Chikate, A. C. Abhyankar, H. M. Pathan and R. S. Devan, *J. Mater. Sci.: Mater. Electron.*, 2016, **27**, 12446–12451.
- 72 S. A. Pawar, R. S. Devan, D. S. Patil, V. V. Burungale, T. S. Bhat, S. S. Mali, S. W. Shin, J. E. Ae, C. K. Hong, Y. R. Ma, J. H. Kim and P. S. Patil, *Electrochim. Acta*, 2014, **117**, 470–479.
- 73 R. S. Devan, Y.-R. Ma, M. A. More, R. T. Khare, V. V. Antad, R. A. Patil, V. P. Thakare, R. S. Dhayal and L. Schmidt-Mende, *RSC Adv.*, 2016, **6**, 98722–98729.
- 74 R. A. Patil, R. S. Devan, Y. Liou and Y.-R. Ma, *Sol. Energy Mater. Sol. Cells*, 2016, **147**, 240–245.
- 75 R. S. Devan, V. P. Thakare, V. V. Antad, P. R. Chikate, R. T. Khare, M. A. More, R. S. Dhayal, S. I. Patil, Y.-R. Ma and L. Schmidt-Mende, *ACS Omega*, 2017, **2**, 2925–2934.
- 76 N. G. Park, J. van de Lagemaat and A. J. Frank, *J. Phys. Chem. B*, 2000, **104**, 8989–8994.
- 77 S. S. Mali, R. S. Devan, Y. R. Ma, C. A. Betty, P. N. Bhosale, R. P. Panmand, B. B. Kale, S. R. Jadkar, P. S. Patil, J. H. Kim and C. K. Hong, *Electrochim. Acta*, 2013, **90**, 666–672.
- 78 S. A. Pawar, D. S. Patil, U. T. Pawar, R. S. Devan, M. M. Karanjkar, Y. R. Ma, S. W. Shin, J. H. Kim and P. S. Patil, *J. Mater. Sci.: Mater. Electron.*, 2015, **26**, 2595–2604.
- 79 A. Kojima, K. Teshima, Y. Shirai and T. Miyasaka, *J. Am. Chem. Soc.*, 2009, **131**, 6050–6051.
- 80 N. Jain, A. Mary, V. Manjunath, R. Sakla, R. S. Devan, D. A. Jose and A. R. Naziruddin, *Eur. J. Inorg. Chem.*, 2021, 5014–5023.
- 81 H. S. Kim, C. R. Lee, J. H. Im, K. B. Lee, T. Moehl, A. Marchioro, S. J. Moon, R. Humphry-Baker, J. H. Yum,

- J. E. Moser, M. Gratzel and N. G. Park, *Sci. Rep.*, 2012, **2**, 591.
- 82 G. K. Pinheiro, R. B. Serpa, L. V. de Souza, M. L. Sartorelli, F. T. Reis and C. R. Rambo, *Colloids Surf., A*, 2017, **527**, 89–94.
- 83 L. Qiu, Z. Zhuang, S. Yang, W. Chen, L. Song, M. Ding, G. Xia, P. Du and J. Xiong, *Mater. Res. Bull.*, 2018, **106**, 439–445.
- 84 W. J. Ke, G. J. Fang, J. Wang, P. L. Qin, H. Tao, H. W. Lei, Q. Liu, X. Dai and X. Z. Zhao, *ACS Appl. Mater. Interfaces*, 2014, **6**, 15959–15965.
- 85 A. E. Shalan, S. Narra, T. Oshikiri, K. Ueno, X. Shi, H. P. Wu, M. M. Elshaniwany, E. W. G. Diao and H. Misawa, *Sustainable Energy Fuels*, 2017, **1**, 1533–1540.
- 86 J.-F. Li, Z.-L. Zhang, H.-P. Gao, Y. Zhang and Y.-L. Mao, *J. Mater. Chem. A*, 2015, **3**, 19476–19482.
- 87 T. S. Bhat, R. S. Devan, S. S. Mali, A. S. Kamble, S. A. Pawar, I. Y. Kim, Y. R. Ma, C. K. Hong, J. H. Kim and P. S. Patil, *J. Mater. Sci.: Mater. Electron.*, 2014, **25**, 4501–4511.
- 88 H.-C. Hsieh, J. Yu, S.-P. Rwei, K.-F. Lin, Y.-C. Shih and L. Wang, *Thin Solid Films*, 2018, **659**, 41–47.
- 89 S. H. Lin, Y. H. Su, H. W. Cho, P. Y. Kung, W. P. Liao and J. J. Wu, *J. Mater. Chem. A*, 2016, **4**, 1119–1125.
- 90 S. S. Mali, C. S. Shim, H. K. Park, J. Heo, P. S. Patil and C. K. Hong, *Chem. Mater.*, 2015, **27**, 1541–1551.
- 91 I. S. Kim, R. T. Haasch, D. H. Cao, O. K. Farha, J. T. Hupp, M. G. Kanatzidis and A. B. F. Martinson, *ACS Appl. Mater. Interfaces*, 2016, **8**, 24310–24314.
- 92 L. Cojocaru, S. Uchida, Y. Sanehira, J. Nakazaki, T. Kubo and H. Segawa, *Chem. Lett.*, 2015, **44**, 674–676.
- 93 Q. Q. Gao, S. W. Yang, L. Lei, S. D. Zhang, Q. P. Cao, J. J. Xie, J. Q. Li and Y. Liu, *Chem. Lett.*, 2015, **44**, 624–626.
- 94 S. Dharani, H. K. Mulmudi, N. Yantara, P. T. T. Trang, N. G. Park, M. Gratzel, S. Mhaisalkar, N. Mathews and P. P. Boix, *Nanoscale*, 2014, **6**, 1675–1679.
- 95 P. Zhou, W. N. Li, T. H. Li, T. L. Bu, X. P. Liu, J. Li, J. He, R. Chen, K. P. Li, J. Zhao and F. Z. Huang, *Micromachines*, 2017, **8**, 55.
- 96 D. Zhong, B. Cai, X. L. Wang, Z. Yang, Y. D. Xing, S. Miao, W. H. Zhang and C. Li, *Nano Energy*, 2015, **11**, 409–418.
- 97 Y. Xiao, C. Wang, K. K. Kondamareddy, N. Cheng, P. Liu, Y. Qiu, F. Qi, S. Kong, W. Liu and X.-Z. Zhao, *ACS Appl. Energy Mater.*, 2018, **1**, 5453–5462.
- 98 H. Lu, B. Gu and S. Fang, *Sustainable Energy Fuels*, 2021, **5**, 880–885.
- 99 M. Thambidurai, H. A. Dewi, P. C. Harikesh, S. Foo, K. M. Muhammed Salim, N. Mathews and C. Dang, *ACS Appl. Energy Mater.*, 2018, **1**, 5847–5852.
- 100 W. Okada, T. Suga, K. Oyaizu, H. Segawa and H. Nishide, *ACS Appl. Energy Mater.*, 2019, **2**, 2848–2853.
- 101 G. Ren, W. Han, Z. Li, C. Liu, L. Shen and W. Guo, *Sol. Energy*, 2019, **193**, 220–226.
- 102 K. Wang, Z. Zhang, L. Wang, K. Chen, L. Tao, Y. Zhang and X. Zhou, *ACS Appl. Energy Mater.*, 2021, **4**, 3255–3264.
- 103 B. Wang, M. Zhang, X. Cui, Z. Wang, M. Rager, Y. Yang, Z. Zou, Z. L. Wang and Z. Lin, *Angew. Chem., Int. Ed.*, 2020, **59**, 1611–1618.
- 104 B. Wang, J. Yang, L. Lu, W. Xiao, H. Wu, S. Xiong, J. Tang, C. Duan and Q. Bao, *Adv. Mater. Interfaces*, 2020, **7**, 1901964.
- 105 M. Batmunkh, T. J. Macdonald, C. J. Shearer, M. Bat-Erdene, Y. Wang, M. J. Biggs, I. P. Parkin, T. Nann and J. G. Shapter, *Adv. Sci.*, 2017, **4**, 1600504.
- 106 C. Huang, C. Liu, Y. Di, W. Li, F. Liu, L. Jiang, J. Li, X. Hao and H. Huang, *ACS Appl. Mater. Interfaces*, 2016, **8**, 8520–8526.
- 107 A. Apostolopoulou, D. Sygkridou, A. Rapsomanikis, A. N. Kalarakis and E. Stathatos, *Sol. Energy Mater. Sol. Cells*, 2017, **166**, 100–107.
- 108 X. Deng, Y. Wang, Y. Chen, Z. Cui and C. Shi, *J. Solid State Chem.*, 2019, **275**, 206–209.
- 109 M. Thambidurai, F. Shini, J. Y. Kim, C. Lee and C. Dang, *Mater. Lett.*, 2020, **274**, 128003.
- 110 H. Nagaoka, F. Ma, D. W. deQuillettes, S. M. Vorpahl, M. S. Glaz, A. E. Colbert, M. E. Ziffer and D. S. Ginger, *J. Phys. Chem. Lett.*, 2015, **6**, 669–675.
- 111 S. Wang, B. Liu, Y. Zhu, Z. Ma, B. Liu, X. Miao, R. Ma and C. Wang, *Sol. Energy*, 2018, **169**, 335–342.
- 112 Z. L. Zhang, J. F. Li, X. L. Wang, J. Q. Qin, W. J. Shi, Y. F. Liu, H. P. Gao and Y. L. Mao, *RSC Adv.*, 2017, **7**, 13325–13330.
- 113 X. L. Wang, Z. L. Zhang, J. Q. Qin, W. J. Shi, Y. F. Liu, H. P. Gao and Y. L. Mao, *Electrochim. Acta*, 2017, **245**, 839–845.
- 114 X. Yao, J. H. Liang, Y. L. Li, J. S. Luo, B. Shi, C. C. Wei, D. K. Zhang, B. Z. Li, Y. Ding, Y. Zhao and X. D. Zhang, *Adv. Sci.*, 2017, **4**, 1700008.
- 115 Y. M. Li, Y. Guo, Y. H. Li and X. F. Zhou, *Electrochim. Acta*, 2016, **200**, 29–36.
- 116 G. Xiao, C. Shi, K. Lv, C. Ying and Y. Wang, *ACS Appl. Energy Mater.*, 2018, **1**, 2576–2581.
- 117 H. Sun, D. Xie, Z. Song, C. Liang, L. Xu, X. Qu, Y. Yao, D. Li, H. Zhai, K. Zheng, C. Cui and Y. Zhao, *ACS Appl. Mater. Interfaces*, 2020, **12**, 22853–22861.
- 118 M. Kim, I.-W. Choi, S. J. Choi, J. W. Song, S.-I. Mo, J.-H. An, Y. Jo, S. Ahn, S. K. Ahn, G.-H. Kim and D. S. Kim, *Joule*, 2021, **5**, 659–672.
- 119 B. J. Kim, D. H. Kim, Y. Y. Lee, H. W. Shin, G. S. Han, J. S. Hong, K. Mahmood, T. K. Ahn, Y. C. Joo, K. S. Hong, N. G. Park, S. Lee and H. S. Jung, *Energy Environ. Sci.*, 2015, **8**, 916–921.
- 120 W. M. Qiu, U. W. Paetzold, R. Gehlhaar, V. Smirnov, H. G. Boyen, J. G. Tait, B. Conings, W. M. Zhang, C. B. Nielsen, I. McCulloch, L. Froyen, P. Heremans and D. Cheyns, *J. Mater. Chem. A*, 2015, **3**, 22824–22829.
- 121 D. Yang, R. X. Yang, J. Zhang, Z. Yang, S. Z. Liu and C. Li, *Energy Environ. Sci.*, 2015, **8**, 3208–3214.
- 122 Y. H. Chu, H. K. Cai, L. K. Huang, Z. X. Xing, Y. Y. Du, J. Ni, J. Li and J. J. Zhang, *Phys. Status Solidi A*, 2019, **216**, 1800669.
- 123 B. Conings, L. Baeten, T. Jacobs, R. Dera, J. D’Haen, J. Manca and H. G. Boyen, *Appl. Mater.*, 2014, **2**, 081505.
- 124 Q. Jiang, X. Zhang and J. You, *Small*, 2018, **14**, 1801154.

- 125 W. Ke, G. Fang, Q. Liu, L. Xiong, P. Qin, H. Tao, J. Wang, H. Lei, B. Li, J. Wan, G. Yang and Y. Yan, *J. Am. Chem. Soc.*, 2015, **137**, 6730–6733.
- 126 L. Kavan, L. Steier and M. Grätzel, *J. Phys. Chem. C*, 2017, **121**, 342–350.
- 127 E. H. Anaraki, A. Kermanpur, L. Steier, K. Domanski, T. Matsui, W. Tress, M. Saliba, A. Abate, M. Grätzel, A. Hagfeldt and J.-P. Correa-Baena, *Energy Environ. Sci.*, 2016, **9**, 3128–3134.
- 128 J.-Y. Chen, C.-C. Chueh, Z. Zhu, W.-C. Chen and A. K. Y. Jen, *Sol. Energy Mater. Sol. Cells*, 2017, **164**, 47–55.
- 129 Z. Chen, G. Yang, X. Zheng, H. Lei, C. Chen, J. Ma, H. Wang and G. Fang, *J. Power Sources*, 2017, **351**, 123–129.
- 130 J. Ma, X. Zheng, H. Lei, W. Ke, C. Chen, Z. Chen, G. Yang and G. Fang, *Solar RRL*, 2017, **1**, 1700118.
- 131 X. Fan, Y. Rui, X. Han, J. Yang, Y. Wang and Q. Zhang, *J. Power Sources*, 2020, **448**, 227405.
- 132 B. Taheri, E. Calabrò, F. Matteocci, D. Di Girolamo, G. Cardone, A. Liscio, A. Di Carlo and F. Brunetti, *Energy Technol.*, 2020, **8**, 1901284.
- 133 Q. Jiang, Z. Chu, P. Wang, X. Yang, H. Liu, Y. Wang, Z. Yin, J. Wu, X. Zhang and J. You, *Adv. Mater.*, 2017, **29**, 1703852.
- 134 C. M. Gao, S. Yuan, B. Q. Cao and J. H. Yu, *Chem. Eng. J.*, 2017, **325**, 378–385.
- 135 X. Liu, K. W. Tsai, Z. Zhu, Y. Sun, C. C. Chueh and A. K. Y. Jen, *Adv. Mater. Interfaces*, 2016, **3**, 1600122.
- 136 Y. Li, J. Zhu, Y. Huang, F. Liu, M. Lv, S. Chen, L. Hu, J. Tang, J. Yao and S. Dai, *RSC Adv.*, 2015, **5**, 28424–28429.
- 137 J. Xie, K. Huang, X. Yu, Z. Yang, K. Xiao, Y. Qiang, X. Zhu, L. Xu, P. Wang, C. Cui and D. Yang, *ACS Nano*, 2017, **11**, 9176–9182.
- 138 H. Tang, Q. Cao, Z. He, S. Wang, J. Han, T. Li, B. Gao, J. Yang, D. Deng and X. Li, *Solar RRL*, 2020, **4**, 1900415.
- 139 J. J. Yoo, G. Seo, M. R. Chua, T. G. Park, Y. Lu, F. Rotermund, Y.-K. Kim, C. S. Moon, N. J. Jeon, J.-P. Correa-Baena, V. Bulović, S. S. Shin, M. G. Bawendi and J. Seo, *Nature*, 2021, **590**, 587–593.
- 140 R. Ramarajan, M. Kovendhan, K. Thangaraju, D. P. Joseph and R. R. Babu, *Appl. Surf. Sci.*, 2019, **487**, 1385–1393.
- 141 J. Bahadur, A. H. Ghahremani, B. Martin, T. Druffel, M. K. Sunkara and K. Pal, *Org. Electron.*, 2019, **67**, 159–167.
- 142 L. Xiong, M. Qin, G. Yang, Y. Guo, H. Lei, Q. Liu, W. Ke, H. Tao, P. Qin, S. Li, H. Yu and G. Fang, *J. Mater. Chem. A*, 2016, **4**, 8374–8383.
- 143 J. Liang, Z. Chen, G. Yang, H. Wang, F. Ye, C. Tao and G. Fang, *ACS Appl. Mater. Interfaces*, 2019, **11**, 23152–23159.
- 144 Y. Chen, X. Zuo, Y. He, F. Qian, S. Zuo, Y. Zhang, L. Liang, Z. Chen, K. Zhao, Z. Liu, J. Gou and S. Liu, *Adv. Sci.*, 2021, **8**, 2001466.
- 145 S. Zhang, H. Gu, S.-C. Chen and Q. Zheng, *J. Mater. Chem. C*, 2021, **9**, 4240–4247.
- 146 J.-J. Cao, K.-L. Wang, C. Dong, X.-M. Li, W.-F. Yang and Z.-K. Wang, *Org. Electron.*, 2021, **88**, 105972.
- 147 J. Tian, J. Zhang, X. Li, B. Cheng, J. Yu and W. Ho, *Solar RRL*, 2020, **4**, 2000090.
- 148 J. Ye, Y. Li, A. A. Medjahed, S. Pouget, D. Aldakov, Y. Liu and P. Reiss, *Small*, 2021, **17**, 2005671.
- 149 G. Yang, H. Lei, H. Tao, X. Zheng, J. Ma, Q. Liu, W. Ke, Z. Chen, L. Xiong, P. Qin, Z. Chen, M. Qin, X. Lu, Y. Yan and G. Fang, *Small*, 2017, **13**, 1601769.
- 150 E. Halvani Anaraki, A. Kermanpur, M. T. Mayer, L. Steier, T. Ahmed, S.-H. Turren-Cruz, J. Seo, J. Luo, S. M. Zakeeruddin, W. R. Tress, T. Edvinsson, M. Grätzel, A. Hagfeldt and J.-P. Correa-Baena, *ACS Energy Lett.*, 2018, **3**, 773–778.
- 151 W. Gong, H. Guo, H. Zhang, J. Yang, H. Chen, L. Wang, F. Hao and X. Niu, *J. Mater. Chem. C*, 2020, **8**, 11638–11646.
- 152 J. A. Hong, E. D. Jung, J. C. Yu, D. W. Kim, Y. S. Nam, I. Oh, E. Lee, J.-W. Yoo, S. Cho and M. H. Song, *ACS Appl. Mater. Interfaces*, 2020, **12**, 2417–2423.
- 153 Z. Lv, L. He, H. Jiang, X. Ma, F. Wang, L. Fan, M. Wei, J. Yang, L. Yang and N. Yang, *ACS Appl. Mater. Interfaces*, 2021, **13**, 16326–16335.
- 154 H. Xia, X. Li, J. Zhou, B. Wang, Y. Chu, Y. Li, G. Wu, D. Zhang, B. Xue, X. Zhang, Y. Hu, H. Zhou and Y. Zhang, *ACS Appl. Energy Mater.*, 2020, **3**, 3186–3192.
- 155 B. Gao, Q. Cao, X. Pu, J. Yang, J. Han, S. Wang, T. Li, Z. He and X. Li, *Appl. Surf. Sci.*, 2021, **546**, 148711.
- 156 B. Tu, Y. Shao, W. Chen, Y. Wu, X. Li, Y. He, J. Li, F. Liu, Z. Zhang, Y. Lin, X. Lan, L. Xu, X. Shi, A. M. C. Ng, H. Li, L. W. Chung, A. B. Djurišić and Z. He, *Adv. Mater.*, 2019, **31**, 1805944.
- 157 S. Zhang, H. Si, W. Fan, M. Shi, M. Li, C. Xu, Z. Zhang, Q. Liao, A. Sattar, Z. Kang and Y. Zhang, *Angew. Chem., Int. Ed.*, 2020, **59**, 11573–11582.
- 158 Y. Yang, H. Lu, S. Feng, L. Yang, H. Dong, J. Wang, C. Tian, L. Li, H. Lu, J. Jeong, S. M. Zakeeruddin, Y. Liu, M. Grätzel and A. Hagfeldt, *Energy Environ. Sci.*, 2021, **14**, 3447–3454.
- 159 J. Luo, Y. Wang and Q. Zhang, *Sol. Energy*, 2018, **163**, 289–306.
- 160 P. R. Chikate, P. K. Bankar, R. J. Choudhary, Y. R. Ma, S. I. Patil, M. A. More, D. M. Phase, P. M. Shirage and R. S. Devan, *RSC Adv.*, 2018, **8**, 21664–21670.
- 161 P. R. Chikate, K. D. Daware, D. S. Gayhane, Y. R. Ma, R. J. Choudhary, S. I. Patil, M. A. More, D. M. Phase, S. W. Gosavi, P. M. Shirage and R. S. Devan, *ChemistrySelect*, 2018, **3**, 7891–7899.
- 162 P. R. Chikate, A. Sharma, S. R. Rondiya, R. W. Cross, N. Y. Dzade, P. M. Shirage and R. S. Devan, *New J. Chem.*, 2021, **45**, 1404–1414.
- 163 J. H. Lin, R. A. Patil, R. S. Devan, Z. A. Liu, Y. P. Wang, C. H. Ho, Y. Liou and Y. R. Ma, *Sci. Rep.*, 2014, **4**, 6967.
- 164 N. L. Tarwal, A. V. Rajgure, A. I. Inamdar, R. S. Devan, I. Y. Kim, S. S. Suryavanshi, Y. R. Ma, J. H. Kim and P. S. Patil, *Sens. Actuators, A*, 2013, **199**, 67–73.
- 165 P. R. Chikate, K. D. Daware, S. S. Patil, P. N. Didwal, G. S. Lole, R. J. Choudhary, S. W. Gosavi and R. S. Devan, *New J. Chem.*, 2020, **44**, 5535–5544.
- 166 N. L. Tarwal, R. S. Devan, Y. R. Ma, R. S. Patil, M. M. Karanjkar and P. S. Patil, *Electrochim. Acta*, 2012, **72**, 32–39.
- 167 D. Y. Son, J. H. Im, H. S. Kim and N. G. Park, *J. Phys. Chem. C*, 2014, **118**, 16567–16573.

- 168 P. Wang, J. Zhao, J. Liu, L. Wei, Z. Liu, L. Guan and G. Cao, *J. Power Sources*, 2017, **339**, 51–60.
- 169 Z.-L. Tseng, C.-H. Chiang and C.-G. Wu, *Sci. Rep.*, 2015, **5**, 13211.
- 170 K.-M. Lee, S. H. Chang, K.-H. Wang, C.-M. Chang, H.-M. Cheng, C.-C. Kei, Z.-L. Tseng and C.-G. Wu, *Sol. Energy*, 2015, **120**, 117–122.
- 171 K. Mahmood, B. S. Swain and H. S. Jung, *Nanoscale*, 2014, **6**, 9127–9138.
- 172 J. Yang, B. D. Siempelkamp, E. Mosconi, F. De Angelis and T. L. Kelly, *Chem. Mater.*, 2015, **27**, 4229–4236.
- 173 X. Dong, H. Hu, B. Lin, J. Ding and N. Yuan, *Chem. Commun.*, 2014, **50**, 14405–14408.
- 174 J. Dong, J. Shi, D. Li, Y. Luo and Q. Meng, *Appl. Phys. Lett.*, 2015, **107**, 073507.
- 175 J. Song, E. Zheng, L. Liu, X.-F. Wang, G. Chen, W. Tian and T. Miyasaka, *ChemSusChem*, 2016, **9**, 2640–2647.
- 176 L. X. Zhenyun Zhang and J. Qi, *Chin. Phys. B*, 2021, **30**, 038801.
- 177 Z.-L. Tseng, C.-H. Chiang, S.-H. Chang and C.-G. Wu, *Nano Energy*, 2016, **28**, 311–318.
- 178 J. Dong, Y. Zhao, J. Shi, H. Wei, J. Xiao, X. Xu, J. Luo, J. Xu, D. Li, Y. Luo and Q. Meng, *Chem. Commun.*, 2014, **50**, 13381–13384.
- 179 X. Zhao, H. Shen, Y. Zhang, X. Li, X. Zhao, M. Tai, J. Li, J. Li, X. Li and H. Lin, *ACS Appl. Mater. Interfaces*, 2016, **8**, 7826–7833.
- 180 Y.-Z. Zheng, E.-F. Zhao, F.-L. Meng, X.-S. Lai, X.-M. Dong, J.-J. Wu and X. Tao, *J. Mater. Chem. A*, 2017, **5**, 12416–12425.
- 181 T. Y. Su, Y. H. Zheng, Z. W. Ma, L. Cheng, X. L. Xu, F. P. Zhang, G. Yu and Z. G. Sheng, *Chemistryselect*, 2018, **3**, 363–367.
- 182 C. Liu, W. Wu, D. Zhang, Z. Li, G. Ren, W. Han and W. Guo, *J. Mater. Chem. A*, 2021, **9**, 12161–12168.
- 183 M. K. A. Mohammed and M. Shekargoftar, *Sustainable Energy Fuels*, 2021, **5**, 540–548.
- 184 Z. Wang, X. Zhu, J. Feng, C. Wang, C. Zhang, X. Ren, S. Priya, S. Liu and D. Yang, *Adv. Sci.*, 2021, **8**, 2002860.
- 185 Q. Z. An, P. Fassl, Y. J. Hofstetter, D. Becker-Koch, A. Bausch, P. E. Hopkinson and Y. Vaynzof, *Nano Energy*, 2017, **39**, 400–408.
- 186 P. Chen, X. Yin, M. Que, Y. Yang and W. Que, *RSC Adv.*, 2016, **6**, 57996–58002.
- 187 P. Zhang, F. Yang, G. Kapil, Q. Shen, T. Toyoda, K. Yoshino, T. Minemoto, S. S. Pandey, T. Ma and S. Hayase, *Org. Electron.*, 2018, **62**, 615–620.
- 188 M. Tai, X. Zhao, H. Shen, Y. Guo, M. Zhang, Y. Zhou, X. Li, Z. Yao, X. Yin, J. Han, X. Li and H. Lin, *Chem. Eng. J.*, 2019, **361**, 60–66.
- 189 X. Yin, W. Que, D. Fei, H. Xie and Z. He, *Electrochim. Acta*, 2013, **99**, 204–210.
- 190 V. Manjunath, Y. K. Reddy, S. Bimli, R. J. Choudhary and R. S. Devan, *Mater. Today Commun.*, 2022, **32**, 104061.
- 191 N. Kitchamsetti, M. Samtham, P. N. Didwal, D. Kumar, D. Singh, S. Bimli, P. R. Chikate, D. A. Basha, S. Kumar, C. J. Park, S. Chakraborty and R. S. Devan, *J. Power Sources*, 2022, **538**, 231525.
- 192 N. Kitchamsetti, Y. R. Ma, P. M. Shirage and R. S. Devan, *J. Alloys Compd.*, 2020, **833**, 155134.
- 193 N. Kitchamsetti, P. N. Didwal, S. R. Mulani, M. S. Patil and R. S. Devan, *Heliyon*, 2021, **7**, e07297.
- 194 N. Kitchamsetti, R. J. Choudhary, D. M. Phase and R. S. Devan, *RSC Adv.*, 2020, **10**, 23446–23456.
- 195 M. S. Patil, N. Kitchamsetti, S. R. Mulani, S. R. Rondiya, N. G. Deshpande, R. A. Patil, R. W. Cross, N. Y. Dzade, K. K. Sharma, P. S. Patil, Y. R. Ma, H. K. Cho and R. S. Devan, *J. Taiwan Inst. Chem. Eng.*, 2021, **122**, 201–209.
- 196 L. Z. Zhu, Z. P. Shao, J. J. Ye, X. H. Zhang, X. Pan and S. Y. Dai, *Chem. Commun.*, 2016, **52**, 970–973.
- 197 C. Y. Sun, L. Guan, Y. P. Guo, B. J. Fang, J. M. Yang, H. A. Duan, Y. J. Chen, H. Li and H. Z. Liu, *J. Alloys Compd.*, 2017, **722**, 196–206.
- 198 A. Roy, P. Selvaraj, P. Sujatha Devi and S. Sundaram, *Mater. Lett.*, 2018, **219**, 166–169.
- 199 Y. Guo, Y. Xue, C. Geng, C. Li, X. Li and Y. Niu, *J. Phys. Chem. C*, 2019, **123**, 16075–16082.
- 200 S. S. Shin, E. J. Yeom, W. S. Yang, S. Hur, M. G. Kim, J. Im, J. Seo, J. H. Noh and S. I. Seok, *Science*, 2017, **356**, 167–171.
- 201 S. S. Shin, J. H. Suk, B. J. Kang, W. Yin, S. J. Lee, J. H. Noh, T. K. Ahn, F. Rotermund, I. S. Cho and S. I. Seok, *Energy Environ. Sci.*, 2019, **12**, 958–964.
- 202 R. Dileep K, M. K. Rajbhar, A. Ashina, E. Ramasamy, S. Mallick, T. N. Rao and G. Veerappan, *Mater. Chem. Phys.*, 2021, **258**, 123939.
- 203 Y. J. Hu, C. Wang, Y. Tang, L. Huang, J. X. Fu, W. M. Shi, L. J. Wang and W. G. Yang, *J. Alloys Compd.*, 2016, **679**, 32–38.
- 204 A. Bera, K. W. Wu, A. Sheikh, E. Alarousu, O. F. Mohammed and T. Wu, *J. Phys. Chem. C*, 2014, **118**, 28494–28501.
- 205 M. Neophytou, M. De Bastiani, N. Gasparini, E. Aydin, E. Ugur, A. Seitkhan, F. Moruzzi, Y. Choiae, A. J. Ramadan, J. R. Troughton, R. Hallani, A. Savva, L. Tsetseris, S. Inal, D. Baran, F. Laquai, T. D. Anthopoulos, H. J. Snaith, S. De Wolf and I. McCulloch, *ACS Appl. Energy Mater.*, 2019, **2**, 8090–8097.
- 206 N. Tsvetkov, B. C. Moon, J. Lee and J. K. Kang, *ACS Appl. Energy Mater.*, 2020, **3**, 344–351.
- 207 C. Wang, Y. Tang, Y. Hu, L. Huang, J. Fu, J. Jin, W. Shi, L. Wang and W. Yang, *RSC Adv.*, 2015, **5**, 52041–52047.
- 208 T. Mahmoudi, Y. Wang and Y.-B. Hahn, *Adv. Energy Mater.*, 2020, **10**, 1903369.
- 209 X. Luo, J. Ding, J. Wang and J. Zhang, *J. Mater. Res.*, 2020, **35**, 2158–2165.
- 210 Y. Okamoto and Y. Suzuki, *J. Phys. Chem. C*, 2016, **120**, 13995–14000.
- 211 J. Qin, Z. Zhang, W. Shi, Y. Liu, H. Gao and Y. Mao, *ACS Appl. Mater. Interfaces*, 2018, **10**, 36067–36074.
- 212 H. Guo, H. Chen, H. Zhang, X. Huang, J. Yang, B. Wang, Y. Li, L. Wang, X. Niu and Z. Wang, *Nano Energy*, 2019, **59**, 1–9.

- 213 H. Guo, H. Zhang, J. Yang, W. Gong, H. Chen, H. Wang, X. Liu, F. Hao, X. Niu and Y. Zhao, *ACS Appl. Energy Mater.*, 2020, **3**, 6889–6896.
- 214 L. S. Oh, D. H. Kim, J. A. Lee, S. S. Shin, J. W. Lee, I. J. Park, M. J. Ko, N. G. Park, S. G. Pyo, K. S. Hong and J. Y. Kim, *J. Phys. Chem. C*, 2014, **118**, 22991–22994.
- 215 A. Bera, A. D. Sheikh, M. A. Haque, R. Bose, E. Alarousu, O. F. Mohammed and T. Wu, *ACS Appl. Mater. Interfaces*, 2015, **7**, 28404–28411.
- 216 W. X. Li, Q. H. Jiang, J. Y. Yang, Y. B. Luo, X. Li, Y. R. Hou and S. Q. Zhou, *Sol. Energy Mater. Sol. Cells*, 2017, **159**, 143–150.
- 217 S. S. Mali, C. S. Shim, H. Kim and C. K. Hong, *J. Mater. Chem. A*, 2016, **4**, 12158–12169.
- 218 W. Xu, L. Zheng, T. Zhu, L. Liu and X. Gong, *ACS Appl. Mater. Interfaces*, 2019, **11**, 34020–34029.
- 219 A. Pang, D. Shen, M. Wei and Z.-N. Chen, *ChemSusChem*, 2018, **11**, 424–431.
- 220 M. M. Lee, J. Teuscher, T. Miyasaka, T. N. Murakami and H. J. Snaith, *Science*, 2012, **338**, 643–647.
- 221 E. Edri, S. Kirmayer, D. Cahen and G. Hodes, *J. Phys. Chem. Lett.*, 2013, **4**, 897–902.
- 222 S. D. Stranks, G. E. Eperon, G. Grancini, C. Menelaou, M. J. P. Alcocer, T. Leijtens, L. M. Herz, A. Petrozza and H. J. Snaith, *Science*, 2013, **342**, 341–344.
- 223 J. M. Ball, M. M. Lee, A. Hey and H. J. Snaith, *Energy Environ. Sci.*, 2013, **6**, 1739–1743.
- 224 S. H. Hwang, J. Roh, J. Lee, J. Ryu, J. Yun and J. Jang, *J. Mater. Chem. A*, 2014, **2**, 16429–16433.
- 225 N. Aeineh, A.-F. Castro-Méndez, P. J. Rodríguez-Cantó, R. Abargues, E. Hassanabadi, I. Suarez, A. Behjat, P. Ortiz, J. P. Martínez-Pastor and I. Mora-Seró, *ACS Omega*, 2018, **3**, 9798–9804.
- 226 Y. Zhao, J. Wei, H. Li, Y. Yan, W. Zhou, D. Yu and Q. Zhao, *Nat. Commun.*, 2016, **7**, 10228.
- 227 Y. Numata, Y. Sanehira and T. Miyasaka, *ACS Appl. Mater. Interfaces*, 2016, **8**, 4608–4615.
- 228 D. Wang, Q. Chen, H. Mo, J. Jacobs, A. Thomas and Z. Liu, *Mater. Adv.*, 2020, **1**, 2057–2067.
- 229 H.-C. Kwon, A. Kim, H. Lee, D. Lee, S. Jeong and J. Moon, *Adv. Energy Mater.*, 2016, **6**, 1601055.
- 230 M. Xu, W. Ji, Y. Sheng, Y. Wu, H. Cheng, J. Meng, Z. Yan, J. Xu, A. Mei, Y. Hu, Y. Rong and H. Han, *Nano Energy*, 2020, **74**, 104842.
- 231 Y. Qiang, Y. Xie, Y. Qi, P. Wei, H. Shi, C. Geng and H. Liu, *Sol. Energy*, 2020, **201**, 523–529.
- 232 X. Dong, X. Fang, M. H. Lv, B. C. Lin, S. Zhang, J. N. Ding and N. Y. Yuan, *J. Mater. Chem. A*, 2015, **3**, 5360–5367.
- 233 D. Q. Bi, S. J. Moon, L. Haggman, G. Boschloo, L. Yang, E. M. J. Johansson, M. K. Nazeeruddin, M. Gratzel and A. Hagfeldt, *RSC Adv.*, 2013, **3**, 18762–18766.
- 234 K. Wang, Y. T. Shi, Q. S. Dong, Y. Li, S. F. Wang, X. F. Yu, M. Y. Wu and T. L. Ma, *J. Phys. Chem. Lett.*, 2015, **6**, 755–759.
- 235 X. Wang, L.-L. Deng, L.-Y. Wang, S.-M. Dai, Z. Xing, X.-X. Zhan, X.-Z. Lu, S.-Y. Xie, R.-B. Huang and L.-S. Zheng, *J. Mater. Chem. A*, 2017, **5**, 1706–1712.
- 236 M. Qin, J. Ma, W. Ke, P. Qin, H. Lei, H. Tao, X. Zheng, L. Xiong, Q. Liu, Z. Chen, J. Lu, G. Yang and G. Fang, *ACS Appl. Mater. Interfaces*, 2016, **8**, 8460–8466.
- 237 X. Ling, J. Yuan, D. Liu, Y. Wang, Y. Zhang, S. Chen, H. Wu, F. Jin, F. Wu, G. Shi, X. Tang, J. Zheng, S. Liu, Z. Liu and W. Ma, *ACS Appl. Mater. Interfaces*, 2017, **9**, 23181–23188.
- 238 W. Hu, T. Liu, X. Yin, H. Liu, X. Zhao, S. Luo, Y. Guo, Z. Yao, J. Wang, N. Wang, H. Lin and Z. Guo, *J. Mater. Chem. A*, 2017, **5**, 1434–1441.
- 239 M. F. García-Sánchez, A. Ortiz, G. Santana, M. Bizarro, J. Peña, F. Cruz-Gandarilla, M. A. Aguilar-Frutis and J. C. Alonso, *J. Am. Ceram. Soc.*, 2010, **93**, 155–160.
- 240 T. Inoue, M. Osonoe, H. Tohda, M. Hiramatsu, Y. Yamamoto, A. Yamanaka and T. Nakayama, *J. Appl. Phys.*, 1991, **69**, 8313–8315.
- 241 T. Suzuki, I. Kosacki, H. U. Anderson and P. Colomban, *J. Am. Ceram. Soc.*, 2001, **84**, 2007–2014.
- 242 R. Fang, S. Wu, W. Chen, Z. Liu, S. Zhang, R. Chen, Y. Yue, L. Deng, Y.-B. Cheng, L. Han and W. Chen, *ACS Nano*, 2018, **12**, 2403–2414.
- 243 A. Pang, J. Li, X.-F. Wei, Z.-W. Ruan, M. Yang and Z.-N. Chen, *Nanoscale Adv.*, 2020, **2**, 4062–4069.
- 244 J. Yang, J. Xu, Q. Zhang, Z. Xue, H. Liu, R. Qin, H. Zhai and M. Yuan, *RSC Adv.*, 2020, **10**, 18608–18613.
- 245 Z. Xing, S.-H. Li, B.-S. Wu, X. Wang, L.-Y. Wang, T. Wang, H.-R. Liu, M.-L. Zhang, D.-Q. Yun, L.-L. Deng, S.-Y. Xie, R.-B. Huang and L.-S. Zheng, *J. Power Sources*, 2018, **389**, 13–19.
- 246 R. Meng, X. Feng, Y. Yang, X. Lv, J. Cao and Y. Tang, *ACS Appl. Mater. Interfaces*, 2019, **11**, 13273–13278.
- 247 Z. Guo, L. Gao, C. Zhang, Z. Xu and T. Ma, *J. Mater. Chem. A*, 2018, **6**, 4572–4589.
- 248 T. Hu, S. Xiao, H. Yang, L. Chen and Y. Chen, *Chem. Commun.*, 2018, **54**, 471–474.
- 249 L. Ottaviano, L. Lozzi, M. Passacantando and S. Santucci, *Surf. Sci.*, 2001, **475**, 73–82.
- 250 L. Weinhardt, M. Blum, M. Bär, C. Heske, B. Cole, B. Marsen and E. L. Miller, *J. Phys. Chem. C*, 2008, **112**, 3078–3082.
- 251 D. S. Dalavi, R. S. Devan, R. A. Patil, R. S. Patil, Y. R. Ma, S. B. Sadale, I. Kim, J. H. Kim and P. S. Patil, *J. Mater. Chem. C*, 2013, **1**, 3722–3728.
- 252 M. Gillet, K. Aguir, C. Lemire, E. Gillet and K. Schierbaum, *Thin Solid Films*, 2004, **467**, 239–246.
- 253 K. Mahmood, B. S. Swain, A. R. Kirmani and A. Amassian, *J. Mater. Chem. A*, 2015, **3**, 9051–9057.
- 254 F. Wang, Y. Zhang, M. Yang, J. Du, L. Yang, L. Fan, Y. Sui, X. Liu and J. Yang, *J. Power Sources*, 2019, **440**, 227157.
- 255 X. Li, Y. Liu, V. O. Eze, T. Mori, Z. Huang, K. P. Homewood, Y. Gao and B. Lei, *Sol. Energy Mater. Sol. Cells*, 2019, **196**, 157–166.
- 256 F. Wang, M. Yang, Y. Zhang, J. Du, D. Han, L. Yang, L. Fan, Y. Sui, Y. Sun, X. Meng and J. Yang, *Chem. Eng. J.*, 2020, **402**, 126303.
- 257 Y. Guo, T. Liu, N. Wang, Q. Luo, H. Lin, J. Li, Q. Jiang, L. Wu and Z. Guo, *Nano Energy*, 2017, **38**, 193–200.

- 258 W. Zhu, Q. Zhang, C. Zhang, D. Chen, L. Zhou, Z. Lin, J. Chang, J. Zhang and Y. Hao, *Dalton Trans.*, 2018, **47**, 6404–6411.
- 259 A. K. Chandiran, M. Abdi-Jalebi, A. Yella, M. I. Dar, C. Y. Yi, S. A. Shivashankar, M. K. Nazeeruddin and M. Gratzel, *Nano Lett.*, 2014, **14**, 1190–1195.
- 260 G. S. Han, H. S. Chung, B. J. Kim, D. H. Kim, J. W. Lee, B. S. Swain, K. Mahmood, J. S. Yoo, N. G. Park, J. H. Lee and H. S. Jung, *J. Mater. Chem. A*, 2015, **3**, 9160–9164.
- 261 X. Guo, Z. Lin, J. Ma, Z. Hu, J. Su, C. Zhang, J. Zhang, J. Chang and Y. Hao, *J. Power Sources*, 2019, **438**, 226981.
- 262 X. Zhang, J. Li, Z. Bi, K. He, X. Xu, X. Xiao, Y. Zhu, Y. Zhan, L. Zhong, G. Xu and H. Yu, *J. Alloys Compd.*, 2020, **836**, 155460.
- 263 S. An, P. Chen, F. Hou, Q. Wang, H. Pan, X. Chen, X. Lu, Y. Zhao, Q. Huang and X. Zhang, *Sol. Energy*, 2020, **196**, 409–418.
- 264 E. Aydin, M. De Bastiani, X. Yang, M. Sajjad, F. Aljamaan, Y. Smirnov, M. N. Hedhili, W. Liu, T. G. Allen, L. Xu, E. Van Kerschaver, M. Morales-Masis, U. Schwingenschlögl and S. De Wolf, *Adv. Funct. Mater.*, 2019, **29**, 1901741.
- 265 J.-H. Kim, T.-Y. Seong, K.-B. Chung, C. S. Moon, J. H. Noh, H.-J. Seok and H.-K. Kim, *J. Power Sources*, 2019, **418**, 152–161.
- 266 R. A. Rani, A. S. Zoofakhar, A. P. O'Mullane, M. W. Austin and K. Kalantar-Zadeh, *J. Mater. Chem. A*, 2014, **2**, 15683–15703.
- 267 J. H. Lin, R. A. Patil, M. A. Wu, L. G. Yu, K. D. Liu, W. T. Gao, R. S. Devan, C. H. Ho, Y. Liou and Y. R. Ma, *J. Mater. Chem. C*, 2014, **2**, 8667–8672.
- 268 A. Kogo, Y. Numata, M. Ikegami and T. Miyasaka, *Chem. Lett.*, 2015, **44**, 829–830.
- 269 J. Feng, Z. Yang, D. Yang, X. Ren, X. Zhu, Z. Jin, W. Zi, Q. Wei and S. Liu, *Nano Energy*, 2017, **36**, 1–8.
- 270 D. Shen, W. Zhang, Y. Li, A. Abate and M. Wei, *ACS Appl. Nano Mater.*, 2018, **1**, 4101–4109.
- 271 X. Ye, H. Ling, R. Zhang, Z. Wen, S. Hu, T. Akasaka, J. Xia and X. Lu, *J. Power Sources*, 2020, **448**, 227419.
- 272 R. Li, X. Huo, X. Han, Z. Wang, M. Zhang and M. Guo, *Appl. Surf. Sci.*, 2021, **542**, 148728.
- 273 L. Wang, W. F. Fu, Z. W. Gu, C. C. Fan, X. Yang, H. Y. Li and H. Z. Chen, *J. Mater. Chem. C*, 2014, **2**, 9087–9090.
- 274 M. Abulikemu, J. Barbé, A. El Labban, J. Eid and S. Del Gobbo, *Thin Solid Films*, 2017, **636**, 512–518.
- 275 D.-B. Li, L. Hu, Y. Xie, G. Niu, T. Liu, Y. Zhou, L. Gao, B. Yang and J. Tang, *ACS Photonics*, 2016, **3**, 2122–2128.
- 276 M. D. Que, L. L. Zhu, Y. W. Yang, J. Liu, P. Chen, W. Chen, X. T. Yin and W. X. Que, *J. Power Sources*, 2018, **383**, 42–49.
- 277 Z. L. Lu, X. J. Pan, Y. Z. Ma, Y. Li, L. L. Zheng, D. F. Zhang, Q. Xu, Z. J. Chen, S. F. Wang, B. Qu, F. Liu, Y. D. Huang, L. X. Xiao and Q. H. Gong, *RSC Adv.*, 2015, **5**, 11175–11179.
- 278 H. Wang, F. Yang, N. Li, M. A. Kamarudin, J. Qu, J. Song, S. Hayase and C. J. Brabec, *ACS Sustainable Chem. Eng.*, 2020, **8**, 8848–8856.
- 279 T. Cao, P. Huang, K. Zhang, Z. Sun, K. Zhu, L. Yuan, K. Chen, N. Chen and Y. Li, *J. Mater. Chem. A*, 2018, **6**, 3435–3443.
- 280 J. Xiong, Y. Qi, Q. Zhang, D. Box, K. Williams, J. Tatum, P. Das, N. R. Pradhan and Q. Dai, *ACS Appl. Energy Mater.*, 2021, **4**, 1815–1823.
- 281 O. Malinkiewicz, A. Yella, Y. H. Lee, G. M. Espallargas, M. Graetzel, M. K. Nazeeruddin and H. J. Bolink, *Nat. Photonics*, 2014, **8**, 128–132.
- 282 Z. R. Yang, J. S. Xie, V. Arivazhagan, K. Xiao, Y. P. Qiang, K. Huang, M. Hu, C. Cui, X. G. Yu and D. R. Yang, *Nano Energy*, 2017, **40**, 345–351.
- 283 Y. Bai, H. Yu, Z. L. Zhu, K. Jiang, T. Zhang, N. Zhao, S. H. Yang and H. Yan, *J. Mater. Chem. A*, 2015, **3**, 9098–9102.
- 284 X. F. Zeng, T. W. Zhou, C. Q. Leng, Z. G. Zang, M. Wang, W. Hu, X. S. Tang, S. R. Lu, L. A. Fang and M. Zhou, *J. Mater. Chem. A*, 2017, **5**, 17499–17505.
- 285 C. Liu, K. Wang, P. C. Du, T. Y. Meng, X. F. Yu, S. Z. D. Cheng and X. Gong, *ACS Appl. Mater. Interfaces*, 2015, **7**, 1153–1159.
- 286 J. Ciro, S. Mesa, J. I. Uribe, M. A. Mejia-Escobar, D. Ramirez, J. F. Montoya, R. Betancur, H. S. Yoo, N. G. Park and F. Jaramillo, *Nanoscale*, 2017, **9**, 9440–9446.
- 287 Y. Liu, Z. Xu, S. L. Zhao, B. Qiao, Y. Li, Z. L. Qin and Y. Q. Zhu, *Acta Phys. Sin.*, 2017, **66**, 118801.
- 288 Y. Liu, B. Long, R. Chen, S. Huang, W. Ou-Yang and X. Chen, *ACS Appl. Energy Mater.*, 2021, **4**, 3812–3821.
- 289 A. A. Said, J. Xie and Q. Zhang, *Small*, 2019, **15**, 1900854.
- 290 D. Wang, T. Ye and Y. Zhang, *J. Mater. Chem. A*, 2020, **8**, 20819–20848.
- 291 H. S. Kim, J. W. Lee, N. Yantara, P. P. Boix, S. A. Kulkarni, S. Mhaisalkar, M. Gratzel and N. G. Park, *Nano Lett.*, 2013, **13**, 2412–2417.
- 292 K. Mahmood, B. S. Swain and A. Amassian, *Adv. Mater.*, 2015, **27**, 2859–2865.
- 293 L. F. Zhu, Y. Z. Xu, J. J. Shi, H. Y. Zhang, X. Xu, Y. H. Zhao, Y. H. Luo, Q. B. Meng and D. M. Li, *RSC Adv.*, 2016, **6**, 82282–82288.
- 294 F. Cai, L. Yang, Y. Yan, J. Zhang, F. Qin, D. Liu, Y.-B. Cheng, Y. Zhou and T. Wang, *J. Mater. Chem. A*, 2017, **5**, 9402–9411.
- 295 M. M. Tavakoli, P. Yadav, R. Tavakoli and J. Kong, *Adv. Energy Mater.*, 2018, **8**, 1800794.
- 296 M. Kim, G.-H. Kim, T. K. Lee, I. W. Choi, H. W. Choi, Y. Jo, Y. J. Yoon, J. W. Kim, J. Lee, D. Huh, H. Lee, S. K. Kwak, J. Y. Kim and D. S. Kim, *Joule*, 2019, **3**, 2179–2192.
- 297 M. Jeong, I. W. Choi, E. M. Go, Y. Cho, M. Kim, B. Lee, S. Jeong, Y. Jo, H. W. Choi, J. Lee, J.-H. Bae, S. K. Kwak, D. S. Kim and C. Yang, *Science*, 2020, **369**, 1615–1620.
- 298 J. Jeong, M. Kim, J. Seo, H. Lu, P. Ahlawat, A. Mishra, Y. Yang, M. A. Hope, F. T. Eickemeyer, M. Kim, Y. J. Yoon, I. W. Choi, B. P. Darwich, S. J. Choi, Y. Jo, J. H. Lee, B. Walker, S. M. Zakeeruddin, L. Emsley, U. Rothlisberger, A. Hagfeldt, D. S. Kim, M. Grätzel and J. Y. Kim, *Nature*, 2021, **592**, 381–385.
- 299 H. Huang, P. Cui, Y. Chen, L. Yan, X. Yue, S. Qu, X. Wang, S. Du, B. Liu, Q. Zhang, Z. Lan, Y. Yang, J. Ji, X. Zhao, Y. Li, X. Wang, X. Ding and M. Li, *Joule*, 2022, **6**, 2186–2202.

- 300 M. H. Kumar, N. Yantara, S. Dharani, M. Graetzel, S. Mhaisalkar, P. P. Boix and N. Mathews, *Chem. Commun.*, 2013, **49**, 11089–11091.
- 301 D. Liu and T. L. Kelly, *Nat. Photonics*, 2014, **8**, 133–138.
- 302 C. Y. Chang, K. T. Lee, W. K. Huang, H. Y. Siao and Y. C. Chang, *Chem. Mater.*, 2015, **27**, 5122–5130.
- 303 M. M. Tavakoli, R. Tavakoli, P. Yadav and J. Kong, *J. Mater. Chem. A*, 2019, **7**, 679–686.
- 304 Y. W. Noh, I. S. Jin, K. S. Kim, S. H. Park and J. W. Jung, *J. Mater. Chem. A*, 2020, **8**, 17163–17173.
- 305 S. Leng, L. Wang, X. Wang, Z. Zhang, J. Liang, Y. Zheng, J. Jiang, Z. Zhang, X. Liu, Y. Qiu and C.-C. Chen, *Solar RRL*, 2021, **5**, 2100285.
- 306 Y. Wu, J. X. Song, X. R. Wu, C. F. Qiu, X. X. Yin, L. Hu, Z. Su, Y. Z. Jin, J. J. Chen and Z. F. Li, *Chem. Commun.*, 2022, **58**, 9266–9269.
- 307 Q. Jiang, L. Zhang, H. Wang, X. Yang, J. Meng, H. Liu, Z. Yin, J. Wu, X. Zhang and J. You, *Nat. Energy*, 2016, **2**, 16177.
- 308 K. Liu, S. Chen, J. Wu, H. Zhang, M. Qin, X. Lu, Y. Tu, Q. Meng and X. Zhan, *Energy Environ. Sci.*, 2018, **11**, 3463–3471.
- 309 C. Ma and N.-G. Park, *ACS Energy Lett.*, 2020, **5**, 3268–3275.
- 310 H. Min, D. Y. Lee, J. Kim, G. Kim, K. S. Lee, J. Kim, M. J. Paik, Y. K. Kim, K. S. Kim, M. G. Kim, T. J. Shin and S. Il Seok, *Nature*, 2021, **598**, 444–450.
- 311 M. Kim, J. Jeong, H. Z. Lu, T. K. Lee, F. T. Eickemeyer, Y. H. Liu, I. W. Choi, S. J. Choi, Y. Jo, H. B. Kim, S. I. Mo, Y. K. Kim, H. Lee, N. G. An, S. Cho, W. R. Tress, S. M. Zakeeruddin, A. Hagfeldt, J. Y. Kim, M. Gratzel and D. S. Kim, *Science*, 2022, **375**, 302.
- 312 S. S. Shin, W. S. Yang, J. H. Noh, J. H. Suk, N. J. Jeon, J. H. Park, J. S. Kim, W. M. Seong and S. I. Seok, *Nat. Commun.*, 2015, **6**, 7410.
- 313 S. Bao, J. Wu, X. He, Y. Tu, S. Wang, M. Huang and Z. Lan, *Electrochim. Acta*, 2017, **251**, 307–315.
- 314 J. Dou, Y. Zhang, Q. Wang, A. Abate, Y. Li and M. Wei, *Chem. Commun.*, 2019, **55**, 14673–14676.
- 315 F. Sadegh, S. Akin, M. Moghadam, V. Mirkhani, M. A. Ruiz-Preciado, Z. Wang, M. M. Tavakoli, M. Graetzel, A. Hagfeldt and W. Tress, *Nano Energy*, 2020, **75**, 105038.
- 316 Q. Zhang, K. Williams, J. Tatum, F. Han, X. Zhu and Q. Dai, *J. Renewable Sustainable Energy*, 2021, **13**, 063501.
- 317 X. H. Liu, Y. Zhang, M. Chen, C. X. Xiao, K. G. Brooks, J. X. Xia, X. X. Gao, H. Kanda, S. Kinge, A. M. Asiri, J. M. Luther, Y. Q. Feng, P. J. Dyson and M. K. Nazeeruddin, *ACS Appl. Mater. Interfaces*, 2022, **14**, 23297–23306.
- 318 Y. Tang, R. Roy, Z. H. Zhang, Y. C. Hu, F. Yang, C. C. Qin, L. L. Jiang and H. R. Liu, *Sol. Energy*, 2022, **231**, 440–446.
- 319 A. Culu, I. C. Kaya and S. Sonmezoglu, *ACS Appl. Energy Mater.*, 2022, **5**, 3454–3462.
- 320 S. Ranjan, R. Ranjan, A. Tyagi, K. S. Rana, A. Soni, H. K. Kodali, V. Dalal, A. Singh, A. Garg, K. S. Nalwa and R. K. Gupta, *ACS Appl. Energy Mater.*, 2022, **5**, 2679–2696.
- 321 M. J. Paik, Y. Lee, H.-S. Yun, S.-U. Lee, S.-T. Hong and S. I. Seok, *Adv. Energy Mater.*, 2020, **10**, 2001799.
- 322 Y. Sanehira, N. Shibayama, Y. Numata, M. Ikegami and T. Miyasaka, *ACS Appl. Mater. Interfaces*, 2020, **12**, 15175–15182.
- 323 K.-M. Lee, W.-J. Lin, S.-H. Chen and M.-C. Wu, *Org. Electron.*, 2020, **77**, 105406.
- 324 W. Hu, W. Zhou, X. Lei, P. Zhou, M. Zhang, T. Chen, H. Zeng, J. Zhu, S. Dai, S. Yang and S. Yang, *Adv. Mater.*, 2019, **31**, 1806095.
- 325 F. Xie, J. Zhu, Y. Li, D. Shen, A. Abate and M. Wei, *J. Power Sources*, 2019, **415**, 8–14.
- 326 A. Khorasani, M. Marandi, A. Irajizad and N. Taghavinia, *Electrochim. Acta*, 2019, **297**, 1071–1078.
- 327 X. Chen, L. J. Tang, S. Yang, Y. Hou and H. G. Yang, *J. Mater. Chem. A*, 2016, **4**, 6521–6526.
- 328 H. Lu, Y. Ma, B. Gu, W. Tian and L. Li, *J. Mater. Chem. A*, 2015, **3**, 16445–16452.
- 329 J. Kruszynska, J. Ostapko, V. Ozkaya, B. Surucu, O. Szawcow, K. Nikiforow, M. Holdynski, M. M. Tavakoli, P. Yadav, M. Kot, G. P. Kolodziej, M. Wlazlo, S. Satapathi, S. Akin and D. Prochowicz, *Adv. Mater. Interfaces*, 2022, **9**, 2200575.
- 330 Z. Arshad, S. Wageh, T. Maiyalagan, M. Ali, U. Arshad, A. Noorul, M. B. Qadir, F. Mateen and A. G. Al-Sehemi, *Ceram. Int.*, 2022, **48**, 24363–24371.
- 331 K. Chen, W. Tang, Y. Chen, R. Yuan, Y. Lv, W. Shan and W.-H. Zhang, *J. Energy Chem.*, 2021, **61**, 553–560.
- 332 Z. Yang, Q. Fan, T. Shen, J. Jin, W. Deng, J. Xin, X. Huang, X. Wang and J. Li, *Sol. Energy*, 2020, **204**, 223–230.
- 333 R. Azmi, S. Hwang, W. Yin, T.-W. Kim, T. K. Ahn and S.-Y. Jang, *ACS Energy Lett.*, 2018, **3**, 1241–1246.
- 334 J. H. Heo, M. H. Lee, H. J. Han, B. R. Patil, J. S. Yu and S. H. Im, *J. Mater. Chem. A*, 2016, **4**, 1572–1578.
- 335 C. Zhang, Q. X. Zhuang, H. Y. Li, C. Gong, H. X. Wang, R. Li, H. X. Li, Z. Y. Zhang, H. Yang, J. Z. Chen and Z. G. Zang, *Sol. RRL*, 2022, 2200512.
- 336 Q. X. Zhuang, H. X. Wang, C. Zhang, C. Gong, H. Y. Li, J. Z. Chen and Z. G. Zang, *Nano Res.*, 2022, **15**, 5114–5122.
- 337 J. B. Wu, C. Zhen and G. Liu, *Rare Met.*, 2022, **41**, 361–367.
- 338 C. Zhang, H. X. Wang, H. Y. Li, Q. X. Zhuang, C. Gong, X. F. Hu, W. S. Cai, S. Y. Zhao, J. Z. Chen and Z. G. Zang, *J. Energy Chem.*, 2021, **63**, 452–460.
- 339 Z. Xu, Y. Jiang, Z. Li, C. Chen, X. Kong, Y. Chen, G. Zhou, J.-M. Liu, K. Kempa and J. Gao, *ACS Appl. Energy Mater.*, 2021, **4**, 1887–1893.
- 340 J. Song, G. Li, D. Wang, W. Sun, J. Wu and Z. Lan, *Solar RRL*, 2020, **4**, 1900558.
- 341 H. X. Wang, H. Y. Li, S. L. Cao, M. Wang, J. Z. Chen and Z. G. Zang, *Solar RRL*, 2020, **4**, 2000226.
- 342 M. Hu, L. Zhang, S. She, J. Wu, X. Zhou, X. Li, D. Wang, J. Miao, G. Mi, H. Chen, Y. Tian, B. Xu and C. Cheng, *Solar RRL*, 2020, **4**, 1900331.
- 343 L. Xiong, M. Qin, C. Chen, J. Wen, G. Yang, Y. Guo, J. Ma, Q. Zhang, P. Qin, S. Li and G. Fang, *Adv. Funct. Mater.*, 2018, **28**, 1706276.
- 344 W.-Q. Wu, D. Chen, Y.-B. Cheng and R. A. Caruso, *Solar RRL*, 2017, **1**, 1700117.
- 345 X. K. Yang, W. H. Zhao, M. J. Li, L. F. Ye, P. F. Guo, Y. X. Xu, H. Guo, H. W. Yu, Q. Ye, H. Y. Wang, D. Harvey,

- D. Shchukin, M. J. Feng, T. C. Sum and H. Q. Wang, *Adv. Funct. Mater.*, 2022, **32**, 2112388.
- 346 J. L. Liu, Y. J. Guan, S. Liu, S. Li, C. X. Gao, J. K. Du, C. Qiu, D. Y. Li, D. Y. Zhang, X. D. Wang, Y. F. Wang, Y. Hu, Y. G. Rong, A. Y. Mei and H. W. Han, *ACS Appl. Energy Mater.*, 2021, **4**, 11032–11040.
- 347 M. Zheng, W. Xu, H. Yuan and J. Wu, *J. Alloys Compd.*, 2020, **823**, 153730.
- 348 X. Luo, Y. Li, K. Liu and J. Zhang, *Solid State Sci.*, 2020, **108**, 106387.
- 349 J. Dou, D. Shen, Y. Li, A. Abate and M. Wei, *ACS Appl. Mater. Interfaces*, 2019, **11**, 36553–36559.
- 350 Y. Gao, Y. Wu, Y. Liu, C. Chen, X. Shen, X. Bai, Z. Shi, W. W. Yu, Q. Dai and Y. Zhang, *Solar RRL*, 2019, **3**, 1900314.
- 351 J. Sun, Y. Li, N. Tang, Y. Zhou, X. Zhang, X. Lu, X. Gao, J. Gao, L. Shui, S. Wu and J.-M. Liu, *ACS Appl. Energy Mater.*, 2020, **3**, 3328–3336.
- 352 M. M. Tavakoli, D. Prochowicz, P. Yadav and R. Tavakoli, *Phys. Status Solidi RRL*, 2020, **14**, 2000062.
- 353 F. Wang, Y. Zhang, M. Yang, J. Du, L. Xue, L. Yang, L. Fan, Y. Sui, J. Yang and X. Zhang, *Nano Energy*, 2019, **63**, 103825.
- 354 B. Yang, M. Wang, X. F. Hu, T. W. Zhou and Z. G. Zang, *Nano Energy*, 2019, **57**, 718–727.
- 355 J. Jiang, S. Wang, X. Jia, X. Fang, S. Zhang, J. Zhang, W. Liu, J. Ding and N. Yuan, *RSC Adv.*, 2018, **8**, 12823–12831.
- 356 S. F. Shaikh, H.-C. Kwon, W. Yang, R. S. Mane and J. Moon, *J. Alloys Compd.*, 2018, **738**, 405–414.
- 357 M. Kim, T. N. Murakami, T. W. Kim, S. Kim, H. Tampo, M. Chikamatsu and H. Segawa, *Chem. Lett.*, 2018, **47**, 1350–1353.
- 358 G. Tong, Z. Song, C. Li, Y. Zhao, L. Yu, J. Xu, Y. Jiang, Y. Sheng, Y. Shi and K. Chen, *RSC Adv.*, 2017, **7**, 19457–19463.
- 359 Y. Hou, C. O. R. Quiroz, S. Scheiner, W. Chen, T. Stubhan, A. Hirsch, M. Halik and C. J. Brabec, *Adv. Energy Mater.*, 2015, **5**, 1501056.
- 360 W. Chen, Y. Wu, Y. Yue, J. Liu, W. Zhang, X. Yang, H. Chen, E. Bi, I. Ashraful, M. Grätzel and L. Han, *Science*, 2015, **350**, 944–948.
- 361 C. T. Zuo and L. M. Ding, *Small*, 2015, **11**, 5528–5532.
- 362 N. Wijeyasinghe, A. Regoutz, F. Eisner, T. Du, L. Tsetseris, Y.-H. Lin, H. Faber, P. Pattanasattayavong, J. Li, F. Yan, M. A. McLachlan, D. J. Payne, M. Heeney and T. D. Anthopoulos, *Adv. Funct. Mater.*, 2017, **27**, 1701818.
- 363 H. Zhang, H. Wang, W. Chen and A. K. Y. Jen, *Adv. Mater.*, 2017, **29**, 1604984.
- 364 D. S. Dalavi, R. S. Devan, R. S. Patil, Y. R. Ma and P. S. Patil, *Mater. Lett.*, 2013, **90**, 60–63.
- 365 R. A. Patil, R. S. Devan, J. H. Lin, Y. Liou and Y. R. Ma, *Sci. Rep.*, 2013, **3**, 3070.
- 366 R. A. Patil, C. P. Chang, R. S. Devan, Y. Liou and Y. R. Ma, *ACS Appl. Mater. Interfaces*, 2016, **8**, 9872–9880.
- 367 N. Kitchamsetti, P. R. Chikate, R. A. Patil, Y. R. Ma, P. M. Shirage and R. S. Devan, *CrystEngComm*, 2019, **21**, 7130–7140.
- 368 N. Kitchamsetti, M. S. Ramteke, S. R. Rondiya, S. R. Mulani, M. S. Patil, R. W. Cross, N. Y. Dzade and R. S. Devan, *J. Alloys Compd.*, 2021, **855**, 157337.
- 369 R. A. Patil, R. S. Devan, J. H. Lin, Y. R. Ma, P. S. Patil and Y. Liou, *Sol. Energy Mater. Sol. Cells*, 2013, **112**, 91–96.
- 370 D. S. Dalavi, R. S. Devan, R. S. Patil, Y. R. Ma, M. G. Kang, J. H. Kim and P. S. Patil, *J. Mater. Chem. A*, 2013, **1**, 1035–1039.
- 371 K. H. Parmar, V. Manjunath, S. Bimli, P. R. Chikate, R. A. Patil, Y. R. Ma and R. S. Devan, *Chin. J. Phys.*, 2022, **77**, 143–150.
- 372 P. Docampo, J. M. Ball, M. Darwich, G. E. Eperon and H. J. Snaith, *Nat. Commun.*, 2013, **4**, 2761.
- 373 J. Cui, F. Meng, H. Zhang, K. Cao, H. Yuan, Y. Cheng, F. Huang and M. Wang, *ACS Appl. Mater. Interfaces*, 2014, **6**, 22862–22870.
- 374 S. Seo, I. J. Park, M. Kim, S. Lee, C. Bae, H. S. Jung, N. G. Park, J. Y. Kim and H. Shin, *Nanoscale*, 2016, **8**, 11403–11412.
- 375 J. Tang, D. Jiao, L. Zhang, X. Zhang, X. Xu, C. Yao, J. Wu and Z. Lan, *Sol. Energy*, 2018, **161**, 100–108.
- 376 Z. Zhu, Y. Bai, T. Zhang, Z. Liu, X. Long, Z. Wei, Z. Wang, L. Zhang, J. Wang, F. Yan and S. Yang, *Angew. Chem., Int. Ed.*, 2014, **53**, 12571–12575.
- 377 T. Abzieher, S. Moghadamzadeh, F. Schackmar, H. Eggers, F. Sutterlütü, A. Farooq, D. Kojda, K. Habicht, R. Schmager, A. Mertens, R. Azmi, L. Klotz, J. A. Schwenzer, M. Hetterich, U. Lemmer, B. S. Richards, M. Powalla and U. W. Paetzold, *Adv. Energy Mater.*, 2019, **9**, 1802995.
- 378 T. J. Routledge, M. Wong-Stringer, O. S. Game, J. A. Smith, J. E. Bishop, N. Vaenas, B. G. Freestone, D. M. Coles, T. McArdle, A. R. Buckley and D. G. Lidzey, *J. Mater. Chem. A*, 2019, **7**, 2283–2290.
- 379 B. Zhao, L. C. Lee, L. Yang, A. J. Pearson, H. Lu, X.-J. She, L. Cui, K. H. L. Zhang, R. L. Z. Hoye, A. Karani, P. Xu, A. Sadhanala, N. C. Greenham, R. H. Friend, J. L. MacManus-Driscoll and D. Di, *ACS Appl. Mater. Interfaces*, 2018, **10**, 41849–41854.
- 380 V. Manjunath, S. Bimli, K. H. Parmar, P. M. Shirage and R. S. Devan, *Sol. Energy*, 2019, **193**, 387–394.
- 381 Z. Liu, J. Chang, Z. Lin, L. Zhou, Z. Yang, D. Chen, C. Zhang, S. Liu and Y. Hao, *Adv. Energy Mater.*, 2018, **8**, 1703432.
- 382 X. Yin, J. Zhai, L. Song, P. Du, N. Li, Y. Yang, J. Xiong and F. Ko, *ACS Appl. Mater. Interfaces*, 2019, **11**, 44308–44314.
- 383 U. K. Thakur, P. Kumar, S. Gusarov, A. E. Kobryn, S. Riddell, A. Goswami, K. M. Alam, S. Savela, P. Kar, T. Thundat, A. Meldrum and K. Shankar, *ACS Appl. Mater. Interfaces*, 2020, **12**, 11467–11478.
- 384 M. Feng, M. Wang, H. Zhou, W. Li, X. Xie, S. Wang, Z. Zang and S. Chen, *ACS Appl. Energy Mater.*, 2020, **3**, 9732–9741.
- 385 A. M. Elseman, L. Luo and Q. L. Song, *Dalton Trans.*, 2020, **49**, 14243–14250.
- 386 C. C. Boyd, R. C. Shallcross, T. Moot, R. Kerner, L. Bertoluzzi, A. Onno, S. Kavadiya, C. Chosy, E. J. Wolf, J. Werner, J. A. Raiford, C. de Paula, A. F. Palmstrom,

- Z. J. Yu, J. J. Berry, S. F. Bent, Z. C. Holman, J. M. Luther, E. L. Ratcliff, N. R. Armstrong and M. D. McGehee, *Joule*, 2020, **4**, 1759–1775.
- 387 F. Khan, B. D. Rezgui and J. H. Kim, *Sol. Energy*, 2020, **209**, 226–234.
- 388 Y. Wang, T. Mahmoudi and Y.-B. Hahn, *Adv. Energy Mater.*, 2020, **10**, 2000967.
- 389 Z. Hu, D. Chen, P. Yang, L. Yang, L. Qin, Y. Huang and X. Zhao, *Appl. Surf. Sci.*, 2018, **441**, 258–264.
- 390 P. S. Chandrasekhar, Y.-H. Seo, Y.-J. Noh and S.-I. Na, *Appl. Surf. Sci.*, 2019, **481**, 588–596.
- 391 J. H. Lee, Y. W. Noh, I. S. Jin, S. H. Park and J. W. Jung, *J. Power Sources*, 2019, **412**, 425–432.
- 392 Y. Xie, K. Lu, J. Duan, Y. Jiang, L. Hu, T. Liu, Y. Zhou and B. Hu, *ACS Appl. Mater. Interfaces*, 2018, **10**, 14153–14159.
- 393 J. Zhang, W. Mao, X. Hou, J. Duan, J. Zhou, S. Huang, W. Ou-Yang, X. Zhang, Z. Sun and X. Chen, *Sol. Energy*, 2018, **174**, 1133–1141.
- 394 Y. Wei, K. Yao, X. Wang, Y. Jiang, X. Liu, N. Zhou and F. Li, *Appl. Surf. Sci.*, 2018, **427**, 782–790.
- 395 D. Di Girolamo, N. Phung, M. Jošt, A. Al-Ashouri, G. Chistiakova, J. Li, J. A. Márquez, T. Unold, L. Korte, S. Albrecht, A. Di Carlo, D. Dini and A. Abate, *Adv. Mater. Interfaces*, 2019, **6**, 1900789.
- 396 J. H. Lee, Y. W. Noh, I. S. Jin and J. W. Jung, *Electrochim. Acta*, 2018, **284**, 253–259.
- 397 X. Wan, Y. Jiang, Z. Qiu, H. Zhang, X. Zhu, I. Sikandar, X. Liu, X. Chen and B. Cao, *ACS Appl. Energy Mater.*, 2018, **1**, 3947–3954.
- 398 X. Chen, L. Xu, C. Chen, Y. Wu, W. Bi, Z. Song, X. Zhuang, S. Yang, S. Zhu and H. Song, *J. Power Sources*, 2019, **444**, 227267.
- 399 M.-A. Park, I. J. Park, S. Park, J. Kim, W. Jo, H. J. Son and J. Y. Kim, *Curr. Appl. Phys.*, 2018, **18**, S55–S59.
- 400 W. Chen, F.-Z. Liu, X.-Y. Feng, A. B. Djurišić, W. K. Chan and Z.-B. He, *Adv. Energy Mater.*, 2017, **7**, 1700722.
- 401 X. Yin, J. Han, Y. Zhou, Y. Gu, M. Tai, H. Nan, Y. Zhou, J. Li and H. Lin, *J. Mater. Chem. A*, 2019, **7**, 5666–5676.
- 402 P.-C. Chen and S.-H. Yang, *ACS Appl. Energy Mater.*, 2019, **2**, 6705–6713.
- 403 B. Parida, S. Yoon, J. Ryu, S. Hayase, S. M. Jeong and D.-W. Kang, *ACS Appl. Mater. Interfaces*, 2020, **12**, 22958–22970.
- 404 G. Li, Y. Jiang, S. Deng, A. Tam, P. Xu, M. Wong and H.-S. Kwok, *Adv. Sci.*, 2017, **4**, 1700463.
- 405 W.-C. Lai, K.-W. Lin, Y.-T. Wang, T.-Y. Chiang, P. Chen and T.-F. Guo, *Adv. Mater.*, 2016, **28**, 3290–3297.
- 406 W.-C. Lai, K.-W. Lin, T.-F. Guo, P. Chen and Y.-Y. Liao, *Appl. Phys. Lett.*, 2018, **112**, 071103.
- 407 J. Kim, H. R. Lee, H. P. Kim, T. Lin, A. Kanwat, A. R. B. Mohd Yusoff and J. Jang, *Nanoscale*, 2016, **8**, 9284–9292.
- 408 P. Zhou, B. Li, Z. Fang, W. Zhou, M. Zhang, W. Hu, T. Chen, Z. Xiao and S. Yang, *Solar RRL*, 2019, **3**, 1900164.
- 409 S. Wang, B. Zhang, D. Feng, Z. Lin, J. Zhang, Y. Hao, X. Fan and J. Chang, *J. Mater. Chem. C*, 2019, **7**, 9270–9277.
- 410 X. Xia, Y. Jiang, Q. Wan, X. Wang, L. Wang and F. Li, *ACS Appl. Mater. Interfaces*, 2018, **10**, 44501–44510.
- 411 F. P. Gokdemir Choi, H. Moeini Alishah, S. Bozar, C. Kahveci, M. Canturk Rodop and S. Gunes, *Sol. Energy*, 2021, **215**, 434–442.
- 412 Y. Du, C. Xin, W. Huang, B. Shi, Y. Ding, C. Wei, Y. Zhao, Y. Li and X. Zhang, *ACS Sustainable Chem. Eng.*, 2018, **6**, 16806–16812.
- 413 Y. Liu, J. Duan, J. Zhang, S. Huang, W. Ou-Yang, Q. Bao, Z. Sun and X. Chen, *ACS Appl. Mater. Interfaces*, 2020, **12**, 771–779.
- 414 X. Yin, J. Zhai, P. Du, N. Li, L. Song, J. Xiong and F. Ko, *ChemSusChem*, 2020, **13**, 1006–1012.
- 415 W. Han, G. Ren, Z. Li, M. Dong, C. Liu and W. Guo, *J. Energy Chem.*, 2020, **46**, 202–207.
- 416 L. Xu, M. Qian, C. Zhang, W. Lv, J. Jin, J. Zhang, C. Zheng, M. Li, R. Chen and W. Huang, *Nano Energy*, 2020, **67**, 104244.
- 417 H. Sun, X. Hou, Q. Wei, H. Liu, K. Yang, W. Wang, Q. An and Y. Rong, *Chem. Commun.*, 2016, **52**, 8099–8102.
- 418 L. Xu, M. Qian, Q. Lu, H. Zhang and W. Huang, *Mater. Lett.*, 2019, **236**, 16–18.
- 419 Z. Liu, T. He, K. Liu, Q. Zhi and M. Yuan, *RSC Adv.*, 2017, **7**, 26202–26210.
- 420 H. T. Peng, W. H. Sun, Y. L. Li, S. Y. Ye, H. X. Rao, W. B. Yan, H. P. Zhou, Z. Q. Bian and C. H. Huang, *Nano Res.*, 2016, **9**, 2960–2971.
- 421 K. Eom, I. H. Yoo, Q. A. Sial and H. Seo, *Curr. Appl. Phys.*, 2021, **23**, 62–67.
- 422 Z. Liu, T. He, K. Liu, J. Wang, Y. Zhou, J. Yang, H. Liu, Y. Jiang, H. Ma and M. Yuan, *J. Mater. Chem. A*, 2017, **5**, 24282–24291.
- 423 T. H. Schloemer, J. A. Raiford, T. S. Gehan, T. Moot, S. Nanayakkara, S. P. Harvey, R. C. Bramante, S. Dunfield, A. E. Louks, A. E. Maughan, L. Bliss, M. D. McGehee, M. F. A. M. van Hest, M. O. Reese, S. F. Bent, J. J. Berry, J. M. Luther and A. Sellinger, *ACS Energy Lett.*, 2020, **5**, 2349–2360.
- 424 X. Yao, W. Xu, X. Huang, J. Qi, Q. Yin, X. Jiang, F. Huang, X. Gong and Y. Cao, *Org. Electron.*, 2017, **47**, 85–93.
- 425 T. Lei, H. Dong, J. Xi, Y. Niu, J. Xu, F. Yuan, B. Jiao, W. Zhang, X. Hou and Z. Wu, *Chem. Commun.*, 2018, **54**, 6177–6180.
- 426 C.-C. Chang, J.-H. Tao, C.-E. Tsai, Y.-J. Cheng and C.-S. Hsu, *ACS Appl. Mater. Interfaces*, 2018, **10**, 21466–21471.
- 427 L. Xu, H. Wang, X. Feng, Y. Zhou, Y. Chen, R. Chen and W. Huang, *Adv. Photonics Res.*, 2021, 2000132.
- 428 X. Yao, J. Qi, W. Xu, X. Jiang, X. Gong and Y. Cao, *ACS Omega*, 2018, **3**, 1117–1125.
- 429 D. Li, C. Tong, W. Ji, Z. Fu, Z. Wan, Q. Huang, Y. Ming, A. Mei, Y. Hu, Y. Rong and H. Han, *ACS Sustainable Chem. Eng.*, 2019, **7**, 2619–2625.
- 430 M. M. Tepliakova, A. N. Mikheeva, L. A. Frolova, A. G. Boldyreva, A. Elakshar, A. V. Novikov, S. A. Tsarev, M. I. Ustinova, O. R. Yamilova, A. G. Nasibulin, S. M. Aldoshin, K. J. Stevenson and P. A. Troshin, *J. Phys. Chem. Lett.*, 2020, **11**, 5563–5568.
- 431 S. Chu, R. Zhao, R. Liu, Y. Gao, X. Wang, C. Liu, J. Chen and H. Zhou, *Semicond. Sci. Technol.*, 2018, **33**, 115016.

- 432 J. A. Raiford, R. A. Belisle, K. A. Bush, R. Prasanna, A. F. Palmstrom, M. D. McGehee and S. F. Bent, *Sustainable Energy Fuels*, 2019, **3**, 1517–1525.
- 433 Y.-H. Lou and Z.-K. Wang, *Nanoscale*, 2017, **9**, 13506–13514.
- 434 Z. Liu, T. He, H. Wang, X. Song, H. Liu, J. Yang, K. Liu and H. Ma, *RSC Adv.*, 2017, **7**, 18456–18465.
- 435 D. Wang, N. K. Elumalai, M. A. Mahmud, M. Wright, M. B. Upama, K. H. Chan, C. Xu, F. Haque, G. Conibeer and A. Uddin, *Org. Electron.*, 2018, **53**, 66–73.
- 436 T.-H. Yeh, H.-Y. Lee and C.-T. Lee, *J. Alloys Compd.*, 2020, **822**, 153620.
- 437 J. Li, J. Qin, X. Liu, M. Ren, J. Tong, N. Zheng, W. Chen and Y. Xia, *Sol. Energy*, 2020, **211**, 1102–1109.
- 438 M. Cheng, Y. Li, M. Safdari, C. Chen, P. Liu, L. Kloo and L. Sun, *Adv. Energy Mater.*, 2017, **7**, 1602556.
- 439 S. S. Kanakillam, S. Shaji, B. Krishnan, S. Vazquez-Rodriguez, J. A. A. Martinez, M. I. M. Palma and D. A. Avellaneda, *Appl. Surf. Sci.*, 2020, **501**, 144223.
- 440 A. E. Shalan, T. Oshikiri, S. Narra, M. M. Elshanawany, K. Ueno, H.-P. Wu, K. Nakamura, X. Shi, E. W.-G. Diao and H. Misawa, *ACS Appl. Mater. Interfaces*, 2016, **8**, 33592–33600.
- 441 A. Huang, L. Lei, J. Zhu, Y. Yu, Y. Liu, S. Yang, S. Bao, X. Cao and P. Jin, *Langmuir*, 2017, **33**, 3624–3634.
- 442 A. Bashir, S. Shukla, J. H. Lew, S. Shukla, A. Bruno, D. Gupta, T. Baikie, R. Patidar, Z. Akhter, A. Priyadarshi, N. Mathews and S. G. Mhaisalkar, *Nanoscale*, 2018, **10**, 2341–2350.
- 443 Y. Zhou, X. Zhang, X. Lu, X. Gao, J. Gao, L. Shui, S. Wu and J.-M. Liu, *Solar RRL*, 2019, **3**, 1800315.
- 444 Y. Zhang, J. Ge, B. Mahmoudi, S. Förster, F. Syrowatka, A. W. Maijenburg and R. Scheer, *ACS Appl. Energy Mater.*, 2020, **3**, 3755–3769.
- 445 C.-H. Chiang, C.-C. Chen, M. K. Nazeeruddin and C.-G. Wu, *J. Mater. Chem. A*, 2018, **6**, 13751–13760.
- 446 F. P. Gökdemir Choi, *J. Mater. Sci.: Mater. Electron.*, 2021, **32**, 8136–8148.
- 447 B. Li, Y. Rui, J. Xu, Y. Wang, J. Yang, Q. Zhang and P. Müller-Buschbaum, *J. Colloid Interface Sci.*, 2020, **573**, 78–86.
- 448 Y. Dou, D. Wang, G. Li, Y. Liao, W. Sun, J. Wu and Z. Lan, *ACS Appl. Mater. Interfaces*, 2019, **11**, 32159–32168.
- 449 M. Heinemann, B. Eifert and C. Heiliger, *Phys. Rev. B: Condens. Matter Mater. Phys.*, 2013, **87**, 115111.
- 450 J. S. Shaikh, R. C. Pawar, R. S. Devan, Y. R. Ma, P. P. Salvi, S. S. Kolekar and P. S. Patil, *Electrochim. Acta*, 2011, **56**, 2127–2134.
- 451 T. Eom, S. Kim, R. E. Agbenyeke, H. Jung, S. M. Shin, Y. K. Lee, C. G. Kim, T.-M. Chung, N. J. Jeon, H. H. Park and J. Seo, *Adv. Mater. Interfaces*, 2021, **8**, 2170006.
- 452 Z.-K. Yu, W.-F. Fu, W.-Q. Liu, Z.-Q. Zhang, Y.-J. Liu, J.-L. Yan, T. Ye, W.-T. Yang, H.-Y. Li and H.-Z. Chen, *Chin. Chem. Lett.*, 2017, **28**, 13–18.
- 453 W. L. Yu, F. Li, H. Wang, E. Alarousu, Y. Chen, B. Lin, L. F. Wang, M. N. Hedhili, Y. Y. Li, K. W. Wu, X. B. Wang, O. F. Mohammed and T. Wu, *Nanoscale*, 2016, **8**, 6173–6179.
- 454 Q. Yu, J. Pan, J. Mei, Z. Chen, P. Wang, P. Wang, J. Wang, C. Song, Y. Zheng and C. Li, *J. Mater. Sci.*, 2021, **56**, 5736–5747.
- 455 Y. Guo, H. Lei, L. Xiong, B. Li and G. Fang, *J. Mater. Chem. C*, 2017, **5**, 8033–8040.
- 456 L.-C. Chen, C.-C. Chen, K.-C. Liang, S. H. Chang, Z.-L. Tseng, S.-C. Yeh, C.-T. Chen, W.-T. Wu and C.-G. Wu, *Nanoscale Res. Lett.*, 2016, **11**, 402.
- 457 I. Y. Y. Bu, Y.-S. Fu, J.-F. Li and T.-F. Guo, *RSC Adv.*, 2017, **7**, 46651–46656.
- 458 A. Savva, I. T. Papadas, D. Tsikritzis, G. S. Armatas, S. Kennou and S. A. Choulis, *J. Mater. Chem. A*, 2017, **5**, 20381–20389.
- 459 Y.-J. Chen, M.-H. Li, J.-C.-A. Huang and P. Chen, *Sci. Rep.*, 2018, **8**, 7646.
- 460 Q. Sun, S. Zhou, X. Shi, X. Wang, L. Gao, Z. Li and Y. Hao, *ACS Appl. Mater. Interfaces*, 2018, **10**, 11289–11296.
- 461 W. Sun, Y. Li, S. Ye, H. Rao, W. Yan, H. Peng, Y. Li, Z. Liu, S. Wang, Z. Chen, L. Xiao, Z. Bian and C. Huang, *Nanoscale*, 2016, **8**, 10806–10813.
- 462 Y. Ma, Y. Zhang, H. Zhang, H. Lv, R. Hu, W. Liu, S. Wang, M. Jiang, L. Chu, J. Zhang, X. A. Li, R. Xia and W. Huang, *Appl. Surf. Sci.*, 2021, **547**, 149117.
- 463 Z. Zhuang, L. Qiu, L. Dong, Y. Chen, Z. Chu, X. Ma, P. Du and J. Xiong, *Polym. Compos.*, 2020, **41**, 2145–2153.
- 464 M. A. Islam, Y. A. Wahab, M. U. Khandaker, A. Alsubaie, A. S. A. Almalki, D. A. Bradley and N. Amin, *Crystals*, 2021, **11**, 389.
- 465 A. M. Elseman, M. S. Selim, L. Luo, C. Y. Xu, G. Wang, Y. Jiang, D. B. Liu, L. P. Liao, Z. Hao and Q. L. Song, *ChemSusChem*, 2019, **12**, 3808–3816.
- 466 C.-C. Tseng, L.-C. Chen, L.-B. Chang, G.-M. Wu, W.-S. Feng, M.-J. Jeng, D. W. Chen and K.-L. Lee, *Sol. Energy*, 2020, **204**, 270–279.
- 467 C. Liu, X. Zhou, S. Chen, X. Zhao, S. Dai and B. Xu, *Adv. Sci.*, 2019, **6**, 1801169.
- 468 Y.-J. Chen, M.-H. Li, J.-C.-A. Huang and P. Chen, *J. Mater. Chem. C*, 2018, **6**, 6280–6286.
- 469 J. Kim, Y. Lee, B. Gil, A. J. Yun, J. Kim, H. Woo, K. Park and B. Park, *ACS Appl. Energy Mater.*, 2020, **3**, 7572–7579.
- 470 K. Deepthi Jayan and V. Sebastian, *Int. J. Energy Res.*, 2021, **45**, 16618–16632.
- 471 A. Kumar and S. Singh, *Mod. Phys. Lett. B*, 2020, **34**, 2050258.
- 472 M. I. Hossain, F. H. Alharbi and N. Tabet, *Sol. Energy*, 2015, **120**, 370–380.
- 473 J. E. Castellanos-Águila, L. Lodeiro, E. Menéndez-Proupin, A. L. Montero-Alejo, P. Palacios, J. C. Conesa and P. Wahnón, *ACS Appl. Mater. Interfaces*, 2020, **12**, 44648–44657.
- 474 J. X. M. Zheng-Johansson, I. Ebbsjö and R. L. McGreevy, *Solid State Ionics*, 1995, **82**, 115–122.
- 475 A. Pishtshev and S. Z. Karazhanov, *J. Chem. Phys.*, 2017, **146**, 064706.
- 476 S. Uthayaraj, D. G. B. C. Karunarathne, G. R. A. Kumara, T. Murugathas, S. Rasalingam, R. M. G. Rajapakse,

- P. Ravirajan and D. Velauthapillai, *Materials*, 2019, **12**, 2037.
- 477 J. A. Christians, R. C. M. Fung and P. V. Kamat, *J. Am. Chem. Soc.*, 2014, **136**, 758–764.
- 478 X. Li, J. Yang, Q. Jiang, W. Chu, D. Zhang, Z. Zhou and J. Xin, *ACS Appl. Mater. Interfaces*, 2017, **9**, 41354–41362.
- 479 J. Song, W. Hu, Z. Li, X.-F. Wang and W. Tian, *Sol. Energy Mater. Sol. Cells*, 2020, **207**, 110351.
- 480 D. B. Khadka, Y. Shirai, M. Yanagida and K. Miyano, *Sol. Energy Mater. Sol. Cells*, 2020, **210**, 110486.
- 481 S. Gharibzadeh, B. A. Nejjand, A. Moshaii, N. Mohammadian, A. H. Alizadeh, R. Mohammadpour, V. Ahmadi and A. Alizadeh, *ChemSusChem*, 2016, **9**, 1929–1937.
- 482 W. Y. Chen, L. L. Deng, S. M. Dai, X. Wang, C. B. Tian, X. X. Zhan, S. Y. Xie, R. B. Huang and L. S. Zheng, *J. Mater. Chem. A*, 2015, **3**, 19353–19359.
- 483 G. A. Sepalage, S. Meyer, A. Pascoe, A. D. Scully, F. Huang, U. Bach, Y.-B. Cheng and L. Spiccia, *Adv. Funct. Mater.*, 2015, **25**, 5650–5661.
- 484 H. Wang, Z. Yu, X. Jiang, J. Li, B. Cai, X. Yang and L. Sun, *Energy Technol.*, 2017, **5**, 1836–1843.
- 485 W. Sun, S. Ye, H. Rao, Y. Li, Z. Liu, L. Xiao, Z. Chen, Z. Bian and C. Huang, *Nanoscale*, 2016, **8**, 15954–15960.
- 486 J. Cao, B. Wu, J. Peng, X. Feng, C. Li and Y. Tang, *Sci. China: Chem.*, 2019, **62**, 363–369.
- 487 Y. Chen, J. Chu, L. Li, A. S. Yerramilli, Y. He, H. Yang, Y. Shen and T. L. Alford, *J. Mater. Sci.: Mater. Electron.*, 2021, **32**, 12929–12938.
- 488 H. Javaid, V. V. Duzhko and D. Venkataraman, *ACS Appl. Energy Mater.*, 2021, **4**, 72–80.
- 489 D. Saranin, P. Gostischev, D. Tatarinov, I. Ermanova, V. Mazov, D. Muratov, A. Tameev, D. Kuznetsov, S. Didenko and A. Di Carlo, *Materials*, 2019, **12**, 1406.
- 490 M. M. Byranvand, T. Kim, S. Song, G. Kang, S. U. Ryu and T. Park, *Adv. Energy Mater.*, 2018, **8**, 1702235.
- 491 S. Ye, H. Rao, Z. Zhao, L. Zhang, H. Bao, W. Sun, Y. Li, F. Gu, J. Wang, Z. Liu, Z. Bian and C. Huang, *J. Am. Chem. Soc.*, 2017, **139**, 7504–7512.
- 492 M. M. Salah, K. M. Hassan, M. Abouelatta and A. Shaker, *Optik*, 2019, **178**, 958–963.
- 493 S. Z. Haider, H. Anwar, S. Manzoor, A. G. Ismail and M. Wang, *Curr. Appl. Phys.*, 2020, **20**, 1080–1089.
- 494 P. Pattanasattayavong, G. O. N. Ndjawa, K. Zhao, K. W. Chou, N. Yaacobi-Gross, B. C. O'Regan, A. Amassian and T. D. Anthopoulos, *Chem. Commun.*, 2013, **49**, 4154–4156.
- 495 S. Ito, S. Tanaka, H. Vahlman, H. Nishino, K. Manabe and P. Lund, *ChemPhysChem*, 2014, **15**, 1194–1200.
- 496 S. Chavhan, O. Miguel, H.-J. Grande, V. Gonzalez-Pedro, R. S. Sánchez, E. M. Barea, I. Mora-Seró and R. Tena-Zaera, *J. Mater. Chem. A*, 2014, **2**, 12754–12760.
- 497 A. S. Subbiah, A. Halder, S. Ghosh, N. Mahuli, G. Hodes and S. K. Sarkar, *J. Phys. Chem. Lett.*, 2014, **5**, 1748–1753.
- 498 S. Y. Ye, W. H. Sun, Y. L. Li, W. B. Yan, H. T. Peng, Z. Q. Bian, Z. W. Liu and C. H. Huang, *Nano Lett.*, 2015, **15**, 3723–3728.
- 499 J. W. Jung, C.-C. Chueh and A. K. Y. Jen, *Adv. Energy Mater.*, 2015, **5**, 1500486.
- 500 I. S. Yang, M. R. Sohn, S. D. Sung, Y. J. Kim, Y. J. Yoo, J. Kim and W. I. Lee, *Nano Energy*, 2017, **32**, 414–421.
- 501 J. Wang, S. Gong, Z. Chen and S. Yang, *ACS Appl. Mater. Interfaces*, 2021, **13**, 22684–22693.
- 502 M. Lyu, J. Chen and N.-G. Park, *J. Solid State Chem.*, 2019, **269**, 367–374.
- 503 J. Liu, S. K. Pathak, N. Sakai, R. Sheng, S. Bai, Z. Wang and H. J. Snaith, *Adv. Mater. Interfaces*, 2016, **3**, 1600571.
- 504 P. Qin, S. Tanaka, S. Ito, N. Tetreault, K. Manabe, H. Nishino, M. K. Nazeeruddin and M. Grätzel, *Nat. Commun.*, 2014, **5**, 3834.
- 505 Q. Xi, G. Gao, H. Zhou, Y. Zhao, C. Wu, L. Wang, P. Guo and J. Xu, *Nanoscale*, 2017, **9**, 6136–6144.
- 506 I. Zimmermann, P. Gratia, D. Martineau, G. Grancini, J.-N. Audinot, T. Wirtz and M. K. Nazeeruddin, *J. Mater. Chem. A*, 2019, **7**, 8073–8077.
- 507 G. A. Sepalage, S. Meyer, A. R. Pascoe, A. D. Scully, U. Bach, Y.-B. Cheng and L. Spiccia, *Nano Energy*, 2017, **32**, 310–319.
- 508 J. Kim, Y. Lee, A. J. Yun, B. Gil and B. Park, *ACS Appl. Mater. Interfaces*, 2019, **11**, 46818–46824.
- 509 N. Arora, M. I. Dar, A. Hinderhofer, N. Pellet, F. Schreiber, S. M. Zakeeruddin and M. Grätzel, *Science*, 2017, **358**, 768–771.
- 510 C. Liu, L. Zhang, Y. Li, X. Zhou, S. She, X. Wang, Y. Tian, A. K. Y. Jen and B. Xu, *Adv. Funct. Mater.*, 2020, **30**, 1908462.
- 511 Y. Xu, Y. Tian, M. Hou, Y. Wu, Y. Ding, Y. Zhao, X. Zhang and G. Hou, *J. Phys. Chem. C*, 2020, **124**, 27977–27984.
- 512 I. S. Yang, S. Lee, J. Choi, M. T. Jung, J. Kim and W. I. Lee, *J. Mater. Chem. A*, 2019, **7**, 6028–6037.
- 513 M. Kim, A. Alfano, G. Perotto, M. Serri, N. Dengo, A. Mezzetti, S. Gross, M. Prato, M. Salerno, A. Rizzo, R. Sorrentino, E. Cescon, G. Meneghesso, F. Di Fonzo, A. Petrozza, T. Gatti and F. Lamberti, *Commun. Mater.*, 2021, **2**, 6.
- 514 P. Xu, J. Liu, J. Huang, F. Yu, R. Zhang, C.-H. Li, Y.-X. Zheng and J.-L. Zuo, *Solar RRL*, 2021, **5**, 2000777.
- 515 I. S. Jin, J. H. Lee, Y. W. Noh, S. H. Park and J. W. Jung, *Inorg. Chem. Front.*, 2019, **6**, 2158–2166.
- 516 L. Xu, Y. Li, C. Zhang, Y. Liu, C. Zheng, W. Lv, M. Li, Y. Chen, W. Huang and R. Chen, *Sol. Energy Mater. Sol. Cells*, 2020, **206**, 110316.
- 517 I. S. Jin, S. H. Park, K. S. Kim and J. W. Jung, *J. Alloys Compd.*, 2020, **847**, 156512.
- 518 S. Z. Haider, H. Anwar and M. Wang, *Phys. Status Solidi A*, 2019, **216**, 1900102.
- 519 B. Gil, A. J. Yun, Y. Lee, J. Kim, B. Lee and B. Park, *Electron. Mater. Lett.*, 2019, **15**, 505–524.
- 520 F. Igbari, M. Li, Y. Hu, Z.-K. Wang and L.-S. Liao, *J. Mater. Chem. A*, 2016, **4**, 1326–1335.
- 521 I. Y.-Y. Bu, Y.-C. Lu, Y.-S. Fu and C.-T. Hung, *Optik*, 2020, **210**, 164505.
- 522 H. Zhang, H. Wang, H. Zhu, C.-C. Chueh, W. Chen, S. Yang and A. K. Y. Jen, *Adv. Energy Mater.*, 2018, **8**, 1702762.
- 523 W. A. Dunlap-Shohl, T. B. Daunis, X. Wang, J. Wang, B. Zhang, D. Barrera, Y. Yan, J. W. P. Hsu and D. B. Mitzi, *J. Mater. Chem. A*, 2018, **6**, 469–477.

- 524 S. Akin, Y. Liu, M. I. Dar, S. M. Zakeeruddin, M. Grätzel, S. Turan and S. Sonmezoglu, *J. Mater. Chem. A*, 2018, **6**, 20327–20337.
- 525 P.-L. Qin, Q. He, C. Chen, X.-L. Zheng, G. Yang, H. Tao, L.-B. Xiong, L. Xiong, G. Li and G.-J. Fang, *Solar RRL*, 2017, **1**, 1700058.
- 526 B. Yang, D. Ouyang, Z. Huang, X. Ren, H. Zhang and W. C. H. Choy, *Adv. Funct. Mater.*, 2019, **29**, 1902600.
- 527 S. Jeong, S. Seo and H. Shin, *RSC Adv.*, 2018, **8**, 27956–27962.
- 528 I. T. Papadas, A. Savva, A. Ioakeimidis, P. Eleftheriou, G. S. Armatas and S. A. Choulis, *Mater. Today Energy*, 2018, **8**, 57–64.
- 529 B. Lee, A. J. Yun, J. Kim, B. Gil, B. Shin and B. Park, *Adv. Mater. Interfaces*, 2019, **6**, 1901372.
- 530 Y. Chen, Z. Yang, X. Jia, Y. Wu, N. Yuan, J. Ding, W.-H. Zhang and S. Liu, *Nano Energy*, 2019, **61**, 148–157.
- 531 Y. Chen, W. Tang, Y. Wu, R. Yuan, J. Yang, W. Shan, S. Zhang and W.-H. Zhang, *Solar RRL*, 2020, **4**, 2000344.
- 532 D. Ouyang, C. Chen, Z. Huang, L. Zhu, Y. Yan and W. C. H. Choy, *ACS Appl. Mater. Interfaces*, 2021, **13**, 16611–16619.
- 533 J. Tirado, C. Roldán-Carmona, F. A. Muñoz-Guerrero, G. Bonilla-Arboleda, M. Ralaizarisoa, G. Grancini, V. I. E. Queloz, N. Koch, M. K. Nazeeruddin and F. Jaramillo, *Appl. Surf. Sci.*, 2019, **478**, 607–614.
- 534 R. Hu, R. Zhang, Y. Ma, W. Liu, L. Chu, W. Mao, J. Zhang, J. Yang, Y. Pu and X. A. Li, *Appl. Surf. Sci.*, 2018, **462**, 840–846.
- 535 J. Li, C. Kuang, M. Zhao, C. Zhao, L. Liu, F. Lu, N. Wang, C. Huang, C. Duan, H. Jian, L. Yao and T. Jiu, *Inorg. Chem.*, 2018, **57**, 8375–8381.
- 536 L. S. Khanzada, I. Levchuk, Y. Hou, H. Azimi, A. Osvet, R. Ahmad, M. Brandl, P. Herre, M. Distaso, R. Hock, W. Peukert, M. Batentschuk and C. J. Brabec, *Adv. Funct. Mater.*, 2016, **26**, 8300–8306.
- 537 Z.-J. Zhou, Y.-Q. Deng, P.-P. Zhang, D.-X. Kou, W.-H. Zhou, Y.-N. Meng, S.-J. Yuan and S.-X. Wu, *Solar RRL*, 2019, **3**, 1800354.
- 538 G. Y. Ashebir, C. Dong, Z. Wan, J. Qi, J. Chen, Q. Zhao, W. Chen and M. Wang, *J. Phys. Chem. Solids*, 2019, **129**, 204–208.
- 539 M. Jamil, A. Ali, K. Mahmood, M. I. Arshad, S. Tahir, M. Ajazun Nabi, S. Ikram, N. Amin and S. Hussain, *J. Alloys Compd.*, 2020, **821**, 153221.
- 540 B. Koo, H. Jung, M. Park, J. Y. Kim, H. J. Son, J. Cho and M. J. Ko, *Adv. Funct. Mater.*, 2016, **26**, 5400–5407.
- 541 A. J. Huckaba, P. Sanghyun, G. Grancini, E. Bastola, C. K. Taek, L. Younghui, K. P. Bhandari, C. Ballif, R. J. Ellingson and M. K. Nazeeruddin, *ChemistrySelect*, 2016, **1**, 5316–5319.
- 542 J. Ge, C. R. Grice and Y. F. Yan, *J. Mater. Chem. A*, 2017, **5**, 2920–2928.
- 543 A. Ioakeimidis, I. T. Papadas, D. Tsikritzis, G. S. Armatas, S. Kennou and S. A. Choulis, *APL Mater.*, 2019, **7**, 021101.
- 544 J. H. Lee, I. S. Jin, Y. W. Noh, S. H. Park and J. W. Jung, *ACS Sustainable Chem. Eng.*, 2019, **7**, 17661–17670.
- 545 I. T. Papadas, A. Ioakeimidis, G. S. Armatas and S. A. Choulis, *Adv. Sci.*, 2018, **5**, 1701029.
- 546 B. Huang, Y. Cheng, H. Lei, L. Hu, Z. Li, X. Huang, L. Chen and Y. Chen, *Chem. Commun.*, 2021, **57**, 4015–4018.
- 547 B. Tan, S. R. Raga, A. S. R. Chesman, S. O. Furer, F. Zheng, D. P. McMeekin, L. Jiang, W. Mao, X. Lin, X. Wen, J. Lu, Y.-B. Cheng and U. Bach, *Adv. Energy Mater.*, 2019, **9**, 1901519.
- 548 M. Li, Z. K. Wang, Y. G. Yang, Y. Hu, S. L. Feng, J. M. Wang, X. Y. Gao and L. S. Liao, *Adv. Energy Mater.*, 2016, **6**, 1601156.
- 549 S. N. Habisreutinger, T. Leijtens, G. E. Eperon, S. D. Stranks, R. J. Nicholas and H. J. Snaith, *Nano Lett.*, 2014, **14**, 5561–5568.
- 550 G. Li, J. Song, D. Wang, W. Sun, J. Wu and Z. Lan, *J. Power Sources*, 2021, **481**, 229149.
- 551 W. Sun, P. Yuan, S. Wang, Y. Du, J. Zou, F. Cao, Z. Lan and J. Wu, *Electrochim. Acta*, 2021, **380**, 138233.
- 552 Z. Zhao, L. Yuan, J. Huang, J. Shi, Y. Cao, W. Zi and W. Zhang, *Org. Electron.*, 2020, **78**, 105557.
- 553 P. Li, M. I. Omer Mohamed, C. Xu, X. Wang and X. Tang, *Org. Electron.*, 2020, **78**, 105582.
- 554 Z. Niu, E. Zheng, H. Dong, G. A. Tosado and Q. Yu, *ACS Appl. Energy Mater.*, 2020, **3**, 9656–9666.
- 555 J. W. Liu, S. Pathak, T. Stergiopoulos, T. Leijtens, K. Wojciechowski, S. Schumann, N. Kausch-Busies and H. J. Snaith, *J. Phys. Chem. Lett.*, 2015, **6**, 1666–1673.
- 556 Z. K. Wang, M. Li, D. X. Yuan, X. B. Shi, H. Ma and L. S. Liao, *ACS Appl. Mater. Interfaces*, 2015, **7**, 9645–9651.
- 557 X. Zhou, M. Hu, C. Liu, L. Zhang, X. Zhong, X. Li, Y. Tian, C. Cheng and B. Xu, *Nano Energy*, 2019, **63**, 103866.
- 558 H. Yi, D. Wang, L. Duan, F. Haque, C. Xu, Y. Zhang, G. Conibeer and A. Uddin, *Electrochim. Acta*, 2019, **319**, 349–358.
- 559 E. H. Jung, N. J. Jeon, E. Y. Park, C. S. Moon, T. J. Shin, T.-Y. Yang, J. H. Noh and J. Seo, *Nature*, 2019, **567**, 511–515.
- 560 X. Wang, T. Ederth and O. Inganäs, *Langmuir*, 2006, **22**, 9287–9294.
- 561 M. J. Jeong, K. M. Yeom, S. J. Kim, E. H. Jung and J. H. Noh, *Energy Environ. Sci.*, 2021, **14**, 2419–2428.
- 562 D. Bi, L. Yang, G. Boschloo, A. Hagfeldt and E. M. Johansson, *J. Phys. Chem. Lett.*, 2013, **4**, 1532–1536.
- 563 S. Valero, S. Collavini, S. F. Völker, M. Saliba, W. R. Tress, S. M. Zakeeruddin, M. Grätzel and J. L. Delgado, *Macromolecules*, 2019, **52**, 2243–2254.
- 564 K. Lee, H. Yu, J. W. Lee, J. Oh, S. Bae, S. K. Kim and J. Jang, *J. Mater. Chem. C*, 2018, **6**, 6250–6256.
- 565 K.-C. Wang, P.-S. Shen, M.-H. Li, S. Chen, M.-W. Lin, P. Chen and T.-F. Guo, *ACS Appl. Mater. Interfaces*, 2014, **6**, 11851–11858.
- 566 J. W. Jung, C.-C. Chueh and A. K.-Y. Jen, *Adv. Mater.*, 2015, **27**, 7874–7880.
- 567 X. Yin, P. Chen, M. Que, Y. Xing, W. Que, C. Niu and J. Shao, *ACS Nano*, 2016, **10**, 3630–3636.
- 568 K. Wang, C. Wu, Y. Hou, D. Yang, T. Ye, J. Yoon, M. Sanghadasa and S. Priya, *Energy Environ. Sci.*, 2020, **13**, 3412–3422.

- 569 J. Yang, Q. Cao, Z. He, X. Pu, T. Li, B. Gao and X. Li, *Nano Energy*, 2021, **82**, 105731.
- 570 L. Li, X. R. Zhang, H. P. Zeng, X. Zheng, Y. Zhao, L. Luo, F. X. Liu and X. Li, *Chem. Eng. J.*, 2022, **443**, 136405.
- 571 H. Wang, Z. Yu, J. Lai, X. Song, X. Yang, A. Hagfeldt and L. Sun, *J. Mater. Chem. A*, 2018, **6**, 21435–21444.
- 572 K. Ramachandran, C. Jeganathan and S. Karuppuchamy, *J. Alloys Compd.*, 2021, **881**, 160530.
- 573 R. P. Srivastava, H. S. Jung and D. Y. Khang, *Nanomaterials*, 2022, **12**, 1467.
- 574 L. Lin, L. Jiang, P. Li, B. Fan and Y. Qiu, *J. Phys. Chem. Solids*, 2019, **124**, 205–211.
- 575 V. Arjun, K. P. Muthukumar, K. Ramachandran, A. Nithya and S. Karuppuchamy, *J. Alloys Compd.*, 2022, **923**, 166285.
- 576 Q. Guo, C. Wang, J. Li, Y. Bai, F. Wang, L. Liu, B. Zhang, T. Hayat, A. Alsaedi and Z. A. Tan, *Phys. Chem. Chem. Phys.*, 2018, **20**, 21746–21754.
- 577 X. Yao, H. Geng, Y. Gu, H. Cui, G. Guan and M. Han, *J. Phys. Chem. C*, 2021, **125**, 23474–23482.
- 578 S. Park, D. W. Kim and S. Y. Park, *Adv. Funct. Mater.*, 2022, **32**, 2200437.
- 579 G. D. Li, K. M. Deng, Y. F. Dou, Y. S. Liao, D. Wang, J. H. Wu and Z. Lan, *Sol. Energy*, 2019, **193**, 111–117.
- 580 X. Yan, J. H. Zheng, L. L. Zheng, G. H. Lin, H. D. Lin, G. Chen, B. B. Du and F. Y. Zhang, *Mater. Res. Bull.*, 2018, **103**, 150–157.
- 581 J. Yun, J. Jun, H. Yu, K. Lee, J. Ryu, J. Lee and J. Jang, *J. Mater. Chem. A*, 2017, **5**, 21750–21756.
- 582 J. H. Kim, P. W. Liang, S. T. Williams, N. Cho, C. C. Chueh, M. S. Glaz, D. S. Ginger and A. K. Y. Jen, *Adv. Mater.*, 2015, **27**, 695–701.
- 583 F. P. G. Choi, *J. Mater. Sci.: Mater. Electron.*, 2021, **32**, 8136–8148.
- 584 A. B. Huang, L. Lei, Y. Yu, Y. Liu, S. W. Yang, S. H. Bao, X. Cao and P. Jin, *Nanotechnology*, 2017, **28**, 20LT02.
- 585 K. Ramachandran, C. Jeganathan, G. P. Kalaignan and S. Karuppuchamy, *Ceram. Int.*, 2021, **47**, 17883–17894.
- 586 G. Kim, N. Kwon, D. Lee, M. Kim, M. Kim, Y. Lee, W. Kim, D. Hyeon, B. Kim, M. S. Jeong, J. Hong and J. Yang, *ACS Appl. Mater. Interfaces*, 2022, **14**, 5203–5210.
- 587 B. R. Krishna, G. Veerappan, P. Bhyrappa, C. Sudakar and E. Ramasamy, *Mater. Adv.*, 2022, **3**, 2000–2010.
- 588 Y. P. Liao, N. Tian, J. L. Wang, D. S. Yao, G. Y. Zheng, B. Zhou, Y. H. Yang and F. Long, *ACS Appl. Energy Mater.*, 2022, **5**, 9542–9548.
- 589 U. Er, K. C. Icli and M. Ozenbas, *J. Solid State Electrochem.*, 2020, **24**, 293–304.
- 590 S. S. Mali, J. V. Patil and C. K. Hong, *J. Mater. Chem. A*, 2019, **7**, 10246–10255.
- 591 H. Wang, H. A. Dewi, T. M. Koh, A. Bruno, S. Mhaisalkar and N. Mathews, *ACS Appl. Mater. Interfaces*, 2019, **12**, 484–493.
- 592 T. H. Chowdhury, M. Akhtaruzzaman, M. E. Kayesh, R. Kaneko, T. Noda, J.-J. Lee and A. Islam, *Sol. Energy*, 2018, **171**, 652–657.
- 593 H. Javaid, N. Heller, V. V. Duzhko, N. Hight-Huf, M. D. Barnes and D. Venkataraman, *ACS Appl. Energy Mater.*, 2022, **5**, 8075–8083.
- 594 F. Behrouznejad, M. Forouzandeh, R. Khosroshahi, K. Meraji, M. N. Badrabad, M. Dehghani, X. G. Li, Y. Q. Zhan, Y. Liao, Z. J. Ning and N. Taghavinia, *Solar RRL*, 2020, **4**, 564.
- 595 F. Ansari, M. Salavati-Niasari, O. Amiri, N. Mir, B. A. Nejand and V. Ahmadi, *Ind. Eng. Chem. Res.*, 2020, **59**, 743–750.
- 596 Y. Hou, L. J. Tang, H. W. Qiao, Z. R. Zhou, Y. L. Zhong, L. R. Zheng, M. J. Chen, S. Yang and H. G. Yang, *J. Mater. Chem. A*, 2019, **7**, 20905–20910.



Effect of low energy argon ion irradiation on work function of AISI 304L stainless steel

Ashish B. Thorat¹ · Sneha P. Kandare¹ · Shalaka A. Kamble¹ · Mayuri M. Attarde² · Avinash V. Rokade¹ · Fakir Mohammad D. Attar³ · Sunil G. Kulkarni⁴ · Vikas L. Mathe¹ · Vasant N. Bhoraskar¹ · Sanjay D. Dhole¹ · Shailendra S. Dahiwale¹

Received: 21 September 2022 / Accepted: 11 April 2023

© The Author(s), under exclusive licence to Springer-Verlag GmbH, DE part of Springer Nature 2023

Abstract

The effect of low-energy Ar⁺ ion irradiation on the work function of stainless steel AISI 304L (SS-304L) was studied by varying energy and fluence of Ar⁺ ion. The irradiation of Ar⁺ ions on stainless steel creates several vacancies in the target material which resulted a change in work function. The retarding field diode method was used for the measurement of work function. Results reveal work function decreases with an increase in ion energy (for fixed ion fluence) of irradiated Ar⁺ ion. Furthermore, it was observed that at varying ion fluence (for fixed ion energy) the decrease in work function value was more prominently, but at higher fluence, it again increases. In both (energy and fluence) cases of irradiation, the displacement per atom (DPA) in the material has been estimated with the stopping range using the SRIM-2013.00 program and is correlated with the experimental observation. Overall, the maximum work function was observed to be decreased by ~7.28% relative to the pristine sample in the case of fluence variation keeping the energy constant at 30 keV. The results indicate that low-energy ion irradiation can be utilized for work function modulation of materials and can be optimized by controlling ion fluence. The results are useful for further understanding of corrosion rate of materials and the data are extremely important for various nuclear reactors, where these materials are used.

Keywords Low energy ion irradiation · DPA · Work function · SS-304L

1 Introduction

Stainless Steel is an important material for many decades due to its good stability, specific material properties, easy fabrication, broad applicability in circuital parts, etc. Due to the long durability and stability of stainless steel, it has a very high demand in metallurgical processes, construction,

various engineering applications, etc. [1, 2]. However, Stainless steel is a corrosive metal when it comes in contact with a humid environment. M. Stratmann et al. investigated the kinetics of corrosion rate and corrosion potential of the metals, such as iron and steel, during drying of wetted metal surfaces. They have shown if the surface kept in humid environment the voltage drop across the oxide scale formed on top of the iron surface is small as a result corrosion rate changes [3]. M. Briceno et al. reported ion irradiation on 304 stainless steel which forms defects on the mobility of dislocations, dislocation sources and newly generated dislocations. In this work they have reported that mobility of dislocations is altered due to ion irradiation and in depth analysis is given for the same [4]. The content of Chromium (Cr) and Nickel (Ni) in stainless steel is responsible for its superior corrosion resistance [5]. Austenitic stainless steel used in biomaterials engineering application. Reports are available on the measurements made for the corrosion resistance with electropolishing methods for austenitic stainless steel [6, 7]. To protect from corrosion of austenitic stainless

✉ Sanjay D. Dhole
sanjay@physics.unipune.ac.in

✉ Shailendra S. Dahiwale
ssd@physics.unipune.ac.in

¹ Department of Physics, Savitribai Phule Pune University, Pune 411007, India

² Department of Physics, The Poona Gujarati Kelvani Mandal's, Haribhai V. Desai College, Pune 411002, India

³ Department of Physics, AKI's Poona College, Camp, Pune 411001, India

⁴ Department of Physics, Willingdon College, Vishrambag, Sangli 416 415, India

steel, electrochemical treatment was also been used [8]. Earlier, Akos Horvath et al. investigated the behaviour of work function for the stainless-steel material by H^+ and Ar^+ ions irradiation. It was found that the stability of corrosion depends on the work function of the material as well as on the projectile ion species [9]. Controlling the corrosion rate is of prime importance from the application point of view.

The metal or semiconductors when exposed to high energy radiation leads to the formation of lattice defects, such as vacancies as well as dislocation loops near the interface. As a result of which materials properties may get altered [10–12]. G. D. Tolstolutskaia et al. studied the nano hardness and microstructural changes in SS-316 austenitic stainless steel by influence of different gaseous (hydrogen, helium, argon) ion irradiation. They found that regardless of the type of incident energetic ions; the formation of radiation-induced dislocation structure is responsible for hardening of the steel [13]. They further extended their work for the swelling behavior of 18Cr10NiTi austenitic stainless steel irradiated with energetic Ar^+ ions which shows changing behavior of microstructure and swelling occur after 0.7–1.4 MeV Ar^+ irradiations in the temperature range of 550–700 °C to doses between of 40 and 105 DPA. He revealed that microstructure strongly based on Ar^+ concentration, implantation temperature and level of displacements per atom [14]. The heavy ion irradiation causes a change in the magnetic properties of the soft magnetic alloys as a result of a reduction in coercivity and removal of anisotropy [15]. Stainless steel is an important material for accelerators as well as nuclear reactors. In the accelerators or nuclear reactors, the material gets exposed to various radiation, such as the proton, neutron, or ions. Exposure to such radiation causes activations and deteriorations in the physical and chemical properties of the materials [16]. Very recently 247 MeV Ar ions irradiation on martensitic steel (SIMP) material was reported by Cunfeng Yao et al. They reported that due to ion irradiation thickness of surface oxides increases with modification in microstructure of oxides [17]. Austenitic stainless steel (ASS) was irradiated with 1.1 MeV Nitrogen ions which show a hardening behavior after irradiation reported by Chaoliang Xu et al. [18]. Thus, as mentioned above, there is a massive scope of the stainless-steel material in various fields, such as construction, metallurgy, biomedical, nuclear reactors, electronic, etc. However, stainless-steel material has tendency that they easily gets corroded due to various reasons and thus their properties gets degraded. Various physical and chemical approaches are used to reduce the corrosion of this material. In this work also, our aim is to explore the effect of ion irradiation on SS-304L work function, which is related to corrosion property.

A very few reports are available for Ar^+ ions irradiation on stainless steel. In the present work we report the effect of

Ar^+ ion irradiation on the SS-304L material. The Paper is divided into two part. In first part, study on Ar^+ ion irradiation on the work function of SS-304L at different ion energy Ar^+ ion (keeping the ion fluence fix) was carried out and in second part of study on Ar^+ ion irradiation on the work function of SS-304L at different ion fluences (keeping ion energy fix at 30 keV) was carried out. For both the cases, we studied the variation in work function along with the calculations of DPA. The observed variation in work function is implied to change the corrosion property.

2 Experimental method

2.1 Sample preparation

In the present work, a piece of SS-304L material of size 10 mm × 10 mm × 0.5 mm was cut and taken directly for experiments. The cleaning of samples was done with soap water, ethanol, and ultra-sonication for 5 min at room temperature. The sample was further sonicated for 60 min in isopropanol at room temperature. After that, the samples were left for drying overnight under ambient conditions.

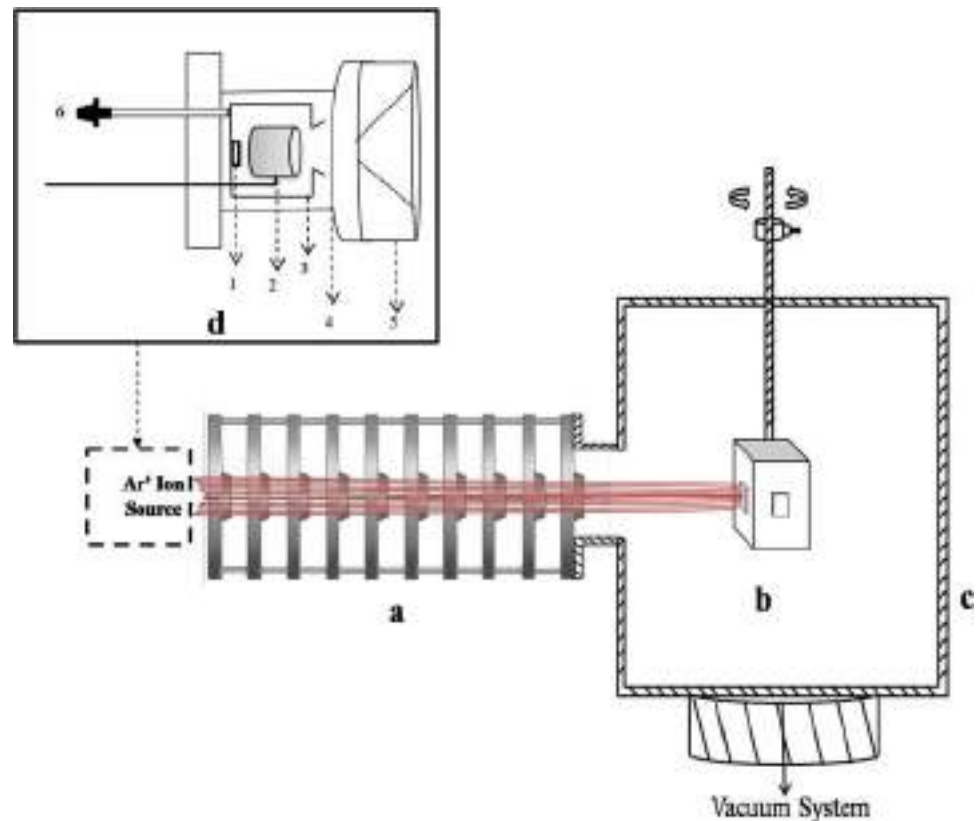
2.2 Ion irradiation

The indigenously developed low energy (5–100 keV) ion irradiation facility at the Department of Physics, Savitribai Phule Pune University was used for ion irradiation purpose. Figure 1 shows a schematic view of the ion irradiation facility. In this system, the penning ionization gauge (PIG) type gaseous ion source is used to get the ion species.

Gaseous ion sources primarily consist of cylindrical anodes and cathodes. It is a cold cathode discharge type ion source. In the cathode region, the gas to be ionized is injected through a gas needle valve. The cathode is a hollow cylinder made from mild steel (MS). Inside the cathode cylinder, a hollow thin anode cylinder is placed. A Neodymium permanent magnet (NdFeB) is placed at the center of the cathode bottom face. The detailed schematic of the ion source is shown in inset of Fig. 1d.

Potential difference of about 3 kV is applied between the cathode and anode. When gas is fed into the cathode region, the stray electrons gets accelerated and collide with neutral gas atoms while traveling toward the anode, thereby creating electric discharge. Electrons from first ionization further get accelerated and gain enough energy to knock out electrons from other neutrals atoms. This continuous process creates a plasma at the central part of anode. The permanent magnet helps in increasing the density and sustaining the plasma. Finally, the ions are extracted from the plasma by applying suitable potential to extraction electrode.

Fig. 1 Schematic view of ion irradiation facility of energy ranging 5–100 keV. **a** Ion accelerator tube with ion source. **b** Sample holder cube. **c** Experimental Chamber placed on the vacuum system. **d** Schematic of the penning ionization gauge (PIG) type gaseous ion source 1—Magnet, 2—Anode, 3—Cathode, 4—Nylon Case, 5—Extractor, 6—Gas Inlet



The total potential drops due to resistor chain across anode and last electrode of accelerator from where ions are extracted and falls on the sample holder results in the total ion energy, which is the kinetic energy of ions. The ion energy can be varied by increasing the high-voltage between anode and last extraction electrode. The ion fluence can be varied by varying ion irradiation time.

The SS-304L sample was placed on the copper sample holder and it was suspended with Wilson port. The desired Ar^+ ion energy was used for the sample irradiation. The ion current density was $3.53 \mu\text{A}\cdot\text{cm}^{-2} \pm 0.015\%$ and it was kept constant throughout the experiment under the vacuum pressure of 4×10^{-4} Pa. Before irradiation, the base pressure in the chamber was maintained at 1×10^{-4} Pa. At a time four samples were placed on a hollow cubical sample holder, one sample placed on each face of the cube (leaving the top and bottom face empty). One by one each sample was exposed to the Ar^+ ion beam by rotating the sample holder by 90° without breaking vacuum pressure. These irradiated samples were then used for further analysis.

2.3 DPA calculations

Estimation of ion distribution in the target material was computed using the Monte Carlo simulation Code with SRIM-13.00 Software. The dislocation of the target atoms

in the solid phase of a material by bombarding ions creates vacancies. The vacancies created per ion per unit length give the displacement per ion per unit length. The SRIM-13.00 also estimates stopping energy and projected range of ions in the matter along with vacancies created per ion per unit length [19–22]. The total number of displaced atoms in a unit volume over a total number of atoms in the material gives a DPA [9, 23, 24].

The ion energy, angle of incidence of ions, elemental composition, and atomic density of target material are the required parameters to find out the full cascade of ion distribution in the target material which was used as input for SRIM-13.00. The angle of incidence for ion was kept at 0° and atomic density input for SS-304L was 7.78 g/cm^3 . All the results recorded from SRIM-13.00 were the average of 9999 ion trajectories. The required calculation of DPA was done by following Eq. 1 given by Akos Horvath et al [18]

$$\text{Peak Area} = \int_{x_c - x_1}^{x_c + x_2} \text{DPA}(x) dx. \quad (1)$$

Here, x_c is the projectile depth, where we get a maximum of $\text{DPA}(x)$, full-width half maxima (FWHM) have been computed in the region which is denoted by $x_1 + x_2$ for the $\text{DPA}(x)$ distribution.

2.4 Measurement of work function

Work function measurement for SS-304L samples was carried out using retarding field diode method with the help of a low energy electron beam. The design of the electron gun is similar to that as discussed by Klauser and Bas [25]. Work function measurement of a variety of samples viz. metals, semiconductors are well-known and reported earlier, and [26, 27] almost similar method applies to insulators too.

In the present work, work function measurement system used consists of an electron gun and sample manipulator assembly enclosed in the Stainless-Steel high vacuum chamber. The polycrystalline gold sample was used as a reference sample which was placed on the sample manipulator along with other samples. The work function of gold ($\phi = 4.9$ eV) was taken as a reference for calculating the work function of the pristine and irradiated SS-304L samples. In the retarding field diode method, the sample was kept at a negative potential relative to cathode, i.e., filament of the electron gun. When the sample and filament are at the same potential, the sample sees the electron above its vacuum level, with a kinetic energy (Eq. 2) equal to

$$\text{K.E.} = 11 - \phi_S, \quad (2)$$

where 11 is the kinetic energy of electrons (in eV) ejected from the electron gun and ϕ_S is sample's work function.

However, if we apply a retarding potential (V_R) to a sample, the sample current will reduce in magnitude, and approach a zero value when the vacuum level approaches the electron kinetic energy. Prior to this same measurement is done for reference sample. Using the plot of sample current vs retarding potential on a semi-logarithmic scale one obtains the value of the work function by measuring the shift of the linear region of the graph compared to a reference sample. The work function of SS-304L samples were measured before and after Ar^+ ions irradiation for two different conditions, (i) at varying ion energy keeping, ion fluence constant and (ii) at varying ion fluence keeping the ion energy constant. These work function measurements were carried out at vacuum pressure of 3×10^{-4} Pa.

2.5 Electrochemical measurement

The AUTOLAB PGSTAT302N was used for the corrosion J–V test using three-electrode cell measurement. Platinum (Pt) foil was used as a counter electrode, a Silver/Silver Chloride (Ag/AgCl) was used as a reference electrode, and a stainless-steel specimen (surface area of 1×1 cm²) was used as the working electrode. Potentiodynamic polarization was used to investigate the corrosion stability of AISI 304L stainless steel in the range of -0.5 to 0.5 V at a scan

rate of 1 mV/s vs Ag/AgCl at ambient temperature. Tafel extrapolation method was used for the corrosion rate analysis. The corrosion behavior of AISI 304L stainless steel was studied with polarization experiments in an aqueous solution of 0.05 M NaCl [28–31].

3 Results and discussion

3.1 Work function analysis

To calculate the work-function using the retarding field diode method (described in Sect. 2.4), initially sample current (I_S) was measured as a function of retarding potential (V_R). Graph of sample current as a function of retarding potential is shown in Fig. 2A.

As the retarding potential was increased the sample current was decreased for all the samples, as it was expected. However, it was observed that with increase in the ion irradiation energy, the change in sample current increased with respect to pristine sample. Furthermore, no significant difference in sample current within the irradiated samples (for all the irradiated samples) was observed at any energy. To understand the effect more clearly, a log plot of sample current vs retarding potential was plotted and is shown in Fig. 2B.

It can be seen from the graph that there is a change in values of current for pristine sample compared to irradiation samples at any typical value of retarding potential. By taking the linear and parallel part of the low current region, considering gold sample as reference, we estimated the work-function values. From the estimated values, variation in work-function (ϕ) was plotted as a function of ion energy and is shown in Fig. 3A.

As evident from the figure, it can be clearly seen that there is substantial change in work function value between pristine and first irradiated sample (i.e., 10 keV); however, no significant change in the work-function values was observed as we increase ion energy (within the irradiated samples). This may be because, the energy and the fluences we are using here are only able to sputter the top surface of the SS-304L and further change in energy does not affect the work-function values. The maximum depth for 40 keV argon ion in SS-304L sample is ~ 19 nm. As fluence is constant for all the energies used for irradiation, the major damage or defects per unit length is not changing substantially. The defects are mainly created by number of ions falling per unit area of the sample. Therefore, even if we change the energy from 10 to 40 keV it is not affecting work function values as a result we observe almost constant work function within irradiated samples. To verify our argument, we made DPA calculations using SRIM 13.00 software. We performed the calculations for displacement damage as a function of depth

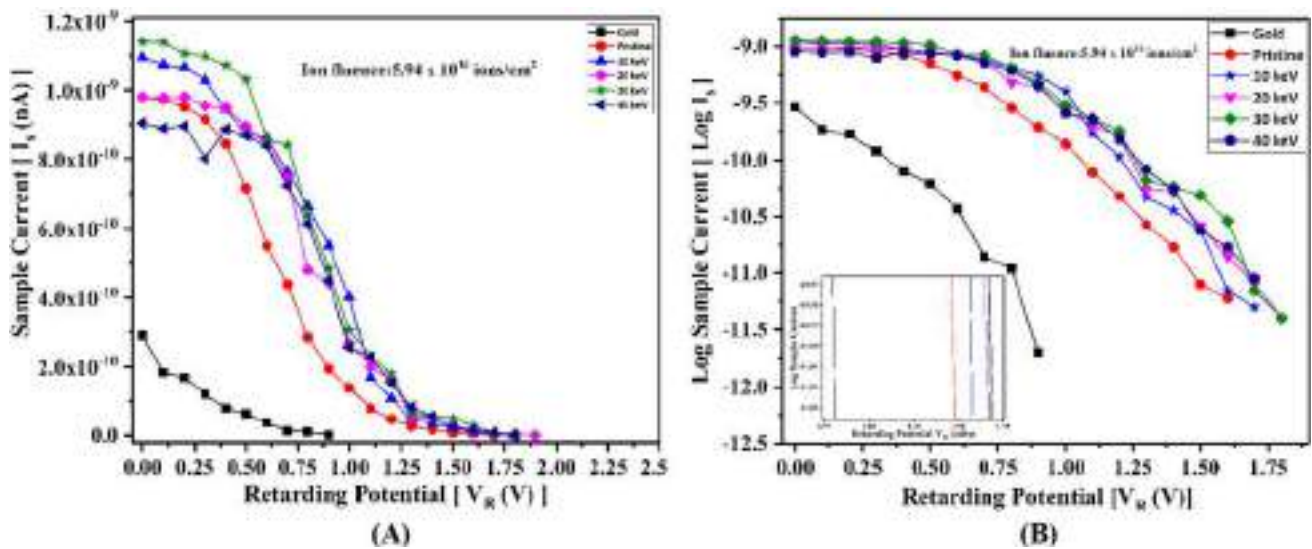
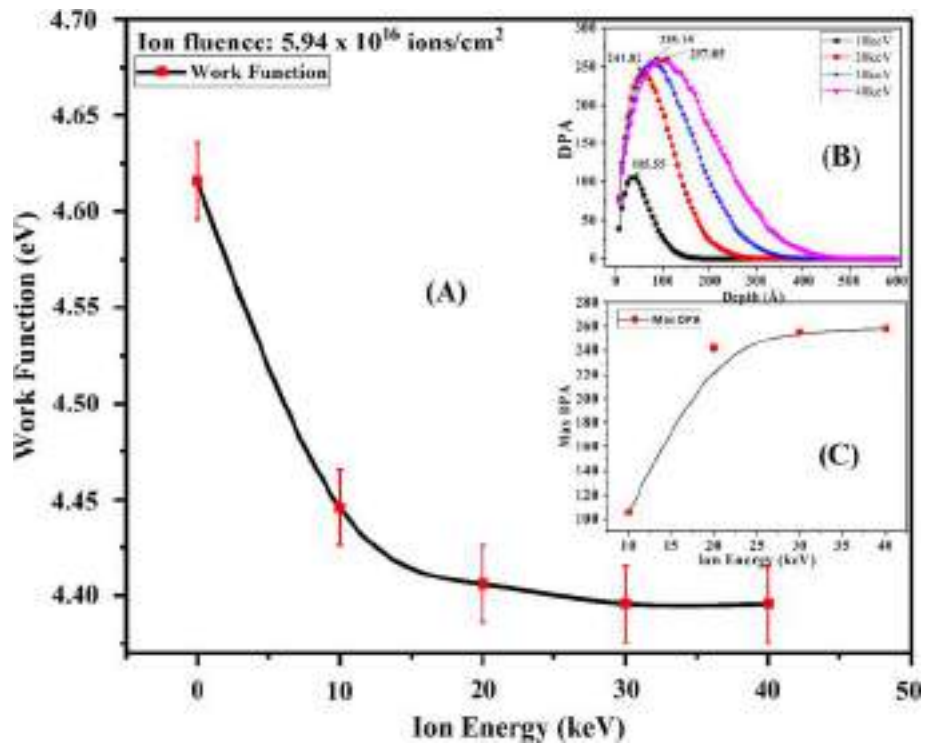


Fig. 2 Graph of A sample current I_s (nA) as a function of retarding potential V_R (V), B $\log I_s$ as a function of retarding potential V_R for pristine and samples irradiated at different ion energies keeping ion fluence constant

Fig. 3 Graph of A work function as a function of ion energy, B distribution of DPA as a function of depth, and C Max DPA as a function of ion energy at constant ion fluence 5.94×10^{16} ions/cm²



for Ar^+ ion in SS-304L samples at varying ion energy (keeping fluence constant).

In this specific case, ion energy was varied and fluence was kept constant (5.94×10^{16} ions/cm²). With increasing ion energy from 20 to 40 keV, the DPA value has changed from 241.82 to 257.8, i.e., only 6% change has been observed. DPA is correlated with damage in the surface of the material, which in turn changes the Wigner Seitz

radius thereby affecting the work function value. Because of the lower damage, the change in the Wigner Seitz radius is smaller, which results in an insignificant change in the work function values, as can be seen in Fig. 3A. The sputtering yield estimated from SRIM for the ion energy 10 keV was obtained to be 5.12 atoms/ion, whereas for ion energy 40 keV it is 4.80 atoms/ion. Change in sputtering

yield is also not significant, which may be the other reason behind insignificant change in the work function values.

Figure 3B shows that as the Ar^+ ion energy is increased the penetration depth increases and the peak of DPA curve also increases. For 40 keV the peak of DPA curve is obtained at 100 Å. Furthermore, we checked the max DPA as a function of increasing ion energy, as shown in Fig. 3C. From the graph it is observed that the maximum DPA saturates at higher energies.

Both calculation results agree with our experimentally observed work-function values. It can be correlated as follows, since the displacement damage created by 10 keV and 40 keV ions is almost same, the change in work function which is related to displacement damage also remains constant. Now, the work function (Φ) is also related to electrostatic potential ($\delta\phi$) of the metal surface and the electron fermi energy (ϵ_f) by the relation given in Eq. 3:

$$\Phi = \delta\phi - \epsilon_f, \quad (3)$$

$\delta\phi$, ϵ_f both are related to Wigner–Seitz radius (r_s) for given metal, as a decreasing exponential function [9, 28–30]. In general, r_s defined as a radius of sphere, whose volume is equal to mean volume per atom in a solid. Now, if r_s increases, $\delta\phi$, ϵ_f both may decrease and depending upon whether your $\delta\phi$ or ϵ_f is dominating work-function will change. In our experimental observation, among the irradiated sample the work-function (Φ) is not changing. This may be because, as we increase the energy, the damage/displacements are neither affecting $\delta\phi$ nor ϵ_f (within the irradiated samples) as ion fluence is constant. However, as compare

to pristine sample, certainly some defects/displacement has been created on the surface of the SS-304L due to irradiation, which has increased r_s , which resulted in decrease in $\delta\phi$ and ϵ_f eventually showing reduction in work-function Φ .

To verify our above argument, we further performed second set of experiment in which ion energy was kept constant and ion fluence was varied.

In this set of experiment, ion energy was kept constant at 30 keV and the ion fluence from varied from 9.9×10^{14} ions/cm² to 1.18×10^{17} ions/cm². Figure 4A shows measured sample current as a function of retarding potential. It was observed that there was a gradual increase and then a decrease in the sample current values to make it close to zero with individual retarding potential values for individual ion fluences. To get more clarity at low current region (close to zero) a log plot was plotted. Figure 4B shows samples Log current as a function of retarding potential. It is observed that irradiated samples current were retarded for higher values as a result the differences in retarding potential were higher.

From both the graphs, it is not very clear how much it has affected the surface, so we estimated the work-function values as a function of fluence, at constant ion energy of 30 keV. The graph is shown in Fig. 5A. We can clearly observe that with increase in ion fluence the work-function value has decreased lowest up to 4.27 eV for the ion fluence of 5.94×10^{16} ions/cm² and then gradually increased back up to 4.45 eV for the ion fluence of 1.18×10^{17} ions/cm².

These results clearly indicate the definite effect of ion fluence on the surface and subsurface region of the material, which resulted in the work-function change. As it was

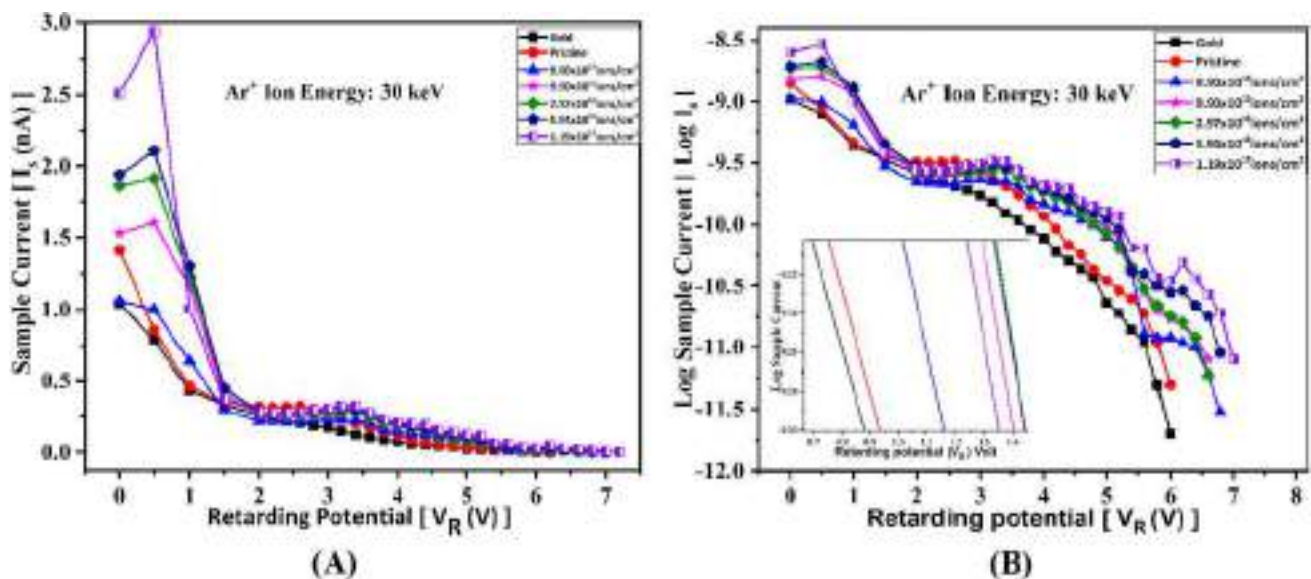
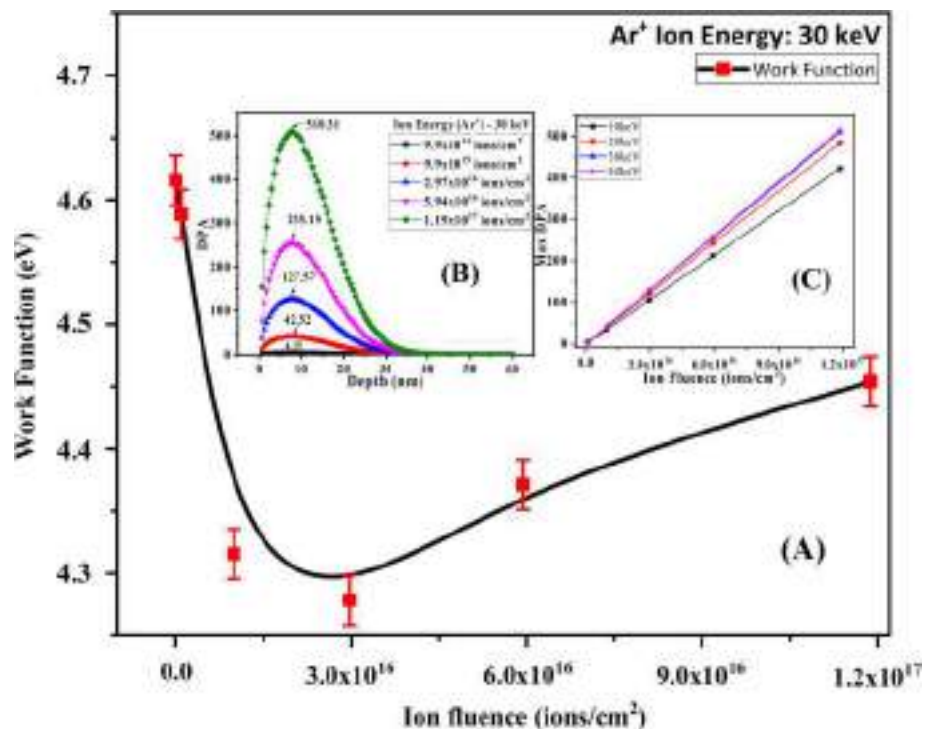


Fig. 4 Graph of **A** sample current I_s (nA) as a function of retarding potential V_R , **B** log (I_s) as a function of retarding potential V_R for various ion fluences at constant ion energy 30 keV

Fig. 5 Graph of **A** work function as a function of ion fluence **B** Distribution of DPA determined for 30 keV Ar⁺ ion irradiation, and **C** Max DPA as a function of ion fluence at constant ion energy 30 keV



argument in previous section that the fluence, i.e., number of ions falling per unit area plays a role in creating defect/displacement which might result in change in work-function values seems to be true. However, it is showing a non-linear behaviour of initial decrease and then increase in the work-function with increase in the ion fluence, which needs to be understood.

For this purpose, we again plotted the DPA values as a function of depth and ion fluence, and is shown in Fig. 5B, C, respectively. Figure 5B shows the area under the curve keeps on increasing with increase in the ion fluence without change in the depth value. In addition, from Fig. 5C, we can see that, as the fluence increases the DPA increases linearly. Thus, both the results indicate that, the number of displacements increases with increase in the ion fluences. This increase in the defects have resulted in decrease in the work-function. However, this is not following, what we have observed experimentally. Experimentally we observe that initially there is decrease in work function up to certain fluence and then it increases with fluence. This decrease and increasing trend of work-function can be again be explained on the basis of Wigner–Seitz radius following the relation given by Eq. 3. As the fluence is increasing at initial stages, i.e., at low fluence, change in r_s is due to both $\delta\varphi$ and ϵ_f (where both are competing). After certain threshold of fluence $\delta\varphi$ dominates as compare to change in ϵ_f , which results in increase in work-function (Φ) [32].

In contrast with previous observations for change of work function as function of ion energy, when ion fluence is varied

(keeping ion energy constant 30 keV), the DPA change is 91.67%. Which resulted in change in Wigner Seitz radius in a significant way causing change in work function values. These results indicate that ion fluence variations dominate modification of work function. Similar results are also been observed by Ákos Horváth et al. [9] and are in agreements with these experimental findings.

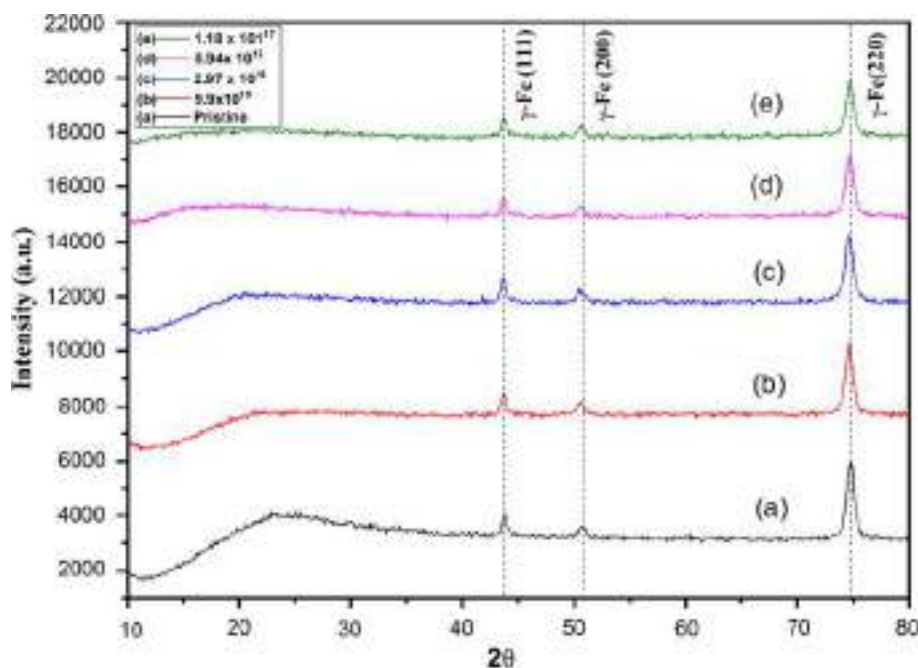
3.2 XRD analysis

Figure 6 shows the XRD pattern for pristine and irradiated AISI 304L SS samples with different ion fluences pristine (a), 9.9×10^{15} ions/cm² (b), 2.97×10^{16} ions/cm² (c), 5.94×10^{16} ions/cm² (d), and 1.18×10^{17} ions/cm² (e), respectively. XRD peaks observed at 2θ values 43.7°, 50.7°, 74.8° corresponds to (111), (200), (220) planes indicating austenitic γ -Fe phase accordance with the JCPDS card No: (00–003–0397) [33–38]. It has been observed that with increase in ion fluence, the peak intensities are decreasing. The peak intensity of highest fluence decreased up to 32% compared with pristine sample.

3.3 SEM Analysis

Figure 7 shows SEM (Surface morphology) of pristine and irradiated AISI 304L stainless steel samples for Fig. 7A Pristine (B) 9.9×10^{15} ions/cm² (C) 2.97×10^{16} ions/cm², (D) 5.94×10^{16} ions/cm² and (E) 1.18×10^{17} ions/cm², respectively. Figure 7A of pristine and Fig. 7B of 9.9×10^{15} ions/

Fig. 6 X-ray diffraction patterns of AISI 304L SS material before and after Ar^+ ion irradiation at various ion fluences



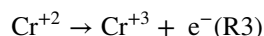
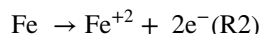
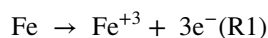
cm^2 irradiated sample shows a smooth surface. Figure 7C of 2.97×10^{16} ions/ cm^2 irradiated sample shows little rough surface with line formation. Further increase in ions fluence, Fig. 7D, shows highest roughness with line formation and the highest fluence sample, Fig. 7E, shows quite smooth surface; however, as we increase the ion fluence the roughness goes on increasing up to the ion fluence of 5.94×10^{16} ions/ cm^2 and then at highest ion fluence, the roughness has been decreased.

3.4 Potentiodynamic polarization studies

As work-function is related to corrosion rate, we further performed the corrosion test experiments to validate our findings. Figure 8A shows potentiodynamic polarization curve for pristine and irradiated samples. The corrosion potential (E_{corr}) and corrosion current density (I_{corr}) were obtained from the polarization curve and the values are tabulated in Table 1. From the graph it was observed that as the ion fluence increases, corrosion potential values also increased (shifted right) and corrosion current values were decreased. All measured values of I_{corr} and E_{corr} obtained from the Tafel extrapolation method [34, 39, 40] have been tabulated in Table 1. The graph was further utilized for the calculation of correction resistance and corrosion rate. Figure 8B shows a corrosion resistance and corrosion rate as a function of ion fluence at constant ion energy. The corrosion resistance increases, whereas corrosion rates decrease with an increase in ion fluence. The obtained results are in corroboration with our work function values as explained in previous section.

The E_{corr} of all irradiated samples was shifted to more positive as compared to pristine (-0.128 V vs Ag/AgCl), meaning improvement in the corrosion resistance. With an increase in ion fluence from 9.90×10^{15} to 1.18×10^{17} ions/ cm^2 E_{corr} value shifted toward positive -0.106 V vs Ag/AgCl to -0.093 V vs Ag/AgCl, respectively. The 1.18×10^{17} ions/ cm^2 sample exhibits most positive corrosion potential with corresponding lowest corrosion current of 5.42×10^{-7} A/ cm^2 . This positive shift of corrosion potential and reduction in corrosion current implies reduction in surface oxidation of samples with increase in ion fluence. The corrosion current indicates oxidative dissolution of sample species during interaction of electrolyte with sample surface. Herein, the decrease of corrosion current with ion fluence shows less dissolution of sample preventing conversion of Fe to $\text{Fe}^{+3}/\text{Fe}^{+2}$. This might have happened because of damage created by ions on AISI 304L SS surface, resulting in restriction of Fe to $\text{Fe}^{+3}/\text{Fe}^{+2}$ [29–31].

During the anodic polarization process the following reactions (R) may occur:



Hence from these results, i.e., change in work function due to variation in ion energy (keeping fluence constant) and change in work function due to variation in ion fluence (keeping ion energy constant), we can conclude that ion fluence plays a major role in controlling the work function values. We can either increase or decrease the cofunction by

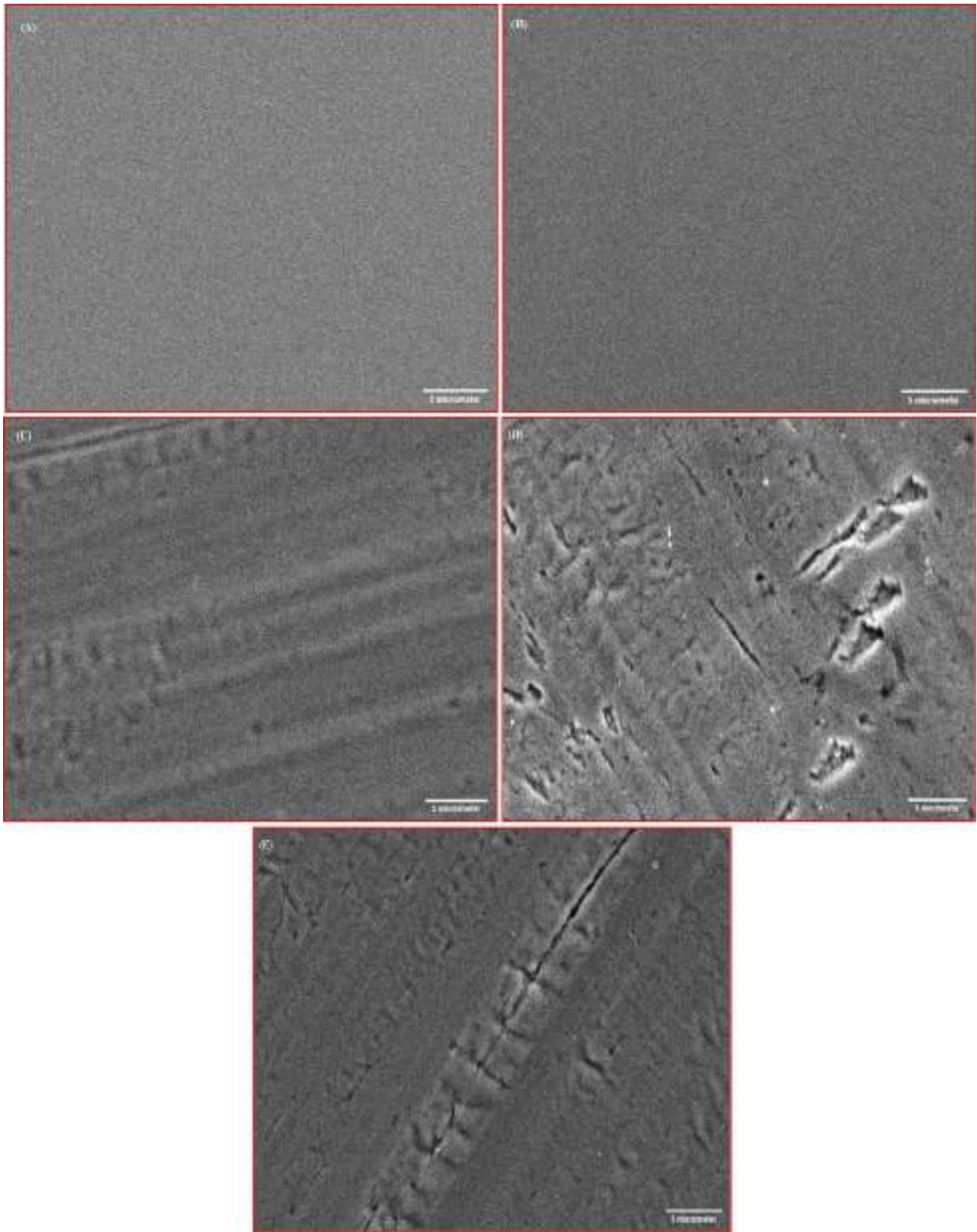


Fig. 7 SEM images of AISI 304L SS samples of **A** pristine, **B** 9.9×10^{15} ions/cm², **C** 2.97×10^{16} ions/cm², **D** 5.94×10^{16} ions/cm², and **E** 1.18×10^{17} ions/cm² ion fluences

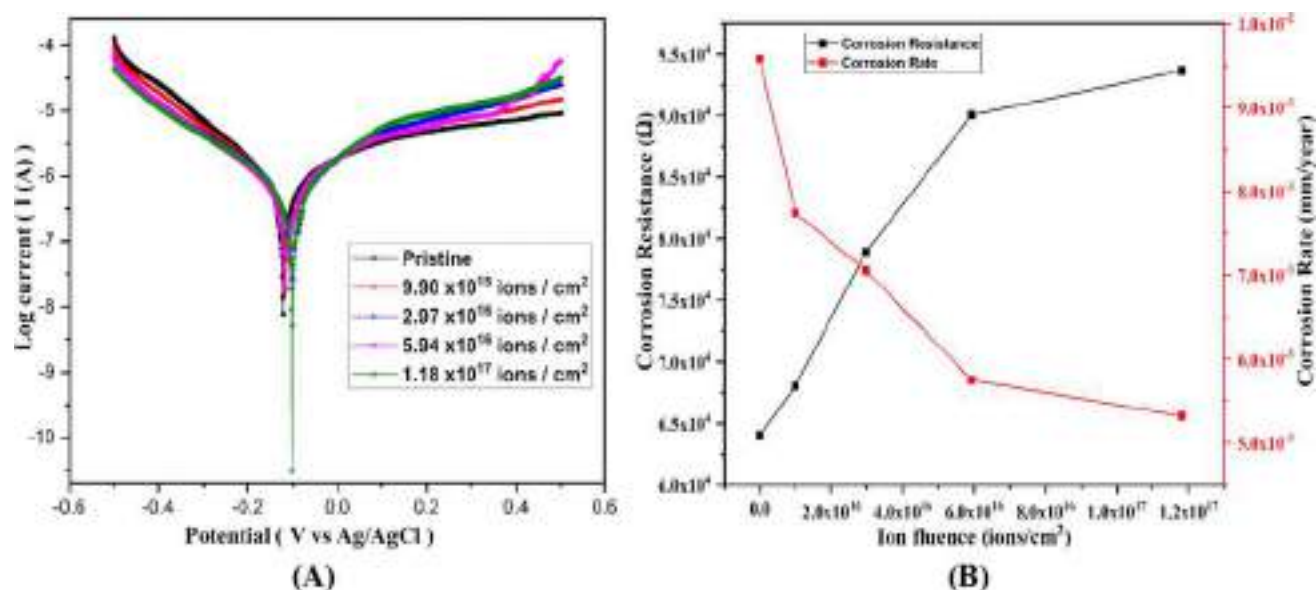


Fig. 8 A Potentiodynamic polarization curve for various ion fluences and **B** corrosion resistance and Corrosion rate as a function of ion fluence at a constant ion energy 30 keV

choosing the suitable fluence values. We can either increase or decrease the cofunction by choosing the suitable fluence values. As it is known that, work-function is related to corrosion rate too, thus we can also control the corrosion of given sample by properly tuning the ion fluence in the given energy range.

4 Conclusion

The energetic ion induced displacement/damage depends on the energy of incoming ions and its fluence, for a particular material. The irradiation effect due to variation in ion energy and ion fluence on work function of SS-304L samples was explored. Variation in ion irradiation energy up to 40 keV, does not affect the work function of samples. Whereas, if the energy is kept constant and fluence is change it modifies the work-function substantially. This change in work-function are related to displacement/damage created by primary ions,

which resulted in increase of Wigner–Seitz radius, which is due to change in electrostatic potential ($\delta\phi$) and the electron fermi energy (ϵ_f) of the SS-304L. The results are useful to control the corrosion stability of stainless-steel material which is applicable in aged nuclear reactors, construction industry, electrical industry, transportation industry and the places, where corrosion stability is required.

Acknowledgements The financial support from the Science and Engineering Research Board, New Delhi, for the development of low energy ion irradiation system under a project (SB/EMEQ-401/2014) is gratefully acknowledged by S. S. Dahiwal. A. B. Thorat acknowledges to Council of Scientific and Industrial Research (CSIR), India for Senior research fellowship award. A. B. Thorat thankful to Dr. Babasaheb Ambedkar National Research Fellowship (BARTI/Fellowship/BANRF-2018/19-20/3036) for financial support (BANRF-2018). S. A. Kamble thankful to SR/WOS-A/PM-110/2018 Women Scientist-A DST, India for financial support. AVR thank SPPU PDF (Grant No. SPPUPDF/ST/PH/2021/0005). One of the authors ABT is thankful to Prof. S.R. Jadar and Prof. V.L. Mathe, Department of Physics, S. P. Pune University, Pune-411007 for provided access to the electrochemical measurement system and work function measurement system, respectively.

Data availability The authors declare that the data supporting the findings of this study are available within the paper.

Declarations

Conflict of interest The authors declare that they have no conflicts of interest.

References

1. L. Gardner, Thin-Walled Struct. **141**, 208 (2019)

Table 1 Obtained values of E_{corr} and I_{corr} for AISI 304L stainless steel material with various ion fluences

Ion fluence (ions/cm ²)	E_{corr} (V vs Ag/AgCl)	I_{corr} (A/cm ²)
Pristine	-0.128	8.24×10^{-7}
9.90×10^{15}	-0.106	6.38×10^{-7}
2.97×10^{16}	-0.103	6.07×10^{-7}
5.94×10^{16}	-0.097	4.95×10^{-7}
1.18×10^{17}	-0.093	5.42×10^{-7}

2. N.R. Baddoo, J. Constr. Steel Res. **64**, 1199 (2008)
3. M. Stratmann, H. Streckel, Corros. Sci. **30**, 681 (1990)
4. M. Briceño, J. Fenske, M. Dadfarnia, P. Sofronis, I.M. Robertson, J. Nucl. Mater. **409**, 18 (2011)
5. J.H. Park, Y. Kang, Steel Res. Int. **88**, 1 (2017)
6. T. Hryniewicz, K. Rokosz, Anti-Corros. Methods Mater. **61**, 57 (2014)
7. R. Rokicki, T. Hryniewicz, C. Pulletikurthi, K. Rokosz, N. Munroe, J. Mater. Eng. Perform. **24**, 1634 (2015)
8. K. Rokosz, T. Hryniewicz, S. Raaen, J. Valiček, Teh. Vjesn. **22**, 125 (2015)
9. Á. Horváth, N. Nagy, G. Vértesy, R. Schiller, Mater. Chem. Phys. **217**, 541 (2018)
10. A. Kaleem, S. Bashir, M. Akram, R. Amir, K. Mahmood, M.S. Rafique, S. Naseem, S. Riaz, M. Sarwar, A. Tariq, Appl. Phys. A Mater. Sci. Process. **128**, 1 (2022)
11. A. Thorat, K. Tikote, M. Bhadane, A. Phatangare, V. Bhoraskar, S. Dhole, S. Dahiwal, Opt. Mater. (Amst). **128**, 112349 (2022)
12. L. Bischoff, W. Pilz, B. Schmidt, Appl. Phys. A Mater. Sci. Process. **104**, 1153 (2011)
13. G. D. Tolstolutskaia, S. A. Karpov, G. Y. Rostova, B. S. Sungurov, and G. N. Tolmachova, J. V.N. Karazin Kharkiv Natl. Univ. Ser. "Physics" **66** (2015).
14. G.D. Tolstolutskaia, S.A. Karpov, A.S. Kalchenko, I.E. Kopanets, A.V. Nikitin, V.N. Voyevodin, Probl. At. Sci. Technol. **126**, 27 (2020)
15. R. Dubey, A. Gupta, P. Sharma, N. Darowski, G. Schumacher, J. Magn. Magn. Mater. **310**, 2491 (2007)
16. E. Mustafin, T. Seidl, A. Plotnikov, I. Strašák, M. Pavlovič, M. Miglierini, S. Stanček, A. Fertman, A. Lančok, Radiat. Eff. Defects Solids **164**, 460 (2009)
17. C. Yao, H. Zhang, H. Chang, Y. Sheng, T. Shen, Y. Zhu, L. Pang, M. Cui, K. Wei, Y. Xu, D. Wang, C. Liu, Z. Ma, L. Zhao, W. Yan, T. Peng, J. Li, C. Qin, Z. Wang, Corros. Sci. **195**, 109953 (2022)
18. C. Xu, X. Liu, Y. Li, W. Qian, W. Jia, Q. Quan, J. Yin, Nucl. Technol. **00**, 1 (2022)
19. J.F. Ziegler, Nucl. Instrum. Methods Phys. Res. Sect. B Beam Interact. Mater. Atoms **219–220**, 1027 (2004)
20. J.F. Ziegler, M.D. Ziegler, J.P. Biersack, Nucl. Instrum. Methods Phys. Res. Sect. B Beam Interact. Mater. Atoms **268**, 1818 (2010)
21. R.E. Stoller, M.B. Toloczko, G.S. Was, A.G. Certain, S. Dwaraknath, F.A. Garner, Nucl. Instrum. Methods Phys. Res. Sect. B Beam Interact. Mater. Atoms **310**, 75 (2013)
22. J. F. Ziegler, M. D. Ziegler, and J. P. Biersack, Nucl. Instrum. Methods Phys. Res. Sect. B Beam Interact. Mater. Atoms **268**, 1818 (2010).
23. Á. Horváth, N. Nagy, G. Vértesy, R. Schiller, Nucl. Instrum. Methods Phys. Res. Sect. B Beam Interact. with Mater. Atoms **466**, 12 (2020)
24. S.K. Singh, V.V.S. Kumar, P. Kumar, Appl. Phys. A Mater. Sci. Process. **127**, 1 (2021)
25. S.J. Klauser, E.B. Bas, J. Phys. E. **12**, 841 (1979)
26. T.M. Bhawe, S.V. Bhoraskar, J. Vac. Sci. Technol. B Microelectron. Nanom. Struct. **16**, 2073 (1998)
27. N.R. Rajopadhye, S.V. Bhoraskar, J. Mater. Sci. Lett. **5**, 603 (1986)
28. L. Hamadou, A. Kadri, N. Benbrahim, Corros. Sci. **52**, 859 (2010)
29. S. Ningshen, U. Kamachi Mudali, S. Ramya, B. Raj, Corros. Sci. **53**, 64 (2011)
30. P. Dhaiveegan, N. Elangovan, T. Nishimura, N. Rajendran, RSC Adv. **6**, 47314 (2016)
31. Y. Zhang, H. Luo, Q. Zhong, H. Yu, J. Lv, Chinese J. Mech. Eng. (English Ed.) **32**, 27 (2019).
32. N.D. Lang, W. Kohn, Phys. Rev. B **3**, 1215 (1971)
33. L. Wang, J. Sun, P. Li, J. Sun, Y. Lv, B. Jing, S. Li, S. Ji, Z. Wen, Int. J. Hydrogen Energy **37**, 5876 (2012)
34. S. Sabooni, H. Rashtchi, A. Eslami, F. Karimzadeh, M.H. Enayati, K. Raeissi, A.H.W. Ngan, R.F. Imani, Int. J. Mater. Res. **108**, 552 (2017)
35. S.Y. Lee, E.W. Huang, W. Woo, C. Yoon, H. Chae, S.G. Yoon, Metals (Basel). **5**, 2109 (2015)
36. F.J. Baldenebro-Lopez, C.D. Gomez-Esparza, R. Corral-Higuera, S.P. Arredondo-Rea, M.J. Pellegrini-Cervantes, J.E. Ledezma-Sillas, R. Martinez-Sanchez, J.M. Herrera-Ramirez, Materials (Basel). **8**, 451 (2015)
37. F. Modiri, H. Savaloni, J. Theor. Appl. Phys. **14**, 223 (2020)
38. G. Shit, P. Bhaskar, S. Ningshen, A. Dasgupta, U.K. Mudali, A.K. Bhaduri, AIP Conf. Proc. **1832**, 4 (2017)
39. Z. Shi, M. Liu, A. Atrens, Corros. Sci. **52**, 579 (2010)
40. A.R. El-Sayed, H.S. Mohran, H.M. El-Lateef, Metall. Mater. Trans. A Phys. Metall. Mater. Sci. **43**, 619 (2012)

Publisher's Note Springer Nature remains neutral with regard to jurisdictional claims in published maps and institutional affiliations.

Springer Nature or its licensor (e.g. a society or other partner) holds exclusive rights to this article under a publishing agreement with the author(s) or other rightsholder(s); author self-archiving of the accepted manuscript version of this article is solely governed by the terms of such publishing agreement and applicable law.



Isomeric cross sections of the (n, α) reactions on the ^{90}Zr , ^{93}Nb and ^{92}Mo isotopes measured for 13.73 MeV–14.77 MeV and estimated for 10 MeV–20 MeV neutron energies

F.M.D. Attar^{a, **}, G.T. Bholane^b, T.S. Ganesapandy^b, S.D. Dhole^{b, *}, V.N. Bhoraskar^b

^a Department of Physics, AKI's Poona College, Pune, 411001, India

^b Department of Physics, S.P. Pune University, Pune, 411007, India

ARTICLE INFO

Keywords:

Isomeric cross-section
Gamma spectroscopy
Activation analysis
EMPIRE-3.2
TALYS-1.8
Nuclear model calculations

ABSTRACT

Isomeric cross sections for the $^{90}\text{Zr}(n, \alpha)^{87}\text{Sr}^m$, $^{93}\text{Nb}(n, \alpha)^{90}\text{Y}^m$ and $^{92}\text{Mo}(n, \alpha)^{89}\text{Zr}^m$ reactions were measured at five neutron energies over the range 13.73 MeV–14.77 MeV using the activation technique in combination with high resolution γ -ray spectrometry. In the present work, the cross sections are measured for the $^{90}\text{Zr}(n, \alpha)^{87}\text{Sr}^m$ and $^{93}\text{Nb}(n, \alpha)^{90}\text{Y}^m$ reactions are referenced to the $^{27}\text{Al}(n, \alpha)^{24}\text{Na}$ standard reaction cross section whereas those measured for $^{92}\text{Mo}(n, \alpha)^{89}\text{Zr}^m$ reaction are referenced to the $^{56}\text{Fe}(n, p)^{56}\text{Mn}$ standard reaction cross section. The cross sections for these reactions were also theoretically estimated using the EMPIRE-3.2 and TALYS 1.8 codes over the neutrons energy range of 10 MeV–20 MeV and matched with the experimental cross sections by making a proper choice of the model parameters. A minimum eight different sets of these statistical model calculations were performed by using the consistent sets of model parameters along with the pre-equilibrium mechanism in addition to the direct-reaction and the statistical Hauser–Feshbach (HF) compound nucleus ones. The measured cross sections for these three reactions increase with the increase in neutron energy from 13.73 MeV to 14.77 MeV. As the proton number increased by one when we go from zirconium to niobium or from niobium to molybdenum, the probability of alpha particle emission also increases at each corresponding neutron energy. The present results indicate that the measured cross section at each neutron energy for the $^{92}\text{Mo}(n, \alpha)^{89}\text{Zr}^m$ reaction is found to be the highest as compared to the other two reactions whereas, for the $^{90}\text{Zr}(n, \alpha)^{87}\text{Sr}^m$ reaction, the measured cross section is found to be the lowest as compared to the other two reactions studied. The results obtained from the present measurement are found to be in good agreement with the calculated reaction cross section based on theoretical models and also with the work reported by earlier authors.

1. Introduction

The measurement of isomeric cross sections in the neutron-induced reactions with the use of the activation technique is an effective method for knowing mainly the details of (n, α) reactions. This work is also of importance for both the basic and applied research including nuclear technology, and most of these cross sections are given in the EXFOR database (Otuka et al., 2014). The cross sections for different nuclear reactions such as (n, p) , (n, α) , $(n, 2n)$, (n, np) have remained a field of interest for the past few decades (Attar et al., 2008, 2014; Avrigeanu et al., 2006; Semkova et al., 2010). EXFOR compilation shows that several measurements are exist near 14 MeV neutron energy,

however the available cross section data in literature within the neutron energy range of 13.73 MeV–14.77 MeV are very much scattered.

Measurements of cross sections for the emission of α particles in reactions induced by fast neutrons for neutron-rich nuclei with $N > 50$ for the mass region around 90 are of considerable interest in testing the nuclear models. At higher neutron energies up to 20 MeV this data is important in several fields of applications such as Accelerator-Driven Systems (ADS) for energy production and transmutation of nuclear waste, for medical therapy and in many other field. Moreover, knowledge of these cross sections for the emission of α -particle is also important for assessing the radiation damage in fusion reactors as zirconium, niobium and molybdenum are used as constituents of structural

* Corresponding author.

** Corresponding author.

E-mail addresses: fmdattar@gmail.com (F.M.D. Attar), sanjay@physics.unipune.ac.in (S.D. Dhole).

<https://doi.org/10.1016/j.apradiso.2022.110192>

Received 29 July 2021; Received in revised form 21 February 2022; Accepted 8 March 2022

Available online 11 March 2022

0969-8043/© 2022 Elsevier Ltd. All rights reserved.

materials in fusion reactors (Zinkle and Busby, 2009). For example, zirconium is used in cladding of uranium fuel elements and also as a hardening agent in alloys required for nuclear reactors. Molybdenum is an excellent structural metal particularly when the operations are to be made at elevated temperatures. Moreover, it is also used for neutronic applications, such as controlled nuclear fusion devices. The niobium is used as a first wall and structural material in the experimental fusion reactors. This acts as an effective microalloying element for steel. Similarly, niobium metal can increase the toughness, strength, formability and weldability of the micro alloyed steel. The alloy of niobium-zirconium is also used for fabricating fuel element claddings of the pressurized water reactors. As these elements are used in reactor technology, the cross-sections for neutron induced reactions are important. Neutron induced reaction cross sections provide the data for the evaluation of processes in these materials under irradiation in reactors and is also of particular importance in the hydrogen and helium gas production through (n, p) and (n, α) reactions.

In the present work, the activation technique has been used to measure the cross sections for the $^{90}\text{Zr}(n, \alpha)^{87}\text{Sr}^m$, $^{93}\text{Nb}(n, \alpha)^{90}\text{Y}^m$ and $^{92}\text{Mo}(n, \alpha)^{89}\text{Zr}^m$ reactions at 13.73 MeV, 14.07 MeV, 14.42 MeV, 14.68 MeV and 14.77 MeV neutron energies. All the three reactions studied have positive Q values and zero threshold energies (IAEA Nuclear Data Center). These three target nuclei in the mass region ~ 90 constitute excellent test cases for nuclear models in the neutron energy range from 10 MeV to 20 MeV.

Since many reaction channels are opened in the neutron energy range above 14 MeV, the experimental results are compared with the theoretically calculated cross-sections up to the neutron energy of 20 MeV by using global and local-parameter approaches, which take into account direct reaction, pre-equilibrium emission (PE), and statistical Hauser-Feshbach (HF) models compound nucleus contributions. The parameter databases obtained by global optimization within the computer codes EMPIRE-3.2 (Herman et al., 2007) and TALYS 1.8 (Koning et al., 2008a) and have been used over the neutron energy range from 10 MeV to 20 MeV.

Attempts were also made to use different values of the parameters like nucleon potential namely neutron and alpha particle, level density, level density parameter and nuclear models, etc., to match the theoretically estimated cross sections with the cross sections measured in the present work as well as those reported literature data compiled in EXFOR (Otuka et al., 2014). The comparison of various calculations including their sensitivity to model approaches and parameters will be complemented by an analysis of recent data measurements.

2. Experiment

2.1. Neutron irradiation

The neutron irradiation work was carried out at the 14 MeV neutron generator laboratory (Bhoraskar, 1989), Department of Physics, Savitribai Phule Pune University, Pune, India. The 14 MeV neutrons were produced by bombarding deuterium ions having an energy of 175 keV on an 8 Ci tritium target. On the tritium target, the deuterium beam had a diameter of about 4 mm and current of about 100 μA . For the study of $^{90}\text{Zr}(n, \alpha)^{87}\text{Sr}^m$, $^{93}\text{Nb}(n, \alpha)^{90}\text{Y}^m$ and $^{92}\text{Mo}(n, \alpha)^{89}\text{Zr}^m$ reactions, the samples were made from natural ZrO_2 (99.99%) powder, Nb_2O_5 (99.99%) powder and the molybdenum (14.84%) target was in the form of a metal foil respectively. For the study of all the three reactions, the samples were prepared for neutron irradiation by packing in a polyethylene bag. The polyethylene bag was folded in such a way that the size of the sample was close to 10 mm \times 10 mm. Following this procedure three sets of samples were made in which each set had five samples. In each experiment performed for each reaction, the samples were irradiated with neutrons by placing them at 0°, 30°, 60°, 90° and 120° angular positions at a distance of 50 mm from the tritium target (Mandal et al., 2012).

For the measurement of $^{90}\text{Zr}(n, \alpha)^{87}\text{Sr}^m$ and $^{93}\text{Nb}(n, \alpha)^{90}\text{Y}^m$ reaction cross-sections, aluminum in the form of a metal foil (99.99%) was used as monitor element and the $^{27}\text{Al}(n, \alpha)^{24}\text{Na}$ reaction was chosen as a monitor reaction. Each respective sample (ZrO_2 and Nb_2O_5) was made by sandwiching 1 gm of element powder between two aluminum foils with total weight 0.2 gm measured with a microbalance at an accuracy of $\pm 10 \mu\text{g}$. For the $^{92}\text{Mo}(n, \alpha)^{89}\text{Zr}^m$ reaction the molybdenum samples in the form of metal foils were used and the $^{56}\text{Fe}(n, p)^{56}\text{Mn}$ reaction was chosen as a monitor reaction. Each sample was prepared by taking 0.5 gm of molybdenum foil and 0.3 gm of Fe powder in a polyethylene bag. Five such samples for each element were placed at 0°, 30°, 60°, 90° and 120° angular positions relative to deuterium ion beam direction. The energy of neutrons at these positions correspond to 14.77 MeV, 14.68 MeV, 14.42 MeV, 14.07 MeV and 13.73 MeV (IAEA TECDOC, 2020). These samples of Zr, Nb and Mo were irradiated for a period of 3600 s, 3000 s and 600 s respectively. Two more sets of irradiations were carried out for each sample following the same procedure. After the irradiation the samples were immediately transferred to the counting room.

2.2. Measurement of the γ -ray activity

The induced γ -ray activities of the irradiated samples were measured with a HPGe detector. The γ -ray detection efficiency and energy calibration of this detector was performed with a Canberra make Multi Gamma Standard MGS-3 γ -ray source. Initially the γ -ray activity of the sample irradiated at 0° was measured. Later on, the γ -ray activities of the samples irradiated at 30°, 60°, 90° and 120° were measured in sequence. A total period of 30 s was kept between the end of counting the γ -ray activity of first sample and the start of counting the γ -ray activity of second sample. Accordingly, the total cooling time for each sample was accounted while estimating the actual induced γ -ray activity. The decay data of the radioisotopes $^{87}\text{Sr}^m$, $^{90}\text{Y}^m$, $^{89}\text{Zr}^m$, ^{24}Na and ^{56}Mn produced via the $^{90}\text{Zr}(n, \alpha)^{87}\text{Sr}^m$, $^{93}\text{Nb}(n, \alpha)^{90}\text{Y}^m$, $^{92}\text{Mo}(n, \alpha)^{89}\text{Zr}^m$, $^{27}\text{Al}(n, \alpha)^{24}\text{Na}$ and $^{56}\text{Fe}(n, p)^{56}\text{Mn}$ reactions respectively are given in Table 1 (National Nuclear Data Center, 1996).

The induced photo-peak activity of 0.388 MeV γ -ray from $^{87}\text{Sr}^m$ and 1.369 MeV γ -ray from ^{24}Na was measured for a period of 1200 s. The induced photo-peak activity of 0.48 MeV γ -ray from $^{90}\text{Y}^m$ and 1.369 MeV γ -ray from ^{24}Na was measured for a period of 1800 s. Similarly, the induced photo-peak activity of 0.588 MeV γ -ray from $^{89}\text{Zr}^m$ and 0.847 MeV γ -ray from ^{56}Mn was measured for a period of 60 s.

3. Data analysis

Fig. 1, Fig. 2 and Fig. 3 show the gamma-ray spectra of $^{87}\text{Sr}^m$ and ^{24}Na , $^{90}\text{Y}^m$ and ^{24}Na and $^{89}\text{Zr}^m$ and ^{56}Mn respectively, produced via neutron induced reactions. The spectra shown in these figures are background subtracted and therefore the area under each photo peak is proportional to the respective γ -ray activity induced in the sample. The activation cross sections for the $^{90}\text{Zr}(n, \alpha)^{87}\text{Sr}^m$, $^{93}\text{Nb}(n, \alpha)^{90}\text{Y}^m$ and

Table 1

The decay data of the radioisotopes produced in neutron induced reactions (National Nuclear Data Center, 1996).

Nuclear Reaction	Abundance (%)	Half-life	E_γ (MeV)	f_d (%)
$^{90}\text{Zr}(n, \alpha)^{87}\text{Sr}^m$	51.45 \pm 0.40	2.815 \pm 0.012 h.	0.388	82.19 \pm 0.22
$^{93}\text{Nb}(n, \alpha)^{90}\text{Y}^m$	100	3.19 \pm 0.06 h	0.48	90.5 \pm 0.3
$^{92}\text{Mo}(n, \alpha)^{89}\text{Zr}^m$	14.649 \pm 0.106	4.161 \pm 0.010 m	0.588	89.62 \pm 0.17
$^{27}\text{Al}(n, \alpha)^{24}\text{Na}$	100	14.997 \pm 0.012 h	1.369	99.99
$^{56}\text{Fe}(n, p)^{56}\text{Mn}$	91.754 \pm 0.106	2.5789 \pm 0.0001 h	0.847	98.85 \pm 0.30

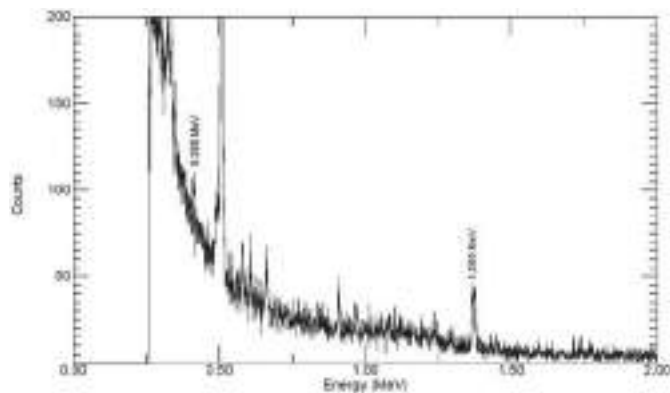


Fig. 1. γ -ray spectra of $^{87}\text{Sr}^m$ and ^{24}Na radio nuclei produced by irradiating ^{90}Zr and ^{27}Al respectively with 13.73 MeV neutrons.

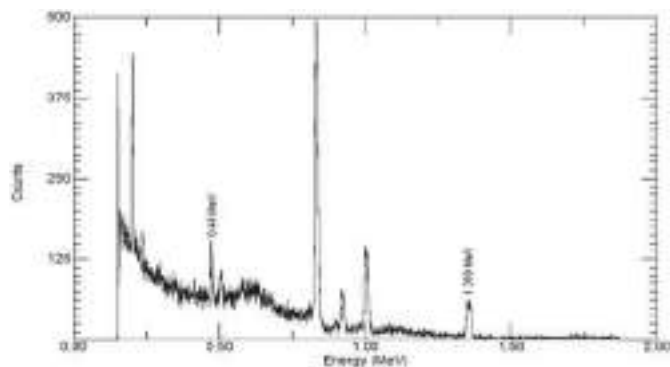


Fig. 2. γ -ray spectra of $^{90}\text{Y}^m$ and ^{24}Na radio nuclei produced by irradiating ^{93}Nb and ^{27}Al respectively with 13.73 MeV neutrons.

$^{92}\text{Mo}(n, \alpha)^{89}\text{Zr}^m$ reactions were obtained at 13.73–14.77 MeV neutron energies using the activation formula given by the following activation expression (1),

$$\sigma_m = \sigma_M \frac{A \varepsilon_M f_d \lambda}{A_M \varepsilon f_d \lambda_M} \frac{N_M (1 - e^{-\lambda_M t_1}) e^{-\lambda_M t_2} (1 - e^{-\lambda_M t_3})}{N (1 - e^{-\lambda t_1}) e^{-\lambda t_2} (1 - e^{-\lambda t_3})} \quad (1)$$

where σ_m is the isomeric reaction cross section, A is the number of counts under the photopeak, f_d is the photon disintegration probability, ε is the detector efficiency, σ_M is the cross section for monitor reaction, λ is the decay constant, N is the number of atoms of the isotope of the element, t_1 is the irradiation time, t_2 is the cooling time, and t_3 is the period for which the γ -activity is measured. The quantity with the subscript M stands for the monitor reaction.

By considering the uncertainties involved in the measurement of each parameter, the error analysis was carried out using the quadrature method (Taylor, 1982). The flux of the low energy neutrons ($E_n < 10$ MeV) in the D-T reaction is about two orders of magnitude lower than that at 14 MeV (Kawade et al., 2003). In the present work, the contributions of the low energy neutrons in the cross sections of all the three reactions studied are negligible and were therefore not taken into account. Similarly, the effects of the multiple scattering of neutrons and the inhomogeneities were also not taken into account as the errors induced by these processes are negligibly small. For different parameters, the estimated errors are as follows; (i) detector efficiency ($\sim 1.5\%$) (ii) self-absorption of gamma-rays ($< 2\text{--}5\%$) (Hubbell and Seltzer, 2004) (iii) neutron energy distribution ($< 1\%$) (iv) absolute gamma-ray intensity ($< 2.1\%$) and (v) reference reaction cross section of $^{27}\text{Al}(n, \alpha)^{24}\text{Na}$ ($< 1.1\%$) (Filatenkov et al., 1999) and reference reaction cross section of $^{56}\text{Fe}(n, p)^{56}\text{Mn}$ ($2\text{--}3.7\%$) (Filatenkov et al., 1999).

4. Nuclear model based reaction cross section calculations

The theoretical isomeric cross sections for the $^{90}\text{Zr}(n, \alpha)^{87}\text{Sr}^m$, $^{93}\text{Nb}(n, \alpha)^{90}\text{Y}^m$ and $^{92}\text{Mo}(n, \alpha)^{89}\text{Zr}^m$ reactions were estimated over 10 MeV–20 MeV neutron energies by using statistical nuclear reaction models using the EMPIRE-3.2 (Herman et al., 2007) and TALYS-1.8 codes (Koning et al., 2008a) to investigate if a consistent description can be obtained by the use of these codes. The calculations were performed in the framework of the direct-reaction, PE and statistical Hauser–Feshbach (HF) models in which a minimum of eight different sets of calculations of cross sections for these three reactions were performed by considering the pre-equilibrium mechanism, namely the exciton

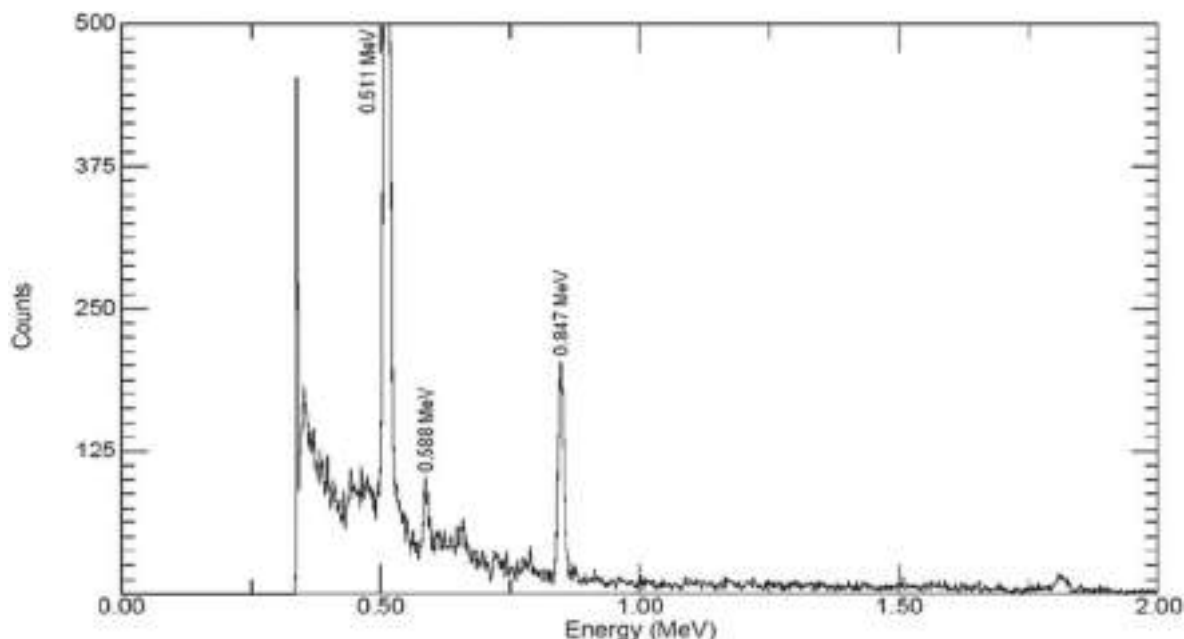


Fig. 3. γ -ray spectra of $^{89}\text{Zr}^m$ and ^{56}Mn radio nuclei produced by irradiating ^{92}Mo and ^{56}Fe respectively with 13.73 MeV neutrons.

model PCROSS code (Iwamoto and Harada, 1982) of EMPIRE-3.2 and the two-component exciton model (Koning and Duijvestijn, 2004) of TALYS-1.8. The first four sets of calculations were performed by means of the computer code EMPIRE-3.2 and the other four sets of calculations were performed by using the TALYS-1.8 code. In these codes, a number of options are available mainly for the nuclear level density, the nucleon potentials etc. Initially the choice of the parameters was made to obtain a good matching between the theoretical cross sections with those measured in the present work for neutron beam energies between 13.73 MeV and 14.77 MeV by considering the possible reaction channels depending on the compound nucleus excitation energy. Using these consistent sets of input parameter options, the theoretical cross sections of these reactions were estimated between 10 MeV and 20 MeV by the EMPIRE-3.2 and TALYS-1.8 codes, as these models make use of structure and model parameters.

4.1. The EMPIRE-3.2 code

The cross sections of the $^{90}\text{Zr}(n, \alpha)^{87}\text{Sr}^m$, $^{93}\text{Nb}(n, \alpha)^{90}\text{Y}^m$ and $^{92}\text{Mo}(n, \alpha)^{89}\text{Zr}^m$ reactions were estimated using the EMPIRE-3.2 code over the neutron energy range of 10 MeV–20 MeV in which all the transmission coefficients for the incident nucleon emission were calculated within the coupled channel approach using ECIS-06 (Raynal, 1994). The calculations of cross sections were carried out using the microscopic combinatorial level density by (Goriely et al., 2007) obtained from the Hartree-Fock-Bogoliubov method and considering the pre-equilibrium mechanism as defined in the exciton model (Griffin, 1966) as implemented in PCROSS code (Iwamoto and Harada, 1982). While employing the exciton model, the calculations were performed by choosing the values 1.5 (default) and 3 for the mean free path multiplier namely the MFP parameter. Moreover, in these calculations, for each MFP parameter value, the optical potentials for incident neutrons given by Koning (Koning and Delaroche, 2003) and by Strohmaier (1981) were separately used along with the alpha potential given by Avrigeanu (Avrigeanu et al., 1994) for the outgoing alpha particle. Hence there are two sets for each MFP value chosen in PCROSS code and each set of model parameters was used for estimating the cross sections over the neutron energy range of 13.73 MeV–14.77 MeV. Moreover for the $^{93}\text{Nb}(n, \alpha)^{90}\text{Y}^m$ reaction, the calculations were also performed by considering multistep compound model (Nishioka et al., 1986) along with the MFP parameter values 1.5 and 3 in the PCROSS code.

A comparison between the estimated cross sections with those measured in the present work provided important information about the best option of the input parameters available. Using all these best options of the input parameters and their combinations, the cross sections for the $^{90}\text{Zr}(n, \alpha)^{87}\text{Sr}^m$, $^{93}\text{Nb}(n, \alpha)^{90}\text{Y}^m$ and $^{92}\text{Mo}(n, \alpha)^{89}\text{Zr}^m$ reactions were successfully reproduced from 10 MeV to 20 MeV neutron energy using the EMPIRE-3.2 code.

4.2. The TALYS-1.8 code

The TALYS-1.8 code was also used for estimating the cross sections for the $^{90}\text{Zr}(n, \alpha)^{87}\text{Sr}^m$, $^{93}\text{Nb}(n, \alpha)^{90}\text{Y}^m$ and $^{92}\text{Mo}(n, \alpha)^{89}\text{Zr}^m$ reactions over the neutron energy range of 10 MeV–20 MeV in which all the optical model calculations were performed by ECIS-06 (Raynal, 1994). The calculations of the cross sections for these reactions were carried out using the level density model by (Hilaire et al., 2012), which uses temperature dependent combinatorial level densities with the DIM Gogny force given by Hartree-Fock-Bogolyubov calculations. Moreover these calculations were performed implementing the preequilibrium mechanism via the exciton model (Koning and Duijvestijn, 2004) and by using the local, global optical model parameters of neutrons as given by Koning (Koning and Delaroche, 2003) and for the alpha particle as given by Avrigeanu (Avrigeanu et al., 1994). For all three reactions, the calculations were performed using a sensitive parameter for the alpha particle emission namely Cstrip (Kalbach, 2005) with the assigned

values of 1.6 and 1.8. For each value of Cstrip, two sets of calculations were performed, one by using the neutron local potential and the other set by using the neutron global potential. Moreover for the $^{93}\text{Nb}(n, \alpha)^{90}\text{Y}^m$ reaction, the calculations were also performed by considering the additional parameters colldamp (Hilaire et al., 2012; Koning et al., 2008b) and ctmglobal (Gilbert and Cameron, 1965) along with a Cstrip value of 0.04.

Initially, the calculations were carried out using all the input parameters mentioned above to find out the consistent best option set. The parameters that produced theoretical cross sections close to those measured over 13.73 MeV–14.77 MeV were used for estimating the cross sections for the $^{90}\text{Zr}(n, \alpha)^{87}\text{Sr}^m$, $^{93}\text{Nb}(n, \alpha)^{90}\text{Y}^m$ and $^{92}\text{Mo}(n, \alpha)^{89}\text{Zr}^m$ reactions from 10 MeV to 20 MeV neutron energy.

5. Results and discussion

The experimental cross sections for the $^{90}\text{Zr}(n, \alpha)^{87}\text{Sr}^m$, $^{93}\text{Nb}(n, \alpha)^{90}\text{Y}^m$ and $^{92}\text{Mo}(n, \alpha)^{89}\text{Zr}^m$ reactions were obtained over the neutron energies of 13.73 MeV–14.77 MeV by substituting the values of all the experimental parameters and constants in the activation expression (1) and the values of the cross sections for each reaction under study are given in Table 2. It is evident from Table 2 that, the cross sections of (i) $^{90}\text{Zr}(n, \alpha)^{87}\text{Sr}^m$ reaction varies from 3 mb to 4.2 mb, (ii) $^{93}\text{Nb}(n, \alpha)^{90}\text{Y}^m$ reaction varies from 5 mb to 7 mb and (iii) $^{92}\text{Mo}(n, \alpha)^{89}\text{Zr}^m$ reaction varies from 5.8 mb to 8 mb.

The theoretical cross sections for the $^{90}\text{Zr}(n, \alpha)^{87}\text{Sr}^m$, $^{93}\text{Nb}(n, \alpha)^{90}\text{Y}^m$ and $^{92}\text{Mo}(n, \alpha)^{89}\text{Zr}^m$ reactions obtained using EMPIRE-3.2 and TALYS-1.8 are given in Table 3, Table 4 (a and b) and Table 5 respectively. In the present work, most of the theoretically estimated cross-sections for the three reactions studied are close to the measured cross-sections within the experimental error bar.

On comparing the theoretically estimated isomeric cross sections with the respective measured isomeric cross sections given in Table 3, it is observed that the cross sections estimated by the EMPIRE-3.2 code using the MFP parameter value 3 and that estimated by the TALYS-1.8 code using the Cstrip parameter with a value of 1.8 are in good agreement with the corresponding isomeric cross sections measured in the present work from 13.73 MeV to 14.77 MeV as compared to the other sets of input parameter options used. Using the consistent set of input parameters given in Table 3, the cross sections of the $^{90}\text{Zr}(n, \alpha)^{87}\text{Sr}^m$ reaction were also estimated using EMPIRE-3.2 and TALYS-1.8 codes and the results are given in Fig. 4. In addition, the cross sections measured in the present work and those reported in literature (BarreiraFilho and Fanger, 1982; Blosser et al., 1955; Bramlitt and Fink, 1963; Brolley et al., 1955; Dóczy et al., 1998; Filatenkov, 2016; Fujino et al., 1977; Gonçalves et al., 1987; Grallert et al., 1993; Husain et al., 1970; Ibn Majah et al., 2001; Ikeda et al., 1988; Marcinkowski et al., 1990; Molla et al., 1991; Mukherjee and Bakhr, 1963; Osman, K.T.; Habbani, 1996; Raics et al., 1991; Reed, 1960; Sailer et al., 1977; Semkova et al., 2010; Sigg and Kuroda, 1975; Srinivasa Rao et al., 1978) are also plotted in Fig. 4. The plots in Fig. 4 show that, the theoretical cross sections obtained using almost all the best options of input model parameters of the EMPIRE-3.2 and TALYS-1.8 codes mentioned in Table 3 are in good agreement with the cross sections measured in the

Table 2

Measured cross sections of the $^{90}\text{Zr}(n, \alpha)^{87}\text{Sr}^m$, $^{93}\text{Nb}(n, \alpha)^{90}\text{Y}^m$ and $^{92}\text{Mo}(n, \alpha)^{89}\text{Zr}^m$ reactions over 13.73 MeV–14.77 MeV neutron energies.

Neutron energy (MeV)	Measured isomeric cross section (mb)		
	$^{90}\text{Zr}(n, \alpha)^{87}\text{Sr}^m$	$^{93}\text{Nb}(n, \alpha)^{90}\text{Y}^m$	$^{92}\text{Mo}(n, \alpha)^{89}\text{Zr}^m$
13.73 ± 0.11	3.0 ± 0.3	5.0 ± 0.4	5.8 ± 0.3
14.07 ± 0.11	3.4 ± 0.3	5.5 ± 0.5	6.3 ± 0.3
14.42 ± 0.10	3.7 ± 0.3	5.9 ± 0.5	6.8 ± 0.4
14.68 ± 0.08	4.0 ± 0.3	6.1 ± 0.5	7.5 ± 0.4
14.77 ± 0.08	4.2 ± 0.3	7.0 ± 0.6	8.0 ± 0.4

Table 3

Cross sections for $^{90}\text{Zr}(n, \alpha)^{87}\text{Sr}^m$ reaction estimated over 13.73 MeV–14.77 MeV neutron energies using EMPIRE-3.2 and TALYS 1.8 codes along with cross sections measured in the present work.

Neutron energy (MeV)	Measured isomeric cross section (mb)	Theoretical isomeric cross section (mb)							
		EMPIRE-3.2				TALYS 1.8			
		MFP 1.5		MFP 3		Cstrip a 1.6		Cstrip a 1.8	
		neutron potential by Strohmaier	neutron global potential by Koning	neutron potential by Strohmaier	neutron global potential by Koning	neutron local potential by Koning	neutron global potential by Koning	neutron local potential by Koning	neutron global potential by Koning
13.73	3.0 ± 0.3	3.13	2.72	3.08	2.68	2.49	2.57	2.65	2.73
14.07	3.4 ± 0.3	3.36	2.93	3.36	2.94	2.94	3.03	3.13	3.22
14.42	3.7 ± 0.3	3.60	3.14	3.64	3.19	3.26	3.36	3.45	3.56
14.68	4.0 ± 0.3	3.80	3.32	3.89	3.42	3.69	3.80	3.91	4.03
14.77	4.2 ± 0.3	3.88	3.40	3.99	3.51	3.84	3.96	4.07	4.19

Table 4a

Cross sections for $^{93}\text{Nb}(n, \alpha)^{90}\text{Y}^m$ reaction estimated over 13.73 MeV–14.77 MeV neutron energies using EMPIRE-3.2 code along with cross sections measured in the present work.

Neutron energy (MeV)	Measured isomeric cross section (mb)	Theoretical isomeric cross section (mb) using EMPIRE-3.2 code							
		MFP 1.5				MFP 3			
		MSC 0		MSC 1		MSC 0		MSC 1	
		neutron potential by Strohmaier	neutron global potential by Koning	neutron potential by Strohmaier	neutron global potential by Koning	neutron potential by Strohmaier	neutron global potential by Koning	neutron potential by Strohmaier	neutron global potential by Koning
13.73	5.0 ± 0.4	4.17	3.59	4.35	3.75	4.17	3.59	5.12	4.48
14.07	5.5 ± 0.5	4.25	3.66	4.45	3.84	4.25	3.66	5.25	4.60
14.42	5.9 ± 0.5	4.21	3.64	4.42	3.81	4.21	3.64	5.29	4.64
14.68	6.1 ± 0.5	4.22	3.65	4.43	3.83	4.22	3.65	5.33	4.69
14.77	7.0 ± 0.6	4.23	3.66	4.45	3.85	4.23	3.66	5.37	4.72

Table 4b

Cross sections for $^{93}\text{Nb}(n, \alpha)^{90}\text{Y}^m$ reaction estimated over 13.73 MeV–14.77 MeV neutron energies using TALYS 1.8 code along with cross sections measured in the present work.

Neutron energy (MeV)	Measured isomeric cross section (mb)	Theoretical isomeric cross section (mb) using TALYS 1.8 code					
		Cstrip a 0.04 + colldamp + ctmglobal		Cstrip a 1.6 + colldamp + ctmglobal		Cstrip a 1.8 + colldamp + ctmglobal	
		neutron local potential by Koning	neutron global potential by Koning	neutron local potential by Koning	neutron global potential by Koning	neutron local potential by Koning	neutron global potential by Koning
		13.73	5.0 ± 0.4	5.56	5.53	25.55	25.50
14.07	5.5 ± 0.5	6.11	6.07	27.05	26.99	29.73	29.67
14.42	5.9 ± 0.5	6.74	6.69	28.62	28.54	31.42	31.35
14.68	6.1 ± 0.5	7.13	7.06	29.20	29.10	32.03	31.93
14.77	7.0 ± 0.6	7.09	7.02	29.10	29.01	31.93	31.84

Table 5

Cross sections for $^{92}\text{Mo}(n, \alpha)^{89}\text{Zr}^m$ reaction estimated over 13.73 MeV–14.77 MeV neutron energies using EMPIRE-3.2 and TALYS 1.8 codes along with cross sections measured in the present work.

Neutron energy (MeV)	Measured isomeric cross section (mb)	Theoretical isomeric cross section (mb)							
		EMPIRE-3.2				TALYS 1.8			
		MFP 1.5		MFP 3		Cstrip a 1.6		Cstrip a 1.8	
		neutron potential by Strohmaier	neutron global potential by Koning	neutron potential by Strohmaier	neutron global potential by Koning	Koning neutron local potential	neutron global potential by Koning	Koning neutron local potential	neutron global potential by Koning
13.73	5.8 ± 0.3	6.16	5.40	6.36	5.61	5.88	5.85	6.32	6.30
14.07	6.3 ± 0.3	6.53	5.73	6.83	6.04	6.62	6.60	7.12	7.09
14.42	6.8 ± 0.4	6.88	6.06	7.28	6.45	7.23	7.20	7.75	7.72
14.68	7.5 ± 0.4	7.04	6.21	7.46	6.62	7.98	7.95	8.56	8.52
14.77	8.0 ± 0.4	7.13	6.29	7.58	6.73	7.90	7.86	8.45	8.42

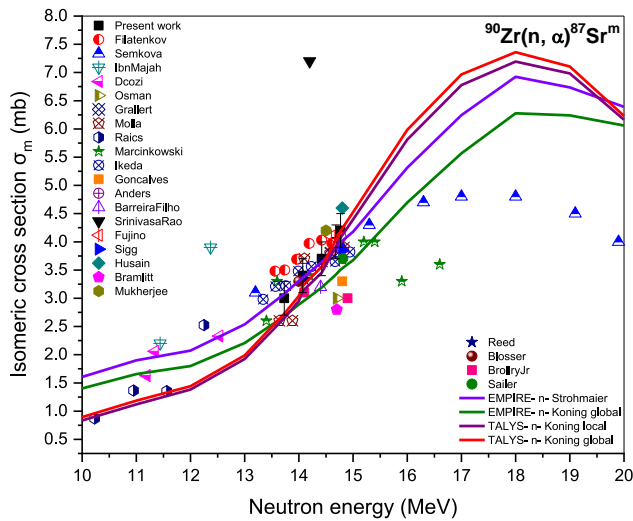


Fig. 4. Cross sections for $^{90}\text{Zr}(n, \alpha)^{87}\text{Sr}^m$ reaction at different neutron energies (i) measured in the present work and (ii) estimated over 10 MeV–20 MeV neutron energies using consistent set of input model parameters of EMPIRE-3.2 and TALYS 1.8 codes in the present work. A few literatures cross sections are plotted for comparison.

present work as well as with most of those reported in literature (Anders et al., 1985; BarreiraFilho and Fanger, 1982; Dóczi et al., 1998; Filatenkov, 2016; Fujino et al., 1977; Gonçalves et al., 1987; Grallert et al., 1993; Husain et al., 1970; Ibn Majah et al., 2001; Ikeda et al., 1988; Marcinkowski et al., 1990; Molla et al., 1991; Mukherjee and Bakhru, 1963; Osman, K.T.; Habbani, 1996; Raics et al., 1991; Reed, 1960; Sailer et al., 1977; Semkova et al., 2010; Sigg and Kuroda, 1975) between 10 MeV and 16.3 MeV.

The cross sections measured by Semkova (Semkova et al., 2010) above 16.5 MeV are found to be lower than those estimated theoretically using both codes, whereas the cross sections measured by IbnMajah (Ibn Majah et al., 2001) at 12.37 MeV and by SrinivasaRao (Srinivasa Rao et al., 1978) at 14.2 MeV are found to higher than the theoretically estimated cross sections. Moreover, the cross sections measured by Marcinkowski (Marcinkowski et al., 1990) at 15.9 MeV and at 16.6 MeV, by Bramlitt (Bramlitt and Fink, 1963) and by Brolley Jr (Brolley et al., 1955) are found to be lower as compared to the theoretically estimated values. The overall picture shows a well determined production cross section of the $^{87}\text{Sr}^m$ isomer for the (n, α) reaction on ^{90}Zr .

The cross sections for the $^{93}\text{Nb}(n, \alpha)^{90}\text{Y}^m$ reaction were calculated using some additional parameters available in both codes as compared to the set of input parameters which were used for the other two (n, α) reactions of the present study. This is mainly because the theoretical cross sections for this reaction obtained using EMPIRE-3.2 or TALYS-1.8 are found to be much lower or much higher than the presently measured cross sections respectively.

Table 4-a gives a summary of the cross sections for the $^{93}\text{Nb}(n, \alpha)^{90}\text{Y}^m$ reaction measured in the present work and estimated using the EMPIRE-3.2 code. It is observed from Table 4-a that the variation in the obtained isomeric cross sections is very small using all the options of the input parameters used in the theoretical calculations as compared to the variation in the measured isomeric cross sections, which is 2 mb over the whole neutron energy range. In the present work, out of all the input parameter options used in the theoretical calculations, only the option with MFP 3 and MSC 1 renders the theoretical cross-section values close to the measured ones at 13.73 MeV and 14.07 MeV. For the remaining three higher neutron energies, the theoretical cross sections are found to be lower than the corresponding measured ones. Similarly, Table 4-b gives a summary of the cross sections for the $^{93}\text{Nb}(n, \alpha)^{90}\text{Y}^m$ reaction measured in the present work and estimated using the TALYS-1.8 code

by considering the different values for the Cstrip parameter along with colldamp, ctmglobal and the neutron local as well as global potentials by Koning. It is observed from Table 4-b that the cross-sections obtained using the Cstip parameter value 0.04 are close to the one measured in the present work as compared to any other set of input parameter options which resulted very large values at each neutron energy.

Similarly, using the consistent set of the input parameters given in Table 4-a and Table 4-b, the cross sections of the $^{93}\text{Nb}(n, \alpha)^{90}\text{Y}^m$ reaction were estimated using EMPIRE-3.2 and TALYS-1.8 codes and the results are shown in Fig. 5. In addition, the cross sections measured in the present work and those reported in literature (Alford et al., 1961; Anders et al., 1985; Bramlitt and Fink, 1963; Dóczi et al., 1998; Fessler et al., 2000; Filatenkov, 2016; Gaiser et al., 1979; Garlea et al., 1992; Harper and Alford, 1982; Husain et al., 1970; Ikeda et al., 1988; Jianzhou et al., 1977; Kim et al., 1986; Levkovskii et al., 1970; Lu et al., 1970; Mannan and Qaim, 1988; Molla et al., 1991; Pasha et al., 2019; Ryves and Kol-kowski, 1981; Turkiewicz, 1975; Wölfle et al., 1988) are also plotted in Fig. 5. The plots in Fig. 5 show that, the theoretical cross sections obtained using almost all the best options of input model parameters of EMPIRE-3.2 and TALYS-1.8 codes mentioned in Table 4-a and Table 4-b are close to the cross sections measured in the present work within the uncertainties as well as to most of those reported in literature (Alford et al., 1961; Anders et al., 1985; Bramlitt and Fink, 1963; Dóczi et al., 1998; Fessler et al., 2000; Filatenkov, 2016; Gaiser et al., 1979; Garlea et al., 1992; Harper and Alford, 1982; Husain et al., 1970; Ikeda et al., 1988; Jianzhou et al., 1977; Kim et al., 1986; Lu et al., 1970; Mannan and Qaim, 1988; Molla et al., 1991; Pasha et al., 2019; Ryves and Kol-kowski, 1981; Turkiewicz, 1975; Wölfle et al., 1988) between 10 MeV and 19 MeV. The cross sections measured by Woelfle (Wölfle et al., 1988) between 12.55 MeV and 13.35 MeV and above 18.5 MeV are found to be higher than those estimated theoretically using both codes. However, the cross sections measured by Woelfle between 15.8 MeV and 17 MeV lies between the theoretical cross sections estimated using both codes. Moreover, the cross sections measured by Levkovskii (Levkovskii et al., 1970) are found to be lower than the theoretically estimated cross sections. The overall picture shows a well determined production cross section of the $^{90}\text{Y}^m$ isomer for the (n, α) reaction on ^{93}Nb .

Table 5 gives a summary of the cross sections for $^{92}\text{Mo}(n, \alpha)^{89}\text{Zr}^m$ reaction measured in the present work and estimated theoretically. On comparing the theoretically estimated cross sections with the respective

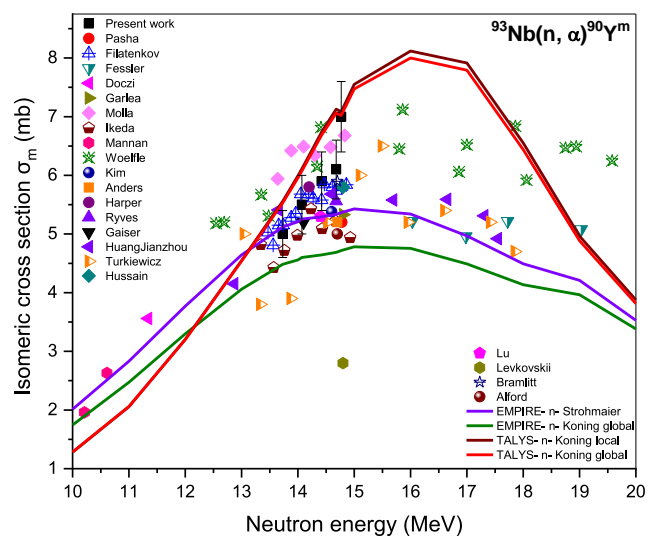


Fig. 5. Cross sections for $^{93}\text{Nb}(n, \alpha)^{90}\text{Y}^m$ reaction at different neutron energies (i) measured in the present work and (ii) estimated over 10 MeV–20 MeV neutron energies using consistent set of input model parameters of EMPIRE-3.2 and TALYS 1.8 codes in the present work. A few literatures cross sections are plotted for comparison.

measured ones given in Table 5, it is observed that the agreement is quite satisfactory as compared to any other set of input parameter options used.

Using the consistent set of input parameters given in Table 5, the theoretical cross sections of the $^{92}\text{Mo}(n, \alpha)^{89}\text{Zr}^m$ reaction are shown in Fig. 6. In addition, the cross sections measured in the present work and those reported in literature (Amemiya et al., 1982; Filatenkov, 2016; Fujino et al., 1977; Garlea et al., 1992; Hasan et al., 1972; Ikeda et al., 1988; Kanda, 1972; Lu et al., 1970; Marcinkowski et al., 1986; Qaim et al., 1974; Rao et al., 1981; Reimer et al., 2005; Sigg and Kuroda, 1975) are also plotted in Fig. 6. The plots in Fig. 6 show that, the theoretical cross sections obtained using almost all the best options of input model parameters of EMPIRE-3.2 and TALYS-1.8 codes mentioned in Table 5 are also in good agreement with most of those reported in literature (Amemiya et al., 1982; Filatenkov, 2016; Ikeda et al., 1988; Marcinkowski et al., 1986; Sigg and Kuroda, 1975) between 13 MeV and 15.9 MeV. The cross sections measured by Reimer (Reimer et al., 2005), Garlea (Garlea et al., 1992), SrinivasaRao (Rao et al., 1981), Fujino (Fujino et al., 1977), most of the measured cross sections by Kanda (Kanda (1972), Hasan (Hasan et al., 1972) and Qaim (Qaim et al., 1974) are found to be lower than those estimated theoretically using both codes as well as earlier works mainly. In addition, the cross section measured by Lu (Lu et al., 1970) is found to be higher than those estimated theoretically using both codes. The overall picture shows a well determined production cross section of the $^{89}\text{Zr}^m$ isomer for the (n, α) reaction on ^{92}Mo .

From the results shown in Figs. 4–6, it can be observed that the theoretical cross sections for all the three reactions studied are found to decrease around and above 17 MeV as other reaction channels are beginning to emerge.

The measured cross sections for these three reactions increase with the increase in neutron energy. Moreover, from the results of Table 2 it is quite interesting to know that, as the proton number increased by one when we go from zirconium to niobium or from niobium to molybdenum, the probability of alpha particle emission also increased with the neutron energy. The present results indicate that the measured cross section at each neutron energy for the $^{92}\text{Mo}(n, \alpha)^{89}\text{Zr}^m$ reaction is found to be the highest as compared to the other two reactions whereas, for the $^{90}\text{Zr}(n, \alpha)^{87}\text{Sr}^m$ reaction it is found to be the lowest as compared to the other two reactions studied. This is mainly due to the increase in coulomb repulsion between the protons as we go from zirconium to molybdenum via niobium, because the percentage increase in the proton number is quite large as compared to percentage increase in the number of neutrons in a target nucleus which are responsible for compensating the coulomb repulsion between the protons. Therefore, these cross sections for the emission of α particles in these three reactions induced by fast neutrons for neutron-rich nuclei with $N > 50$ in the mass region ~ 90 are found to be useful in testing the nuclear models. The results obtained from the measurement are compared with new model calculations and also with works by other authors and good agreement was found to exist between the experimental data and the new model calculations.

6. Conclusions

The isomeric cross sections for the $^{90}\text{Zr}(n, \alpha)^{87}\text{Sr}^m$, $^{93}\text{Nb}(n, \alpha)^{90}\text{Y}^m$ and $^{92}\text{Mo}(n, \alpha)^{89}\text{Zr}^m$ reactions were measured at five neutron energies over the range of 13.73 MeV–14.77 MeV, using the neutron activation technique. The results obtained were compared with new model based calculated values and also with earlier works reported by other authors and were found to be in good agreement. The measured cross sections increase with the neutron energy from 13.73 MeV to 14.77 MeV. From the results of the present study, it can be concluded that as the proton number increases by one, from zirconium to niobium, or from niobium to molybdenum, the probability of alpha particle emission also increases at each corresponding neutron energy. Moreover, the theoretical cross-

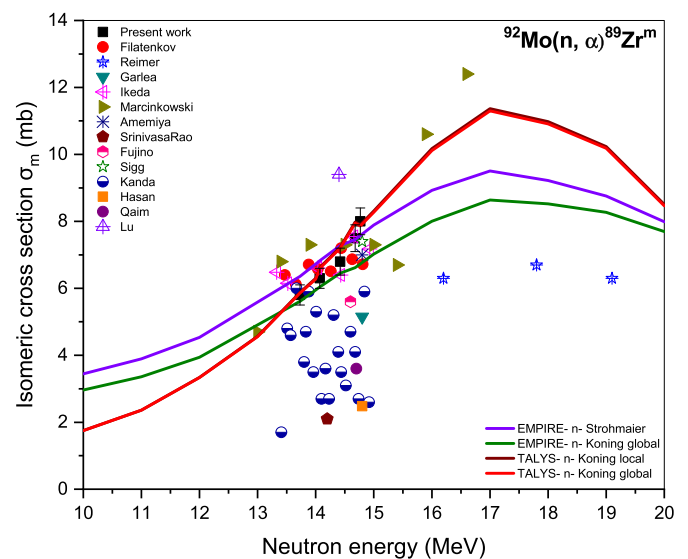


Fig. 6. Cross sections for $^{92}\text{Mo}(n, \alpha)^{89}\text{Zr}^m$ reaction at different neutron energies (i) measured in the present work and (ii) estimated over 10 MeV–20 MeV neutron energies using consistent set of input model parameters of EMPIRE-3.2 and TALYS 1.8 codes in the present work. A few literatures cross sections are plotted for comparison.

sections obtained using the mean free path multiplier namely MFP for EMPIRE-3.2 and those obtained using a sensitive parameter for alpha particle emission, namely Cstrip for TALYS-1.8, plays an important role in getting the cross-section values close to the measured ones in the present work. These experimental results are important for reactor technology applications and constitute an addition to the EXFOR database.

CRedit author statement

F. M. D. Attar: Methodology; Data curation; Writing - original draft; Software; Project administration; Funding acquisition.

G.T. Bholane: Writing - review & editing; Investigation; Software; Formal analysis.

T.S. Ganesapandy: Software, Visualization; Writing - review & editing; Validation.

S.D. Dhole: Funding acquisition; Project administration; Writing - review & editing; Supervision; Investigation; Resources.

V.N. Bhoraskar: Conceptualization; Methodology; Writing - review & editing; Supervision; Investigation; Validation; Formal analysis.

Declaration of competing interest

The authors declare that they have no known competing financial interests or personal relationships that could have appeared to influence the work reported in this paper.

Acknowledgements

One of the authors [F.M.D. Attar] gratefully acknowledges the financial assistance by DST FIST sanction no. SR/FST/College-328/2016. Author [S. D. Dhole] is thankful to SERB-DST sanction number: EMR/2017/002497 and DAE-BRNS sanction number: 36(6)/14/49/2016-BRNS for the financial support. The author F.M.D. Attar wish to express sincere thanks to Dr. Iqbal N. Shaikh (Vice-Principal), Dr. Aftab Anwar Shaikh (Principal) of the Poona College, Pune and AKI Trust, Mumbai for the encouragement, support and help for carrying out research work.

References

- Avrigneanu, V., Chuvaev, S.V., Eichin, R., Filatenkov, A.A., Forrest, R.A., Freiesleben, H., Herman, M., Koning, A.J., Seidel, K., 2006. Pre-equilibrium reactions on the stable tungsten isotopes at low energy. *Nucl. Phys.* 765, 1–28.
- Avrigneanu, V., Hodgson, P.E., Avrigneanu, M., 1994. Global optical potentials for emitted alpha particles. *Phys. Rev. C* 49, 2136–2141. <https://doi.org/10.1103/PhysRevC.49.2136>.
- Hubbell, J.H., Seltzer, S.M., 2004. Tables of x-Ray Mass Attenuation Coefficients and Mass Energy-Absorption Coefficients 1 keV to 20 MeV for Elements $z = 1$ to 92 and 48 Additional Substances of Dosimetric Interest.
- Alford, W.L., Koehler, D.R., Mandeville, C.E., 1961. Evidence for an isomeric state of ${}^{90}\text{Y}$. *Phys. Rev.* 123, 1365–1368. <https://doi.org/10.1103/PhysRev.123.1365>.
- Amemiya, S., Ishibashi, K., Katoh, T., 1982. Neutron activation cross section of molybdenum isotopes at 14.8 MeV. *J. Nucl. Sci. Technol.* 19, 781–788. <https://doi.org/10.1080/1881248.1982.9734218>.
- Anders, B., Bahal, B.M., Pepelnik, R., 1985. Measurements of 14 MeV Neutron Activation Cross Section at KORONAR, GKSS-85-E-24, 1985 Rept. Ges.
- Attar, F.M.D., Mandal, R., Dhole, S.D., Saxena, A., Ashokkumar, Ganesan, S., Kailas, S., Bhoraskar, V.N., 2008. Cross-sections for formation of ${}^{89}\text{Zr}$ through ${}^{90}\text{Zr}(n,2n){}^{89}\text{Zr}$ reaction over neutron energy range 13.73 MeV to 14.77 MeV. *Nucl. Phys.* 802, 1–11.
- Attar, F.M.D., Dhole, S.D., Bhoraskar, V.N., 2014. Cross sections of the n,p phantom $\{\text{rule}(0.16em)\{0ex\}\}$ reaction on the ${}^{78}\text{Se}$ and ${}^{80}\text{Se}$ isotopes $\{\text{mathrm}\{Se\}$ isotopes measured for 13.73 MeV to 14.77 MeV and estimated for 10 MeV to 20 MeV neutron energies. *Phys. Rev. C* 90, 64609. <https://doi.org/10.1103/PhysRevC.90.064609>.
- BarreiraFilio, J.L., Fanger, H.-U., 1982. Measurements of neutron activation cross sections at 14.4 MeV for ZN-68 and ZR-90. 82. Ges.Kernen.-Verwertung, Schiffbau und Schiffahrt, p. E-8.
- Bhoraskar, V.N., 1989. A facility for 14-MeV neutron irradiation and activation analysis. *Indian J. Pure Appl. Phys.* 27, 648–655.
- Blosser, H.G., Goodman, C.D., Handley, T.H., Randolph, M.L., 1955. 14-MeV $(n, \text{ensuremath}\{\alpha\})$ Cross-Section Measurements. *Phys. Rev.* 100, 429–430. <https://doi.org/10.1103/PhysRev.100.429.2>.
- Bramlitt, E.T., Fink, R.W., 1963. Rare nuclear reactions induced by 14.7-MeV neutrons. *Phys. Rev.* 131, 2649–2663. <https://doi.org/10.1103/PhysRev.131.2649>.
- Brolley, J.E., Bunker, M.E., Cochran, D.R.F., Henkel, R.L., Mize, J.P., Starner, J.W., 1955. 14-MeV $(n, \text{ensuremath}\{\alpha\})$ Cross Sections in Zirconium. *I. Phys. Rev.* 99, 330. <https://doi.org/10.1103/PhysRev.99.330>. Dóczy et al., 1998 Dóczy, R., Semkova, V., Fenyvesi, A., Yamamoto, N., Buczkó, C.M., Csikai, J., 1998. Excitation functions of some (n,p) and (n,α) reactions from threshold to 16 MeV. *Nucl. Sci. Eng.* 129, 164–174. <https://doi.org/10.13182/NSE98-A1970>.
- Fessler, A., Plompen, A.J.M., Smith, D.L., Meadows, J.W., Ikeda, Y., 2000. Neutron activation cross-section measurements from 16 to 20 MeV for isotopes of F, Na, Mg, Al, Si, P, Cl, Ti, V, Mn, Fe, Nb, Sn, and Ba. *Nucl. Sci. Eng.* 134, 171–200. <https://doi.org/10.13182/NSE99-14>.
- Filatenkov, A.A., 2016. USSR Report to the INDC, 0460, 2016.
- others Filatenkov, A.A., Chuvaev, S.V., Aksenov, V.N., Yakovlev, V.A., Malyshev, A. V., Vasil'ev, S.K., Avrigneanu, M., Avrigneanu, V., Smith, D.L., Ikeda, Y., 1999. Khlopin Radiat. Inst., Leningrad Reports.
- Fujino, Y., Hyakutake, M., Kumabe, I., 1977. Activation cross sections on zirconium and molybdenum isotopes induced by 14.6 MeV neutrons. *Jpn. Rep. to NEANDC*, No. 51, 60.
- Gaiser, J.E., Alford, W.L., Skelton, R.T., 1979. Neutron cross sections for Nb-93(n,alpha) Y-90-m and Se-80(n,alpha)Se-79-m at 14.1-MeV. *Bull. Am. Phys. Soc.* 24.
- Garlea, I., Miron-Garlea, Chr, Rosu, H.N., Fodor, G., V. R., 1992. Integral neutron cross sections measured around 14 MeV. *Rev. Roum. Phys.* 37, 19.
- Gilbert, A., Cameron, A.G.W., 1965. A composite nuclear-level density formula with shell corrections. *Can. J. Phys.* 43, 1446–1496. <https://doi.org/10.1139/p65-139>.
- Gonçalves et al., 1987 Gonçalves, I.F., Schram, Z., Papp, Z., Daroczy, S., 1987. (n,p) , (n,α) and $(n,2n)$ reaction cross-sections for some isotopes of Zr, Pd, and Cd at 14.8 MeV. *Int. J. Radiat. Appl. Instrum. Appl. Radiat. Isot.* 38, 989–991. [https://doi.org/10.1016/0883-2889\(87\)90274-7](https://doi.org/10.1016/0883-2889(87)90274-7).
- Goriely, S., Samyn, M., Pearson, J.M., 2007. Further explorations of Skyrme-Hartree-Fock-Bogoliubov mass formulas. VII. Simultaneous fits to masses and fission barriers. *Phys. Rev. C* 75, 64312. <https://doi.org/10.1103/PhysRevC.75.064312>.
- Grallert, A., Csikai, J., Buczkó, C.M., Shaddad, I., 1993. IAEA Nucl.Data section report to the I.N.D.C, 286, p. 131, 1993.
- Griffin, J.J., 1966. Statistical model of intermediate structure. *Phys. Rev. Lett.* 17, 478–481. <https://doi.org/10.1103/PhysRevLett.17.478>.
- Harper, R.C., Alford, W.L., 1982. Experimental and theoretical neutron cross sections at 14 MeV. *J. Phys. G Nucl. Phys.* 8, 153–160. <https://doi.org/10.1088/0305-4616/8/1/014>.
- Hasan, S.S., Prasad, R., Seghal, M.L., 1972. The 14.8 MeV neutron cross sections for enriched isotopes of ${}^{82}\text{Se}$, ${}^{92}\text{Mo}$, ${}^{117}\text{Sn}$, ${}^{128}\text{Te}$ and ${}^{130}\text{Te}$. *Nucl. Phys.* 181, 101–105. [https://doi.org/10.1016/0375-9474\(72\)90903-7](https://doi.org/10.1016/0375-9474(72)90903-7).
- Herman, M., Capote, R., Carlson, B.V., Obložinský, P., Sin, M., Trkov, A., Wienke, H., Zerkin, V., 2007. (EMPIRE): nuclear reaction model code system for data evaluation. *Nucl. Data Sheets* 108, 2655.
- Hilaire, S., Girod, M., Goriely, S., Koning, A.J., 2012. Temperature-dependent combinatorial level densities with the DIM Gogny force. *Phys. Rev. C* 86, 64317.
- Husain, L., Bari, A., Kuroda, P.K., 1970. Neutron activation cross sections at 14.8 MeV for rubidium, strontium, zirconium, and niobium. *Phys. Rev. C* 1, 1233–1236. <https://doi.org/10.1103/PhysRevC.1.1233>.
- IAEA TECDOC, 2020. Reference Neutron Activation Library, TECDOC Series. INTERNATIONAL ATOMIC ENERGY AGENCY, Vienna.
- Ibn Majah, M., Chiadli, A., Sudár, S., Qaim, S.M., 2001. Cross sections of (n,p) , (n,α) and $(n,2n)$ reactions on some isotopes of zirconium in the neutron energy range of 10–12 MeV and integral tests of differential cross section data using a 14 MeV $d(\text{Be})$ neutron spectrum. *Appl. Radiat. Isot.* 54, 655–662. [https://doi.org/10.1016/S0969-8043\(00\)00299-2](https://doi.org/10.1016/S0969-8043(00)00299-2).
- Ikeda, Y., Konno, C., Oishi, K., Nakamura, T., Miyade, H., Kawade, K., Yamamoto, H., Katoh, T., 1988. JAERI Reports, vol. 1312, 1988.
- Iwamoto, A., Harada, K., 1982. Mechanism of cluster emission in nucleon-induced preequilibrium reactions. *Phys. Rev. C* 26, 1821–1834.
- JAEA Nuclear Data Center. Nuclear Data Center JAEA. n.d. [WWW Document]. URL. <http://nucleardata.nuclear.lu.se/database/masses>.
- Jianzhou, H., Yunfeng, C., Wenrong, Z., Baolin, C., 1977. Activation function of fast neutron induced nuclear reaction for Ni-58 and Nb-93. *At. Energy Sci. Technol.* 11, 211.
- Kalbach, C., 2005. Preequilibrium reactions with complex particle channels. *Phys. Rev. C* 71, 34606. <https://doi.org/10.1103/PhysRevC.71.034606>.
- Kanda, Y., 1972. The excitation functions and isomer ratios for neutron-induced reactions on ${}^{92}\text{Mo}$ and ${}^{90}\text{Zr}$. *Nucl. Phys.* 185, 177–195. [https://doi.org/10.1016/0375-9474\(72\)90558-1](https://doi.org/10.1016/0375-9474(72)90558-1).
- Kawade, K., Sakane, H., Kasugai, Y., Shibata, M., Iida, T., Takahashi, A., Fukahori, T., 2003. Measurement method of activation cross-sections of reactions producing short-lived nuclei with 14 MeV neutrons. *Nucl. Instrum. Methods Phys. Res. Sect. A Accel. Spectrometers, Detect. Assoc. Equip.* 496, 183–197. [https://doi.org/10.1016/S0168-9002\(02\)01617-0](https://doi.org/10.1016/S0168-9002(02)01617-0).
- Kim, Y.S., Kim, N.B., Chung, K.H., Bak, H.I., 1986. Measurement of Nb-93(n,na)Y-89m, Nb-93(n,a)Y-90m and Nb-93(n,2n)Nb-92m cross sections for 14 MeV neutrons. *J. Kor. Nucl. Soc.* 18, 92.
- Koning, A.J., Delaroche, J.P., 2003. Local and global nuclear optical models from 1 keV to 200 MeV. *Nucl. Phys.* 713, 231–310. [https://doi.org/10.1016/S0375-9474\(02\)01321-0](https://doi.org/10.1016/S0375-9474(02)01321-0).
- Koning, A.J., Duijvestijn, M.C., 2004. A global pre-equilibrium analysis from 7 to 200 MeV based on the optical model potential. *Nucl. Phys.* 744, 15–76. <https://doi.org/10.1016/j.nuclphysa.2004.08.013>.
- Koning, A.J., Duijvestijn, M.C., Hilaire, S., 2008a. TALYS-10. EDP Sciences, France.
- Koning, A.J., Hilaire, S., Goriely, S., 2008. Global and local level density models. *Nucl. Phys.* 810, 13–76. <https://doi.org/10.1016/j.nuclphysa.2008.06.005>. Levkovskii et al., 1970 Levkovskii, V.N., Vinit'skaya, G.P., Kovel'skaya, G.E., 1970. Cross sections for (n,p) and (n,α) reactions with 14.8-MeV neutrons. *Sov. J. Nucl. Phys.* 10, 25. Lu et al., 1970 Lu, W., RanaKumar, N., Fink, R.W., 1970. Activation Cross Sections for (n, p) , (n, α) , (n, pn) and (n, nd) reactions, and $(n, \text{ensuremath}\{\alpha\})$ Reactions in the Region of $Z=40$ $\{\text{mathrm}\{to\}$ 58 $\}$ at 14.4 MeV. *Phys. Rev. C* 1, 358–361. <https://doi.org/10.1103/PhysRevC.1.358>.
- Mandal, R., Radhu Pansare, G., Sengupta, D., Nagesh Rao Bhoraskar, V., 2012. Angular distribution of neutron flux around the tritium target of 14 MeV neutron generator. *J. Phys. Soc. Jpn.* 81, 104006. <https://doi.org/10.1143/JPSJ.81.104006>.
- Mannan, A., Qaim, S.M., 1988. Activation cross section and isomeric cross-section ratio for the ${}^{93}\text{Nb}(n, \text{ensuremath}\{\alpha\}){}^{90}\text{mY}$ process. *Phys. Rev. C* 38, 630–632. <https://doi.org/10.1103/PhysRevC.38.630>.
- Marcinkowski, A., Stankiewicz, K., Garuska, U., Herman, M., 1986. Cross section of fast neutron induced reactions on molybdenum isotopes. *Z. Phys. A, Hadron. Nucl.* 323, 91. Marcinkowski et al., 1990 Marcinkowski, A., Garuska, U., Hoang, H.M., Kielan, D., Zwiegliński, B., 1990. Cross sections of the (np) reaction on zirconium isotopes. *Nucl. Phys.* 510, 93–105. [https://doi.org/10.1016/0375-9474\(90\)90289-X](https://doi.org/10.1016/0375-9474(90)90289-X).
- Molla, N.I., Miah, R.U., Rahman, M., Aysha, A., 1991. Excitation functions of some (np) , $(n,2n)$ and (n,α) reactions on nickel, zirconium and niobium isotopes in the energy range 13.63–14.83 MeV. *Conf. Conf. Nucl. Data Sci. Technol., Juelich* 355, 1991, (1991). p. 355.
- Mukherjee, S.K., Bakhrū, H., 1963. Proceedings of nuclear and solid state Physics symposium, Bombay, India, p. 244, 1963, EXFOR 31330.002.
- National Nuclear Data Center, 1996. Information Extracted from the N. 2 database National Nuclear Data Center, Information Extracted from the NuDat 2 Database.
- Nishioka, H., Verbaarschot, J.J.M., Weidenmüller, H.A., Yoshida, S., 1986. Statistical theory of precompound reactions: the multistep compound process. *Ann. Phys.* 172, 67–99. [https://doi.org/10.1016/0003-4916\(86\)90020-5](https://doi.org/10.1016/0003-4916(86)90020-5).
- Osman, K.T., Habbani, F.I., 1996. Sudanese Report to the I.N.D.C. No.001, 1996.
- Otuka, N., Dupont, E., Semkova, V., Pritychenko, B., Blokhin, A.I., Aikawa, M., Babykina, S., Bossant, M., Chen, G., Dunaeva, S., Forrest, R.A., Fukahori, T., Furutachi, N., Ganesan, S., Ge, Z., Gritzay, O.O., Herman, M., Hlaváč, S., Kató, K., Lalremruata, B., Lee, Y.O., Makinaga, A., Matsumoto, K., Mikhaylyukova, M., Pikulina, G., Pronyaev, V.G., Saxena, A., Scherer, O., Simakov, S.P., Soppera, N., Suzuki, R., Takács, S., Tao, X., Taova, S., Tárkányi, F., Varlamov, V.V., Wang, J., Yang, S.C., Zerkin, V., Zhuang, Y., 2014. Towards a more complete and accurate experimental nuclear reaction data library (EXFOR): international collaboration between nuclear reaction data centres (NRDC). *Nucl. Data Sheets* 120, 272–276. <https://doi.org/10.1016/j.nds.2014.07.065>. Pasha et al., 2019 Pasha, I., Basavanna, R., Yerranguntla, S.S., Suryanarayana, S.V., Karkera, M., Naik, H., Karantha, M.P., Danu, L.S., Bishnoi, S., Patel, T., Kumar, R., 2019. ${}^{93}\text{Nb}(n,2n){}^{92}\text{mNb}$, ${}^{93}\text{Nb}(n,\alpha){}^{90}\text{mY}$ and ${}^{92}\text{Mo}(n,p){}^{92}\text{mNb}$ reactions at 14.78 MeV and covariance analysis. *J. Radioanal. Nucl. Chem.* 320, 561–568. <https://doi.org/10.1007/s10967-019-06510-z>.

- Qaim, S.M., Wölfle, R., Stöcklin, G., 1974. Radiochemical investigations of fast neutron-induced low-yield nuclear reactions. *J. Radioanal. Chem.* 21, 395–405. <https://doi.org/10.1007/BF02516324>.
- Raics, P., Nagy, S., Szegedi, S., Kornilov, N.V., Kagalenko, A.B., 1991. Cross section measurements of neutron induced reactions on the zirconium isotopes in the energy range of 5.4 to 12.3 MeV. *Conf. Nucl. Data Sci. Technol., Juelich 660, 1991, (1991)*. p. 660.
- Rao, C.V.S., Das, N.L., Rao, B.V.T., Rao, J.R., 1981. Activation cross-sections for 14.2 MeV neutrons on molybdenum. *Phys. Scripta* 24, 935–937. <https://doi.org/10.1088/0031-8949/24/6/004>.
- Raynal, J., 1994. Notes on ECIS94, CEA Saclay Report No. CEA-N-2772.
- Reed, C.H., 1960. Div. of Tech. Info. U.S. AEC Reports. No.11929.
- Reimer, P., Avrigeanu, V., Chuvaev, S.V., Filatenkov, A.A., Glodariu, T., Koning, A., Plompen, A.J.M., Qaim, S.M., Smith, D.L., Weigmann, H., 2005. Reaction mechanisms of fast neutrons on stable Mo isotopes below 21 MeV. *Phys. Rev. C* 71, 44617. <https://doi.org/10.1103/PhysRevC.71.044617>.
- Ryves, T.B., Kolkowski, P., 1981. The Nb(n, 2n), Nb(n,α) and Nb(n, n') cross sections at 14 MeV. *J. Phys. G Nucl. Phys.* 7, 529–534. <https://doi.org/10.1088/0305-4616/7/4/012>.
- Sailer et al., 1977 Sailer, K., Daroczy, S., Raics, P., Nagy, S., 1977. The cross sections of (n,2n), (np), (n,α) reactions for 14.8 MeV neutrons on isotopes of Cr and Zr. *All Union Conf. Neutron Phys., Kiev 1, 246, 18-22 Apr 1977*.
- Semkova, V., Bauge, E., Plompen, A.J.M., Smith, D.L., 2010. Neutron activation cross sections for zirconium isotopes. *Nucl. Phys.* 832, 149–169. <https://doi.org/10.1016/j.nuclphysa.2009.10.133>.
- Sigg and Kuroda, 1975 Sigg, R.A., Kuroda, P.K., 1975. 14-8 MeV neutron-induced (n, 2n), np) and (n, α) cross-sections for some closed shell nuclides. *J. Inorg. Nucl. Chem.* 37, 631–636. [https://doi.org/10.1016/0022-1902\(75\)80511-2](https://doi.org/10.1016/0022-1902(75)80511-2).
- Srinivasa Rao, C.V., Lakshmana Das, N., Thirumala Rao, B.V., Rama Rao, J., 1978. Fluctuations in the systematics of (n,2n) reaction cross sections in the low mass region; Fast neutron cross-sections of fusion reactor interest. 21. *Nucl. Phys. Solid State Phys. Symp., Bombay 2, 113*.
- Strohmaier, B., 1981. IAEA Advisory Group Meeting on Nuclear Data for Radiation Damage Assessment and Related Safety Aspects. October 1981. International Atomic Energy Agency, Vienna, pp. 12–16 (IAEA).
- Taylor, J.R., 1982. *An Introduction to Error Analysis*. University Science Books Mill Valley, p. 57.
- Turkiewicz, 1975 Turkiewicz, J., 1975. Preliminary values of cross-sections for (na) reactions on the P-31, Mn-55, Co-59, As-75 and Nb-93. *Priv. Commun. Name Turkiewicz*.
- Wölfle, R., Mannan, A., Qaim, S.M., Liskien, H., Widera, R., 1988. Excitation functions of $^{93}\text{Nb}(n, 2n)^{92}\text{mNb}$, $^{93}\text{Nb}(n, \alpha)^{90}\text{mY}$, $^{139}\text{La}(n, \alpha)^{136}\text{Cs}$ and $^{181}\text{Ta}(n, p)^{181}\text{Hf}$ reactions in the energy range of 12.5–19.6 MeV. *Int. J. Radiat. Appl. Instrum. Appl. Radiat. Isot.* 39, 407–412. [https://doi.org/10.1016/0883-2889\(88\)90071-8](https://doi.org/10.1016/0883-2889(88)90071-8).



Covariance analysis and measurements of photon and neutron induced nuclear reaction cross sections of gallium isotopes

T. S. Ganesapandy¹, G. T. Bholane¹, A. B. Phatangare¹, F. M. D. Attar², S. S. Dahiwale¹, S. V. Suryanarayana³, V. N. Bhoraskar¹, S. D. Dhole^{1,a}

¹ Department of Physics, Savitribai Phule Pune University, Pune 411007, India

² Department of Physics, AKI's Poona College, Camp, Pune 411001, India

³ Nuclear Physics Division, Bhabha Atomic Research Centre, Mumbai 400085, India

Received: 16 October 2021 / Accepted: 5 June 2022

© The Author(s), under exclusive licence to Società Italiana di Fisica and Springer-Verlag GmbH Germany, part of Springer Nature 2022

Abstract The production cross sections of $^{69}\text{Ga}(n,p)^{69}\text{Zn}^m$, $^{69}\text{Ga}(n,2n)^{68}\text{Ga}$, $^{71}\text{Ga}(n,p)^{71}\text{Zn}^m$ and $^{71}\text{Ga}(n,2n)^{70}\text{Ga}$ reactions at 14.77 ± 0.17 neutron energy and the bremsstrahlung spectrum averaged cross sections of $^{69}\text{Ga}(\gamma,n)^{68}\text{Ga}$ and $^{71}\text{Ga}(\gamma,n)^{70}\text{Ga}$ reactions at 15 MeV bremsstrahlung end point energy were measured using offline gamma spectrometry. Uncertainties in the measured cross sections were reported with a detailed covariance analysis. The experimental results were compared with previously reported experimental data from the EXFOR database and the evaluated nuclear data libraries ENDF/B-VIII.0, JENDL-5 and TENDL-2019. Theoretical nuclear model calculations were performed with the TALYS-1.95 code with default and optimized input parameters to fit with the experimental data. The measured cross sections were found to be in good agreement with the literature and theoretical calculations.

1 Introduction

Gallium-68 (^{68}Ga) is an important Positron Emission Tomography (PET) radioisotope that decays with a half-life of 67.71 min [1] and is used for diagnostic imaging in oncological applications [2–6]. The short half-life of ^{68}Ga makes it an ideal radioisotope for clinical use [7]. ^{68}Ga is used as one of the theranostic twins along with Lutetium-177 (^{177}Lu) [8], here ^{68}Ga -labelled compounds [9] are used for diagnostic imaging and ^{177}Lu -labelled compounds [10] target the somatostatin receptor.

^{68}Ga can be prepared indirectly from its long-lived parent Germanium-68 which has a half-life of 271 days. ^{68}Ga can also be produced directly in cyclotrons by bombarding (1) solid/liquid enriched zinc targets with either protons [11, 12] or deuterium ions [13, 14] and (2) solid copper targets with alpha particles [15, 16]. Alternatively, ^{68}Ga can also be produced directly by bombarding solid Gallium targets with either 14 MeV neutrons from a neutron generator via the $^{69}\text{Ga}(n,2n)^{68}\text{Ga}$ nuclear reaction [17–19] or 15 MeV photons from a medical Linear accelerator (LINAC) via the $^{69}\text{Ga}(\gamma,n)^{68}\text{Ga}$ nuclear reaction [20]. Table 1 illustrates the recent experimental studies on the production of ^{68}Ga .

A few authors [19, 23–25] have experimentally measured the neutron-induced reaction cross sections on Gallium target at multiple neutron energies in the energy range 9.44–18.7 MeV. The uncertainties reported by Pu et al. [25] is 4%, by Bormann et al. [24] is 10%, by Nesaraja et al. [23] is 28% and Raut et al. [19] is 3%. Several authors [17, 18, 26, 27] have measured the neutron-induced reaction cross sections on Gallium target in the neutron energy range 13.5–14.9 MeV. However, the reported uncertainties vary from 5 to 20%. There are large discrepancies in the reported data hence there is a need to make precise measurements for neutron induced reactions on Gallium. So far, only one experimental study [20] of photon-induced reactions on Gallium target has been done and there is no data available for the same on the EXFOR database [28] for bremsstrahlung of end-point energy 15 MeV.

In the present work the production cross sections for $^{69}\text{Ga}(n,p)^{69}\text{Zn}^m$, $^{69}\text{Ga}(n,2n)^{68}\text{Ga}$, $^{71}\text{Ga}(n,p)^{71}\text{Zn}^m$ and $^{71}\text{Ga}(n,2n)^{70}\text{Ga}$ reactions are measured at 14.77 ± 0.17 MeV neutron energy with $^{27}\text{Al}(n,\alpha)^{24}\text{Na}$ as the monitor reaction, and the bremsstrahlung spectrum averaged cross section for $^{69}\text{Ga}(\gamma,n)^{68}\text{Ga}$ and $^{71}\text{Ga}(\gamma,n)^{70}\text{Ga}$ reactions are measured using 15 MeV bremsstrahlung photons with $^{197}\text{Au}(\gamma,n)^{196\text{g+m}}\text{Au}$ as the monitor reaction using the activation technique and off-line gamma-ray spectrometry. Theoretical calculations for neutron induced reactions on Gallium from reaction 13–17 MeV using the TALYS-1.95 [29] nuclear code were compared along with the evaluated cross section data files from ENDF/B-VIII.0 [30], JENDL-5 [31], TENDL-2019 [32] libraries and experimental data from the EXFOR database [28].

^a e-mail: sanjay@physics.unipune.ac.in (corresponding author)

Table 1 Recent studies for the production of ^{68}Ga

Nuclear reaction	Threshold energy (MeV)	Projectile energy range (MeV)	Authors
$^{68}\text{Zn}(p,n)^{68}\text{Ga}$	3.758	20	Szelecsényi et al. [21]
$^{68}\text{Zn}(d,2n)^{68}\text{Ga}$	6.103	20–24	Zolbadral et al. [13], Simeckova et al. [14]
$^{65}\text{Cu}(\alpha,n)^{68}\text{Ga}$	6.183	15–42	Hermanne et al. [15], Shahid et al. [22], Szelecsényi et al. [21]
$^{69}\text{Ga}(n,2n)^{68}\text{Ga}$	10.464	11–15	Pachauu et al. [17], Luo et al. [18]
$^{69}\text{Ga}(\gamma,n)^{68}\text{Ga}$	10.314	70	Schupp et al. [20]

Table 2 Timing details of the present experiment at 14.77 MeV neutron energy

Reaction	Irradiation time (secs)	Cooling time (secs)	Counting time (secs)
$^{69}\text{Ga}(n,p)^{69\text{m}}\text{Zn}$	3600	10,020	1809
$^{69}\text{Ga}(n,2n)^{68}\text{Ga}$	3600	3916	2254
$^{71}\text{Ga}(n,p)^{71\text{m}}\text{Zn}$	3600	10,020	1809
$^{71}\text{Ga}(n,2n)^{70}\text{Ga}$	3600	3916	2254

2 Experimental details

2.1 Measurements of production cross sections of nuclear reactions on Gallium induced by 14.77 MeV neutrons

The neutron induced cross sections on Gallium were measured via the activation analysis technique with 14.77 ± 0.17 MeV neutrons. The neutron irradiation work was carried out at the 14 MeV neutron generator facility [33], Department of Physics, Savitribai Phule Pune University, Pune, India. The 14 MeV neutron generator is a 250 kV DC electrostatic accelerator and the deuterium ions are produced by an RF ion source [34]. The 14 MeV neutron beam was produced through the $^3\text{H}(d,n)^4\text{He}$ ($Q = 17.589$ MeV) reaction i.e. by bombarding ~ 175 keV deuteron beam on an 8 Ci tritium target. Pure aluminium (99.99% purity) foils were used as monitor element for the measurement of cross sections of the reactions. The neutron flux was determined with the $^{27}\text{Al}(n,\alpha)^{24}\text{Na}$ reference reaction [35]. For the measurement of the gamma-ray activity a coaxial HPGe(30%) detector cooled by a liquid nitrogen cryostat was used. The resolution of the detector was measured as 1.49 keV at 1332.5 keV of ^{60}Co . The detector was connected to an Ortec EASY-MCA-8 K Multichannel Analyzer through an amplifier. The Ortec-make Maestro software was used for the data acquisition and peak area analysis. To avoid contamination, the detector surface was covered with 0.1 mm thick mylar sheet. Eu-152 standard source was used for the energy calibration of the HPGe detector. The calibration source was kept at 45 mm from the central area of the detector surface. The dead time of the detector was kept below 2% throughout the counting of the irradiated samples by placing them at 5 cm from the surface of the detector.

For the measurement of production cross sections, samples were prepared with powder of pure Ga_2O_3 (99.99%) wrapped in pure aluminium foil as monitor element. Each sample was prepared by sandwiching a known weight of element-powder, and then packing in a polyethylene bag. By folding the polyethylene bag, wrapped between two aluminium foils the sample size of $10 \text{ mm} \times 10 \text{ mm}$ was made. Three such samples were made and used in the present experiment. For the activation experiment, the gallium sample was mounted at 0° with respect to the incident deuterium beam, where the neutron energy corresponds to 14.77 ± 0.17 MeV. The neutron energy of 14.77 MeV was predetermined for the particular sample irradiation position from the ratio of the cross-section of $^{90}\text{Zr}(n, 2n)^{89}\text{Zr}^g$ reaction to the cross-section of $^{93}\text{Nb}(n, 2n)^{92}\text{Nb}^m$ reaction [36]. The spread in the neutron energy arises from the dimensions of the Al foil used for the neutron flux measurements, target geometry and the distance between the two. The half angle subtended by the Al foil corresponds to a neutron energy spread of 0.17 MeV. The deuterium ion beam current on the target was $\sim 80 \mu\text{A}$ at 175 kV accelerating voltage. The sample was irradiated with neutrons for 3600 s.

The gamma-ray activity of the neutron irradiated samples was measured by mounting the sample at the marked position in front of the pre-calibrated HPGe detector. The experiment was repeated 3 times and the cross sections of the reaction were obtained by taking average of three measurements, following the same procedure. Typical recorded gamma-ray spectrum for Ga and Al samples irradiated by 14.77 MeV neutrons are shown in Fig. 1, along with the timing details where t_{irr} is the irradiation time, t_{cool} is the cooling time and t_{count} is the counting time. The details of the irradiation time, cooling time and counting time are shown in Table 2. The nuclear data used for the reactions are given in Table 3.

Fig. 1 The typically recorded spectra for the Ga sample and Al monitor element irradiated by 14.77 MeV neutrons

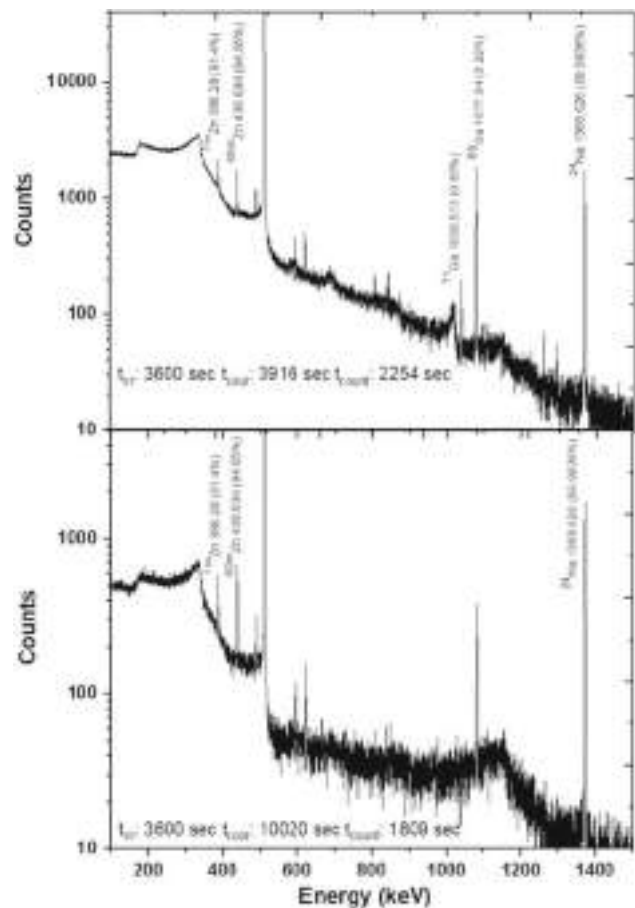


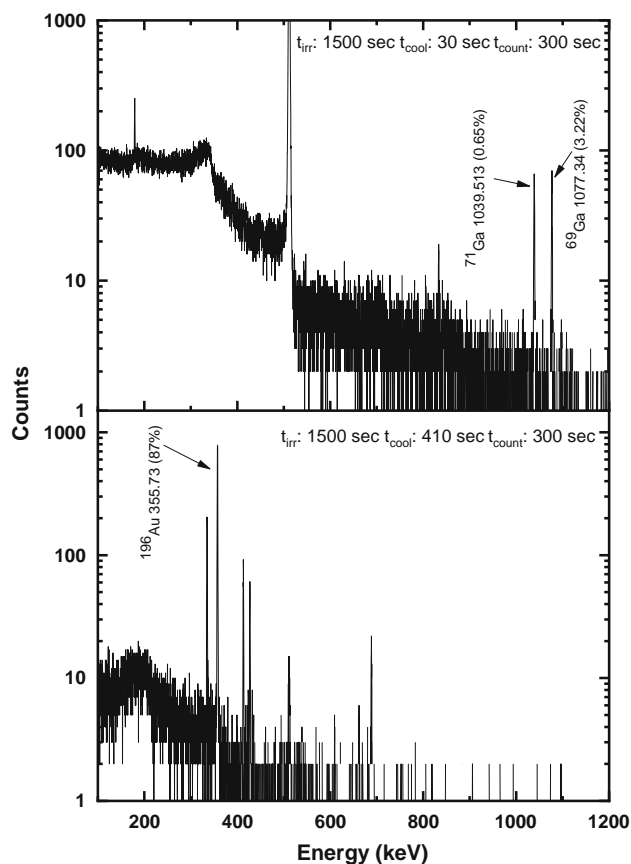
Table 3 Decay data adopted in the present work [37–43]

Reaction	Threshold (MeV)	$T_{1/2}$	Decay mode	E_γ (keV)	I_γ (%)
$^{69}\text{Ga}(n,p)^{69}\text{Zn}^m$	0.129	13.756 ± 0.018 h	IT (99.967%)	438.634	94.85 ± 0.07
$^{69}\text{Ga}(n,2n)^{68}\text{Ga}$	10.464	67.71 ± 0.08 m	ec β^+ (100%)	1077.34	3.22 ± 0.03
$^{71}\text{Ga}(n,p)^{71}\text{Zn}^m$	2.057	3.96 ± 0.05 h	β^- (100%)	386.28	91.40 ± 0.21
$^{71}\text{Ga}(n,2n)^{70}\text{Ga}$	9.432	21.14 ± 0.05 m	β^- (99.59%)	1039.513	0.65 ± 0.05
$^{27}\text{Al}(n,\alpha)^{24}\text{Na}$	3.249	14.997 ± 0.012 h	β^- (100%)	1368.626	99.9936 ± 0.0015
$^{69}\text{Ga}(\gamma,n)^{68}\text{Ga}$	10.314	67.71 ± 0.08 m	ec β^+ + (100%)	1077.34	3.22 ± 0.03
$^{71}\text{Ga}(\gamma,n)^{70}\text{Ga}$	9.301	21.14 ± 0.05 m	B^- (99.59%)	1039.513	0.65 ± 0.05
$^{197}\text{Au}(\gamma,n)^{196g}\text{Au}$	8.073	6.1669 ± 0.0006 d	ec β^+ + (93%)	355.73	87 ± 3

2.2 Measurements of production cross sections of nuclear reactions on Gallium induced by bremsstrahlung of 15 MeV end-point energy

For the measurements of $^{69}\text{Ga}(\gamma,n)^{68}\text{Ga}$ and $^{71}\text{Ga}(\gamma,n)^{70}\text{Ga}$ reaction cross sections, $^{197}\text{Au}(\gamma,n)^{196g+m}\text{Au}$ reaction was used as the monitor reaction at 15 MeV bremsstrahlung end-point energy. The experiment was carried out using the medical linear electron accelerator at Dr. Vikhe Patil Memorial Hospital, Ahmednagar, India. The bremsstrahlung of 15 MeV end point energy was obtained by operating the medical linear electron accelerator in 15 MV photon mode. The photon beam field size was 5 cm × 5 cm at the isocenter (Source to Skin Distance = 100 cm on the patient table). The sample of Gallium was made by packing around 1 g of natural Ga₂O₃ powder (99.99% pure) in 10 mm × 10 mm polyethylene bag and such three samples were made. For bremsstrahlung flux monitoring a gold foil of weight 0.5 g and of dimensions 10 mm × 10 mm having thickness 0.025 mm was used. The Gallium sample and Gold monitor was placed at a distance 100 cm from tungsten converter. Both the sample and the monitor were irradiated by 15 MeV bremsstrahlung radiations produced by bombarding the tungsten target with 15 MeV electron beam at 5 μA current

Fig. 2 The typically recorded spectra for the Ga sample and Au monitor element irradiated by 15 MeV bremsstrahlung photons



for an irradiation time of 25 min. A constant dose rate of 670 ± 10 cGy/min was maintained during irradiation. After irradiation the Ga sample and the Au monitor were transferred to the control room where they were cooled and then counted separately. The gamma-ray activity of the Ga sample and Au monitor was measured by the HPGe detector with an 8 k multi-channel analyser system. Typical recorded gamma-ray spectrum for Ga and Au samples irradiated by 15 MeV bremsstrahlung photons are shown in Fig. 2, along with the timing details where t_{irr} is the irradiation time, t_{cool} is the cooling time and t_{count} is the counting time.

3 Data analysis

3.1 Detector calibration and uncertainty

The efficiency calibration of the HPGe detector was carried out with a standard ^{152}Eu source of known activity ($A_0 = 4336.98 \pm 86.74$ Bq as on 1 Oct. 1999). The absolute efficiency ε for the point source placed at a distance of 45 mm from the end-cap of the detector is given by the expression

$$\varepsilon = \frac{CK_C}{A_0 e^{-\lambda T} I_\gamma \Delta t} \tag{1}$$

where C is the count obtained for a counting time ($\Delta t = 5200$ s) for a particular gamma-line of ^{152}Eu having a decay intensity I_γ , A_0 is the activity of ^{152}Eu source at the time of manufacture, T is the time between date of manufacture to the beginning of counting and K_C is the correction factor for the coincidence summing effect. The coincidence summing correction and the absolute efficiency thus obtained for point source geometry was transferred to absolute efficiency for the samples of finite size using EFFTRAN code [44]. The data used in Eq. 1 to obtain efficiency $\varepsilon(E_\gamma)$ at each of the eight identified γ -rays of Eu-152 are presented in Table 4. Taylor series expansion of detector efficiency (Eq. 1) as a function of four attributes, $\varepsilon(E_\gamma) = f(C, N_0, I_\gamma, t_{1/2})$:

$$\left(\frac{\Delta \varepsilon_i}{\varepsilon_i}\right)^2 = \left(\frac{\Delta C_i}{C_i}\right)^2 + \left(\frac{\Delta A_0}{A_0}\right)^2 + \left(\frac{\Delta I_{\gamma i}}{I_{\gamma i}}\right)^2 + \left(T \ln 2 \frac{\Delta t_{1/2}}{t_{1/2}^2}\right)^2 \tag{2}$$

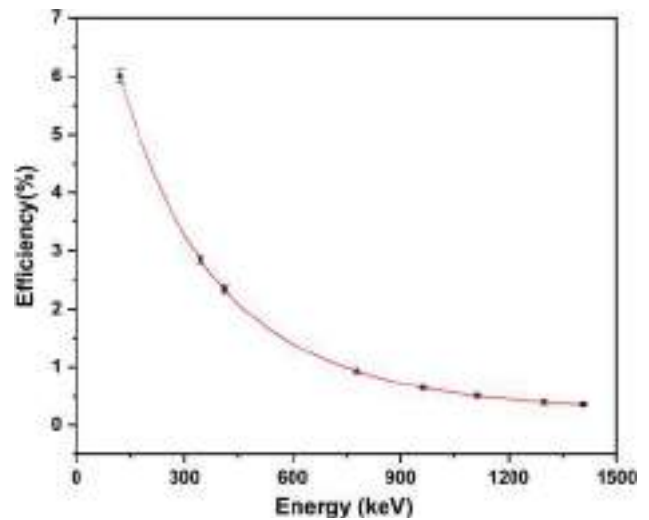
Table 4 Efficiency calibration of HPGe detector with a ¹⁵²Eu standard source

E_γ (keV)	I_γ (%)	C	K_C	$\varepsilon(E_\gamma)$
121.8	28.53 ± 0.016	$123,085 \pm 427$	1.0465	5.999 ± 0.126
344.8	26.59 ± 0.20	$55,854 \pm 307$	1.0297	2.847 ± 0.063
411.1	2.237 ± 0.013	4352 ± 100	1.0711	2.333 ± 0.081
778.9	12.93 ± 0.08	$16,959 \pm 171$	1.0419	0.931 ± 0.028
964.1	14.51 ± 0.07	$15,809 \pm 163$	1.0345	0.648 ± 0.021
1112.1	13.67 ± 0.08	$11,002 \pm 166$	1.0199	0.510 ± 0.018
1299.1	1.633 ± 0.01	1130 ± 59	1.0422	0.402 ± 0.040
1408.0	20.87 ± 0.09	$15,712 \pm 178$	1.0265	0.361 ± 0.013

Table 5 Correlation matrix for the measured detector efficiency at the calibration points

E_γ (KeV)	Efficiency	Correlation matrix								
121.8	5.999 ± 0.126	1								
344.8	2.847 ± 0.063	0.858	1							
411.1	2.333 ± 0.081	0.549	0.522	1						
778.9	0.931 ± 0.028	0.638	0.606	0.388	1					
964.1	0.648 ± 0.021	0.582	0.554	0.355	0.412	1				
1112.1	0.510 ± 0.018	0.521	0.495	0.317	0.368	0.336	1			
1299.1	0.402 ± 0.040	0.192	0.182	0.117	0.135	0.124	0.111	1		
1408.0	0.361 ± 0.013	0.541	0.515	0.330	0.383	0.350	0.313	0.115	1	

Fig. 3 Measured detector efficiency along with interpolated detector efficiency fitting curve



where the expansion terms are as stated in ref. [45]. The covariance matrix for detector efficiencies was generated with the sandwich formula

$$(V_\varepsilon)_{ij} = \sum_{r=1}^4 e_{ir} S_{ijr} e_{jr} \tag{3}$$

where e_{ir} , e_{jr} are the diagonal matrices and S_{ijr} are the micro correlation matrices between e_{ir} and e_{jr} due to the r th attribute as stated in ref. [46]. For uncorrelated elements (C_i , $I_{\gamma i}$), the micro correlation matrix is given as a $(n \times n)$ unit matrix and for completely correlated elements (A_0 , $t_{1/2}$), the micro correlation matrix is given as a $(n \times n)$ square matrix with each element as 1. The covariance matrix generated with Eqs. 1 and 2 is given in Table 5. The interpolated detector efficiency fitting curve and measured detector efficiency is plotted in Fig. 3.

Table 6 Interpolated efficiencies with uncertainty and the correlation matrix for the sample and the monitor reaction

E_γ (KeV)	Efficiency	Correlation matrix				
386.28	2.509 ± 0.087	1				
438.634	2.157 ± 0.102	0.974	1			
1039.513	0.571 ± 0.015	0.442	0.293	1		
1077.34	0.537 ± 0.015	0.476	0.331	0.993	1	
1368.626	0.374 ± 0.011	0.491	0.385	0.650	0.668	1

The efficiencies of the detector at required points of energies were generated with a linear parametric function [46] by varying m from 1 to 8

$$\ln \varepsilon_i = \sum_{i=1}^m p_m (\ln E_i)^{m-1} \quad (4)$$

The best quality of fit was achieved for $m = 6$, with $\frac{\chi^2}{8-6} = 1.14 \approx 1$, where p_m 's are the parameters of the fitting function, m is the order of the fitting function and E_i is the energy of γ -lines in MeV. In order to estimate the efficiencies corresponding to γ -rays emitted from the decay of the reaction products ^{68}Ga , ^{70}Ga , ^{24}Na , ^{27}Mg , $^{69\text{m}}\text{Zn}$ and $^{71\text{m}}\text{Zn}$ the following linear parametric model was used

$$\ln \varepsilon = -5.101 - 1.695(\ln E) + 0.17(\ln E)^2 + 0.749(\ln E)^3 + 0.448(\ln E)^4 + 0.093(\ln E)^5 \quad (5)$$

The interpolated efficiencies and the corresponding correlation matrix for characteristic γ lines for the sample and the monitor reaction are given in Table 6. Table 6 has been generated from Table 5 following Sect. III.A. Efficiency Calibration of HPGe Detector Using ^{152}Eu Standard Gamma-Ray Source of Ref. [45].

3.2 Calculation of the correction factors

The induced activity in irradiated samples was corrected for coincidence summing effects and gamma ray self-attenuation. The Coincidence summing correction factor f_c was calculated with the TrueCoinc code [47]. The total efficiency curve for the HPGe detector was calculated by counting the standard gamma sources ^{22}Na , ^{57}Co , ^{60}Co and ^{137}Cs each for a period of 3600 s and was given as an input to the TrueCoinc code. The self-attenuation coefficients f_s due to interactions of gamma rays within the sample thickness is given by

$$f_s = \frac{\mu t}{1 - e^{-\mu t}} \quad (6)$$

where μ is the linear attenuation coefficient in cm^{-1} for the irradiated sample and t is the thickness of the sample in cm. The mass attenuation coefficient μ/ρ for individual elements (Gallium, Oxygen, Aluminium and Gold) was obtained by interpolating the curves from the NIST Standard Reference Database [48]. The μ/ρ for the compound Ga_2O_3 was calculated using

$$(\mu/\rho)_{\text{Ga}_2\text{O}_3} = W_{\text{Ga}}(\mu/\rho)_{\text{Ga}} + W_{\text{O}}(\mu/\rho)_{\text{O}} \quad (7)$$

where W is fraction of the element by weight in the compound Ga_2O_3 and (μ/ρ) is the mass attenuation coefficient of the element. Therefore, the correction factor CF for induced activity in sample is given by

$$CF = f_c \times f_s \quad (8)$$

The calculated self-attenuation coefficients f_s and the coincidence summing correction factor f_c are given in Table 7 for Ga_2O_3 sample, Al and Au monitor.

3.3 Covariance analysis and measurement of (n,p) and (n,2n) reaction cross sections of ^{69}Ga and ^{71}Ga induced by 14.77 MeV neutrons

In the present work cross sections of $^{69}\text{Ga}(n,2n)^{68}\text{Ga}$, $^{71}\text{Ga}(n,2n)^{70}\text{Ga}$, $^{69}\text{Ga}(n,p)^{69}\text{Zn}^{\text{m}}$ and $^{71}\text{Ga}(n,p)^{71}\text{Zn}^{\text{m}}$ reactions were measured at 14.77 ± 0.17 MeV neutron energy with $^{27}\text{Al}(n,\alpha)^{24}\text{Na}$ as the monitor reaction. The cross section was determined using the neutron activation equation [49]

$$\sigma_x = \sigma_m \frac{CF_x \varepsilon_m C_x a_m A_x M_m I_{\gamma m} f_m}{CF_m \varepsilon_x C_m a_x A_m M_x I_{\gamma x} f_x} \quad (9)$$

Table 7 Self-attenuation coefficient f_s and coincidence summing correction factor f_c for sample and monitor reaction products

Product nuclide	E_γ (keV)	Sample	f_c	f_s	CF
^{68}Ga	1077.34	Ga_2O_3	1.0235	1.0185	1.0424
$^{69}\text{Zn}^m$	438.634	Ga_2O_3	1	1.0290	1.0290
^{70}Ga	1039.513	Ga_2O_3	1.0593	1.0188	1.0792
$^{71}\text{Zn}^m$	386.28	Ga_2O_3	1.2135	1.0313	1.2516
^{24}Na	1368.626	Al foil	1	1.0003	1.0003
^{196}gAu	355.73	Au foil	1.0288	1.0253	1.0548

Table 8 Fractional uncertainties (%) in various parameters used to obtain cross sections

Reaction	C_s	C_m	$I_{\gamma s}$	$I_{\gamma m}$	$\eta_{m,s}$	$f_{\lambda s}$	$f_{\lambda m}$	M_s	M_m	a_s	A_s	A_m	σ_m
1 $^{69}\text{Ga}(n,p)^{69}\text{Zn}^m$	3.7773	0.7565	0.0738	0.0015	0.3944	0.1237	0.0697	0.0231	0.2017	0.0149	0.0014	7.41E-05	0.5
2 $^{69}\text{Ga}(n,2n)^{68}\text{Ga}$	0.6621	0.7565	0.9316	0.0015	0.0189	0.0478	0.0697	0.0231	0.2017	0.0149	0.0014	7.41E-05	0.5
3 $^{71}\text{Ga}(n,p)^{71}\text{Zn}^m$	4.7839	0.7565	2.2975	0.0015	0.3901	0.2934	0.0697	0.0231	0.2017	0.0225	0.0014	7.41E-05	0.5
4 $^{71}\text{Ga}(n,2n)^{70}\text{Ga}$	2.1120	0.7565	7.6923	0.0015	0.0203	0.0001	0.0697	0.0231	0.2017	0.0225	0.0014	7.41E-05	0.5
Cor(1,2)	0	1	0	1	0.207	0	1	1	1	1	1	1	1
Cor(1,3)	0	1	0	1	0.969	0	1	1	1	0	1	1	1
Cor(1,4)	0	1	0	1	0.181	0	1	1	1	0	1	1	1
Cor(2,3)	0	1	0	1	0.362	0	1	1	1	0	1	1	1
Cor(2,4)	0	1	0	1	0.988	0	1	1	1	0	1	1	1
Cor(3,4)	0	1	0	1	0.345	0	1	1	1	1	1	1	1

where the subscript x denotes the sample reaction parameters and subscript m denotes the monitor reaction parameters. Here $\sigma_m = 111.5 \pm 0.42\text{mb}$ is taken from the IRDFF-II evaluated data file at 14.77 MeV. CF is the correction factor due to the coincidence summing effects and the gamma ray self-attenuation, ε is the detector efficiency, C is the photo peak counts, a is the isotopic abundance, A is the atomic mass, M is the mass, I_γ is the branching ratio of γ -ray taken from [37] and f is the timing factor. The timing factor f is given by

$$f = \frac{(1 - e^{-\lambda t_{irr}})(e^{-\lambda t_{cool}})(1 - e^{-\lambda t_{count}})}{\lambda} \tag{10}$$

where λ is the decay constant, t_{irr} is the irradiation time, t_{cool} is the cooling time and t_{count} is the counting time.

The measured cross section calculated using Eq. 9 contains uncertainty [49] contributed by parameters observed with uncertainty. The parameters with uncertainty are the monitor cross section (σ_m), efficiency ($\varepsilon_m, \varepsilon_x$), counts (C_m, C_x), isotopic abundance (a_m, a_x), atomic mass (A_m, A_x), mass (M_m, M_x), intensity ($I_{\gamma m}, I_{\gamma x}$) and timing factor (f_m, f_x). The uncertainty in the detector efficiencies is further reduced by adopting $\eta_{m,x} = \varepsilon_m / \varepsilon_x$ [49] and the partial uncertainty in $\eta_{m,x}$ is $\frac{\Delta \eta_{m,x}}{\eta_{m,x}} = \text{cov}(\varepsilon_m) + \text{cov}(\varepsilon_x) - 2\text{cov}(\varepsilon_m, \varepsilon_x)$. The uncertainty in the time factor f is propagated as

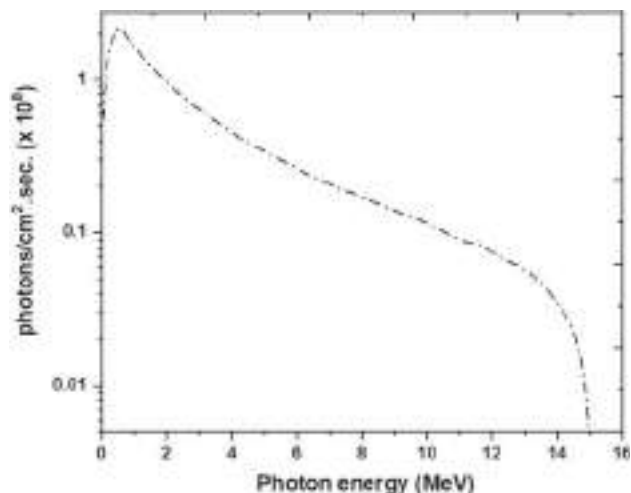
$$\left(\frac{\Delta f}{f}\right)^2 = \left(\frac{\Delta \lambda}{\lambda}\right)^2 \left(\frac{\lambda t_{irr} e^{-\lambda t_{irr}}}{1 - e^{-\lambda t_{irr}}} - \lambda t_{cool} + \frac{\lambda t_{count} e^{-\lambda t_{count}}}{1 - e^{-\lambda t_{count}}} - 1\right)^2 \tag{11}$$

where the uncertainty in the decay constant λ is $\Delta \lambda = \frac{(\ln 2 \Delta T_{1/2})}{(T_{1/2})^2}$ and the uncertainty in half-life is obtained from the ENDSF library [50]. The partial uncertainties for each parameter of Eq. 9 and their correlations are given in Table 8. From Table 8, the correlation due to different attributes was assigned 0 for uncorrelated and assigned 1 for fully correlated. The fractional uncertainties of the measured cross sections were calculated by taking the quadratic sum of the fractional uncertainties.

Table 9 Correction factor (CT_φ) for integrated flux along with the threshold energy

Reaction	Threshold energy (MeV)	CT_φ
$^{197}\text{Au}(\gamma, n)^{196\text{g}}\text{Au}$	8.073	
$^{69}\text{Ga}(\gamma, n)^{68}\text{Ga}$	10.314	0.4853
$^{71}\text{Ga}(\gamma, n)^{70}\text{Ga}$	9.301	0.6944

Fig. 4 Bremsstrahlung spectrum with end point energy of 15 MeV simulated with GEANT4



3.4 Covariance analysis and the measurements of production cross sections of nuclear reactions on Gallium induced by bremsstrahlung of 15 MeV end-point energy

In the present work bremsstrahlung spectrum averaged cross sections of $^{69}\text{Ga}(\gamma, n)^{68}\text{Ga}$ and $^{71}\text{Ga}(\gamma, n)^{70}\text{Ga}$ reactions were measured using the ratio method at bremsstrahlung of 15 MeV end-point energy with $^{197}\text{Au}(\gamma, n)^{196\text{g+m}}\text{Au}$ as monitor reaction. Here the cross section was determined with the modified Eq. 9,

$$\langle \sigma_x \rangle = \sigma_m \frac{C F_x \varepsilon_m C_x a_m A_x M_m I_{\gamma m} f_m}{C F_m \varepsilon_x C_m a_x A_m M_x I_{\gamma x} f_x CT_\varphi} \tag{12}$$

where the parameters have the same meaning as in Eq. 9 and I_γ is the branching ratio of γ -ray taken from [43]. CT_φ is the flux ratio used to normalize the cross sections due to the monitor and targets having different threshold energies as given in Table 9. σ_m in Eq. 12 is the average value of the cross section for the monitor reaction from threshold energy to the endpoint bremsstrahlung energy was calculated using

$$\langle \sigma_m \rangle = \frac{\int_{E_m}^{E_{\max}} \varphi(E) \sigma(E) dE}{\int_{E_m}^{E_{\max}} \varphi(E) dE} \tag{13}$$

where $\sigma(E)$ is taken from interpolated values of [51] from threshold energy for the monitor reaction to 15 MeV bremsstrahlung end point energy and the photon flux $\varphi(E)$ was taken from the simulated bremsstrahlung spectrum Fig. 4. The calculated σ_m is $137.61 \pm 5.87\text{mb}$.

The flux ratio is given as

$$CT_\varphi = \frac{\int_{E_x}^{E_{\max}} \varphi(E) dE}{\int_{E_m}^{E_{\max}} \varphi(E) dE} \tag{14}$$

where $E_{\max} = 15\text{MeV}$, E_x is the threshold energy for the sample reaction and E_m is the threshold energy for the monitor reaction. $\varphi(E)$ was taken from the bremsstrahlung spectrum in Fig. 4 simulated with the Monte Carlo based GEANT4 code [52]. The photon flux was estimated using a similar approach from our previous works [53, 54]. The bremsstrahlung spectrum for 15 MeV electrons bombarding a 0.1 mm thick tungsten target at 5 μA beam and the geometry of our experimental setup was considered for the simulation. The bremsstrahlung spectrum was estimated at a distance of 100 cm from the tungsten target. The default physics models of GEANT4 code with EMStandardPhysics physics list were used for the simulation.

Table 10 Fractional uncertainties (%) in various parameters used to obtain cross sections

Reaction	C_s	C_m	$I_{\gamma s}$	$I_{\gamma m}$	$\eta_{m,s}$	$f_{\lambda s}$	$f_{\lambda m}$	M_s	M_m	a_s	A_s	A_m	σ_m
1 $^{69}\text{Ga}(\gamma,n)^{68}\text{Ga}$	9.0580	2.4799	0.9317	3.4483	0.0113	0.0001	0.0001	0.0232	0.1000	0.0150	0.0014	0.0003	4.3
2 $^{71}\text{Ga}(\gamma,n)^{70}\text{Ga}$	4.9808	2.4799	7.6923	3.4483	0.0119	0.0001	0.0001	0.0232	0.1000	0.0226	0.0014	0.0003	4.3
Cor(1,2)	0	1	0	1	0.988	0	1	1	1	0	1	1	0

The uncertainty in the parameters from Eq. 12 are for monitor cross section σ_m and the other parameters follows from Eq. 9. The uncertainty in cross section σ_m is 4.3% with uncertainty in interpolated values for reference excitation function 8% and the simulated bremsstrahlung spectrum by GEANT4 code having an uncertainty of 9% [55]. The partial uncertainties for each parameter of Eq. 12 and their correlations are given in Table 10. From Table 10, the correlation due to different attributes was assigned 0 for uncorrelated and assigned 1 for fully correlated. The fractional uncertainties of the measured cross sections were calculated by taking the quadratic sum of the fractional uncertainties.

4 Nuclear model calculations

The excitation functions for $^{69}\text{Ga}(n,p)^{69}\text{Zn}^m$, $^{69}\text{Ga}(n,2n)^{68}\text{Ga}$, $^{71}\text{Ga}(n,p)^{71}\text{Zn}^m$ and $^{71}\text{Ga}(n,2n)^{70}\text{Ga}$ reactions were calculated from 13 to 17 MeV using the TALYS-1.95 nuclear reaction code [29]. The TALYS-1.95 code can be used for nuclear reactions that involve incident projectiles as gammas, neutrons, protons, deuterons and α -particles in the incident energy range from 1 keV to 200 MeV. A similar approach to our earlier work [56] that involves chi-squared validation of calculated cross sections with experimental data from the EXFOR database was done. $384 = 6 \times 2 \times 4 \times 8$ excitation functions were calculated with different combinations of 6 level density models [57–62], 2 nucleon-nucleus optical model potentials [63], 4 pre-equilibrium models [64] and 8 γ -ray strength functions [65–71] available TALYS-1.95 code. A single set of models was chosen based on brute-force chi-square fitting. The uncertainty due to statistical calculations was studied by randomly varying the value of a chosen set of parameters between $\pm X\%$ of its central value [72]. The value of X for parameter uncertainties is determined by comparison with existing experimental uncertainties [73]. 1000 such calculations were carried out for each reaction to determine the uncertainty band in calculated excitation function due to parameter uncertainties.

The excitation functions for $^{69}\text{Ga}(\gamma,n)^{68}\text{Ga}$ and $^{71}\text{Ga}(\gamma,n)^{70}\text{Ga}$ reactions were calculated for photon energies from reaction threshold to 15 MeV with the TALYS-1.95 code using the default constant temperature model for calculating nuclear level densities, with eight available gamma-ray strength functions as given below.

- (1) GSF-1: Generalized Lorentzian of Kopecky and Uhl [65]
- (2) GSF-2: Generalized Lorentzian of Brink and Axel [66, 67]
- (3) GSF-3: Hartee-Fock-BCS tables [69]
- (4) GSF-4: Hartree-Fock-Bogolyubov tables [69]
- (5) GSF-5: Hybrid model of Goriely [68]
- (6) GSF-6: Goriely TDHFB [71]
- (7) GSF-7: Temperature dependent relativistic mean field [70]
- (8) GSF-8: Gogny D1M HFB + quasi-random-phase approximation [70]

5 Results and discussions

The measured neutron induced reaction cross sections on gallium, the covariance matrix and the correlation matrix generated with Eq. 2 and Table 8 are presented in Table 11. We have compared our measured cross sections with the previously reported experimental data from the EXFOR database. The measured data was also compared with the evaluated cross section data from the ENDF/B-VIII.0, JENDL-5 and TENDL-2019 libraries and the calculations with TALYS-1.95 nuclear code in Table 12. For convenience, the cross sections from TENDL-2019 evaluation are represented by a thin black solid line, ENDF/B-VIII.0 evaluation by a black dotted line, the JENDL-5 evaluation by a violet dotted line, TALYS-1.95 95% upper confidence level by a red dashed line, TALYS-1.95 95% lower confidence level by a black dashed line and the region between the above two dashed lines is filled in Figs. 5, 6, 7, 8. Normalisation was carried out for the earlier reported experimental data with respect to the recent evaluated cross section data for monitor reactions from IRDFF-II [35]. For the experimental data where monitor cross section was not reported, normalization was not performed and was not compared with our work.

The measured photon induced reaction cross sections on gallium and the correlation matrix generated with Eq. 2 and Table 10 are presented in Table 13. There are no photon induced cross sections reported in the EXFOR database.

Table 11 Covariance matrix and correlation matrix for measured cross sections

Reaction	Cross section (barns)	Correlation matrix			
$^{69}\text{Ga}(n,p)^{69}\text{Zn}^m$	0.02137 ± 0.00084	1			
$^{69}\text{Ga}(n,2n)^{68}\text{Ga}$	0.78958 ± 0.01165	0.151	1		
$^{71}\text{Ga}(n,p)^{71}\text{Zn}^m$	0.00903 ± 0.00049	0.048	0.109	1	
$^{71}\text{Ga}(n,2n)^{70}\text{Ga}$	1.17808 ± 0.09462	0.028	0.073	0.02	1

Table 12 Measured neutron induced reactions cross section(barns) compared with evaluated data libraries [30, 32] and TALYS-1.95 calculations

Reaction	Present work	TALYS-1.95	ENDF/B-VIII.0	TENDL-2019	JENDL-5
$^{69}\text{Ga}(n,p)^{69}\text{Zn}^m$	0.02137 ± 0.00084	0.0194 ± 0.0009		0.0227	0.0289
$^{69}\text{Ga}(n,2n)^{68}\text{Ga}$	0.78958 ± 0.01165	0.8189 ± 0.0487	0.9268	0.8676	0.8351
$^{71}\text{Ga}(n,p)^{71}\text{Zn}^m$	0.00903 ± 0.00049	0.0108 ± 0.0003		0.014	0.0119
$^{71}\text{Ga}(n,2n)^{70}\text{Ga}$	1.17808 ± 0.09462	1.0786 ± 0.0382	1.0077	1.0618	1.0189

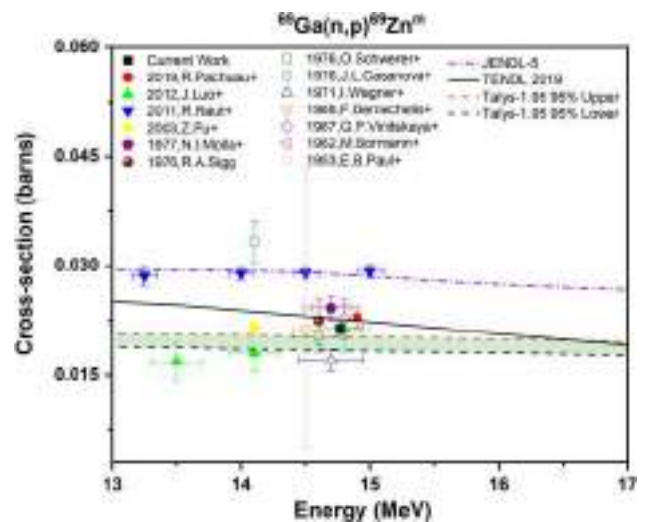
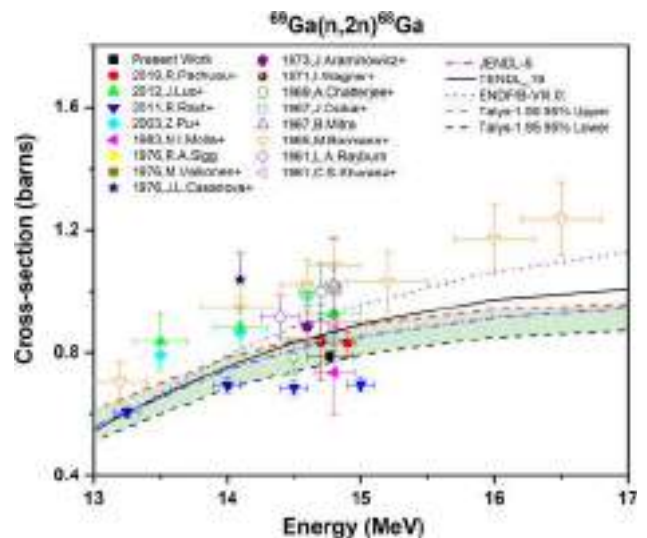
Fig. 5 A comparison of the experimental $^{69}\text{Ga}(n,p)^{69}\text{Zn}^m$ reaction cross sections with the evaluated JENDL-5, TENDL-2019 data and theoretical values using TALYS-1.95**Fig. 6** A comparison of the experimental $^{69}\text{Ga}(n,2n)^{68}\text{Ga}$ reaction cross sections with the evaluated ENDF/B-VIII.0, JENDL-5, TENDL-2019 data and theoretical values using TALYS-1.95

Fig. 7 A comparison of the experimental $^{71}\text{Ga}(n,p)^{71}\text{Zn}^m$ reaction cross sections with the evaluated JENDL-5, TENDL-2019 data and theoretical values using TALYS-1.95

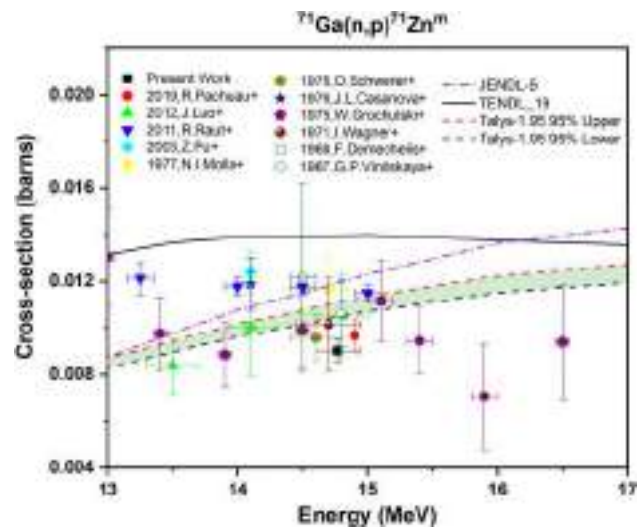


Fig. 8 A comparison of the experimental $^{71}\text{Ga}(n,2n)^{70}\text{Ga}$ reaction cross sections with the evaluated ENDF/B-VIII.0, JENDL-5, TENDL-2019 data and theoretical values using TALYS-1.95

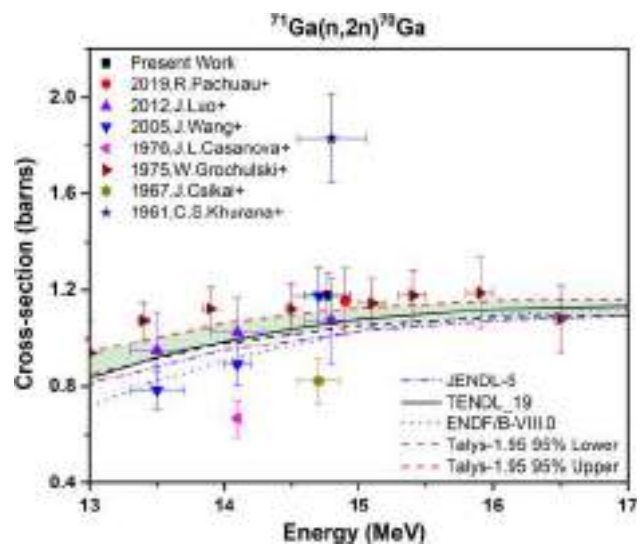


Table 13 Correlation matrix for measured bremsstrahlung spectrum averaged cross section

Reaction	Cross section (barns)	Correlation matrix
$^{69}\text{Ga}(\gamma,n)^{68}\text{Ga}$	0.02171 ± 0.00237	1
$^{71}\text{Ga}(\gamma,n)^{70}\text{Ga}$	0.04117 ± 0.00452	0.305

5.1 The $^{69}\text{Ga}(n,p)^{69}\text{Zn}^m$ reaction

Figure 5 shows our measured cross section for the $^{69}\text{Ga}(n,p)^{69}\text{Zn}^m$ reaction at 14.77 ± 0.17 MeV neutron energy along with the reported experimental data from the EXFOR database and the evaluated data from the ENDF/B-VIII.0, JENDL-5 and TENDL-2019 libraries. For this reaction, Pachuaui et al. [17], Luo et al. [18], Raut et al. [19], Molla et al. [26], Sigg et al. [74], Schwerer et al. [75], Wagner et al. [76], Demechelis et al. [77] and Bormann et al. [24] adopted $^{27}\text{Al}(n,\alpha)^{24}\text{Na}$ reaction as the monitor reaction. Pu et al. [25] adopted $^{93}\text{Nb}(n,2n)^{93}\text{Nb}^m$ reaction as the monitor reaction. Nesaraja et al. [78] adopted $^{56}\text{Fe}(n,p)^{56}\text{Mn}$ reaction as the monitor reaction. Casanova et al. [79] and Vinitkaya et al. [80] adopted $^{63}\text{Cu}(n,2n)^{62}\text{Cu}$ reaction as the monitor reaction. Reported cross section data were normalised at respective neutron energies with respect to IRDFF-II data for respective the monitor reactions. All the reported cross sections after normalization with IRDFF-II evaluated reference monitor data varied by less than 5%. As shown in the Fig. 5, cross sections reported by Luo et al. [18] and Vinitkaya et al. [80] whose neutron energies overlap with our value are in good agreement with our result. Our measured cross section does not correspond with those reported by Pachuaui et al. [17], Molla et al. [26], Schwerer et al. [75] and Wagner et al. [76]. Our measured cross section is in good agreement with TALYS-1.95

calculations and TENDL-2019 within the experimental error. However, the JENDL-5 evaluation is higher than our measured cross section.

5.2 The $^{69}\text{Ga}(n,2n)^{68}\text{Ga}$ reaction

Figure 6 shows the measured cross section for $^{69}\text{Ga}(n,2n)^{68}\text{Ga}$ reaction at 14.77 ± 0.17 MeV neutron energy along with reported experimental data from the EXFOR database and the evaluated data from ENDF/B-VIII.0 and TENDL-2019 libraries. For this reaction, Pachuau et al. [17], Luo et al. [18], Raut et al. [19], Molla et al. [81], Sigg et al. [74], Wagner et al. [76], Bormann et al. [24] adopted $^{27}\text{Al}(n,\alpha)^{24}\text{Na}$ reaction as monitor reaction. Pu et al. [25] adopted $^{93}\text{Nb}(n,2n)^{93}\text{Nb}^m$ reaction as monitor reaction. Csikai et al. [27] and Valkonen et al. [82] adopted $^{27}\text{Al}(n,p)^{27}\text{Mg}$ reaction as monitor reaction whereas Khurana et al. [83] adopted $^{56}\text{Fe}(n,p)^{56}\text{Mn}$ reaction as monitor reaction. Casanova et al. [79], Araminowicz et al. [84], Chatterjee et al. [85], Mitra [86] and Rayburn [87] adopted $^{63}\text{Cu}(n,2n)^{62}\text{Cu}$ reaction as monitor reaction. Reported cross section data was normalised at the respective neutron energies with respect to the IRDFF-II data for the respective monitor reactions. Cross sections reported by Chatterjee et al. [85] and Csikai et al. [27] after normalization with IRDFF-II changed by $\sim 9\%$ of the original values. However, all other cross sections varied by less than 5%. As shown in the Fig. 6, cross sections reported by Molla et al. [81], Valkonen et al. [82], and Wagner et al. [76] whose neutron energies overlap with our value are in good agreement with our result. Our measured cross section shows a large deviation with those reported by Luo et al. [18], Pu et al. [25], Sigg et al. [74], Araminowicz et al. [84] Chatterjee et al. [85], Csikai et al. [27], Mitra [86] Bormann et al. [24] and Khurana et al. [83]. Our measured cross section is in good agreement with the TALYS-1.95 calculations within the experimental error, while the ENDF/B-VIII.0 and JENDL-5, TENDL-2019 evaluations are higher than our measured cross section.

5.3 The $^{71}\text{Ga}(n,p)^{71}\text{Zn}^m$ reaction

Figure 7 shows our measured cross section for $^{71}\text{Ga}(n,p)^{71}\text{Zn}^m$ reaction at 14.77 ± 0.17 MeV neutron energy along with reported experimental data from the EXFOR database and evaluated data from ENDF/B-VIII.0 and TENDL-2019 libraries. For this reaction, Pachuau et al. [17], Luo et al. [18], Raut et al. [19], Nesaraja et al. [23], Molla et al. [26], Schwerer et al. [75], Wagner et al. [76], and Demechelis et al. [77] adopted $^{27}\text{Al}(n,\alpha)^{24}\text{Na}$ reaction as monitor reaction. Pu et al. [25] adopted $^{93}\text{Nb}(n,2n)^{93}\text{Nb}^m$ reaction as monitor reaction while Grochulski et al. [88] adopted $^{56}\text{Fe}(n,p)^{56}\text{Mn}$ reaction as monitor reaction. Casanova et al. [79] and Vinitzkaya et al. [80] adopted $^{63}\text{Cu}(n,2n)^{62}\text{Cu}$ reaction as monitor reaction. Reported cross section data were normalised at respective neutron energies with respect to the IRDFF-II data for respective monitor reactions. Reported cross sections varied by less than 5% after normalization.

As shown in the Fig. 7, cross sections reported by Pachuau et al. [17] whose neutron energies overlap with our value are in good agreement with our result. Our measured cross section do not correspond with those reported by Luo et al. [18], Molla et al. [26], Wagner et al. [76] and Vinitzkaya et al. [80]. Our measured cross section is in good agreement with TALYS-1.95 calculations and TENDL-2019 within the experimental error. However, our measured cross section is lower than the JENDL-5 evaluation.

5.4 The $^{71}\text{Ga}(n,2n)^{70}\text{Ga}$ reaction

Figure 8 shows the measured cross section for $^{71}\text{Ga}(n,2n)^{70}\text{Ga}$ reaction at 14.77 ± 0.17 MeV neutron energy along with reported experimental data from the EXFOR database and evaluated data from ENDF/B-VIII.0 and TENDL-2019 libraries. For this reaction, Pachuau et al. [17], Luo et al. [18], Wang et al. [89] and Nesaraja et al. [23] adopted $^{27}\text{Al}(n,\alpha)^{24}\text{Na}$ reaction as monitor reaction while Csikai et al. [27] adopted $^{27}\text{Al}(n,p)^{27}\text{Mg}$ reaction as monitor reaction. Casanova et al. [79] and Vinitzkaya et al. [80] adopted $^{63}\text{Cu}(n,2n)^{62}\text{Cu}$ reaction as monitor reaction while Grochulski et al. [88] adopted $^{56}\text{Fe}(n,p)^{56}\text{Mn}$ reaction as monitor reaction. The reported cross section was normalised at respective neutron energies with respect to IRDFF-II data for respective monitor reactions. Cross sections reported by Csikai et al. [27] and Khurana et al. [83] after normalization with IRDFF-II changed by 9–55% of the original values. However, all other reported cross sections after normalisation varied by less than 5%.

As shown in the Fig. 8, cross sections reported by Pachuau et al. [17], Luo et al. [18], and Wang et al. [89] whose neutron energies overlap with our value are in good agreement with our result. Our measured cross section shows a large deviation with those reported by Csikai et al. [27] and Khurana et al. [83]. Our measured cross section is in good agreement with TALYS-1.95 calculations within the experimental error, while the ENDF/B-VIII.0, JENDL-5 and TENDL-2019 evaluations are lower than our measured cross section.

5.5 The $^{69}\text{Ga}(\gamma,n)^{68}\text{Ga}$ and $^{71}\text{Ga}(\gamma,n)^{70}\text{Ga}$ reaction

In the present work, the bremsstrahlung spectrum averaged cross sections of $^{69}\text{Ga}(\gamma,n)^{68}\text{Ga}$ and $^{71}\text{Ga}(\gamma,n)^{70}\text{Ga}$ reactions, have been measured relative to the cross section of $^{197}\text{Au}(\gamma,n)^{196\text{g+m}}\text{Au}$ reaction monitor. A detailed covariance analysis for measured cross section has been done. The total uncertainties in the measured cross sections of $^{69}\text{Ga}(\gamma,n)^{68}\text{Ga}$ and $^{71}\text{Ga}(\gamma,n)^{70}\text{Ga}$ reactions are 10.486% and 10.571% respectively, having a correlation of 30%. The bremsstrahlung spectrum averaged cross section σ for

Fig. 9 A comparison of the experimental bremsstrahlung spectrum averaged cross sections of $^{69}\text{Ga}(\gamma, n)^{68}\text{Ga}$ reaction cross section with the evaluated TENDL-2019 data and theoretical values for 8 γ -ray strength functions using TALYS-1.95

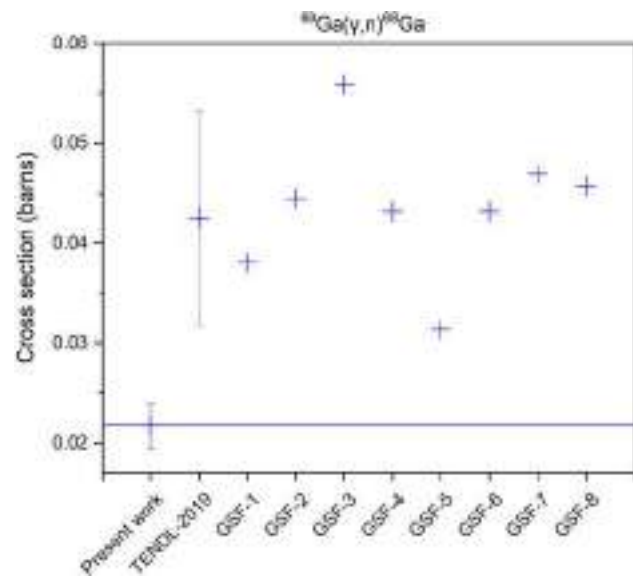
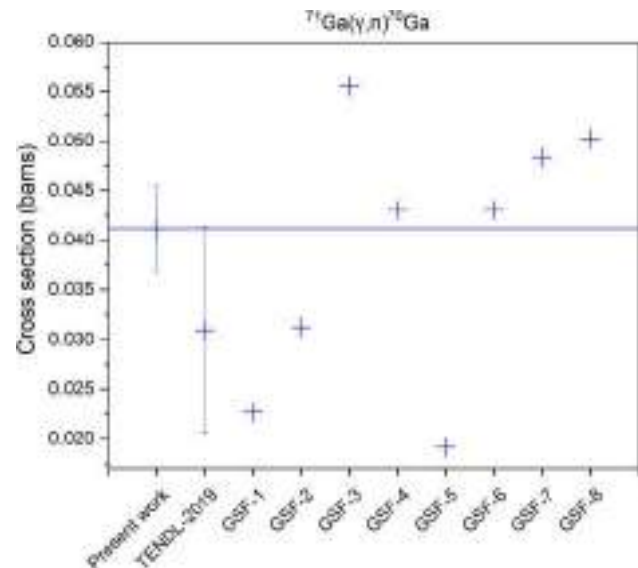


Fig. 10 A comparison of the experimental bremsstrahlung spectrum averaged cross sections of $^{71}\text{Ga}(\gamma, n)^{70}\text{Ga}$ reaction cross section with the evaluated TENDL-2019 data and theoretical values for 8 γ -ray strength functions using TALYS-1.95



the $^{69}\text{Ga}(\gamma, n)^{68}\text{Ga}$ and $^{71}\text{Ga}(\gamma, n)^{70}\text{Ga}$ reaction at the 15 MeV bremsstrahlung endpoint energy have been measured for the first time. The energy dependant cross section from TENDL-2019 and TALYS-1.95 calculations with eight different gamma-ray strength functions (GSF-1 to GSF-8) have been converted to the bremsstrahlung spectrum averaged cross section for bremsstrahlung with end point energy of 15 MeV by using Eq. 14 and compared with our result in Figs. 9 and 10. It is observed from our work that for the $^{69}\text{Ga}(\gamma, n)^{68}\text{Ga}$ reaction, the measured bremsstrahlung spectrum averaged cross section is lower than TENDL-2019 and (GSF-1 to GSF-8) calculations. This could be related to the correction factor for threshold energy and the shape of the reference excitation function of the $^{197}\text{Au}(\gamma, n)^{196\text{g+m}}\text{Au}$ monitor reaction. For $^{71}\text{Ga}(\gamma, n)^{70}\text{Ga}$ reaction our measured bremsstrahlung spectrum averaged cross section is in agreement with TENDL-2019, GSF-4 and GSF-6 within the experimental error. However, it was lower than GSF-3, GSF-7 and GSF-8 while higher than GSF-1, GSF-2 and GSF-5.

6 Conclusions

Cross sections for $^{69}\text{Ga}(n, p)^{69}\text{Zn}^m$, $^{69}\text{Ga}(n, 2n)^{68}\text{Ga}$, $^{71}\text{Ga}(n, p)^{71}\text{Zn}^m$ and $^{71}\text{Ga}(n, 2n)^{70}\text{Ga}$ reactions were measured at 14.77 ± 0.17 MeV neutron energy with $^{27}\text{Al}(n, \alpha)^{24}\text{Na}$ reaction as the monitor reaction, and the bremsstrahlung spectrum averaged cross section for $^{69}\text{Ga}(\gamma, n)^{68}\text{Ga}$ and $^{71}\text{Ga}(\gamma, n)^{70}\text{Ga}$ reactions were measured using 15 MeV bremsstrahlung photons with $^{197}\text{Au}(\gamma, n)^{196\text{g+m}}\text{Au}$ reaction as the monitor reaction using activation technique and off-line gamma-ray spectrometry. A detailed covariance analysis was performed for determination of uncertainty in the measured cross section inclusive of the contribution from

various sources. The experimental results were compared with the previously reported EXFOR data that had been normalized by the latest IRDFF-II monitor data and the evaluated nuclear data libraries ENDF/B-VIII.0, JENDL-5, TENDL-2019. The measured cross sections were found to be in good agreement with certain literature and theoretical calculations with the TALYS-1.95 code. The bremsstrahlung induced reaction cross sections are reported for the first time at 15 MeV end point energy.

Acknowledgements The authors [S. D. Dhole and V. N. Bhoraskar] gratefully acknowledge the financial assistance for research work in the field of neutron and photon induced nuclear reactions by BRNS, Mumbai sanction number: 36(6)/14/49/2016-BRNS and SERB-DST, New Delhi sanction number: EMR/2017/002497. The authors are grateful to Dr. Bhushan Nikam and the management of Dr. Vikhe Patil Memorial Hospital, Ahmednagar, India for providing the medical LINAC for the experiments. The authors are grateful to the anonymous reviewers who have contributed greatly to the improvement of this article.

Data availability statement This manuscript has associated data in a data repository. [Authors' comment: All the data of the present study are contained in this article.]

References

- M.-M. Bé, V.P. Chechev, Nucl. Instrum. Methods Phys. Res. Sect. A Accel. Spectrom. Detect. Assoc. Equip. **728**, 157 (2013)
- S.R. Banerjee, M.G. Pomper, Appl. Radiat. Isot. Incl. Data Instrum. Methods Use Agric. Ind. Med. **76**, 2 (2013)
- S. Fanti, V. Ambrosini, P. Tomassetti, P. Castellucci, G. Montini, V. Allegri, G. Grassetto, D. Rubello, C. Nanni, R. Franchi, Biomed. Pharmacother. **62**, 667 (2008)
- R.P. Baum, H.R. Kulkarni, Theranostics **2**, 437 (2012)
- M. Meisenheimer, Y. Saenko, E Eppard, in *Med Isot*, ed by S.A.R. Naqvi M.B. Imrani (IntechOpen, Rijeka, 2021).
- I. Velikyan, Molecules **20**, 12913 (2015)
- B.W. Tsang, C.J. Mathias, M.A. Green, J. Nucl. Med. **34**, 1127–1131 (1993)
- R.A. Werner, C. Bluemel, M.S. Allen-Auerbach, T. Higuchi, K. Herrmann, Ann. Nucl. Med. **29**, 1 (2015)
- A.R. Haug, R. Cindea-Drimus, C.J. Auernhammer, M. Reincke, B. Wängler, C. Uebleis, G.P. Schmidt, B. Göke, P. Bartenstein, M. Hacker, J. Nucl. Med. **53**, 1686 (2012)
- R. Valkema, S.A. Pauwels, L.K. Kvols, D.J. Kwekkeboom, F. Jamar, M. de Jong, R. Barone, S. Walrand, P.P.M. Kooij, W.H. Bakker, J. Lasher, E.P. Krenning, J. Nucl. Med. **46**(Suppl 1), 83S (2005)
- A. Hermanne, N. Walravens, and O. Cicchelli, in *Nucl. Data Sci. Technol.*, ed by S. M. Qaim (Springer, Berlin, 1992), pp. 616–618
- F. Tárkányi, F. Szelecsényi, Z. Kovács, S. Sudár, Radiochim. Acta **50**, 19 (1990)
- Z. Tsoodol, M. Aikawa, I. Dagvadorj, T. Khishigjargal, N. Javkhantugs, Y. Komori, H. Haba, Appl. Radiat. Isot. **159**, 109095 (2020)
- E. Simecková, EPJ Web Conf. **146**, 11034 (2017)
- A. Hermanne, R. Adam Rebeles, F. Tárkányi, S. Takács, Phys. Res. Sect. B Beam Interact. Mater Atoms **356–357**, 28 (2015)
- S. Mukherjee, B. Bindu Kumar, N.L. Singh, Pramana **49**, 253 (1997)
- R. Pachuau, B. Lalremruata, A. Gandhi, S.V. Suryanarayana, B.K. Nayak, A. Kumar, L.S. Danu, Nucl. Phys. A **992**, 121613 (2019)
- J. Luo, R. Liu, L. Jiang, Radiochim. Acta **100**, 231 (2012)
- R. Raut, A.S. Crowell, B. Fallin, C.R. Howell, C. Huibregtse, J.H. Kelley, T. Kawano, E. Kwan, G. Rusev, A.P. Tonchev, W. Tornow, D.J. Vieira, J.B. Wilhelm, Phys. Rev. C **83**, 44621 (2011)
- F.D. Schupp, C.B. Colvin, D.S. Martin, Phys. Rev. **113**, 1095 (1959)
- F. Szelecsényi, Z. Kovács, K. Nagatsu, K. Fukumura, K. Suzuki, and K. Mukai, **100**, 5 (2012)
- A. Shahid, K. Kim, G. Kim, M. Zaman, M. Nadeem, Phys. Res. Sect. B Beam Interact. Mater Atoms **358**, 160 (2015)
- C. Nesaraja, K.-H. Linse, S. Spellerberg, S. Sudar, A. Suhaimi, S.M. Qaim, Radiochim. Acta **86**, 1 (1999)
- M. Bormann, E. Fretwurst, P. Schehka, G. Wrege, H. Büttner, A. Lindner, H. Meldner, Nucl. Phys. **63**, 438 (1965)
- Z. Pu, J. Yang, X. Kong, Appl. Radiat. Isot. **58**, 723 (2003)
- N.I. Molla, S.M. Qaim, Nucl. Phys. A **283**, 269 (1977)
- J. Csikai, G. Pető, Acta Phys. Acad. Sci. Hungaricae **23**, 87 (1967)
- N. Otuka, E. Dupont, V. Semkova, B. Pritychenko, A.I. Blokhin, M. Aikawa, S. Babykina, M. Bossant, G. Chen, S. Dunaeva, R.A. Forrest, T. Fukahori, N. Furutachi, S. Ganesan, Z. Ge, O.O. Gritzay, M. Herman, S. Hlavač, K. Katō, B. Lalremruata, Y.O. Lee, A. Makinaga, K. Matsumoto, M. Mikhaylyukova, G. Pikulina, V.G. Pronyaev, A. Saxena, O. Schwerer, S.P. Simakov, N. Soppera, R. Suzuki, S. Takács, X. Tao, S. Taova, F. Tárkányi, V.V. Varlamov, J. Wang, S.C. Yang, V. Zerkin, Y. Zhuang, Nucl. Data Sheets **120**, 272 (2014)
- A. J. Koning, M. C. Duijvestijn, and S. Hilaire, *TALYS-10* (EDP Sciences, France, 2008)
- D.A. Brown, M.B. Chadwick, R. Capote, A.C. Kahler, A. Trkov, M.W. Herman, A.A. Sonzogni, Y. Danon, A.D. Carlson, M. Dunn, D.L. Smith, G.M. Hale, G. Arbanas, R. Arcilla, C.R. Bates, B. Beck, B. Becker, F. Brown, R.J. Casperson, J. Conlin, D.E. Cullen, M.-A. Descalle, R. Firestone, T. Gaines, K.H. Guber, A.I. Hawari, J. Holmes, T.D. Johnson, T. Kawano, B.C. Kiedrowski, A.J. Koning, S. Kopecky, L. Leal, J.P. Lestone, C. Lubitz, J.I. Márquez Damián, C.M. Mattoon, E.A. McCutchan, S. Mughabghab, P. Navratil, D. Neudecker, G.P.A. Nobre, G. Noguere, M. Paris, M.T. Pigni, A.J. Plompen, B. Pritychenko, V.G. Pronyaev, D. Roubtsov, D. Rochman, P. Romano, P. Schillebeeckx, S. Simakov, M. Sin, I. Sirakov, B. Sleaford, V. Sobes, E.S. Soukhovitskii, I. Stetcu, P. Talou, I. Thompson, S. Van der Marck, L. Welsch-Sherill, D. Wiarda, M. White, J.L. Wormald, R.Q. Wright, M. Zerkle, G. Žerovnik, Y. Zhu, Nucl. Data Sheets **148**, 1 (2018)
- O. Iwamoto, N. Iwamoto, K. Shibata, A. Ichihara, S. Kunieda, F. Minato, S. Nakayama, EPJ Web Conf. **239**, 9002 (2020)
- A.J. Koning, D. Rochman, J.-C. Sublet, N. Dzysiuk, M. Fleming, S. van der Marck, Nucl. Data Sheets **155**, 1 (2019)
- V.N. Bhoraskar, Indian J. Pure Appl. Phys. **27**, 648 (1989)
- S.S. Jayantha Kumar, V.K. Chindhade, V.N. Bhoraskar, Pramana **22**, 453 (1984)
- A. Trkov, P.J. Griffin, S.P. Simakov, L.R. Greenwood, K.I. Zolotarev, R. Capote, D.L. Aldama, V. Chechev, C. Destouches, A.C. Kahler, C. Konno, M. Košťál, M. Majerle, E. Malambu, M. Ohta, V.G. Pronyaev, V. Radulović, S. Sato, M. Schulc, E. Šimečková, I. Vavtar, J. Wagemans, M. White, H. Yashima, Nucl. Data Sheets **163**, 1 (2020)
- V.E. Lewis, K.J. Zieba, Nucl. Instrum. Methods **174**, 141 (1980)
- A. Sonzogni, (2015)
- M.F. Koskinas, F.W. Lacerda, I.T. Matos, T.S. Nascimento, I.M. Yamazaki, M.N. Takeda, M.S. Dias, Appl. Radiat. Isot. **87**, 118 (2014)

39. C.D. Nesaraja, Nucl. Data Sheets **115**, 1 (2014)
40. K.S. Krane, Appl. Radiat. Isot. **70**, 1649 (2012)
41. K. Abusaleem, B. Singh, Nucl. Data Sheets **112**, 133 (2011)
42. M. Shamsuzzoha Basunia, Nucl. Data Sheets **112**, 1875 (2011)
43. H. Xiaolong, Nucl. Data Sheets **108**, 1093 (2007)
44. T. Vidmar, Phys. Res. Sect. A Accel. Spectrom. Detect. Assoc. Equip. **550**, 603 (2005)
45. B.S. Shivashankar, S. Ganesan, H. Naik, S.V. Suryanarayana, N.S. Nair, K.M. Prasad, Nucl. Sci. Eng. **179**, 423 (2015)
46. L.P. Geraldo, D.L. Smith, Phys. Res. Sect. A Accel. Spectrom. Detect. Assoc. Equip. **290**, 499 (1990)
47. S. Sudar, IAEA-TECDOC-1275, International Atomic Energy Agency, (2002), pp. 37–48
48. J. Hubbell and S. Seltzer, <http://physics.nist.gov/PhysRefData/XrayMassCoef/Cover.html> (1995)
49. N. Otuka, B. Lalremruata, M.U. Khandaker, A.R. Usman, L.R.M. Punte, Radiat. Phys. Chem. **140**, 502 (2017)
50. T. W. Burrows, <https://www.Nndc.Bnl.Gov/Ensd/> (2021)
51. N. Iwamoto, K. Kosako, and T. Murata, in *IAEA-Conf 2016-004* (2016), pp. 53–58.
52. J. Allison, K. Amako, J. Apostolakis, H. Araujo, P.A. Dubois, M. Asai, G. Barrand, R. Capra, S. Chauvie, R. Chytracek, G.A.P. Cirrone, G. Cooperman, G. Cosmo, G. Cuttone, G.G. Daquino, M. Donszelmann, M. Dressel, G. Folger, F. Foppiano, J. Generowicz, V. Grichine, S. Guatelli, P. Gumplinger, A. Heikkinen, I. Hrivnacova, A. Howard, S. Incerti, V. Ivanchenko, T. Johnson, F. Jones, T. Koi, R. Kokoulin, M. Kossov, H. Kurashige, V. Lara, S. Larsson, F. Lei, O. Link, F. Longo, M. Maire, A. Mantero, B. Mascialino, I. McLaren, P.M. Lorenzo, K. Minamimoto, K. Murakami, P. Nieminen, L. Pandola, S. Parlati, L. Peralta, J. Perl, A. Pfeiffer, M.G. Pia, A. Ribon, P. Rodrigues, G. Russo, S. Sadilov, G. Santin, T. Sasaki, D. Smith, N. Starkov, S. Tanaka, E. Tcherniaev, B. Tome, A. Trindade, P. Truscott, L. Urban, M. Verderi, A. Walkden, J.P. Wellisch, D.C. Williams, D. Wright, H. Yoshida, IEEE Trans. Nucl. Sci. **53**, 270 (2006)
53. T.S. Ganesapandy, G.T. Bholane, A.B. Phatangare, F.M.D. Attar, S.S. Dahiwal, S.V. Suryanarayana, V.N. Bhoraskar, and S.D. Dhole, Nucl. Phys. A **122445** (2022)
54. G.T. Bholane, T.S. Ganesapandy, A.B. Phatangare, V.D. Bharud, B.J. Patil, S.S. Dahiwal, S.V. Suryanarayana, V.N. Bhoraskar, S.D. Dhole, Appl. Radiat. Isot. **174**, 109739 (2021)
55. J. Allison, K. Amako, J. Apostolakis, P. Arce, M. Asai, T. Aso, E. Bagli, A. Bagulya, S. Banerjee, G. Barrand, B.R. Beck, A.G. Bogdanov, D. Brandt, J.M.C. Brown, H. Burkhardt, P. Canal, D. Cano-Ott, S. Chauvie, K. Cho, G.A.P. Cirrone, G. Cooperman, M.A. Cortés-Giraldo, G. Cosmo, G. Cuttone, G. Depaola, L. Desorgher, X. Dong, A. Dotti, V.D. Elvira, G. Folger, Z. Francis, A. Galoyan, L. Garnier, M. Gayer, K.L. Genser, V.M. Grichine, S. Guatelli, P. Guèye, P. Gumplinger, A.S. Howard, I. Hřivnáčová, S. Hwang, S. Incerti, A. Ivanchenko, V.N. Ivanchenko, F.W. Jones, S.Y. Jun, P. Kaitaniemi, N. Karakatsanis, M. Karamitros, M. Kelsey, A. Kimura, T. Koi, H. Kurashige, A. Lechner, S.B. Lee, F. Longo, M. Maire, D. Mancusi, A. Mantero, E. Mendoza, B. Morgan, K. Murakami, T. Nikitina, L. Pandola, P. Paprocki, J. Perl, I. Petrović, M.G. Pia, W. Pokorski, J.M. Quesada, M. Raine, M.A. Reis, A. Ribon, A. Ristić Fira, F. Romano, G. Russo, G. Santin, T. Sasaki, D. Sawkey, J.I. Shin, I.I. Strakovsky, A. Taborda, S. Tanaka, B. Tomé, T. Toshito, H.N. Tran, P.R. Truscott, L. Urban, V. Uzhinsky, J.M. Verbeke, M. Verderi, B.L. Wendt, H. Wenzel, D.H. Wright, D.M. Wright, T. Yamashita, J. Yarba, H. Yoshida, Phys. Res. Sect. A Accel. Spectrom. Detect. Assoc. Equip. **835**, 186 (2016)
56. T.S. Ganesapandy, G.T. Bholane, A.B. Phatangare, V.D. Bharud, S.S. Dahiwal, F.M.D. Attar, V.N. Bhoraskar, S.D. Dhole, Appl. Radiat. Isot. **176**, 109813 (2021)
57. A. Gilbert, A.G.W. Cameron, Can. J. Phys. **43**, 1446 (1965)
58. W. Dilg, W. Schantl, H. Vonach, M. Uhl, Nucl. Phys. A **217**, 269 (1973)
59. S. Goriely, F. Tondeur, J.M. Pearson, At. Data Nucl. Data Tables **77**, 311 (2001)
60. S. Goriely, S. Hilaire, A.J. Koning, Phys. Rev. C **78**, 64307 (2008)
61. A.V. Ignatyuk, J.L. Weil, S. Raman, S. Kahane, Phys. Rev. C **47**, 1504 (1993)
62. S. Hilaire, M. Girod, S. Goriely, A.J. Koning, Phys. Rev. C **86**, 64317 (2012)
63. A.J. Koning, J.P. Delaroche, Nucl. Phys. A **713**, 231 (2003)
64. A.J. Koning, M.C. Duijvestijn, Nucl. Phys. A **744**, 15 (2004)
65. J. Kopecky, M. Uhl, Phys. Rev. C **41**, 1941 (1990)
66. D. Brink, Nucl. Phys. **4**, 215 (1957)
67. P. Axel, Phys. Rev. **126**, 671 (1962)
68. S. Goriely, Phys. Lett. B **436**, 10 (1998)
69. E. Khan, S. Goriely, D. Allard, E. Parizot, T. Suomijärvi, A.J. Koning, S. Hilaire, M.C. Duijvestijn, Astropart. Phys. **23**, 191 (2005)
70. M. Martini, S. Hilaire, S. Goriely, A.J. Koning, S. Péru, Nucl. Data Sheets **118**, 273 (2014)
71. D.P. Arteaga, P. Ring, Phys. Rev. C **77**, 34317 (2008)
72. D.L. Smith, *ANL/NDM-159* (Argonne National Laboratory, 2005)
73. A.J. Koning, D. Rochman, Nucl. Data Sheets **113**, 2841 (2012)
74. R.A. Sigg, *Fast Neutron Induced Reaction Cross Sections and Their Systematics* (United States, 1976)
75. O. Schwerer, M. Winkler-Rohatsch, G. Winkler, Oesterr. Akad. Wiss. Math-Naturw. Kl Anzeiger **113**, 153 (1976)
76. I. Wagner, M. Uhl, Oesterr. Akad. Wiss. **108**, 185 (1971)
77. F. Demichelis, M. Guidetti, E. Miraldi, C. Oldano, Nuovo Cim. B **58**, 177 (1968)
78. C.D. Nesaraja, S. Sudár, S.M. Qaim, Phys. Rev. C **68**, 24603 (2003)
79. J.L. Casanova, M.L. Sanchez, An. Fis. **72**, 186 (1976)
80. G.P. Vinitzkaya, V.N. Levkovskii, V.V. Sokolskii, Yad. Fiz. **6**, 240 (1967)
81. N.I. Molla, M.M. Islam, M.M. Rahman, S. Khatun, *Measurement of Cross-Sections for Neutron Induced Reactions at 14 MeV* (1983)
82. M. Valkonen, *Studies of 14 MeV Neutron Activation Cross Sections with Special Reference to the Capture Reaction* (Finland, 1976).
83. C.S. Khurana, H.S. Hans, Nucl. Phys. **28**, 560 (1961)
84. J. Araminowicz, J. Dresler, *INR-1464* (Institute of Nuclear Research, Warszawa, 1973), pp. 14–18
85. A. Chatterjee, A. Nath, and A.M. Ghose, in *Nucl. Solid State Phys. Symp.* (1969), p. 117
86. B. Mitra, Indian J. Phys. **41**, 752 (1967)
87. L.A. Rayburn, Phys. Rev. **122**, 168 (1961)
88. W. Grochulski, S. El-Konsol, A. Marcinkowski, Acta Phys. Pol. **6**, 139 (1975)
89. J. Wang, X. Wang, T. Su, Phys. Rev. C **72**, 37604 (2005)



Measurements and estimation of cross sections of neutron and bremsstrahlung induced nuclear reactions for neodymium isotopes with covariance analysis

G.T. Bholane^a, T.S. Ganesapandy^a, A.B. Phatangare^a, F.M.D. Attar^b,
S.S. Dahiwalé^a, S.V. Suryanarayana^c, V.N. Bhoraskar^a, S.D. Dhole^{a,*}

^a Department of Physics, S. P. Pune University, Pune 411007, India

^b Department of Physics, AKI's Poona College, Camp, Pune 411001, India

^c Nuclear Physics Division, Bhabha Atomic Research Centre, Mumbai 400085, India

Received 9 October 2021; received in revised form 20 January 2022; accepted 21 January 2022

Available online 29 January 2022

Abstract

The cross sections of the nuclear reactions $^{142}\text{Nd}(n,2n)^{141}\text{Nd}$, $^{148}\text{Nd}(n,2n)^{147}\text{Nd}$, $^{150}\text{Nd}(n,2n)^{149}\text{Nd}$, $^{142}\text{Nd}(n,2n)^{141\text{m}}\text{Nd}$ and $^{146}\text{Nd}(n,p)^{146}\text{Pr}$ at 14.77 MeV neutron energy and the cross section of the $^{142}\text{Nd}(\gamma,n)^{141}\text{Nd}$, $^{148}\text{Nd}(\gamma,n)^{147}\text{Nd}$ and $^{150}\text{Nd}(\gamma,n)^{149}\text{Nd}$ nuclear reaction at 10 and 15 MeV bremsstrahlung endpoint energies were measured using offline gamma spectroscopy. The photon-induced cross sections are reported for the first time at 10 MeV and 15 MeV bremsstrahlung endpoint energies. The uncertainties in the measured data were calculated using covariance analysis. The experimental results were compared with the previously reported EXFOR data and with the evaluated nuclear data libraries ENDF/B.-VIII.0, JEFF-3.3, JENDL-4.0, CENDL-3.2 and TENDL-2019. The theoretical nuclear model calculations were performed using the TALYS-1.95 code with default and optimized input parameters tuned to reproduce the present and literature data. The present data are in good agreement with other literature and evaluated data. The results are useful for the development of particle accelerators, reactors and the EXFOR database.

© 2022 Elsevier B.V. All rights reserved.

* Corresponding author.

E-mail address: sanjay@physics.unipune.ac.in (S.D. Dhole).

Keywords: Neutron activation analysis; Photon activation analysis; Covariance analysis; Correlation coefficients; TALYS-1.95

1. Introduction

The knowledge of cross sections of the nuclear reactions induced by neutrons and photons is required for several fields of science, such as nuclear structure, model calculations and nuclear reaction theory. Measurements of neutron-induced nuclear reaction cross sections around 14 MeV energy are of great importance for fusion reactor design. Similarly, measurements of cross sections of photon-induced nuclear reactions are significant for evaluating the radiation damage to the structural materials. Furthermore, due to unavailability of photon sources insufficient data are available for the cross sections of photon-induced nuclear reactions. Recently, due to the development of medium energy linear and cyclic electron accelerators, bremsstrahlung beams are readily available. The photonuclear reactions are also important to produce neutrons via (γ, n) reactions. The (γ, n) reactions have high values of cross sections in the 8–15 MeV photon energy range around the giant dipole resonance region [1]. Therefore, the measurements of cross sections for the nuclear reactions induced by the neutrons and photons are of high importance.

Neodymium is an important rare earth element, which occurs naturally as 7 stable isotopes having mass numbers (with relative abundances in brackets) 142(27.152%), 143(12.174%), 144(23.798%), 145(8.293%), 146(17.189%), 148(5.756%) and 150(5.638%). It has various practical applications such as permanent magnets, lasers and glass [2–5] and is also used as a monitor for burnup analysis of spent nuclear fuel [6,7].

The experimentally measured neutron-induced nuclear reaction cross sections of neodymium isotopes have been reported in the EXFOR database by the authors [8,9,18–27,10,28–33,11–17]. Similarly, the photon-induced reaction cross sections on neodymium isotopes have been reported by four authors [34–37]. Most of these cross sections were reported before 1990, which contain discrepancies, whereas the covariance analysis with detailed report of partial uncertainties has not been reported by most of the authors. The discrepancies in the data are due to the use of detectors having poor energy resolution (beta counting or NaI(Tl)), counting methods and nuclear parameters used. The data evaluators also face difficulty in finding the uncertainties with its breakdown [38]. Therefore, more accurate measurements of the cross sections of nuclear reactions on neodymium isotopes is necessary.

In the present work, we report on the cross sections of four $(n, 2n)$ and one (n, p) nuclear reactions at 14.77 MeV neutron energy and two (γ, n) nuclear reactions at 10 MeV bremsstrahlung endpoint energy and three (γ, n) nuclear reactions at 15 MeV bremsstrahlung endpoint energy, followed by covariance analysis for each reaction. The (γ, n) cross sections using 10 and 15 MeV bremsstrahlung photons are reported for the first time. The measured cross sections are compared with the available literature data from the EXFOR [39] database and also with the evaluated nuclear data libraries ENDF/B.-VIII.0 [40], JEFF-3.3 [41], JENDL-4.0 [42], CENDL-3.2 [43] and TENDL-2019 [44]. The theoretical model calculations for these nuclear reaction cross sections were performed with the TALYS-1.95 [45] nuclear model code with optimized parameters of the code. The measured cross sections are in good agreement with the literature data, TALYS-1.95 calculations and evaluated nuclear data. An elaborate description of the methods employed in the present work is given in the following sections.

2. Experimental details

2.1. Sample preparation

The samples were made from a pure (99.9%) Nd_2O_3 powder of natural isotopic abundance. 2 grams of powder was measured with a microbalance with an accuracy of $\pm 10 \mu\text{g}$, which was covered in a polyethylene bag. The polyethylene bag was folded in such a way so that size of the powder sample was close to 10 mm x 10 mm. The sample used for neutron irradiation was wrapped with a pure aluminum foil weighing 0.3 grams, for neutron flux monitoring. For bremsstrahlung irradiation, a gold foil of 0.5 gm and size 10 mm x 10 mm was placed along with the neodymium samples, for monitoring bremsstrahlung flux.

2.2. Irradiation

The neutron irradiation experiment of the Nd_2O_3 sample wrapped with the aluminum foil was carried out at the 14 MeV Neutron Generator Laboratory, Department of Physics, Savitribai Phule Pune University, India [46]. The 14 MeV neutrons were produced by bombarding deuterium ions with an energy of 175 keV on an 8 Ci tritium target. At the termination of the deuterium beam at the tritium target, the beam had a 4 mm diameter and a beam current of $\sim 100 \mu\text{A}$. The Neodymium sample was mounted at 0° with respect to the incident deuterium beam, where the neutron energy corresponds to $14.77 \pm 0.17 \text{ MeV}$. The neutron flux and energy distribution were determined by activation analysis with $^{27}\text{Al}(n,\alpha)^{24}\text{Na}$ nuclear reaction. The uncertainty in the neutron energy is derived from the uncertainty in the cross section of (n,α) reaction, detector efficiency and sample geometry [47]. The sample was irradiated for a period of 3600 seconds. After the irradiation the sample was transferred to the gamma ray counting room.

The bremsstrahlung irradiation experiment of the Nd_2O_3 samples along with the gold foil was carried out with the medical linear electron accelerator at Dr. Vikhe Patil Memorial Hospital, Ahmednagar, India. The Medical LINAC is used for medical applications, having a monochromatic electron beam of current $5 \mu\text{A}$ and energy spread less than 0.5%. The bremsstrahlung photons were generated by bombarding the high energy electron beam on a tungsten target. The operators had setup the collimators of the system to give a field size of 5 cm X 5 cm at the patient table situated at 100 cm from the tungsten target. The samples were placed in the given field area on the patient table. The samples were irradiated one by one with bremsstrahlung beams of 10 MeV and 15 MeV endpoint energies, for a period of 1500 seconds. A constant dose rate of $580 \pm 10 \text{ cGy/min}$ and $670 \pm 10 \text{ cGy/min}$ was maintained for 10 MeV and 15 MeV energies respectively. After the irradiation, samples were brought for gamma spectroscopy with the HPGe detector in the control room of the medical LINAC.

2.3. Measurement of γ -ray activity

After irradiation, the samples were transferred to the counting room for gamma spectroscopy. The gamma ray activity of the samples was measured with a lead shielded and pre-calibrated HPGe detector having 30% relative efficiency and 1.5 keV energy resolution at 1.33 MeV gamma energy. The data acquisition was carried out with an Ortec Manufactured Easy MCA 8k coupled with PC based Maestro software. For the measurements of different products generated through $(n,2n)$, (n,p) and (γ,n) reactions with neodymium, a proper cooling time and counting time plan had been implemented because the half-life of the products varies from 62 seconds to 10.98 days.

Table 1

Details of the irradiation, cooling, counting time and threshold energy of the reactions.

Reaction	Projectile Radiation	Irradiation Time (seconds)	Cooling Time (seconds)	Counting Time (seconds)	Threshold Energy E_{th} (MeV)
$^{142}\text{Nd}(n,2n)^{141}\text{Nd}$	14.77 MeV Neutrons	3600	1860	5485	9.899
$^{148}\text{Nd}(n,2n)^{147}\text{Nd}$		3600	73380	3600	7.382
$^{150}\text{Nd}(n,2n)^{149}\text{Nd}$		3600	1860	5485	7.375
$^{142}\text{Nd}(n,2n)^{141m}\text{Nd}$		3600	40	62	10.66
$^{146}\text{Nd}(n,p)^{146}\text{Pr}$		3600	360	1750	3.490
$^{142}\text{Nd}(\gamma,n)^{141}\text{Nd}$	Bremsstrahlung 15 MeV	1500	692	372	9.829
$^{150}\text{Nd}(\gamma,n)^{149}\text{Nd}$		1500	692	372	7.375
$^{148}\text{Nd}(\gamma,n)^{147}\text{Nd}$		1500	121820	3600	7.332
$^{150}\text{Nd}(\gamma,n)^{149}\text{Nd}$	Bremsstrahlung	1500	340	425	7.375
$^{148}\text{Nd}(\gamma,n)^{147}\text{Nd}$	10 MeV	1500	54360	3600	7.332

Table 2

Nuclear spectroscopic data for the different radioisotopes produced [48–54].

Nuclide	Half-life	Decay Mode	E_γ (keV)	I_γ (%)
^{141}Nd	2.49 ± 0.03 h	ec β^+ (100%)	1126.91	0.80 ± 0.03
^{147}Nd	10.98 ± 0.01 d	β^- (100%)	531.016	13.4 ± 0.3
^{149}Nd	1.728 ± 0.001 h	β^- (100%)	211.309	25.9 ± 1.4
^{141m}Nd	62 ± 8 sec	IT (99.95%)	756.51	91.6
^{146}Pr	24.09 ± 0.1 m	β^- (100%)	453.86	46 ± 3
^{27}Mg	9.458 ± 0.012 m	β^- (100%)	843.76	71.80 ± 0.2
^{24}Na	14.997 ± 0.012 h	β^- (100%)	1368.626	99.9936 ± 0.0015
^{196}Au	6.1669 ± 0.0006 d	ec β^+ (93%)	355.73	87 ± 3

Here, the cooling time means the time from the end of the irradiation to the start of the gamma counting. The details of the irradiation, cooling and counting time used for different reactions are given in **Table 1**. The details of the nuclear spectroscopic data for the different radioisotopes produced are given in **Table 2**. The decay data was adopted from the ENSDF library [48–54]. The typical recorded spectra of neutron irradiated Nd+Al and 10 and 15 MeV bremsstrahlung irradiated Nd and Au samples are shown in **Fig. 1**, **Fig. 2** and **Fig. 3** respectively. The details of the irradiation time (t_1), cooling time (t_2) and counting time (t_3) are also given in these figures.

3. Data analysis

3.1. Efficiency calibration for HPGe detector

The HPGe detector used for the gamma spectroscopy was calibrated using the standard ^{152}Eu γ source. The ^{152}Eu γ source has a half-life of 13.517 years [55] and initial activity $A_0 = 4336.98$ Bq on 1 Oct. 1999. The detection efficiency of the HPGe detector was calculated by the **Eq. (1)**.

$$\varepsilon = K_c \frac{C}{A_0 I_\gamma e^{-\lambda T} \Delta t} \quad (1)$$

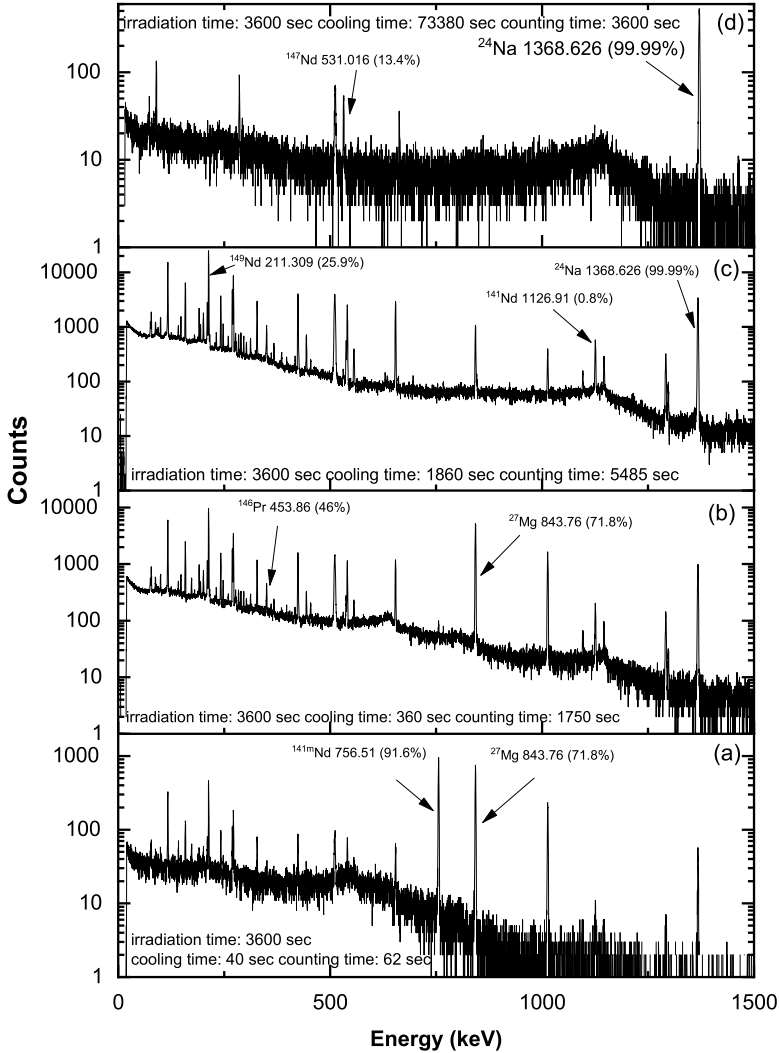


Fig. 1. Gamma ray spectra of the 14.77 MeV neutron irradiated neodymium and aluminum sample.

where, ϵ is the geometry dependent efficiency, C is observed counts for a particular γ energy, A_0 is the initial activity of the source at the time of manufacture, I_γ is the absolute intensity of the gamma peak, λ is the decay constant of the source, T is the time elapsed from the manufacturing of the source to the start of the counting, $\Delta t = 3600$ seconds is the live time of the detector and K_c is the correction factor for the coincidence summing effect calculated by the EFFTRAN code [56]. The efficiency was transferred from a point source geometry to a finite source geometry by the EFFTRAN code, as the ^{152}Eu γ source has a finite geometry. For calibration of the detector, the ^{152}Eu γ source was placed at 50 mm from the surface of the detector to avoid large coincidence summing errors. The details of the γ energies, intensities [55] and transferred efficiency ϵ are given in Table 3. The efficiency calibration curve is shown in Fig. 4.

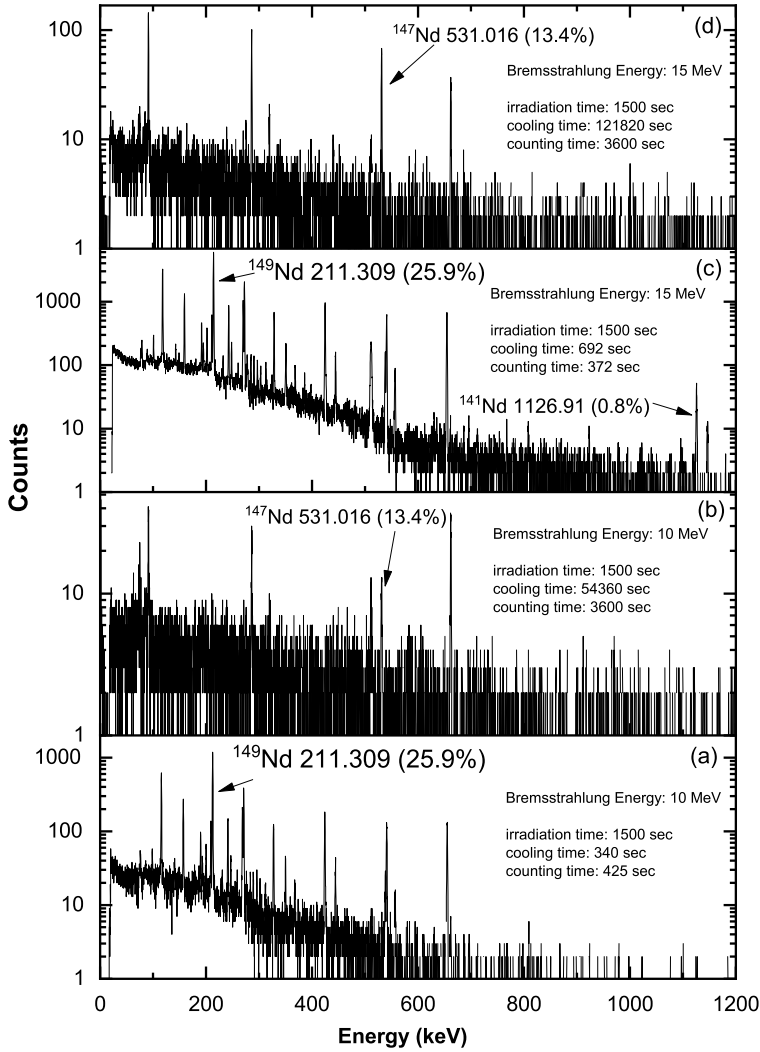


Fig. 2. Gamma ray spectra for the bremsstrahlung irradiated neodymium samples.

The covariance analysis for the detection efficiencies of the HPGe detector was performed following the procedure given by Refs. [38,57–59]. The efficiency can be written as a function of the four attributes $\epsilon = (C, A_0, I_\gamma, T_{1/2})$ and can be expanded as **Eq. (2)**.

$$\left(\frac{\Delta\epsilon_i}{\epsilon_i}\right)^2 = \left(\frac{\Delta C_i}{C_i}\right)^2 + \left(\frac{\Delta A_0}{A_0}\right)^2 + \left(\frac{\Delta I_{\gamma i}}{I_{\gamma i}}\right)^2 + (t\Delta\lambda)^2 \quad (2)$$

where, ΔC_i , ΔA_0 , $\Delta I_{\gamma i}$ and $\Delta\lambda$ are the uncertainties in C_i , A_0 , $I_{\gamma i}$ and decay constant λ respectively.

The partial uncertainties due to the four attributes ($C, A_0, I_\gamma, T_{1/2}$) and total uncertainty in detection efficiency at the corresponding γ energy is given in **Table 4**. The covariance matrix for the detector efficiencies is given in **Table 5**. The uncertainty at the corresponding energy

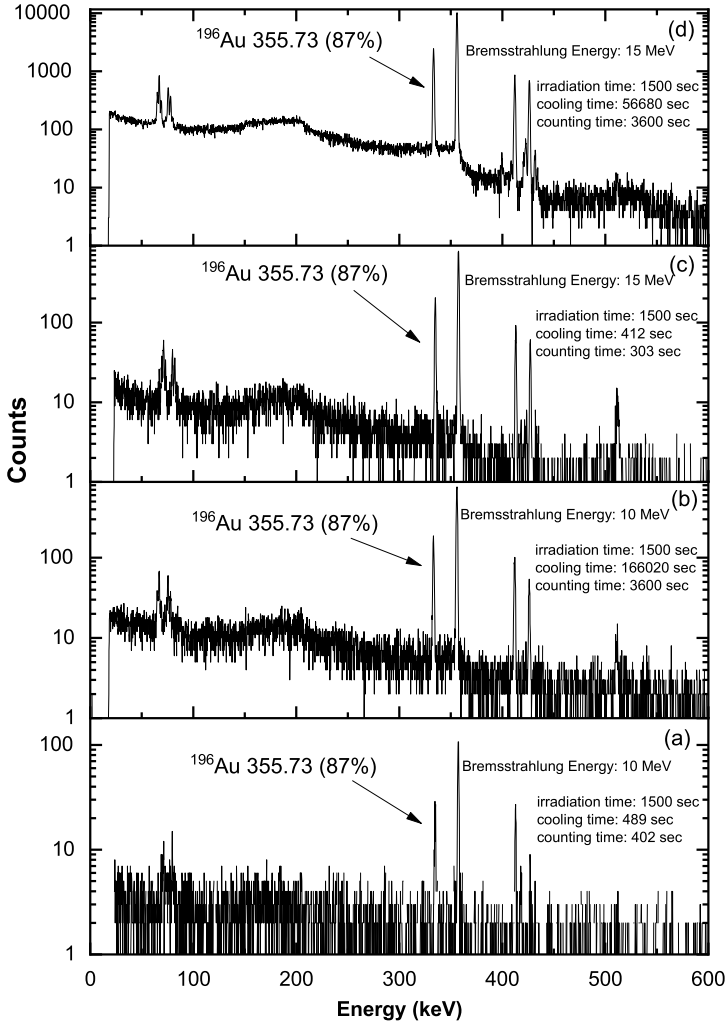


Fig. 3. Gamma ray spectra for the bremsstrahlung irradiated gold samples.

Table 3
 Detector efficiency at corresponding gamma energies and intensities from ^{152}Eu γ source and coincidence summing correction factor.

E_γ (keV)	I_γ (%)	K_c	ϵ (%)
121.7817	28.53 ± 0.16	1.0465	5.97907
244.6974	7.55 ± 0.04	1.0663	3.83048
443.9606	2.827 ± 0.014	1.0589	2.21235
778.9045	12.93 ± 0.08	1.0419	0.97215
867.38	4.23 ± 0.03	1.0768	0.77537
964.057	14.51 ± 0.07	1.0345	0.64487
1112.076	13.67 ± 0.08	1.0199	0.52811
1408.013	20.87 ± 0.09	1.0265	0.36541

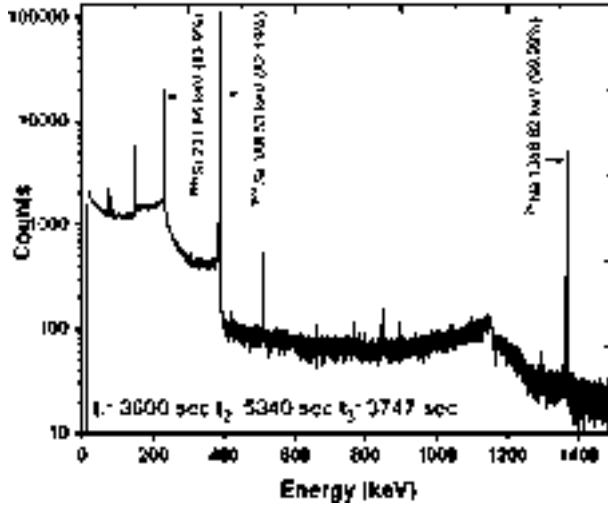


Fig. 1. The typically recorded spectrum for the Sr sample and Al monitor element irradiated by 14.77 MeV neutrons.

deuteron beam on an 8 Ci tritium target. The neutron flux was determined with the $^{27}\text{Al}(n,\alpha)^{24}\text{Na}$ reference monitor reaction [27]. The calculated neutron flux was $\sim 10^8 \text{ n/cm}^2\cdot\text{sec}$. The strontium sample was mounted at 0° with respect to the incident deuterium beam where the neutron energy corresponds to $14.77 \pm 0.17 \text{ MeV}$ [28]. The deuterium ion beam current on the tritium target was $\sim 60 \mu\text{A}$ at 175 kV accelerating voltage. The sample was irradiated with neutrons for an hour and then immediately transferred to the counting room where it was cooled.

The gamma-ray activity of the irradiated samples were measured with a coaxial HPGc (30%) detector cooled by a liquid nitrogen cryostat. The energy resolution of the detector was measured as 1.49 keV at the 1332.5 keV peak of ^{60}Co gamma source. The detector was connected to an Ortec EASY-MCA-8K Multichannel Analyser through an amplifier. The Ortec-make Maestro software was used for the data acquisition and the dead time was maintained below 2%. Eu-152 standard source was used for energy calibration of the HPGc detector. The calibration source was kept at 50 mm from the central area of the detector surface. The gamma-ray activity of the neutron irradiated samples was measured by mounting the sample at the marked position in front of the pre-calibrated HPGc detector. Typical recorded gamma-ray spectrum for Sr and Al samples irradiated by 14.77 MeV neutrons are shown in Fig. 1, along with the timing details where t_1 is the irradiation time, t_2 is the cooling time and t_3 is the counting time. The details of the irradiation time, cooling time and counting time are given in Table 1. The nuclear data used for the reactions are given in Table 2.

2.2. Measurements of 15 MeV bremsstrahlung induced nuclear reaction cross sections for Strontium

Samples of pure SrO_2 (99.99%) powder of known weight and natural isotopic abundance were prepared. Au foil (0.5 gm), of the same size as the samples was placed along with the samples for monitoring the bremsstrahlung flux. The bremsstrahlung irradiation experiment of the samples was carried out with the medical linear electron accelerator at Dr. Vikhe Patil Memorial Hospital, Ahmednagar, India. The Medical LINAC is capable of delivering a monochromatic electron

Table 1
Timing details of the samples irradiated with 14.77 MeV neutrons.

Reaction	Irradiation time (secs)	Cooling time (secs)	Counting time (secs)
$^{88}\text{Sr}(n,2n)^{87}\text{Sr}^m$	3600	5340	3747
$^{88}\text{Sr}(n,p)^{88}\text{Rb}$	3600	30	1385
$^{88}\text{Sr}(n,\alpha)^{85}\text{Kr}$	3600	77040	7232
$^{86}\text{Sr}(n,2n)^{85}\text{Sr}^m$	3600	1480	3807
$^{86}\text{Sr}(n,2n)^{85}\text{Sr}^g$	3600	77040	7232
$^{84}\text{Sr}(n,2n)^{83}\text{Sr}$	3600	77040	7232

Table 2
Decay data adopted in the present work [5,29–31] along with threshold energy.

Reaction	Threshold (MeV)	$T_{1/2}$	Decay mode	E_γ (keV)	I_γ (%)
$^{88}\text{Sr}(n,2n)^{87}\text{Sr}^m$	11.632	2.815 ± 0.012 h	IT (99.7%)	388.531	82.19 ± 0.22
$^{88}\text{Sr}(n,p)^{88}\text{Rb}$	4.582	17.773 ± 0.018 m	β^- (100%)	898.03	14.4 ± 0.24
$^{88}\text{Sr}(n,\alpha)^{85}\text{Kr}$	0.804	4.480 ± 0.008 h	β^- (78.8%)	151.195	75.2 ± 0.5
$^{86}\text{Sr}(n,2n)^{85}\text{Sr}^m$	11.859	67.63 ± 0.04 m	IT (86.6%)	231.86	83.9 ± 0.4
$^{86}\text{Sr}(n,2n)^{85}\text{Sr}^g$	11.625	64.849 ± 0.007 d	ec (100%)	514.0048	96 ± 4
$^{84}\text{Sr}(n,2n)^{83}\text{Sr}$	12.065	32.41 ± 0.03 h	ec β^+ (100%)	762.65	26.7 ± 2.2

Table 3
Timing details of the samples irradiated with bremsstrahlung of 15 MeV end point energy.

Reaction	Irradiation time (secs)	Cooling time (secs)	Counting time (secs)
$^{88}\text{Sr}(\gamma,n)^{87}\text{Sr}^m$	1500	146	600
$^{86}\text{Sr}(\gamma,n)^{85}\text{Sr}^m$	1500	146	600

beam of current 5 μA with an energy spread of less than 0.5%. The bremsstrahlung radiation was generated by bombarding the high energy electron beam on a tungsten target. A field size of 5 cm \times 5 cm was setup by the operators at the patient table 100 cm from the source. The samples were placed in this field on the patient table. Both the Sr sample and Au monitor were irradiated simultaneously with bremsstrahlung of 15 MeV endpoint energies of dose rate 670 ± 10 cGy/min for 1500 seconds. Samples were taken to the control room after irradiation for counting. The gamma-ray activity of the irradiated samples was measured with a pre-calibrated HPGe (30%) detector one after the other. Typical recorded gamma-ray spectrum for Sr sample irradiated with bremsstrahlung of 15 MeV end point energy is shown in Fig. 2, along with the timing details. The timing details of the present experiment are given in Table 3. The nuclear data used for the reactions are given in Table 2.

3. Data analysis

3.1. Calibration and estimation of the efficiency of the HPGe detector

The calibration of the HPGe detector was carried out with a standard ^{152}Eu source of known activity ($A_0 = 4336.98 \pm 86.74$ Bq as on 1 Oct. 1999). The absolute efficiency ε for the point

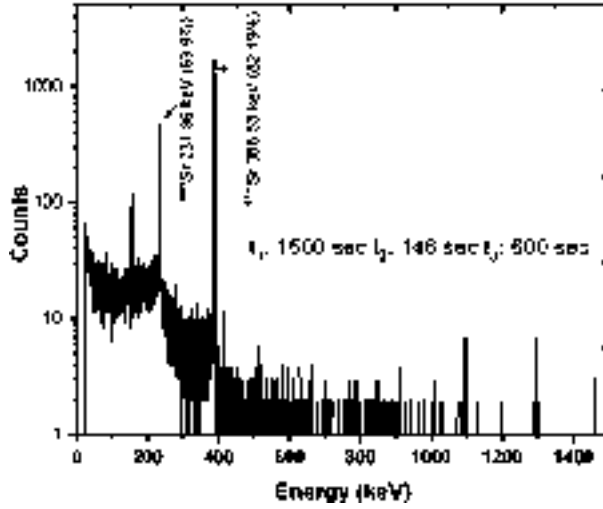


Fig. 2. The typically recorded spectrum for the Sr sample irradiated by bremsstrahlung of 15 MeV end-point energy.

Table 4
HPGe detector efficiency calibration with ¹⁵²Eu standard source.

E_γ (keV)	I_γ (%)	C	K_C	$\varepsilon(E_\gamma)$
121.78	28.53 ± 0.016	73933 ± 296	1.0465	5.039 ± 0.103
344.28	26.59 ± 0.20	36812 ± 209	1.0297	2.692 ± 0.059
778.9	12.93 ± 0.08	8763 ± 110	1.0711	1.318 ± 0.032
964.08	14.51 ± 0.07	8185 ± 105	1.0419	1.097 ± 0.027
1112.07	13.67 ± 0.08	6960 ± 107	1.0345	0.990 ± 0.026
1408.01	20.87 ± 0.09	8630 ± 97	1.0265	0.804 ± 0.019

source placed at a distance of 55 mm from the end-cap of the detector is given by the expression

$$\varepsilon = \frac{CK_C}{A_0 e^{-\lambda T} I_\gamma \Delta t} \tag{1}$$

where C is the count obtained for a counting time ($\Delta t = 3600$ seconds) for a particular gamma-line of ¹⁵²Eu having a decay intensity I_γ . A_0 is the activity of ¹⁵²Eu source at the time of manufacture, T is the time between date of manufacture to the beginning of counting and K_C is the correction factor for the coincidence summing effect. Absolute efficiency was obtained from EFFTRAN code [32]. Efficiency $\varepsilon(E_\gamma)$ at each of the six identified γ -rays of Eu-152 are presented in Table 4. The uncertainty in efficiency was calculated with the Taylor series expansion of detector efficiency (equation (1)) from Ref. [33]. The interpolated detector efficiency fitting curve and measured detector efficiency is plotted in Fig. 3.

The efficiencies of the detector at required points of energies were generated with a linear parametric function [34]

$$\ln \varepsilon_i = \sum_m p_m (\ln E_i)^{m-1} \quad 1 \leq m \leq 6 \tag{2}$$

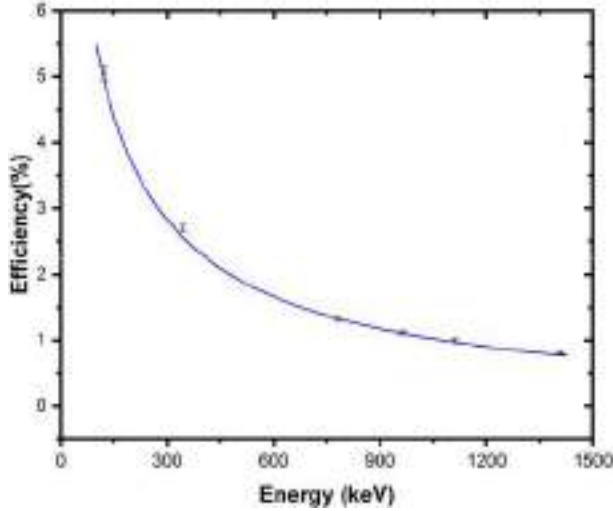


Fig. 3. Measured detector efficiency with interpolated detector efficiency curve.

Table 5

Interpolated sample efficiencies with uncertainty and correlation matrix for the sample and the monitor reaction.

E_γ (keV)	Efficiency	Correlation matrix							
151.195	4.612 ± 0.099	1.000							
231.86	3.608 ± 0.084	0.977	1.000						
388.53	2.439 ± 0.053	0.932	0.936	1.000					
514.0048	1.921 ± 0.042	0.845	0.820	0.967	1.000				
762.65	1.36 ± 0.03	0.748	0.688	0.886	0.971	1.000			
843.76	1.244 ± 0.028	0.750	0.682	0.875	0.962	0.998	1.000		
898.03	1.178 ± 0.026	0.758	0.687	0.872	0.956	0.995	0.999	1.000	
1368.626	0.828 ± 0.019	0.870	0.809	0.797	0.765	0.761	0.786	0.809	1.000

The best quality of fit was achieved for $m = 4$, with $\frac{\chi}{6-4} = 1.06 \approx 1$. In order to estimate the efficiencies corresponding to γ -rays emitted from the decay of the reaction products $^{87}\text{Sr}^m$, ^{88}Rb , ^{85}Kr , $^{85}\text{Sr}^m$, $^{85}\text{Sr}^g$, ^{83}Sr , ^{24}Na and ^{27}Mg , the following linear parametric model was used

$$\ln \varepsilon = -4.534403 - 0.856484 \ln E + 0.067139 \ln E^2 + 0.059392 \ln E^3 \quad (3)$$

The interpolated efficiencies and the corresponding correlation matrix for characteristic γ lines for the sample and the monitor reaction are given in Table 5.

3.2. Measurement of $(n,2n)$, (n,p) and (n,α) reaction cross sections on natural strontium target

The cross sections of $^{88}\text{Sr}(n,2n)^{87}\text{Sr}^m$, $^{88}\text{Sr}(n,p)^{88}\text{Rb}$, $^{88}\text{Sr}(n,\alpha)^{85}\text{Kr}$, $^{86}\text{Sr}(n,2n)^{85}\text{Sr}^m$, $^{86}\text{Sr}(n,2n)^{85}\text{Sr}^g$ and $^{84}\text{Sr}(n,2n)^{83}\text{Sr}$ reactions were measured at 14.77 ± 0.17 MeV neutron energy relative to $^{27}\text{Al}(n,\alpha)^{24}\text{Na}$ monitor reaction. The cross section was determined with the neutron activation equation [35]

$$\sigma_s = \sigma_m \frac{\varepsilon_m C_s a_m A_s I_{\gamma m} M_m f_m C F_s}{\varepsilon_s C_m a_s A_m I_{\gamma s} M_s f_s C F_m} \quad (4)$$

Table 6
Correction factors (CF) for self-attenuation and coincidence summing for sample and monitor.

Product nuclide	E_γ (keV)	Sample	CF
$^{87}\text{Sr}^m$	388.53	SrO ₂	1.021
^{88}Rb	898.03	SrO ₂	1.011
^{85}Kr	151	SrO ₂	1.013
$^{85}\text{Sr}^m$	231.86	SrO ₂	1.041
$^{85}\text{Sr}^g$	514.0048	SrO ₂	1.017
^{83}Sr	762.65	SrO ₂	1.021
^{24}Na	1368.626	Al foil	1.001
^{27}Mg	843.76	Al foil	1.003
^{196}Au	355.73	Au foil	1.055

where, the subscript s denotes sample reaction parameters and subscript m denotes the monitor reaction parameters. Here $\sigma_m = 111.5 \pm 0.42$ mb is taken from the IRDFF-II evaluated data file at 14.77 MeV. ϵ is the detector efficiency, C is the photo peak counts, a is the isotopic abundance, A atomic mass, I_γ is the branching ratio of γ -ray taken from [36], M is the mass, f is the timing factor and CF is the correction factor due to coincidence summing effects and gamma ray self-attenuation. The timing factor f is given by

$$f = \frac{(1 - e^{-\lambda t_1})(e^{-\lambda t_2})(1 - e^{-\lambda t_3})}{\lambda} \quad (5)$$

where, λ is the decay constant, t_1 is the irradiation time, t_2 is the cooling time and t_3 is the counting time. The Coincidence summing correction factor f_c was calculated by the TrueCoinc code [37]. The total efficiency curve for the HPGe detector was obtained from the TrueCoinc code. The self-attenuation coefficients f_s due to interactions of gamma rays within the sample thickness is given by

$$f_s = \frac{\mu t}{1 - e^{-\mu t}} \quad (6)$$

where μ is the linear attenuation coefficient in cm^{-1} for the irradiated sample and t is the thickness of the sample in cm. The mass attenuation coefficient μ/ρ for individual elements (Strontium, Oxygen, Aluminium and Gold) was obtained by interpolating the curves from the NIST Standard Reference Database [38]. The μ/ρ for the compound SrO₂ was calculated using

$$(\mu/\rho)_{\text{SrO}_2} = \sum_i W_i (\mu/\rho)_i \quad (7)$$

where W_i is fraction of the i th element by weight in the compound SrO₂ and $(\mu/\rho)_i$ is the mass attenuation coefficient of the i th element. CF for induced activity in sample is given by

$$CF = f_c \times f_s \quad (8)$$

The calculated self-attenuation coefficients f_s and coincidence summing correction factor f_c are given in Table 6 for SrO₂ sample, Al and Au monitor.

The measured cross section calculated with equation (4) contains uncertainty [35] contributed by parameters observed with uncertainty. The partial uncertainties for each parameter of equation (4) and their correlations are given in Table 7 following Sec. 4.1.4 of Ref. [35]. The fractional uncertainties in atomic mass for sample and monitor are negligible.

Table 7

Uncertainty in measured cross sections obtained with fractional uncertainties (%) in various parameters.

Reaction	C_s	C_m	I_{γ_s}	I_{γ_m}	$\eta_{m,s}$	f_{λ_s}	f_{λ_m}	M_s	M_m	a_s	σ_m
1 $^{88}\text{Sr}(n,2n)^{87}\text{Sr}^m$	1.1125	0.5163	0.2677	0.0015	0.1171	0.168	0.0708	0.05	0.1008	0.0121	0.5
2 $^{88}\text{Sr}(n,p)^{88}\text{Rb}$	2.3103	0.2856	1.6667	0.0015	0.0019	0.0158	0.0761	0.05	0.1008	0.0121	0.5
3 $^{88}\text{Sr}(n,\alpha)^{85}\text{Kr}$	9.6234	0.4868	0.6649	0.0015	0.4664	0.4523	0.0046	0.05	0.1008	0.0121	0.5
4 $^{86}\text{Sr}(n,2n)^{85}\text{Sr}^m$	1.4513	0.6813	0.4768	0.0015	0.3046	0.0107	0.0711	0.05	0.1008	0.1014	0.5
5 $^{86}\text{Sr}(n,2n)^{85}\text{Sr}^g$	3.6021	0.4628	0.4167	0.0015	0.0704	0.0107	0.0046	0.05	0.1008	0.1014	0.5
6 $^{84}\text{Sr}(n,2n)^{83}\text{Sr}$	7.7079	0.4628	8.2397	0.0015	0.0331	0.0472	0.0046	0.05	0.1008	1.7857	0.5
Cor(1, 2)	0	1	0	1	1	1	1	1	1	1	1
Cor(1, 3)	0	1	0	1	1	1	1	1	1	1	1
Cor(1, 4)	0	1	0	1	1	1	1	1	1	0	1
Cor(1, 5)	0	1	0	1	1	1	1	1	1	0	1
Cor(1, 6)	0	1	0	1	1	1	1	1	1	0	1
Cor(2, 3)	0	1	0	1	1	1	1	1	1	1	1
Cor(2, 4)	0	1	0	1	1	1	1	1	1	0	1
Cor(2, 5)	0	1	0	1	1	1	1	1	1	0	1
Cor(2, 6)	0	1	0	1	1	1	1	1	1	0	1
Cor(3, 4)	0	1	0	1	1	1	1	1	1	0	1
Cor(3, 5)	0	1	0	1	1	1	1	1	1	0	1
Cor(3, 6)	0	1	0	1	1	1	1	1	1	0	1
Cor(4, 5)	0	1	0	1	1	1	1	1	1	1	1
Cor(4, 6)	0	1	0	1	1	1	1	1	1	0	1
Cor(5, 6)	0	1	0	1	1	1	1	1	1	0	1

Table 8

Correction factor (CT_φ) and the threshold energy for monitor and sample reactions.

Reaction	Threshold energy (MeV)	CT_φ
$^{197}\text{Au}(\gamma,n)^{196}\text{Au}$	8.073	
$^{88}\text{Sr}(\gamma,n)^{87m}\text{Sr}$	11.113	0.34
$^{86}\text{Sr}(\gamma,n)^{85m}\text{Sr}$	11.492	0.29

3.3. Measurement of (γ,n) reaction cross sections for natural strontium target

The average cross sections of $^{88}\text{Sr}(\gamma,n)^{87m}\text{Sr}$ and $^{86}\text{Sr}(\gamma,n)^{85m}\text{Sr}$ reactions were measured using the ratio method [39] at bremsstrahlung of 15 MeV end-point energy with $^{197}\text{Au}(\gamma,n)^{196}\text{Au}$ as the monitor reaction. Here, the cross section was determined with the equation

$$\sigma_x = \langle \sigma_m \rangle \frac{CF_x \varepsilon_m C_x a_m A_x I_{\gamma m} M_m f_m}{CF_m \varepsilon_x C_m a_x A_m I_{\gamma x} M_s f_x CT_\varphi} \quad (9)$$

where the parameters have the same meaning as in equation (4) and I_γ is the branching ratio of γ -ray taken from Refs. [5,30,40]. CT_φ is the flux ratio used to normalise the cross sections due to the monitor and targets having different threshold energies and is given in Table 8.

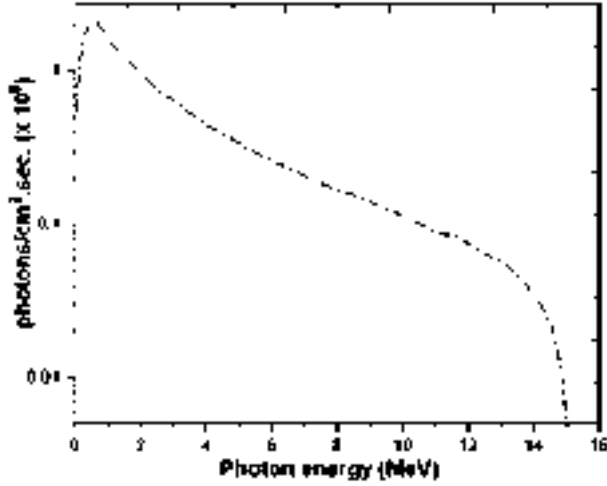


Fig. 4. GEANT4 simulated bremsstrahlung spectrum of 15 MeV end point energy.

The flux ratio is given as

$$CT_{\varphi} = \frac{\int_{E_x}^{E_{\max}} \varphi(E) dE}{\int_{E_m}^{E_{\max}} \varphi(E) dE} \quad (10)$$

where $E_{\max} = 15$ MeV, E_x is the threshold energy for the sample and E_m is the threshold energy for the sample. $\varphi(E)$ was taken from the bremsstrahlung spectrum Fig. 4 simulated using Monte Carlo based GEANT4 code [41]. The Geant4 simulations were performed by default physics models with EMStandardPhysics physics list. The bremsstrahlung photons incident on the sample surface was estimated by adopting the LINAC geometry of the experiment. The dose deposited on the patient table was correlated with the simulated dose deposit to obtain the photon flux as in Refs. [42,43].

$$\langle \sigma_m \rangle = \frac{\int_{E_m}^{E_{\max}} \varphi(E) \sigma(E) dE}{\int_{E_m}^{E_{\max}} \varphi(E) dE} \quad (11)$$

$\langle \sigma_m \rangle$ in equation (9) is the average value of the cross section for the monitor reaction from threshold energy to 15 MeV and $\varphi(E)$ is taken from the simulated bremsstrahlung spectrum Fig. 4 and $\sigma(E)$ is taken from interpolated cross section of $^{197}\text{Au}(\gamma, n)^{196}\text{Au}$ reaction in Ref. [44] from threshold energy for the monitor reaction to 15 MeV bremsstrahlung end point energy.

Here $\langle \sigma_m \rangle = 158.93 \pm 4.76$ mb is calculated from equation (11). The partial uncertainties for each parameter of equation (9) and their correlations are given in Table 9. The fractional uncertainties in atomic mass for sample and timing factor for monitor are negligible. The fractional uncertainties of the measured cross sections were calculated as the quadratic sum of the fractional uncertainties.

4. Nuclear model calculations

The excitation functions for $^{88}\text{Sr}(n,2n)^{87}\text{Sr}^m$, $^{88}\text{Sr}(n,p)^{88}\text{Rb}$, $^{88}\text{Sr}(n,\alpha)^{85}\text{Kr}$, $^{86}\text{Sr}(n,2n)^{85}\text{Sr}^m$, $^{86}\text{Sr}(n,2n)^{85}\text{Sr}^g$ and $^{84}\text{Sr}(n,2n)^{83}\text{Sr}$ reactions were calculated from reaction threshold to 20 MeV

Table 9

Fractional uncertainties (%) in various parameters used to obtain cross sections.

Reaction	C_s	C_m	$I_{\gamma s}$	$I_{\gamma m}$	$\eta_{m,s}$	$f_{\lambda s}$	M_s	M_m	a_s	A_m	σ_m
1 $^{88}\text{Sr}(\gamma,n)^{87m}\text{Sr}$	0.9892	2.4799	0.2677	3.4483	0.0621	0.3961	0.05	0.1	0.1014	0.0003	3.
2 $^{86}\text{Sr}(\gamma,n)^{85m}\text{Sr}$	2.5868	2.4799	0.4768	3.4483	0.0363	0.0491	0.05	0.1	0.0121	0.0003	3.
Cor(1,2)	0	1	0	1	1	1	1	1	0	1	0

with the TALYS-1.95 statistical model code [22]. The TALYS-1.95 code can be used for nuclear reactions that involve incident projectiles such as gammas, neutrons, protons, deuterons and α -particles in the incident energy range from 1 keV to 200 MeV. The TALYS-1.95 calculations of the present work are based on the contributions of the compound nucleus theory, direct reactions, optical model potentials and pre-equilibrium processes. An elaborate description of the TALYS-1.95 code can be found in Ref. [22]. Inelastic scattering for 14 MeV neutrons has both compound and direct-like components. The latter is described by the Distorted Wave Born Approximation (DWBA). At energies above the threshold of the (n,2n) channel, the direct-like components' contribution to the inelastic scattering dominates the former. There are 384 model combinations in TALYS-1.95 code. These correspond to the combinations of six level density models [45–50], two nucleon-nucleus optical model potentials [51], four pre-equilibrium models [52] and eight γ -ray strength functions [53–59]. Chi-squared validation of calculated cross sections with experimental data from the EXFOR database was done to determine a consistent parameter set [60]. The uncertainty band in the optimised parameter set was studied based on Refs. [61,62]. Here, parameters of the level density model and optical model potential were assigned an uncertainty based on the above. 1000 calculations were performed to determine the uncertainty in the excitation functions by randomly varying the value of the aforementioned parameters within the optimised parameter set between $\pm X\%$ of its central value. The neutron energies were binned at intervals of 1 MeV. The statistical mean corresponding to 1000 values of cross section and the standard deviation (SD) for each energy bin was calculated. The uncertainty in theoretical calculations was expressed as the percentage SD per unit calculated cross-section per bin multiplied by 1.96 to determine the 95% confidence interval. The direct-like component was accounted for by DWBA calculations. The pre-equilibrium contributions were accounted for by the two-component exciton model [52]. The default local optical model parameters in the present work are the parameterisation of Koning and Delaroche [51]. The level densities are described by the generalised superfluid model [49]. The gamma-ray transmission coefficients are calculated through the energy-dependent gamma-ray strength function given by Brink–Axel [54,55].

The excitation functions for $^{88}\text{Sr}(\gamma,n)^{87}\text{Sr}^m$ and $^{86}\text{Sr}(\gamma,n)^{85}\text{Sr}^m$ were calculated for photon energies from reaction threshold to 20 MeV using TALYS-1.95 code with the default constant temperature model for calculating nuclear level densities, with the eight available gamma-ray strength functions as given below

- (1) GSF-1: Generalised Lorentzian of Kopecky and Uhl [53]
- (2) GSF-2: Generalised Lorentzian of Brink and Axel [54,55]
- (3) GSF-3: Hartree-Fock-BCS tables [57]
- (4) GSF-4: Hartree-Fock-Bogolyubov tables [57]
- (5) GSF-5: Hybrid model of Goriely [56]
- (6) GSF-6: Goriely TDHFB [59]

Table 10

Measured cross sections with the covariance matrix and correlation matrix.

Reaction	Cross section (barns)	Covariance matrix ($\times 10^{-4}$)						Correlation matrix					
$^{88}\text{Sr}(n,2n)^{87}\text{Sr}^{\text{m}}$	0.2772 ± 0.0038	1.88						1					
$^{88}\text{Sr}(n,p)^{88}\text{Rb}$	0.0148 ± 0.0004	0.41	8.46					0.1	1				
$^{88}\text{Sr}(n,\alpha)^{85}\text{Kr}$	0.00127 ± 0.00012	0.63	0.4	93.96				0.05	0.01	1			
$^{86}\text{Sr}(n,2n)^{85}\text{Sr}^{\text{m}}$	0.2881 ± 0.0051	0.63	0.45	0.73	3.16			0.27	0.09	0.04	1		
$^{86}\text{Sr}(n,2n)^{85}\text{Sr}^{\text{g}}$	0.7427 ± 0.0274	0.5	0.39	0.52	0.6	13.63		0.1	0.04	0.01	0.09	1	
$^{84}\text{Sr}(n,2n)^{83}\text{Sr}$	0.6552 ± 0.0749	0.5	0.39	0.51	0.58	0.47	130.96	0.03	0.01	0.01	0.03	0.01	1

Table 11

Measured cross section at 14.77 ± 0.17 MeV neutron energy compared with the evaluated data of the TENDL-2019 library [23] and TALYS-1.95 calculations.

Reaction	Present work (barns)	TALYS-1.95 (barns)	TENDL-2019 (barns)
$^{88}\text{Sr}(n,2n)^{87}\text{Sr}^{\text{m}}$	0.2772 ± 0.0038	0.2587 ± 0.0288	0.2466
$^{88}\text{Sr}(n,p)^{88}\text{Rb}$	0.0148 ± 0.0004	0.0132 ± 0.0014	0.0165
$^{88}\text{Sr}(n,\alpha)^{85}\text{Kr}$	0.00127 ± 0.00012	0.00011 ± 0.00010	0.00127
$^{86}\text{Sr}(n,2n)^{85}\text{Sr}^{\text{m}}$	0.2881 ± 0.0051	0.2841 ± 0.0308	0.2557
$^{86}\text{Sr}(n,2n)^{85}\text{Sr}^{\text{g}}$	0.7427 ± 0.0274	0.7849 ± 0.0625	0.7181
$^{84}\text{Sr}(n,2n)^{83}\text{Sr}$	0.6552 ± 0.0749	0.5553 ± 0.0833	0.5244

(7) GSF-7: T-dependent relativistic mean field [58]

(8) GSF-8: Gogny DIM HFB + quasi-random-phase approximation [58]

5. Results and discussion

The covariance matrix and the correlation matrix of the measured neutron-induced reaction cross sections for strontium are presented in Table 10. Normalisation is carried out for earlier reported experimental data with respect to the recent evaluated cross section data for monitor cross section from the IRDFF-II [27] database. The measured cross sections for $^{88}\text{Sr}(n,2n)^{87}\text{Sr}^{\text{m}}$, $^{88}\text{Sr}(n,p)^{88}\text{Rb}$, $^{88}\text{Sr}(n,\alpha)^{85}\text{Kr}$, $^{86}\text{Sr}(n,2n)^{85}\text{Sr}^{\text{m}}$, $^{86}\text{Sr}(n,2n)^{85}\text{Sr}^{\text{g}}$ and $^{84}\text{Sr}(n,2n)^{83}\text{Sr}$ reactions are compared with the normalised experimental data from the EXFOR database. The measured data is also compared with the cross section reported by evaluated cross section data from the TENDL-2019 [23] library and statistical model calculations with the TALYS-1.95 nuclear code in Table 11. For all the reactions in the present study, the TALYS-1.95 calculations were done with generalised the superfluid model for level densities (ldmodel 3), the exciton model for pre-equilibrium contributions (preeqmode 2), the generalised lorentzian of Brink and Axel (strength 2) and the local nucleon nucleus potential of Koning and Delaroche (localomp y). The optimised TALYS-1.95, the cross sections from the TENDL-2019 evaluation are represented by a thin black solid line, ENDF/B-VIII.0 evaluation by a black dotted line, TALYS-1.95 95% upper confidence level by a red dotted, TALYS-1.95 95% lower confidence level by a black dashed line and the region between the above two dashed lines is filled in Fig. 5 to Fig. 8. For experimental data where monitor cross section is not available on the EXFOR database, normalisation is not performed and compared with the present work.

The covariance matrix and the correlation matrix for measured photon-induced reaction cross sections on strontium are presented in Table 12. The TENDL-2019 evaluated data is compared

Table 12
Covariance matrix and correlation matrix for measured cross sections.

Reaction	Cross section (barns)	Covariance matrix ($\times 10^{-4}$)		Correlation matrix	
$^{88}\text{Sr}(\gamma, n)^{87}\text{Sr}^m$	0.01566 ± 0.00083	28.274		1	
$^{86}\text{Sr}(\gamma, n)^{85}\text{Sr}^m$	0.01146 ± 0.00066	27.075	33.976	0.873	1

Table 13

Measured average cross section (σ) for $^{88}\text{Sr}(\gamma, n)^{87}\text{Sr}^m$ and $^{86}\text{Sr}(\gamma, n)^{85}\text{Sr}^m$ reactions at 15 MeV bremsstrahlung end-point energy.

Reaction	Present work (barns)	TALYS-1.95 calculations (barns)							
		GSF-1	GSF-2	GSF-3	GSF-4	GSF-5	GSF-6	GSF-7	GSF-8
$^{88}\text{Sr}(\gamma, n)^{87}\text{Sr}^m$	0.01566 ± 0.00083	0.02449	0.03142	0.04857	0.03336	0.02115	0.03336	0.03405	0.04597
$^{86}\text{Sr}(\gamma, n)^{85}\text{Sr}^m$	0.01146 ± 0.00066	0.02586	0.03378	0.03894	0.03575	0.02319	0.03575	0.03368	0.04344

with TALYS-1.95 calculations for eight different gamma strength functions (GSF-1 to GSF-8) and the present work is presented in Table 13.

5.1. The $^{88}\text{Sr}(n, 2n)^{87}\text{Sr}^m$ reaction

In Fig. 5 the measured cross section for $^{88}\text{Sr}(n, 2n)^{87}\text{Sr}^m$ reaction at 14.77 ± 0.17 MeV neutron energy is plotted along with reported experimental data from the EXFOR database and evaluated data from the TENDL-2019 library. For this reaction, Filatenkov et al. [63], Muyao et al. [64], Molla et al. [65], Dabek et al. [66], Rao et al. [67], Holub et al. [68], Husain et al. [17] and Strohal et al. [19] adopted $^{27}\text{Al}(n, \alpha)^{24}\text{Na}$ reaction as monitor reaction. He et al. [14] and Konno et al. [69] adopted $^{93}\text{Nb}(n, 2n)^{93}\text{Nb}^m$ reaction as a monitor reaction, while Minetti et al. [70] adopted $^{63}\text{Cu}(n, 2n)^{62}\text{Cu}$ reaction as a monitor reaction. Rao et al. [16] adopted $^{56}\text{Fe}(n, p)^{56}\text{Mn}$ reaction as monitor reaction. Reported cross section data are normalised at respective neutron energies with respect to IRDFF-II data for respective monitor reactions.

As shown in the Fig. 5, cross sections reported by Dabek et al. [66], Molla et al. [65], Konno et al. [69], Guozhu et al. [14] and Filatenkov et al. [71] whose neutron energies overlap with the present value are in good agreement with the present result within reported experimental uncertainty. Our measured cross section does not correspond with those reported by Zhou et al. [64], Husain et al. [17] and Minetti et al. [70]. The measured cross section is in good agreement with TALYS-1.95 calculations and the TENDL-2019 evaluation within the error bar.

5.2. The $^{88}\text{Sr}(n, p)^{88}\text{Rb}$ reaction

Fig. 6 shows the measured cross section for $^{88}\text{Sr}(n, p)^{88}\text{Rb}$ reaction at 14.77 ± 0.17 MeV neutron energy along with reported experimental data from the EXFOR database and evaluated data from the TENDL-2019 library. For this reaction, Kasugai et al. [72], Dabek et al. [66], Molla et al. [65], Tikku et al. [73], Husain et al. [17] and Strohal et al. [19] adopted $^{27}\text{Al}(n, \alpha)^{24}\text{Na}$ reaction as a monitor reaction. Guozhu-He et al. [14] adopted $^{93}\text{Nb}(n, 2n)^{93}\text{Nb}^m$ reaction as monitor reaction, whereas Levkovskii et al. [74,75] adopted $^{65}\text{Cu}(n, 2n)^{64}\text{Cu}$ reaction as monitor reaction. Gupta et al. [76], Dresler et al. [77], Rao et al. [16] and Prasad et al. [78] adopted $^{56}\text{Fe}(n, p)^{56}\text{Mn}$

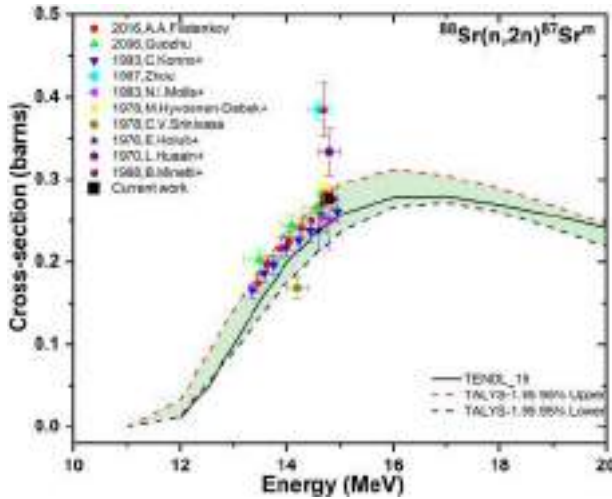


Fig. 5. Comparison of the experimental $^{88}\text{Sr}(n,2n)^{87}\text{Sr}^m$ reaction cross sections with the evaluated TENDL-2019 data and theoretical values calculated with TALYS-1.95. (For interpretation of the colours in the figure(s), the reader is referred to the web version of this article.)

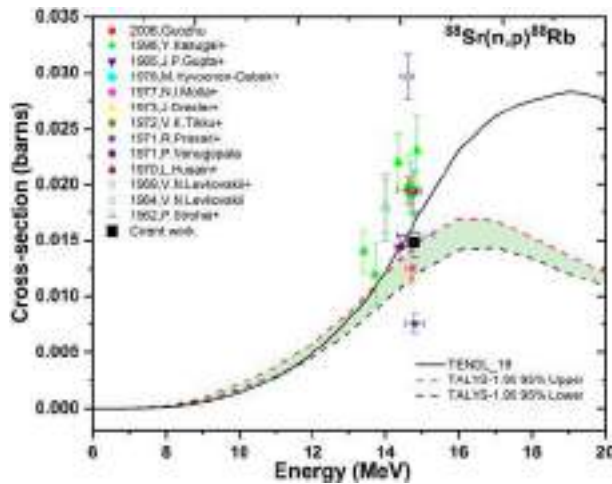


Fig. 6. Comparison of $^{88}\text{Sr}(n,p)^{88}\text{Rb}$ reaction experimental cross sections with the evaluated TENDL-2019 data and theoretical values using TALYS-1.95.

reaction as a monitor reaction. Reported cross section data are normalised at respective neutron energies with respect to IRDFF-II data for respective monitor reactions.

As shown in the Fig. 6, cross sections for $^{88}\text{Sr}(n,p)^{88}\text{Rb}$ reaction reported by Gupta et al. [76] and Levkovskii et al. [75], whose neutron energies overlap with the present value are in good agreement with the present result. The measured cross section shows a large deviation with those reported by Guozhu-He et al. [14], Kasugai et al. [72], Dabek et al. [66], Molla et al. [65], Dresler et al. [77], Tikku et al. [73], Prasad et al. [78], Husain et al. [17] and Strohal et al. [19]. However,

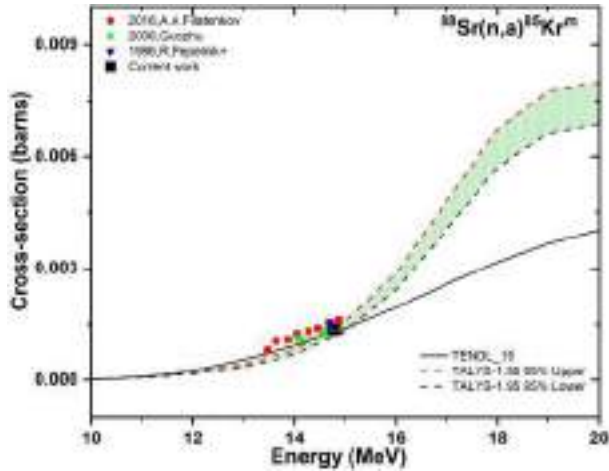


Fig. 7. Comparison of experimental $^{88}\text{Sr}(n,\alpha)^{85}\text{Kr}^m$ reaction cross sections with the evaluated TENDL-2019 data and theoretical values using TALYS-1.95.

the measured cross section is in good agreement with TALYS-1.95 calculations and the TENDL-2019 evaluation within the error bar.

5.3. The $^{88}\text{Sr}(n,\alpha)^{85}\text{Kr}^m$ reaction

In Fig. 7 the measured cross section for $^{88}\text{Sr}(n,\alpha)^{85}\text{Kr}^m$ reaction at 14.77 ± 0.17 MeV neutron energy is plotted along with reported experimental data from the EXFOR database and evaluated data from the TENDL-2019 library. For this reaction, Filatenkov et al. [63], Peplnik et al. [79] and Strohal et al. [19] adopted $^{27}\text{Al}(n,\alpha)^{24}\text{Na}$ reaction as a monitor reaction. He et al. [14] adopted $^{93}\text{Nb}(n,2n)^{93}\text{Nb}^m$ reaction as a monitor reaction. Reported cross section data are normalised at respective neutron energies with respect to IRDFF-II data for respective monitor reactions.

The present results for $^{88}\text{Sr}(n,\alpha)^{85}\text{Kr}^m$ reaction are in good agreement with the reported experimental cross sections of Filatenkov et al. [71], Guozhu-He et al. [14] and Peplnik et al. [79]. Moreover, the measured cross section matches with TALYS-1.95 calculations and the TENDL-2019 evaluation within the error bar.

5.4. The $^{86}\text{Sr}(n,2n)^{85}\text{Sr}^m$ reaction

Fig. 8 shows our measured cross section for $^{86}\text{Sr}(n,2n)^{85}\text{Sr}^m$ reaction at 14.77 ± 0.17 MeV neutron energy along with reported experimental data from the EXFOR database and evaluated data from the TENDL-2019 library. For this reaction, Ma Hui-Fang et al. [80], Dabek et al. [66], Rao et al. [81], Holub et al. [68], Husain et al. [17], Rieder et al. [82] and Strohal et al. [19] adopted $^{27}\text{Al}(n,\alpha)^{24}\text{Na}$ reaction as a monitor reaction. Luo et al. [83], Guozho-He et al. [14] and Konno et al. [69] adopted $^{93}\text{Nb}(n,2n)^{93}\text{Nb}^m$ reaction as a monitor reaction. Rao et al. [16] adopted $^{56}\text{Fe}(n,p)^{56}\text{Mn}$ reaction as monitor reaction. Reported cross section data are normalised at respective neutron energies with respect to IRDFF-II data for respective monitor reactions.

As shown in the Fig. 8, cross sections for $^{86}\text{Sr}(n,2n)^{85}\text{Sr}^m$ reaction reported by Holab et al. [68] and Strohal et al. [19], whose neutron energies overlap with the present value are in good

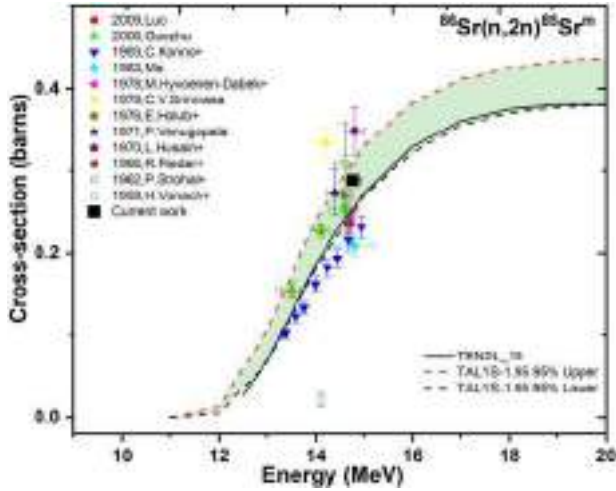


Fig. 8. Comparison of $^{86}\text{Sr}(n,2n)^{85}\text{Sr}^{\text{III}}$ reaction experimental cross sections with the evaluated TENDL-2019 data and theoretical values using TALYS-1.95.

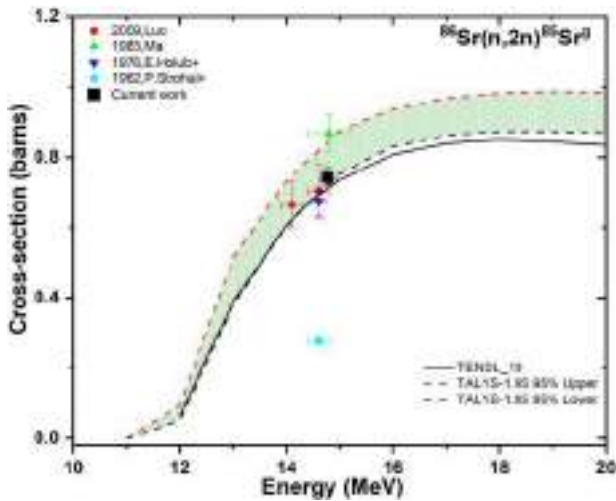


Fig. 9. Comparison of experimental $^{86}\text{Sr}(n,2n)^{85}\text{Sr}^{\text{II}}$ reaction cross sections with the evaluated TENDL-2019 data and theoretical values using TALYS-1.95.

agreement with the present result. Our measured cross section shows a large deviation with those reported by Luo et al. [83], Guozhu-He et al. [14], Konno et al. [69], Ma Hui-Fang et al. [80], Dabek et al. [66], Rao et al. [81], Rao et al. [16], Husain et al. [17] and Rieder et al. [82]. The measured cross section is in good agreement with TALYS-1.95 calculations within the error bar, however they are higher than the evaluated excitation function by the TENDL-2019 library.

5.5. The $^{86}\text{Sr}(n,2n)^{85}\text{Sr}^{\text{g}}$ reaction

Fig. 9 shows the measured cross section for $^{86}\text{Sr}(n,2n)^{85}\text{Sr}^{\text{g}}$ reaction at 14.77 ± 0.17 MeV neutron energy along with reported experimental data from the EXFOR database and evaluated

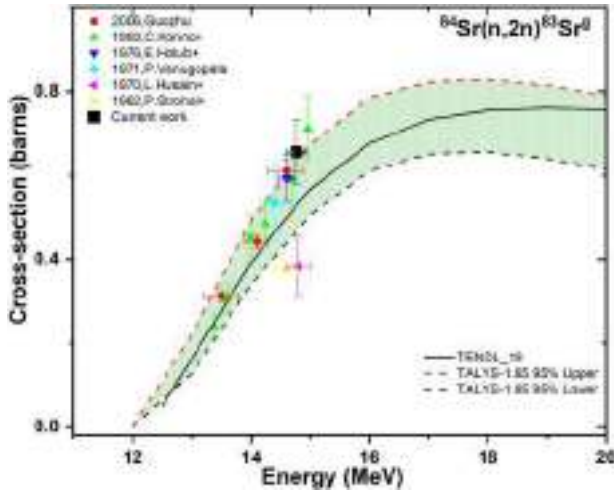


Fig. 10. Comparison of experimental $^{84}\text{Sr}(n,2n)^{83}\text{Sr}^g$ reaction cross sections with the evaluated TENDL-2019 data and theoretical values using TALYS-1.95.

data from the TENDL-2019 library. For this reaction, Hui-Fang et al. [80], Holub et al. [68] and Strohal et al. [19] adopted $^{27}\text{Al}(n,\alpha)^{24}\text{Na}$ reaction as a monitor reaction. Luo et al. [83], adopted $^{93}\text{Nb}(n,2n)^{93}\text{Nb}^m$ reaction as a monitor reaction. Reported cross section data are normalised at respective neutron energies with respect to IRDFF-II data for respective monitor reactions.

The present results for $^{86}\text{Sr}(n,2n)^{85}\text{Sr}^g$ reaction are in good agreement with the reported experimental cross sections of Luo et al. [83]. However, the experimental results reported by Ma et al. [80], Holub et al. [68] and Strohal et al. [19] show large deviations from our results. TALYS-1.95 calculations agree with the present results within the error bar, while the evaluated excitation function by the TENDL-2019 library predicts a lower cross section for 14.77 MeV neutron energy for the $^{86}\text{Sr}(n,2n)^{85}\text{Sr}^g$ reaction.

5.6. The $^{84}\text{Sr}(n,2n)^{83}\text{Sr}^g$ reaction

Fig. 10 shows our measured cross section for $^{84}\text{Sr}(n,2n)^{83}\text{Sr}^g$ reaction at 14.77 ± 0.17 MeV neutron energy along with reported experimental data from the EXFOR database and evaluated data from the TENDL-2019 library. For this reaction, He et al. [14] and Konno et al. [69] adopted $^{93}\text{Nb}(n,2n)^{93}\text{Nb}^m$ reaction as a monitor reaction Rao et al. [16] adopted $^{56}\text{Fe}(n,p)^{56}\text{Mn}$ reaction as a monitor reaction. Holub et al. [68], Husain et al. [17] and Strohal et al. [19] adopted $^{27}\text{Al}(n,\alpha)^{24}\text{Na}$ reaction as a monitor reaction. Reported cross section data are normalised at respective neutron energies with respect to IRDFF-II data for respective monitor reactions.

For $^{84}\text{Sr}(n,2n)^{83}\text{Sr}^g$ reaction, the present results are in good agreement with Guozho-He et al. [14], Konno et al. [69] and Holub et al. [68]. However, the present results do not agree the reported data of Husain et al. [17] and Strohal et al. [19]. The above two reported data do not follow the TENDL-2019 evaluation for the same reaction. The present results match with the general trend of the excitation function for the $^{84}\text{Sr}(n,2n)^{83}\text{Sr}^g$ reaction and the TALYS-1.95 calculations. The TENDL-2019 evaluation is lower than most normalised experimental data above 14 MeV neutron energy.

5.7. The $^{88}\text{Sr}(\gamma, n)^{87}\text{Sr}^{\text{m}}$ and $^{86}\text{Sr}(\gamma, n)^{85}\text{Sr}^{\text{m}}$ reaction

The average cross sections of $^{88}\text{Sr}(\gamma, n)^{87}\text{Sr}^{\text{m}}$ and $^{86}\text{Sr}(\gamma, n)^{85}\text{Sr}^{\text{m}}$ reactions have been measured relative to the cross section of $^{197}\text{Au}(\gamma, n)^{196}\text{Au}^{\text{m}}$ monitor reaction at 15 MeV Bremsstrahlung endpoint energy. The total uncertainties in the measured cross sections of $^{88}\text{Sr}(\gamma, n)^{87}\text{Sr}^{\text{m}}$ and $^{86}\text{Sr}(\gamma, n)^{85}\text{Sr}^{\text{m}}$ reactions are 5.37% and 5.81% respectively with a detailed covariance analysis. The energy dependant cross section from the TENDL-2019 library and TALYS-1.95 calculations with eight different gamma-ray strength functions have been converted to the average cross section for bremsstrahlung with end point energy of 15 MeV by using equation (11) and compared with the present result in Table 13. It is observed from the present work that for both $^{88}\text{Sr}(\gamma, n)^{87}\text{Sr}^{\text{m}}$ and $^{86}\text{Sr}(\gamma, n)^{85}\text{Sr}^{\text{m}}$ reactions, the measured average cross section is not in agreement with the TENDL-2019 evaluation and GSF-1 to GSF-8 although they are of the same order of magnitude of the present results.

6. Conclusions

Cross sections for $^{88}\text{Sr}(n, 2n)^{87}\text{Sr}^{\text{m}}$, $^{88}\text{Sr}(n, p)^{88}\text{Rb}$, $^{88}\text{Sr}(n, \alpha)^{85}\text{Kr}$, $^{86}\text{Sr}(n, 2n)^{85}\text{Sr}^{\text{m}}$, $^{86}\text{Sr}(n, 2n)^{85}\text{Sr}^{\text{g}}$ and $^{84}\text{Sr}(n, 2n)^{83}\text{Sr}$ reactions have been measured at 14.77 ± 0.17 MeV neutron energy with $^{27}\text{Al}(n, \alpha)^{24}\text{Na}$ and $^{27}\text{Al}(n, p)^{27}\text{Mg}$ as monitor reactions. In addition, the average cross sections for $^{88}\text{Sr}(\gamma, n)^{87}\text{Sr}^{\text{m}}$ and $^{86}\text{Sr}(\gamma, n)^{85}\text{Sr}^{\text{m}}$ reactions have been measured using 15 MeV bremsstrahlung photons from a medical LINAC with $^{197}\text{Au}(n)^{196}\text{Au}$ as a monitor reaction with Activation Technique and off-line gamma-ray spectroscopy. Uncertainty in measured cross section is determined with a detailed covariance analysis. The results from the present work were compared with available normalised EXFOR experimental data and evaluated nuclear data from the TENDL-2019 library. The measured cross sections are found to be in good agreement with certain literature and statistical model calculations with the TALYS-1.95 code. The results of the present study validate nuclear model approaches with increased predictive power. The photonuclear reaction cross sections are reported for the first time at 15 MeV bremsstrahlung end point energy. The present results highlight alternative production routes for $^{87}\text{Sr}^{\text{m}}$ and $^{85}\text{Sr}^{\text{g}}$.

CRedit authorship contribution statement

T.S. Ganesapandy: Data curation, Formal analysis, Investigation, Methodology, Software, Validation, Writing – original draft. **G.T. Bholane:** Data curation, Formal analysis, Software, Validation. **A.B. Phatangare:** Resources, Visualization. **F.M.D. Attar:** Formal analysis. **S.S. Dahiwal:** Funding acquisition, Resources. **S.V. Suryanarayana:** Conceptualization, Funding acquisition. **V.N. Bhoraskar:** Conceptualization, Project administration, Supervision. **S.D. Dhole:** Funding acquisition, Investigation, Project administration, Resources, Supervision, Writing – review & editing.

Declaration of competing interest

The authors declare that they have no known competing financial interests or personal relationships that could have appeared to influence the work reported in this paper.

Acknowledgements

The authors [S.D. Dhole and V.N. Bhoraskar] gratefully acknowledge the financial assistance for research work in the field of neutron-induced and photon-induced nuclear reactions by BRNS, Mumbai sanction number: 36(6)/14/49/2016-BRNS and SERB-DST, New Delhi sanction number: EMR/2017/002497. The authors are grateful Dr. Bhushan Nikam and the management of Dr. Vikhe Patil Memorial Hospital, Ahmednagar, India for providing the medical LINAC for the experiments.

References

- [1] F. Tárkányi, A. Hermanne, F. Ditrói, S. Takács, A.V. Ignatyuk, I. Spahn, S. Spellerberg, *Eur. Phys. J. A* 57 (2021) 21.
- [2] R.L. Meckelnburg, *J. Nucl. Med.* 5 (1964), 929 LP.
- [3] N.A. Kostenikov, B.L. Zhuikov, V.M. Chudakov, Y.R. Iliuschenko, S.V. Shatik, V.V. Zaitsev, D.S. Sysoev, A.A. Stanzhevskiy, *Brain Behav.* 9 (2019) e01212.
- [4] E.K. Reddy, R.G. Robinson, C.M. Mansfield, *J. Natl. Med. Assoc.* 78 (1986) 27.
- [5] T.D. Johnson, W.D. Kulp, *Nucl. Data Sheets* 129 (2015) 1.
- [6] J.F. Allen, J. Pinajian, *Int. J. Appl. Radiat. Isot.* 16 (1965) 319.
- [7] L. Rosenthal, *Radiology* 84 (1965) 75.
- [8] S.A. Kandil, I. Spahn, B. Scholten, Z.A. Saleh, S.M.M. Saad, H.H. Coenen, S.M. Qaim, *Appl. Radiat. Isot.* 65 (2007) 561.
- [9] T. Ido, A. Hermanne, F. Ditrói, Z. Szűcs, I. Mahunka, F. Tárkányi, *Nucl. Instrum. Methods Phys. Res., Sect. B, Beam Interact. Mater. Atoms* 194 (2002) 369.
- [10] F. Tárkányi, S.M. Qaim, G. Stöcklin, *Int. J. Radiat. Appl. Instrum., Part A, Appl. Radiat. Isot.* 39 (1988) 135.
- [11] F. Rösch, S.M. Qaim, G. Stöcklin, *Radiochim. Acta* 61 (1993) 1.
- [12] K. Sakamoto, M. Dohniwa, K. Okada, *Int. J. Appl. Radiat. Isot.* 36 (1985) 481.
- [13] F. Tárkányi, S.M. Qaim, G. Stöcklin, *Int. J. Radiat. Appl. Instrum., Part A, Appl. Radiat. Isot.* 41 (1990) 91.
- [14] G. He, J. Luo, Z. Liu, X. Kong, *Ann. Nucl. Energy* 33 (2006) 37.
- [15] A.M. Goryachev, G.N. Zalesnyy, *Vopr. Teor. Yader. Fiz.* 8 (1982) 121.
- [16] P.V. Rao, R.E. Wood, J.M. Palms, R.W. Fink, *Phys. Rev. C* 3 (1971) 629.
- [17] L. Husain, A. Bari, P.K. Kuroda, *Phys. Rev. C* 1 (1970) 1233.
- [18] M. Bormann, E. Fretwurst, P. Schehka, G. Wrege, H. Büttner, A. Lindner, H. Meldner, *Nucl. Phys.* 63 (1965) 438.
- [19] P. Strohal, N. Cindro, B. Eman, *Nucl. Phys.* 30 (1962) 49.
- [20] T.D. Thiep, T.T. An, N.T. Khai, P.V. Cuong, N.T. Vinh, *J. Radioanal. Nucl. Chem.* 286 (2010) 161.
- [21] R. Mandal, G. Radhu Pansare, D. Sengupta, V. Nagesh Rao Bhoraskar, *J. Phys. Soc. Jpn.* 81 (2012) 104006.
- [22] A.J. Koning, M.C. Duijvestijn, S. Hilaire, in: *TALYS-10*, EDP Sciences, France, 2008.
- [23] A.J. Koning, D. Rochman, J.-C. Sublet, N. Dzysiuk, M. Fleming, S. van der Marck, *Nucl. Data Sheets* 155 (2019) 1.
- [24] N. Otuka, E. Dupont, V. Semkova, B. Pritychenko, A.I. Blokhin, M. Aikawa, S. Babykina, M. Bossant, G. Chen, S. Dunaeva, R.A. Forrest, T. Fukahori, N. Furutachi, S. Ganesan, Z. Ge, O.O. Gritzay, M. Herman, S. Hlavač, K. Katō, B. Lalremruata, Y.O. Lee, A. Makinaga, K. Matsumoto, M. Mikhaylyukova, G. Pikulina, V.G. Pronyaev, A. Saxena, O. Schwerer, S.P. Simakov, N. Soppera, R. Suzuki, S. Takács, X. Tao, S. Taova, F. Tárkányi, V.V. Varlamov, J. Wang, S.C. Yang, V. Zerkin, Y. Zhuang, *Nucl. Data Sheets* 120 (2014) 272.
- [25] V.N. Bhoraskar, *Indian J. Pure Appl. Phys.* 27 (1989) 648.
- [26] S.S. Jayantha Kumar, V.K. Chindhade, V.N. Bhoraskar, *Pramana* 22 (1984) 453.
- [27] A. Trkov, P.J. Griffin, S.P. Simakov, L.R. Greenwood, K.I. Zolotarev, R. Capote, D.L. Aldama, V. Chechev, C. Destouches, A.C. Kahler, C. Konno, M. Košťál, M. Majerle, E. Malambu, M. Ohta, V.G. Pronyaev, V. Radulović, S. Sato, M. Schulc, E. Šimečková, I. Vavtar, J. Wagemans, M. White, H. Yashima, *Nucl. Data Sheets* 163 (2020) 1.
- [28] Reference Neutron Activation Library, International Atomic Energy Agency, Vienna, 2020.
- [29] A. Negret, B. Singh, *Nucl. Data Sheets* 124 (2015) 1.
- [30] B. Singh, J. Chen, *Nucl. Data Sheets* 116 (2014) 1.
- [31] E.A. McCutchan, A.A. Sonzogni, *Nucl. Data Sheets* 115 (2014) 135.
- [32] T. Vidmar, *Nucl. Instrum. Methods Phys. Res., Sect. A, Accel. Spectrom. Detect. Assoc. Equip.* 550 (2005) 603.

- [33] B.S. Shivashankar, S. Ganesan, H. Naik, S.V. Suryanarayana, N.S. Nair, K.M. Prasad, Nucl. Sci. Eng. 179 (2015) 423.
- [34] L.P. Geraldo, D.L. Smith, Nucl. Instrum. Methods Phys. Res., Sect. A, Accel. Spectrom. Detect. Assoc. Equip. 290 (1990) 499.
- [35] N. Otuka, B. Lalremruata, M.U. Khandaker, A.R. Usman, L.R.M. Punte, Radiat. Phys. Chem. 140 (2017) 502.
- [36] A. Sonzogni, AIP Conf. Proc. 769 (2005) 574.
- [37] S. Sudar, in: "TrueCoinc" Software Utility for Calculation of the True Coincidence Correction, International Atomic Energy Agency (IAEA), 2002.
- [38] J. Hubbell, S. Seltzer, <http://Physics.Nist.Gov/PhysRefData/XrayMassCoef/Cover.Html>, 1995.
- [39] S. Yang, K. Kim, M. Zaman, H. Naik, G. Kim, T.-Y. Song, Y.-O. Lee, S.G. Shin, Y.-U. Key, M.-H. Cho, J. Radioanal. Nucl. Chem. 300 (2014) 367.
- [40] H. Xiaolong, Nucl. Data Sheets 108 (2007) 1093.
- [41] J. Allison, K. Amako, J. Apostolakis, H. Araujo, P.A. Dubois, M. Asai, G. Barrand, R. Capra, S. Chauvie, R. Chytracsek, G.A.P. Cirrone, G. Cooperman, G. Cosmo, G. Cuttone, G.G. Daquino, M. Donszelmann, M. Dressel, G. Folger, F. Foppiano, J. Generowicz, V. Grichine, S. Guatelli, P. Gumplinger, A. Heikkinen, I. Hrivnacova, A. Howard, S. Incerti, V. Ivanchenko, T. Johnson, F. Jones, T. Koi, R. Kokoulin, M. Kossov, H. Kurashige, V. Lara, S. Larsson, F. Lei, O. Link, F. Longo, M. Maire, A. Mantero, B. Mascialino, I. McLaren, P.M. Lorenzo, K. Minamimoto, K. Murakami, P. Nieminen, L. Pandola, S. Parlati, L. Peralta, J. Perl, A. Pfeiffer, M.G. Pia, A. Ribon, P. Rodrigues, G. Russo, S. Sadilov, G. Santin, T. Sasaki, D. Smith, N. Starkov, S. Tanaka, E. Tcherniaev, B. Tome, A. Trindade, P. Truscott, L. Urban, M. Verderi, A. Walkden, J.P. Wellisch, D.C. Williams, D. Wright, H. Yoshida, IEEE Trans. Nucl. Sci. 53 (2006) 270.
- [42] G.T. Bholane, T.S. Ganesapandy, A.B. Phatangare, V.D. Bharud, B.J. Patil, S.S. Dahiwal, S.V. Suryanarayana, V.N. Bhoraskar, S.D. Dhole, Appl. Radiat. Isot. 174 (2021) 109739.
- [43] G.T. Bholane, T.S. Ganesapandy, A.B. Phatangare, F.M.D. Attar, S.S. Dahiwal, S.V. Suryanarayana, V.N. Bhoraskar, S.D. Dhole, Nucl. Phys. A 1020 (2022) 122399.
- [44] C. Plaisir, F. Hannachi, F. Gobet, M. Tarisien, M.M. Aléonard, V. Méot, G. Gosselin, P. Morel, B. Morillon, Eur. Phys. J. A 48 (2012) 68.
- [45] A. Gilbert, A.G.W. Cameron, Can. J. Phys. 43 (1965) 1446.
- [46] W. Dilg, W. Schantl, H. Vonach, M. Uhl, Nucl. Phys. A 217 (1973) 269.
- [47] S. Goriely, F. Tondeur, J.M. Pearson, At. Data Nucl. Data Tables 77 (2001) 311.
- [48] S. Goriely, S. Hilaire, A.J. Koning, Phys. Rev. C 78 (2008) 64307.
- [49] A.V. Ignatyuk, J.L. Weil, S. Raman, S. Kahane, Phys. Rev. C 47 (1993) 1504.
- [50] S. Hilaire, M. Girod, S. Goriely, A.J. Koning, Phys. Rev. C 86 (2012) 64317.
- [51] A.J. Koning, J.P. Delaroche, Nucl. Phys. A 713 (2003) 231.
- [52] A.J. Koning, M.C. Duijvestijn, Nucl. Phys. A 744 (2004) 15.
- [53] J. Kopecky, M. Uhl, Phys. Rev. C 41 (1990) 1941.
- [54] D. Brink, Nucl. Phys. 4 (1957) 215.
- [55] P. Axel, Phys. Rev. 126 (1962) 671.
- [56] S. Goriely, Phys. Lett. B 436 (1998) 10.
- [57] E. Khan, S. Goriely, D. Allard, E. Parizot, T. Suomijärvi, A.J. Koning, S. Hilaire, M.C. Duijvestijn, Astropart. Phys. 23 (2005) 191.
- [58] M. Martini, S. Hilaire, S. Goriely, A.J. Koning, S. Péru, Nucl. Data Sheets 118 (2014) 273.
- [59] D.P. Arteaga, P. Ring, Phys. Rev. C 77 (2008) 34317.
- [60] T.S. Ganesapandy, J.J. Jeremiah, S.S. Dahiwal, S.D. Dhole, V.N. Bhoraskar, Appl. Radiat. Isot. 150 (2019).
- [61] D.L. Smith, in: Covariance Matrices for Nuclear Cross Sections Derived from Nuclear Model Calculations, 2005.
- [62] A.J. Koning, D. Rochman, Nucl. Data Sheets 113 (2012) 2841.
- [63] A.A. Filatenkov, in: Neutron Activation Cross Sections Measured at KRI in Neutron Energy Region 13.4–14.9 MeV, 2016.
- [64] Z. Muyao, Z. Yongfa, W. Chuanshan, Z. Lu, C. Yitai, Z. Shuxin, Z. Shenjin, X. Kuanzhong, Z. Shenmuo, C. Xueshi, Z. Yiping, Y. Qinguan, Chin. J. Nucl. Phys. 9 (1987) 34.
- [65] S. Molla, N.I. Mizanul Islam, M. Mizanur Rahman, M. Khatun, in: Measurement of Cross Section for Neutron Induced Reactions at 14 MeV via Activation Technique, 1983.
- [66] M. Hyvönen-Dabek, M. Tarvainen, P. Holmberg, J. Radioanal. Chem. 46 (1978) 357.
- [67] C.V. Srinivasa Rao, N. Lakshmana Das, B.V. Thirumala Rao, J. Rama Rao, in: 21 Nucl. Phys. and Solid State Phys. Symp., Bombay, 1978, p. 113.
- [68] E. Holub, N. Cindro, J. Phys. G Nucl. Phys. 2 (1976) 405.

- [69] C. Konno, Y. Ikeda, K. Oishi, K. Kawade, H. Yamamoto, H. Maekawa, Activation Cross Section Measurements at Neutron Energy from 13.3 to 14.9 MeV, 1993.
- [70] B. Minetti, A. Pasquarelli, Nucl. Phys. A 118 (1968) 449.
- [71] A.A. Filatenkov, S.V. Chuvaev, V.N. Aksenov, V.A. Yakovlev, A.V. Malyshev, S.K. Vasil'ev, M. Avrigeanu, V. Avrigeanu, D.L. Smith, Y. Ikeda, et al., Rept: Khlopin Radiev. Inst., Leningrad Reports, No. 252, 1999.
- [72] Y. Kasugai, H. Yamamoto, K. Kawade, T. Iida, Ann. Nucl. Energy 25 (1998) 23.
- [73] V.K. Tikku, H. Singh, B. Sethi, in: 15. Nucl. and Solid State Phys. Symp., 1972, p. 115.
- [74] V.N. Levkovskii, J. Exp. Theor. Phys. 45 (1964) 213.
- [75] V.N. Levkovskii, Sov. J. Nucl. Phys. 8 (1969) 4.
- [76] J.P. Gupta, H.D. Bhardwaj, R. Prasad, Pramana 24 (1985) 637.
- [77] J. Dresler, Cross Sections of the (n, p) Reactions at 14.6 MeV for 13 Nuclides, 1973.
- [78] R. Prasad, D.C. Sarkar, Nuovo Cimento A 3 (1971) 467.
- [79] R. Pepelnik, 14 MeV Neutron Activation Cross Sections, 1986.
- [80] M. Hui-Fang, High Energy Phys. Nucl. Phys. 7 (1983) 639.
- [81] C.V. Srinivasa Rao, in: 21. Nucl. Phys. and Solid State Phys. Symp., Bombay, 1978, p. 113.
- [82] R. Rieder, Acta Phys. Austriaca 23 (1966) 42.
- [83] J. Luo, F. Tuo, X. Kong, J. Radioanal. Nucl. Chem. 279 (2009) 443.



Peer Reviewed Refereed
and UGC Listed Journal
(Journal No. 40776)



ISSN 2277 - 5730

AN INTERNATIONAL MULTIDISCIPLINARY
QUARTERLY RESEARCH JOURNAL

AJANTA

Volume - XI, Issue - II
April - June - 2022
English Part - I

Impact Factor / Indexing
2020 - 6.306
www.sjifactor.com



Ajanta Prakashan


CONTENTS OF ENGLISH PART - I


S. No.	Title & Author	Page No.
1	Democracy and Society Dr. Vikas Singh	1-6
2	Issues in Indian Higher Education Policy: Achieving Full Potential By 2030 Deore Sujata Agnihotri Ganesh	7-22
3	Impact of Regionalism on Indian Society Dr. S. R. Manza	23-29
4	Mobile Cultures/Nationality and Literature Today Dr. Pradnya Kale	30-33
5	Causes and Remedies of Regional Imbalances Dr. P. N. Dapke	34-37
6	Rabindranath Tagore's Nationalism in Contemporary Context of India: An Interrogation of <i>Nationalism in India</i> Dr. Rupali Prabhakar Palodkar	38-41
7	Good Governance and Administrative Practices Dr. Hemchandra Narsingrao Deshmukh	42-49
8	Physical Shopping Vs Digitalized Shopping: A Comparative Study Ms. Surbhi Bhardwaj	50-57
9	Women Empowerment and Democracy Asst. Prof. Maimanat Jahan Ara	58-63
10	Indian Federalism in 21 st Century: Issues and Challenges Dr. Ahmad Shamshad	64-79
11	Regionalism in India: Its Different Dimensions, Meaning and Suggestive Measures Dr. Wahida Abdul Razzak Shaikh	80-86
12	Importance of English as Language of Communication Karuna B. Ghoble	87-88

10. Indian Federalism in 21st Century: Issues and Challenges

Dr. Ahmad Shamshad

Assistant Professor, Department of Political Science, Aki's Poona College of Arts,
Science & Commerce Camp, Pune.

Abstract

Government is an important part of the state but the form of government of all the states is not the same. The form of government is selected keeping in mind the particular circumstances and needs of the country. This is the reason that the government of one country is unitary and that of some is federal. In a unitary system, the entire power is vested in the center and in a federal system, the entire power is divided between the center and the states. Federalism or federal form of government is the most suitable form for a vast and pluralistic country like India. It tries to facilitate the socio-political cooperation between two sets of identities through various structural mechanisms of 'shared rule'.

Key Words - Federal, Unitary, Bicameral, Unicameral

Introduction

Federalism was introduced in India by the Government of India Act, 1935. While drafting the Constitution of Indian, the framers wanted to give a federal look to it considering the pluralistic characteristics of India. The Constitution contains certain integral federal features such as two governments; division of powers between the union and its constituents; supremacy of the Constitution; rigidity of the Constitution; independent Judiciary; bicameralism etc. Unlike the true federal states like the USA, Indian federation was not a result of a contract between several sovereign-units but a product of conversion of a unitary system into a federal system.

Historical Background of Federalism

Federalism in India is a historical progress. Under the present constitution, the federal configuration and its tangible operation can be understood only on the broad canvas of its long expedition. The word "federal" is derived from the Latin "phodus/foedus", meaning "covenant".

It symbolizes the ideas of promise, obligation and undertaking; and consequently, the federal idea is based on cooperation, reciprocity and mutuality. Federalism is a way of separating

powers so that central and local governments are harmonized and autonomous within a domain. To be clear, federalism calls for a constitutional mechanism (a parts) to bring about unity in diversity by toning the different forces of centripetal and centrifugal trends in the country for the attainment of conjoint national goals.

In India, between 321 and 185 BC in Magadha, the Maurya's assimilated for the first time several kingdoms and republics, which may be the first subcontinental state in Indian history and starting with the land revenue system of Mughals & Sher Shah and taking shape with Akbar's division of his empire into 12 Subas or Provinces, it provides a classic example of a federal government.

Federalism is the result of historical development. It stems from the need for unity of some independent states, which are not able to deal with external threats at the private level. Their union makes possible the promotion of their security and economic interests. However, these states do not completely relinquish their independence.

The factors driving the formation of a federation are the idea of national unity, discussions on common economic interests and international prestige. Federalism is a modern concept. However, its theory and practice are no older than the American Federation, which came into existence in 1787.

The federal idea is such a scheme of government, in which the attached states form a federation and they are neither separate nor united from each other. In this perspective, this concept is very ancient and was put into practice in ancient Greece. But it has been implemented on a large scale during the last two centuries and in modern times, the US Constitution of 1787 is considered the first experiment in establishing a federal system of government. Subsequently, federalism as a mode of political organization was incorporated into the Constitution of Switzerland, the Dominion of Canada and the Commonwealth of Australia and India.

Federalism in India

After the Third Round Table Conference* also flopped significantly, the British government issued a White Paper in March 1933, proposing a new Indian constitution with an accountable government in the provinces and the principle of dyarchy at the centre. As a result of the publication of the White Paper, in April 1933 Her Majesty's Government appointed a Joint Select Committee of both the Houses of Parliament to evaluate and survey the proposals for the

White Papers. These proposals were enacted into law and received the assent of the British Crown and eventually became the basis for the Government of India Act of 1935.

The significance of the 1935 Act lies in the fact that the provinces were endowed with a legal personality under a national plan, and that the character of the national plan was ultimately a federal system. This meant ending the principle of dyarchy at the provincial level and retaining it at the centre.

But the federal structure that India is following today is different from that which the British brought to us. The greatest indication of federalism in India lies in the history of its foundation in 1947, when after the partition of Pakistan from the Indian subcontinent, all the provinces, presidencies and princely states were united under a single document of accession, which shows that all these dependent states came together to be called the former sovereign (sovereign) or one nation-state. India's growth and journey as a federal country can be broadly understood by dividing it into two parts: constitutional/legal provisions and the face of federalist India brought in by the judiciary.

Constitutional Character of Federalism in India: Unitary vs Federal

According to Article 1 of the Indian Constitution, India is a union of states. On the other hand, the system of government is federal. Indian federalism has its origins from the Canadian system, whereas the Indian Federation is not established by the consent or agreement of the states, as well as the right of the states to secede from the union.

Due to the more powerful central government, the true nature of the Indian Union has been brought into controversy, while there is no unanimity on the definition of a federal state. Now the question arises that which state is federal or unitary? To know the answer to this question, it is necessary to know the characteristics of federal and unitary systems.

The Constitution of India is unique with respect to its extreme extent and substance. The uniqueness of the Indian Constitution also lies in the fact that though it is federal in character, it declares India to be a union of states. The constitution provides for single citizenship as in the United Kingdom and unlike the United States which provides for dual citizenship. Single citizenship gives the Constitution a unitary facet where all citizens are united under a single identity as an "Indian".

The Constitution of India establishes a dual polity with jurisdiction to make laws on various subjects which is divided between the central and state governments. The distinguishing

feature here is that the rest of the powers are in the hands of the central government. This feature, which is different from other countries, makes Indian federalism a bit complicated to fathom (intricate). Another feature which marks India as a federal country in nature is the written Constitution. The Indian Constitution is the longest and largest Constitution in the world which clearly defines everything from rights to remedies. It strengthens the federal nature of the country and assures security to the state and citizens.

Powers in the country are divided into three pillars of democracy: the legislature, the executive, and the judiciary. These three props are complementary and supplementary with an independent judiciary which is the protector of the supremacy of the Constitution and gets to the bottom of the differences between the center and the states or 2 states. This guarantees a rigorous remedial system.

The judiciary, though independent, is an integrated institution and thus gives the Constitution the essence of a unitary government. Other terms of the same Constitution provide for the President to appoint the constitutional heads (Governors) of all the states, and they hold their office according to the will of the President.

The Constitution of India is both stern and flexible at the same time. The rigidity of the constitution is an indispensable feature of federalism. But the same rigid constitution has affected a century of amendments, less than 75 years after independence. The Constitution provides for a bicameral legislature consisting of an upper house (Rajya Sabha) and a lower house (Lok Sabha).

The Rajya Sabha is the stand-in for the states of the Indian Union, while the Lok Sabha represents the people of India as a whole. The Rajya Sabha (even though a less powerful chamber) is required to maintain federal stability by protecting the interests of the states against unnecessary interference from the Centre.

Apart from the above provisions, the following provisions of the Constitution also make India a federal Nation.

Important Features- Federal vs Unitary

Federal	Unitary
<p>Dual government In a unitary state, there is only one national government, whereas in a federal state there are two governments - one national and the other state government. In India there is a</p>	<p>Despite the features of the federal system, the Indian Constitution has not been considered as a full federal constitution because there are some such provisions in the Indian Constitution, which are the proof of being unitary. The features that</p>

central government and other state governments. In other words, the dual government system has been established by the Indian Constitution.

The division of Power

Division of powers between the center and the states is the main feature of the union government. Subjects of national importance have been given to the central government and those of local importance to the state governments. That is why there are three lists in the Constitution of India, which are as follows - (i) Union List, (ii) State List, and; (iii) Concurrent List.

Supremacy of the Constitution

The Indian Constitution is considered the supreme law of the country. It is the duty of every person to follow the laws made according to the Constitution. No government official or the ruler of the country can do any work against the Constitution. The Parliament or the State Legislature cannot make any law which is against any article of the Constitution. The Supreme Court and High Courts of India have been given the power of judicial review. According to this, the court can declare as unconstitutional such law of Parliament or such order of the executive which violates any provision mentioned in the constitution.

Bicameral Legislature

Under the federal government, the legislature must be bicameral. Usually, the lower house represents the people and the upper house represents the states of the union. The lower house is called the Lok Sabha and the upper house is called the Rajya Sabha.

Independent Judiciary

give a unitary form to the Indian Constitution are as follows-

One constitution

In India, there is only one Constitution for the center and the states. There is a federal system in countries like America and Switzerland, there are separate constitutions of the states, whereas in India there is only one constitution for the whole country, in which there is a provision regarding the system of governance of the center and the states.

Residuary power

The Constitution of India has given residuary powers to the Central Government as per Article 248. Residual power means any matter which is not mentioned in any of the three lists, i.e., Union, State & Concurrent List. This arrangement is available in the Canadian Constitution.

Constitutional Amendment

The center has more powers than the states in relation to amending the Constitution. Most of the part of the Constitution can be changed by the Parliament by a simple majority by certain method. There is very little part of the constitution, in which amendment is necessary to support the legislatures of at least half of the states. Therefore, the central government has the superiority even in the amendment of the constitution, which is the main feature of the unitary system.

Division of Powers

The division of powers in the Constitution is in favour of the Centre. Very important subjects have been mentioned in the Union List than in the State List. Apart from this, the total number of subjects in the Union List is 97, while 66 subjects of less importance have been listed in the State List. Apart from this, a total of 47 subjects are listed in the concurrent list. The Center or the



possibly resulting in a major worldwide recession and a spike in worldwide oil and gas price levels. Rising global commodity prices, if sustained or worsened, have the potential to produce fast and extended hyperinflation in several nations.

Continued price increases may aggravate poverty and food shortages for certain populations, especially in import-dependent Middle Eastern and African nations (e.g., Egypt, Lebanon, Libya, and Yemen). These trends may potentially exacerbate political unrest and create migratory problems in certain areas (Khudaykulova, Yuanqiong, & Khudaykulov, 2022). This highlights that this impact of war is longstanding and will be lasting in the world and both in Ukraine and Russia individual. Along with harming the well-being of the people and their houses, these war zone issues will also affect a lot to the economic stability of the world. Especially the sanctions that are being imposed on Russia along with its counter-sanctions are all likely to lead to a major imbalance on both the national and international levels.

The Russia-Ukraine war has had a significant impact on the region and beyond, with consequences in various areas:

Humanitarian: The conflict has had a devastating humanitarian impact, with thousands of people killed and millions displaced from their homes. It has also led to the breakdown of essential services such as healthcare, education, and access to clean water.

Economic: The conflict has had a significant impact on the economies of both Russia and Ukraine, as well as on the wider region. It has disrupted trade and investment, damaged infrastructure, and resulted in significant costs for reconstruction and recovery.

Political: The conflict has led to the destabilization of the region and has strained relations between Russia and Ukraine, as well as between Russia and Western countries. It has also challenged the principles of international law, such as respect for territorial integrity and sovereignty.

Security: The conflict has had wider implications for security, with the potential for the conflict to escalate and for tensions to spread beyond the region. It has also led to the militarization of the region and an increase in arms production and sales.

Diplomatic: The conflict has led to increased tensions between Russia and Western countries, resulting in the imposition of sanctions on Russia by the United States and European Union. The conflict has also tested the ability of international organizations such as the United Nations to resolve conflicts and promote peace.

CONCLUSION

The beginning of the Russia- Ukraine started with the wish of Ukraine to enter into the NATO which Russia was completely against off. Although the head strong decision of both the countries and the long-standing history of Russia on constant acts of war have turned the fears of the world to come true. This war and its longstanding attacks have affected both the countries as well other countries on the international level. The most evident impact of this war is concerned with the loss of life and people in this. Apart from this the disruption in the global supply chain due to the sanctions on Russia by the Western countries have resulted into the major imbalance of import and export on the international level. It has also indeed resulted into hyperinflation making it difficult for the people to afford their basic necessities.

The conflict has its roots in political, economic, and security issues, with Ukraine seeking closer ties with the West while Russia seeks to maintain its influence over Ukraine. The conflict has resulted in a significant humanitarian impact, with thousands of people killed and millions displaced from their homes. It has also had a significant economic impact, disrupting trade and investment, and leading to significant costs for reconstruction and recovery. The conflict has challenged the principles of



international law and has strained relations between Russia and Western countries. Despite numerous ceasefire agreements and diplomatic efforts to resolve the conflict, a lasting peace remains elusive, and the conflict continues to be a source of tension and instability in the region.

REFERENCES

1. ANNA, C. (2022). Russia's war on Ukraine: Impact on food security and EU response. <https://policycommons.net/artifacts/2325136/russias-war-on-ukraine/3085667/>
2. Balbaa, M. E., Eshov, M., & Ismailova, N. (2022). The Impacts of Russian Ukrainian War on the Global Economy in the frame of digital banking networks and cyber attacks. https://www.researchgate.net/profile/Muhammad-Balbaa/publication/360658201_The_Impacts_of_Russian-Ukrainian_War_on_the_Global_Economy/links/6400eaf20d98a97717d0c3d8/The-Impacts-of-Russian-Ukrainian-War-on-the-Global-Economy.pdf
3. Balbaa, M. E., Eshov, M., & Ismailova, N. (2022). The Impacts of Russian-Ukrainian War on the Global Economy. Advance online publication. DOI: DOI, 10. https://www.researchgate.net/profile/Muhammad-Balbaa/publication/360074361_The_Impacts_of_Russian-Ukrainian_War_on_the_Global_Economy/links/6260411cbca601538b5a325f/The-Impacts-of-Russian-Ukrainian-War-on-the-Global-Economy.pdf
4. Garicano, L., Rohner, D., & Weder, B. (Eds.). (2022). Global Economic Consequences of the War in Ukraine Sanctions, Supply Chains and Sustainability. Centre for Economic Policy Research. https://cepr.org/system/files/publication-files/172987-global_economic_consequences_of_the_war_in_ukraine_sanctions_supply_chains_and_sustainability.pdf
5. Kammer, A., Azour, J., Selassie, A. A., Goldfajn, I., & Rhee, C. (2022). How war in Ukraine is reverberating across world's regions. Washington: IMF, March, 15, 2022. <https://joserobertoafonso.com.br/wp-content/uploads/2022/03/How-War-in-Ukraine-Is-Reverberating-Across-Worlds-Regions-%E2%80%93-IMF-Blog.pdf>
6. Khudaykulova, M., Yuanqiong, H., & Khudaykulov, A. (2022). Economic consequences and implications of the Ukraine-russia war. *International Journal of Management Science and Business Administration*, 8(4), 44-52. https://www.researchgate.net/profile/Bojan-Obrenovic/publication/362057842_Economic_Consequences_and_Implications_of_the_Ukraine-Russia_War/links/62d3bff85aab971198b63e2c/Economic-Consequences-and-Implications-of-the-Ukraine-Russia-War.pdf
7. Mariotti, S. (2022). A warning from the Russian–Ukrainian war: avoiding a future that rhymes with the past. *Journal of Industrial and Business Economics*, 49(4), 761-782. <https://link.springer.com/article/10.1007/s40812-022-00219-z>
8. Mbah, R. E., & Wasum, D. F. (2022). Russian-Ukraine 2022 War: A review of the economic impact of Russian-Ukraine crisis on the USA, UK, Canada, and Europe. *Advances in Social Sciences Research Journal*, 9(3), 144-153. https://www.researchgate.net/profile/Ruth-Endam-Mbah/publication/359512955_Russian-Ukraine_2022_War_A_Review_of_the_Economic_Impact_of_Russian-Ukraine_Crisis_on_the_USA/links/6241fcdd21077329f2dd2c3d/Russian-Ukraine-2022-War-A-Review-of-the-Economic-Impact-of-Russian-Ukraine-Crisis-on-the-USA.pdf



9. Nitions, U. (2022). Global Impact of war in Ukraine on food, energy and finance systems. United Nations. <https://news.un.org/pages/wp-content/uploads/2022/04/UN-GCRG-Brief-1.pdf>
10. Orhan, E. (2022). The effects of the Russia-Ukraine war on global trade. *Journal of International Trade, Logistics and Law*, 8(1), 141-146.
<http://jital.org/index.php/jital/article/view/277>
11. Ozili, P. K. (2022). Global economic consequence of Russian invasion of Ukraine. Available at SSRN. https://papers.ssrn.com/sol3/papers.cfm?abstract_id=4064770
12. Pereira, P., Bašić, F., Bogunovic, I., & Barcelo, D. (2022). Russian-Ukrainian war impacts the total environment. *Science of The Total Environment*, 837, 155865.
<https://www.sciencedirect.com/science/article/pii/S004896972202962X>
13. World Trade Organisation. (2021) The Crisis in Ukraine Implications of the war for global trade and development.
https://www.wto.org/english/res_e/booksp_e/imparctukraine422_e.pdf

Volume 96, No. 01(II), 2023

(New Series)

ISSN : 0972-0766



(Established in 1804)

**JOURNAL
OF THE
ASIATIC SOCIETY OF MUMBAI**
(A UGC - CARE Listed Journal)

Editors

Parineets Deshpande

Ambarish Khare

Published by

The Asiatic Society of Mumbai

Town Hall, Mumbai- 400 001.

Maharashtra State (INDIA)

2023

Volume 96 for 2023
(New Series)
ISSN : 0972-0766

**JOURNAL
OF THE
ASIATIC SOCIETY OF MUMBAI**

Editors
Parineets Deshpande
Ambarish Khare

Published by
The Asiatic Society of Mumbai
Town Hall, Mumbai- 400 001.
Maharashtra State (INDIA)
2023

London Agents
ARTHUR PROBSTHAIN
41, Great Russell Street, London, WCB, 3PL

JOURNAL OF ASIATIC SOCIETY OF MUMBAI

Volume 96 for 2023

(For the year 2023)

CONTENTS

Articles

- | | | | |
|----|--|--|----|
| 1 | A STUDY OF CHARACTERS, LANGUAGE & SOCIAL CLASS IN BERNARD SHAW'S PYGMALION | Dr. Abdul Saleem | 1 |
| 2 | FAMILY FOCUSED PSYCHOTHERAPEUTIC INTERVENTIONS TO ENHANCE PARENTCHILD RELATIONSHIP AMONG ADOLESCENT | Dr. Freda Cota Pereira | 9 |
| 3 | HUMAN RIGHTS AND WOMEN EMPOWERMENT: ISSUES AND PERSPECTIVES SPECIAL REFERENCE TO AGARTALA MUNICIPAL AREA | Mr. Kalipadha Debnath | 16 |
| 4 | A BRIEF CASE STUDY OF HIMALAYA DRUG COMPANY'S CLOSED DIVISION IN JALGAON DISTRICT OF MAHARASHTRA | Dr. Khalid Arshad & Dr. Aftab Alam | 21 |
| 5 | DETERMINING FACTORS OF INCOME OF THE FEMALE HEADED HOUSEHOLDS OF THE IN MULLAITIVU DISTRICT OF SRI LANKA | Gnanasubramaniam
Gnanachandran &
Dr.J.A.Arul Chellakumar | 27 |
| 6 | IMPACT OF MIGRATION: A CRITICAL ANALYSIS | Dr. Mukhtar Shaikh | 35 |
| 7 | THE ANGLO FRENCH SAGA: WAR AND DIPLOMACY IN 17TH AND 18TH CENTURY | Dr Zoheb Hasan | 40 |
| 8 | THE COST OF MATERIALISTIC LIFESTYLE: MONEY, MIND AND MORALITY | Zameer Salim Sayyed | 45 |
| 9 | KAMALA DAS: THE VOICE OF THE SUBALTERN | Dr. Vinita Basantani &
Ms. Zeenat B.Merchant | 49 |
| 10 | COMPARATIVE ANALYSIS OF THE GLOBAL INNOVATION CAPACITY: A STUDY ON BRICS COUNTRIES | Ms. Lizette D'Costa | 52 |
| 11 | INNOVATIVE DEVELOPMENT IN ECONOMIC WITH RESPECT TO MACRO ECONOMICS | Dr. Thombre Kailas
Arjunrao | 60 |
| 12 | A STUDY ON CULTURE AND HERITAGE OF INDIA. | Imran Hussain | 64 |
| 13 | QUALITY OF WORK-LIFE IN BANKING SECTOR | Nishi Shah, Dr. Divya
Jain, Miti Suchak &
Charvi Joshi | 68 |



IMPACT OF MIGRATION: A CRITICAL ANALYSIS

Dr. Mukhtar Shaikh

Assistant Professor, Department of Political Science, Poona College of Arts, Science & Commerce,
Pune

Abstract

Human beings are social animals who have survived throughout history only due to their constant ability to migrate. Migration refers to the process of people moving from one place to another, typically for permanent or semi-permanent settlement. There are many reasons why people migrate, including seeking better economic opportunities, political or social instability, environmental factors such as natural disasters or climate change, family reunification, and education. People who migrate are often referred to as migrants, and they may face a variety of challenges and barriers, including language and cultural differences, legal and bureaucratic hurdles, and discrimination. Governments and international organizations play a key role in managing migration and ensuring that it is safe, orderly, and humane. This can include policies to protect the rights of migrants, promote integration and inclusion, and address the root causes of migration, such as poverty, inequality, and conflict. Although this process of migration has indeed been the reason for the cause of a lot of issues on a wide scale. This paper has been developed to understand these major issues. The aim of this research paper is to focus on the major issues of immigration. They are related to changes in the labour market, changes in the demand and supply for labourers, financial drains, health issues, and a raise in crime rates. Apart from this, the paper has also highlighted the emerging issues related to migration which is concerned with children.

Introduction

Migration is the movement of individuals from one location to the next, either within or even across national boundaries. Individuals move for a variety of causes, including better economic possibilities, fleeing violence or oppression, reuniting with family and friends, or furthering their education. Migration can occur in numerous ways, including voluntary or forced movement, internal or international migration, and temporary or permanent migration. Refugees, for instance, may be compelled to escape their home nation because of warfare or oppression and claim refuge in some other nation, or economic migrants may relocate to some other nation in quest of better job possibilities (Charles et al., 2018). Migration is indeed a continual phenomenon that has sparked political discussion throughout the globe. The Individuals that had left their respective homelands willingly for financial or some other causes, or people who have been compelled to leave their respective countries (refugees, displaced persons, etc.), have demonstrated a consistent rising pattern.

Handling people migration is among the most difficult tasks for landing nations globally, both developed and developing. It is compounded in cities, where migrants often seek a higher standard of living. The reasons and pathways of migrant flow for various forms of migration are hard to tell apart, providing challenges for governments (Borkowska et al., 2018). This process of migration may both have beneficial and bad consequences both for migrants and the cultures they migrate to and from. On the one side, migration may boost cultural exchange, economic progress, and variety. Migration, on the other side, can cause societal conflicts, exploitation, and prejudice. This paper will further discuss and evaluate different kinds of issues that the process of migration develops will be discussed in detail.

Study Area

A study area is the specific geographic place or area getting investigated in a research endeavor. The research topic or goals often determine the study area, which might be different according to the extent and emphasis of the investigation. The study area of this paper is the global concept. The entire concept of migration and its effects will be discussed by applying global concepts. How the overall process of migration is affecting society on the global level will be discussed in this paper.

Result and Discussions

Long-term and expanding research on the phenomenon of migration and mobility indicates that movement is in significant part tied to broader global financial, sociological, geopolitical, and technical



shifts impacting several important policy concerns. As globalisation trends develop, such alterations increasingly influence the way we live as we go about our daily routines - in our employment, in our homes, and in our communal and religious life (World Economic Forum, 2017). Due to the continual advancement of distance-shrinking technology, a growing number of individuals are capable of obtaining knowledge, commodities, and service from across the world. In the past few years, the different issues of both security and financial ability have led to an increasing number of migrants on the global level. Foreign migrants make up an insignificant proportion of the global demographic (approximately 3.3% in 2015). Among the 244 million global migrants registered in 2015, 58% reside in affluent countries, with 85 million coming from underdeveloped countries (OCED, 2014). Throughout the last 25 years, Asia, Europe, and North America have had the greatest increases in the number of foreign migrants, acquiring over 27 million apiece, or nearly 1.1 million more migrants every year. In recent years, an array of nations has indeed been open to periodic immigration. In 2015, more than 70% had strategies either to preserve or not intervene to modify the number of foreign migrants, whereas roughly 13% have measures to decrease immigration and 12% had strategies to increase it. In 2015, roughly one-third of all governments have anti-emigration laws. On the international level, there have indeed been both positive and negative reactions from countries, society and government officials from all across the globe (WHO. n.d). The negative approach to the process of migration or the person who has immigrated is connected to the issues that are developed due to migration.

Among the different issues, one of the major issues that the process of migration has developed is concerned with health. Refugee and migrant health issues are comparable with those experienced by the overall population, although some categories might experience them with greater frequency. Unexpected accidents, hypothermia, wounds, stomach ulcers, cardiac diseases, pregnancy- and delivery-related difficulties, diabetes, and hypertension comprise the most common medical problems among recently arriving refugees and migrants. Female refugees and migrants have unique problems, notably in the areas of maternity, infant, and immunization coverage, including reproductive and sexual health, and abuse (Duncan & Popp, 2017). The hazards linked to population migrations, such as psychological illnesses, reproductive health issues, greater newborn mortality, dietary illnesses, drug misuse, drunkenness, and witnessing an assault, make refugees and migrants more vulnerable to nosocomial illnesses (NCDs). Many times it is difficult for the host country to provide the necessary support for this kind of health issue (IOM, 2020). Almost every country has a planned healthcare system that works along with its population and its demographic. Providing necessary support and extra services to this sudden number of people indeed becomes more difficult for people on a wide scale.

Apart from the health issues related to migration other areas like the labour market, economic well-being and social peace and crime also need to take into consideration. One such important area where the process of migration is affecting or resulting in the development of serious issues is the labour market (OHCHR, 2013). Whilst the flow of migrants generally corresponds to economic strength, particularly from constructing to developed economies, the issue is whether migrants themselves contribute to the prosperity of the recipient economic system or if their existence robs natives of employment opportunities and/or symbolizes a hardship to residents. If prices are inflexible, a basic model of labour availability and demand might indicate that migration, depicted as a simple change in the supply of workers with a downward-sloping labour quantity demanded and all else being constant, will cut native wages or drive out their job (OHCHR, 2013). This issue of taking on native jobs in the labour market led to further hatred among the native people against the migrants leading to major social and political issues on the international level.

Another major source of public concern about immigrants is the potential influence on government finances, especially if they're net recipients or net beneficiaries of social payments. According to studies and conclusions, this fear seems to be more prominent in public views than that of the effect migration has on income and employment. The idea that immigrants strain public finances can explain why, in so many advanced countries, richer persons are frequently in favour of curbing migration, even though owners of capital were probably going to benefit from the inflow of workers (Koczan et al., 2021). In the near term, migrants typically place a price on the target country, particularly in terms of social inclusion and support, as well as the duration required to find work. Refugees have higher expenses, whereas financial immigrants face less. For a long time, immigrants have been less

expensive than locals regarding medical services since individuals prefer to relocate while they're still young. If migrants effectively integrate into the labour market, then have a net beneficial influence on governmental finances over time (Koczan et al., 2021). In aging countries, the immigration of young workers might alleviate the budgetary viability pressures on pension schemes while also assisting in the payment of seniors' medical expenditures.

Another significant public worry regarding migration's influence on recipient nations is the link connecting criminal activity and immigration. Generally, communities with high rates of crime have a higher proportion of immigrants (Amelina, 2022). Yet, when the demographic characteristics of something like the cities are controlled for or auxiliary factors are included, immigration seems to have a minimal to substantial direct influence on violent crime. Individuals' criminal behaviour, especially that of immigrants, is heavily influenced by labour market options. People in the Becker-Ehrlich model of crime logically select between crime and legal labour force activity based on the prospective rewards within each choice. The "return" of criminality is calculated by weighing the likelihood of being discovered and punished against the income from formal employment. If indeed the latter overcomes the latter, a person will act criminally (Edo et al., 2020). In the migration setting, the model implies that incorporation into formal business decreases the likelihood of migrants committing crimes. Among all of these one of the merging issues in concern with migration is related to children.

Deportation and forceful removal of unaccompanied minor migrants and refugees are major causes for worry. This large-scale deportation procedure, which is the result of aggressive regional border security measures, mainly in Europe and North America, externalizes the protection obligations assigned to child migrants to authorities that are ill-equipped to carry things out. Human rights organizations have raised substantial child welfare issues about all of these rules, notably the lack of any systematic investigation of the best interest of kids or the potential threats at home (Li, 2022). UNICEF claimed in 2017 that kids made up 9% of the estimated 400,000 migrants trapped in Libya, with 14,000 of them traveling alone. Amnesty International stated in May 2018 that there were over 33 operational prison camps in Libya, including over 7,000 migrants (many more of them minors) held in custody. Of the lack of resettlement options in Europe or abroad, the European Union, African Union, and United Nations organizations have concentrated their attention on repatriating migrants who want to leave imprisonment and return home (Pruitt, 2021). The International Organization for Migration (IOM) has supported the repatriation of approximately 23,000 migrants from Libya, along with a few kids. Attempts are indeed being undertaken to guarantee that evaluations of the economic interest of deported kids are done before departure, as well as to deal with the absence of assistance available to returns or their families after they reach their destination country.

Migration can have a significant impact on both the sending and receiving communities. Some of the positive impacts of migration include:

1. **Economic growth and development:** Migration can lead to an increase in the labor force, which can contribute to economic growth and development. Migrants often take up low-paying jobs that are hard to fill, and in doing so, contribute to the overall productivity of the economy.
2. **Cultural exchange and diversity:** Migration can bring people from different cultural backgrounds together, leading to cultural exchange and diversity. This can enrich the social fabric of a community and promote understanding and tolerance.
3. **Remittances:** Migrants often send money back to their families and communities, which can help to alleviate poverty and support development projects.
4. **Innovation and knowledge transfer:** Migrants often bring new ideas and skills to their new communities, which can contribute to innovation and knowledge transfer.

However, there are also negative impacts associated with migration, including:

1. **Brain drain:** Migration can lead to a loss of skilled workers from the sending country, which can exacerbate skills shortages and hinder development.
2. **Social tensions and conflicts:** Migration can lead to social tensions and conflicts between migrants and the receiving community, particularly if the migrants are seen as a threat to jobs or cultural norms.



3. Exploitation and discrimination: Migrants are often vulnerable to exploitation and discrimination, particularly if they are undocumented or working in low-paying jobs.
4. Economic and social costs: Migration can impose economic and social costs on both the sending and receiving communities, particularly if the migrants require social services or contribute to congestion and environmental degradation.

Overall, the impact of migration depends on a range of factors, including the characteristics of the migrants, the policies of the sending and receiving countries, and the attitudes of the communities involved.

Conclusion

This paper has indeed helped in highlighting some of the major issues related to the process of migration for both the immigrants and the hosting nation. As per the analysis, some of the major issues that have been highlighted are concerned with demand in labour markets and the ability of immigrants to take over the native peoples' jobs. Apart from this the financial drainage and the health issues caused by the immigrants along with the growth in crime rates are also one of the most significant issues that can be highlighted. The paper has also highlighted some of the emerging issues which are concerned with child immigrants who have no proper guidance or alone move on their own. Managing and engaging these kids in the right places is becoming difficult for the authorized on a wide scale. Although necessary efforts are being adopted all across the places.

References

- Amelina, A. (2022). Knowledge production for whom? Doing migrations, coloniality and standpoints in non-hegemonic migration research. *Ethnic and Racial Studies*, 45(13), 2393-2415. <https://www.tandfonline.com/doi/abs/10.1080/01419870.2022.2064717>
- Borkowska, K., Ketuly, K. A., Mohammad, S. A., Azizi, N., & Mwaikokesya, M. (2018). Migration and its impact on developing countries. *Strengthening Urban Engagement of Universities in Africa and Asia (SUEUAA): Thematic Paper Series*, 1-17. https://www.researchgate.net/profile/Sizar-Dosky/publication/326583533_Migration_and_Its_Impact_on_Developing_Countries/links/5b577e820f7e9bc79a609a51/Migration-and-Its-Impact-on-Developing-Countries.pdf
- Charles, A., Galal, H., & Guna, D. (2018). Preparing Cities to Manage Migration. A policy brief from the Think20 Migration Task Force, CARI and CIPPEC, Buenos Aires. <https://www.g20-insights.org/wp-content/uploads/2018/07/preparing-cities-to-manage-migration-1532526982.pdf>
- Duncan, H. O. W. A. R. D., & Popp, I. O. A. N. A. (2017). World migration report 2018. https://publications.iom.int/fr/system/files/pdf/wmr_2018_en_chapter10.pdf
- Edo, A., Ragot, L., Rapoport, H., Sardoschau, S., Steinmayr, A., & Sweetman, A. (2020). An introduction to the economics of immigration in OECD countries. *Canadian Journal of Economics/Revue canadienne d'économique*, 53(4), 1365-1403. <https://onlinelibrary.wiley.com/doi/abs/10.1111/caje.12482>
- IOM. (2020) *WORLD MIGRATION REPORT 2020*. https://publications.iom.int/system/files/pdf/wmr_2020.pdf
- Koczan, Z., Peri, G., Pinat, M., & Rozhkov, D. (2021). The impact of international migration on inclusive growth: A review. https://papers.ssrn.com/sol3/papers.cfm?abstract_id=4026261
- Li, A. (2022). The effects of adult child migration and migration duration on the emotional health of rural elders in China. *Ageing & Society*, 1-24. <https://www.cambridge.org/core/journals/ageing-and-society/article/effects-of-adult-child-migration-and-migration-duration-on-the-emotional-health-of-rural-elders-in-china/0B6C64CEFB52CC720BDDB34083470F29>
- Mishra, S. B., & Alok, S. (2022). Handbook of research methodology. <http://74.208.36.141:8080/jspui/bitstream/123456789/1319/1/BookResearchMethodology.pdf>
- OCED. (2014) *Is migration good for the economy?* <https://www.oecd.org/migration/OECD%20Migration%20Policy%20Debates%20Numero%202.pdf>



- OHCHR. (2013) *Migration and human rights IMPROVING HUMAN RIGHTS-BASED GOVERNANCE OF INTERNATIONAL MIGRATION*.
https://www.ohchr.org/sites/default/files/Documents/Issues/Migration/MigrationHR_improvingHR_Report.pdf
- Pandey, P., & Pandey, M. M. (2021). *Research methodology tools and techniques*. Bridge Center.
<http://dspace.vnbrims.org:13000/jspui/bitstream/123456789/4666/1/RESEARCH%20METHODOLOGY%20TOOLS%20AND%20TECHNIQUES.pdf>
- Pruitt, L. J. (2021). Children & migration: Political constructions and contestations. *Global Policy*, 12(5), 592-602. <https://onlinelibrary.wiley.com/doi/abs/10.1111/1758-5899.13011>
- WHO. n.d. *MIGRATION AND HEALTH: KEY ISSUES*.
https://www.euro.who.int/data/assets/pdf_file/0005/293270/Migration-Health-Key-Issues-.pdf
- World Economic Forum. (2017) *Migration and Its Impact on Cities*.
https://www3.weforum.org/docs/Migration_Impact_Cities_report_2017_low.pdf



राष्ट्रहिताय संस्कृतम्

Kavikulaguru Kalidas Sanskrit University
Ramtek, Dist. Nagpur, Maharashtra

Peer Reviewed

**Journal of
Fundamental &
Comparative Research**

UGC CARE Listed Journal

शोधसंहिता

New Research Frontiers

Research Journal
ISSN No. 2277-7067

Journal of Fundamental & Comparative Research

शोधसंहिता

A Peer Reviewed Bi-annual Interdisciplinary Research
Journal of the University

UGC CARE Listed Journal
New Research Frontiers

- Patron -

Prof. Shrinivasa Varkhedī
Vice Chancellor

- Chief Editor -

Prof. Madhusudan Penna
Director, Research & Publication

- Editor -

Dr. Rajendra C. Jain
Dept. of Sanskrit Language & Literature



कविकुलगुरु कालिदास

KAVIKULAGURU KALIDAS SANSKRIT UNIVERSITY
RAMTEK

19	STRUCTURAL DESIGN OF WIND TURBINE BLADE PROFILES USING FINITE ELEMENT ANALYSIS	114
20	HERMENEUTICS OF CULTURE IN MAHESH DATTANI'S <i>DANCE LIKE A MAN</i>	126
21	SOCIAL MEDIA AND DEMOCRACY	130
22	MACRO TO MICRO WEDDING – A BIRD EYE VIEW	134
23	CHANGING TRENDS POST COVID ON THE WORK LOAD IMPACTING THE PERFORMANCE OF HOUSEKEEPING STAFF IN HOTELS	140
24	PLANT DISEASE DETECTION PAPER	146
25	जनजातीय विकास योजनाओं का लोहरा जनजाति पर प्रभाव : एक समाजशास्त्रीय अध्ययन	157
26	CORPORATE SOCIAL RESPONSIBILITY IN RURAL DEVELOPMENT SECTOR: AN INTRODUCTION	162
27	A CALL FOR COUNSELLING POLICY AND IMPLEMENTATION ON HUMAN TRAFFICKING	169
28	JUVENILE JUSTICE (CARE AND PROTECTION) ACT, 2015: A CRITICAL ANALYSIS	176
29	LEGAL ISSUES OF SOCIAL MEDIA PRIVACY IN DEMOCRATIC COUNTRIES – A COMPARATIVE STUDY	185
30	FAIR AND SPEEDY TRIAL IN CONTEXT OF RIGHTS AN ACCUSED	191
31	ANALYSIS OF JOB SATISFACTION OF EMPLOYEES BASED ON DIFFERENT TYPES OF HOSPITALS IN AHMEDNAGAR DISTRICT	196
32	SURVEY OF LITERATURE RELATED TO JOB SATISFACTION OF EMPLOYEES WORKING IN HOSPITALS	202

“SOCIAL MEDIA AND DEMOCRACY”

Dr. Mukhtar Shaikh, Dept. of Political Science AKIs Poona College, Camp Pune.

Abstract: *There are many media of communication. There are many methods and ways of communication as individual communication and group communication. Social media is one of the effective media of group communication. Press is one of the most affecting social media in India. In democratic countries, the media is known as the "fourth Pillar" to keep an eye on the activities of the legislature, executive and judiciary. Since the 18th century, especially since the time of the American Independence Movement and the French Revolution, the media has played an important role in reaching out to and informing the public. If the media plays a positive role, then any person, organization, group and country can be made economically, socially, culturally and politically prosperous. Since, the press has played a very important role in the strengthening of democracy in any country that freedom of the press has been considered important for a healthy and strong democracy, but the irony is that for the past few years there has been a continuous decrease in the matter of press freedom. In the case of freedom of the press, a sensational report of the American watchdog Freedom House came out this year, which revealed that there has been a decrease in press freedom for the last one and a half decades. The current paper through a light on social media and democracy.*

Key Words: *Society, social media, democracy, role, press, journalist etc.*

Introduction: In the present times, the utility, importance and role of media is continuously increasing. No society, government, class, institution, group, person can move forward by neglecting the media. Media has become an indispensable necessity in today's life. If we see what is called a society, then the fact comes to the fore that we cannot call a group of people or an unrelated human being as a society. Society means the mutual fabric of relationships, in which communities of rational and thoughtful human beings exist.

Media is a comprehensive system which includes printing press, journalists, electronic media, radio, cinema, internet etc. If we talk about the role of media in the society, it means that what is the media contributing directly and indirectly to the society and what positive and negative effects it is having on the society during the discharge of its responsibilities.

Looking at its impact, it is clear that with the increase in the power, importance and usefulness of the media in the society, its positive effects have increased considerably, but at the same time its negative effects have also emerged.

While the media has contributed to making the public fearlessly aware, exposing corruption, logical control over power and promotion of public interest works, it tarnished its role by being caught in the web of greed, fear, malice, competition, maliciousness and political machinations have also done. Adoption of yellow journalism for personal or institutional vested interests, exploitation of others by blackmail, giving attention to spicy news and distorting news, publishing news inciting riots, giving double meaning to events and statements, fear or greedily flattering the ruling party, unnecessarily praising and glorifying someone and criticizing someone else are being done by the media nowadays. Exaggerating the accident and sensitive issues, ignoring the news related to 'honesty, morality, conscientiousness and courage' have the common features of the media today. This behaviour of the media creates a situation of disorder and imbalance in the society.

In the matter of freedom of the press, today the situation has changed a lot and for the last few years, conspiracies are being made to blunt or break this weapon in the form of a pen. Today, Journalists are the most threatened by political, criminal and terrorist groups and India is no exception in this matter. It is ironic that in newsrooms around the world, there has been an increase in fear and tension caused by government and private groups.

Social Media and Democracy: Social Media affects democracy. The reason for this is that through this the public is getting more information and people are becoming aware. Due to Corona, political parties have been able to convey their views to the public only through virtual meetings in elections. With the connection of social media, one can also participate in debates by sitting in their respective areas. This is the only link because of which people are connected with each other. The major problem of social media is fake which must be stopped. Not only in India but all over the world, the pen has been considered more powerful than the sword and more effective than the edge of the sword, because of its vigilance, many big scams have been exposed in the last few decades in many countries including India.

It is the result of the power of the pen that many a times big industrialists, leaders and giants of various fields who are involved in wrong deeds come down to the floor in a single stroke. If we look at history, in the 1970s, when America's famous 'Watergate' scandal was busted, American President Richard Nixon was also forced to step down. The same situation has been seen in India too, when due to the alertness of the press, high-ranking leaders like Union Ministers and Chief Ministers, who have held very important positions, have been jailed in various cases of corruption.

Underlining the role and power of the press in India, Akbar Allahabadi once said, "Neither pull the bow, nor the sword, when the cannon is in competition, then take out the newspaper." The meaning of his statement was that the pen is more powerful than cannon, sword and any other weapon. The country's first Prime Minister Pt. Jawaharlal Nehru had also said in one of his addresses on December 3, 1950, "Instead of banning the press, I would like to have a completely free press despite all the dangers of misuse of its freedom because Freedom is not just a slogan but an integral part of democracy.

Antisocial activities are reaching the youth through the Internet, due to which there is a continuous decrease in morality, culture and civilization in them. In view of all this, it has become necessary to discuss the role of media.

Indian Scenario of Social Media: In India, the situation is getting worse day- by-day in terms of freedom can be gauged from the annual report of 'Reporters Without Borders'. In the report released by the same organization in the year 2009, where India was at 109th position in terms of press freedom, in a decade it has dropped 31 places to reach 140th position. According to the facts presented in this report about the freedom of the press in India, where India was at 136th position in 2017 and 138th position in 2018 in terms of press freedom, now it has slipped two places and reached 140th position. Undoubtedly, this decline in the freedom of the press does not bode well for a healthy democracy. According to the organization, hatred against journalists is turning into violence around the world, which has increased the fear of journalists around the world. The direct and clear indication of the decrease in the freedom of the press is that the right to freedom of expression, which is enshrined in the basic spirit of democracy, is gradually decreasing.

According to the report, Norway has the best position in terms of press freedom. Apart from Norway, Finland, Sweden, the Netherlands, Denmark, Switzerland, New Zealand, Jamaica, Belgium and Costa Rica also occupy the top positions in press freedom countries, while Turkmenistan, North Korea, Eritrea, China, Vietnam, Sudan, Syria, Djibouti, the condition of press freedom is worst in countries like Saudi Arabia, Laos etc. Pakistan has moved from 139th to 142nd position while Bangladesh has also slipped from 146th to 150th position.

On various occasions, not only in India but all over the world, journalists have to pay the price of truth even by giving their lives. At least six journalists were killed in India last year, according to a report by Reporters Without Borders. Apart from this, there were fatal attacks on many journalists and many journalists also had to face 'hate campaign' on social media. Although perhaps the number of killing of 15-20 journalists in a year around the world would not shock people that much, but if we look into the depth of the matter, it becomes clear that how bad the situation is. Some time ago, a report by the International Federation of Journalists revealed that more than 2300 journalists have been killed in the

last two and a half decades since 1990, out of which only 112 journalists were killed in the year 2015. Given. A Reporters Without Borders report on India reveals that one of the current states of press freedom in India is violence against journalists, including police violence, attacks by Maoists, reprisals from criminal groups or corrupt politicians. Its direct and clear meaning is that if something wrong or unethical is happening anywhere, which is being suppressed or hidden and a journalist tries to expose it, then he is putting his life at risk because to curb such journalists, all kinds of unethical methods of money, price, punishment, discrimination are used, and if they do not agree, sometimes elaborate arrangements are made to suffocate such journalists.

Killing journalists has been considered as the last and cruellest way to put pressure on the media. Although, the freedom of the press has not been provided separately in the Indian Constitution, but its freedom is also inherent in the freedom of expression and freedom of the citizens, and in case of danger to the unity and integrity of the country, this freedom can also be obstructed, but such Even when no situation is created, the killing of journalists in the country and journalism becoming challenging is never in the interest of democracy, rather it can be clearly considered as an attempt by some forces to demolish the fourth pillar of the democratic system.

Media and Leadership: Media provides leadership to the society in many ways. This affects the ideology of the society. Media should also be present in the role of motivator so that society and governments get inspiration and guidance. Media is also the protector of the interests of different sections of the society. He also plays the role of a watchdog of the society's policy, traditions, beliefs and civilization and culture. Different sections of the society get information about the various incidents happening all over the world only through the media. Therefore, he should present the information objectively in the right perspective.

Media's Role in Society: Media also plays a big role in the imbalance and balance of the society through its news. Media can develop a sense of peace, harmony, harmony and courtesy in the society through its role. In times of social tension, conflicts, differences, wars and riots, the media should act in a very restrained manner. Media also plays an important role in inculcating the feeling of devotion and unity towards the nation. In honour of the martyrs, the media should take an active part in broadcasting inspiring and encouraging news. Media can also play the role of social worker through various social works. By providing public assistance at the time of earthquake, flood or other natural or man-made calamities, it can do a great service to humanity. Media should also come forward to promote good practices

Conclusion: The role of the media should be as an agency providing accurate information. Society gets information about the events happening all over the world through the media. That's why it should be the endeavour of the media that this information should be realistic. There should be no attempt to present information by distorting or corrupting it. For the benefit and information of the society, the information should be presented before the public in its original and pure form. The presentation of the media should be such that it can guide the society. The presentation of news and events should be in such a way that the public can be guided. Good articles, editorials, informative information, best entertainment etc. should be included in the news only then the right direction can be given to the society.

References:

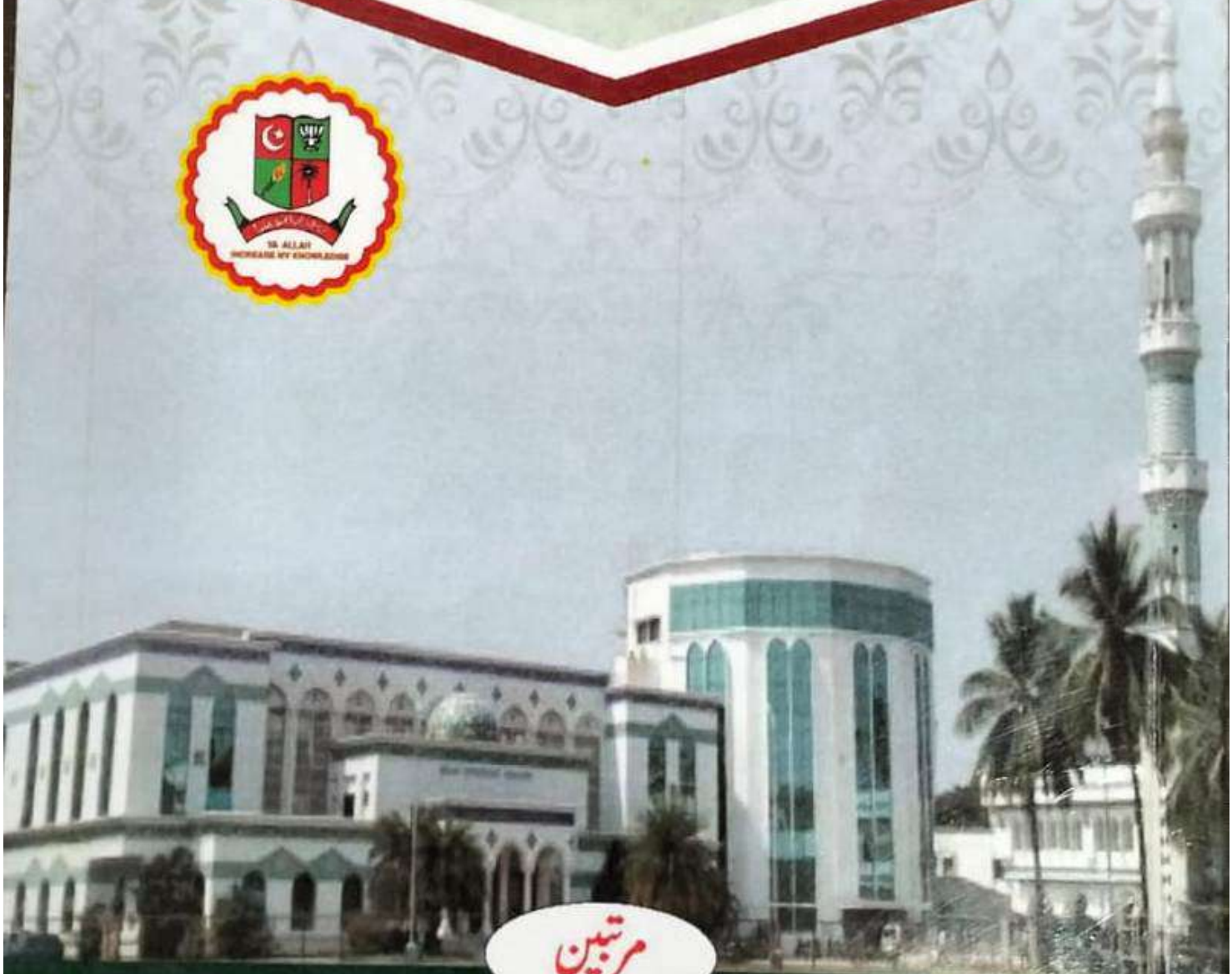
1. AlSayyad, Nezar; Guvenc, Muna (2013-10-10). "Virtual Uprisings: On the Interaction of New Social Media, Traditional Media Coverage and Urban Space during the 'Arab Spring'". *Urban Studies*. 52 (11): 2018–2034. doi:10.1177/0042098013505881. ISSN 0042-0980. S2CID 145777087.
2. Chomsky, Noam (2002). *Manufacturing Consent: The Political Economy of the Mass Media*. Pantheon. ISBN 978-0375714498.

3. Exoo, Calvin F. (2010). *The Pen and the Sword: Press, War, and Terror in the 21st Century*. California: Sage Publications. ISBN 978-1-4129-5360-3.
4. Fahim, Kareem; Mona El-Naggar (January 25, 2011). "Violent Clashes Mark Protests Against Mubarak's Rule". *The New York Times*.
5. Hazen, Don and Julie Winokur, ed. (1997). *We the Media - A Citizen's Guide to Fighting for Media Democracy*. New York: The New Press. ISBN 1-56584-380-0
6. Lazar, Marina-Irina (2015). "Reinforcing Democracy through Internet and Social Networks Participation: Votes, Voters and Elected Behavioral Outcomes in Romanian Presidential Elections". *Revista de Stiinte Politice*: 63–72. ProQuest 1697772455 – via ProQuest.
7. Shane, Scott (January 29, 2011). "Spotlight Again Falls on Web Tools and Change". *The New York Times*.
8. Thornham, Sue (2007). *Women, Feminism and Media*. Edinburgh: Edinburgh University Press. p. 97. ISBN 978-0-7486-2071-5.
9. Wheeler, Mark; Iosifidis, Petros. "The Public Sphere and Network Democracy: Social movements and Political Change?". *Global Media Journal*. 13 (25). Retrieved 21 February 2019.
10. Mack, Ott, Robert L., Brian L. (2014). *Critical Media Studies: An Introduction Second Edition*. West Sussex, UK: Wiley-Blackwell. ISBN 978-1-118-55397-8.

شعبہ اردو نیوکالج کے عالمی ویبپینار میں پیش گئے مقالات کا مجموعہ

سوغاتِ ادب

(شعری ادب)



مرتبین

ساحب حسین ندوی

ڈاکٹر طیب خرازی

جوش - انقلاب، شباب اور فطرت کا شاعر

ڈاکٹر عبد الباقی اویسی

اسوسیٹ پروفیسر ایمین خیر الاسلام پانچاگان
آف آرٹس سائنس اینڈ کامرس کیمپ یونے

جوش بیسویں صدی کے اردو کے عظیم شاعر ہیں جنہوں نے اپنی جذبہ بانی و انقلابی شاعری سے ایک انقلاب پیدا کیا ملک کی جدوجہد آزادی میں اردو زبان کے جیالے شاعروں اور ادیبوں نے اپنے اپنے حصہ دیا۔ ان میں جوش کا نام خاص طور پر لیا جاتا ہے انہوں نے اپنی جذبہ بانی و انقلابی شاعری سے اردو میں ایک نیا جہاں پیدا کیا جس کی وجہ سے انہیں شاعر انقلاب، شاعر شباب، شاعر جذبات کے علاوہ شاعر علم کہا جانے لگا ان کی پرشور اور توانا آواز کا اندازہ ان کے اس شعر سے ہوتا ہے۔

کام ہے میرا تعمیر نام ہے شباب

میرا فخر و انقلاب و انقلاب و انقلاب

جوش کے اجداد افغانی نسل کے سرداروں میں سے تھے جو نواب غازی الدین خاں کے مہمان کھنڈو آئے اور یہیں فوج میں ملازم ہوئے اور وہ یہیں سکونت پذیر ہو گئے۔ جوش کے پردادا نواب غازی خاں گویا و داد احمد خاں اور والد ماجد بشیر حسن خاں وہ نہ صرف صاحب سیف تھے بلکہ عالی علم صاحب دیوان بھی تھے ایسے علمی و ادبی گھرانے میں ۲۵ دسمبر ۱۸۹۸ء کو جوش ملیح آباد (کھنڈو) میں جنم لیا۔ ادبی ماحول میں ان کی پرورش ہونے کی وجہ سے انہیں شاعری ورثے میں ملی تھی جس پر ان کو بطور طور پر ناز تھا۔ ان کا مقبول عام شعر ان کی شاعرانہ عظمت کی ترجمانی کرتا ہے ملاحظہ فرمائے۔

شاعری کیوں نہ ماں آئے مجھے

میرا فن خاندانی ہے

جوش چھوٹی ہی عمر میں ہی اپنی شاعری کا باقاعدہ آغاز کر دیا تھا۔ ابتدا میں مزید کھنڈو کے شاعرانہ رعبے بعد میں وہ اپنے وجدان ذوق کو رہنما بنا کر مشق سخن کرتے رہے جس کی وجہ سے ان کی شاعری

پر وہ ان چہرہ حق نگین، ان کی ادبی شخصیت شاعری، تنقید، خاکے، انکشاف و آزادی اور سوانح نگاری کے اقل پر چھائی ہوئی ہے۔

جوش اپنے زمانے کے قادر الکلام شاعر تھے انہوں نے اپنی شاعری کے متعلق خودنوشت یادوں کی بارات میں لکھا ہے "میں شاعری کے پیچھے نہیں دوڑا بلکہ خود شاعری نے میرا نقاب کیا ہے۔" جوش نے اپنا اولین مجموعہ کلام "روح ادب" میں اپنی شاعری کے بارے میں ایسے نمایاں خودخالی وضع کیے ہیں۔ مثلاً فخر کی آزادی، حسن تخیل، لطیف گوئی اور بے تکلفی جیسی شاعرانہ خصوصیات ہیں جو کسی دوسرے شعراء کے مجموعہ کلام میں عموماً کم ہی پائی جاتی ہے۔

۱۹۱۹ء میں جوش کے والد کے انتقال کے بعد جائیداد کی تقسیم ہوئی تو ان کی آمدنی کے ذرائع محدود ہونے لگے چونکہ ان کی پرورش جاگیردارانہ ماحول میں ہوئی تھی ان کے مزاج میں علمانہ رویہ ہونے کی وجہ سے وہ کسی کے ہاں ملازمت کرنا گوارا نہیں کرتے تھے۔

وقت اور حالات سے انسان کو خبردار کرنا ہونا چاہیے۔ جوش کو کلر معاش دامن گیر ہوئی ان دنوں حیدرآباد و دکن علم و ادب کا مرکز بنا ہوا تھا، شعر و سخن کے چرچے عام تھے۔ مقامی شعراء میں عبدالقادر صدیقی حسرت، مولوی اکبر علی اور احمد جمال نورانی وغیرہ جیسی شخصیات کے علاوہ ہندوستان کے شعراء، ارباب مولانا وحید الدین سلیم، مولوی عبدالحق علی حیدر علیا، مولانا اور مولانا ایساہی برنی وغیرہ جیسی ہستیوں کی وجہ سے دکن ادب کا دلستان بنا ہوا تھا۔ ان ہی دنوں جوش بھی حیدرآباد و دکن آئے یہاں کی ادبی فضا، تہذیب و تمدن اور انسان قدر دانی سے انہیں جانے نہیں دیا اس دور میں حیدرآباد میں جامعہ عثمانیہ علم و ادب کی عظیم درس گاہ قائم ہو چکی تھی اس جامعہ کی مقبولیت ہندوستان بھر کے کونے کونے میں ہونے لگی اس جامعہ میں ایک دارترجمہ کا شعبہ بھی تھا یہاں ایک ایسا شعبہ تھا جہاں سائنسی علوم کے ترجمہ داروں زبان میں ہوا کرتے تھے۔ محمد آصفیہ کی سرکاری زبان اردو رہنے کی وجہ سے اس زبان کی خوب پذیرائی ہوتی رہی خوب پھیلنے پھولنے کا مواقع میسر آئے ان دنوں علامہ اقبال اور جوش کے درمیان مراسم تھے علامہ اقبال کی دربار آصفیہ تک رسائی حاصل بھی کیا جاتا ہے کہ انہوں نے ہی ریاست حیدرآباد کے وزیر اعظم مہاراجہ کرشن پرشاد سے جوش کی ملازمت کے لیے سفارش کی تھی جس پر ۱۹۲۳ء میں نواب میر عثمان علی خاں شاہ وگن نے دارترجمہ کے شعبہ میں علم کی حیثیت سے مامور کیا۔ جوش کی قسمت کا ستارہ چمک اٹھا بیٹھیں سے ان کی سفر زندگی نئی شروعات ہوئی حیدرآباد دکن کے ادبی ماحول میں ان کی شاعرانہ صلاحیتوں اور لیاقت کے جوہر نکھرنے لگے وہ ہر جگہ محفل شعر و سخن میں شرکت کرتے رہے اور دانش حاصل کرتے رہے۔

SAUGHAT-E-ADAB (Sheri Asnaf)

Compiled By
Dr. MOHD TAYYAB ALI
Assit. Professor, Department of Urdu,
The New College3 (Autonomous), Chennai-14

SAJID HUSSAIN
Assit. Professor, Department of Urdu,
The New College3 (Autonomous), Chennai-14

سوغات ادب (شعری ادب)	:	نام کتاب
ڈاکٹر طیب خراوی / ساجد حسین ندوی	:	مرتبین
سے ایم پروسس چھپتی۔	:	طباعت
ساجد حسین ندوی	:	سرورق
2022	:	سن اشاعت
شعبہ اردو، نیوکالج، چھپتی	:	زیر اہتمام
بھنگریہ ماہنامہ تعلیمی سفر لا تور، مہاراشٹر، انڈیا	:	آئی ایس بی این
500	:	تعداد
Rs. 400	:	قیمت

ISBN No. : 978-81-954282-3-6

ملنے کا پتہ

شعبہ اردو، نیوکالج (خود مختار) چھپتی

Dept. of Urdu, The New College, Chennai - 14

E-mail : thenewcollegeurdudpt@gmail.com

ISBN No. : 978-81-954282-3-6

فہرست مضامین

صفحہ نمبر	مضمون نگار	عناوین
6	ڈاکٹر طیب خراوی	مقدمہ
14	پروفیسر سید سجاد حسین	کلیدی خطبہ "اردو کی شعری اصناف"
24	ساجد حسین ندوی	اردو ادب میں شہ نگاری کی اہمیت و افادیت
29	ڈاکٹر امداد نقی	صحت نعت
37	ڈاکٹر سید وحی اللہ نقیاری مری	اردو کی ایک متروک منصف سخن سرشتی
45	ڈاکٹر سید سلیم اللہ حسینی	چہ بے اردو نزل ایک جائزہ
52	ڈاکٹر محمد ابراہیم الہانی	آزاد نظم نثر اور روایت
58	ڈاکٹر عبدالباری اعجاز	جوگس - انتخاب، شباب اور فطرت کا شاعر
66	ڈاکٹر حنا آفرین	تیرے سلطان پیری کی نزل کوئی
73	ڈاکٹر فیروزہ ایس۔ خان	ریاضت خیر آبادی خیرات کا شاعر
80	ڈاکٹر مسرت حمزہ لون	علاسا اقبال کا تصور خودی
89	ڈاکٹر عارث حمزہ لون	اردو شاعری میں لہجوں کی انفرادیت
96	ڈاکٹر ساجد صدیقی	اقبال کی شاعری میں تصور جہ دوزن
106	ڈاکٹر شاکر کوثر	شہریار کی نظموں میں مصری مسائل کی عکاسی
112	ڈاکٹر مرثیہ اقبال	مرشد آباد میں مرثیہ نگاری کی روایت
122	ڈاکٹر شائین الہم خان	منصف غزل میں شعرا سے پہلے اردو کی خدمات
129	ڈاکٹر گلزار احمد رت	عوامی شاعرانہ کبیر آبادی کی نظم نگاری
133	ڈاکٹر سیم احمد قاسمی	اردو قصیدہ نگاری میں شاعر مداحی کا کردار

ISBN No. : 978-81-954282-3-6

شاعری اور ادب کی دنیا ہے۔ ان کا بیچم غلامانہ ذہن میں انقلاب پیدا کرنے کی ترغیب دیتا ہے۔
ہاں میں جذبہ وطنی پیدا کرتا ہے۔ ان کی انقلابی شاعری کا ثور انگریز دشمنی ہے۔
سنو بسٹان زلف گئی خدا کیا آرہی ہے آسمان سے
کر آزادی کا لہر بہتر ہے غلامی کی حیات جاویداں سے

خوب کو جذبہ پیدا دیتا ہوں
قوم کے ہاتھوں میں تھوڑ دیتا ہوں

جوش کی شاعری ہر جہت پر پورے ہوئے ہے وہ خلوص و محبت کا پیکر تھے۔ وہ زندوں اور
آئے تھے۔ وہ شاعری کی افادیت اور منصب سے بخوبی واقف تھے وہ بے غرض بے لوث انسانوں کی
طرح ہر ایک سے محبت کیا کرتے تھے۔ ان کی شاعری میں ہر طبقے کے لوگوں کے لیے پیام ملتا ہے۔ ان
شاعری میں شہسوار کی چنگاری سلگتی رہتی ہے جس سے زندگی کی حقیقی تصویر نظر آتی ہے جس پر
حزوری جوش کی نظموں میں سے اس نظم کا اندازہ پورا موثر معلوم ہوتا ہے لیکن ہم جب موت اور
حزوری کے حقیقی جوش کی خیالات انور سے سمجھیں تو یہاں چند باتیں سامنے آتی ہیں ایک وہ شہسوار
حسین و شہب کی محبوب میں جو کیفیت ہوتی ہے وہ جگ نما ہے انہوں نے عورت کی تصویر کو
میں جو شہسوار کی ہے وہ بڑی مستزکن ہے۔

مست ہے مجھ کو گزرنے کے واسطے
آسمان جان غم کو واقف رکھنی کرے
ان جگمگ پر اور پیڑ ہو جھنگلے کے لیے
پارکی سے جو اٹھ سکتی نہ ہو کابل کا پار
مظنی جھانچے سے قر و غلب کے واسطے
پڑ نغین کا عالم اور ہنر آہ آہ
جوش کی شاعری میں فرحیں اور مزوروں کی حمایت میں گرچہ بہت کچھ لکھا ہے لیکن وہ اپنے
نیا اور غلب کے ہاں نظر کے عصارے پوری طرح آزاد نہ ہو سکے ان کی شاعری میں ترکیب کا
غیر معمول کے فنائی رہتے تھے۔ جوش کی شاعری میں انکار کی وسعت نہیں ہے وہ معمولی بات کو شاعرانہ
انفا سے بیان کر دیتے ہیں کہ بعض اوقات وہ خود فیصلہ نہیں کر پاتے کہ کیا کیا چاہتے تھے۔

ہم ایسے اہل نظر کو جوتے حق کے لیے
اگر رسول نہ ہوتے تو صبح کافی تھی
ڈاکٹر ابو محمد محمد جوش کے بارے میں کہتے ہیں۔

"جوش نے سماجی مسائل کی طرف توجہ کی ہے انھیں وہ اداری کا تذکرہ ان
کی نظموں کا ایک خاص موضوع رہا ہے۔ بعض کو تاجپوں کے باوجود انہوں نے
حزوروں اور کسانوں کی زندگی کی تصویریں جس انداز سے پیش کی ہیں وہ انھیں
محسوس تو کیا ہے۔ سرمایہ داری کی مخالفت اور عوام و فلاح کے رجحانات جس
تفصیل و شدت کے ساتھ انھوں نے اپنی نظموں میں پیش کیے ہیں بلاشبہ ان
کے ادبیات میں ہے۔" (ادبی تحقیق و تنقید، ڈاکٹر ابو محمد محمد جوش، ص ۲۸)

ترقی پسند شعراء کا ذکر آتے ہی جوش کا نام بھی سناؤ زمین پر ابھر آتا ہے۔ حقیقت یہ ہے کہ اردو میں تر
قی پسند تحریک کو پورا ان چھ سالے میں جوش کا عہد غلامانہ ہے۔ اس تحریک سے ان کا ابتدا ہی سے
تعلق رہا ہے اور وہ اس تحریک کے آخر تک ساتھ رہ کر نظم نگاری کو فروغ دیتے رہے۔ انہوں نے اپنی
نظموں میں "ترقی پسند نظریات کو اجاگر کیا ہے ان کی نظموں میں اس زمانے میں رونما ہونے والے
سماجی سیاسی اور سماجی برائیوں کو دیکھا جاسکتا ہے۔ انہوں نے اپنی مقصدی اور موضوعاتی نظموں کے
اور ایسے انقلابی رجحانات کو بخوبی پیش کیا ہے۔ وہ اپنی نظریہ شاعری میں عام انسانوں کی سادہ زندگی کی
حسین طریقے کی منظر کشی کی ہے۔ مثال کے طور پر ان کی مشہور نظموں میں شکستہ زمانہ کا خواب،
ایسٹ انڈیا کمپنی کے فرزندوں کے نام، ام فریب، دو بیگانی ہزار اور بجلی شب وغیرہ ایسی نظمیں ہیں جس
میں انقلاب و بغاوت اور حقیقت پسندی کی عمدہ عکاسی کی گئی ہے۔ ان نظموں میں انقلابی جوش کا منظر بھی
دکھا ہے۔ شکستہ زمانہ کا خواب نظم میں جوش کی انقلابی کیفیت کا بہترین اظہار ہوتا ہے۔

کیا ہند کا زمانہ کاب نہ رہا ہے گویا رہی ہیں آہ
آنکائے ہیں شاہد یکم قیدی اور تو رہے ہیں لٹھریں
دیواروں کے نیچے آکر یوں بیٹھ آئے ہیں زمینی
سینوں میں سما تم بجلی کا آنکھوں میں بھٹکتی شمشیریں
بھوکوں کی نظر میں بجلی ہے تو یوں کے وہاںے غلطے ہیں
تقدیر کے لب کو جنش ہے م تو رہی ہیں قدوریں
کیا ان کو بھر بھی کہ سینوں سے جو خون بر آیا کرتے تھے

جوش جامد عثمانیہ کے شعبہ دارالترجمہ میں تقریباً پندرہ (۱۵) سالوں تک فرض منصبی پر فائز رہا۔ انہیں دینے دے انہیں زبان اور اسلوب پر قدرت رہنے کی وجہ سے وہ انگریزی ادب کی کتابوں اور زبان میں ترجمے کرتے رہے۔ جوش کی تند مزاجی اور حاکمانہ رویے نے انہیں شہادتِ شہداء سے دور رکھا اور وقت انسانِ شہرت کے نشے میں اپنے فرض اور مرتے کو بھول جاتا ہے۔ جوش نے سربراہ حکومت اعلیٰٰ منظور نظام میر عثمان علی خاں بہادر کے جشن ساگر و گلابھی اس نظم کے آفرین شاعر گستاخانہ الفاظ کہ

بھی جوش کے جوش کی مدح فرما
بھی دلہروں کی شہداء خوانیاں کر

یہ میر عثمان علی خاں کو بہت ناگوار گذار پہلے ہی سے وہ جوش کے سیاسی شعبدہ بازی اور غصے کے بارے میں انہیں بہت سی اطلاعات موصول ہو رہی تھیں جس سے وہ ناخوش تھے۔ لہذا انہیں ۱۹۳۱ء میں جوش کو ان کے عہدہ سے برطرف کر کے حیدرآباد دکن سے پھیل جانے کا حکم صادر کر دیا گیا۔ حیدرآباد دکن کی فرخانی اور مہاراجہ برائے صلاحیت کا اندازہ لگاتے کہ انہوں نے جوش کے لیے مہلتیں مانگی کیا تاکہ ان کی گزر بسر آسانی ہو سکے۔ جوش کو اپنے عہدہ سے برطرفی کے بعد مالی دشواریوں کا سامنا پڑا لیکن انہوں نے نواب میر عثمان علی خاں شاہ دکن کی فرخانی کا اعتراف اپنی تصنیف "یادوں کی یادوں میں" لکھ کر لیا ہے۔ ملاحظہ ہوں۔

"میری یہ بڑی نمک خرازی ہوگی کہ اگر میں اس امر کا اعتراف نہ کروں کہ شعبہ دارالترجمہ کی وابستگی نے مجھ کو جس علمی فائدہ پہنچایا ہے اور خصوصیت کے ساتھ علامہ طباطبائی، علامہ عہادی اور مرزا ہادی رسوا کے فیضان بہت نے مجھے بیسودا کو میرے جہل پر مطالعہ کر کے مجھ کو ذوق مطالعہ پر ماسور کیا۔" (یادوں کی یادوں میں ص ۱۷۵)

جوش حیدرآباد سے وطنی منتقل ہو گئے وہاں وہ پیشہ صحافت سے وابستہ ہو گئے۔ وہ آزادانہ طور پر شاعری کرنے لگے ایک طرف تو وہ ملازمت کی قید سے آزاد ہوئے ان کی ذہنی و قلمی پختگی اور جس وقت وہ بہت لگنے دوسری طرف وہ کھلی فضاء میں سانس لینے لگے یہاں ان سے نئی نئی تجربیں آتی گریں۔ جوش نے جوش سے بہت متاثر تھے جس کا انہوں نے اپنی شاعری میں کھل کر اظہار کیا ہے۔ جوش کی شاعری کے کی پہلو میں ان کی شاعری میں انقلاب، شباب، رومانیت، جذبہ اور مہم جوئی کا رنگ نظر آتا ہے۔ انہوں نے اپنی شاعری کی ابتدا غزل گوئی سے کی تھی لیکن وہ نظم کے جذبہ میں

مقام بنالیا۔ غزل ان کی پسندیدہ صنف تھی انہوں نے غزل کو نیا رنگ و آہنگ اور نیا لہجہ عطا کیا ہے۔ غزل میں حسن و عشق کو موضوع بنا لیا ہے مومنا غزل میں ایسا تہ و نثر و مہیات کا اظہار کیا جاتا ہے لیکن جوش نے مرادنی اور نامحرمیوں کے بجائے عزم اور حوصلہ مندی کو بخوبی شاعری میں جوش کیا ہے۔ وہ غزل کے معانی میں حسن کے اسیر نہ تھے ان کی غزلوں کی یہ خصوصیات ہیں کہ غزل میں رنگاری اور تنوع کو ملحوظ رکھا ہے انہوں نے اس صنف میں داخلیت سے زیادہ خارجیت کو زیادہ اہمیت دی ہے اور راجی عقائد کی تقلید سے گریز کرتے ہوئے اپنی انفرادیت کے تحت ایک نئی زبان کی تخلیق کی ہے۔ جوش کے یہاں مشابہت کی گہرائی تخیل اور الفاظ کی ہم آہنگی ملتی ہے۔ انہوں نے نظموں کی طرح غزلوں میں بھی بیابکان انداز سے لکھائی رنگ و آہنگ کو اپنایا ہے۔

جوش کی غزلیہ شاعری کے متعلق ڈاکٹر سید حامد حسین رقمطراز ہیں۔

"جوش نے صنف غزل کا حلقہ بگوش ہونے سے جس طرح انکار کیا ہے وہ بجائے خود ایک بے یقین ذہین کی کارفرمائی تھی جوش نے جہاں یہ محسوس کیا ہے کہ لکھنا غزل میں فرسودہ مضامین کی دلدل خاکس ہوا کرتی ہے وہاں اس بات کا بھی شدت کے ساتھ احساس ہوا ہے کہ غزل کی فرسودہ ساقی گری رند بلد فوش کو تا آسودگی کے سوا کچھ دے سکتی ہے جوش نے بقدر ظرافت اپنے خود بتانے کے لیے جوش کہتے ہیں۔"

مومنہ کلام

سوزِ غم دے کے مجھے اس نے یہ ارشاد کیا
وہ کریں بھی تو کن انقلاب میں تیرا شکوہ
دل کو چوٹیوں نے بھی جبین سے رہنے نہ دیا
اسے میں سو جان سے اس طرزِ حکم کے تار
جا تجھے کھٹکتا ہر سے آزاد کیا
جن کو تیری نگاہ لطف نے بہا دیا کیا
جب چلی سرد ہوا میں نے تجھے یاد کیا
پھر تو فرمائیے کیا آپ نے ارشاد کیا

اتنا مانوس ہوں فطرت سے کل جب چنگی
بجھ کے میں نے یہ کہا مجھ سے کچھ ارشاد کیا
بجھ کو تو ہوش نہیں تم کو خبر ہو شائد
لوگ کہتے ہیں کہ تم نے مجھے بہا دیا کیا
جوش کے یہاں اقبال کی طرح فلسفی گہرائی ہے نہ جذبہ بیداری مگر کلام میں ملاح و بھونڈی گن گرتی ضرور ملتی ہے، وہ انسانی حقوق کیلئے اپنی آواز بلند کرتے ہیں ان پر ہونے والے ظلم و استبداد کا خلاف ایک بیات فارم پر منتج ہونے کا بیجا مہم دیتے ہیں۔ اس کے علاوہ ہندوستان کی جدوجہد آزادی میں جوش کی انقلابی

اک وہ زہی بے رنگی سے جھلکیں گی ہزاروں تصویریں
کیا ان کو خبر تھی زہر و زہر رکھتے تھے جو روح ملت کو
ابٹس گئے زمیں سے مار سہہ بڑھیں گی ملک شمشیریں

جوش غزل اور نظم کے میدان میں اپنی شاعرانہ جوہر نکھرتے گئے وہیں پر انھوں نے صنف ہائے ادب
بھی اپنی شاعرانہ صلاحیتوں کا سدھ مظاہر کیا ہے مستند و مشہور روایتی گو شعراء میر انیس، درویش اور امجد علی صاحب
کے بعد جوش کا بھی نام نمایاں حیثیت سے لیا جاتا ہے۔ ان کے رباعیات کا اندازہ مگر شعراء سے لے کر
بے جب ہم ان کی رباعیات کا مطالعہ کرتے ہیں ہم شمیم کی جھلک غریبیت کی شکل میں نظر آتی ہے۔
صنف رباعی میں وہ کسی ایک نقطہ پر قائم نہیں رہے وہ کبھی حسن و عشق کے نغمے گانے میں تو کبھی سنجیدگی
دیتے ہیں تو کبھی انہی انصاف اور مساوات کی تعلیم بھی دیتے ہیں انہوں نے اپنی رباعیات میں ہر قسم
موضوعات تعلیم بھی دیتے ہیں اس فن میں جوش کے چند مشہور رباعیات ملاحظہ ہوں۔

خینے تری زندگی پہ دل جلتا ہے صرف ایک تبسم کے لیے کلاں
خینے نے کہا کہ اس چمن میں ہاوا یہ ایک تبسم بھی کے ملت
کیا عرف مسلمان کے پیارے ہیں حسین پراخ تو نوح جہر کے تارے ہیں کلاں
انسان کو بیدار تو ہو لینے دو ہر قوم پیکارے گی ہمارے ہیں کلاں

تو مار کو غم کروں تو مرہم بچے بچہ کو فتنار دوں تو زخم بچے
قدرت نے وہ بخشی ہے کرامت مجھ کو شعلے کے نچوڑ دوں تو شہم بچے
جوش شاعری کے علاوہ نثر نگاری میں یدِ طولیٰ رکھتے تھے۔ وہ علمی ادبی گہرائی کے چشم بچے
ہونے کی وجہ سے انھیں اردو، فارسی، ہندی اور انگریزی زبانوں پر قدرت حاصل تھی۔ اس قدر ادا
صلاحیتوں کی بدولت انھوں نے قوی اردو لغت ترتیب و تالیف کو بخوبی انجام دیں۔ شعبہ دارالترجمہ
جہانگیر آباد میں انھیں ترجمہ، ایڈیٹنگ اور دیگر سائنسی و فنی علوم کو اردو زبان میں تراجم کروانے کا
میں صلاحیت سے بے طرف کیے جانے کے بعد انہوں نے قلم اور صحافت کے پیشے سے وابستگی رکھی۔
۱۹۵۲ء میں سالانہ گیم کا اجرا کیا گیا یہ دو سالوں تک نکلتا رہا۔ مالی حالات بہتر نہ ہونے کی وجہ سے
کرتا رہا۔ بعد میں حکومت ہنگامہ رسالہ "آج کل" کے مدیر کی حیثیت سے خدمات انجام دیتے رہے
جہاں بھی وہ زیادہ توں تک وابستہ نہیں رہے۔ ۱۹۵۵ء میں پاکستان ہجرت کر گئے یہاں بھی انھوں نے

اپنی علمی و ادبی صلاحیتوں کو بروئے کار لانے یہاں وہ انجمن ترقی اردو پورا سے منسلک رہے حراج میں
ظہیر آباد رہنے کی وجہ سے بہت جلد کارہ کئی بھی کر لی۔ وہ اپنے تخصص کی مناسبت سے حراج میں جمعیہ کی
امتازت اور غور و فکر مضر بہت کم ہے حراج میں اداب الہی پین جذبات اور اشتعال بہت زیادہ تھا۔

جوش نے اپنی خودنوشت "یادوں کی بارات" کی تکمیل کی جب تصنیف شائع ہوئی ادبی اور سیاسی
حلقوں میں اس کی بڑی وحموم رہی یہ کتاب شہرت کے بجائے تنقید کا شکار رہی۔ "یادوں کی بارات" جوش
کی ایسی تصنیف ہے جس میں انھوں نے کئی نامور شخصیتوں کی فنی زندگی کے راز کھولے ہیں جب تصنیف
منظر عام پر آئی تو مصنف کے کئی مطلقوں میں واوانا بچا جس کی وجہ سے ان کی شخصیت متنازع بن گئی۔ یادوں
کی بارات سے پہلے انہوں نے جو اپنے مقام بنایا تھا بعد اسے انہوں نے کھو دیا بعض کلمے ذہن کے لوگوں
میں اور ادبی حلقوں میں اس کی کافی پذیرائی ہوئی رہی۔ اس تصنیف کے علاوہ جوش کے کئی شعری مجموعے
روح ادب، شاعر کی راہیں، نقش و نگار، شعلہ و شبنم، فکر و نگار، ہنون و حکمت، عرش و فرش، حرف و حکایت،
آیات و نعمات، رزمی اور گنگ، موسم بہا، سیف و سحر، موحد و منکر، نجوم و جواہر، آواز حق، خلیفہ اسلام،
صحن و انقلاب، فقر و فقرہ، کے علاوہ مرثیوں میں عروس ادب، محراب و مضرب، دیوان عشق اور
فانیت کے علاوہ نثری تصانیف میں مقالات زرین، اورانی سحر، جذبات و لطرت، مقالات جوش
امکانات جوش وغیرہ قابل ذکر ہیں۔ یہ ادبی تخلیقات آج ہمارے لیے ادبی سرمایے سے کم نہیں جوش کا
شعری اور نثری ادب قابل قدر ضرور ہے لیکن یہ سچ حقیقت ہے کہ جوش کی نثر میں ان کی شاعری انھیں
راہ نہیں آتی اس لیے انھیں اپنی خودنوشت میں اس بات کا اظہار کرنا پڑا۔

اردو ادب میں جوش کی حیثیت تہا زہر شاعر رہی ہے ان کے فن کا تجربہ کرتے وقت ارباب ادب
نے بڑی بے احتیاجی سے کام لیا ہے، اس ضمن میں ہندوین ادب کا وہ یہ متعلقہ نہیں رہا لیکن ان کی
شاعرانہ عظمت اور شخصیت اپنی جگہ سلسلہ ہے۔ جوش کی علمی و ادبی خدمات کو سراہتے ہوئے حکومت ہند
نے پدم بھوشن ایوارڈ سے سرفراز کیا اور بعد ازاں حکومت پاکستان نے ۲۰۱۳ء میں ریاضی اعزاز پلاٹ
اقتیاز سے نوازا کہ ان کی شاعری اور شخصیت کو زندہ جاوید کر دیا۔ ہندوستان کے اس عظیم شاعر کا انتقال
بڑی ملک پاکستان میں ہوا لیکن سوگ ساری دنیا میں منایا گیا۔ خاص طور پر ہندوستان میں وہ سبھی کے
قابل فخر سہوت تھے سبھی ان کی شخصیت اور فن کو جاملی تھی۔ ان کی طوب پڑھائی گئی ہوئی یہ اور بات ہے
کہ شخص کردار کمزوریوں اور تہذیبی حراج کی وجہ سے بدنام زمانہ بھی رہے لیکن ان کی شعری و نثری خدمات
ہمارے ادبی سرمایے ہے۔





ماہنامہ **فہرست** اتر پردیش اردو اکادمی لکھنؤ

مارچ ۲۰۲۳ء



75
आज़ादी का
अमृत महोत्सव

اتر پردیش اردو اکادمی

خبرنامہ

ترتیب

۲	ایڈیٹر	اداریہ
۳	ذاکر حسین ذاکر	جنگ آزادی کے اہم موڑ
۱۳	مجاہد سید	غزل
۱۳	انس مسرور انصاری	غزل
۱۳	ڈاکٹر ابرار احمد	اردو رپورٹاژ: فن اور روایت
۲۲	ڈاکٹر محمود کاکوروی	رباعیاں
۲۳	شعیب نظام	غزل
۲۳	فراق جلال پوری	غزل
۲۴	شمیم اقبال خاں	پہلی مسلم معلمہ فاطمہ شیخ...
۲۸	معید رہبر لکھنوی	غزل
۲۸	شاداب شبیری	غزل
۲۹	اشفاق برادر	شعائیں (افسانہ)
۳۱	مبصر	تبصرہ
۳۱	سید محمود حسن	تبرک (محفوظ رحمانی)

جلد : ۵۱ مارچ ۲۰۲۳ء شماره : ۹

سرپرست : چودھری کیف الوری (چیرمین)

ایڈیٹر : ایس۔ مناظر عادل حسن

معاون : محمد معاذ اختر احسن (پرنٹنگ)

زر سالانہ : پچاس روپے - 50/-

قیمت فی شماره : پانچ روپے - 5/-

upurduakademi3@gmail.com

www.upurduakademi.in

خط و کتابت و ترسیل زر کا پتہ

سکرٹری، اتر پردیش اردو اکادمی، دہلی، بھوتی کھنڈ،

گومتی نگر لکھنؤ۔ 226010

فون نمبر: 0522-4022 924

ایس۔ مناظر عادل حسن، ایڈیٹر، پرنٹ اور پبلشر نے اسپریشن پرنٹ ہاؤس، لاٹوش روڈ، لکھنؤ سے چھپوا کر دفتر اکادمی، واقع دہلی بھوتی کھنڈ، گومتی نگر لکھنؤ سے شائع کیا۔

ڈاکٹر ابرار احمد

اسٹنٹ پروفیسر، شعبہ اردو، عربی و فارسی
پونا کالج آف آرٹس، سائنس اینڈ کامرس، کمپ، پونے

اردو رپورتاژ: فن اور روایت

* Reportage: Writing intended to give an account of observed or documented events." (The Oxford English Dictionary P. 475)

(ایسی تحریر جو مشاہدات یا دستاویزی واقعات پر مشتمل ہو، رپورتاژ کہلاتی ہے۔)

Webster Third News International Dictionary میں رپورتاژ کے بارے میں لکھا ہے۔

" Writing intended to give a factual and detailed account of directly observed or carefully documented events and scenes." (Webster Third News International Dictionary P. 1925)

(ایسی تحریر جو راست مشاہدات اور محتاط دستاویزی واقعات و مناظر کی سچی تفصیل بیان کرتی ہو رپورتاژ ہے۔)

کشاف تنقیدی اصطلاحات میں ابوالعجاز حفیظ صدیقی

نے رپورتاژ پر تبصرہ کرتے ہوئے لکھا ہے:

رپورتاژ اردو غیر افسانوی نثر کی ایک اہم صنف ہے۔ ناول اور افسانہ کی طرح یہ صنف بھی مغرب کے زیر اثر اردو میں داخل ہوئی ہے لیکن اردو ادیبوں نے اسے اردو کے عین مزاج کے مطابق برتنے کی کوشش کی جس کے باعث اس نے بہت ہی کم وقت میں اخباری رپورٹ سے علاحدہ ایک صنف کا درجہ حاصل کر لیا۔

رپورتاژ فرانسیسی زبان کا لفظ ہے۔ فرانسیسی میں اس کا تلفظ Reportage ہے جس کے لیے انگریزی میں Report مستعمل ہے۔ اردو میں اس جدید صنف کو "رپورتاژ" کے نام سے موسوم کیا گیا ہے۔ یہ صحافتی رپورٹ سے یکسر علاحدہ صنف ہے۔ اس میں صحافتی خوبیاں تو موجود ہوتی ہیں لیکن اس کا فن خالص ادبی ہوتا ہے۔ اس صنف ادب میں خیالات و تصورات کے بالمقابل مشاہدات و تجربات کو فوقیت دی جاتی ہے۔ یہ ایک ایسا نثری ہیانیہ ہے جس میں صحافت، ادبیت اور افسانویت کا حسین امتزاج پایا جاتا ہے۔ اس صنف کی تعریف ماہرین لغات و فن نے اپنے اپنے انداز میں پیش کی ہیں۔ آکسفورڈ انگلش ڈکشنری میں رپورتاژ کے معنی یوں درج ہیں۔